

Advances in Organometallic Chemistry

EDITED BY

F. G. A. STONE

DEPARTMENT OF CHEMISTRY
BAYLOR UNIVERSITY
WACO, TEXAS

ROBERT WEST

DEPARTMENT OF CHEMISTRY
UNIVERSITY OF WISCONSIN
MADISON, WISCONSIN

VOLUME 36



ACADEMIC PRESS

A Division of Harcourt Brace & Company

San Diego New York Boston
London Sydney Tokyo Toronto

This book is printed on acid-free paper. ∞

Copyright © 1994 by ACADEMIC PRESS, INC.

All Rights Reserved.

No part of this publication may be reproduced or transmitted in any form or by any means, electronic or mechanical, including photocopy, recording, or any information storage and retrieval system, without permission in writing from the publisher.

Academic Press, Inc.

525 B Street, Suite 1900, San Diego, California 92101-4495

United Kingdom Edition published by

Academic Press Limited

24–28 Oval Road, London NW1 7DX

International Standard Serial Number: 0065-3055

International Standard Book Number: 0-12-031136-4

PRINTED IN THE UNITED STATES OF AMERICA

94 95 96 97 98 99 QW 9 8 7 6 5 4 3 2 1

Contributors

Numbers in parentheses indicate the pages on which the authors' contributions begin.

JAMES R. BOWSER (57), Department of Chemistry, State University of New York at Fredonia, Fredonia, New York 14063

NEIL J. COVILLE (95), Centre for Applied Chemistry and Chemical Technology, Department of Chemistry, University of the Witwatersrand, Johannesburg 2001, South Africa

HOLGER FRIEDRICH (229), Anorganisch-Chemisches Institut, Technische Universität München, D-85747 Garching, Germany

HERMANN HANDWERKER (229), Anorganisch-Chemisches Institut, Technische Universität München, D-85747 Garching, Germany

ANTHONY F. HILL (159), Department of Chemistry, Imperial College of Science, Technology, and Medicine, South Kensington, London SW7 2AY, United Kingdom

COLIN J. SCHAUVERIEN (283), Koninklijke/Shell Laboratorium, Amsterdam (Shell Research B. V.), 1031 CM Amsterdam, The Netherlands

DAVID WHITE (95), Centre for Applied Chemistry and Chemical Technology, Department of Chemistry, University of the Witwatersrand, Johannesburg 2001, South Africa

ROBERT E. WILLIAMS (1), Loker Hydrocarbon Research Institute, University of Southern California, Los Angeles, California 90089

CHRISTIAN ZYBILL (229), Anorganisch-Chemisches Institut, Technische Universität München, D-85747 Garching, Germany

Early Carboranes and Their Structural Legacy

ROBERT E. WILLIAMS

*Loker Hydrocarbon Research Institute,
University of Southern California, University Park,
Los Angeles, California, 90089-1661*

I. Background and Introduction	1
II. Carboranes, Carbocations, and Polyboranes	9
III. Skeletal Electron Pair Bonds Identified by <i>styx</i> and <i>Chop-Styx</i>	18
IV. Classification Based on Geometry, Empirical Formula, and Electron Pair Bond Relationships	22
V. Polyborane Lewis Base Adducts	30
VI. Electron Counting	31
VII. Carborane Nomenclature	31
VIII. <i>nido</i> -Carboranes and Related Compounds	32
A. <i>nido</i> -6-Vertex Compounds	32
B. <i>nido</i> -4-Vertex Compounds	33
C. <i>nido</i> -5-Vertex Compounds	34
D. <i>nido</i> -7-, -8-, and -9-Vertex Compounds.	34
E. <i>nido</i> -10-Vertex Compounds	35
F. <i>nido</i> -11- and -12-Vertex Compounds	36
G. <i>nido</i> -2-Vertex Compounds	39
IX. <i>arachno</i> -Carboranes and Related Compounds	40
A. <i>arachno</i> -9-Vertex Compounds	41
B. <i>arachno</i> -10-, -11-, and -12-Vertex Compounds	42
C. <i>arachno</i> -8-Vertex Compounds	44
D. <i>arachno</i> -7-, -6-, and -5-Vertex Compounds	45
E. <i>arachno</i> -4-Vertex Compounds	45
F. <i>arachno</i> -3-Vertex Compounds	46
G. <i>arachno</i> -2-Vertex Compounds	46
X. <i>hypho</i> -Carboranes and Related Compounds.	47
A. <i>hypho</i> -6-Vertex Compounds	48
B. <i>hypho</i> -5-Vertex Compounds	48
C. <i>hypho</i> -4-Vertex Compounds	48
D. <i>hypho</i> -3-Vertex Compounds	48
XI. Conclusion	49
References.	49

I

BACKGROUND AND INTRODUCTION

Carboranes are mixed hydrides of carbon and boron in which atoms of both elements feature in the electron deficient polyhedral molecular skeleton. Fulfilling an invitation to chronicle the evolution of their chemis-

try has not been without problems. However, a number of pleasant surprises have been brought into focus in retracing the last 40 years. Prior to the 1950s there were no recognized carboranes; however, by the end of the 1950s, examples of two or three *kinds* of carboranes had been discovered. Our small group on the west coast of the United States (1) discovered the first carboranes, i.e., the *closo*-carboranes, 1,5- $\text{C}_2\text{B}_3\text{H}_5$ (**1**), 1,2- $\text{C}_2\text{B}_4\text{H}_6$ (**2**), 1,6- $\text{C}_2\text{B}_4\text{H}_6$ (**3**), and 2,4- $\text{C}_2\text{B}_5\text{H}_7$ (**4**) (2–5) although in a low, synthetically useless, combined yield of less than 2%. The correct structures, deduced (3–5) from their ^{11}B NMR spectra, are illustrated in Fig. 1 along with selected, but incorrect, classical alternatives (**A**, **B**, **C**, **D**, and **E**) favored at the time by traditionalists to avoid five coordinate carbons and multicenter bonding. Throughout this article, with a few obvious exceptions, the *sticks* in the *ball* and *stick* illustrations represent connections rather than bonds. As multicenter bonds are invariably present there are more connections than electron pair bonds.

Shortly thereafter, other groups of investigators (6–18) in the Eastern United States, as well as a group in Russia (19–21), reported the discovery of the much larger (10 boron) icosahedral *closo*-carborane, 1,2- $\text{C}_2\text{B}_{10}\text{H}_{12}$ (**6**) (Fig. 2), in much higher yields. Somewhat more reasonable, but still incorrect, suggested structures (**F**, **G**, **H**, and **I**) are also displayed in Fig. 2. Interestingly, nonclassical multicentered bonding was not rejected in the B_{10} portion of the molecule as the structure of $\text{B}_{10}\text{H}_{14}$ was well known.

The majority of the structural patterns, the emphasis of this article, became evident from structural studies on the more illuminating smaller *closo*-carboranes (Fig. 1), while the overwhelming majority of carborane synthetic chemistry was subsequently derived from reactions involving the more important icosahedral *closo*-carboranes (Figs. 2 and 3). As this account concentrates on structural patterns, as opposed to synthesis, the smaller *closo*-carboranes get top billing. We cover first the entire range of *closo*-carboranes (Figs. 1 through 7) and return for a more detailed discussion later.

Once the nonclassical structures, (**1**) to (**8**), had been established and accepted for the *closo*- $\text{C}_2\text{B}_n\text{H}_{n+2}$ series, wherein $n = 3, 4, 5$, and 10, it seemed reasonable that an intermediate sized species could be prepared, namely a derivative of $\text{C}_2\text{B}_6\text{H}_8$ (**9**) (22), wherein $n = 6$ (Fig. 4). By this time classical structural alternatives had been abandoned and only nonclassical cluster structures with multicenter bonds were considered (see Fig. 4).

The remaining medium sized *closo*-carboranes, $\text{C}_2\text{B}_7\text{H}_9$ (**10**), 1,2- $\text{C}_2\text{B}_8\text{H}_{10}$ (**11**), 1,6- $\text{C}_2\text{B}_8\text{H}_{10}$ (**12**), 1,10- $\text{C}_2\text{B}_8\text{H}_{10}$ (**13**) (all in Fig. 5), and $\text{C}_2\text{B}_9\text{H}_{11}$ (**14**) (in Fig. 6) were prepared by Hawthorne and co-workers (23) by the degradation of the icosahedral compounds. The incorrect structure for the monoanion *closo*- $\text{CB}_{10}\text{H}_{11}]^-$ is illustrated as **Q**, in Fig. 6, while

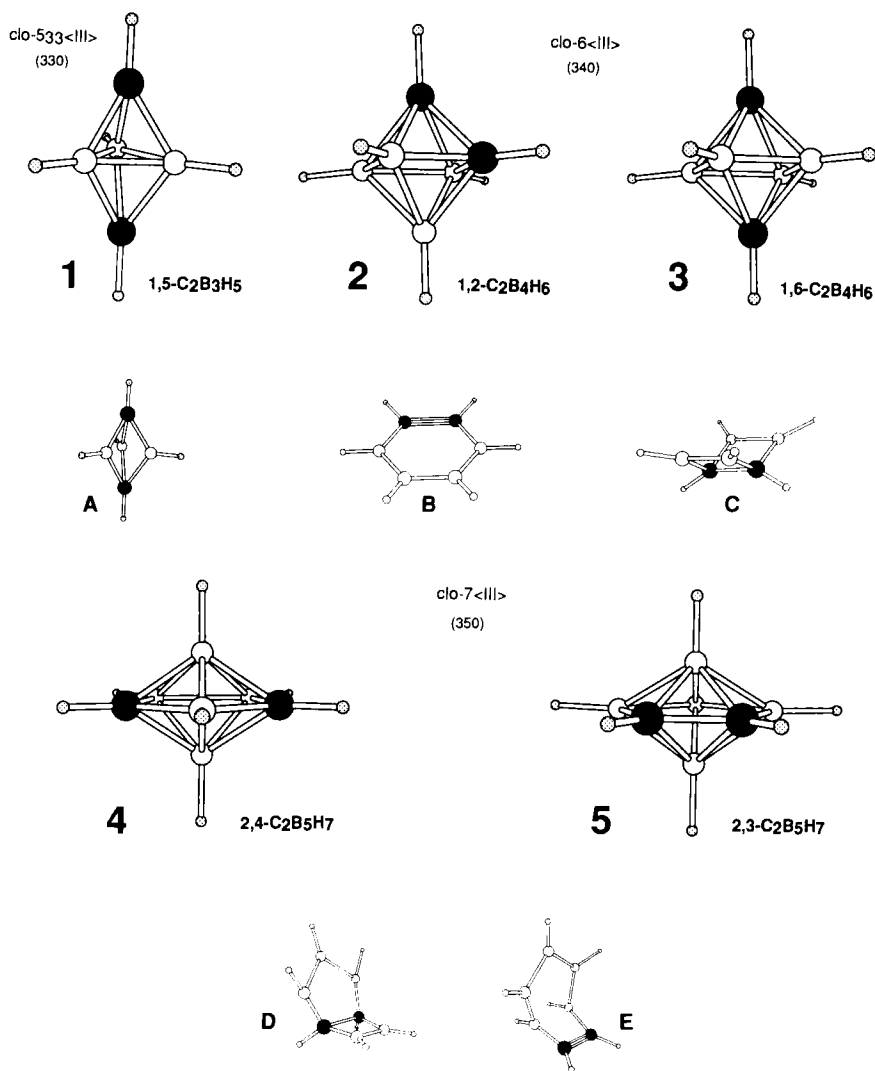


FIG. 1. Smaller *closo*-carboranes: $1,5\text{-C}_2\text{B}_3\text{H}_5$ (**1**), $1,2\text{-C}_2\text{B}_4\text{H}_6$ (**2**), $1,6\text{-C}_2\text{B}_4\text{H}_6$ (**3**), $2,4\text{-C}_2\text{B}_5\text{H}_7$ (**4**), $2,3\text{-C}_2\text{B}_5\text{H}_7$ (**5**), and the classical alternatives, **A**, **B**, **C**, **D**, and **E**.

the correct structure (**20**) is shown in Fig. 7 (23,24), along with the other monocarba-*closo*-carborane species.

Long before humans crossed the Bering Straits from Asia into North America, the Los Angeles basin was home to exposed pools of hydrocarbons, the La Brea Tar Pits. Oil deposits, deep under what is now Long

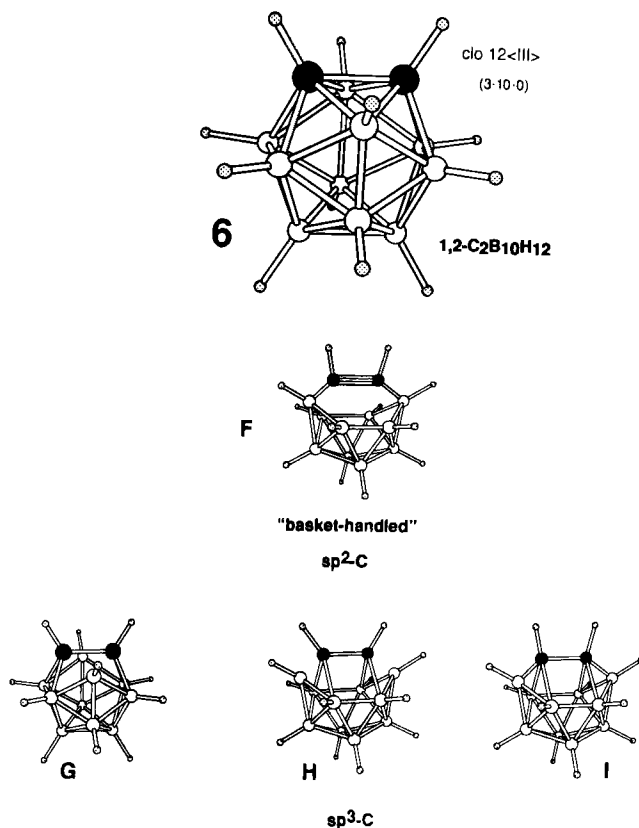


FIG. 2. The structure of the icosahedral *closo*-carborane, 1,2- $\text{C}_2\text{B}_{10}\text{H}_{12}$ (**6**) and its incorrect alternatives, **F**, **G**, **H**, and **I**.

Beach in Southern California, leaked to the surface and appeared as small lakes of hydrocarbons amidst Cypress and Pine groves on a sage brush plain in Los Angeles over 20 miles to the north. The volatile components evaporated and a sticky asphaltic, optically smooth mass remained. At times, water, sand, or dust collected over the surface and grasses masked the edges; a more certain death trap is difficult to imagine. The pursued and their pursuers encountering the tar were quickly ensnared, entombed, and embalmed. In this century, the bones of many predators, extinct for over 10 thousand years, such as 11-ft-tall flat-faced bears, giant American lions, saber-toothed tigers (*Smilodon fatalis*), dire wolves and their prey, horses, camels, enlarged versions of ground sloths, and the Antique bison, as well as mammoths and mastodons, have been recovered from the

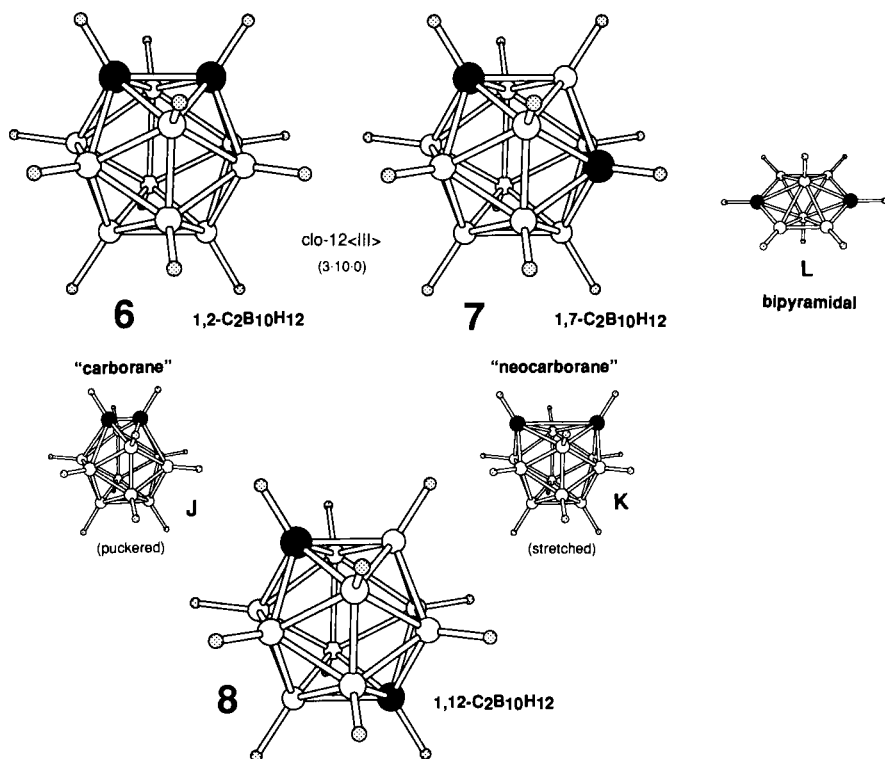


FIG. 3. The icosahedral *closo*-carboranes, $1,2\text{-C}_2\text{B}_{10}\text{H}_{12}$ (**6**) (at one time thought to be the puckerred "carborane," **J**), $1,7\text{-C}_2\text{B}_{10}\text{H}_{12}$ (**7**) (at one time thought to be the stretched "neocarborane," **K**), and $1,12\text{-C}_2\text{B}_{10}\text{H}_{12}$ (**8**).

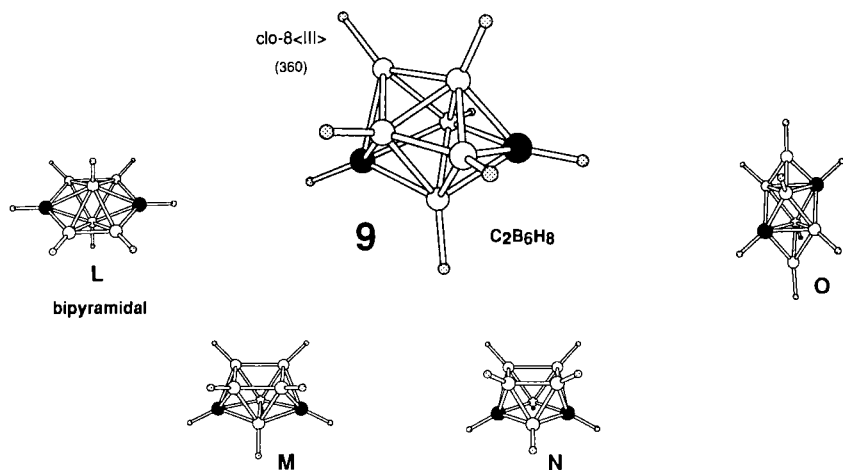


FIG. 4. The intermediate-sized *closo*-carborane, $\text{C}_2\text{B}_6\text{H}_8$ (**9**) and its fanciful deltahedral alternatives, **L**, **M**, **N**, and **O**.

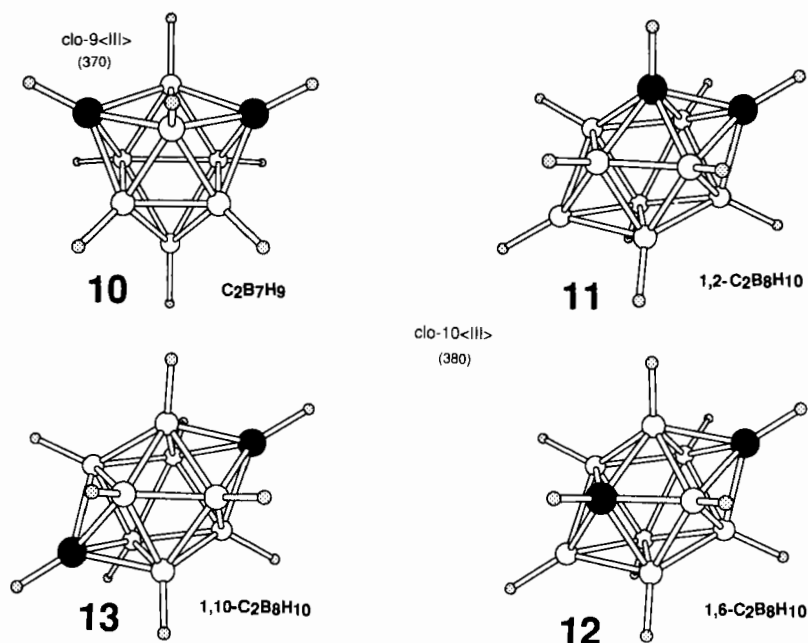


FIG. 5. The medium-sized *closo*-carboranes, $C_2B_7H_9$ (10), $1,2-C_2B_8H_{10}$ (11), $1,6-C_2B_8H_{10}$ (12), and $1,10-C_2B_8H_{10}$ (13).

long congealed tar and reassembled, their soft tissues incorporated into the asphalt.

Most of the early paleontology was directed by Chester Stock (1892–1950) (28) of the University of California, Berkeley, and the Califor-

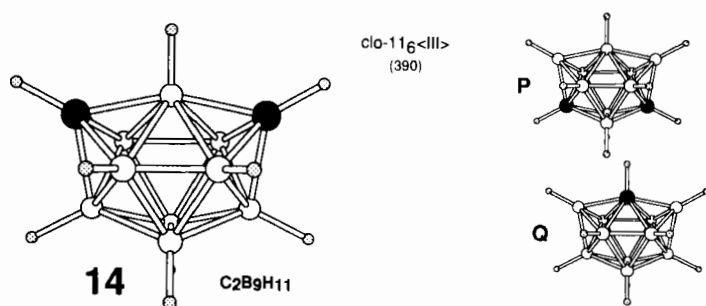


FIG. 6. The *closo*-carborane, $C_2B_9H_{11}$ (14) and related incorrect carbon location isomers P and Q.

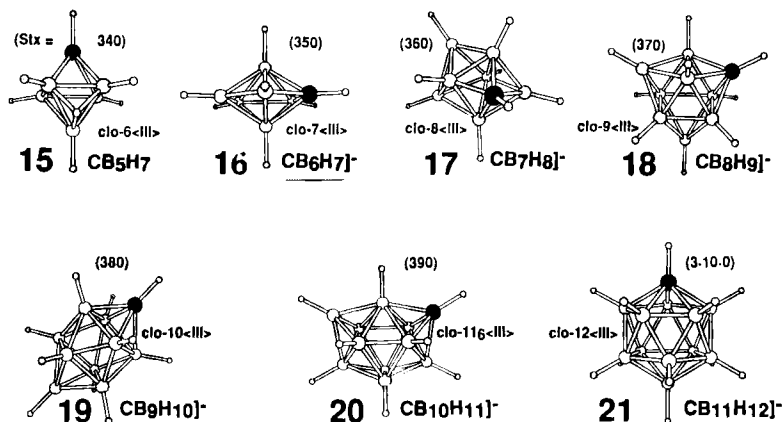


FIG. 7. The monacarba-*closo*-carborane, CB_5H_7 (15) (27) and the related *closo*-anions, $\text{CB}_6\text{H}_7]^-$ (16), $\text{CB}_7\text{H}_8]^-$ (17), $\text{CB}_8\text{H}_9]^-$ (18), $\text{CB}_9\text{H}_{10}]^-$ (19), $\text{CB}_{10}\text{H}_{11}]^-$ (20) (26), and $\text{CB}_{11}\text{H}_{12}]^-$ (21).

nia Institute of Technology. His original collections are on display in the Page Museum at the La Brea Tar Pits.

Chemists of today, gazing into these tar pits, cannot help but wonder how many different types and kinds of compounds, primarily hydrocarbons, must exist in each handful of such tar; surely hundreds, perhaps tens of thousands. Today, DNA, ^{13}C , and ^{14}C analyses are furnishing information on the faunal relationships between ancient and modern species, their normal temperatures during their lifetime, and the years since their death.

Of more recent vintage and enshrined at the University of Southern California is Anton B. Burg, the first American born, exclusively American educated, *hydroboron* chemist and boron chemistry's link with its classical past. It was Anton Burg who, seeking pure boron by the Weintraub electric-arc method, was able to modify it into the first *reasonable*-yield synthesis of diborane, B_2H_6 (29). He subsequently obtained the support of his mentor, Hermann I. Schlesinger, for a critical restudy and extension of the works of the great German chemist, Professor Alfred Stock, the father of boron hydride chemistry (28). Indeed, Alfred Stock then adopted for his own use the Burg–Schlesinger diborane synthesis.

Although Alfred Stock reported in 1923 (30) and reviewed in his 1933 book (31) that diborane and ethylene reacted to produce aromatic smelling substances (no doubt the products of hydroboration), it was Burg (29) who first systematically hydroborated double bonds by reacting diborane,

B_2H_6 , with the carbonyl moieties of aldehydes, ketones, and esters, i.e., $CH_3CH=O$, $(CH_3)_2C=O$, and $HC(=O)OCH_3$, and by identifying the dialkoxyborane products, $(RO)_2BH$. Hurd (32) quantified the reactions of diborane with olefins (hydroboration of $C=C$ double bonds) by identifying the trialkylborane products, Bu_3B and Et_3B , produced from the reactions of diborane with butene and ethylene in the gas phase. Subsequently the elegant and exhaustive extension of the Burg–Hurd hydroboration reaction to olefins in solution by H. C. Brown (propelled by his discovery that ethers were catalysts) plus his discovery of the hydroboration rearrangement (33) [see brachiation below (34)] enabled him to develop the broad chemistry of hydroboration for which he was awarded the Nobel Prize for Chemistry in 1979.

Since hydrocarbons are compounds of carbon and hydrogen, and boron hydrides are compounds of boron and hydrogen, then perhaps it is appropriate that the first carboranes (hybrid compounds of carbon, boron and hydrogen) were discovered (2–5) in Pasadena, California (1), during the middle 1950s, in close proximity to Anton B. Burg and just across town from the La Brea Tar Pits.

In the early 1950s, Lipscomb (35) and Kasper *et al.* (36) elucidated the structures of pentaborane, B_5H_9 , and decaborane, $B_{10}H_{14}$, with certainty and had popularized the idea that boron hydrides, or polyboranes, had polyhedral cage structures. It was noted that the structure of pentaborane resembled a fragment of a regular octahedron and that the structure of decaborane could be viewed as a fragment of an icosahedron, the polyhedra already known to be present in elemental boron. The concept of three-center two-electron ($3c-2e$) bonds had come into vogue, suggested by Longuet-Higgins (37) and popularized by Lipscomb (38).

In the early 1950s, it was thought that the United States could develop a long-range aircraft that would utilize a lightweight boron hydride or a boron hydride derivative as its fuel and to that end, massive governmental expenditures had been authorized (39). During these investigations, carried out under a government-imposed veil of secrecy, it was found that none of the pure polyboranes had optimum physical characteristics for a fuel and it was thought that perhaps certain hydrocarbon derivatives of selected polyboranes would have the required properties. Alkyl derivatives of boron hydrides were envisioned for this purpose, not carboranes.

Many hydrocarbons and polyboranes were mixed together and caused to react in various ways. Alkyl polyboranes such as ethyldecaborane, $C_2H_5B_{10}H_{13}$, and propylpentaborane, $C_3H_7B_5H_8$ (1,6–8), as well as numerous alkyl and polyalkyl derivatives of diborane, $R_xB_2H_{6-x}$ (40), were produced and tested as possible high-energy fuels.

II

CARBORANES, CARBOCATIONS, AND POLYBORANES

The first process known to produce carboranes took place in the Pasadena laboratory of Olin Mathieson Corporation (1) under the sponsorship of the U.S. Office of Naval Research. It involved a reaction between B_2H_6 and acetylene. Such a mixture explodes if sparked or ignited with a hot wire, producing primarily intractable solids and hydrogen. In addition, however, something less than 1% of the boron was found to be incorporated in volatile products containing boron and carbon as well as hydrogen. The mass spectra of these "unknown" compounds revealed that they were not simple alkyl derivatives of polyboranes.

The positive ion mass spectrometer had come into usage by the early 1950s and its availability enabled the identification of many compounds formed only in trace amounts. Subjecting these volatile products to mass spectroscopic analysis enabled Landesman (39,41) to tentatively identify (~ 1953) molecular species such as $C_2B_3H_x$, $C_2B_4H_y$, and $C_2B_5H_z$ as components in these mixtures; the identities of x , y and z were then unknown.

Later, Keilin *et al.* (4,34) observed that the same compounds were produced from the reaction between pentaborane, B_5H_9 , and acetylene in a silent electric discharge (plasma?) apparatus, i.e., Burg's original equipment for producing B_2H_6 from BCl_3 and H_2 . Moreover, it was found that the values of y and z in $C_2B_4H_y$ and $C_2B_5H_z$ were 6 (or greater) and 7 (or greater), respectively. The mass spectrometers available circa 1953 were of such an ionizing voltage that the parent ions of several hydrogen-rich polyboranes such as B_2H_6 , B_4H_{10} , and B_5H_{11} , i.e., those molecules that contained BH_2 groups, could not be detected. Hence only the minimum numbers of hydrogens associated with the borons and carbons in the parent compounds could be established with certainty; then there was always the possibility that one or two hydrogens would not be detected.

The writer, assisted by the late C. David Good (42) (a one-time graduate student of Anton Burg), repeated the Keilin synthesis in 1956 and accumulated sufficient material for separation and spectroscopic analysis. The infrared and ^{11}B NMR spectra indicated that BHB bridge hydrogens as well as BH_2 and CH_2 groups were absent from these products, and the data suggested, moreover, that all skeletal borons were in tetrahedral sp^3 environments rather than planar sp^2 configurations. The sharp mass spectral *cut offs* of the boron monoisotopic spectra (43) were also indicative of "hydrogen-poor" molecules (e.g., resembling aromatic hydrocarbons) that were resistant to fragmentation.

We concluded (3a–3d) that the empirical formulae had to be $C_2B_3H_5$ (**1**), $C_2B_4H_6$ (**2**) and (**3**), and $C_2B_5H_7$ (**4**) (Fig. 1). On the basis of the ^{11}B NMR spectra, we concluded that the structures of these compounds must be three-dimensional, nonclassical, and deltahedral (44) (with the carbons occupying low coordination vertices and nonadjacent in the most stable isomers) rather than two-dimensional, classical, and more or less “flat” like benzene or cyclohexane; see **A**, **B**, **C**, **D**, and **E** in Fig. 1. A patent was filed in 1959 (2a), only covering $C_2B_3H_5$ (**1**), as several chemist–administrators and patent lawyers were squeamish about the correctness of our structures for (**2**), (**3**), and (**4**) favoring instead structures more like **B**, **C**, **D**, and **E**. In the patent, $C_2B_3H_5$ is described as containing two *identical CH groups* and three *identical BH groups* but the lawyers would not take the risk of suggesting structures such as (**1**) or **A**; conversations circa 1490 between Columbus and Ferdinand and Isabella spring to mind.

These events took place some 40 years ago, we were young and flexible, influenced strongly by Lipscomb, and our imaginations not yet cross-linked. The carbon placement patterns (wherein carbon prefers (a) low coordinated and (b) nonadjacent sites) were easily deduced from the structures illustrated in Fig. 1. However, these patterns were not accepted by many investigators (e.g., **P** in Fig. 6) (**23**) until the late 1960s and a number of younger authors are unaware of this generality (see **Q** in Fig. 6 versus (**20**) in Fig. 7) (26).

The structures in Fig. 1 were made public on September 8, 1961 (3a,3b). Seventeen days later Lipscomb included them in a paper he submitted to the Proceedings of the National Academy of Science (3c) and shortly thereafter theoretical calculations were carried out (1962) by Hoffmann and Lipscomb (3d), following which they concluded that our proposed structures for 1,5- $C_2B_3H_5$, 1,6- $C_2B_4H_6$, and 2,4- $C_2B_5H_7$ represented the most stable structures for those compounds. They extrapolated their calculations to include the larger compound, $C_2B_{10}H_{12}$ (at that time formally unreported in the open literature), and supported an icosahedral structure based on its probable similarity to the dianion $B_{12}H_{12}]^{2-}$ whose structure had been anticipated by Lipscomb *et al.* (45) and by Longuet-Higgins and Roberts (46).

The discoveries of the icosahedral carboranes (Figs. 2 and 3) took place independently of the smaller carboranes (47). It has always been intriguing that the icosahedral carboranes, having been kept secret in government sponsored work in the U.S.A. for over 5 years, became public in both the U.S.A. (papers submitted in January through July, 1963 to *Inorganic Chemistry*) (10–12) and in the former USSR (papers submitted on August 24, and September 28, 1963) (21) at almost the same time. Surprisingly the Russians (21) interpreted their X-ray data as supporting the incorrect

structure incorporating a bidentate, —CH=CH— , group (**F** in Fig. 2), which was also favored by at least one U.S.A. group in the absence of X-ray data (see below). Between the end of World War II and the breakup of the Soviet Union, both the U.S.A. and the USSR kept close watch on each other's research progress. With the recent dissolution of the USSR and the opening of its KGB records we may learn one day why the dates of publication almost coincide.

All of the smaller carboranes (Fig. 1), as well as the icosahedral carboranes (Figs. 2 and 3), were temporarily designated as military secrets following their discovery. For this reason, 5 or 6 years passed between structural projections and declassification for publication. The results of this delay were mixed, in that while time was allowed for the correct deltahedral structures to be adjudicated before publication, many of the original participants became otherwise occupied (and several may have been ignored) when their work was eventually written up and published. The full story on the discovery of the icosahedral carboranes (Figs. 2 and 3) consequently has not yet been completely elucidated nor can it be reported here with authority. Based on published matter, "hearsay," and 30- to 40-year-old recollections, the following sequence of events can be offered.

In Fig. 2 is displayed the correct structure of the $1,2\text{-C}_2\text{B}_{10}\text{H}_{12}$ icosahedral carborane (**6**) as well as several incorrect structures that were proposed at the time of discovery. Four structures that were progressively less appealing to the traditional chemical community were suggested. These candidate structures would have incorporated either a bivalent group, —CH=CH— , **F** (with classical three-coordinate carbons), tetravalent groups, >CH—CH< , **G** and **H** (with classical four-coordinate μ^2 carbons), or (less desirable) each of the carbon atoms is μ^3 , ≡CH—CH≡ , **I** (with nonclassical five-coordinate carbons).

The correct structure was found to be that of $1,2\text{-C}_2\text{B}_{10}\text{H}_{12}$ (**6**), which incorporates an even less attractive (to the traditionalists) ≡CH—CH≡ group with two neighboring nonclassical six-coordinate, μ^4 , carbons.

As with the *aberrant structures* for $\text{C}_2\text{B}_3\text{H}_5$, $\text{C}_2\text{B}_4\text{H}_6$, and $\text{C}_2\text{B}_5\text{H}_7$ (**A**, **B**, **C**, and **D** in Fig. 1) the more familiar classical, electron-precise thinking, died slowly. The traditionalists viewed the hydrocarbon part and tried to give it a conventional or classical structure. They considered it sufficiently arcane that *inorganic* polyboranes unequivocally had polyhedral fragment structures, increasingly identified with seditious terms such as nonclassical, electron-deficient and incorporating three-center two-electron ($3c\text{--}2e$) bonds, etc., but to think that the familiar, conforming, well-behaved *organic* hydrocarbon moieties would also be involved in such nontraditional electron-deficient $3c\text{--}2e$ bonding was virtually incomprehensible!

In retrospect, an alkyl derivative of $1,2\text{-C}_2\text{B}_{10}\text{H}_{12}$, of unknown structure at the time, must have been synthesized in the late 1950s as various patent filings refer to the preexistence of such a compound. Bobinski (9) or Rose (48) of Reaction Motors Division of Thiokol Chemical Corporation apparently carried out the first synthesis between isopropenylacetylene and $\text{B}_{10}\text{H}_{12}(\text{NCCH}_3)_2$, but the correct structure remained in a state of flux (at least in the minds of many investigators) up to the time the Reaction Motors–Thiokol manuscripts were submitted to *Inorganic Chemistry* for publication in January through July of 1963.

Recruited as a referee, and benefiting from having previously deduced the structures of the much more easily characterized smaller *closo*-carboranes of Fig. 1, we argued for the icosahedral structures, illustrated in Figs. 2 and 3, as simple extensions of the series, *closo*- $\text{C}_2\text{B}_n\text{H}_{n+2}$, as typified in Fig. 1. From most of the originally submitted manuscripts (one or two were never published completely) it is now obvious that most investigators (including Heying and co-workers from Olin Mathieson Chemical Corporation) supported the correct icosahedral structures illustrated in Figs. 2 and 3 by early 1963. However, others still considered some of the alternatives (**F**, **G**, **H**, **I**, **J**, and **K**) as reasonable as late as July 1963.

In August of 1963 a paper *supporting the correct icosahedral structures* with six-coordinate carbons (Fig. 3) was submitted for publication by Schroeder and Vickers (13), which should have ended the debate for all time. In 1964, however, Zakharkin *et al.* reaffirmed their support for the bidentate “basket-handle,” —CH=CH— , structure, **F** in Fig. 3 (with classical three-coordinate carbons) (21), for $\text{C}_2\text{B}_{10}\text{H}_{12}$. Lipscomb *et al.* quickly responded with data supporting the icosahedral structure (15,16). Disputes concerning classical versus nonclassical carbons in electron deficient clusters (see below) seem to incite outrage, more akin to religious zealotry than science.

Now, more than 30 years later, Paetzold *et al.* (49a) have recently reported the icosahedral azaborane, $\text{NB}_{11}\text{H}_{12}$ (isoelectronic and isostructural with $\text{C}_2\text{B}_{10}\text{H}_{12}$), which incorporates an unprecedented six-coordinate nitrogen (totally unthinkable in the early 1960s outside of metal nitride chemistry)! Would it be heresy to suggest that a metastable *closo*-icosahedral oxygen analog, $\text{:OB}_{11}\text{H}_{11}$ or the related cation, $\text{OB}_{11}\text{H}_{12}]^+$ (with a six-coordinate oxygen), may one day be reported? Following submission of this review the related anion, *nido*- $\text{B}_{11}\text{H}_{12}]^-$, was reported by Frange *et al.* (49b).

The final acceptance of the more symmetrical icosahedral structure, (**6**) in Fig. 2, for the 10-boron “carborane,” ultimately shown to be $1,2\text{-C}_2\text{B}_{10}\text{H}_{12}$, amusingly received a setback when a second compound with

the same empirical formula, transiently named “neocarborane,” was discovered (see Fig. 3). It was suggested in 1963 that carborane and neocarborane were static isomers of $C_2B_{10}H_{12}$ that merely differed from each other by the length of their CC bonds. Carborane, **J**, was considered to have an ultra short CC bond (i.e., puckered), which allowed five-atom exocyclic derivatives to be formed involving the two carbons while neocarborane, **K**, with the long CC bond disallowed the formation of five-atom exocyclic derivatives. Carborane and neocarborane would truly have been examples of the *bond stretch isomers* later contemplated by Chatt *et al.* in 1971 (50) and Hoffmann and Stohrer in 1972 (51) and which were recently discussed by Mayer under the title “Fact or Fiction” (52). Carborane, **J**, was actually 1,2- $C_2B_{10}H_{12}$ (**6**) and neocarborane, **K**, was ultimately shown to be its isomer 1,7- $C_2B_{10}H_{12}$ (**7**) (53).

The smaller *closo*-carboranes, $C_2B_3H_5$ (**1**) and the $C_2B_4H_6$ isomers (**2**) and (**3**) and 2,4- $C_2B_5H_7$ (**4**) all have bipyramidal structures that monotonically increase from *trigonal*, to *tetragonal* (octahedron) to *pentagonal* bipyramids, respectively, as opposed to the traditionalist favored classical structures, (**A**, **B**, **C**, **D**, and **E** in Fig. 1). It might *speciously* have been anticipated that the structure of the next larger *species*, $C_2B_6H_8$, would naturally have a *hexagonal* bipyramidal structure (**L** in Fig. 4) rather than our proposed (22) most-spherical structure (**9**). In fact the hexagonal bipyramidal structure, **L**, for a static $C_2B_6H_8$ would fit the experimental ^{11}B NMR spectrum quite well (22); i.e., the four lower coordinate (4k) borons should be found at lower field while the two higher coordinated (6k) borons should be found at higher field in a 4 : 2 ratio as is observed.

The terms 4k and 6k indicate the numbers of other *skeletal* borons and carbons to which the atom under consideration is connected; *endoterminal groups, exoterminal groups, and bridging groups are not included in this count*. We deliberately utilize two distinct accounting systems; the generally more important connectivity system 2k, 3k, 4k, 5k, and 6k enumerates the number of other *skeletal* atoms to which a given atom is connected, *before* any terminal or bridging groups are attached. These values (2k to 6k) tend to indicate where various skeletal heteroatoms are most likely to reside and the subsequent disposition of bridge and endohydrogens in the thermodynamically most stable skeletal configurations in the absence of overriding factors. In contrast, the coordination number system (CN) includes *all* atoms within *bonding* distance of a given atom, *after* terminal and bridging groups are attached.

To further complicate the issue two additional static structures, clo-8(IV), **M**, and clo-8(IV + IV), **N**, (see Fig. 4), were also compatible with the ^{11}B NMR spectrum, the former having four 4k borons and two 5k borons in a 4 : 2 ratio and the latter having six 4k borons (but of two kinds)

in the ratio of 4:2 as is illustrated in Fig. 4. An even less acceptable bicapped trigonal antiprism, **O**, was considered even though it would have been expected to display a reversed 2:4 ratio in the ^{11}B NMR spectrum (low field to high) rather than the 4:2 ratio observed.

The term clo-8(IV) is the shorthand designation for a *closo*-compound (based on electron count) with eight-skeletal borons and carbons with a four (IV)-membered open face, while the designation clo-8(IV + IV) refers to an Archimedian antiprism and differs in having two square (IV-gonal) open faces. The most spherical structure (**9**), as well as candidates **L** and **O**, would all be described as clo-8(III) configurations as their largest apertures are triangles (III-gons).

In spite of the three candidate static structures, all of which were simplistically compatible with the ^{11}B NMR spectrum without additional rationalization, the presence of *two* 6k vertices in one case and square open faces in the other two isomers made all three unacceptable in our view. Consequently, in 1965 we proposed the most spherical, dodecahedral (bisdisphenoidal) alternative, 1,7- $\text{C}_2\text{B}_6\text{H}_8$ (**9**) only (22), with four 4k vertices and four 5k vertices even though the anticipated 2:2:2 ^{11}B NMR spectrum was not observed. We assumed that either coincidental overlap of signals or fluxional behavior made the anticipated 2:2:2 pattern simplify into the 4:2 ^{11}B NMR spectrum observed experimentally. Hoffmann subsequently endorsed structure (**9**) as the most stable on the basis of calculations (55). Later (1966) Hawthorne and co-workers also reported $\text{C}_2\text{B}_6\text{H}_8$ (23). They favored the Archimedian antiprism, clo-8(IV + IV), configuration, **N**, in Fig. 4. Our predicted (22) bisdisphenoidal deltahedral configuration (**9**) for 1,7- $\text{C}_2\text{B}_6\text{H}_8$ was confirmed in the crystal (56) (X ray) and recently supported theoretically (*ab initio*/IGLO/NMR) for the same structure in solution (57,58).

The *ab initio* treatment optimizes one or more candidate structures, and the IGLO calculations generate ^{11}B and ^{13}C NMR chemical shift values for the various optimized candidate structures. Success is achieved when, and if, one set of the predicted and the experimentally observed chemical shift values match almost exactly.

Skeletal atoms that donate *more* skeletal electrons than their neighboring atoms tend to occupy the more electron rich vertices that have the *smaller numbers* of connections. Thus carbon (a three skeletal electron donor; 3 SED) preempts less-connected 3k and 4k vertices while 5k vertices are tolerated. In contrast, boron (only a two skeletal electron donor; 2 SED) occupies greater-connected 4k and 5k vertices with even 6k vertices being tolerated in rare instances.

The only set of cases where borons in 6k sites are found includes the isostructural clo-11(III) series, *closo*- $\text{C}_2\text{B}_9\text{H}_{11}$ (**14**), *closo*- $\text{CB}_{10}\text{H}_{11}]^-$ (**20**)

and *closo*- $B_{11}H_{11}]^{2-}$, each of which incorporates one 6k boron site. *closo*- $C_2B_9H_{11}$ was discovered by Hawthorne and co-workers (59) who assigned the correct structure (**14**) illustrated (60) in Fig. 6, but not before it was suggested by a referee (59) that a higher coordinated pair of vertices for the carbons (**P** in Fig. 6) was also compatible with the spectrum. The remaining *closo*-species, $C_2B_7H_9$ (**10**) and $C_2B_8H_{10}$ (**12**), and (**13**) (isomers) were identified by 1966.

Within the same time frame (1950s and early 1960s), organic chemists investigating carbocations, notably Winstein *et al.*, were proposing structures incorporating nonclassical five-coordinate carbons involved in multicenter bonding (61) for several electron-deficient hydrocarbon cations, namely the *hypho*-trishomocyclopropenium (**22**) and *arachno*-2-norbornyl (**23**) carbocations (Fig. 8). These structures were proposed to incorporate CCC $3c-2e$ bonds in their most stable configurations and even CHC $3c-2e$ bonds during rearrangement. Decades of resistance to such unsavory suggestions ensued, which have been summarized in H. C. Brown's 1977 book, "The Non-Classical Ion Problem" (62) with a commentary by Paul v. R. Schleyer. On the other side of the debate, ^{13}C and 1H NMR studies by Olah *et al.* (in the early 1970s) of stable carbocations in superacids and magic acid (61) clearly dispelled any reasonable objections to electron-deficient, nonclassical carbocations by unequivocally proving the nonclassical structure of the 2-norbornyl cation with a centrally located CCC $3c-2e$ bond (61*a,b*)! Such a structure has recently been confirmed by an x-ray crystallographic study of the salt of a methyl derivative (61*c*).

The author suggested (1962) (34) that hybrid *arachno*-carborane configurations (Fig. 9), with dynamic BHC $3c-2e$ bonds, participated as undetectable intermediates (**24**) or transition states in the *brachiation* of boron atoms along hydrocarbon chains to explain H. C. Brown's hydroboration rearrangement (33). This mechanism was initially greeted with skepticism,

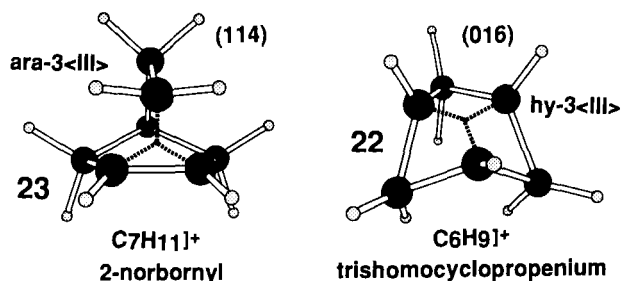


FIG. 8. The nonclassical structures of trishomocyclopropenium (**22**) and 2-norbornyl (**23**) cations.

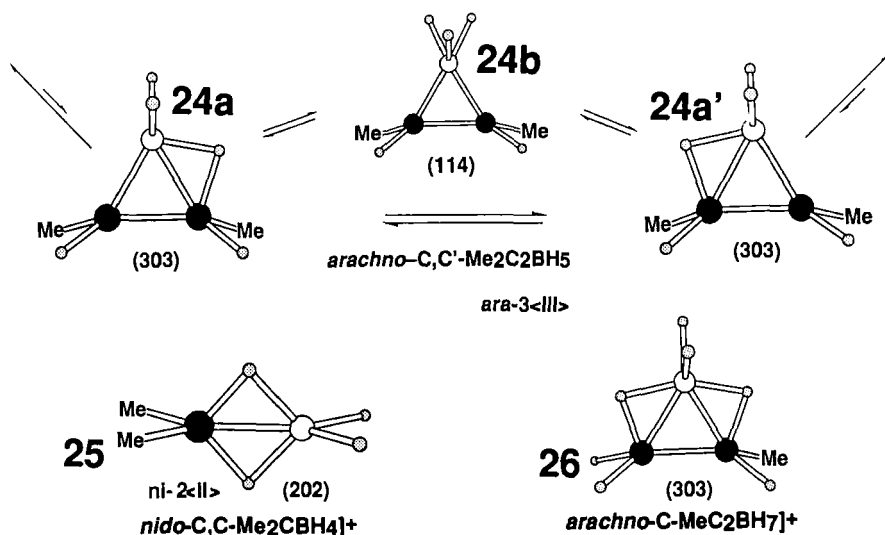


FIG. 9. The Brachiation intermediates (24a) and (24b) and the carborane cations (25) and (26).

but was ultimately proved to be correct by Rickborn and Wood (1971 and 1983) (34).

Recently, stable cations with static BHC 3c-2e bonds have been observed (¹¹B NMR) at very low temperatures in superacid solutions by Williams *et al.* (63,64). These unusual BHC bridge hydrogens are found in isoelectronic and isostructural carborane analogs of the well-known polyboranes *nido*-B₂H₆ and *arachno*-B₃H₈]⁻. The carborane analogs are the cations, *nido*-Me₂CBH₄]⁺ (25) and *arachno*-MeC₂BH₇]⁺ (26) in Fig. 9.

Weiss (65) was the first to synthesize a *nido*-carborane. He produced *nido*-C₂B₄H₈ (32) (Fig. 10), in the late 1950s by the long-term, low-temperature heating of a mixture of B₅H₉ and acetylene and determined its empirical formula. Its hexaborane-like structure was deduced (Fig. 10) from the ¹¹B spectrum (66). Onak subsequently developed a high yield synthesis. Recognition that *nido*-C₂B₄H₈ (32) was isoelectronic and isostructural with hexaborane, B₆H₁₀ (28), foreshadowed the conclusion that the carboranes would structurally resemble the boron hydrides or polyboranes more than they would hydrocarbons, e.g., the many isomers of C₆H₁₀. In Fig. 10 are illustrated hexaborane and the myriad of hexaborane-related carboranes. All show the family resemblance to B₆H₁₀ (28). The numerical *styx* (0260 to 5210) and *Stx* (620) numbers of Fig. 10 are explained below.

The more recently discovered alkyl derivatives of the all-carbon cluster, C₆H₆]²⁺ (29), have hexaborane-like structures (67) reconfirming the con-

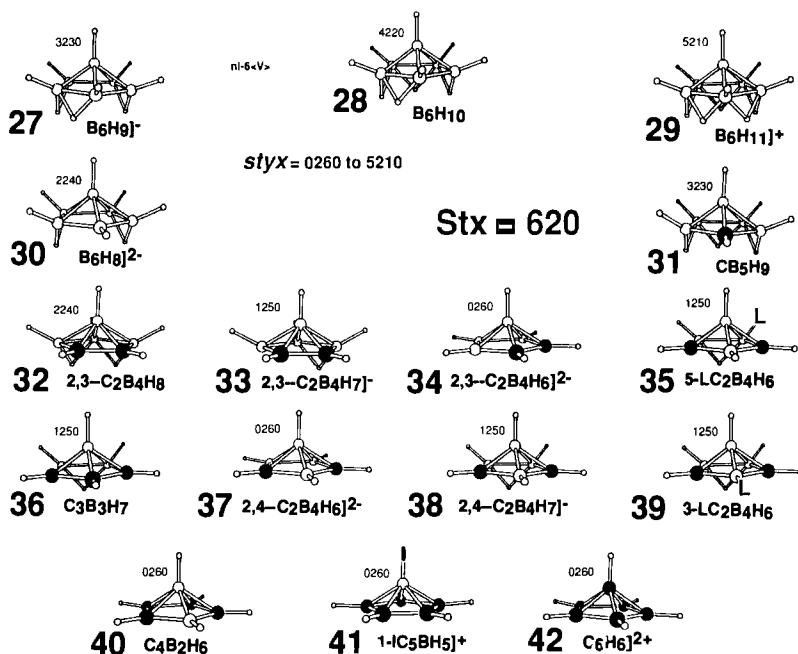


FIG. 10. *nido*-Hexaborane, B_6H_{10} (**28**), and its isoelectronic analogs (**27**, **29–31**, **33–41**), including $C_7B_4H_8$ (**32**) and $C_6H_6]^{2+}$ (**42**).

clusion that the *common denominator* of the compounds illustrated in Fig. 10 is electron deficiency, and whether or not the molecular skeleton is all boron, all carbon, or of mixed boron and carbon atoms is of lesser consequence. If a series of compounds are electron deficient, and assuming that they have the same number of heavy atom $3c-2e$ bonds (e.g., BBB, BBC, BCC, or CCC bonds), then the structures are always quite similar. Thus there is a polyborane–carborane–carbocation continuum of structures that decreases in the number of additional $3c-2e$ bonds in the form of bridge hydrogens in the order mentioned.

In discussing carboranes, polyborane configurations must also be discussed as the structural rules and patterns that pertain to the many examples of polyboranes are directly applicable to the numerous carboranes and to the far less numerous nonclassical carbocations as well.

The carboranes were discovered as by-products in a program whose objective was to develop alkyl derivatives of polyboranes suitable for use as high-energy fuels. Certain *closo*-carboranes turned out to be of superior thermal stability but with low fuel values. In an effort to exploit these unexpected properties, programs were subsequently undertaken for incor-

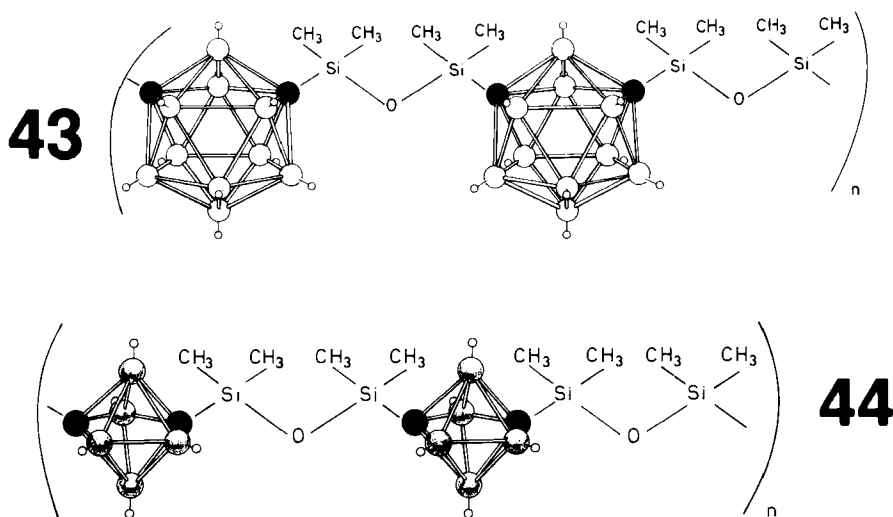


FIG. 11. *closo*-Carborane siloxane copolymers, (43) and (44).

porating selected *closo*-carboranes into polymers for use at high temperatures and/or in other special circumstances. The carborane siloxane polymers, Dexasil™ (43) and Pentasil (44), (Fig. 11) are representative of copolymers (68) that grew out of the discovery of the *closo*-carboranes.

In spite of their high thermal stability and low fuel value, selected alkyl *closo*-carboranes, e.g., *closo*-1-C₆H₁₃-1,2-C₂B₁₀H₁₁, performed unusually well as rocket additives when admixed with other fuel-oxidizer mixtures. These alkyl *closo*-carboranes serve as burn rate enhancers so that even though they do not contribute as high energy fuels, they improve accuracy by substantially shortening the time between ignition and arrival-at-target.

III

SKELETAL ELECTRON PAIR BONDS IDENTIFIED BY *styx* AND CHOP-*Stx*

Among Lipscomb's contributions to polyborane chemistry (see Fig. 12) was the idea that the various polyborane structures could be described as constructed about the vertices of *two* concentric pseudospherical surfaces, the skeletal atoms, occupying adjacent sites (vertices) on the *inner sphere*, while the terminal groups occupy radially identical sites on the *outer sphere* (38). Lipscomb differentiated between the *inner-skeletal* components and the *exoterminal* components. The inner-skeletal compo-

	<1933 STOCK	1954 LIPSCOMB	1959 PARRY & Edwards	<1969 COMMITTEE	1970 WILLIAMS	1971 WADE & Rudolph	1974 SHORE
Empirical Formulae	B_nH_{n+6} B_nH_{n+4}		$B_nH_n(BH_3)_3$ $B_nH_n(BH_3)_2$ $B_nH_n \cdot BH_3$				B_nH_{n+8}
Classification	hydrogen rich / hydrogen poor	open open condensed	<i>nido</i> <i>nido</i> <i>closo</i> **		<i>arachno</i> ** <i>nido</i> <i>closo</i>	Skeletal Electron Counting Rules $n + m$***	<i>hypho</i> **
Structures		Atoms on Concentric Spheres; Icosahedral Fragments; styx rules*			Most Spherical Deltahedra and their Fragments		

- The *styx* rules allow potential structures to be drawn by counting skeletal orbitals ($3s + 3t + 2y + 2x$) and skeletal electrons ($2s + 2t + 2y + 2x$), assuming the skeleton to be built up only from $y + x$ ($2c-2e$) and $s + t$ ($3c-2e$) bonds.
- ** Clovo from Gk. "cage" was later transformed into *closo* ("closed"); *nido* from Gk. nest; *arachno* from Gk. web and *hypho* from Gk. net.
- *** The sum, $n + m$, counts the skeletal electron pairs in B_nH_{n+s+x} ; the values $m = 1, 2, 3, 4$ mean *closo*, *nido*, *arachno*, and *hypho*, respectively; $n = 0$ may be designated as "*capo*"; Wade included transition metal atoms as skeletal vertices and developed rules to count their skeletal electron contributions according to the metal's ligands.

FIG. 12. Evolution of the relationships between class and empirical formulae, geometrical systematics, and skeletal electron accounting.

nents include the skeletal atoms of the core clusters (i.e., the borons and both the bridge hydrogens and endohydrogens) and the skeletal electron pairs that held them together, while the exoterminal components include the exoterminal groups (hydrogens, alkyl groups, Lewis base groups, etc.) and the electron pair bonds that attach the exoterminal groups to the skeletal core cluster.

Lipscomb also developed a method for cataloging the various types and kinds of endoskeletal electron pair bonds that hold the inner sphere atoms together. He coined the acronym *styx* for his method, wherein *s* stands for the number of bridging boron–hydrogen–boron (BHB) $3c-2e$ bonds, the *t* stands for the number of BBB $3c-2e$ bonds, the *y* for the BB $2c-2e$ bonds, and the *x* for the endo BH $2c-2e$ bonds of BH_2 groups. In this fashion, each boron hydride or carborane structure can be identified by a combination of these four numbers and its molecular formula (as an example, see Fig. 10). When expressing the formula B_pH_q , analysis of the boron, hydrogen, and electron numbers leads to the equations $p = s + t$, $q = s + x$, and $s + t + y + x = p + q/2$.

In Fig. 10 (B_6H_{10} and its analogs) each of the empirical formulae is coupled with one of six Lipscomb's *styx* numbers that vary between 0260 and 5210 and that identify the four kinds of architectural *bonds* that hold each of the hexaborane-like skeletal core clusters together. The four *styx* numbers identify, in sequence, the numbers of the skeletal BHB, BBB, BB, and endo-BH bonds (of BH_2 groups), respectively.

We use a simplification (69) of the *styx* treatment in which the bridge hydrogens of the BHB groups are ignored. The bridge hydrogens, BHB (the *s* in *styx*), and BB $2c-2e$ bonds (the *y* in *styx*) are combined under one symbol, *S* ($styx \rightarrow Stx$, where $S = s + y$). It is as if the bridge hydrogens of the BHB groups are chopped off and BB groups remain. The result is that one Chop-*Stx* number, 620, identifies all of the compounds in Fig. 10 (69). As the *S* in the Chop-*Stx* code represents both BHB and BB bonds it is independent of whether bridging hydrogens are present or absent on BB bonds. The 6 in the Chop-*Stx* number 620 (the sum of the BHB and BB bonds) does not reveal the number of bridge hydrogens but in combination with the empirical formulae the number of bridge hydrogens is easily determined. For example, it is obvious from the empirical formula how many hydrogens are in *excess* of the number of heavy skeletal atoms, and since the value of *x* (in *Stx*) reveals how many of that *excess* must be endohydrogens then the difference identifies the number of bridge hydrogens that must be present. Absolutely no information is lost in this description.

All of the many diverse boron hydrides, carboranes, carbocations, and their anions and cations, isoelectronic with *nido*- B_6H_{10} (28), adhere to the

2 3 4 5 6 7 8 9 10 11 12 13 14

Hypho

016 215 414 424 444

Arachno

104 303 502 701 900 920 930
114 313 323 512 522 532 542 552 562 572 582
363 373 383

Nido

202 212 600 610 620 630 640 650 660 670 680 690
411 421 431 441 451 461 471 481 491
222

Closo

300 310 330 340 350 360 370 380 390 3-10-0 3-11-0 3-12-0
131 141

“Capo”

040 060 080 0-10-0
2 3 4 5 6 7 8 9 10 11 12 13 14

FIG. 13. Chop-*Stx* numbers.

Chop-*Stx* number 620 (Fig. 10). This simplifying strategy (69,70) allows entire fields to be organized under the abbreviated Chop-*Stx* notation (Fig. 13) of which *Stx* = 620 is only one small entry. If for some reason Lipscomb's more definitive *styx* information is desired, it is readily reconstituted by a comparison of the *Stx* number and the empirical formula:

Chop-	<i>S</i>	<i>t</i>	<i>x</i>
B_6H_{10}	6	2	0
$(10 - 6) = 4 = (s + x)$	4	2	2
$x = 0$, thus $s = 4$			
$S = 6 = (s + y)$	<i>s</i>	<i>t</i>	<i>y</i>
$s = 4$, thus $y = 2$			<i>x</i>

Lipscomb's

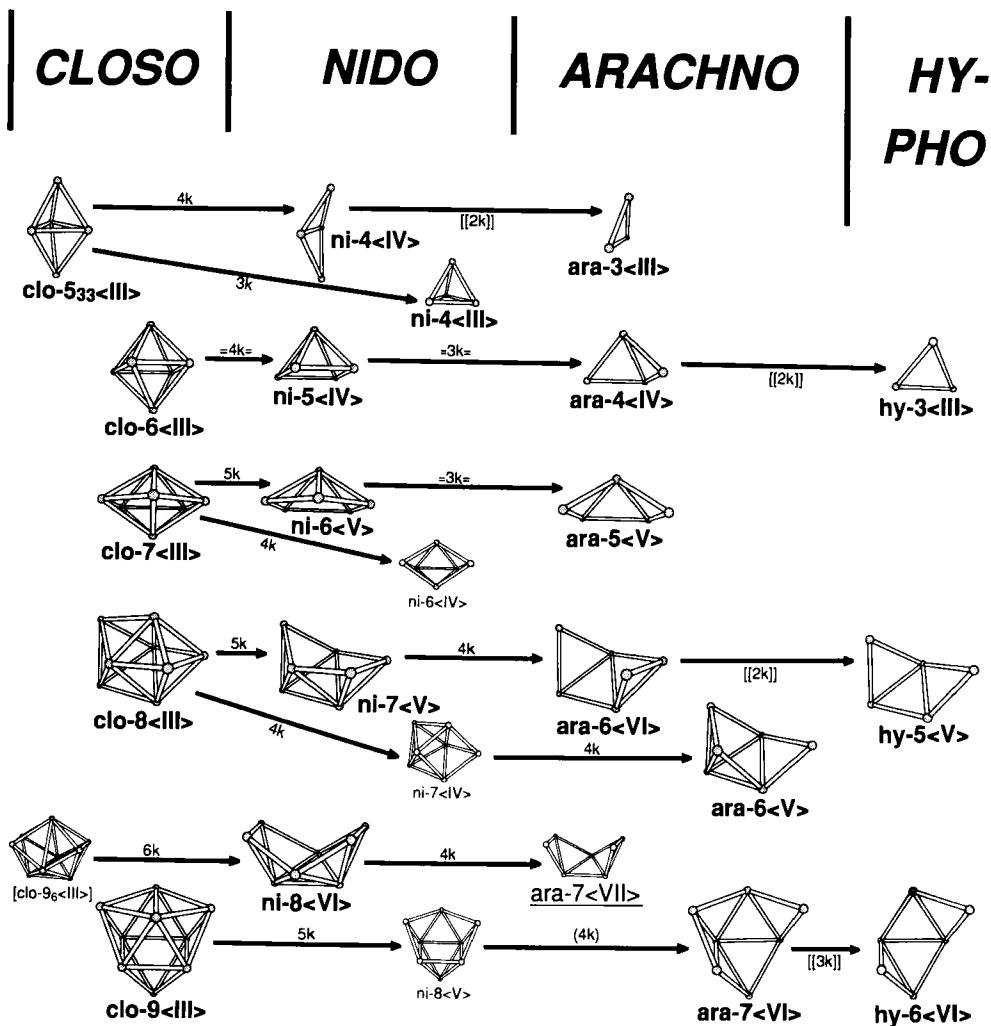


FIG. 14. 1992 geometrical systematics.

IV

CLASSIFICATION BASED ON GEOMETRY, EMPIRICAL FORMULA, AND ELECTRON PAIR BOND RELATIONSHIPS

In 1971 an attenuated version of the deltahedra-deltahedral fragment systematics manuscript was accepted by the journal *Inorganic Chemistry* as correspondence (71). Figure 14 is an expanded version of our 1971

CLOSO

NIDO

ARACHNO

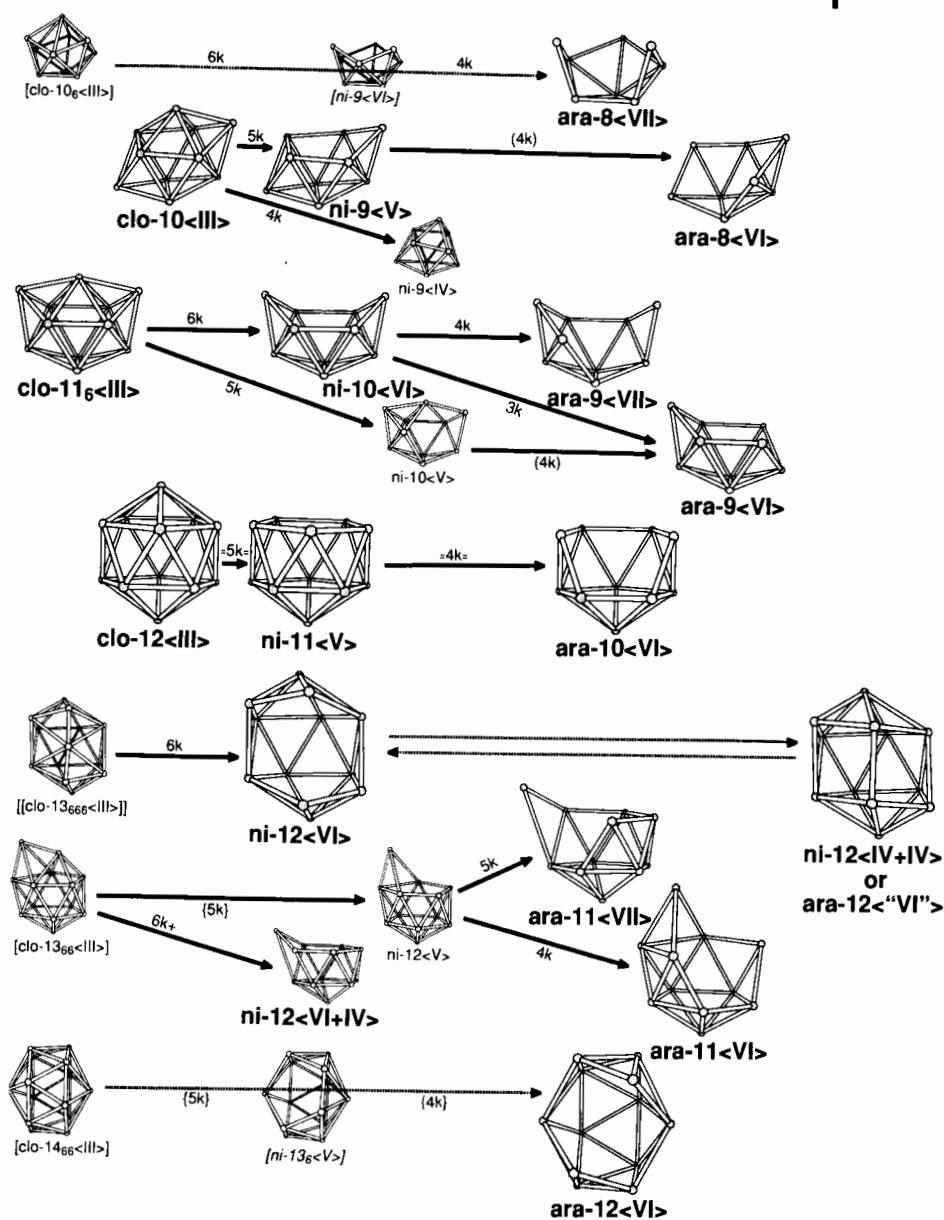


FIG. 14. (continued)

proposal (72). Figure 14 differs in that fragments derived from both smaller (clo-5<III>) and larger (clo-13₆₆<III> and clo-14₆₆<III>) deltahedra as well as fragments derived from the *almost-spherical* deltahedra, clo-9₆<III> and clo-10₆<III> are included (see below).

One original objective (72) for promoting the most-spherical geometrical patterns was to displace the viewpoint that *all* carborane and polyborane configurations could best be derived from the sacrosanct regular icosahedron and the regular octahedron in the case of B₅H₉. Our alternative point of view was that all *nido*-structures could be generated from the one-vertex-larger most-spherical *closo*-deltahedral structure (6 to 12 vertices) by the simple removal of one highest coordinated vertex and that the *arachno*-structures could, in turn, be derived from the *nido*-structures by the removal of one additional high coordination vertex (adjacent to the open face). The shibboleth that all polyboranes and carboranes should best be viewed as fragments of the *sacred* icosahedron was shown to be somewhat flawed (72).

In a footnote (73), the author suggested (74) that the all-carbon cation, *nido*-C₅H₅]⁺, should have a B₅H₉-like structure; see (45) and (48) in Fig. 15. A few months later the same suggestion was made by Hoffmann (75), which was followed by the synthesis of the 1,2-dimethyl derivative of *nido*-C₅H₅]⁺ by Masamune (76) in 1972. Such developments foreshadowed the perception of a continuum of polyborane–carborane–carbocation structures (see Figs. 10 and 14).

Three conclusions have come into focus since 1971 (72): First, the icosahedron-icosahedral fragment rationale is only slightly misleading. Of course the icosahedral fragment rationale is not applicable to the six other *closo*-geometries (clo-6<III> to clo-11<III> in Fig. 14) but it is only completely incorrect for two of the *nido*-configurations, i.e., *nido*-7<V> and *nido*-9<V>, that are within its limited range of forecasting (6 to 11 vertices). Moreover all *arachno*- and *hypho*-configurations may be viewed as fragments of an icosahedron. Second, while our most-spherical deltahedra rational, as far as carbon–boron skeletons are concerned, accounts for almost all of the *closo*-, *nido*-, *arachno*- and *hypho*-configurations, it does not correctly account for the *nido*-8<VI>, the proposed *arachno*-8<VII>, and the *nido*-12<VI> configurations, unless one additional connection is broken in each case.

Third, our 1971 geometrical systematics (72) were endorsed by Wade (77) and subsequently by Rudolph (78) expanded by them to include certain transition element clusters, metal–hydrocarbon π -complexes, and eventually incorporated into what has become known as *Wade's Rules*. Subsequent developments in all of these areas have highlighted the need (where

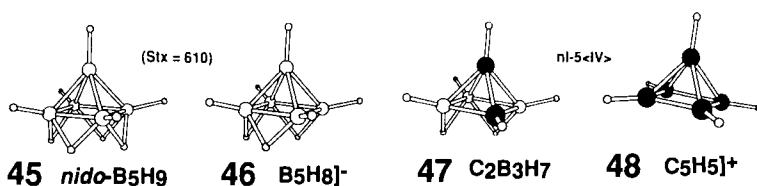


FIG. 15. Compounds related to *nido*-B₅H₉ (**45**), B₅H₈]⁻ (**46**), C₂B₃H₇ (**47**), and C₅H₅]⁺ (**48**).

elements other than boron and carbon are concerned) to think in terms of a wider range of parent deltahedra than were needed in 1971 (72). This has resulted in reference to exceptions to the original rules, which, however, still apply with virtually no exceptions to the carboranes themselves.

The recent 1992-approach (Fig. 14), the *modified* most-spherical deltahedra rationale, harks back to the roots of the most-spherical geometrical systematics (72). The seminal question is: What was the property of the series of most-spherical deltahedra that made them the preferred structural precursors for the *nido*-, *arachno*-, and *hypho*-carboranes? The common denominator was, and is, the homogeneous nature of their vertex connectivities. In the 12-vertex icosahedron all vertices are 5k vertices and in the 6-vertex to 10-vertex, most-spherical deltahedra, all are 4k and 5k vertices (Figs. 14 and 16). Of course two 3k vertices and one 6k vertex are found in the 5-vertex, clo-5₃₃(III), and 11-vertex, clo-11₆(III), deltahedra, respectively, as there are simply no alternative deltahedra incorporating only 4k and 5k vertices. In other words, the deltahedra chosen by nature for electron-deficient clusters of boron and carbon are most-spherical *because* the vertices in such deltahedra are most homogeneous. There is a price exacted for the presence of the two 3k vertices in C₂B₃H₅ (**1**), clo-5₃₃(III), and the one 6k vertex in C₂B₉H₁₁ (**14**), clo-11₆(III). Among all of the *closo*-carboranes, C₂B_nH_{n+2}, the compounds C₂B₃H₅ (**1**) and C₂B₉H₁₁ (**14**), which, by necessity, incorporate 3k and 6k vertices, are much less stable than are all of the other *closo*-carboranes that incorporate only 4k and 5k vertices.

At least two 6k vertices (Figs. 14 and 16) are necessarily present in the best possible *closo*-13₆₆(III) and *closo*-14₆₆(III) deltahedra and we suggest it is much more than coincidence that *closo*-C₂B₁₁H₁₃ and *closo*-C₂B₁₂H₁₄, which would be based on the *closo*-13₆₆(III) and *closo*-14₆₆(III) deltahedra, each incorporating two 6k vertices, have never been observed. Apparently one 6k vertex engenders instability in *closo*-boron-carbon clusters, while such clusters with two 6k vertices are not stable at ambient conditions.

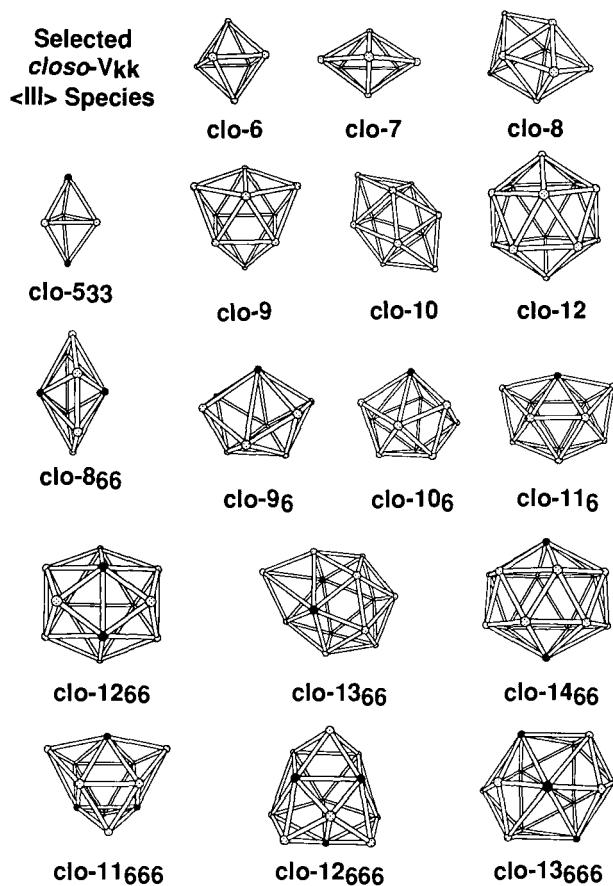


FIG. 16b. Illustrations of the deltahedra of Fig. 16a.

fragments, then the presence of 6k vertices in the parent *closo*-deltahedra becomes inconsequential. Thus these deltahedra containing 6k vertices (undesirable for *closo*-carboranes) may be as acceptable as the most spherical deltahedra in generating the *nido*-, *arachno*-, and *hypho*-fragments, provided the offending 6k vertices are removed or become 5k vertices in the process of vertex removal (see Figs. 16b and 17).

In comparing Figs. 14, 16, and 17, it is seen that the clo-9₆<III> configuration (with one 6k vertex) is unacceptable for the *closo*-species, C₂B₇H₉ (**10**) in Fig. 5 and B₉H₉]²⁻ (which both adopt clo-9<III> configurations), but the second choice, the clo-9₆<III> configuration, is the chosen progeni-

Closo-, Nido-, & Arachno- VERTICES

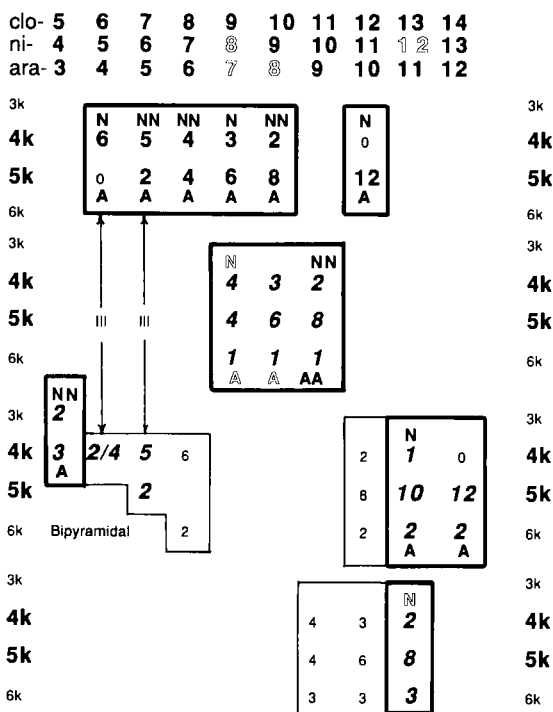


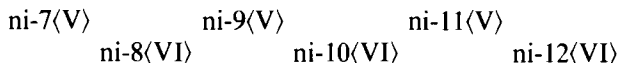
FIG. 17. Deltahedra from which *nido*- and *arachno*-fragments are generated.

tor for the *nido*-8-vertex species related to $C_2B_6H_{10}$ as the offending 6k vertex is removed in generating the ni-8(VI) configuration (Fig. 14). In the same vein, the 6k vertex is unacceptable in the clo-10₆(III) structure for *closo*- $C_2B_8H_{10}$ (11) in Figure 5, or for $B_{10}H_{10}]^{2-}$ (which both adopt the clo-10₆(III) configuration) but the clo-10₆(III) structure could be the deltahedral precursor for the *arachno*-8-vertex species, $C_2B_6H_{12}$ (ara-8(VII)), if the proposed structure turns out to be correct (79).

There are no *closo*-13-vertex carboranes, but the preferred *nido*-12-vertex configuration (for boron-carbon skeletons) can be derived (in a contrived fashion) from the *closo*-13₆₆₆(III) deltahedron as the removal of the central 6k vertex, between the other two 6k vertices, produces a *nido*-fragment with no 6k vertices and the experimentally observed VI-gonal open face (ni-12(VI)) is observed. Similarly, the unacceptable (for exclusively boron-carbon skeletons) clo-14₆₆(III) configuration probably accounts for the *arachno*-12-vertex structure with no 6k vertices, although

no suitable *nido*-13-vertex configuration (without 6k vertices) comes to mind, unless an additional cage connection is also removed.

The preferred open faces for the observed larger *nido*-carboranes alternate between V-gonal and VI-gonal, which may be significant:



In discussing site preferences, it is helpful to clarify cluster forming units by the numbers of skeletal electrons donated (*n*-SED) units. When suitable transition element groups are present, containing elements that donate less skeletal electrons (< 2 SED) than do carbon (3 SED) or boron (2 SED) or are more electropositive than carbon or boron, then compounds derived from configurations incorporating 6k vertices, derived from clo-9₆⟨III⟩, -10₆⟨III⟩, -13₆₆⟨III⟩, and -14₆₆⟨III⟩, are observed but this article involves carboranes, not metallacarboranes. Carbon and boron are three and two skeletal electron donors (3 SEDs and 2 SEDs), respectively.

In Fig. 14, below each of the carbon–boron preferred *nido*-configurations, are the *nido*-configurations with smaller apertures as their molecular skeletons incorporate one more connection, see ni-6⟨IV⟩, ni-7⟨IV⟩, ni-8⟨V⟩, ni-9⟨IV⟩, and probably *nido*-10⟨V⟩. Such configurations are favored by the presence of heteroelements or groups that contribute more skeletal electrons than carbon (4 SEDs or greater) such as nitrogen, phosphorus, sulfur, and selenium (all may be 4 SEDs), but such species are also not carboranes.

I explain the additional connection (69,70,80a) as follows (*caveat emptor*): (a) fewer electrons, i.e., greater electron deficiency, engenders more connections [e.g., B₂H₆ (six electron pairs; nine connections) versus C₂H₆ (seven electron pairs; seven connections) versus N₂H₆ (2 NH₃; eight electron pairs; six connections) (80a); and (b) four skeletal electron donors (4 SEDs), i.e., NH groups or bare sulfurs, are *substantially more reluctant* to contribute their four skeletal electrons *for the same geometrical locations* than are 3 SEDs (carbons) to contribute their three electrons or the 2 SEDs (borons) to contribute their two electrons. As a consequence (even when the numbers of skeletal electron pairs remain constant) the molecule is internally polarized, e.g., the 4 SEDs (the minority of the skeletal atoms) are less electron deficient while (c) the rest of the molecule (the boron majority, i.e., the 2 SEDs) becomes incrementally more electron deficient and (d) the incrementally greater electron deficiency among the majority of the skeletal atoms usually causes one more skeletal connection to be present and thus the open face becomes smaller; see (a) above (80b).

V

POLYBORANE LEWIS BASE ADDUCTS

Having related the polyboranes, carboranes, and carbocations to each other, it should be added that Lewis base adducts of both polyboranes and carboranes also adhere to the geometrical systematics of the polyborane, carborane, carbocation continuum (69,70). For ease of illustration only, consider the addition (hypothetically) of one positively charged proton to several locations within a contrived isotopically labeled anion derived from methylhexaborane, namely $^{13}\text{CH}_3^{11}\text{B}_6\text{H}_8]^-$ (**49**) (620)(see Fig. 18); a number of other $Stx = 620$ compounds are produced.

It is seen in Fig. 18 that the proton could simply add to the anion (**49**) as a bridge hydrogen to form the parent, *nido*-methylhexaborane, $^{13}\text{CH}_3^{11}\text{B}_6\text{H}_9$ (**50**) (620) (80c,81). Second, the proton could hypothetically insert itself into the nucleus of one of the ^{11}B atoms, which would change it to a ^{12}C atom. The product in this case would be the known *nido*- $^{13}\text{CH}_3^{12}\text{CB}_5\text{H}_8$ (**51**) (620) (82), the methyl derivative of the monocarbon carborane structurally related to *nido*- B_6H_{10} (**28**) (620) (see Fig. 10) (83). Third, the proton could notionally have been inserted into the ^{13}C of the methyl group of the anion producing an ^{14}N atom! This would hypothetically produce a Lewis base adduct, *nido*- $\text{H}_3^{14}\text{NB}_6\text{H}_8$ (**52**) (620) (Fig. 18). All are *nido*- $Stx = 620$ species, and would be isoelectronic and should be isostructural except for bridge hydrogen locations.

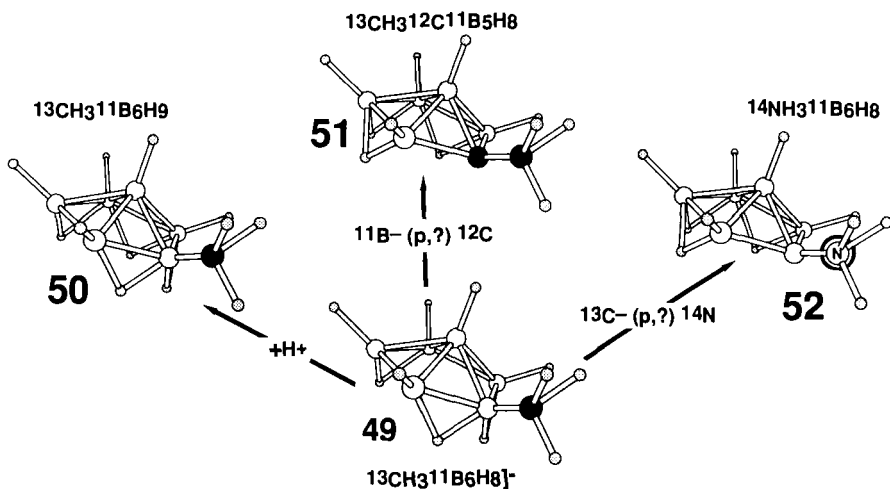


FIG. 18. Addition of protons and the simple "alchemical" transmutation of the elements: $^{13}\text{CH}_3^{11}\text{B}_6\text{H}_8]^-$ (**49**), $^{13}\text{CH}_3^{11}\text{B}_6\text{H}_9$ (**50**), $^{13}\text{CH}_3^{12}\text{CB}_5\text{H}_8$ (**51**), and $^{14}\text{NH}_3^{11}\text{B}_6\text{H}_8$ (**52**).

VI

ELECTRON COUNTING

Skeletal electron counting (Fig. 12) is the essence of both Lipscomb's original *styx* cataloging of the skeletal electron bonds (from which our simplified Chop-*Stx* formalism is derived, Fig. 13) as well as the empirical formula/geometrical systematics of 1971 (72,84), which has been expanded (85) to Fig. 14. Wade was first (77,86) to realize that by switching the focus from geometry plus empirical formula to geometry plus skeletal electron counting (see also Figs. 12 and 14) that clusters containing transition elements and many other heteroatoms could also be encompassed within the same more general unified concept along with clusters involving boron and carbon. In fact, according to Wade, following the publication of our geometrical systematics (72), he originally compared our patterns with clusters in transition element chemistry to discern the differences. He discovered that the similarities vastly outnumbered the differences.

Mingos (87), Stone (88), Rudolph (78), Gimarc and Ott (89), and King (90) have all made significant contributions to the theoretical understanding of the geometrical-electron counting systematics. As a result of these collective efforts the various boron-carbon skeletal cluster patterns have become the primeval touchstone molecules for all electron deficient cluster chemistry. Hoffmann (91) has added frontier orbital considerations to the comparisons between electron deficient isoelectronic and isostructural compounds from both organic and inorganic chemistries. He seems not to identify the polyboranes and carboranes as the missing links between electron deficient organic and electron deficient inorganic chemistries, although Hoffmann and Lipscomb (38) were instrumental in the elucidation of many polyborane structures.

VII

CARBORANE NOMENCLATURE

The term *carborane* was casually coined by the late Carl David Good and the author during a period when we were aware of the four smallest *closo*-carboranes only (Fig. 1) and did not contemplate that larger species (Figs. 2 to 6) would be discovered. We assumed the small *closo*-carboranes (Fig. 1) should be named as symmetrical and unsymmetrical compounds much as 1,2-Me₂B₂H₄ and 1,1-Me₂B₂H₄ had previously been labeled as symmetrical and unsymmetrical dimethyl derivatives of diborane.

Initially, *closo*-1,5- $C_2B_3H_5$ (**1**) was named *symmetrical triboradimethyne* indicating the presence of three identical BH groups and two identical CH groups (Fig. 1). The two isomers of $C_2B_4H_6$, (**2**) and (**3**), were called symmetrical and unsymmetrical tetraboradimethynes and $C_2B_5H_7$ (**4**), pentaboradimethyne. This terminology was used in the original patent (2a) issued on $C_2B_3H_5$ (**1**).

The term dicarbapolyboranes was adopted somewhat later but certainly before anyone realized that the isomers of $C_2B_4H_6$ could be isoelectronic and possibly isostructural with the $B_6H_6]^{2-}$ dianion, which had been forecast theoretically, but not yet isolated.

Gradually, over time, the syllable *poly*- was dropped and the name became dicarbaboranes. The prefix *di*- was deleted when it was realized that related neutral species with up to four and six carbons (later termed *nido*- and *arachno*-carboranes) could be envisioned and the term, *carba*-boranes survived for a time. Eventually, the syllable *ba* was dropped (after someone mentioned it sounded like stuttering in the nursery rhyme "Ba Ba Black Sheep"), and the abbreviated generic term carborane was adopted for lack of a better alternative. IUPAC and the British Royal Society of Chemistry favor the term carbaborane, while the Russian literature generally referred to the carboranes as barenes.

Later, when *closo*-1,2- $C_2B_{10}H_{12}$ (**6**) (Fig. 2) was produced from acetylene and *arachno*- $B_{10}H_{12}(NCCH_3)_2$, the term carborane was strangely ascribed (apparently in confusion) to both boron compounds. Still later, the term carborane was preempted as the specific name of *closo*-1,2- $C_2B_{10}H_{12}$ (**6**), which is still frequently referred to as orthocarborane.

VIII

nido-CARBORANES AND RELATED COMPOUNDS

A. *nido*-6-Vertex Compounds

The first *nido*-carborane, $C_2B_4H_8$ (**32**), and most other *nido*-6-vertex species are related to *nido*-hexaborane-10, B_6H_{10} (Fig. 10). All of the "-cene" compounds such as *nido*-ferrocene, are also isoelectronic and isostructural ($Stx = 620$) with *nido*- B_6H_{10} (**28**). As a comparison only (they are not carboranes) two ni-6(IV) compounds, incorporating four SEDs, are illustrated in Fig. 19. Compounds $N_2B_4H_6$ (**53**) and $S_2(CpCo)_2B_2H_2$ (**54**) are isoelectronic with B_6H_{10} (**28**) but are not isostructural.

There are many other families of *nido*- and *arachno*-carboranes which are structurally related to their *nido*- and *arachno*-polyborane analogs. In

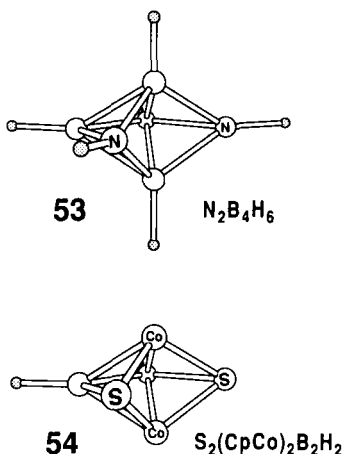


FIG. 19. Compounds for comparison with Fig. 10, $\text{N}_2\text{B}_4\text{H}_6$ (**53**), and $\text{S}_2(\text{CpCo})_2\text{B}_2\text{H}_2$ (**54**).

recent decades, a Czechoslovakian group, headed by Hermanek *et al.* (92) have been extremely prolific in the discovery of new *nido*- and *arachno*-carboranes.

B. *nido*-4-Vertex Compounds

Recently, we (70,93,94) compared the speculative compound, *nido*- $\text{B}_4\text{H}_7]^-$ (**600**) with the known structure reported by Olah and co-workers for homocyclopropenium cation, *nido*- $\text{C}_4\text{H}_5]^+$ (**56**), (411) (95,96) via the *ab initio*/IGLO/NMR method. The results indicate that *nido*- $\text{B}_4\text{H}_7]^-$ (**55**) should also have the structure (411) illustrated in Fig. 20. These structures should be compared with Paetzold's known structure (97) of *nido*- NB_3H_6 (**57**) (222) as well as the structure we predict for Matteson's *nido*- CB_3H_7 (**58**) (411) (98) and our preferred structure for Burg's (99) possible *nido*- $\text{B}_4\text{H}_4\text{L}_2$ (**59**) (222).

The *nido*-deltahedral fragment for the known compounds *nido*- $\text{C}_4\text{H}_5]^+$ (**56**) and *nido*- NB_3H_6 (**57**), ni-4(IV), is exactly that expected following the excision of one high connected 4k vertex from the *closo*-trigonal bipyramid thus extending the original pattern espoused in 1971 (72) and as illustrated in Fig. 14. In contrast, other electron deficient compounds involving other elements than B, C, or N, etc., have ni-4(III) tetrahedral structures derived by the removal of one undesirable 3k vertex from the clo-5(III) deltahedron (Fig. 14) rather than ni-4(IV) configurations.

Perhaps two patterns collide in forecasting *nido*-4-vertex structures, high connected 4k vertex removal *versus* undesirable 3k vertex removal.

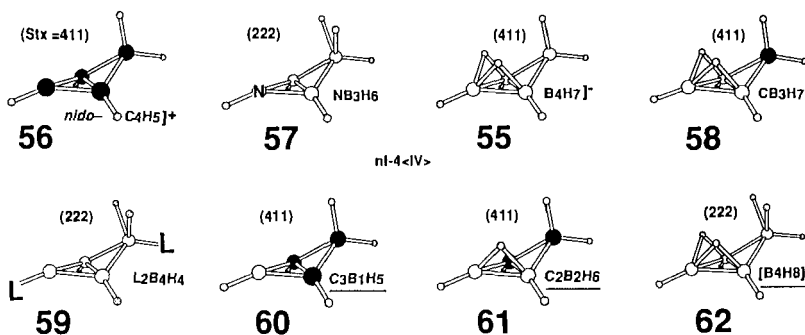


FIG. 20. Compounds (55–61) related to the hypothetical *nido*-B₄H₈ (62).

Projected structures for C₃BH₅ (60), C₂B₂H₆ (61), and B₄H₈ (62) are also illustrated in Fig. 20.

C. *nido*-5-vertex Compounds

The parent structures for the *nido*-species, 1,2-Me₂C₅H₃⁺ (48) (76) and 1,2-Me₂B₅H₇ (45) (100) and the carborane, 1,2-C₂B₃H₇ (47) (101) are illustrated in Fig. 15. All are related to the parent boron hydride, B₅H₉, as well as Fe₃(CO)₉[μ³PMnCp(CO)₂]₂ (102).

D. *nido*-7-, -8- and -9-Vertex Compounds

Figures 21, 22, and 23 are illustrated examples of seven-, eight-, and nine-vertex *nido*-compounds. The only seven-vertex *nido*-carborane known with certainty is Sneddon's (103) diethyl derivative of C₂B₅H₈⁻ (63a) (411), which incorporates an endohydrogen instead of an anticipated (72) bridge hydrogen (Fig. 21). Hosmane's (104) phosphorous derivative, RPC₂B₄H₆ (63b) (630), should also fall into this category.

Among the *nido*-8-vertex compounds, the C₂B₆H₁₀ isomers (64), (65), and (66) (105–109), the C₂B₆H₉⁻ isomers (67) and (68) (109,110), C₄B₄H₈

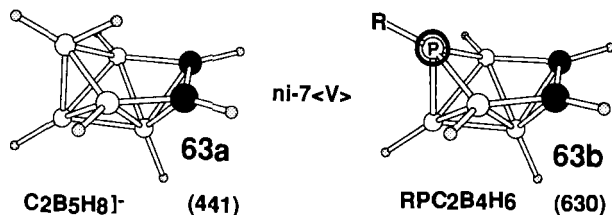
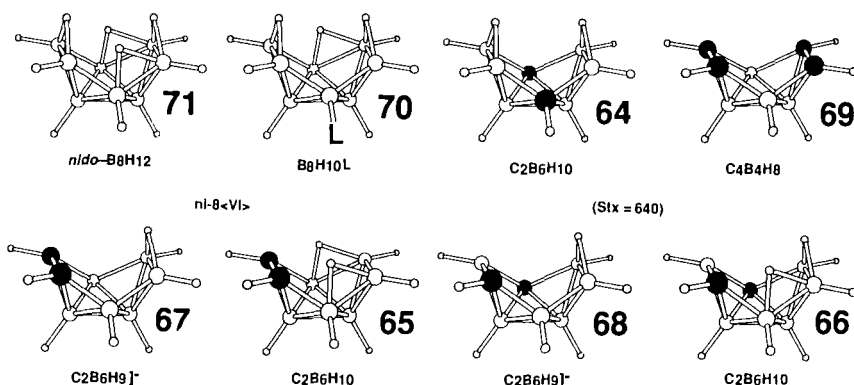


FIG. 21. Compounds (63a, 63b) related to the hypothetical [*nido*-B₇H₁₁].

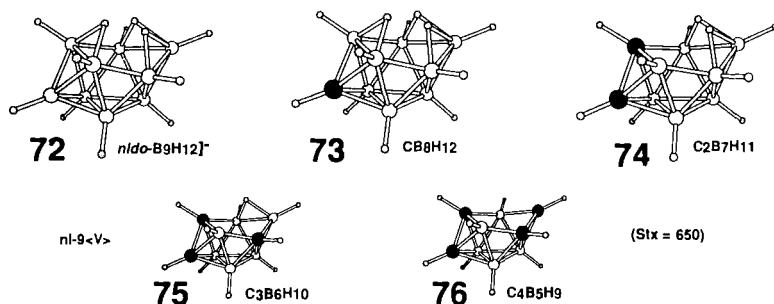
FIG. 22. Compounds (64–71) related to *nido*-B₈H₁₂.

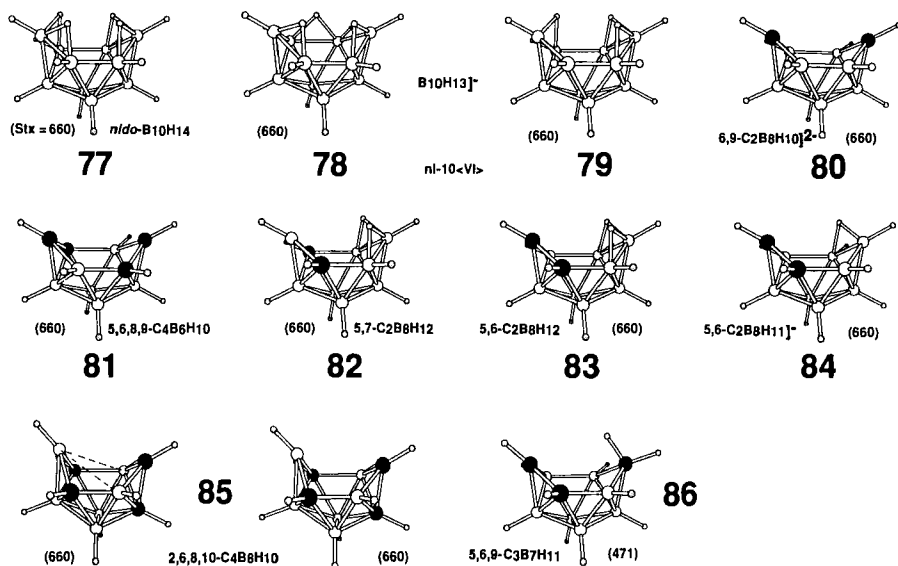
(69) (111,112), B₈H₁₀L (L = Me₃N) (70) (113,114), and B₈H₁₂ (71) (115) have hexagonal (VI-gonal) open faces, ni-8(VI) (Fig. 14). The bridge hydrogens and carbons are associated with low coordinated vertices with the bridge hydrogens having priority (Fig. 22). When a sulfur (4 SED) is incorporated (115), the originally anticipated ni-8(V) configuration (72) is observed.

nido-C₂B₇H₁₁ (74) (116) and *nido* CB₈H₁₂ (73) resemble *nido*-B₉H₁₂]⁻ (72) (117) and have the structures anticipated (72) in Fig. 14; the bridge hydrogens and carbons are all associated with low coordinated vertices (Fig. 23). Predicted structures for unknown compounds C₃B₆H₁₀ (75) and C₄B₅H₉ (76) are included.

E. *nido*-10-Vertex Compounds

In Fig. 24 are illustrated the parent *nido*-decaborane, B₁₀H₁₄ (77), and numerous structurally related carboranes, (78) to (86) (36,118,119); all

FIG. 23. Compounds (72–76) related to the hypothetical *nido*-B₉H₁₃].

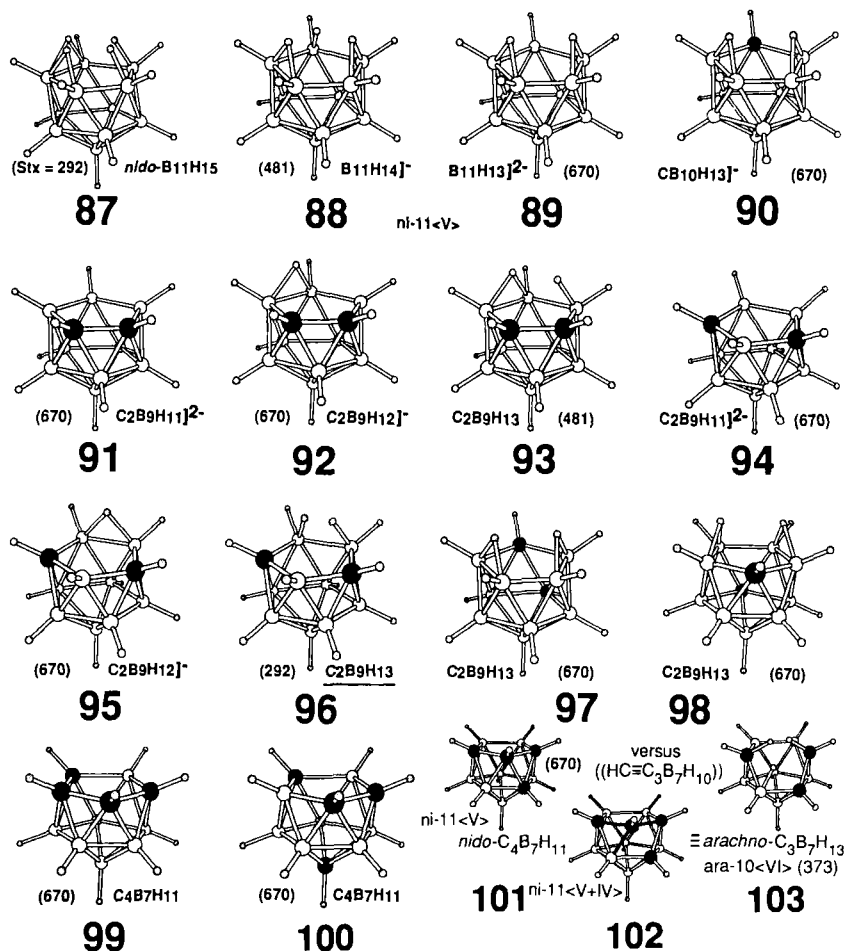
FIG. 24. Compounds (77–86) related to *nido*-B₁₀H₁₄.

have ni-10(VI) configurations. In most cases, the bridging hydrogens are associated with the lowest coordinated vertices and the carbons are either found in the lowest coordinated sites or the carbons are separated with rare exceptions for special reasons, e.g., (85) (120) and (86) (121). Should NB₉H₁₁][−], or SB₉H₁₀][−], or even more likely NB₉H₁₀]^{2−} or SB₉H₉]^{2−} be prepared, ni-10(V) structures are anticipated (69).

F. *nido*-11- and -12-Vertex Compounds

Figure 25 illustrates examples of *nido*-11-vertex compounds. When there are too many “extra” hydrogens around the five membered open face of *nido*-11-vertex compounds, one (or perhaps two) of the excess hydrogens become endohydrogens, rather than bridge hydrogens, i.e., B₁₁H₁₄][−] (88) (122,123), C₂B₉H₁₃ (93), and probably B₁₁H₁₅ (87) (122). All of the compounds (124) in Fig. 25 have ni-11(V) configurations even when nitrogen or phosphorous atoms (4 SED) are present as there is no *nido*-fragment with an IV-gonal open face. As there is no precedent for a triangle of carbons on the surface of any known carborane skeleton, we suggest the proposed structure (101) is more likely than (102). Structure 101 may be considered an alkyl derivative of *arachno*-C₃B₇H₁₃ (103).

Figure 26 shows known and speculative *nido*-12-vertex compounds. In the boxed area in Fig. 26 are illustrated Grimes' isomers (54,125) and

FIG. 25. Compounds (87–103) related to *nido*- $B_{11}H_{15}$.

tautomers of $R_4C_4B_8H_8$ (**104'**) and (**105'**). As the same dianion, *nido*- $C_2B_{10}H_{12}]^{2-}$ (isoelectronic with Grimes' compounds) is produced from both *closo*-1,2- $C_2B_{10}H_{12}$ (**6**) and *closo*-1,7- $C_2B_{10}H_{12}$ (**7**) we assume the structures are quite similar, i.e. (**104**) and (**105**).

The *nido*-12-vertex configuration, optimal for boron–carbon skeletons ($ni-12<VI>$; (**104**) and (**104'**) in Fig. 26), may be generated in two steps from the [$clo-13_{66}<III>$] deltahedron (Fig. 14). First, one five-connected {5k} vertex must be removed, which simultaneously converts the two adjacent 6k vertices in the parent $clo-13_{66}<III>$ deltahedron to two 5k vertices in the $ni-12<V>$ fragment. Subsequently, one additional highly coordi-

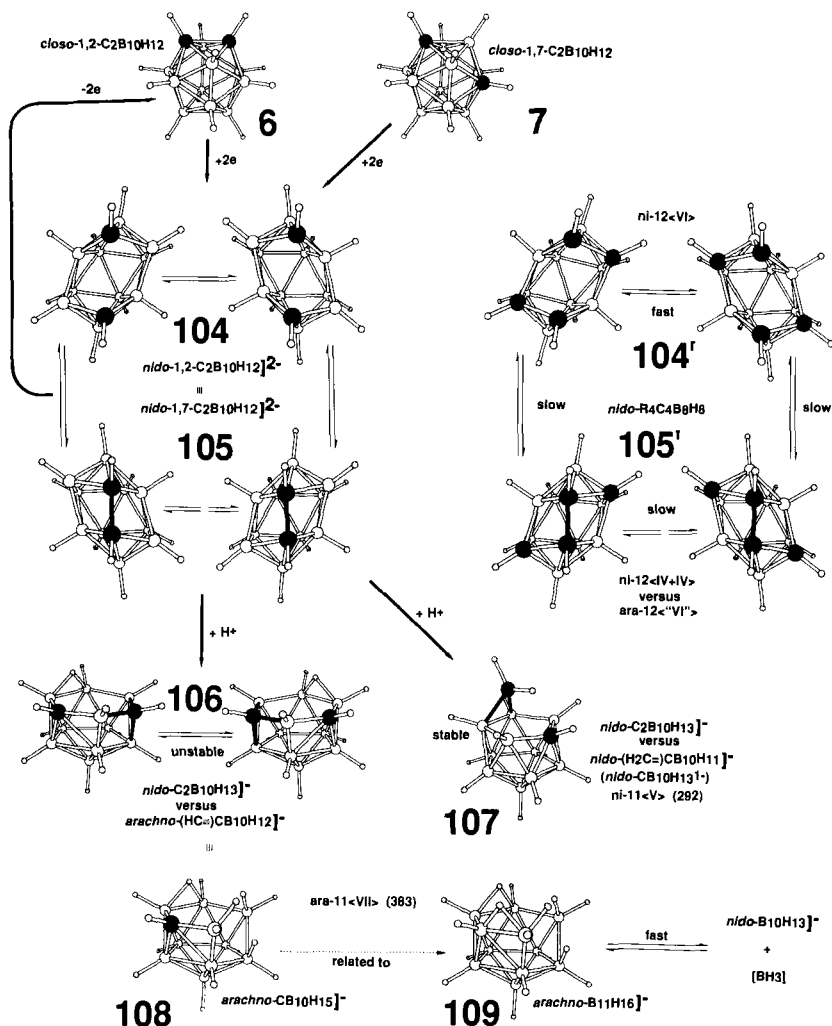


FIG. 26. Compounds (6, 7, 104–109) related to the hypothetical *nido*-B₁₂H₁₆].

nated connection, about the open face, must also be removed to produce the preferred ni-12<VI> configuration characteristic of the *nido*-structure for C₄B₈H₁₂ (**104**) (Fig. 26). Alternatively, the central 6k vertex of the clo-13₆₆₆/III> deltahedron (Fig. 14) may be removed producing the ni-12<VI> configuration in one step, e.g., (**104**) in Fig. 26.

Another configuration speciously results when one 6k vertex is removed from the clo-13₆₆₆/III> deltahedron thereby producing a *notional* “ni-

12(VI*)" fragment (126), which would seemingly leave the other 6k vertex intact. However, this is not to be, when the skeletal atoms are all carbon and boron. Upon protonation of (104) and (105) the stable (107) (127) and unstable (106) isomers of $C_2B_{10}H_{13}]^-$ are produced. In the latter, one additional connection is also removed between the remaining 6k boron and a 4k edge carbon, and this produces a 5k boron and a 3k carbon in (106). As a result there are adjacent VI-gonal and IV-gonal open faces (ni-12(VI+IV)) in this unstable configuration rather than the notional ni-12(VI*) configuration. It is our view that excising the electron precise alkyl carbon ($HC \equiv$ group) in (106) and replacing it with three endohydrogens suggests (106) should be more accurately portrayed as an alkyl derivative of (108) (ara-11(VII); see Fig. 14), which in turn is probably related to the presumed *arachno*- $B_{11}H_{16}]^-$ (109) intermediate involved in the total boron exchange reaction between *nido*- $B_{10}H_{13}]^-$ (78) and (79) in Fig. 24 and diborane, (110) in Fig. 27.

G. *nido*-2-Vertex Compounds

Before leaving the *nido*-compounds, the "misfit polyborane," diborane, B_2H_6 , should be addressed for completeness. Diborane is a *nido*-compound "in name only"; it has architectural features, i.e., BH_2 groups, that are usually associated with *arachno*-compounds rather than *nido*-compounds (Fig. 27). Diborane, B_2H_6 (110), discussed in most textbooks as the smallest and simplest of the boron hydrides, is generally treated as the *parent* of all boron hydrides. This is probably an extrapolation from hydrocarbon chemistry where methane is the smallest and the simplest hydrocarbon and may, in a legitimate sense, be considered the parent of all hydrocarbons.

Had three BH_3 groups trimerized into the unobserved *arachno*- B_3H_9 (through which the thermal decomposition of B_2H_6 is believed to proceed anyway) instead of two BH_3 groups dimerizing into *nido*- B_2H_6 , there would be no misfit. In many respects diborane chemistry is a field unto itself and has less in common with polyborane chemistry than might be expected.

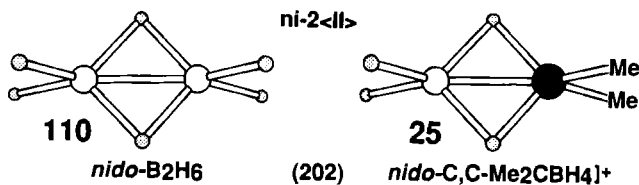
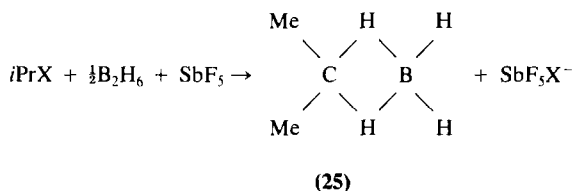


FIG. 27. Diborane derivatives (25, 110).

The *nido*-carborane cation *nido*-C,C-Me₂CBH₄]⁺ (**25**) was prepared and is shown in Fig. 27. It is isoelectronic and isostructural with diborane, B₂H₆, and is prepared from isopropyl cation, Me₂CH]⁺, and diborane (128). This cation incorporates two CHB bridge hydrogens and is stable only at low temperatures in the presence of superacids. Two other legitimate *nido*-compounds incorporate endo hydrogens, for example, the seven-vertex derivative of C₂B₅H₈]⁻ (**63a**) (Fig. 21) and the CH₂ group in C₃B₇H₁₁ (**86**) (Fig. 24).



IX

***arachno*-CARBORANES AND RELATED COMPOUNDS**

In contrast with the *nido*-compounds, most (but not all) *arachno*-carboranes and *arachno*-polyboranes incorporate one or more endohydrogens in their structures. The larger *arachno*-carboranes also differ from the more electron deficient *nido*-compounds and the even more electron deficient *closo*-compounds by having multiple space isomers per empirical formula. By this, we mean not only isomers of a given empirical formula, in which the carbon atoms simply occupy different vertices of a fixed deltahedron or deltahedral fragment (Fig. 1 to 6) but isomers of a given empirical formula that are based upon different deltahedral fragments altogether, and with differently sized open faces.

For example, within the *closo*-compounds with boron-carbon skeletons (Fig. 1), each most spherical deltahedron is unique and when there are isomers, they differ only in the location of the exosubstituent groups or in the locations of the carbon atoms (e.g., 1,2-C₂B₄H₆ (**2**) versus 1,6-C₂B₄H₆ (**3**) in Fig. 1) about the vertices of the most spherical deltahedra characteristic of the variously sized *closo*-compounds. These considerations also apply to the *nido*-compounds with boron-carbon skeletons wherein the locations of carbons and exosubstituent groups may differ but there remains only one preferred *nido*-deltahedral fragment configuration (e.g., 2,3-C₂B₄H₇]⁻ (**33**) versus 2,4-C₂B₄H₇]⁻ (**38**) in Fig. 10), which applies to all similarly sized *nido*-polyboranes, -carboranes and -carbocations.

In contrast, within the *arachno*-compounds, there may be two optional skeletal deltahedral fragments for each size category. In other words, all sufficiently large *arachno*-compounds, from 6 to 12 vertices, have available one deltahedral fragment structure with a VI-gonal open face. In addition, however, deltahedral structures with VII-gonal open faces are known (129) for *arachno*-9-vertex compounds and possibly known for *arachno*-8- (130) and -11-vertex compounds.

A. *arachno*-9-Vertex Compounds

The first *arachno*-carborane was discovered by Hawthorne (131). It was the *arachno*-9-vertex carborane, $C_2B_7H_{13}$ (**112**) (552), and this molecule is compared with a number of isomeric and related carboranes and polyboranes (ni-9(VI)) in Fig. 28. An isomer (**113**) was discovered by Stibr *et al.* (118). The bridge hydrogens tend to be found associated with neighboring low coordinated borons, and the carbons tend to be found in low coordinated sites as expected (72).

Some of the most elegant 1H and ^{11}B studies ever published (132) were carried out on *arachno*- CB_8H_{14} (**115**) and *arachno*- $CB_8H_{13}]^-$ (**116**). Wall-

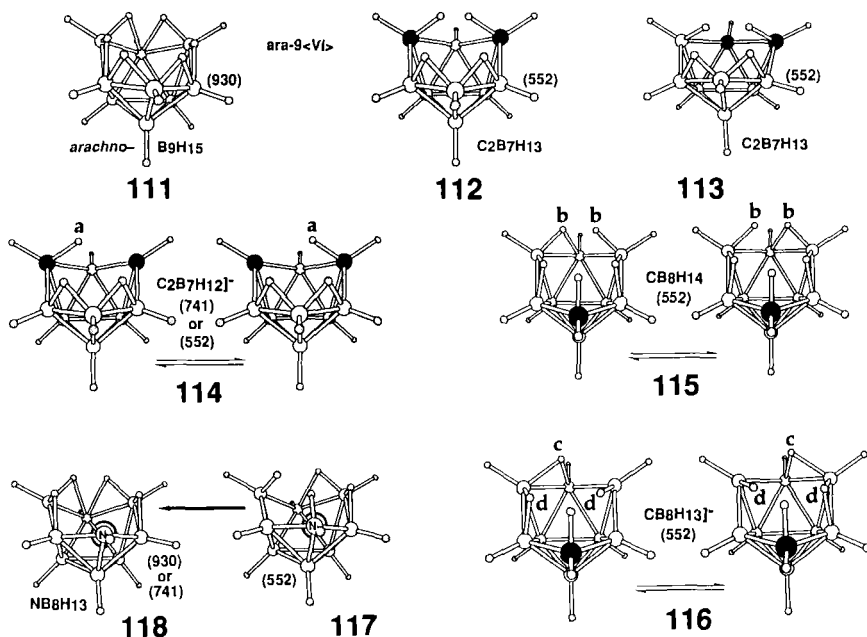


FIG. 28. Compounds (**111**–**118**) related to *arachno*- B_9H_{15} .

bridge *et al.* (132) proved unambiguously (based upon coupling constants) that the bridge-endohydrogen labeled, b, in fluxional (**115**), spent half the time as a bridge hydrogen and half the time as an endohydrogen. In the even more fluxional anion (**116**), the full-time bridge hydrogen, c, is coupled with one boron all the time and two other borons half time each, while the two bridge endohydrogens, d, are half-time endo- and half-time bridging hydrogens as illustrated. Note that there are always two endohydrogens (the **2** in 552) in the examples discussed. We would have anticipated several years ago that the isoelectronic NB_8H_{13} (133) would also have the 552 configuration, e.g., (**117**). Evidently the nitrogen, a 4 SED, is so positively charged in such a situation that the potential endohydrogen (on nitrogen) in (**117**) leaves as a proton and migrates to an available BB bond, converting it into a BHB bridge hydrogen and the structure (**118**) is observed in the crystal. If a lone electron pair remains on the nitrogen (as we anticipate is the case) we should count the lone pair as an endogroup, and *Chop-Stx* would equal 741, but if the skeleton sorbed the electron pair created by the hypothetical departure of the hydrogen from the nitrogen then the *Chop-Stx* value would be 930.

B. *arachno*-10-, -11-, and -12-Vertex Compounds

At the larger end of the range are *arachno*-10-, -11-, and -12-vertex carboranes and polyboranes. Among the *arachno*-10-vertex carboranes are $\text{C}_2\text{B}_8\text{H}_{14}$ (**121**) and the related anion, $\text{C}_2\text{B}_8\text{H}_{13}]^-$ (**120**); both have the expected structures (72,92), see Fig. 29.

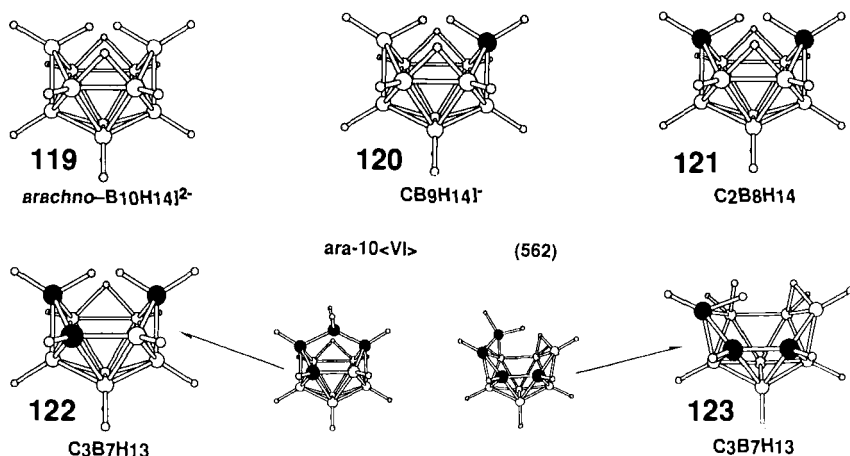


FIG. 29. Compounds (**119–123**) related to the hypothetical $[\text{arachno-B}_{10}\text{H}_{16}]$.

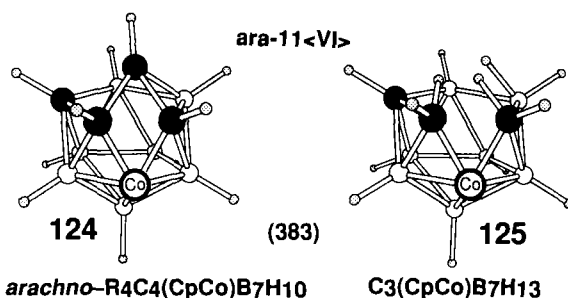


FIG. 30. Compounds (**124**, **125**) related to the hypothetical [*arachno*-B₁₁H₁₇].

In Fig. 29 two other compounds incorporating four carbons are illustrated on a smaller scale (92). In each case we would prefer to view them as alkyl derivatives of 6,7,9-C₃B₇H₁₃ (**122**) and 6,7,8-C₃B₇H₁₃ (**123**) following replacement of the electron-precise CH₂ group with two endohydrogens. The hydrocarbon scaffolding *enforces* unusual bridge and endohydrogen dispositions in (**123**), which would almost certainly tautomerize to resemble (**122**) were it free to do so.

An alkylated derivative of an *arachno*-11-vertex compound, C₃B₈H₁₄ [wherein a BH group is replaced by a CpCo group (134)], has the anticipated *ara*-11<VI> structure illustrated in Fig. 30. In this case an electron precise CH group, in (**124**), is replaced with three endohydrogens to produce (**125**). The structure in Fig. 30 should be compared with structures (**108**) and (**109**) in Fig. 26. An additional connection is missing; compare *ara*-11<VI> versus *ara*-11<VII> in Fig. 14.

Although no 12-vertex *arachno*-structures have been reported, there is one 12-vertex *pseudo nido*-compound (ni-12<IV + IV>) with an isolated electron precise CC bond between the two IV-gonal open faces (54,125) that probably should be considered the prototype for the most probable *arachno*-12-vertex compounds [see (**105**) in Figs. 26 and 31. The anticipated *ara*-12<VI> configuration, (**126**) in Fig. 31, would be produced by removing the isolated electron precise 2c–2e bond (as electron-precise scaffolding) and replacing it with two endohydrogens (70). This produces a VI-gonal open face, *ara*-12<VI>. Such a structure coincides precisely with the structure that would be produced by the removal of a pair of adjacent 5k vertices (between the two 6k vertices) from the most spherical 14-vertex *closo*-deltahedron (Fig. 14). This procedure simultaneously changes the two *overly connected* (6k) vertices of the original *closo*-14-vertex deltahedron into acceptable 5k vertices (see Fig. 31).

Having discussed the larger *arachno*-9-, -10-, -11-, and -12-vertex compounds, it is of interest to compare the less plentiful *arachno*-compounds with fewer than 9 vertices.

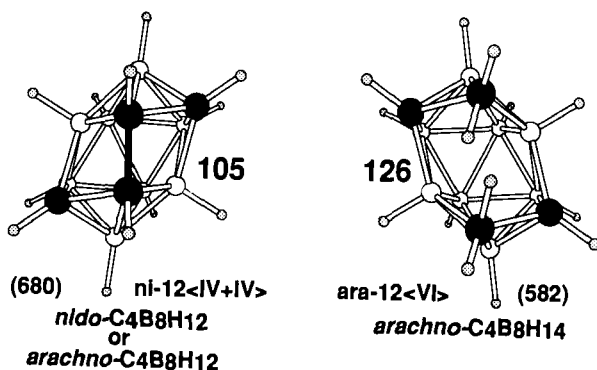


FIG. 31. Compounds (**105**, **126**) related to the hypothetical [*arachno*-B₁₂H₁₈].

C. *arachno*-8-Vertex Compounds

In Fig. 32 are displayed the *arachno*-carborane, C₂B₆H₁₂ (**128**) (130) and the *arachno*-polyborane, B₈H₁₄ (**127**) (135). In accordance with the ¹¹B and ¹H NMR spectra the more open ni-8<VII> structure has been proposed (130) for *arachno*-C₂B₆H₁₂ (**128**) while *arachno*-B₈H₁₄ (**127**) assumes the ni-8<VI> configuration. With one less bridge or endohydrogen to tolerate the two related isomeric anions of *arachno*-C₂B₆H₁₁]⁻, structures (**129**) (136) and (**130**) (137) assume the more compact ara-8<VI> configuration.

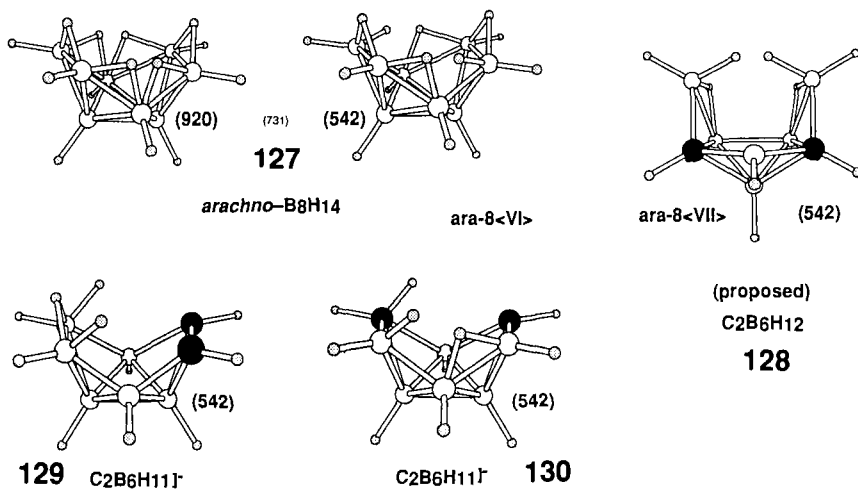


FIG. 32. Compounds (**127**–**130**) related to *arachno*-B₈H₁₄.

D. *arachno*-7-, -6-, and -5-Vertex Compounds

There are no *arachno*-7-, -6-, or -5-vertex carboranes known to date, nor are there any *arachno*-7-vertex polyboranes, however, the *arachno*-polyboranes, B_6H_{12} , $B_6H_{11}]^-$, and B_5H_{11} , are known. Kodama's *arachno*- B_5H_9L and *arachno*- $B_6H_{10}L$ would be isoelectronic with *arachno*- CB_4H_{10} and *arachno*- CB_5H_{11} , respectively (138).

E. *arachno*-4-Vertex Compounds

In Fig. 33 are illustrated the polyborane and hydrocarbon analogs of *arachno*- B_4H_{10} (**131**) (139), *arachno*- $B_4H_9]^-$ (**132**) (140), and *arachno*- $C_4H_7]^+$ (**133**) (61,63). None of these compounds are noted for their stability, all are fluxional, and to date, no *arachno*-4-vertex carboranes are known. On the other hand, allyl groups on boron are known to be fluxional, i.e., the two CH_2 groups of the allyl group become equivalent (141) on an NMR time scale. The intermediate or transition state, in this case would be a derivative of *arachno*- C_3BH_7 (**134**) or the expected carborane intermediate isoelectronic and isostructural with both the *arachno*-borane anion $B_4H_9]^-$ (**132**) and the *arachno*-cation $C_4H_7]^+$ (**133**). We suggest the organometallic intermediates in olefin metathesis and ROMP polymerization (142) also have *arachno*-4-vertex configurations (70) (see (**135**) in Fig. 33).

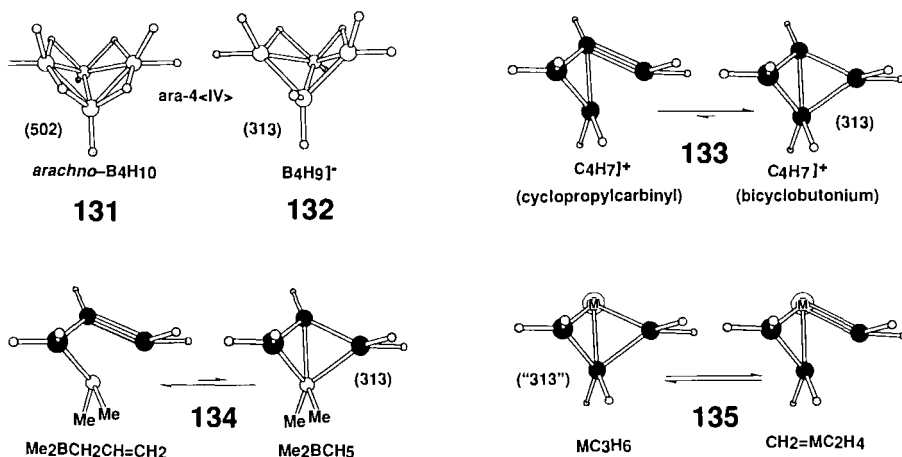


FIG. 33. Compounds (**131**–**135**) related to *arachno*- B_4H_{10} .

F. *arachno*-3-Vertex Compounds

In Fig. 34 are displayed the structures of $B_3H_8]^-$ (**136**) (143), the alkyl anion (**137**), and the brachiation intermediate (**24'**) (33,34) (see Fig. 9); the cation (**26**) and the intermediates (**138**) are presumed to be involved in H and C scrambling in isopropyl cation, to be compared with 2-norbornyl cation [see (**23**) in Fig. 26]. Mixed boron-carbon compounds have been observed in derivatives of Shore's $CB_2H_7]^-$ (**137**) (144,145) and Williams *et. al.*'s (63) alkyl derivative of $C_2BH_8]^+$ (**26**), which incorporate two BHC $3c-2e$ bridge hydrogens (61). A fluxional uncharged alternative structure (**24**) with one boron and two carbons (also containing a BHC $3c-2e$ bridge hydrogen) was invoked by the author (34) and later confirmed by Rickborn and Wood (34) as the primary intermediate in the brachiation of boron along a chain of carbons, i.e., in H.C. Brown's hydroboration rearrangement [see (**24**), Fig. 9]. An organometallic intermediate in Ziegler-Natta polymerization (**139**) probably has an *arachno*-3-vertex configuration also.

G. *arachno*-2-Vertex Compounds

One may also view Shore's anion, (**137**) (144,145) in Fig. 34, from a different perspective by simply assuming that the CH_2 moiety is electron

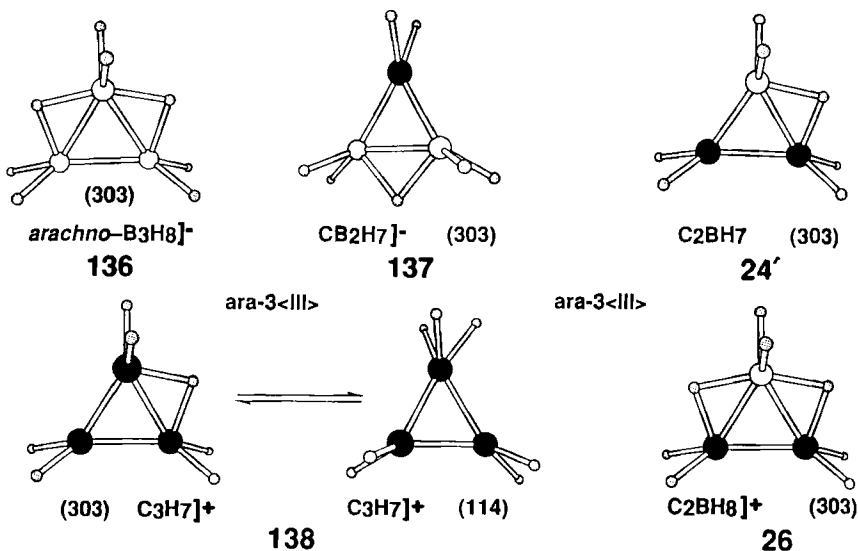


FIG. 34. Compounds (**24'**, **26**, **136**–**138**) related to the hypothetical [*arachno*- B_3H_9].

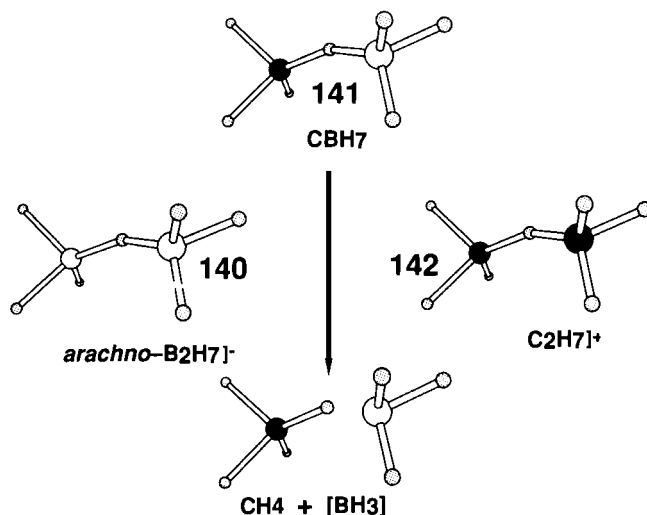


FIG. 35. Compounds (**140–142**) related to *arachno*-B₂H₇]⁻.

precise external scaffolding and replacing the methylene group with two endohydrogens. In this fashion, one may notionally consider Shore's CB₂H₇]⁻ derivative to be a dialkyl derivative of *arachno*-B₂H₇]⁻ (**140**) (*144–146*) in Fig. 35.

Preparing a carborane analog of B₂H₇]⁻ (**140**), i.e., the hypothetical neutral *arachno*-CBH₇ (**141**), would be a difficult synthetic task. It is unlikely that an intermediate compound with a BHC-bridge hydrogen can be synthesized unless very seriously sterically constrained to offset the tendency to dissociate into two neutral portions composed of derivatives of CH₄ and BH₃ (see Fig. 35). Although the parent C₂H₇]⁺ (**142**) is unknown, several sterically constrained peralkyl derivatives of (**142**) are known (*147*).

X

hypho-CARBORANES AND RELATED COMPOUNDS

Shore discovered the first *hypho*-compound, a polyborane anion (*148*). To our knowledge, no neutral *hypho*-polyboranes have been discovered though many neutral hydrocarbons are known that are formally *hypo*-species (e.g., cyclobutane, etc.). *hypho*-B₈H₁₆ and perhaps *hypho*-B₁₀H₁₈,

have been reported but we suspect that these are commo-compounds rather than parent *hypho*-polyboranes.

A. *hypho*-6-Vertex Compounds

hypho-B₆H₁₄ has been reported (149) to have been prepared in high yield, although it cannot be isolated. We suspect that the polymer (B₃H₇)_n was produced instead. Shore has prepared *hypho*-B₆H₁₀L₂ but no related carboranes have been reported. The Czechs have reported (150) the "helmet" anion *hypho*-C₂B₆H₁₃]⁻ and pointed out that if the two electron precise CH₂ groups were replaced with four endo hydrogens that *hypho*-B₆H₁₃]⁻ would result.

B. *hypho*-5-Vertex Compounds

The anion B₅H₁₂]⁻ (151) and Shore's di-Lewis base adduct, B₅H₉L₂ (152), are known and are presumed to be isoelectronic and *partially* isostructural with Hart's non-classical carbocation (153), but no carboranes that are intermediate between these species have been observed.

C. *hypho*-4-Vertex Compounds

hypho-B₄H₁₂ is not anticipated to be stable as both it and the related *arachno*-B₃H₉ would disproportionate into the more stable *nido*-B₂H₆ (110) shown in Fig. 27. *hypho*-B₄H₈L₂ derivatives do exist (154) but, in the opinion of the writer, they might as well be considered to be derivatives of *arachno*-B₃H₇L by considering the pendant electron-precise BH₂L group to be isoelectronic with an electron-precise CH₃ group. No carborane analogs are known.

D. *hypho*-3-Vertex Compounds

Trishomocyclopropenium cation, (22) (155) in Fig. 8, may be considered an alkylated derivative of C₃H₉]⁺, which in turn could be considered isoelectronic and isostructural with the intermediate (156), di-Lewis base adduct of B₃H₇, *hypho*-B₃H₇L₂, but no intermediate carborane analogs have been reported or are anticipated; however, the *hypho*-dianion, B₃H₉]²⁻, might (157) someday be prepared under special conditions. We suggest that an organometallic intermediate in Ziegler-Natta polymerization would be related.

XI

CONCLUSION

In this article I have concentrated on molecules consisting of boron, carbon, and hydrogen, i.e., compounds belonging to the polyborane, carborane, carbocation continuum. For further reading, Hermanek *et al.*, Sneddon *et al.*, and Onak *et al.* have been the most prolific discoverers of new carboranes in recent decades and certain carboranes have an extensive and growing derivative chemistry. Shore *et al.* are the most prolific source of new polyboranes, Kodama and Parry *et al.* for polyborane Lewis base adducts, and Olah *et al.* for new carbocations.

Entire fields neighbor the carborane, polyborane, carbocation continuum and lie beyond the scope of this manuscript; e.g., the metalla- and elementa- derivatives of polyboranes and carboranes have been exploited by Hawthorne *et al.*, Stone *et al.*, Greenwood *et al.*, Hosmane *et al.*, Grimes *et al.*, and Siebert *et al.* Paetzold has rejuvenated the field of azaboranes. Halo and polyhalo derivatives have been studied by Davidson *et al.*, Haubold *et al.*, and Onak *et al.* Others including Gaines *et al.* and Fehlner *et al.* have elucidated mechanisms, etc.; many other investigators have been overlooked. I cannot imagine the next 40 years could be more exciting than the last 40, but perhaps we are sitting in the back row of the balcony and if we can move to center stage the best is yet to come.

The first small *closo*-carboranes of Fig. 1 came to our attention much as one discovers mushrooms: absent the night before, surprisingly present in the morning. Without sufficient appreciation, we leisurely named them carboranes for the esoteric one-of-a-kind curiosities we thought them to be. Had we any perception, at the time, of the vast network of invisible "mycelia" that connected them not only to the many other types and kinds of carboranes (Figs. 2–35) but to the many neighboring fields as well, we surely would have taken naming them more seriously.

ACKNOWLEDGMENT

Support over the years by the U.S. Office of Naval Research (1964–1975) and the Loker Hydrocarbon Research Institute (1984–1993) is gratefully acknowledged. Professors G. A. Olah, R. W. Parry, S. Hermanek, S. G. Shore, K. Wade, F. G. A. Stone, G. K. S. Prakash, P. Paetzold, and T. P. Onak are thanked for sharing their scientific insights.

REFERENCES

- (1) Pasadena California Laboratory of Olin Mathieson Chemical Corporation.
- (2a) Good, C. D. and Williams, R. E., U.S. Patent 3030289 (filed 9/16/ 1959; issued 4/16/ 1962); *Chem. Abstr.*, 57, 12534b.

- (2b) Shapiro, I.; Good, C. D.; Williams, R. E. *J. Am. Chem. Soc.* **1962**, *84*, 3837.
- (3a) Williams, R. E.; Good, C. D.; Shapiro, I. 140th Meeting of the American Chemical Society, Chicago, Sept. 1961; 14 N, p. 36.
- (3b) *Chem. Eng. News* Sept. 11, **1961**.
- (3c) Lipscomb, W. N. *Proc. Natl. Acad. Sci. U.S.A.* **1961**, *47*, 1791 (see especially footnote 9).
- (3d) Hoffmann, R.; Lipscomb, W. N. *J. Chem. Phys.* **1962**, *36*, 3489.
- (4) Shapiro, I.; Keilin, B.; Good, C. D.; Williams, R. E. *J. Am. Chem. Soc.* **1963**, *85*, 3167.
- (5) Onak, T. P.; Gerhart, F. J.; Williams, R. E. *J. Am. Chem. Soc.* **1963**, *85*, 3378.
- (6) Niagara Falls Laboratory of Olin Mathieson Chemical Corporation.
- (7) Reaction Motors Division of Thiokol Chemical Company.
- (8) Redstone Arsenal Division of Rohm and Hass in Huntsville, Alabama.
- (9) Bobinski, J. J. *J. Chem. Educ.* **1964**, *41*, 500.
- (10) Heying, T. L.; Ager, J. W.; Clark, S. L.; Mangold, D. J.; Goldstein, H. L.; Hillman, M.; Polak, R. J.; Szymanski, J. W. *Inorg. Chem.* **1963**, *2*, 1089.
- (11) Fein, M. M.; Bobinski, J.; Mays, N.; Schwartz, N.; Cohen, M. S. *Inorg. Chem.* **1963**, *2*, 1111.
- (12) Grafstein, D.; Dvorak, J. *Inorg. Chem.* **1963**, *2*, 1128.
- (13) Schroeder, H.; Vickers, G. D. *Inorg. Chem.* **1963**, *2*, 1317.
- (14) Grafstein, D.; Dvorak, J. *Inorg. Chem.* **1963**, *2*, 1131.
- (15) Potenza, J. A.; Lipscomb, W. N. *J. Am. Chem. Soc.* **1964**, *86*, 1874.
- (16) Potenza, J. A.; Lipscomb, W. N. *Inorg. Chem.* **1964**, *3*, 1673.
- (17) Pepetti, S.; Heying, T. L. *J. Am. Chem. Soc.* **1964**, *86*, 2295.
- (18) Dunks, G. B.; Wiersema, R. J.; Hawthorne, M. F. *J. Am. Chem. Soc.* **1973**, *95*, 3174.
- (19) Zakharkin, L.; Kalinin, V. *Izv. Akad. Nauk SSSR. Ser. Khim.* **1967**, 194.
- (20) Zakharkin, L. I.; Kalinin, V. N.; Kvasov, B. A.; Synakin, A. P. *Zh. Obshch. Khim.* **1971**, *41*, 1726.
- (21a) Zakharkin, L. I.; Stanko, V. I.; Brattsev, V. A.; Chapovsky, Yu. A.; Struchkov, Yu. T. *Bull. Acad. Sci. USSR (Engl. Transl.)* **1963**, 1911; Zakharkin, L. I.; Stanko, V. I.; Brattsev, V. A.; Chapovsky, Yu. A.; Okhlobystin, O. Yu. *ibid.*, p. 2074; Zakharkin, L. I.; Kalinin, V. N.; Podvistotskaya, L. *Izv. Akad. Nauk SSSR, Ser. Khim.* **1967**, 2310.
- (22) Williams, R. E.; Gerhart, F. J. *J. Am. Chem. Soc.* **1965**, *87*, 3513.
- (23) Tebbe, F. N.; Garrett, P. M.; Young, D. C.; Hawthorne, M. F. *J. Am. Chem. Soc.* **1966**, *88*, 609.
- (24) Knoth, W. H. *J. Am. Chem. Soc.* **1967**, *89*, 1274.
- (25) Onak, T. P.; Drake, R.; Dunks, G. J. *J. Am. Chem. Soc.* **1965**, *87*, 2505.
- (26) Prince, S. R.; Schaeffer, R. O. *J. Chem. Soc., Chem. Commun.* **1968**, 451.
- (27) McKown, G. L.; Don, B. P.; Beaudet, R. A.; Vergamini, P. J.; Jones, L. H. *J. Am. Chem. Soc.* **1976**, *98*, 6909.
- (28) Son of German immigrants to San Francisco whose family business was destroyed by the San Francisco earthquake of 1906; It is not known whether Chester Stock and Alfred Stock were related.
- (29) Burg, A. B. Laboratory Notebooks, University of Chicago, **1934**.
- (30) Stock, A.; Kuss, E. *Chem. Ber.* **1923**, *56*, 808.
- (31) Stock, A. "Hydrides of Boron and Silicon"; Cornell University Press: Ithaca, NY, 1933.
- (32) Hurd, D. T. *J. Am. Chem. Soc.* **1948**, *70*, 2053.
- (33) Brown, H. C. "Hydroboration"; Benjamin, New York, **1962**.
- (34) Williams, R. E. *Inorg. Chem.* **1962**, *1*, 971; Rickborn, B.; Wood, S. E. *J. Am. Chem.*

- Soc.* **1971**, 93, 3940; *J. Org. Chem.* **1983**, 48, 555; Field, L. D.; Gallagher, S. *Tetrahedron Lett.* **1985**, 6125.
- (35) Dulmage, W. J.; Lipscomb, W. N. *Acta Crystallogr.* **1952**, 5, 260.
- (36) Kasper, J. S.; Lucht, C. M.; Harker, D. *Acta Crystallogr.* **1950**, 3, 436.
- (37) Lonquet-Higgins, H. C. *J. Chim. Phys.* **1949**, 46, 268; see also Duffey, G. H. *J. Chem. Phys.* **1951**, 19, 963, footnote p. 964.
- (38) Lipscomb, W. N. "Boron Hybrides"; Benjamin: New York, **1963**.
- (39) Holzmänn, R. T.; Hughes, R. L.; Smith, I. C.; Lawless, E. W. "Production of Boranes"; Academic Press: New York, **1967**; pp. 163–184.
- (40) Callery Chemical Company, Pittsburgh, Pennsylvania.
- (41) Williams, R. E. In "Progress in Boron Chemistry"; Brotherton, R. J.; Steinberg, H., Eds.; Pergamon: Oxford, 1970; Vol. 2, Chapter 2, p. 37.
- (42) Who later tragically died as a consequence of an explosion involving perchlorate rocket fuels.
- (43) Shapiro, I.; Wilson, C. O.; Ditter, J. F.; Lehmann, W. J. In "Borax to Boranes", Adv. Chem. Ser., No. 32; American Chemical Society: Washington, DC, **1961**.
- (44) Deltahedra are polyhedra with exclusively triangular facets.
- (45) Eberhardt, W. H.; Crawford, B. L.; Lipscomb, W. N. *J. Chem. Phys.* **1954**, 22, 989.
- (46) Lonquet-Higgins, H. C.; Roberts, M. De V. *Proc. R. Soc. London, Ser. A* **1955**, 230, 110.
- (47) Their existence was brought to the attention of the writer and his associates but the details were intentionally not made available to them.
- (48) Rose, Carl D. U.S. Patent 3,028,432 (filed 11/13/1959; issued 4/3/1962).
- (49a) Paetzold, P.; Müller, A. H. E.; Runsink, J. *Angew. Chem.* **1991**, 103, 201.
- (49b) Ouassas, A.; Fenet, B.; Frange, B. IMEBORON-VIII (Abstr. CA-13), Knoxville, Tennessee, **1993**.
- (50) Chatt, J.; Muir, L. M.; Muir, K. W., *J. Chem. Soc., Chem. Commun.*, **1971**, 655.
- (51) Stohrer, W.-D.; Hoffmann, R. *J. Am. Chem. Soc.* **1972**, 94, 1661.
- (52) Mayer, J. M. *Angew. Chem. Int. Ed. Eng.* **1992**, 31, 286.
- (53) Interestingly, Grimes' isomers (54) of $R_4C_4B_8H_8$ ($R = Me$ and Et) could be considered as *bond stretch isomers* (50–52) depending on one's point of view. Of course under such a loose definition Kekulé benzene could be considered a bond stretch isomer of Dewar benzene.
- (54) Grimes, R. N. *Adv. Inorg. Radiochem.* **1983**, 26, 55.
- (55) Hoffmann, R. to Williams, R. E. personal correspondence, October 14, **1965**.
- (56) Hart, H.; Lipscomb, W. N. *J. Am. Chem. Soc.* **1967**, 91, 771; *Inorg. Chem.* **1968**, 7, 1070.
- (57) Williams, R. E.; Prakash, G. K. S.; Bausch, J. W., BUSA-2, Durham, NC., June **1990**
- (58) Bausch, J. W.; Prakash, G. K. S.; Williams, R. E. *Inorg. Chem.* **1992**, 31, 3763.
- (59) Berry, T. E.; Tebbe, F. N.; Hawthorne, M. F. *Tetrahedron Lett.* **1965**, 12, 715 (see footnote 3).
- (60) Tsai, C.; Strieb, W. E. *J. Am. Chem. Soc.* **1966**, 88, 4513.
- (61) Olah, G. A.; Prakash, G. K. S.; Williams, R. E.; Field L. D.; Wade, K. "Hypercarbon Chemistry"; Wiley (Interscience): New York, **1987**; Olah, G. A.; Prakash, G. K. S.; Sommer, J., "Superacid Chemistry"; Wiley (Interscience), New York, **1985**; Laube, T. *Angw. Chemie (English)* **1987**, 26, 560.
- (62) Brown, H. C. "The Non-Classical Ion Problem"; commentary by P. v. R. Schleyer. Plenum Press: New York, **1977**.
- (63) Williams, R. E.; Prakash, G. K. S.; Field, L. D.; Olah, G. A. In "Advances in Boron and the Boranes"; Liebman, J. F.; Greenberg, A.; Williams, R. E., Eds.; VCH Publishers: New York, **1988**; Chapter 9, p. 222.

- (64) Williams, R. E. IMEBORON-III (Abstr.), München-Ettal, **1976**; Williams, R. E.; Field, L. D., IMEBORON-IV (Abstr.), Snowbird, Utah, **1979**; Williams, R. E. In "Boron Chemistry"; Parry, R. W.; Kodama, G., Eds.; Pergamon: Oxford, **1980**; p. 1.
- (65) Onak, T. P.; Williams, R. E.; Weiss, H. G. *J. Am. Chem. Soc.* **1962**, *84*, 2830.
- (66) Hoffmann, R., and Lipscomb, W. N. criticized our proposed structure for **32**; see *Inorg. Chem.* **1963**, *2*, 232 and Lipscomb, W. N. to Williams, R. E., personal correspondence, March 5, **1963**, as we did not subscribe to their "open" 3c-2e bonds. Later our proposed structure was confirmed by x-ray analysis [Streib, W. E.; Boer, J. P.; Lipscomb, W. N. *J. Am. Chem. Soc.* **1963**, *85*, 233; *Inorg. Chem.* **1964**, *3*, 1666; and still later Lipscomb *et al.* abandoned their "open" 3c-2e bonds.
- (67) Hogeveen, H.; Kwant, P. W. *Tetrahedron Lett.* **1973**, *19*, 1665.
- (68) Williams, R. E., *J. Pure Appl. Chem.* **1972**, *29*, 569.
- (69) Olah, G. A.; Wade, K.; Williams, R. E., Eds. "Electron Deficient Boron and Carbon Clusters"; Wiley: New York, **1991**; Chapter 2 by R. E. Williams; Williams, R. E. The Loker Symposium on Electron Deficient Compounds at the University of Southern California, Los Angeles, CA, January **1989**; Williams, R. E., IMEBORON-VI, Bechyně Czechoslovakia, June **1987**.
- (70) Williams, R. E. *Chem. Rev.*, **1992**, *92*, 177.
- (71) This final acceptance was expedited by M. F. Hawthorne and followed two years of puerile polemics with four editors and many referees (some were duplicates). The referees' objections were based on (a) the lack of experimental evidence, (b) the inappropriate inclusion of the *organic* carbocation, $C_5H_5^+$, with *inorganic* boron hydrides and (c) resentment over the presumed heretical attack on the sacredness of the icosahedron as the basic building model for all boron chemistry.
- (72) Williams, R. E. *Inorg. Chem.* **1971**, *10*, 210.
- (73) Footnote 7 of Williams (72).
- (74) This suggestion (the $C_5H_5^+$ structure) had been removed from the text, as a concession to more than one referee who felt such an outrageous proposal should prevent publication; it was reinsinuated into the final galley proof (73) as footnote 7.
- (75) Stohrer, W. D.; Hoffmann, R. *J. Am. Chem. Soc.* **1972**, *94*, 1661.
- (76) Masamune, S.; Sakai, M.; Ona, H.; Jones, A. J. *J. Am. Chem. Soc.* **1972**, *94*, 8956.
- (77) Wade, K. *J. Chem. Soc., Chem. Commun.* **1971**, 792.
- (78) Rudolph, R. W.; Pretzer, W. R. *Inorg. Chem.* **1972**, *11*, 1974.
- (79) Recent *ab Initio*/IGLO/ ^{11}B NMR calculations by two groups do not support this structure: (a) Onak, T. P.; Williams, R. E. and (b) Bausch, J. W.; Sneddon, L., both to be published, **1994**.
- (80a) Espoused at a lecture at Cal Tech in the early 1950's by either the speaker or a member of the audience (both forgotten).
- (80b) In actuality it is probable that one of the 4-SED atoms retains one skeletal electron pair as an endo-lone pair which would convert an Stx compound into a *de facto* $(S - 2)(t + 1)(x + 1)$ compound where the 1 in $x + 1$ represents an endo lone pair on the 4 SED (\cong a deprotonated endo hydrogen).
- (80c) Notice how the bridge hydrogens favor neighboring the methyl group in both **(49)** and **(50)** but the two more remote hydrogens in **(50)** are unsymmetrical!.
- (81) Brice, V. T.; Johnson, H. D., II; Shore, S. G. *J. Am. Chem. Soc.* **1973**, *95*, 6629.
- (82) Onak, T. P.; Dunks, G. B.; Spielman, J. R.; Gerhart, F. J.; Williams, R. E. *J. Am. Chem. Soc.* **1966**, *88*, 2061.
- (83) Note how the bridge hydrogens avoid neighboring the hypothetically produced ^{12}C .
- (84) Williams, R. E. *Adv. Inorg. Chem. Radiochem.* **1976**, *18*, 67.
- (85) Williams, R. E. The Loker Symposium on Electron Deficient Compounds at the University of Southern California, Los Angeles, CA, January **1989**.

- (86) Wade, K. *Adv. Inorg. Chem. Radiochem.* **1976**, 18, 1.
- (87) Mingos, D. M. P.; Wales, D. J. "Introduction to Cluster Chemistry"; Prentice-Hall, Englewood Cliffs, NJ, **1989**; Mingos, D. M. P. *Acc. Chem. Res.* **1984**, 17, 311; Mason, R.; Thomas, K. M.; Mingos, D. M. P. *J. Am. Chem. Soc.* **1973**, 95, 3802.
- (88) Stone, A. J. *Inorg. Chem.* **1981**, 20, 563; *Polyhedron*, **1984**, 3, 1299; Wales, D. J.; Stone, A. J. *Inorg. Chem.* **1987**, 26, 3845.
- (89) Gimarc, B. M.; Ott, J. J. *Inorg. Chem.* **1986**, 25, 2708.
- (90) King, R. B. *Inorg. Chim. Acta*, **1981** 49, 237.
- (91) Hoffmann, R., "Bridges between Inorganic and Organic Chemistry"; Nobel Lecture, **1981**, reviewed in *Science* **1981**, 211, 995.
- (92) Stibr, B. *Chem. Rev.* **1992**, 92, 225; Plešek, J. *ibid.*, p. 269; Hermanek, S. *ibid.*, p. 325.
- (93) Rasul, G.; Prakash, G. K. S.; Williams, R. E.; Kodama, G.; Parry, R. W. Detailed *ab initio*/IGLO/NMR results will be reported elsewhere.
- (94) Kodama, G.; Parry, R. W. *J. Am. Chem. Soc.* **1972**, 94, 407.
- (95) Olah, G. A.; Staral, J. S.; Spear, R. J.; Liang, G. J. *J. Am. Chem. Soc.* **1975**, 97, 5489.
- (96) Schindler, M. *J. Am. Chem. Soc.* **1987**, 109, 1024.
- (97) Paetzold, P.; Redenz-Stormans, B.; Boese, R.; Buhl, M.; Schleyer, P. v. R., *Angew. Chem., Int. Ed. Engl.* **1990**, 29, 1059.
- (98) Matteson, D. S.; Mattschei, P. K. *Inorg. Chem.* **1973**, 12, 2472.
- (99) The compound $((\text{CH}_3)_2\text{N})_2\text{B}_4\text{H}_6$ was reported (of unknown structure) by Burg, A. B. *J. Am. Chem. Soc.* **1957**, 79, 2129; We propose that the structure might be $((\text{CH}_3)_2\text{NH})_2\text{B}_4\text{H}_4$ or more generally $\text{L}_2\text{B}_4\text{H}_4$.
- (100) Tucker, P. M.; Onak, T. P.; Leach, J. B. *Inorg. Chem.* **1970**, 9, 1430.
- (101) Franz, D. A.; Grimes, R. N. *J. Am. Chem. Soc.* **1970**, 92, 1438; **1972**, 94, 412.
- (102) Koide, Y.; Bautista, M. T.; White, P. S.; Schauer, C. K. *Inorg. Chem.* **1992**, 31, 3690.
- (103) Beck, J. S.; Quintana, W.; Sneddon, L. G. *Organometallics* **1988**, 7, 1015.
- (104) Hosmane, N. S.; Lu, K.-J.; Cowley, A. H.; Mardones, M. A. *Inorg. Chem.* **1991**, 30, 1325.
- (105) Gotcher, A. J.; Ditter, J. F.; Williams, R. E. *J. Am. Chem. Soc.* **1973**, 95, 7514; Reilly, T.; Burg, A. B. *Inorg. Chem.* **1974**, 13, 1250.
- (106) Bausch, J. W.; Prakash, G. K. S.; Williams, R. E., BUSA-II Meeting, Research Triangle Park NC, June 9, **1990**.
- (107) Bausch, J. W.; Prakash, G. K. S.; Bühl, M.; Schleyer, P. v. R.; Williams, R. E. *Inorg. Chem.* **1992**, 31, 3060.
- (108) Onak, T. P., to be published.
- (109) Kang, S. O.; Bausch, J. W.; Carroll, P. J.; Sneddon, L. G. *J. Am. Chem. Soc.* **1992**, 114, 6248.
- (110) Onak, T. P.; Tseng, J.; Tran, D.; Herrera, S.; Chan, B.; Arias, J.; Diaz, M. *Inorg. Chem.* **1992**, 31, 3910.
- (111) Fehlner, T. P. *J. Am. Chem. Soc.* **1977**, 99, 8355; **1980**, 102, 3424.
- (112) Siebert, W.; El-Essawi, M. E. M. *Chem. Ber.* **1979**, 112, 1480.
- (113) Briguglio, J. J.; Carroll, P. J.; Corcoran, E. W.; Sneddon, L. G. *Inorg. Chem.* **1986**, 25, 4621.
- (114) Zimmerman, G. J.; Sneddon, L. G.; *J. Am. Chem. Soc.* **1981**, 103, 1102.
- (115) Enrione, R. E.; Boer, P. F.; Lipscomb, W. N. *J. Am. Chem. Soc.*, **1964**, 86, 1451; *Inorg. Chem.*, **1964**, 3, 1659.
- (116) Huffman, J. C.; Streib, W. E. *J. Chem. Soc., Chem. Commun.*, **1972**, 662.
- (117) Siedle, A. R., Ph.D. Thesis, Indiana University, Bloomington, 1973; p. 61; data to be published with Garber, A. R.; Bodner, G. M.; Todd, L. J.
- (118) Stibr, B.; Hermanek, S.; Janousek, Z.; Plzak, Z.; Dolansky, J.; Plešek, J. *Polyhedron*

- 1982, 1, 822; Stibr, B.; Plešek, J.; Zbáková, A. *ibid.*, p. 826; Rietz, R. R.; Schaeffer, R. J. *Am. Chem. Soc.* **1971**, 93, 1263; Garrett, P. M.; Ditta, G. S.; Hawthorne, M. F. *ibid.*, p. 1265.
- (119) Stibr, B.; Plešek, J.; Hermanek, S. *Collect. Czech. Chem. Commun.* **1972**, 37, 2696; Stibr, B.; Janousek, Z.; Base, K.; Hermanek, S.; Plešek, J.; Zakharova, I. A., *ibid.*, **1984**, 49, 1891; Stibr, B.; Plešek, J.; Zbáková, A. *Polyhedron* **1982**, 1, 824; Stibr, B.; Janousek, Z.; Base, K.; Hermanek, S.; Plešek, J.; Zakharova, I. A. *Collect. Czech. Chem. Commun.* **1984**, 49, 1891; Stibr, B.; Jelinek, T.; Plešek, J.; Zbáková, E.; Plzak, Z.; Hermanek, S. *J. Chem. Soc., Chem. Commun.*, **1987**, in press.
- (120) Koster, R.; Seidel, G.; Wrackmeyer, B.; Bläser, D.; Boese, R. *Chem. Ber.* **1991**, 124, 2715; Koster, R.; Seidel, G.; Wrackmeyer, B. *Angew. Chem.* **1985**, 97, 317; *Angew. Chem., Int. Ed. Engl.* **1985**, 24, 326; Koster, R.; Seidel, G.; Horstschäfer, W.; Siebert, W.; Gangmus, B. *Inorg. Synth.*, **1991**, 29.
- (121) Kang, S. O.; Furst, G. T.; Sneddon, L. G., *Inorg. Chem.* **1989**, 28, 2339.
- (122) Getman, T. D.; Krause, J. A.; Shore, S. G. *Inorg. Chem.* **1988**, 27, 2398, footnote 11.
- (123) Once Shore had determined the correct structure of $B_{11}H_{14}^-$ (122) the ^{11}B and 1H NMR data of Howe, D. V.; Jones, C. J.; Wiersema, R. J.; and Hawthorne, M. F. (*Inorg. Chem.* **1971**, 10, 2516), were reinterpreted by the original authors as well as several other groups to support the 481 configuration.
- (124) Stibr, B.; Plešek, J.; Jelinek, T.; Base, K.; Janousek, Z.; Hermanek, S. In "Boron Chemistry"; Hermanek, S., Ed.; World Sci. Publ.: Singapore, **1987**; Astheimer, R. J.; Sneddon, L. G., *Inorg. Chem.* **1983**, 22, 1928.
- (125) Venable, T. L.; Maynard, R. B.; Grimes, R. N. *J. Am. Chem. Soc.* **1989**, 106, 6187; **1984**, 106, 6187; Maynard, R. B.; Sinn, E.; Grimes, R. N. *Inorg. Chem.* **1981**, 20, 1201.
- (126) The asterisk signifies the presence of one 6k vertex.
- (127) Dunks, G. B.; Wiersema, R. J.; Hawthorne, M. F., *J. Am. Chem. Soc.* **1973**, 95, 3174; Tolpin, E. I.; Lipscomb, W. N., *J. Chem. Soc., Chem. Commun.* **1973**, 257; Getman, T. D.; Knobler, C. B.; Hawthorne, M. F., *Inorg. Chem.* **1990**, 29, 158.
- (128) Williams, R. E.; Prakash, G. K. S.; Field, L. D.; Olah, G. A., In "Advances in Boron and the Boranes"; Liebman, J. F.; Greenberg, A.; Williams, R. E., Eds.; VCH Publishers: New York, **1988**; Chapter 9.
- (129) Tippe, A.; Hamilton, W. C. *Inorg. Chem.* **1969**, 8, 464.
- (130) Corcoran, E. W.; Sneddon, L. G., *J. Am. Chem. Soc.* **1985**, 107, 7446.
- (131) Tebbe, F. N.; Garrett, P. M.; Hawthorne, M. F., *J. Am. Chem. Soc.* **1966**, 88, 607.
- (132) Howarth, O. W.; Jasztal, M. J.; Taylor, J. G.; Wallbridge, M. G. H. *Polyhedron* **1985**, 4, 1466.
- (133) Base, K.; Janousek, F.; Plešek, J.; Stibr, B.; Hermanek, S.; Huffman, J.; Ragatz, P.; Schaeffer, R. J. *Chem. Soc., Chem. Commun.* **1975**, 934; **1981**, 1162; *Collect. Czech. Chem. Commun.* **1983**, 48, 804.
- (134) Williams, R. E. In "Electron Deficient Boron and Carbon Clusters"; Olah, G. H.; Wade, K.; Williams, R. E., Eds.; Wiley: New York, 1991; Chapter 2, p. 67.
- (135) Moody, D. C.; Schaeffer, R. O. *Inorg. Chem.* **1976**, 15, 233.
- (136) Jelinek, T.; Stibr, B.; Hermanek, S.; Plešek, J. *J. Chem. Soc., Chem. Commun.* **1989**, 804.
- (137) Onak, T. P. to be published.
- (138) Of course, one may consider benzene (72), benzvalene and Dewar benzene to be arachno-6-vertex compounds as they are members of the arachno- $C_{10}H_6$ B_nH_{n+6} class.
- (139) Nordman, C. E.; Lipscomb, W. N. *J. Chem. Phys.* **1953**, 21, 1856; Jones, M. E.; Hedberg, K.; Shomaker, V. J. *Am. Chem. Soc.* **1953**, 75, 7116; Simmons, N. P. C.; Burg, A. B.; Beaudet, R. A., *Inorg. Chem.*, **1981**, 20, 533.

- (140) Johnson, H. D.; Geanangel, R. A.; Shore, S. G. *Inorg. Chem.* **1970**, *9*, 908.
- (141) Mikhailov, B. M.; Bubnov, Yu. N. "Organoboron Compounds"; Harwood Academic: New York, 1984.
- (142) Grubbs, R. H., et al. *Science* **1990**, *243*, 907; Piers, W. E.; Bercaw, J. E. *J. Am. Chem. Soc.* **1990**, *112*, 9406; Clawson, L.; Soto, J.; Buchwald, S. L.; Stigerwald, M. L.; Grubbs, R. H. *ibid.* **1985**, *107*, 3377.
- (143) Peters, C. R.; Nordman, C. E. *J. Am. Chem. Soc.* **1960**, *82*, 5758; Brellochs, B.; Binder, H. Z. *Naturforsch.* **1988**, *43*, 648.
- (144) Shore, S. G. In "Boron Hydride Chemistry"; Muetterties, E. L., Ed.; Academic Press: New York, **1975**; Chapter 3.
- (145) Gaines, D. F. *Inorg. Chem.* **1963**, *2*, 523.
- (146) Hertz, R. K.; Johnson, H. D.; Shore, S. G. *Inorg. Chem.* **1973**, *12*, 1875; Shore, S. G.; Lawrence, S. H.; Watkins, M. I.; Bau, R. J. *Am. Chem. Soc.*, **1982**, *104*, 7669.
- (147) Kirchen, R. P.; Sorensen, T. S. *Chem. Commun.* **1978**, 769; McMurry, J. E.; Hodge, C. N. *J. Am. Chem. Soc.* **1984**, *106*, 6450; Sun, F.; Sorensen, T. S. *ibid.* **1993**, *115*, 77.
- (148) The various classes, $C_{10-x}B_nH_{n+x}$, were named as follows: Closo ($x = 2$) (Gk. clovo = cage); nido ($x = 4$) (Gk. nest); arachno ($x = 6$) (Gk. web). When Shore discovered an $x = 8$ compound we exhumed the term hypho (Gk. net) which had been our second choice when we selected arachno. The author also suggested other choices, i.e. Groucho, Chico, Harpo and Zeppo, but Shore declined, advising the writer where to place them pending later exploitation.
- (149) Brellochs, B.; Binder, H. *Angew. Chem. Int. Ed. Engl.* **1988**, *27*, 262.
- (150) Jelenek, T.; Plesek, J.; Hermanek, S.; Stibr, B. *Main Group Met. Chem.* **1987**, *10*, 397.
- (151) Rempel, R. J.; Johnson, H. D.; Jaworowsky, I. S.; Shore, S. G. *J. Am. Chem. Soc.* **1975**, *97*, 5398; Bühl, M.; Schleyer, P. v. R.; McKee, M. L. *Heteroatom Chem.* **1991**, *2*, 499.
- (152) Fratini, A. V.; Sullivan, G. W.; Denniston, M. L.; Hertz, R. K.; Shore, S. G. *J. Am. Chem. Soc.* **1974**, *96*, 3013; Mangion, M.; Hertz, R. K.; Denniston, M. L.; Long, J. R.; Clayton, W. R.; Shore, S. G. *ibid.* **1976**, *98*, 449.
- (153) Hart, H.; Kazuya, M.; *Tetrahedron Lett.* **1973**, *42*, 4133.
- (154) Kodama, G.; Mitsuaki, K. *Inorg. Chem.* **1979**, *18*, 3302.
- (155) Masamune, S.; Sakai, M.; Kemp-Jones, A. V.; Nakashima, T. *Can. J. Chem.* **1974**, *52*, 855.
- (156) Paine, R. T.; Parry, R. W. *Inorg. Chem.* **1975**, *14*, 689.
- (157) Shore, S. G., personal communication to R. E. Williams, August **1991**.

Organometallic Derivatives of Fullerenes

JAMES R. BOWSER

*SUNY College at Fredonia
Fredonia, New York 14063*

I.	Introduction	57
A.	General Properties	58
B.	Preparation and Separation of Fullerenes	61
II.	Endohedral Complexes	63
A.	Synthesis and Mechanisms of Formation	63
B.	Evidence for Sequestration	65
C.	Molecular Orbital Calculations	67
III.	Fullerenes with Metal-Containing External Substituents	69
A.	Osmate Esters	69
B.	Platinum Complexes	71
C.	Iridium Complexes	72
D.	Ruthenium Complexes	74
E.	"Naked Metal" Complexes	74
IV.	Interstitial Substitution and Salt Formation	75
A.	Intercalation of Alkali Metals	77
B.	Other Salts	79
V.	Substitution for Framework Carbon	80
A.	Synthesis of Heteroclusters	81
B.	Computational Studies	82
VI.	Conclusions	86
	References	87

I

INTRODUCTION

The first fullerenes were reported in 1985 (1). Since that time, over a thousand research articles that deal with fullerenes, along with more than sixty reviews, have been published (2,3). However, most of these have been written from the perspective of the organic chemist, physical chemist (or physicist), or materials scientist. What about the inorganic/organometallic domain?

The chemical modification of an all-carbon cluster via the addition of a metal or metalloid produces, of course, an organometallic derivative. The term "doping" is commonly encountered in this regard, but has been used to describe a wide variety of processes. The focus of this summary is on the synthesis, structures, and physical and chemical properties of

metal- and metalloid-containing derivatives of large carbon clusters. Relevant literature through November 1992 is reviewed.

There are at least four different ways to incorporate a heteroatom into a fullerene system: endohedrally (i.e., on the inside), externally (as for example by complexation to a metal), by intercalation into the interstices of a solid-state lattice, and by incorporation into the framework itself (either by cluster expansion or by replacement of one or more carbon atoms). Each of these has, to one extent or another, been accomplished in the laboratory, and all have been studied computationally as well.

A symbolism first suggested by Smalley (4,5) is used here for certain doped species. The atoms making up the cluster framework are grouped within parentheses, with the atomic symbol(s) preceded by @; atoms that lie inside the hollow fullerene cage are listed inside the parentheses and before the @. Hence, the formula ($\text{K}@\text{C}_{59}\text{B}$) represents a hybrid, 60-atom cluster surrounding a potassium atom. $\text{K}(@\text{C}_{59}\text{B})$ denotes the potassium salt of the C_{59}B^- anion.

A. General Properties

The ability to modify any chemical system is, of course, dependent on the attributes of that system. A summary of relevant properties for the best known fullerene, C_{60} (buckminsterfullerene or "bucky ball"), is as follows. The cluster is a hollow sphere, with a diameter (defined as the distance between two carbon nuclei *trans* to one another) of about 7.1 Å. The surface consists of a fused network of 20 six-membered and 12 five-membered rings, and there are 120 covalent bonds (90 σ and 30 π). The σ network involves sp^2 -hybridized carbons and is somewhat strained because of the curvature of the surface; the three angles about any carbon sum to 348°, compared to the ideal value of 360° (6). There are two different carbon-carbon bond lengths, with the bonds fusing 2 six-membered rings (and thereby connecting two pentagons) being shorter than the 6-5 junctions. Reported experimental values include 1.401 and 1.458 Å by electron diffraction (7), 1.355 and 1.467 Å from X-ray analysis of a twinned crystal (8), and 1.391 and 1.455 Å from neutron powder diffraction (9) (see Fig. 1).

X-ray diffraction data have been somewhat difficult to obtain because of the crystals' tendency to retain solvent; however, it is now known that under normal conditions of temperature and pressure, C_{60} crystallizes into a face-centered cubic lattice (10). At room temperature the molecules appear to be rapidly spinning ($>10^8$ rotations per second). The unit cell edge length is 14.17 Å, which is consistent with the close packing of (pseudo)spherical molecules 10.02 Å in diameter. The calculated van der

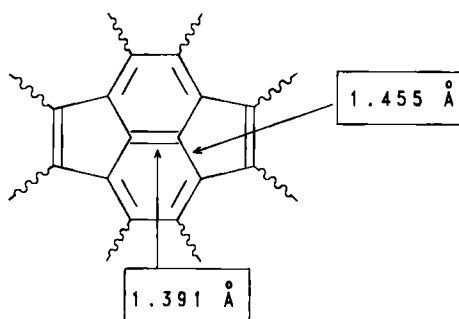


FIG. 1. Bond distances in C_{60} , as determined by neutron powder diffraction [see Ref. (9).]

Waals diameter for the carbons of C_{60} is then 2.94 Å, about 12% smaller than the interplanar spacings (3.35 Å) in graphite (11). Evidence that the intermolecular interactions are of the van der Waals type includes isothermal compressibility data, which are comparable to the interlayer values for graphite (12).

A first-order phase transition to the simple cubic lattice type occurs at about -18°C ; this has been studied by both variable-temperature NMR (13) and DSC (10). Other useful thermal studies have been reported as well. It was established by calorimetry that the standard enthalpy of formation of C_{60} is +545 kcal/mol (14). TGA data indicate thermal degradation beginning at roughly 450°C in air and at about 700°C under an inert atmosphere, depending on the heating rate (15–17).

The C_{60} molecule is diamagnetic, with a HOMO of H_u symmetry (fivefold degeneracy). The LUMO is triply degenerate, with T_{1u} symmetry. The band gap in crystalline C_{60} (*fcc* lattice type) is estimated to be about 1.7 eV (18,19). A partial MO diagram is shown in Fig. 2.

Two noteworthy properties of C_{60} are its moderate ionization energies and high electron affinity. The first ionization energy is about 7.6 eV (20,21)—quite comparable to transition metals such as nickel and silver, and considerably lower than for smaller organic molecules such as ethylene (10.5 eV) and benzene (9.2 eV). Hence, behavior as a Lewis base is to be expected, and electron transfer to produce salts of the C_{60}^{+} cation is not out of the question.

The first electron affinity has been measured to be about 2.65 eV (19,22–26), greater than that of any element except for the halogens. The most comparable molecule appears to be BF_3 (also 2.65 eV). Among organic species, tetracyanoethylene (TCNE, 2.88 eV) makes a reasonably good comparison. The high EA_1 derives, of course, from the low-lying LUMOs. Gas-phase electron addition can be achieved to produce $C_{60}^{\cdot-}$

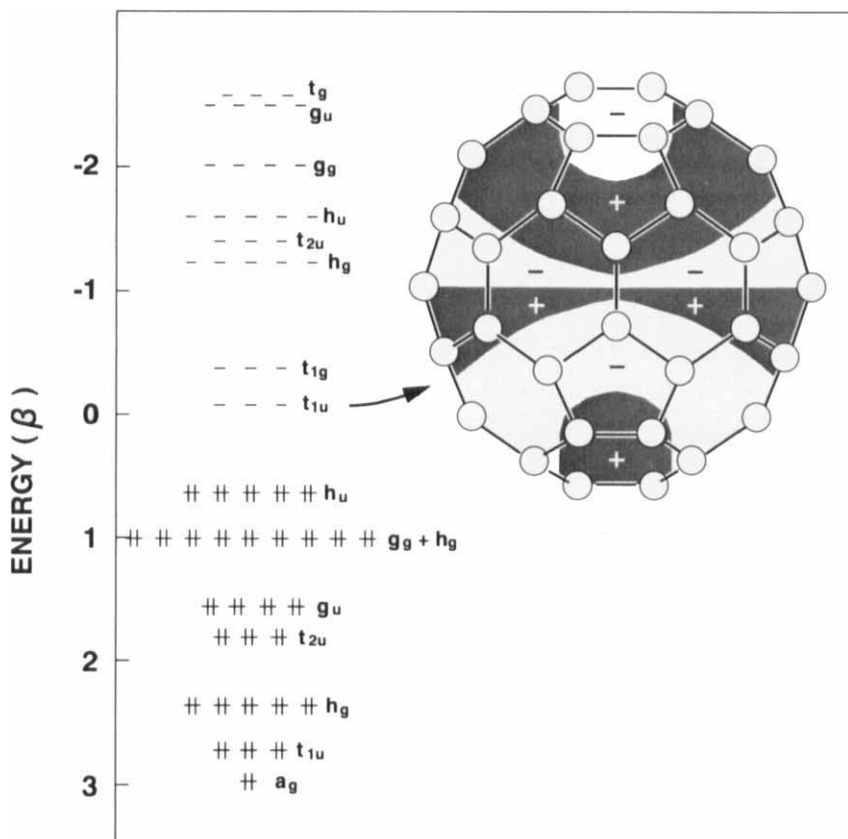


FIG. 2. Hückel energy levels of C_{60} . One orbital contributing to the LUMO level is pictured. [Reproduced with permission from Ref. (6).]

($n = 1$ and 2) as stable, free anions (27). In solution, C_{60} behaves as an oxidizing agent and is easily reduced electrochemically (26,28–30). Most researchers have reported three reversible waves; five were observed (at -0.36 , -0.83 , -1.42 , -2.01 , and -2.60 V referenced to SCE) when benzonitrile was used as the solvent (30).

Among the other fullerenes, the best studied is C_{70} . That cluster is thought to be slightly less stable than C_{60} per mole of carbon. Its ellipsoidal geometry (D_{5h} point group, Fig. 3) was proposed in 1985 (31) and has been confirmed by electron diffraction (32), ^{13}C NMR spectroscopy (33,34), an X-ray crystallographic study of a derivative (35), and by scanning tunneling microscopy (36,37). Larger members of the fullerene family include C_{76} , C_{84} , C_{90} , C_{94} , and C_{100} , up to at least C_{330} (38–40). Also known is

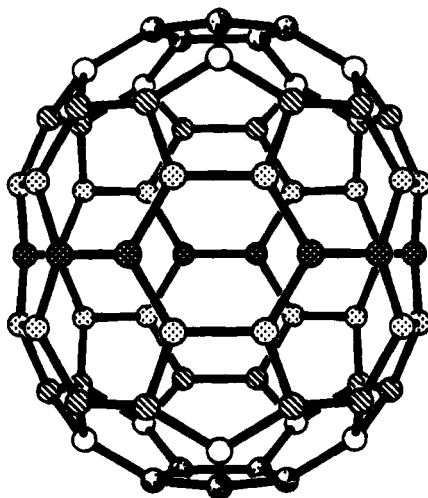


FIG. 3. The structure of C_{70} . [Reproduced with permission from Ref. (120).]

C_{82} , although that species appears to be most common in the presence of one or more metals (see Section II) (41).

B. Preparation and Separation of Fullerenes

There are many known ways to produce fullerenes in the laboratory; they appear to form spontaneously whenever carbon condenses in an inert gas atmosphere (42). The first fullerenes to be recognized as such were synthesized by laser-induced vaporization from a rotating graphite disk (1). In 1990 it was shown that the resistive heating of graphite produces macroscopic quantities of C_{60} and C_{70} (43). Since that time, several research groups have reported improvements in the general procedure. For example, Diederich and co-workers were able to separate the soot produced in this manner into individual clusters that amounted to over 75% of the total soot mass (26). Scrivens *et al.* described a procedure for the collection of gram quantities in 1.5 hour (44). Parker *et al.* used plasma discharge to obtain 44% extractable fullerenes; about one-third of the extract consisted of large clusters having between 84 and 200 atoms (39). It is also possible to obtain laboratory-scale amounts by the controlled pyrolysis of benzene and other aromatic hydrocarbons (45,46). Advances in the synthetic methodology have been such that fullerene generation can now serve as a synthetic experiment in the undergraduate laboratory (47,48). A simple apparatus for this purpose is diagrammed in Fig. 4.

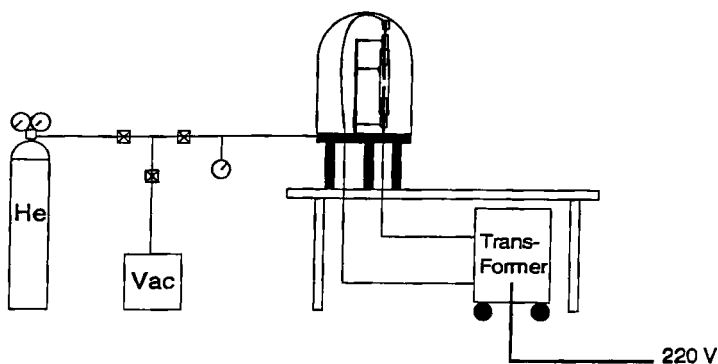


FIG. 4. A simple apparatus for the generation of fullerenes. [Reproduced with permission from Ref. (47).]

Different methods give different product ratios, of course. For example, the electric discharge approach gives fullerene mixtures whose composition depends on the size of the graphite rod, the intensity of the electrical current, and the pressure and nature of the carrier gas (28,49). A typical composition is roughly 70–85% C_{60} and 10–15% C_{70} , with the remainder being larger clusters (44). It was recently reported that ion sputtering and electron beam evaporation of graphite preferentially produce C_{70} and higher fullerenes, with only small amounts of C_{60} (50).

Purification can be a difficult step, but a number of procedures for obtaining pure compounds from soots have been published. Regardless of how the soot is produced, it is customary to extract the fullerenes with boiling benzene or toluene; CS_2 is even more effective, but is more unpleasant and hazardous. Soxhlet or other continuous extraction is very important for good separation (39,51,52). [An alternative method using ultrasound has also been suggested (53).] The isolation of individual products has been accomplished in various ways, including fractional sublimation (15,43,54) and various kinds of chromatography. A few examples are:

- (1) HPLC using a bonded phase C_{18} column, with hexane as the mobile phase (53). Polystyrene gel (55) and a variety of other stationary phases (56–58) have been tried as well.
- (2) Column chromatography using alumina (26,33), silica gel (49), and powdered graphite (59).
- (3) Flash chromatography using a stationary phase of activated charcoal (44).
- (4) Charge-transfer complex chromatography (49,60).

II

ENDOHEDRAL COMPLEXES

It was noted above that the diameter of C_{60} is approximately 7.1 Å. Subtracting twice the van der Waals radius of carbon (roughly 1.7 Å) suggests that the internal cavity is 3.7 Å in diameter, which is easily large enough to permit the sequestration of at least one atom of any element. There are now many known examples of such species. None have been isolated as of this writing, but some progress has been made in this regard (see below). Nor have any crystallographic determinations of endohedral complexes been reported. Hence, the evidence that metals lie inside of rather than external to the cage is limited to observations of chemical reactivity, plus a variety of spectroscopic observations. Such data are sufficiently strong to have convinced most researchers of the existence of such species, although some questions remain (61).

A. Synthesis and Mechanisms of Formation

The first example of what Cioslowski has named endohedral complexes (62) was observed by Smalley's group in 1985 (31). The laser vaporization of a graphite disk impregnated with $LaCl_3$ gave mass spectral evidence for several lanthanum-carbon species, including $(La@C_{60})$, $(La@C_{74})$, and $(La@C_{82})$. Later, the milligram-scale synthesis and partial purification of $(La@C_{82})$ was accomplished. The procedure involved the reaction of 10% La_2O_3 /graphite at 1200°C, followed by sublimation onto a cool copper disk (4,5). The collected material contained both fullerenes and endohedral complexes; addition of hot toluene to the sublimate gave a solution containing $(La@C_{82})$, along with C_{60} , C_{70} , and C_{96} .

An alternate synthesis of $(La@C_{82})$ involves the arc vaporization of a composite graphite/ La_2O_3 rod mixed with a binder (63). The soot that is produced can be extracted with toluene, washed with Et_2O , and dried. The extract is reported to contain 2–4% $(La@C_{82})$ by mass, mixed with C_{60} and C_{70} .

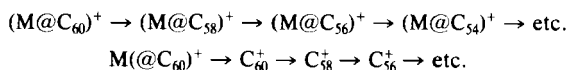
A variety of yttrium-doped cations have been produced by direct laser vaporization of graphite/ Y_2O_3 /fullerene mixtures (64,65). One product obtained in this manner was $(Y@C_{60})$. Later, $(Y@C_{82})$ was produced by a similar process, using yttrium-carbon rods (66,67). Examples of other monometal endohedral complexes include $(Sc@C_{82})$ (68,69), several containing alkali metals (5,31,70), and a host of rare-earth species (71).

The contact arc vaporization of graphite/Fe(CO)₅ mixtures under a helium atmosphere, followed by extraction and column chromatography of the soot produced, led to the observation of (Fe@C₆₀) (72). Various spectroscopic comparisons have been made between that compound and its exohedral isomer (see Section III.E, below).

The larger fullerenes can enclose two or more metals. Examples include the (M₂@C₈₀) family (M = La, Ce, Tb, etc.) (71,73,74). Evidence for the mixed-metal species (YLa@C₈₀) has also been obtained (74). The formulation (M₂@C₈₂) (M = La, Y, Ce, and Tb) appears to yield special stability (66,67,73). Also known are some three-metal clusters, including (Sc₃@C₈₂) (68,69), (La₃@C₁₀₆) (73), and (La₃@C₁₁₂) (73). It has been stated that scandium is incorporated more easily than lanthanum or yttrium (68).

Data describing (U@C₂₈), the smallest endohedral complex yet known (75), have recently been published. A likely structure for C₂₈ has T_d symmetry, with four six-membered rings in a tetrahedral orientation about the geometric center. It was proposed that (U@C₂₈) contains a sequestered metal covalently bonded at those four sites.

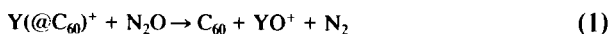
There appear to be two mechanisms by which endohedral complexes are produced. One involves carbon aggregation leading to closure as the cage forms around the metal; this is presumably what occurs when graphite-impregnated mixtures undergo laser vaporization. This method appears to work best for the more electropositive metals (76). However, there is also evidence that small atoms and molecules can become sequestered *after* the cluster has been formed. Such direct implantation appears to occur when fullerene ion beams are accelerated and passed through a chamber containing helium at low pressures (77,78). Large collisional energies cause cage fragmentation; ionizing energies in the range of 35–40 eV appear to give the best results. That this approach produces heteroatoms that are endohedrally located can be deduced from the fragmentation patterns, which typically include heteroatom-containing ions formed by the successive loss of C₂ units (see Scheme 1) (65,79,80). Similar approaches have yielded C₆₀⁺ adducts with D₂, neon, and argon (81,82). Divalent and trivalent cations have also been studied (81–84).



SCHEME 1. Generalized fragmentation patterns for endohedral and exohedral isomers of a monometal derivative of C₆₀.

B. Evidence for Sequestration

What data demonstrate the endohedral nature of these compounds? First, these species show very low chemical activity. Although lanthanum is a lithophilic element and La(III) is a hard Lewis acid, (La@C₈₂) appears to be unreactive toward O₂, H₂O, and NH₃; this strongly suggests sequestration of the metal (4,5,70). In the same way, the stability of (Y@C₆₀) toward oxidation by N₂O is noteworthy. Thus it is possible to prepare the exohedral isomer Y(@C₆₀) by gas-phase ion association and to demonstrate that the reaction



is much more facile for that isomer than for the endohedral complex (64) (see Fig. 5).

FT-ICR experiments show endohedral species to be remarkably stable toward photofragmentation. At high energies, (La@C₆₀)⁺ fragments in the same manner as C₆₀ itself, undergoing successive cage contractions two carbons at a time *without* loss of the metal (4,85,86). For C₆₀ the sequence ends at C₃₂⁺, while the smallest lanthanum-containing fragment observed was (La@C₄₄)⁺ [or possibly (La@C₄₂)⁺] (5). The fragmentations of the molecular ions of (K@C₆₀) and (Cs@C₆₀) again occur in two-carbon sequences, down to (K@C₄₄)⁺ and (Cs@C₄₈)⁺ (70). Calculations and molecular modeling studies suggest that the spheroidal 44- and 48-carbon cages are just barely large enough to accommodate K⁺ and Cs⁺ ions, respectively (4). This behavior is in contrast to that observed for exohedral complexes such as Fe(@C₆₀) (87–89), for which the primary mode of fragmentation involves loss of the metal to give C₆₀⁺ (Scheme 1).

The isomers Fe(@C₆₀) and (Fe@C₆₀) can be differentiated by EXAFS and Mossbauer spectroscopy (72). The EXAFS data for the endohedral compound show *two* relatively short Fe–C distances, at 2.06 and 2.34 Å. The external adduct, as expected, shows only one bonding distance (2.03 Å). The ⁵⁷Fe Mossbauer spectrum of (Fe@C₆₀) consists of a single transition, with an isomer shift of –0.083 mm/sec. This is consistent with zero-valent iron (72).

Supporting evidence has also been obtained from ESR spectroscopy (63,66–69,90). As is shown in Fig. 6, the spectrum of (La@C₈₂) consists of eight lines of equal intensity, centered at *g* = 2.001. The chemical shift is close to that observed for fullerene radical anions (91–94). The eight-line pattern is attributable to coupling to the *I* = $\frac{7}{2}$ ¹³⁹La nucleus, with a hyperfine coupling constant of 1.25 G. There are also weak satellites due

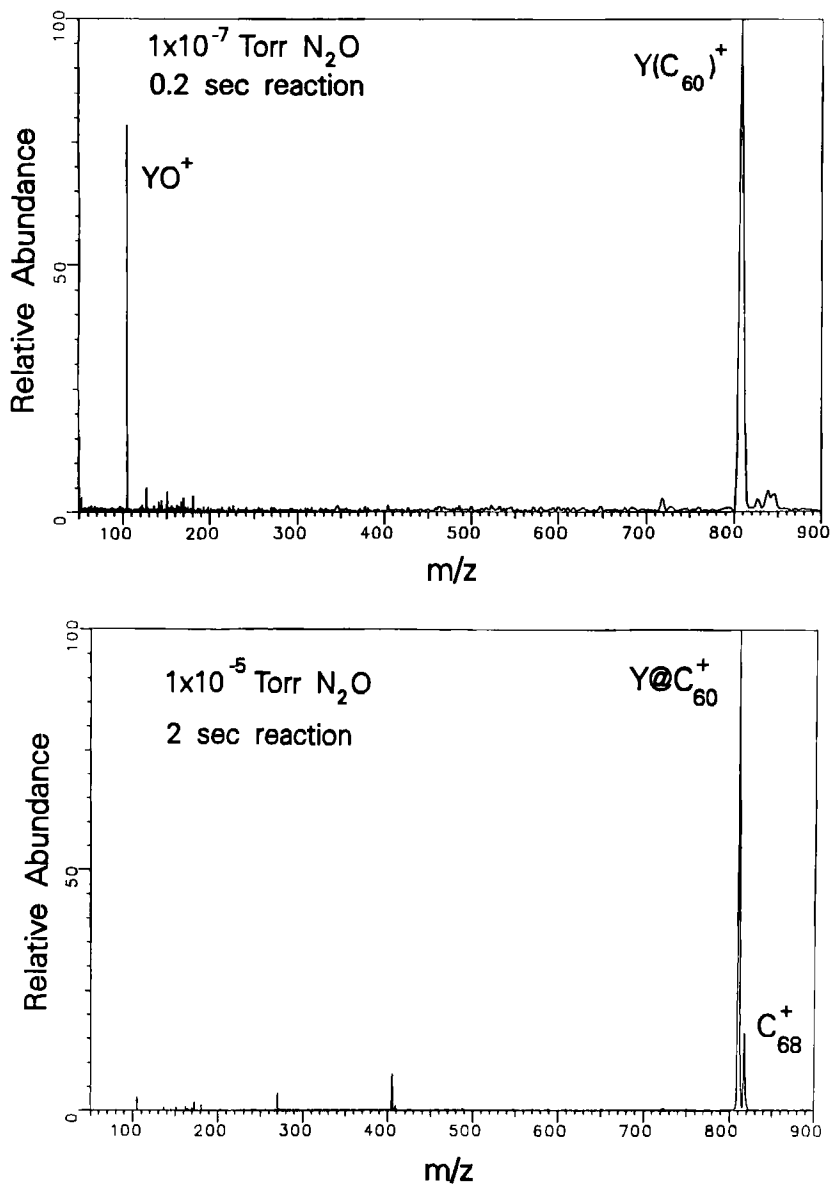


FIG. 5. The different behaviors of the endohedral and exohedral isomers of YC_{60} in the presence of N_2O . $Y(@C_{60})^+$ readily loses the metal (a), but $(Y@C_{60})^+$ does not (b). [Reproduced with permission from Ref. (64).]

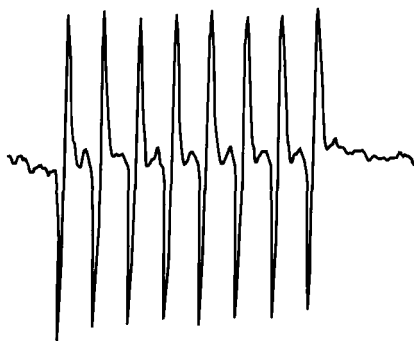


FIG. 6. The ESR spectrum of $(\text{La}@\text{C}_{82})$. [Reproduced with permission from Ref. (90).]

to ^{13}C coupling. It was argued that these data support the ionic formulation $(\text{La}^{3+}@\text{C}_{82}^{3-})$, with the unpaired electron density primarily residing in π -type cage orbitals (90). The spectra of $(\text{Y}@\text{C}_{82})$ (66,67) and $(\text{Sc}@\text{C}_{82})$ (68,69) lead to the same conclusion.

Detailed ESR analyses of the extracts produced from the arc burning of graphite/ Sc_2O_3 composite rods have been reported (68,69). In one case, the spectrum obtained was that of a mixture; in addition to the $(\text{Sc}@\text{C}_{82})$ signal, a 22-line pattern consistent with a computer simulation for $(\text{Sc}_3@\text{C}_{82})$ was observed (68). The three scandiums are spectroscopically equivalent; this might arise either from dynamic averaging or geometric equivalence. By analogy with previously published spectral data for Sc_3 (95), it was suggested that the metals form an equilateral triangle (69). Interestingly, the bimetallic complexes $(\text{Y}_2@\text{C}_{82})$ and $(\text{Sc}_2@\text{C}_{82})$ are ESR-silent (67–69).

C. Molecular Orbital Calculations

Several computational studies of endohedral fullerenes have been carried out. Many of them point in the same general direction: Species having low ionization energies tend to donate electron density to the cage, while those having higher ionization energies do not appear to engage in strong bonding interactions.

Cioslowski used *ab initio* methods to examine the interactions of framework carbons with intercalated atoms, monatomic ions, and small molecules such as H_2 , N_2 , HF , and LiF (62,96). Orbital mixing between the sequestered species and the cluster MOs was found to be negligible; the

interactions were primarily of the induced dipole type. It was predicted that polar molecules are stabilized (for HF, by as much as 14.9 kcal/mol), and nonpolar molecules destabilized, by sequestration. The HOMO and LUMO orbitals are those of the cluster.

Chang *et al.* considered the sequestration of a variety of species by C_{60} , using the Hartree–Fock *ab initio* method (97). Their results suggest a clear relationship between the degree of electron transfer and the ionization energy of the heteroatom; the formulation ($M^+@C_{60}^-$) is applicable for electropositive metals. For example, the calculated charges of the metals (by population analysis) were +1.10 for cesium, +0.99 for potassium, +0.79 for lanthanum, and +0.59 for calcium. Metals with high ionization potentials (Mn and U) and nonmetals (O and F) showed little interaction with the cage.

The electronic structures of lanthanum complexes are of interest because of the possible involvement of $6s$, $5d$, and/or $4f$ orbitals. It has been suggested (97) that the ground state of ($La@C_{60}$) results from the transfer of two electrons from $La(6s)$ to the cage LUMO (T_{1u}). This leaves lanthanum with one valence electron in the $5d$ orbital and assigns the metal a formal charge of $2+$. (As noted above, a charge of +0.79 was obtained from population analysis.) A somewhat different conclusion was reached when ($La@C_{60}$) was studied within the local density approximation (98,99). It was predicted from Mulliken analysis that the metal of ($La@C_{60}$) bears a charge of +2.85, which may be more in accord with the ESR data (90). The LDA calculations indicated that the metal causes destabilization of the HOMO, but does not affect the LUMO level. The calculated ionization energy was 6.9 eV, compared to a calculated IE_1 of 7.8 eV for C_{60} itself. [The experimental ionization energy of ($La@C_{60}$) is less than 6.4 eV (100).]

Endohedral complexes with exactly 82 framework carbon atoms appear to have special stability. This is in contrast to typical compound distributions of “normal” fullerene mixtures, for which the four most abundant species have 60, 70, 84, and 76 carbons, respectively (38). It has been suggested that a delocalized electron count of 84 might correspond to a stable shell closing (5). An 82-carbon cluster would then require two additional electrons, which might be supplied by an encapsulated metal. The existence of the series of compounds ($La_n@C_{84-2n}$) ($n = 0-2$) is then of significance if the lanthanums exist as La^{2+} ions (73).

A slightly different interpretation comes from the determination that the C_{80}^{6-} anion has a large HOMO–LUMO band gap, comparable to that of C_{60} (71,101). Two trivalent metals could supply the “extra” electrons needed for the $6-$ charge.

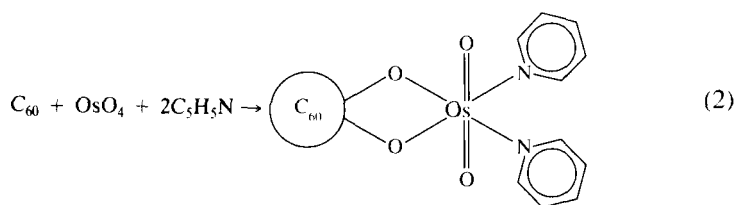
III

FULLERENES WITH METAL-CONTAINING EXTERNAL SUBSTITUENTS

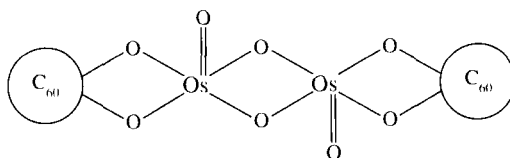
The activity of C_{60} as a ligand might reasonably involve either localized or delocalized π bonds (i.e., the bonding might mimic that of either C_2H_4 or C_6H_6). The evidence accumulated to date points to localized bonding. Consistent with the electron affinity data (see above), tetracyanoethylene has been suggested as a comparable case (102).

A. Osmate Esters

The first metal-containing fullerene derivative (and also the first fullerene to be structurally characterized) was reported by Hawkins and co-workers (35,60,103,104). They reacted C_{60} with osmium tetroxide in the presence of pyridine, utilizing the well-known tendency of OsO_4 to add across $C=C$ double bonds to produce osmate esters:



By varying the reacting ratios, considerable stoichiometric control is possible for this system; 1 : 1, 1 : 2, and 1 : 3 adducts have all been obtained, as well as a dimer:



As can be seen in Fig. 7, the X-ray structure of a substituted pyridine derivative, $(C_{60})OsO_4(4-t-BuC_5H_4N)_2$ demonstrated that the



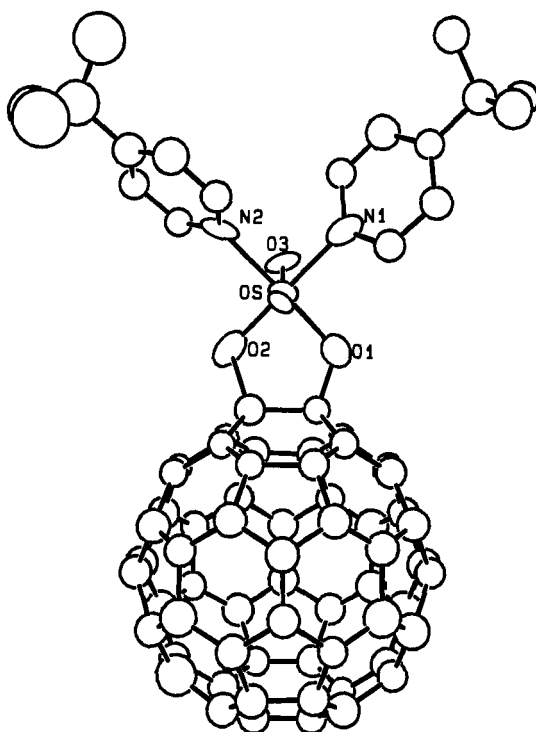


FIG. 7. The structure of $(C_{60})OsO_4(4-t-BuC_5H_5N)_2$. [Reproduced with permission from Ref. (105).]

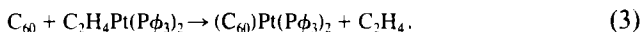
unit adds across a $C=C$ bond at the junction of two hexagons (35). (As the shorter of the two bond types, that site presumably has the greater concentration of π electrons—see Fig. 1.) The soccer-ball structure is distorted, with the two bound carbons pulled outward. This was effectively demonstrated by a histogram of distances from the calculated cluster center (105). The bonds of the two oxygen-linked carbons are elongated, to about 1.53 \AA ; this is compatible with sp^3 -hybridization at those centers.

It was predicted from bond localization energy calculations that addition across a 6,6-double bond should be a general reaction of fullerenes (106). This has been shown to be true for a variety of cases. Among nonmetal reactants, a well-known example is the interaction of C_{60} with molecular oxygen upon UV irradiation, producing the epoxide $C_{60}O$ (107). Similarly, the gas-phase reaction of C_{60}^{2+} with ammonia is thought to produce an aziridine (108), and a bis(bromophenyl) derivative has been isolated and structurally characterized (109). A host of other carbon-based adducts have been prepared as well (109,110).

Several isomers of the bis- complex $C_{60}[OsO_4(py)_2]_2$ were recently reported (111). Assuming that both additions are at 6,6-ring fusions, there are eight possible regioisomers. However, three involve substitution at proximate sites and so are not sterically viable. This leaves five, which is the number observed and separated by preparative scale HPLC. Two of the five were uniquely defined by NMR analysis of ^{13}C -enriched samples. Molecular polarity appears to increase as the bond angle between the osmyl groups decreases.

B. Platinum Complexes

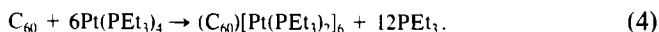
The first example of direct C_{60} ligation to an external metal was provided by Fagan *et al.* (112). The reaction involved displacement of coordinated ethylene by C_{60} in toluene, with the crystalline product obtained in 85% yield:



As was the case for the adducts described above, addition occurs at a 6–6 bond of the fullerene. Platinum(0) was an excellent choice in this regard because of its propensity for π backbonding.

The structure of $(C_{60})Pt(P\phi_3)_2$ is similar in many respects to those of other platinum–olefin complexes. For example, the metal–carbon distances (2.106 and 2.116 Å) are in accord with those in $C_2H_4Pt(P\phi_3)_2$ and $(TCNE)Pt(P\phi_3)_2$ (113,114). The bond angles are also similar and provide information about backbonding (115).

A remarkable, multiple platinum adduct has also been described (116). The reaction of excess $Pt(PEt_3)_4$ with C_{60} gives a hexaplatinum derivative:



The orange, air-sensitive product consists of a single isomer, as evidenced by its NMR spectra (singlet in the ^{31}P spectrum; three resonances in 2 : 2 : 1 intensity ratios for ^{13}C). The X-ray analysis (Fig. 8) showed six η^2 interactions. The metals form an octahedral array, and the point group (ignoring the ethyl substituents) is T_h . The limiting stoichiometry of 6 : 1 is rationalized in the following manner: Each $Pt(PEt_3)_2$ group binds directly across one 6,6-junction and sterically blocks four others. Hence, 6 appropriately positioned metal units either react at or protect all 30 such sites (116). Similar reactions are observed for the nickel and palladium analogs (102).

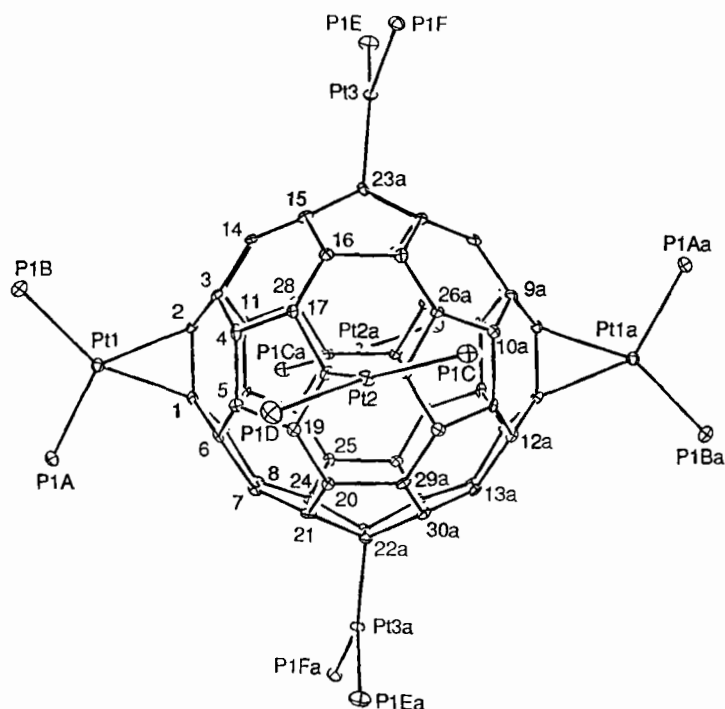


FIG. 8. The structure of the hexametal adduct $(C_{60})[Pt(PEt_3)_6]$. The ethyl groups are not shown. [Reproduced with permission from Ref. (116).]

C. Iridium Complexes

A number of iridium–fullerene complexes have been reported, most of which are derived from Vaska's compound, $Ir(CO)Cl(P\phi_3)_2$. An early example was the adduct $(C_{60})Ir(CO)Cl(P\phi_3)_2$ (117), obtained in 45% yield from the reaction



The structure of this adduct has been crystallographically determined, as has that of a derivative containing a less symmetric phosphine ligand (118). In these species, the local environment about the metal is quite similar to that in smaller adducts such as $(C_2H_4)Ir(CO)Cl(P\phi_3)_2$. As was observed for the osmate ester, the two bound carbons are pulled away from the rest of the cluster, and the bond between them lengthened (to 1.53 Å). The Ir–C distances are about 2.19 Å. The geometry about the metal is approximately octahedral, but with the C–Ir–C angle compressed (to 41°) and the P–Ir–P angle widened (to 113°) from the 90° ideal.

TABLE I
CARBONYL STRETCHING FREQUENCIES FOR
VASKA'S COMPOUND AND SELECTED ADDUCTS^a

Compound	$\nu_{\text{CO}}(\text{cm}^{-1})$
$\text{Ir}(\text{CO})(\text{P}\phi_3)_2\text{Cl}$	1965
$(\text{O}_2)\text{Ir}(\text{CO})(\text{P}\phi_3)_2\text{Cl}$	2005
$(\text{TCNE})\text{Ir}(\text{CO})(\text{P}\phi_3)_2\text{Cl}$	2057
$(\text{C}_2\text{F}_4)\text{Ir}(\text{CO})(\text{P}\phi_3)_2\text{Cl}$	2052
$(\text{C}_{60})\text{Ir}(\text{CO})(\text{P}\phi_3)_2\text{Cl}$	2014
$(\text{C}_{60})[\text{Ir}(\text{CO})(\text{P}\phi_3)_2\text{Cl}]_2$	2001
$(\text{C}_{70})\text{Ir}(\text{CO})(\text{P}\phi_3)_2\text{Cl}$	2002

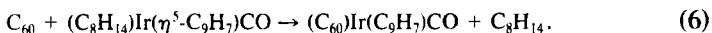
^a Sources: Data taken from Refs. (117) and (119–121).

The vibrational frequency of the carbonyl group is of interest in such adducts; in general, π -acceptor ligands cause ν_{CO} to shift to higher energy upon complexation to Vaska's compound (119). The carbonyl band is found at 1965 cm^{-1} in $\text{Ir}(\text{CO})\text{Cl}(\text{P}\phi_3)_2$ itself; values for several adducts are given in Table I. The measured frequency for $(\text{C}_{60})\text{Ir}(\text{CO})\text{Cl}(\text{P}\phi_3)_2$ is 2014 cm^{-1} , very close to that for $(\text{O}_2)\text{Ir}(\text{CO})\text{Cl}(\text{P}\phi_3)_2$. This correlates with the observation that, as for the dioxygen complex, the process described by Eq. (5) is readily reversed (117).

Balch and co-workers have designed systems in which the phosphine ligand of Vaska's complex is modified by an organic aromatic moiety. The resulting species can act as an effective host for fullerenes (i.e., a "molecular egg crate"). An example is the ligand $\text{C}_6\text{H}_5\text{CH}_2\text{OC}_6\text{H}_4\text{CH}_2\text{P}\phi_2$ (bobP ϕ_2) (118). The interaction of $\text{Ir}(\text{CO})\text{Cl}(\text{bobP}\phi_2)_2$ with C_{60} produced a crystalline aggregate which the two arms of each phosphine ligand reach out to cradle a fullerene unit of an adjacent molecule (see Fig. 9).

Several other fullerene-iridium complexes have been reported, including the double adduct $(\text{C}_{60})\{\text{Ir}(\text{CO})\text{Cl}(\text{PMe}_2\phi)_2\}_2$, which crystallizes into two conformational isomers (120). The adduct of Vaska's compound with C_{70} is also known. The structure of $(\text{C}_{70})\text{Ir}(\text{CO})\text{Cl}(\text{P}\phi_3)_2$ has the same characteristics (including η^2 coordination across a 6,6-ring bond) as that of its smaller relative (121). A solvated double adduct, $(\text{C}_{70})\{\text{Ir}(\text{CO})\text{Cl}(\text{P}\phi\text{Me}_2)_2\}_2 \cdot 3\text{C}_6\text{H}_6$, was synthesized in 60% yield. X-ray diffraction showed that the metals coordinate on opposite sides of the molecule (twofold symmetry) (122).

Shapley and co-workers obtained the indenyl derivative $(\text{C}_{60})\text{Ir}(\text{CO})\text{C}_9\text{H}_7$ (123):



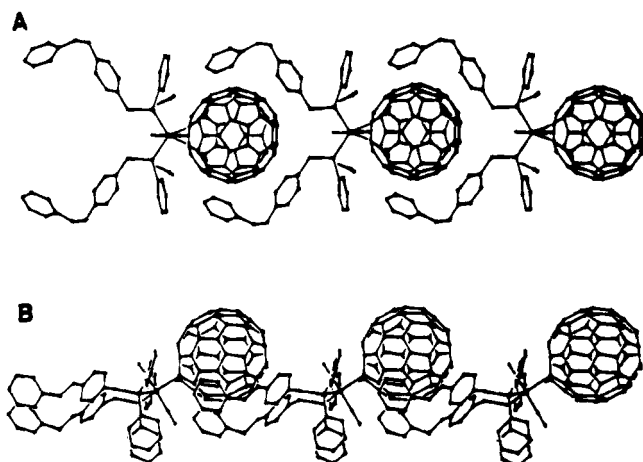


FIG. 9. The structure of $(C_{60})Ir(CO)Cl(bobP\phi_2)_2$. [Reproduced with permission from Ref. (118).]

The product was identified by its 1H NMR and IR spectra. It exhibits a carbonyl stretch at 1998 cm^{-1} , compared to 1954 cm^{-1} for the precursor. This is again consistent with metal-to-ligand backbonding into π^* cluster orbitals, since ν_{CO} is known to be a reflection of the electron density at the metal center for such complexes (123).

D. Ruthenium Complexes

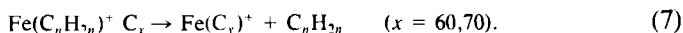
Reactions of fullerenes with ruthenium substrates are limited at present to a few examples. The mixing of C_{60} with a molar excess of the salt $[Cp^*Ru(CH_3CN)_3]^+[O_3SCF_3]^-$ produced a red-brown solid; the proposed formulation is $[(C_{60})\{Cp^*Ru(CH_3CN)_2\}_3]^{3+}[O_3SCF_3]_3^-$ (102,112). The fact that only one acetonitrile ligand was lost per reactant cation contrasts with results for electron-rich systems (102,124) and is again indicative of the π -accepting behavior of C_{60} . Shapley and Koefod have also described a ruthenium- C_{60} complex (125).

E. "Naked Metal" Complexes

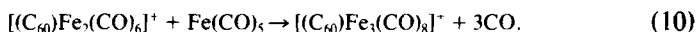
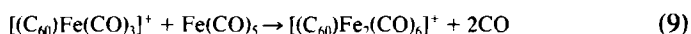
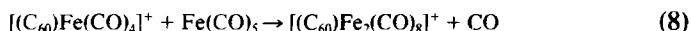
A large number of derivatives of C_{60} in which one or more framework carbons have single atoms or small groups as external substituents are now known. To date, this has primarily been the domain of organic chemists (109,110), but several exohedral metal complexes have been reported as well.

Freiser and co-workers used Fourier transform mass spectrometry to generate a variety of such complexes (87–89,126). Their general approach involves the formation of M^+ ions from pure metal targets by laser desorption, followed by interaction with C_{60} in the vapor state. The “naked metal” complexes $M(C_{60})$ ($M = Co, Ni, Cu, Rh, La$, and VO) were obtained in this manner. The fragmentation behavior of those species is characterized by the facile loss of metal (see Scheme 1) (87,88). Evidence for the nickelocenium-like cation $[Ni(C_{60})_2]^+$ (the first fullerene “sandwich” species) has also been obtained (126).

For the case of iron, an indirect approach was necessary. Fe^+ was generated by laser desorption and reacted with pentane at 1×10^{-6} Torr, producing $Fe(C_nH_{2n})^+$ ions ($n = 2-5$). Those cations then underwent a displacement reaction with C_{60} and C_{70} (88) (see Fig. 10):



$Fe(CO)_5$ has also been used as a source of iron (72,89). Freiser observed the displacement of a carbonyl group by C_{60} and concluded that the Fe^+-C_{60} dissociation energy is about 36.6 kcal/mol (88,89). The formation of higher carbonyl clusters occurred through a series of secondary interactions, for example,



The EXAFS and Mossbauer behavior of $Fe(C_{60})$ and its endohedral isomer were described above (72). EXAFS has also been used as a structural probe for $Y(C_{82})$ (61). It was determined that the metal has six to eight nearest-neighbor carbons at a distance of 2.35 Å. Metal–metal interactions were also observed, at 4.05 ± 0.05 Å. This is strong evidence that the complex is exohedral. Dimers such as $C_{82}Y-X-Y-C_{82}$ (where X is a bridging carbon or oxygen atom) were suggested.

IV

INTERSTITIAL SUBSTITUTION AND SALT FORMATION

Recall that the standard-state lattice of C_{60} is of the face-centered cubic type and therefore contains both octahedral and tetrahedral interstices. Various chemical agents have been incorporated into these interstices. Among other effects, such doping has a profound influence on the electrical

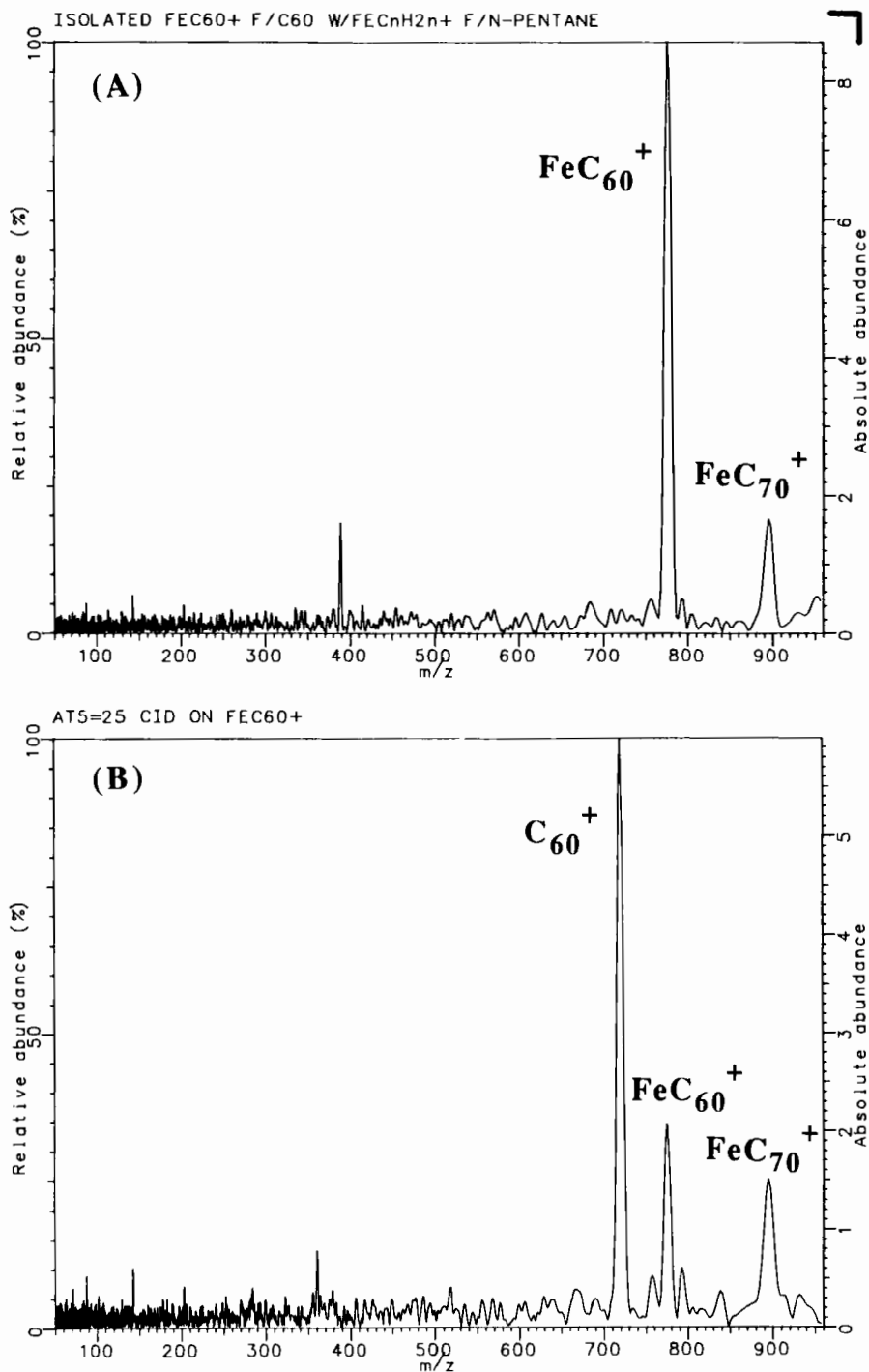


FIG. 10. Fourier transform mass spectra of two "naked metal" clusters. (A) Isolated FeC_{60}^+ and FeC_{70}^+ ; (B) collision-induced dissociation of FeC_{60}^+ at 76 eV, showing facile loss of the metal. [Reproduced with permission from Ref. (88).]

properties of bulk samples. Recall that the band gap between the HOMO and the triply degenerate LUMO is about 1.7 eV (18,19). Hence, at room temperature pure C_{60} acts as an electrical insulator.

A. Intercalation of Alkali Metals

The tetrahedral and octahedral interstices (two and one per formula unit, respectively) are of sufficient size to accommodate a variety of species. For example, numerous structural studies in which the C_{60} lattice acts as a host for solvent molecules such as cyclohexane (127,128), pentane (129), and other molecular species (130) have been reported.

Also important in this regard is the fact that the LUMO level of C_{60} is triply degenerate (T_{1u} symmetry). Electron-donating atoms such as alkali metals are small enough to easily fit into the lattice interstices and lead to the population of those orbitals. It was recognized early on that this has enormous potential in materials science. Fullerenes have π orbitals radiating in all directions, making them excellent candidates for three-dimensional electronic conductors (131).

It is now realized that the interaction of C_{60} with active, monovalent metal atoms typically produces compounds having the stoichiometry M_3C_{60} [i.e., $M_3^+(C_{60}^{3-})$], with the metals occupying all of the tetrahedral and octahedral holes. Photoelectron studies verify that the cage LUMO is then half-filled (132,133). Also accessible (via a change in the lattice type) is the M_6C_{60} stoichiometry, in which the T_{1u} level is completely filled. There is also evidence for a stable $M_4(C_{60})$ phase, with a body-centered tetragonal lattice (134–136).

1. Synthesis

Several synthetic pathways have been established for the incorporation of electropositive metals into fullerene lattices. One method involves the passage of a metal vapor stream over solid C_{60} (137,138). The interaction with potassium is described by the equation



Some other successful synthetic approaches are as follows:

- (1) A mixture of $K_{(s)}$ (in 90-fold excess) with C_{60} was refluxed in toluene under an inert atmosphere, resulting in the precipitation of $K_3(C_{60})$ (139).
- (2) $M_6(C_{60})$ compounds are readily prepared using excess metal reagent at high temperatures. The 3 : 1 salt can then be obtained by a comproportionation reaction at 400–450°C [Eq. (12)] (140):



- (3) Prewighed, stoichiometric amounts of metal and C_{60} were reacted in sealed tubes under helium (141).
- (4) Solid-state electrochemistry was used to study several Li/C_{60} stoichiometries. The process involved the incorporation of lithium atoms from a $Li_{(s)}$ electrode at $80^\circ C$ (142).
- (5) Doping by direct ion implantation, using a silicon or quartz substrate, has been reported (143).

2. Structural Studies

Single-crystal X-ray diffraction and other techniques have established that, as expected, the metals in $K_3(C_{60})$ occupy all the available interstices in the face-centered cubic lattice (see Fig. 11) (141, 144). $K_3(C_{60})$ represents

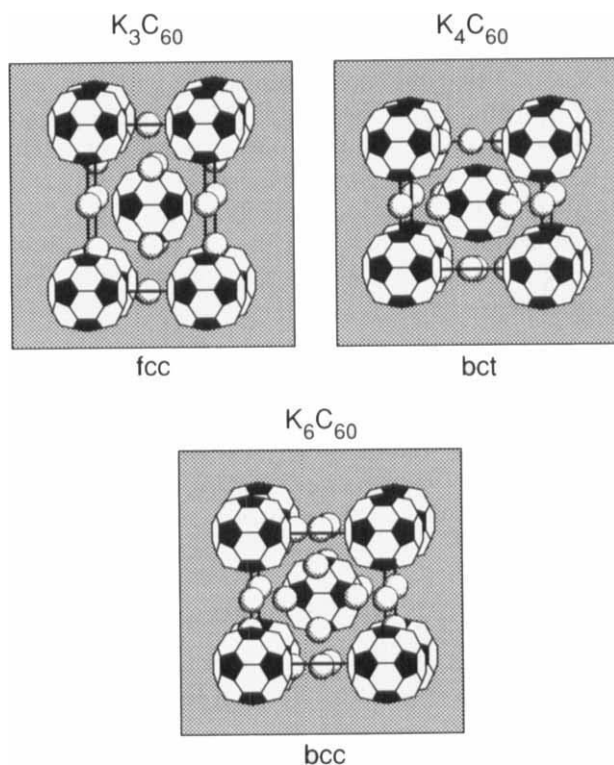


FIG. 11. The solid-state structures of the potassium-doped fullerides $K_n(C_{60})$, $n = 3, 4$, and 6. [Reproduced with permission from Ref. (6).]

a favored stoichiometry, as demonstrated by the fact that samples having the formal composition $K_{1.5}C_{60}$ undergo phase separation to $C_{60} + K_3(C_{60})$ (145).

The high-temperature reaction of C_{60} with excess potassium or cesium produces the $M_6(C_{60})$ salt (6,146,147). In those compounds, the fulleride ions form a body-centered cubic array, with four metals forming a "cross" on each of the six faces (see Fig. 11). This amounts to surrounding each cluster anion with a cage of 24 metal cations (146).

It is possible to follow alkali metal doping by Raman spectroscopy (137,148). It was found that the 1458 cm^{-1} band of C_{60} moves to 1446 cm^{-1} for the tripotassium and 1429 cm^{-1} for the hexapotassium salts. The vibrational frequencies for the $(C_{60})^{6-}$ anion have been calculated (149).

3. Electrical Conductivity

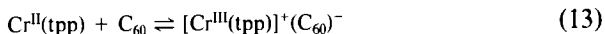
As alkali metals begin to fill the *fcc* lattice interstices, metal-to-cluster charge transfer occurs. Electrons enter the π -antibonding orbitals and the electrical conductivity increases, reaching a maximum at the M_3C_{60} stoichiometry. At room temperature the conductivity is still rather low [about $2 \times 10^2\ \Omega \cdot \text{cm}$ for $K_3(C_{60})$ (138), compared to $7 \times 10^2\ \Omega \cdot \text{cm}$ for graphite and 10^4 – $10^5\ \Omega \cdot \text{cm}$ for metals such as lead and cesium]. However, the conductivity improves dramatically at low temperatures, and $K_3(C_{60})$ becomes superconducting below 18 K (138). $Rb_3(C_{60})$ has a critical temperature of 30 K (138,139,141,150), while $Cs_2Rb(C_{60})$ gives $T_c = 33\text{ K}$ (151). A superconducting transition temperature of 45 K was reported for C_{60} co-doped with rubidium and thallium (152).

If the stoichiometry is increased beyond 3 : 1, the conductivity is reduced. The M_6C_{60} stoichiometry produces an insulator (137,140,146). Details of the electronic structure of crystalline $K_6(C_{60})$ have been calculated (153).

B. Other Salts

The alkali metal-doped fullerenes make the connection between interstitial doping and salt formation quite clear. Related species have been produced by mixing C_{60} with various electron donors. An early example involved the use of bulk electrolysis to obtain a double salt of the C_{60}^- radical anion, $(Ph_4P^+)_2(C_{60}^-(Cl^-))$. The product precipitated as microcrystals at a platinum electrode (93). Later, spectroscopic evidence for a chromium(III) salt, $[Cr(tpp)]^+(C_{60})^-$ (tpp is the dianion of tetraphenylporphyrin) was obtained (91). In solution, the ESR and electrical conductivity data

were consistent with the ionic formulation. The equilibrium



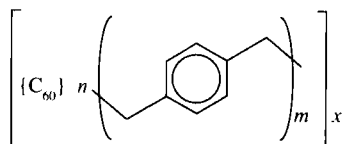
was found to be solvent dependent. The product was favored in THF, while addition of toluene caused the equilibrium to shift to the left. The data suggest that C_{60}^- is a very weakly coordinating anionic ligand (91).

V

SUBSTITUTION FOR FRAMEWORK CARBON

There is considerable interest at present in the synthesis, structures, and properties of fullerene-based systems in which heteroatoms are part of the cluster framework. For a variety of reasons, such hybrid clusters are expected to be at least as interesting as the pure fullerenes themselves. Framework substitution would permit the controlled alteration of the electronic properties of the molecule. For example, doping with an electron-rich atom such as nitrogen should reduce the electron affinity, producing a better nucleophile but a poorer electrophile; replacement of carbon by boron or some other metalloid should have the opposite effect. This is of major interest not only to synthetic chemists, but in materials science as well; C_{60} is readily made semiconducting, and the potential control of solid-state electrical conductivity leads to a wealth of intriguing possibilities (76,154).

Another impetus for studying hybrid clusters concerns their incorporation into polymers. Some success has been achieved for C_{60} itself. An example is the C_{60} -*p*-xylylene copolymer reported by Loy and Assink (155). The xylylene monomer was prepared by thermolysis of paracyclophane and then reacted with C_{60} , producing a brown precipitate.



The structure given above is supported by ^{13}C NMR data. TGA shows that the polymer is cross-linked. Unfortunately, the material is air sensitive.

Polymer formation should be facilitated for framework-doped fullerenes. For example, a *trans* disubstituted cluster such as $(\text{C}_{58}\text{Si}_2)$ could readily be functionalized at the two silicon centers and the functionalized ends then joined together to produce a linear polymer.

There is good reason to believe that it will be experimentally simpler to derivatize hybrid clusters than to derivatize the all-carbon fullerenes. The high electron affinity of C_{60} makes it readily ionized; this appears to complicate both the chemical separation and analysis of its reaction products. An example is the failure (to date) of attempts to isolate $(La@C_{60})$ and other endohedral complexes. Because of their molecular polarity, species such as $(M@C_{59}B)$ might be more amenable to separation by chromatography (5).

A related experimental problem derives from the size and symmetry of C_{60} , which combine to create many sites of identical reactivity. There are two possible isomers for a singly substituted adduct such as $C_{60}O$ or $(C_{60})OsO_4(py)_2$ (resulting from addition at 5,6- or 6,6- ring junctions). For a doubly substituted complex like $(C_{60})[Pt(PEt_3)_2]_2$, there are eight geometric isomers even when consideration is limited to 6,6- ring junctions. The possibilities increase geometrically for higher levels of substitution. As a result, synthetic chemists must be extremely careful about their combining stoichiometries. Even for very simple stoichiometries, the differentiation and separation of isomers can become a formidable problem. Framework heteroclusters provide a possible solution. Compare, for example, the expected reactivity of a hybrid fullerene such as $(C_{58}B_2)$ to that of C_{60} . Based on both chemical intuition and computational studies (see below), it should be possible to limit attack by some nucleophile to the boron centers; this would obviously limit the possibilities for isomerism and therefore simplify the separation and isolation of the product(s).

A. Synthesis of Heteroclusters

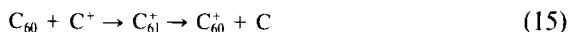
Starting with a homoatomic fullerene, one can visualize two routes to framework-modified derivatives: by the addition of one or more heteroatoms (i.e., cluster expansion) or by substitution of a heteroatom for carbon. The first experimental evidence for the latter was provided by Smalley's group (156). The laser vaporization of a graphite rod that had been impregnated with boron nitride produced mass spectral evidence for clusters formulated as $C_{60-n}B_n$, where n ranges from at least 1 to 6; the strongest ion signal corresponded to $C_{59}B^+$. Seventy-atom hybrid clusters were also observed. In contrast to endohedral complexes, these clusters show relatively high reactivity at the heteroatom site. For example, the boron atoms can be titrated with ammonia to give $C_{60-n}B_n(NH_3)_n$. For $(C_{58}B_2)$ the titration data suggest that the borons are nonadjacent. Photofragmentation again produces ions formed by the loss of two-carbon units. For $(C_{59}B)$, this stepwise process terminates at $C_{31}B^+$. $(C_{58}B_2)$ behaves similarly, but preferentially loses boron after the cluster has shrunk to below 40 atoms.

Although such boron-carbon clusters have not yet been obtained in macroscopic amounts, there is evidence that conversion to endohedral derivatives such as (K@C₅₉B) may facilitate their isolation (5).

Since boron nitride was used as the heteroatom source, it might be expected that nitrogen-containing clusters would also be formed. However, this was not the case (156). It was suggested that clusters such as (C₅₉N) might interact with free nitrogen in the system to produce N₂ (4). However, the synthesis of nitrogen-doped heteroclusters from the contact-arc vaporization of graphite under N₂ or NH₃ atmospheres has been claimed (157). Mass and photoelectron spectroscopic data for C₆₉N, C₆₉N₂, C₇₀N₂, C₅₉N₆, and C_{60-n}N_n (*n* = 1-4) were presented. More recently, the reaction of N⁺ with C₆₀ gave evidence for the C₅₉N⁺ cation, which rapidly eliminates CN (158):



Basic cluster expansion chemistry is beginning to appear. Isotopic labeling studies of the gas-phase sequence



gave evidence that the added carbon joins the framework, rather than being bonded externally (159).

The framework expansion of C₆₀ by the addition of organic moieties was suggested by Wudl's group (160). They used diphenyldiazomethane to produce a series of compounds conforming to the formula C_{60+n}(C₆H₅)_{2n} (*n* = 1-6). Reaction times increased with increasing *n* (about 1 hr for the first addition and 8-10 days for complete substitution to C₆₆Ph₁₂). The regiochemistry is thought to parallel that observed for the platinum derivatives (116); the second addition occurs *para* to the first, and the hexasubstituted product has octahedral symmetry. They reported calculations that suggest that the cluster expansion products are about 30 kcal/mol more stable than isomers that retain the 60-atom cage structure, with Ph₂C groups as substituents (160).

B. Computational Studies

When one considers the formal replacement of one or more framework carbon atoms of C₆₀ with heteroatoms, three questions quickly come to mind:

- (1) What heteroatoms are likely to produce stable clusters?
- (2) What heteroatoms are likely to produce the most interesting and chemically useful molecules?

(3) How will the presence of heteroatoms affect the physical and chemical properties of 60-atom clusters?

Given these considerations, it is not surprising that researchers have focused primarily on carbon's three neighbors in the periodic table—boron, nitrogen, and silicon. Early computational results suggest that, for each of these, substitution appears to be synthetically feasible and should result in stable products.

The Car–Parrinello method (a variation of the LDA approach) was used to investigate the replacement of carbon by boron and nitrogen to give ($C_{59}X$) (161). This type of substitution reduces the icosahedral symmetry all the way to the C_s point group, removing all orbital degeneracies. The dipole moment of ($C_{59}B$) was calculated to be about 1.4 D, oriented *inward* toward the center of the cage; the molecular dipole of $C_{59}N$ was larger (~ 2.2 D) and directed outward. Semiconducting behavior was predicted; the calculated band gaps were about 1.2 eV for ($C_{59}B$) and 0.4 eV for ($C_{59}N$).

Another possibility is the replacement of two-carbon units by isoelectronic B–N fragments. A host of comparisons can be drawn for simpler systems: aminoboranes ($R_2NBR'_2$) have long been compared to alkenes (162); two polymorphs of boron nitride are isostructural with diamond and graphite (163); borazine is a structural and, in many ways, a chemical analog of benzene (164); etc. Hence, compounds having the general formula ($C_{60-2n}B_nN_n$) were of interest to us. Hückel (165) and MNDO (166) computations were carried out on ($C_{58}BN$) (three isomers), ($C_{12}B_{24}N_{24}$), and ($B_{30}N_{30}$) (three isomers). In every case the total cohesive energy was found to be greater than that for C_{60} itself. For the ($C_{58}BN$) system, the most stable isomer we examined features a B–N bond joining two hexagons, while the least stable case has separated boron and nitrogen atoms. Not surprisingly, it was found that there is a general tendency for σ electron density to be transferred toward nitrogen (reflecting its high electronegativity), and for π electrons to move toward boron (because of its formally electron-deficient character). The calculated atomic charges are about +0.05 for boron and –0.14 for nitrogen (165).

The ($B_{30}N_{30}$) formulation would necessarily require a total of at least 12 B–B + N–N bonds. (This is a result of the 12 five-membered rings included in the cluster framework.) Smalley suggested that the weakness of those bond types relative to $C\cdots C$ would destabilize the molecule (156). However, our computational results suggest that this effect is compensated for by the strong B–N interactions. ($C_{12}B_{24}N_{24}$) is of special interest in this regard, since a structure that avoids B–B and N–N linkages can be drawn. That isomer (pictured in Fig. 12) has S_6 symmetry. There

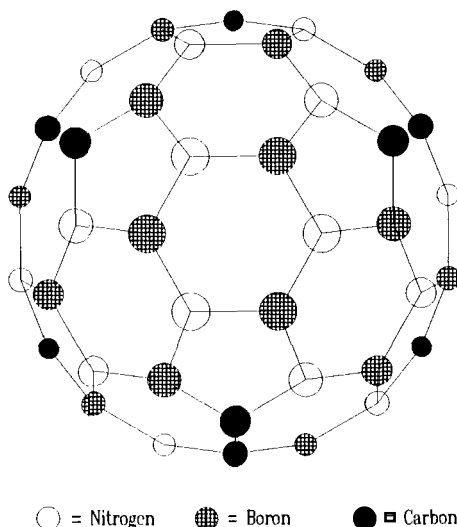


FIG. 12. The calculated structure of "CBN-ball" ($C_{12}B_{24}N_{24}$); only the top two-thirds of the molecule is shown. [Reproduced with permission from Ref. (165).]

are six pairs of CB_2N_2 pentagons, with each pair connected by a carbon-carbon bond. The 20 hexagons subdivide into 12 $C_2B_2N_2$ and 8 B_3N_3 units, with every ring being isoelectronic with its all-carbon counterpart. There are two chemically different kinds of carbons—six nearer the equator and six nearer the pole. There are 6 C-C, 12 B-C, 12 C-N, and 60 B-N nearest-neighbor interactions (165,166).

Systems in which framework carbons are replaced by silicon have also been studied (167,168). The large size and low electronegativity of silicon relative to carbon have predictable effects. In general, compounds belonging to the series $(C_{60-n}Si_n)$ show decreased stability (as measured by total cohesive energies) with increasing n . There is obvious structural distortion, with the silicon atoms protruding from the surface (see Fig. 13). The calculated bond lengths are about 1.74 Å for the Si-C bonds, intermediate between normal single and double bond distances (about 1.88 and 1.69 Å, respectively), and in close agreement with a previously published calculation for silabenzene (SiC_5H_6) (169). For the *ortho* isomer of $(C_{58}Si_2)$, the silicon-silicon bond is calculated to be 2.25 Å, which is again intermediate between typical single and double bond distances (170,171).

The silicons acquire a partial positive charge in all cases; carbons adjacent to silicon are negative, while β carbons are slightly positive—an

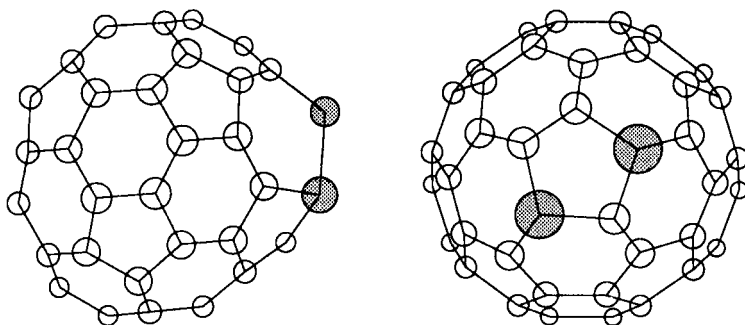
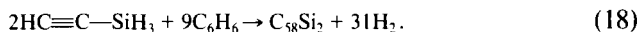
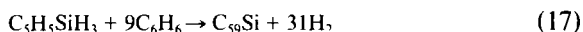


FIG. 13. The calculated structures of *ortho*- and *meta*-isomers of ($C_{58}Si_2$). [Reproduced with permission from Ref. (168).]

effect that is well known in organosilicon chemistry (172). A consequence of this bond polarity, of course, is the generation of molecular dipoles. The calculated dipole moments for *ortho*- and *meta*- (i.e., separated by one carbon) isomers of ($C_{58}Si_2$) are 1.1 and 1.7 D, respectively. The geometric distortions and dipole moments convey the image of “bucky balls with handles”; that is, readily accessed sites of high reactivity (toward nucleophiles at the silicon centers and toward electrophiles at the adjacent carbons). This suggests that such molecules, if and when they are synthesized, will be derivatized readily. The *trans*-isomer (silicons on opposite sides of the cluster) has a dipole moment of zero, and this should facilitate its chromatographic separation from the others.

The synthesis of such hybrid clusters is, of course, a significant problem. One possible option mimics the approach of McKinnon, who showed that macroscopic amounts of C_{60} are produced by the controlled combustion of benzene [idealized Eq. (16)] (45,46). This suggests that the similar treatment of C_6H_6 mixed with small amounts of appropriate silicon-containing compounds might produce silaballs. Two possible examples are silacyclopentadiene and silaacetylene:



The calculated reaction enthalpies (using the MNDO-based methodology) for all of these equations fall into the range of +731 to +753 kcal/mol, with the all-carbon reaction being the most endothermic of the three (167).

VI

CONCLUSIONS

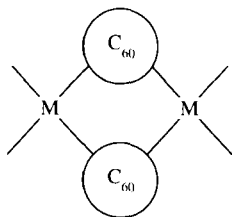
Where do we go from here? Seemingly in all directions at once, based on the burgeoning literature entries. There would appear to be several areas of particular interest to inorganic and organometallic chemists.

A great deal remains to be learned about the behavior of large clusters as ligands. It is already clear that C_{60} and C_{70} are potent π acceptors. What about electron donation? Given that the HOMO levels of these clusters are about 1.5 eV less stable than for benzene, it seems reasonable that analogs of species such as $Cr(C_6H_6)_2$ and $Cr(C_6H_6)(CO)_3$ should be preparable. (It is true that the six-membered rings of fullerenes are nonplanar, but it is also known that geometric distortions occur upon coordination—see Section III.) A related question is whether metal–fullerene interactions are necessarily dihapto. How might species having η^4 or η^6 linkages be synthesized?

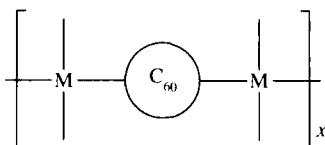
An approach that has not yet been exploited involves the prereduction of a fullerene to its di- or trivalent anion, followed by reaction with a metal [e.g., Eq. (19)]:



The nickelocenium-like cation $[Ni(C_{60})_2]^+$ (126) is an early example of a potentially important group of chemical species—those having two large clusters bound to the same metal center. The chemical and electronic properties of triple-decker complexes analogous to the $[Ni_2(C_5H_5)_3]^+$ cation (173), of bridged binuclear complexes such as



and of linear polymers of the type



would also be of great interest.

Many fascinating and useful fullerene-based studies that lie at the interface of organometallic chemistry and materials science (nanotechnology) can be suggested. For example, studies of the growth of "buckytubes" on electrode tips may have major ramifications (174,175), especially if heteroatoms can be incorporated into the lattice structure (154). Efforts to design new, fullerene-based semi- and superconductors will surely continue. In this regard, technology related to so-called "quantum dots" and "molecular switches" is expected to be important.

Quantum dots are, in essence, zero-dimensional impurities in an otherwise pristine lattice. They show their most useful electronic properties when the dots are less than 10 Å across (176), which makes C₆₀ and its derivatives (~7 Å in diameter) plausible candidates, especially in view of their facile, reversible reduction to anions.

A common approach to nanoscale charge transport (molecular switches) involves conducting polymers. The incorporation of fullerenes into such polymers is being studied both experimentally (177,178) and computationally (179). For example, evidence for photoinduced electron transfer from the excited state of a π -conjugated polymer to the C₆₀ molecule has been obtained (178). It has been argued that charge separation of this type might provide a basis for molecular information storage units (180).

ACKNOWLEDGMENTS

I am grateful to three colleagues in my department—Daniel Jelski, Philip Kumler, and Thomas Janik—for fruitful collaboration, stimulating discussions, and technical help. Financial support from TA instruments, Inc., the SUNY Research Foundation, and the Scholarly Incentive Program of the SUNY College at Fredonia is noted with appreciation.

REFERENCES

- (1) Kroto, H. W.; Heath, J. R.; O'Brien, S. C.; Curl, R. F.; Smalley, R. E. *Nature (London)* **1985**, *318*, 162.
- (2) Three suggested sources are: (a) the March 1992 issue of *Accounts of Chemical Research* (Volume 25, Number 3, containing eleven useful reviews). (b) Hammond, G. S.; Kuck, V. J., Eds. "Fullerenes—Synthesis, Properties, and Chemistry of Large Carbon Clusters," ACS Symp. Ser. 481; American Chemical Society: Washington, DC, 1992. (c) Billups, W. E.; Ciufolini, M. A., Eds. "Buckminsterfullerenes"; VCH Publishers: New York, 1993.
- (3) Comprehensive bibliographical information on fullerenes is available via electronic mail. Richard Smalley of Rice University has produced several editions of "The Almost (but never quite) Complete Buckminsterfullerene Bibliography," a daunting compilation which contained over a thousand entries as of November 1992. The task has now been taken over by Frank Tinker of the Arizona Fullerene Consortium. Requests can be made electronically: email=tinker@physics.arizona.edu.

- (4) Smalley, R. E. In "Fullerenes—Synthesis, Properties, and Chemistry of Large Carbon Clusters", ACS Symp. Ser. 481; Hammond, G. S.; Kuck, V. J., Eds.; American Chemical Society: Washington, DC, 1992; Chapter 10.
- (5) Chai, Y.; Guo, T.; Jin, C.; Haufler, R. E.; Chibante, L. P. F.; Fure, J.; Wang, L.; Alford, J. M.; Smalley, R. E. *J. Phys. Chem.* **1991**, *95*, 7564.
- (6) Haddon, R. C. *Acc. Chem. Res.* **1992**, *25*, 127.
- (7) Hedberg, K.; Hedberg, L.; Bethune, D. S.; Brown, C. A.; Dorn, H. C.; Johnson, R. D.; de Vries, M. *Science* **1991**, *254*, 410.
- (8) Liu, S.; Lu, Y.; Kappes, M. M.; Ibers, J. A. *Science* **1991**, *254*, 408.
- (9) David, W. I. F.; Ibberson, R. M.; Matthewman, J. C.; Prassides, K.; Dennis, T. J. S.; Hare, J. P.; Kroto, H. W.; Taylor, R.; Walton, D. R. M. *Nature (London)* **1991**, *353*, 147.
- (10) Heiney, P. A.; Fischer, J. E.; McGhie, A. R.; Romanow, W. J.; Denenstein, A. M.; McCauley, J. P.; Smith, A. B.; Cox, D. E. *Phys. Rev. Lett.* **1991**, *66*, 2911.
- (11) Fischer, J. E.; Heiney, P. A.; Smith, A. B. *Acc. Chem. Res.* **1991**, *25*, 112.
- (12) Fischer, J. E.; Heiney, P. A.; McGhie, A. R.; Romanow, W. J.; Denenstein, A. M.; McCauley, J. P.; Smith, A. B. *Science* **1991**, *252*, 1288.
- (13) Tycko, R.; Dabbagh, G.; Fleming, R. M.; Haddon, R. C.; Makhija, A. V.; Zahurak, S. M. *Phys. Rev. Lett.* **1991**, *67*, 1886.
- (14) Beckhaus, H. D.; Rüchardt, C.; Kao, M.; Diederich, F.; Foote, C. S. *Angew. Chem.* **1992**, *104*, 69; *Angew. Chem., Int. Ed. Engl.* **1992**, *31*, 63.
- (15) Cox, D. M.; Sherwood, R. D.; Tindall, P.; Creegan, K. M.; Anderson, W.; Martella, D. J. In "Fullerenes—Synthesis, Properties, and Chemistry of Large Carbon Clusters", ACS Symp. Ser. 481; Hammond, G. S.; Kuck, V. J., Eds.; American Chemical Society: Washington, DC, 1992; Chapter 8.
- (16) Malhotra, R.; Lorents, D. C.; Bae, Y. K.; Becker, C. H.; Tse, D. S.; Jusinski, L. E.; Wachsmann, E. D. In "Fullerenes—Synthesis, Properties, and Chemistry of Large Carbon Clusters", ACS Symp. Ser. 481; Hammond, G. S.; Kuck, V. J., Eds.; American Chemical Society: Washington, DC, 1992; Chapter 9.
- (17) Saxby, J. D.; Chatfield, S. P.; Palmisano, A. J.; Vassallo, A. M.; Wilson, M. A.; Pang, L. S. K. *J. Phys. Chem.* **1992**, *96*, 17.
- (18) Saito, S.; Oshiyama, A. *Phys. Rev. Lett.* **1991**, *66*, 2637.
- (19) Haufler, R. E.; Wang, L.-S.; Chibante, L. P. F.; Jin, C.; Conceicao, J.; Chai, Y.; Smalley, R. E. *Chem. Phys. Lett.* **1991**, *179*, 449.
- (20) Zimmerman, J. A.; Eyler, J. R.; Bach, S. B. H.; McElvany, S. W. *J. Chem. Phys.* **1991**, *94*, 3556.
- (21) Lichtenberger, D. L.; Nebesny, K. W.; Ray, C. D.; Huffman, D. R.; Lamb, L. D. *Chem. Phys. Lett.* **1991**, *176*, 203.
- (22) Wang, L.-S.; Conceicao, J.; Jin, C.; Smalley, R. E. *Chem. Phys. Lett.* **1991**, *182*, 5.
- (23) Curl, R. F.; Smalley, R. E. *Science* **1988**, *242*, 1017.
- (24) Haddon, R. C.; Brus, L. E.; Raghavachari, K. *Chem. Phys. Lett.* **1986**, *125*, 459.
- (25) Yang, S. J.; Pelletier, C. L.; Conceicao, J.; Chesnovsky, O.; Smalley, R. E. *Chem. Phys. Lett.* **1987**, *139*, 233.
- (26) Allemand, P.-M.; Koch, A.; Wudl, F.; Rubin, Y.; Diederich, F.; Alvarez, M. M.; Anz, S. J.; Whetten, R. L. *J. Am. Chem. Soc.* **1991**, *113*, 1050.
- (27) Limbach, P. A.; Schweikhard, L.; Cowan, K. A.; McDermott, M. T.; Marshall, A. G.; Coe, J. V. *J. Am. Chem. Soc.* **1991**, *113*, 6795.
- (28) Cox, D. M.; Behal, S.; Disko, M.; Gorun, S. M.; Greaney, M.; Hsu, C. S.; Kollin, E. B.; Millar, J.; Robbins, J.; Bobbins, W.; Sherwood, S. D.; Tindall, P. *J. Am. Chem. Soc.* **1991**, *113*, 2940.

- (29) Dubois, D.; Kadish, K. M.; Flanagan, S.; Haufler, R. E.; Chibante, L. P. F.; Wilson, L. J. *J. Am. Chem. Soc.* **1991**, *113*, 4364.
- (30) Dubois, D.; Kadish, K. M.; Flanagan, S.; Wilson, L. J. *J. Am. Chem. Soc.* **1991**, *113*, 7773.
- (31) Heath, J. R.; O'Brien, S. C.; Zhang, Q.; Liu, Y.; Curl, R. F.; Kroto, H. W.; Smalley, R. E. *J. Am. Chem. Soc.* **1985**, *107*, 7779.
- (32) McKenzie, D. R.; Davis, C. A.; Cockayne, D. J. H.; Muller, D. A.; Vassallo, A. M. *Nature (London)* **1992**, *355*, 622.
- (33) Taylor, R.; Hare, J. P.; Abdul-Sada, A. K.; Kroto, H. W. *J. Chem. Soc., Chem. Commun.* **1990**, 1423.
- (34) Johnson, R. D.; Meijer, G.; Salem, J. R.; Bethune, D. S. *J. Am. Chem. Soc.* **1991**, *113*, 3619.
- (35) Hawkins, J. M.; Meyer, A.; Lewis, T. A.; Loren, S.; Hollander, F. J. *Science* **1991**, *252*, 312.
- (36) Wilson, R. J.; Meijer, G.; Bethune, D. S.; Johnson, R. D.; Chambliss, D. D.; de Vries, M. S.; Hunziker, H. E.; Wendt, H. R. *Nature (London)* **1990**, *348*, 621.
- (37) Wragg, J. L.; Chamberlain, J. E.; White, H. W.; Kratschmer, W.; Huffman, D. R. *Nature (London)* **1990**, *348*, 623.
- (38) Diederich, F.; Ettl, R.; Rubin, Y.; Whetten, R. L.; Beck, R.; Alvarez, M. M.; Anz, S.; Sensharma, D.; Wudl, F.; Khemani, K. C.; Koch, A. *Science* **1991**, *252*, 548.
- (39) Parker, D. H.; Wurz, P.; Chatterjee, K.; Lykke, K. R.; Hunt, J. E.; Pellin, M. J.; Hemminger, J. C.; Gruen, D. M.; Stock, L. M. *J. Am. Chem. Soc.* **1991**, *113*, 7499.
- (40) Lamb, L. D.; Huffman, D. R.; Workman, R. K.; Howells, S.; Chen, T.; Sarid, D.; Ziolo, R. F. *Science* **1992**, *255*, 1413.
- (41) For a review of the higher fullerenes, see Diederich, F.; Whetten, R. L. *Acc. Chem. Res.* **1992**, *25*, 119.
- (42) Smalley, R. E. *Acc. Chem. Res.* **1992**, *25*, 98.
- (43) Kratschmer, W.; Lamb, L. D.; Fostiropoulos, K.; Huffman, D. R. *Nature (London)* **1990**, *347*, 354.
- (44) Scrivens, W. A.; Bedworth, P. V.; Tour, J. M. *J. Am. Chem. Soc.* **1992**, *114*, 7917.
- (45) Howard, J. B.; McKinnon, J. T.; Makarovskiy, Y.; Lafleur, A. L.; Johnson, M. E. *Nature (London)* **1991**, *352*, 139.
- (46) McKinnon, J. T. *J. Phys. Chem.* **1991**, *95*, 8941.
- (47) Iacoe, D. W.; Potter, W. T.; Teeters, D. J. *Chem. Educ.* **1992**, *69*, 663.
- (48) Craig, N. C.; Gee, G. C.; Johnson, A. R. *J. Chem. Educ.* **1992**, *69*, 665.
- (49) Ajie, H.; Alvarez, M. M.; Anz, S. J.; Beck, R. D.; Diederich, F.; Fostiropoulos, K.; Huffman, D. R.; Kratschmer, W.; Rubin, Y.; Schriver, K. E.; Sensharma, D.; Whetten, R. L. *J. Phys. Chem.* **1990**, *94*, 8630.
- (50) Bunshah, R. F.; Jou, S.; Prakash, S.; Doerr, H. J.; Isaacs, L.; Wehrsigs, A.; Yeretizian, C.; Cynn, H.; Diederich, F. *J. Phys. Chem.* **1992**, *96*, 6866.
- (51) Hare, J. P.; Kroto, H. W.; Taylor, R. *Chem. Phys. Lett.* **1991**, *177*, 394.
- (52) Haufler, R. E.; Conceicao, J.; Chibante, L. P. F.; Chai, Y.; Byrne, N. E.; Flanagan, S.; Haley, M. M.; O'Brien, S. C.; Pan, C.; Xiao, Z.; Billups, W. E.; Ciufolini, M. A.; Hauge, R. H.; Margrave, J. L.; Wilson, L. J.; Curl, R. F.; Smalley, R. E. *J. Phys. Chem.* **1990**, *94*, 8634.
- (53) Diack, M.; Hettich, R. L.; Compton, R. N.; Guiochon, G. *Anal. Chem.* **1992**, *64*, 2143.
- (54) Johnson, R. D.; Meijer, G.; Bethune, D. S. *J. Am. Chem. Soc.* **1990**, *112*, 8983.
- (55) Gügel, A.; Becker, M.; Hammel, D.; Mindach, L.; Rader, J.; Simon, T.; Wagner, M.; Müllen, K. *Angew. Chem.* **1992**, *104*, 666; *Angew. Chem., Int. Ed. Engl.* **1992**, *31*, 644.

- (56) Welch, C. J.; Pirkle, W. H. *J. Chromatogr.* **1992**, 609, 89.
- (57) Meier, M. S.; Selegue, J. P. *J. Org. Chem.* **1992**, 57, 1924.
- (58) Jinno, K.; Yamamoto, K.; Ueda, T.; Nagashima, H.; Itoh, K. *J. Chromatogr.* **1992**, 594, 105.
- (59) Vassalo, A. M.; Palmisano, A. J.; Pang, L. S. K.; Wilson, M. A. *J. Chem. Soc., Chem. Commun.* **1992**, 60.
- (60) Hawkins, J. M.; Lewis, T. A.; Loren, D. S.; Meyer, A.; Heath, J. R.; Shibato, Y.; Saykally, R. J. *J. Org. Chem.* **1990**, 55, 6250.
- (61) See, for example, Soderholm, L.; Wurz, P.; Lykke, K. R.; Parker, D. H.; Lytle, F. W. *J. Phys. Chem.* **1992**, 96, 7153.
- (62) Cioslowski, J. *J. Am. Chem. Soc.* **1991**, 113, 4139.
- (63) Johnson, R. D.; de Vries, M. S.; Salem, J.; Bethune, D. S.; Yannoni, C. S. *Nature (London)* **1992**, 355, 239.
- (64) McElvany, S. W. *J. Phys. Chem.* **1992**, 96, 4935.
- (65) McElvany, S. W.; Ross, M. M.; Callahan, J. H. *Acc. Chem. Res.* **1992**, 25, 162.
- (66) Weaver, J. H.; Chai, Y.; Kroll, G. H.; Jin, C.; Ohno, T. R.; Haufler, R. E.; Guo, T.; Alford, J. M.; Conceicao, J.; Chibante, L. P. F.; Jain, A.; Palmer, G.; Smalley, R. E. *Chem. Phys. Lett.* **1992**, 190, 460.
- (67) Shinohara, H.; Sato, H.; Saito, Y.; Ohkohchi, M.; Ando, Y. *J. Phys. Chem.* **1992**, 96, 3571.
- (68) Shinohara, H.; Sato, H.; Ohkohchi, M.; Ando, Y.; Kodama, T.; Shida, T.; Kato, T.; Saito, Y. *Nature (London)* **1992**, 357, 52.
- (69) Yannoni, C. S.; Hoinkis, M.; de Vries, M. S.; Bethune, D. S.; Salem, J. R.; Crowder, M. S.; Johnson, R. D. *Science* **1992**, 256, 1191.
- (70) Weiss, F. D.; Elkind, J. L.; O'Brien, S. C.; Curl, R. F.; Smalley, R. E. *J. Am. Chem. Soc.* **1988**, 110, 4464.
- (71) Gillan, E. G.; Yeretizian, C.; Min, K. S.; Alvarez, M. M.; Whetten, R. L.; Kaner, R. B. *J. Phys. Chem.* **1992**, 96, 6869.
- (72) Pradeep, T.; Kulkarni, G. U.; Kannan, K. R.; Garu Row, T. N.; Rao, C. N. R. *J. Am. Chem. Soc.* **1992**, 114, 2272.
- (73) Alvarez, M. M.; Gilan, E. G.; Holczer, K.; Kaner, R. B.; Min, K. S.; Whetten, R. L. *J. Phys. Chem.* **1991**, 95, 10561.
- (74) Ross, M. M.; Nelson, H. H.; Callahan, J. H.; McElvany, S. W. *J. Phys. Chem.* **1992**, 96, 5231.
- (75) Guo, T.; Diener, M.; Chai, Y.; Alford, M. J.; Haufler, R. E.; McClure, S. M.; Ohno, T.; Weaver, J. H.; Scuseria, G. E.; Smalley, R. E. *Science* **1992**, 257, 1661.
- (76) Smalley, R. E. *Nat. Res. Rev.* **1991**, 43, 3.
- (77) Weiske, T.; Böhme, D. K.; Hrůšák, J.; Kratschmer, W.; Schwarz, H. *Angew. Chem.* **1991**, 103, 898; *Angew. Chem., Int. Ed. Engl.* **1991**, 30, 884.
- (78) Weiske, T.; Hrůšák, J.; Böhme, D. K.; Schwarz, H. *Helv. Chim. Acta* **1992**, 75, 79.
- (79) Ross, M. M.; Callahan, J. H. *J. Phys. Chem.* **1991**, 95, 5720.
- (80) Mowrey, R. C.; Ross, M. M.; Callahan, J. H. *J. Phys. Chem.* **1992**, 96, 4755.
- (81) Caldwell, K. A.; Giblin, D. E.; Gross, M. L. *J. Am. Chem. Soc.* **1992**, 114, 3743.
- (82) Caldwell, K. A.; Giblin, D. E.; Hsu, C. S.; Cox, D.; Gross, M. L. *J. Am. Chem. Soc.* **1991**, 113, 8519.
- (83) Weiske, T.; Hrůšák, J.; Böhme, D. K.; Schwarz, H. *Chem. Phys. Lett.* **1991**, 186, 459.
- (84) Weiske, T.; Böhme, D. K.; Schwarz, H. *J. Phys. Chem.* **1991**, 95, 8451.
- (85) O'Brien, S. C.; Heath, J. R.; Curl, R. F.; Kroto, H. W.; Smalley, R. E. *J. Chem. Phys.* **1988**, 88, 220.

- (86) Radi, P. P.; Bunn, T. L.; Kemper, P. R.; Molchan, M. E.; Bowers, M. T. *J. Chem. Phys.* **1988**, *88*, 2809.
- (87) Huang, Y.; Freiser, B. S. *J. Am. Chem. Soc.* **1991**, *113*, 9418.
- (88) Roth, L. M.; Huang, Y.; Schwedler, J. T.; Cassady, C. J.; Ben-Amotz, D.; Kahr, B.; Freiser, B. S. *J. Am. Chem. Soc.* **1991**, *113*, 6298.
- (89) Jiao, Q.; Huang, S.; Lee, S. A.; Gord, J. R.; Freiser, B. S. *J. Am. Chem. Soc.* **1992**, *114*, 2726.
- (90) Johnson, R. D.; Bethune, D. S.; Yannoni, C. S. *Acc. Chem. Res.* **1992**, *25*, 169.
- (91) Pénicaud, A.; Hsu, J.; Reed, C.; Koch, A.; Khemani, K. C.; Allemand, P.-M.; Wudl, F. *J. Am. Chem. Soc.* **1991**, *113*, 6698.
- (92) Kukolich, S. G.; Huffman, D. R. *Chem. Phys. Lett.* **1991**, *182*, 263.
- (93) Allemand, P.-M.; Srdanov, G.; Koch, A.; Khemani, K.; Wudl, F.; Rubin, Y.; Diederich, F.; Alvarez, M. M.; Anz, S. J.; Whetten, R. L. *J. Am. Chem. Soc.* **1991**, *113*, 2780.
- (94) Keizer, P. M.; Morton, J. R.; Preston, K. F.; Sugden, A. K. *J. Am. Chem. Soc.* **1991**, *113*, 7117.
- (95) Knight, L. B.; Woodward, R. W.; Van Zee, R. J.; Weltner, W. *Chem. Phys. Lett.* **1983**, *94*, 296.
- (96) Cioslowski, J.; Fleischmann, B. *J. Chem. Phys.* **1991**, *94*, 3730.
- (97) Chang, A. H. H.; Ermler, W. C.; Pitzer, R. M. *J. Chem. Phys.* **1991**, *94*, 5004.
- (98) Rosén, A.; Wästberg, B. *J. Am. Chem. Soc.* **1988**, *110*, 8701.
- (99) Rosén, A.; Wästberg, B. *Z. Phys. D: At., Mol. Clusters* **1988**, *12*, 387.
- (100) Cox, D. M.; Trevor, D. J.; Reichmann, K. C.; Kaldor, A. *J. Am. Chem. Soc.* **1986**, *108*, 2457.
- (101) Fowler, P. W. *Chem. Phys. Lett.* **1986**, *131*, 444.
- (102) Fagan, P. J.; Calabrese, J. C.; Malone, B. *Acc. Chem. Res.* **1992**, *25*, 134.
- (103) Hawkins, J. M.; Loren, S.; Meyer, A.; Nunlist, R. *J. Am. Chem. Soc.* **1991**, *113*, 7770.
- (104) Hawkins, J. M.; Meyer, A.; Loren, S.; Nunlist, R. *J. Am. Chem. Soc.* **1991**, *113*, 9394.
- (105) Hawkins, J. M. *Acc. Chem. Res.* **1992**, *25*, 150.
- (106) Amiđ, D.; Trinajstić, N. *J. Chem. Soc., Perkin Trans. 2* **1990**, 1595.
- (107) Creegan, K. M.; Robbins, J. L.; Robbins, W. K.; Millar, J. M.; Sherwood, R. D.; Tindall, P. J.; Cox, D. M.; McCauley, J. P.; Jones, D. R.; Gallagher, R. T.; Smith, A. B. *J. Am. Chem. Soc.* **1992**, *114*, 1103.
- (108) Stry, J. J.; Collbaugh, M. T.; Turos, E.; Garvey, J. F. *J. Am. Chem. Soc.* **1992**, *114*, 7914.
- (109) Wudl, F. *Acc. Chem. Res.* **1992**, *25*, 157, and citations therein.
- (110) Wudl, F. In "Fullerenes—Synthesis, Properties, and Chemistry of Large Carbon Clusters", ACS Symp. Ser. 481; Hammond, G. S.; Kuck, V. J., Eds.; American Chemical Society: Washington, DC, 1992; p. 161.
- (111) Hawkins, J. M.; Meyer, A.; Lewis, T. A.; Bunz, U.; Nunlist, R.; Ball, G. E.; Ebbesen, T. W.; Tanigaki, K. *J. Am. Chem. Soc.* **1992**, *114*, 7954.
- (112) Fagan, P. J.; Calabrese, J. C.; Malone, B. *Science* **1991**, *252*, 1160.
- (113) Cheng, P.-T.; Cook, C. D.; Nyburg, S. C.; Wan, K. Y. *Inorg. Chem.* **1971**, *10*, 2210.
- (114) Panattoni, C.; Bombieri, G.; Belluco, U.; Baddley, W. H. *J. Am. Chem. Soc.* **1968**, *90*, 798.
- (115) See Fagan *et al.* (102), and citations therein.
- (116) Fagan, P. J.; Calabrese, J. C.; Malone, B. *J. Am. Chem. Soc.* **1991**, *113*, 9408.
- (117) Balch, A. L.; Catalano, V. J.; Lee, J. W. *Inorg. Chem.* **1991**, *30*, 3980.
- (118) Balch, A. L.; Catalano, V. J.; Lee, J. W.; Olmstead, M. M. *J. Am. Chem. Soc.* **1992**, *114*, 5455.

- (119) Vaska, L. *Acc. Chem. Res.* **1968**, *1*, 335.
- (120) Balch, A. L.; Lee, J. W.; Noll, B. C.; Olmstead, M. M. *J. Am. Chem. Soc.* **1992**, *114*, 10984.
- (121) Balch, A. L.; Catalano, V. J.; Lee, J. W.; Olmstead, M. M.; Parkin, S. R. *J. Am. Chem. Soc.* **1991**, *113*, 8953.
- (122) Balch, A. L.; Lee, J. W.; Olmstead, M. M. *Angew. Chem.* **1992**, *104*, 1400; *Angew. Chem., Int. Ed. Engl.* **1992**, *31*, 1356.
- (123) Koefod, R. S.; Hudgens, M. F.; Shapley, J. R. *J. Am. Chem. Soc.* **1991**, *113*, 8957.
- (124) Fagan, P. J.; Ward, M. D.; Calabrese, J. C. *J. Am. Chem. Soc.* **1989**, *111*, 1698.
- (125) Shapley, J. R.; Koefod, R. S. "Abstracts of Papers", 201st National Meeting of the American Chemical Society, Atlanta, GA, April 1991.
- (126) Huang, Y.; Freiser, B. S. *J. Am. Chem. Soc.* **1991**, *113*, 8186.
- (127) Gorun, S. M.; Greaney, M. A.; Cox, D. M.; Sherwood, R.; Day, C. S.; Day, V. W.; Upton, R. M.; Briant, C. E. *Proc. Mater. Res. Soc.* **1991**, *206*, 659.
- (128) Gorun, S. M.; Greaney, M. A.; Day, V. W.; Day, C. S.; Upton, R. M.; Briant, C. E. In "Fullerenes—Synthesis, Properties, and Chemistry of Large Carbon Clusters", ACS Symp. Ser. 481; Hammond, G. S.; Kuck, V. J., Eds. American Chemical Society: Washington, DC, 1992; p. 41.
- (129) Fleming, R. M.; Kortan, A. R.; Hessen, B.; Siegrist, T.; Thiel, F. A.; Marsh, P.; Haddon, R. C.; Tycko, R.; Dabbagh, G.; Kaplan, M. L.; Muijsce, A. M. *Phys. Rev. B* **1991**, *44*, 888.
- (130) Assink, R. A.; Schirber, J. E.; Loy, D. A.; Morosin, B.; Carlson, G. A. *J. Mater. Res.* **1992**, *7*, 2136.
- (131) Haddon, R. C.; Hébard, A. F.; Rosseinsky, M. J.; Murphy, D. W.; Glarum, S. H.; Palstra, T. T. M.; Ramirez, A. P.; Duclos, S. J.; Fleming, R. M.; Siegrist, T.; Tycko, R. In "Fullerenes—Synthesis, Properties, and Chemistry of Large Carbon Clusters", ACS Symp. Ser. 481; Hammond, G. S.; Kuck, V. J., Eds.; American Chemical Society: Washington, DC, 1992; Chapter 5.
- (132) Benning, P. J.; Martins, J. L.; Weaver, J. H.; Chibante, L. P. F.; Smalley, R. E. *Science* **1991**, *252*, 1417.
- (133) Wertheim, G. K.; Rowe, J. E.; Buchanan, D. N. E.; Chaban, E. E.; Hébard, A. F.; Dortan, A. R.; Makhija, A. V.; Haddon, R. C. *Science* **1991**, *252*, 1419.
- (134) Stephens, P. W.; Mihaly, L.; Wiley, B.; Huang, S. M.; Kaner, R. B.; Diederich, F.; Whetten, R. L.; Holczer, K. *Phys. Rev. B* **1992**, *45*, 543.
- (135) Zhu, Q.; Zhou, O.; Coustel, N.; Vaughan, G.; McCauley, J. P.; Romanow, W. J.; Fischer, J. E.; Smith, A. B. *Science* **1991**, *254*, 545.
- (136) Fleming, R. M.; Rosseinsky, M. J.; Ramirez, A. P.; Murphy, D. W.; Tully, J. C.; Haddon, R. C.; Siegrist, T.; Tycko, R.; Glarum, S. H.; Marsh, P.; Dabbagh, G.; Zahurak, S. M.; Makhija, A. V.; Hampton, C. *Nature (London)* **1991**, *352*, 701.
- (137) Haddon, R. C.; Hébard, A. F.; Rosseinsky, M. J.; Murphy, D. W.; Duclos, S. J.; Lyons, K. B.; Miller, B.; Rosamilia, J. M.; Fleming, R. M.; Kortan, A. R.; Glarum, S. H.; Makhija, A. V.; Muller, A. J.; Eick, R. H.; Zahurak, S. M.; Tycko, R.; Dabbagh, G.; Theil, F. A. *Nature (London)* **1991**, *350*, 320.
- (138) Hébard, A. F.; Rosseinsky, M. J.; Haddon, R. C.; Murphy, D. W.; Glarum, S. H.; Palstra, T. T. M.; Ramirez, A. P.; Kortan, A. R. *Nature (London)* **1991**, *350*, 600.
- (139) Wang, H. H.; Kini, A. M.; Carlson, K. D.; Williams, J. M.; Lykke, K. R.; Wurz, P.; Parker, D. H.; Pellin, M. J.; Gruen, D. M.; Welp, U.; Kwok, W.-K.; Fleshler, S.; Crabtree, G. W. *Inorg. Chem.* **1991**, *30*, 2839.
- (140) McCauley, J. P.; Zhu, Q.; Coustel, N.; Zhou, O.; Vaughan, G.; Idziak, S. H. J.;

- Fischer, J. E.; Tozer, S. W.; Groski, D. M.; Bykovetz, N.; Lin, C. L.; McGhie, A. R.; Allen, B. H.; Romanow, W. J.; Denenstein, A. M.; Smith, A. B. *J. Am. Chem. Soc.* **1991**, *113*, 8537.
- (141) Holczer, K.; Klein, O.; Huang, S. M.; Kaner, R. B.; Fu, K. J.; Whetten, R. L.; Diederich, F. *Science* **1991**, *252*, 1154.
- (142) Chabre, Y.; Djurado, D.; Armand, M.; Romanow, W. J.; Coustel, N.; McCauley, J. P.; Fischer, J. E.; Smith, A. B. *J. Am. Chem. Soc.* **1992**, *114*, 764.
- (143) Kastner, J.; Kuzmany, H.; Palmethofer, L.; Bauer, P.; Stingeder, G. *Nucl. Instrum. Methods Phys. Res., Sect. B*, **1993**, *80*, 1456.
- (144) Stephens, P. W.; Mihaly, L.; Lee, P. L.; Whetten, R. L.; Huang, S.-M.; Kaner, R. B.; Diederich, F.; Holczer, K. *Nature (London)* **1991**, *351*, 632.
- (145) Tycko, R.; Dabbagh, G.; Rosseinsky, M. J.; Murphy, D. W.; Fleming, R. M.; Ramirez, A. P.; Tully, J. C. *Science* **1991**, *253*, 884.
- (146) Zhou, O.; Fischer, J. E.; Coustel, N.; Kycia, S.; Zhu, Q.; McGhie, A. R.; Romanow, W. J.; McCauley, J. P.; Smith, A. B.; Cox, D. E. *Nature (London)* **1991**, *351*, 462.
- (147) Fischer, J. E.; Heiney, P. A.; Luzzi, D. E.; Cox, D. E. In "Fullerenes—Synthesis, Properties, and Chemistry of Large Carbon Clusters", ACS Symp. Ser. 481; Hammond, G. S.; Kuck, V. J., Eds.; American Chemical Society: Washington, DC, 1992; Chapter 4.
- (148) Duclos, S. J.; Haddon, R. C.; Glarum, S. H.; Hebard, A. F.; Lyons, K. B. *Science* **1991**, *254*, 1625.
- (149) Negri, F.; Orlandi, G.; Zerbetto, F. *Chem. Phys. Lett.* **1992**, *196*, 303.
- (150) Rosseinsky, M. J.; Ramirez, A. P.; Glarum, S. H.; Murphy, D. W.; Haddon, R. C.; Hébard, D. W.; Palstra, T. T. M.; Kortan, A. R.; Zahurak, S. M.; Makhija, A. V. *Phys. Rev. Lett.* **1991**, *66*, 2830.
- (151) Tanigaki, K.; Eddesen, T. W.; Saito, S.; Mizuki, J.; Tsai, J. S.; Kubo, Y.; Kuroshima, S. *Nature (London)* **1991**, *352*, 222.
- (152) Iqbal, Z.; Baughmann, R. J.; Ramakrishna, B. L.; Khare, S.; Murthy, N. S.; Bornemann, H. J.; Morris, D. E. *Science* **1991**, *254*, 826.
- (153) Erwin, S. C.; Pederson, M. R. *Phys. Rev. Lett.* **1991**, *67*, 1610.
- (154) Smalley, R. E. *Mater. Sci. Eng., B*, **1993**, *19*, 1.
- (155) Loy, D. A.; Assink, R. A. *J. Am. Chem. Soc.* **1992**, *114*, 3977.
- (156) Guo, T.; Jin, C.; Smalley, R. E. *J. Phys. Chem.* **1991**, *95*, 4948.
- (157) Pradeep, T.; Vijayakrishna, V.; Santra, A. K.; Rao, C. N. R. *J. Phys. Chem.* **1991**, *95*, 10564.
- (158) Christian, J. F.; Wan, Z.; Anderson, S. *J. Phys. Chem.*, in press.
- (159) Christian, J. F.; Wan, Z.; Anderson, S. *J. Phys. Chem.* **1992**, *96*, 3574.
- (160) Suzuki, T.; Li, Q.; Khemani, K. C.; Wudl, F.; Almarson, Ö. *Science* **1991**, *254*, 1186.
- (161) Andreoni, W.; Fygi, F.; Parrinello, M. *Chem. Phys. Lett.* **1992**, *190*, 159.
- (162) Wiberg, E. *Naturwissenschaften* **1948**, *35*, 182.
- (163) Wells, A. F. "Structural Inorganic Chemistry", 5th ed.; Oxford University Press (Clarendon), London and New York, 1984; pp. 835 and 1060.
- (164) Lappert, M. F.; Power, P. P.; Sanger, A. R.; Srivastava, R. C. "Metal and Metalloid Amides"; Ellis Horwood: Chichester, 1980; Chapter 5.
- (165) Bowser, J. R.; Jelski, D. A.; George, T. F. *Inorg. Chem.* **1992**, *31*, 156.
- (166) Xia, X.; Jelski, D. A.; Bowser, J. R.; George, T. F. *J. Am. Chem. Soc.* **1992**, *114*, 6493.
- (167) Bowser, J. R.; Jelski, D. A.; Xia, X.; George, T. F. "Abstracts of Papers", 22nd Northeast Regional Meeting of the American Chemical Society, Syracuse, NY, June 1992.

- (168) Jelski, D. A.; Bowser, J. R.; Xia, X.; Gao, J.; George, T. F. *J. Cluster Sci.*, **1993**, 4, 173.
- (169) Baldrige, K. K.; Gordon, M. S. *Organometallics* **1988**, 7, 144.
- (170) West, R. *Angew. Chem. Int. Ed. Engl.* **1987**, 26, 1201; *Angew. Chem.* **1987**, 99, 1231.
- (171) Grev, R. S. *Adv. Organomet. Chem.* **1991**, 33, 125.
- (172) For a variety of examples, see Colvin, E. "Silicon Reagents in Organic Synthesis"; Academic Press: New York, 1988.
- (173) Werner, H.; Salzer, A. *Synth. React. Inorg. Met.-Org. Chem.* **1972**, 2, 239.
- (174) Iijima, S. *Nature (London)* **1991**, 354, 56.
- (175) Iijima, S.; Ichihashi, T.; Ando, Y. *Nature (London)* **1992**, 356, 776.
- (176) Reed, M. A. *Sci. Am.* **1993**, 268, 118.
- (177) Sariciftci, N. S.; Smilowitz, L.; Heeger, A. J.; Wudl, F. *Science* **1992**, 258, 1474.
- (178) Morita, S.; Zakhidov, A. A.; Yoshino, K. *Solid State Commun.* **1992**, 82, 249.
- (179) Beleznyay, C.; Jelski, D. A.; Nafai, L.; George, T. F. submitted for publication in *Phys. Rev. Lett.*
- (180) Carter, F. L., Ed. "Molecular Electronic Devices"; Dekker: New York, 1987.

Quantification of Steric Effects in Organometallic Chemistry

DAVID WHITE and NEIL J. COVILLE

*Centre for Applied Chemistry and Chemical Technology
Department of Chemistry
University of the Witwatersrand
Johannesburg 2001
South Africa*

I.	Introduction	95
II.	Quantification of Steric Size Using Physical Measurements	97
	A. Cone Angles	97
	B. Solid Angles	117
	C. Summary	130
III.	Quantification of Steric Size Using Molecular Mechanics Methods	130
	A. Ligand Repulsive Energy, E_R	130
	B. Molecular Mechanics and Steric Size Assessment	133
	C. Steric Effects in Macrocyclic Chemistry	134
IV.	Quantification of Steric Size Using Chemical Methods	134
	A. The Modified Taft Steric Parameter, E_s^*	134
	B. Use of NMR Spectroscopy to Quantify Steric Size.	136
V.	Quantification of the Variation in Steric Effect with Distance	137
VI.	Steric Profiles and Thresholds	142
VII.	Quantification of Steric Size Using Molecular Volumes	145
VIII.	Some Applications of Steric Size Measurements	152
IX.	Conclusion	154
	References.	155

I

INTRODUCTION

The concept of steric size has its origin in the systematic development of organic chemistry in the mid 1850s. This arose out of the attempt to rationalize reactivity patterns in terms of chemical structure. The link between the two phenomena, structure and reactivity, was first recognized in 1872 when Hofmann noted the resistance of triarylamines to undergo alkylation and proposed that this was due to the "bulk" of the substrate (1). A few years later Sachse (2) and Mohr (3) questioned Baeyer's (4) assumption that all cyclic structures were planar, invoking "bulk crowding" as a rationalization for the distortion from planarity. After these initial studies, Kehrmann showed that *o*-substituted quinones were less

reactive than their unsubstituted analogs and ascribed the findings to a *steric effect* (5). In 1894, Meyer laid the foundation for the definition of a *quantifiable steric effect* by noting the presence of steric effects in esterification reactions (6). However, Wegscheider was the first to coin the phrase *steric hindrance* while looking at similar esterification reactions (7). The early recognition of the nature of the steric effect was reviewed by Anschütz in 1928 (8) and extensively elaborated in 1956 in the classic text "Steric Effects in Organic Chemistry" (9). A brief historical discussion of the early development of the steric effect was written by Mosher and Tidwell in 1990 (10).

Interestingly, the quantification of steric effects in organometallic chemistry took a completely different course from studies in organic chemistry. In 1970 Tolman quantified the steric effect in terms of cone angles (11). This method has become the standard for measuring all ligand sizes and the methodology as well as limited data sets of cone angles are listed in many inorganic chemistry textbooks (12).

A variety of new procedures for evaluating steric size in both organic and inorganic chemistry has been reported in the intervening years and it is the aim of this review to report and evaluate both the older and newer methodologies. To our knowledge there has been no general review of the quantification of steric effects in chemistry since the Tolman review of 1977 (13). Our survey of the literature has revealed that the quantification of steric size has evolved with time along quite different lines in the various branches of chemistry. Indeed, the formal link between organic and inorganic (organometallic) steric size measurements has been little discussed or appreciated (14–16). Only in recent studies of cone angles of organic fragments (e.g., rings, alkyl groups) and solid angle measurements (Section II,B) has a merging of approaches become apparent.

In this review only the available literature concerning the *quantification of steric effects* has been covered in depth. No attempt has been made to separate the data derived from the fields of organic or inorganic chemistry. In principle, there is no reason to differentiate between the size measurement of a ligand or an organic substituent. A distinction needs to be made, however, between the *quantification* and the *assessment* of a steric effect. The former term applies, exclusively, to the quantitative analysis of steric effects, whereas the latter refers to the qualitative detection of such effects.

It must be recognized at the outset that, although a steric size can be measured and quantified, the relationship between structure and reactivity is determined by *both steric and electronic effects*. The separation of steric and electronic effects is a nontrivial task and, where appropriate, the methods used to separate these effects are mentioned. This review,

however, does not concern itself with the measurement and assessment of electronic effects.

In general four procedures can be identified to assess and/or quantify steric size: (i) direct *physical* measurement of steric size from a knowledge of atom sizes, bond lengths, and bond angles (for example using cone and solid angles), (ii) inference of relative sizes from some chemical property (for example the rate of hydrolysis of esters), (iii) molecular mechanics models (for example the use of van der Waals repulsion energy as a steric parameter), and (iv) the use of molecular volumes.

II

QUANTIFICATION OF STERIC SIZE USING PHYSICAL MEASUREMENTS

A. Cone Angles

No steric measure has been as widely used and accepted by inorganic chemists as the cone angle concept originally proposed by Tolman (11, 13). The cone angle concept is very elegant in its simplicity and usefulness. Cone angles were initially generated for a specific system and these data have provided a *relative ordering* of steric size that can be generalized to any atom or substituent. Specifically a phosphorus-containing ligand is placed 2.28 Å from a metal and the linear angle, θ , between the vectors tangential to the outermost van der Waals radii of the atoms on the ligand is measured (Fig. 1). This provides a three-dimensional measure of steric size. The M–P value of 2.28 Å was chosen as it is typical of a Ni–P bond distance and the original data were generated for the specific problem of steric size relating to $\text{Ni}(\text{CO})_3\text{L}$ complexes. It is assumed that the relative ordering of ligands by size using this value will hold for all other M–P bond lengths and, consequently, that this *arbitrary* set of data can be used for all metals bound to phosphorus. The method is easy to apply to ligands

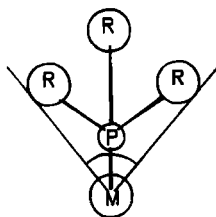


FIG. 1. Measurement of the Tolman cone angle, θ , for a PR_3 ligand. Redrawn from Tolman (13) with permission.

with few conformational degrees of freedom (e.g., PH_3). However, when there are internal degrees of freedom (e.g., about the P–C and C–C bonds in PEt_3) the cone angle was originally measured with the ligand folded back into its *minimum conformation*. This is a significant assumption made in measuring linear angles. However, the assumption appears to correlate well with various experimental parameters associated with steric size. Thus, when Tolman was in doubt as to the steric size of a particular ligand (cone angle), he based his final calculation on the degree of substitution, i.e., the position of the equilibrium, in the following reaction:



For asymmetric ligands, $\text{PR}_1\text{R}_2\text{R}_3$, the total cone angle is defined as the average of the sum of the semivertex angles for each PR_i group (Fig. 2):

$$\theta_{\text{total}} = \frac{2}{3} \sum_{i=1}^3 \frac{\theta_i}{2}, \quad (1)$$

where θ_i is the semivertex angle of PR_i . The measurement of the PPh_3 cone angle was based entirely on the use of CPK models: two-thirds of the cone angle is assumed to come from the outermost van der Waals radius of two phenyl groups in *maximum conformation* (185°) and one in *minimum conformation* (65°). Applying this approach to the $\text{P}(m\text{-tolyl})_3$ a cone angle of 148° is obtained (17). This value is obtained, as for PPh_3 , by taking one maximum cone angle of 194.4° (*meta*-methyl protons), one maximum cone angle for PPh_3 (*ortho*-proton), and one minimum cone angle for PPh_3 (*ipso*-carbon) (Fig. 3).

The limitations of Tolman's approach are well recognized: (i) cone angles may differ substantially with change in conformation of L, (ii) the cone angles are only accurate to within 2° , (iii) there is uncertainty as to whether the conformation chosen is, indeed, the minimum without introducing steric strain, (iv) cylindrical symmetry of the ligand is assumed and so ligand meshing must be ignored, (v) van der Waals and covalent

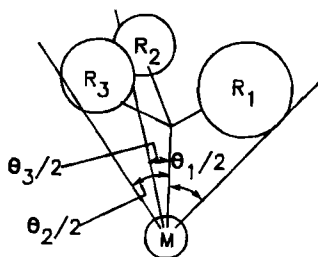


FIG. 2. Measurement of the average Tolman cone angle, θ , for a ligand $\text{PR}_1\text{R}_2\text{R}_3$. The metal-P bond length is 2.28 \AA . Redrawn from Tolman (13) with permission.

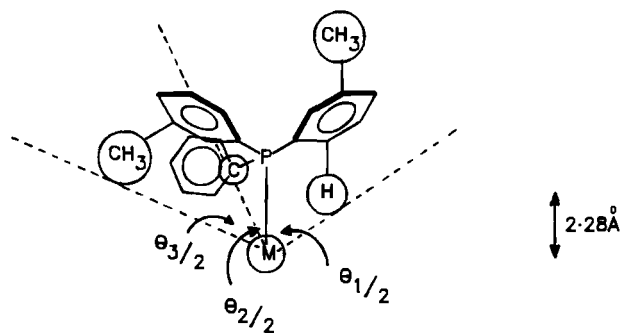


FIG. 3. Measurement of the average Tolman cone angle, θ , for $P(m\text{-tol})_3$. The semivertex angle, $\theta_1/2$, is measured to the *ortho*-hydrogen atom; $\theta_2/2$ is measured to the *ipso*-carbon atom (methyl groups and hydrogens deleted for clarity) and $\theta_3/2$ measured to the *meta*-methyl group.

radii for CPK models were used (e.g., $r_{\text{vdW}}(\text{H}) = 1.00 \text{ \AA}$ not 1.20 \AA), (vi) data are not affected by other ligands surrounding the metal, and (vii) a constant M–P bond length was chosen.

Tolman also recognized that electronic and steric factors are inextricably mixed. Thus, although a steric size can be measured absolutely, *properties* associated with a steric size will be influenced by a mix of steric and electronic factors. He introduced the concept of a *steric/electronic* box, a multivariable statistical approach for taking into account both variables (steric/electronic). Thus, for the dissociation data for $\text{Ni}(\text{CO})_{4-x}\text{L}_x$ complexes, the regression equation, in a multivariable regression, of the surface is

$$z = a\theta + b\nu + c, \quad (2)$$

where θ is the cone angle and ν is the A_1 carbonyl stretching frequency in $\text{Ni}(\text{CO})_3\text{L}$, and a , b , and c are the regression coefficients. The percentage steric character, σ , is then given by

$$\sigma = \frac{a}{a + b} \times 100. \quad (3)$$

For nonplanar surfaces the percentage steric character needs to be defined in terms of partial derivatives:

$$\sigma = \left(\frac{\partial z}{\partial \theta} + \frac{\partial z}{\partial \nu} \right) \times 100. \quad (4)$$

Tolman also measured the sizes of a variety of other ligands commonly encountered in organometallic chemistry (C_5H_5 , CO, CH_3 , and halogens) in precisely an analogous way to the phosphine data.

Yamamoto *et al.* were the first to extend Tolman's work to the measurement of isonitrile cone and fan angles (18). For isonitriles, which do not have cylindrical symmetry, Tolman's cone angle is inappropriate so these authors used the planar width as a measure of the steric bulk of planar ligands (e.g., for 2,6-Me₂C₆H₃NC, xyl-NC). The key assumptions in this approach are: (i) data are derived relative to Rh (M–C distance of 1.92 Å), and C≡N (1.17 Å) and N–C (1.46 Å) bond lengths are based on X-ray crystallographic data, (ii) the M–C≡NR bond is linear, and (iii) the ligand is in the *maximum conformation*. In addition the van der Waals radius of CH₃ was assumed to be 2.00 Å and H 1.20 Å. With these fan angles the authors were able to rationalize the equilibrium between [Rh(CNR)₃Cl] and [Rh(CNR)₄]Cl complexes on the basis, exclusively, of steric effects.

Maitlis, without reporting details, used the Tolman cone angle concept to measure the size of substituted cyclopentadienyl and arene cone angles (19). Using these cone angle data he found that the stabilization of cyclopentadienyl-containing platinum group metal complexes could be rationalized on steric grounds. Cone angles for (η⁵-C₅R₅)Rh(I) and Rh(III) as well as (η⁶-C₆R₆)Rh(O) and Rh(II), R = H, Me, were reported. Maitlis found that the degree of ring proton substitution by alkyl groups resulted in significantly more stable metal cyclopentadienyl complexes. Maitlis also recognized that, although steric effects dominate in the rationalization of this trend, they were not to be used exclusively, as the nature of the leaving group also influenced the results.

Further measurements on the steric sizes of monosubstituted cyclopentadienyl ligands using the Tolman concept were performed by White *et al.* (15). Two methods were employed starting from (i) the metal as apex (θ₁) and (ii) the ring centroid as apex (θ₂) (Fig. 4) and the cone angles of a wide range of commonly encountered C₅H₄R ligands were determined. The cone angles were generated using the software package, ALCHEMY (20), rather than molecular models, with the following assumptions: (i) the cone angle is defined as θ₁ = 2[(4/5)α + (1/5)β], α and β are the half cone angles for C₅H₅ and C₅R₅, respectively; (ii) an M–ring centroid distance of 1.73 Å was chosen. This value corresponds to the Fe–ring centroid distances obtained for a range of [(η⁵-C₅H₄R)Fe(CO)(L)I] complexes (21); (iii) the C₅H₄R ligand was considered to have equivalent C–C (ring centroid–C_{ring} = 1.20 Å) and C–M bond distances; (iv) the atom of the R group directly attached to the ring C atom was assumed to lie in the plane of the ring; (v) for symmetrical substituents (e.g., *t*-Bu), the *maximum* cone angle was measured (i.e., with the C–H bond of the CH₃ group perpendicular to the ring plane); (vi) for unsymmetrical substituents, an *average* cone angle was calculated using the maxima measured in (v);

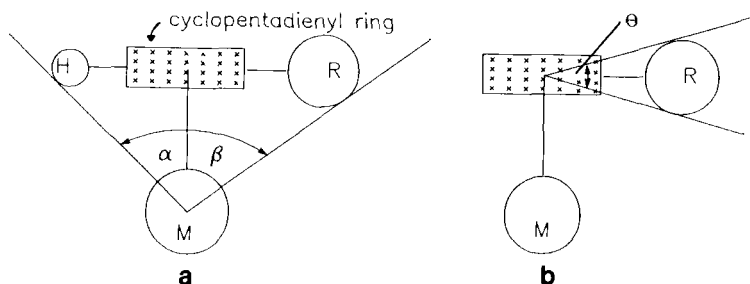


FIG. 4. Measurement of the average cone angle, θ , for a substituted cyclopentadienyl ring. (a) Indicates the measurement of θ_1 (with the metal as apex of the cone). For an n substituted ring, $C_5H_{5-n}R_n$,

$$\theta_1 = \frac{5-n}{5}\alpha + \frac{n}{5}\beta,$$

where α is the cone angle for C_5H_5 and β the cone angle for C_5R_5 . (b) Indicates the measurement of θ_2 with ring centroid as apex.

and (vii) free rotation of the C_5H_4R is assumed, and a hollow, right circular cone is thus implied.

The cone angle measured from the perspective of the cyclopentadienyl ring centroid, θ_2 , was accomplished by two different methods. The first used a procedure similar to that used to generate "ligand profiles" for PR_3 ligands (see Section II,B). The second involved defining a mean plane through the cyclopentadienyl ring carbons and calculating the angle between the vector tangential to the van der Waals radius of the outermost atom and its projection in the plane.

Seligson and Trogler were the first to apply the Tolman concept to amine ligands and used the data to rationalize olefin insertion into Pd–N bonds (22). Tolman's original method was employed: a plexiglass arm cemented to a wooden block was constructed and angles measured with a large protractor (Fig. 5). A metal to nitrogen bond length of 2.20 Å was chosen (average Pd–N bond length as determined from X-ray crystal structures). CPK models were used and the entire system was *calibrated* by reproducing Tolman's phosphine data to within 2° (the accuracy quoted by Tolman in his original work). These authors applied the new cone angle data to the results from crystallographic studies and found that steric effects were the major influence on both the Pd–N distance and the geometrical distortion of the molecule from an idealized square planar geometry. A consideration of kinetic data obtained from the above reaction revealed a steric threshold (see Section V) of ca. 120°. A plot of $\log K$ (the binding constant) versus pK_a versus θ yielded an R^2 of 0.91 for θ values above the steric threshold.

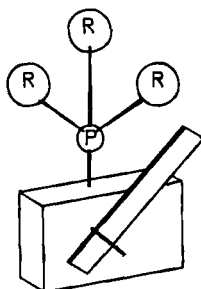


FIG. 5. Cone angle measuring device. Redrawn from Seligson and Trogler (22) with permission.

Recently Marques *et al.* reported linear angles of amines important to the chemistry of aquacobalimin (23). The cone angles were measured in minimum conformation using molecular mechanics with an arbitrary Co-N distance of 1.960 Å. A correlation between cone angle and ΔH^\ddagger was observed.

In 1987 Datta and Sharma proposed that a set of steric measurements for organic ligands generated from the Tolman cone angle approach correlated well with the Dubois steric parameter, E'_s , for organic substituents (14). From six data points these authors found a linear relationship between θ_p (the phosphorus cone angle) and E'_s . In a later publication Datta and Majumdar (14) calculated a series of cone angles for an extended set of alkyl substituents. The major difference in approach to that of Tolman's was that a mathematical (trigonometric) basis was used to assess the steric size. This mathematical methodology was first employed by Imyanitov in 1985 (24). If a *maximum conformation* of the substituent was chosen, the required substituent was considered as built up from a series of fused triangles. By successive applications of the sine and cosine rules a total semivertex angle was calculated (Fig. 6). Datta and Majumdar did not

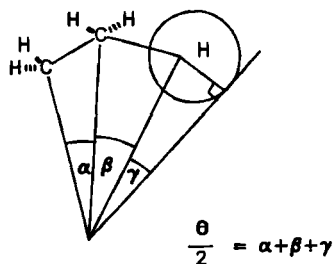


FIG. 6. Calculation of a semivertex angle, $\theta/2$, for an *n*-propyl group in *maximum* conformation by trigonometry. Successive applications of the sine and cosine rules to the three fused triangles allows for evaluation of α , β , and γ .

apply this procedure to the calculation of *hollow cone angles* for substituents like CPh_3 for which this model would also be appropriate. A plot of θ versus E_s (the Taft steric parameter) gave an R^2 of 0.903 and θ vs E_s' an R^2 of 0.908. They were the first to report on the apparently anomalous steric trend detected for the halogens: $\text{F} > \text{I} > \text{Br} > \text{Cl}$. This trend is expected if the van der Waals radii and bond lengths do not change proportionally for the halogens. These authors also could not reproduce Tolman's cone angle for PET_3 as they were considering maximal conformations rather than the minimal used by Tolman. Datta also tested his data by plotting $\log(k/k_0)$ again θ and obtained $R^2 = 0.886$.

There have been many attempts to modify the Tolman cone angle values by correlating the cone angles with chemical and physical properties. For example, Mosbo and co-workers (25) investigated the *cis:trans* ratio of products in $\text{W}(\text{CO})_4\text{LL}'$ complexes to assess steric size. The ligands that were chosen all had similar electronic characteristics. A general decrease in *cis:trans* ratio with increasing size of L' was noticed which the authors believed was due to steric constraints. The correlation revealed two anomalies, for $\text{L} = \text{PET}_3$ and $\text{P}(n\text{-Bu})_3$. The θ value predicted from the equilibrium data was 10° larger than the Tolman values. It was proposed that these differences arose from measurements being based on *minimum conformations* (Tolman). Mosbo and co-workers used molecular mechanics to address the problem of conformation. For details see Section III (26).

Recently Casey and Whiteker used molecular mechanics to design a diphosphine ligand with a bite angle of 120° (27). In Tolman's approach the cone angle for each phosphorus atom (θ) is defined as the sum of the angle between one M-P bond and the vector bisecting the P-M-P bite angle (β) and the cone angle of the nonbridging substituents (11,13) (Fig. 7). To ensure diequatorial bonding in a trigonal bipyramidal arrangement a diphosphine with $\beta = 120^\circ$ was required ($\beta = 90^\circ$ would result in a mix of axial and equatorial chelation). Using molecular mechanics (AMBER force field) to predict the bite angle, a good correlation was observed

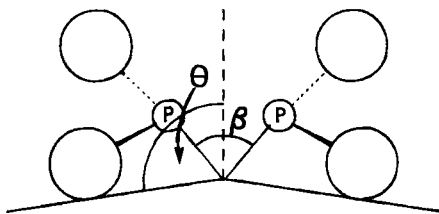


FIG. 7. Illustration of the difference between the bite angle β and the Tolman cone angle θ for a bidentate phosphine. Redrawn from Casey and Whiteker (27) with permission.

between predicted β and that measured directly in crystal structures ($R^2 = 0.85$ over a 50° change in β). This is one of the first recorded uses of molecular mechanics to predict steric effects. These principles were used and the complex [*trans*-1,2-bis((diphenylphosphino)methyl)cyclopropane]irontricarbonyl was synthesized (28). X-ray crystal structure determination revealed a P–Fe–P bite angle of 152.0° . Recently Casey and co-workers have found a correlation between the natural bite angle of chelating diphosphines and regioselectivity in rhodium catalyzed hydroformylation of 1-hexene (29).

Some 10 years after the Tolman review, Stahl and Ernst reported a correction of some of the Tolman cone angles based on enthalpies of dissociation in bis(2,4-dimethylpentadienyl)titanium complexes (30). A plot of the enthalpy of dissociation against θ revealed that the phosphites P(OMe)_3 and P(OEt)_3 as well as PET_3 were all too small to fit the observed thermodynamic data. Thus, these authors proposed the values be increased (to 128° for P(OMe)_3 , 134° for P(OEt)_3 and 137° for PET_3). These corrected data were used by Bosolo and co-workers in a recent publication for the same reasons (31).

The quantification of steric effects has also been applied to organometallic clusters. The first study was reported by Mingos (32) who applied the Tolman linear angle concept to cluster sizes with one modification: the apex of the cone was located at the origin of the cluster polyhedron instead of on the phosphorus atom associated with the ligand (Fig. 8). The approach was semiquantitative as the approximations inherent in the Tolman model were significant when attempting to predict absolute cluster conformations. Data for tetrahedral, octahedral, and icosahedral clusters were presented. The maximum number of ligands found in a particular geometry, n_{max} , was defined as the ideal polyhedral cone angle multiplied

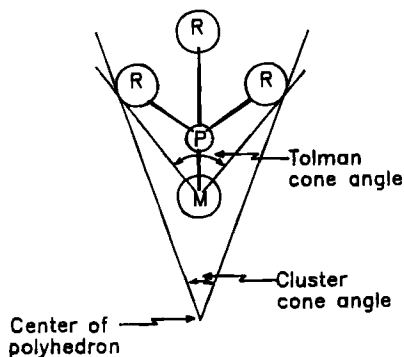


FIG. 8. Illustration of the cluster cone angle. Redrawn from Mingos (32) with permission.

by the number of metal atoms divided by the metal fragment cone angle. The ideal polyhedron cone angles are 109.5° (tetrahedral), 90.0° (octahedral), and 63.9° (icosahedral). When the number of ligands exceeds n_{\max} , steric effects influence complex stability. Under these conditions the cluster may adopt spherical polyhedral geometries. These data were confirmed by an examination of crystal structures. For example $(\eta^5\text{-C}_5\text{H}_5)_6\text{M}_6$ complexes are sterically saturated (cluster cone angle 92° octahedral cone angle 90°), whereas $(\eta^5\text{-C}_5\text{H}_5)_4\text{M}_4$ complexes are sterically unsaturated.

Linear angles for selected phosphines, phosphites, amines, alkyls, isonitriles, cyclopentadienyls, and clusters are given in Tables I–VIII.

TABLE I
STERIC SIZES FOR PR^3 LIGANDS

Ligand	$\theta/^\circ{}^a$	$\theta/^\circ{}^b$	Ω/sr^c	$\Omega/^\circ{}^c$	Ω_s^c	E_R^d
PH_3	87	91.2^e	1.26	74	0.100	
PH_2Ph	101	106.4^e	2.12	97	0.168	
PH_2Me		104.5^e	2.09	96	0.166	
PF_3	104		2.12	97	0.169	
$\text{Me}_2\text{PCH}_2\text{CH}_2\text{PMe}_2$	107					
PH_2Et		111.0^e	2.21	99	0.176	
$\text{PH}_2(o\text{-MePh})$		113.3^e	2.40	104	0.191	
$\text{Et}_2\text{PCH}_2\text{CH}_2\text{PEt}_2$	115					
PCyH_2	115		2.98	117	0.234	32
$\text{PH}_2(i\text{-Pr})$		115.7^e	2.51	106	0.200	
PHMe_2		117.9^e	2.82	113	0.224	
$\text{PH}_2(t\text{-Bu})$		118.3^e	2.88	114	0.229	
PMe_3	118	136.9^e	3.35	124	0.267	39
PHMePh		120.2^e	2.86	114	0.227	
$\text{Ph}_2\text{PCH}_2\text{PPh}_2$	121					
PMe_2Ph	122	141.7^e	3.45	126	0.274	44
		112–	2.79–			
		118^f	3.06^f			
PMe_2Et	123		3.76	133	0.299	48
PCl_3	124		2.51	106	0.199	
$\text{PMe}_2(\text{CF}_3)$	124		3.92	136	0.312	
$\text{Ph}_2\text{PCH}_2\text{CH}_2\text{PPh}_2$	125					
$\text{Ph}_2\text{P}(\text{CH}_2)_3\text{PPh}_2$	127					
PEt_2Me	127		4.04	138	0.322	57
PHPh_2	128		2.75	112	0.219	38
PHEtPh		129.9^e	2.93	116	0.233	
PBr_3	131		2.66	110	0.212	
PPhCl_2		131^g	2.77	112	0.221	
$\text{PMe}_2(i\text{-Pr})$	132		4.15	140	0.331	57
$\text{P}(\text{CH}_2\text{CHCH}_3)_3$		132^g	4.29	143	0.341	

(continued)

TABLE I (continued)

Ligand	$\theta/^\circ$ ^a	$\theta/^\circ$ ^b	Ω/sr ^c	$\Omega/^\circ$ ^c	Ω_s^c	E_R^d
PEt ₃	132	166.4 ^e 137 ^h 119– 130 ^f	4.31 3.09– 3.72 ^f	143	0.344	61
P(<i>n</i> -Pr) ₃	132		4.53	148	0.360	
P(<i>n</i> -Bu) ₃	132		4.53	148	0.360	64
P(CH ₂ CH ₂ CN) ₃		132 ^g	4.69	151	0.373	
PPh ₂ Me	136	117– 126 ^f	3.34 2.99– 3.44 ^f	124	0.266	57
PPhEt ₂	136		3.96	137	0.316	57
PPh(<i>n</i> -Bu) ₂	136		4.85	154	0.386	77
PH(Et) ₂		137.3 ^e	3.24	122	0.258	
P(CF ₃) ₃	137		4.64	150	0.369	
PPh ₂ Cl	138	137 ^g	2.99	117	0.238	48
PMe ₂ (<i>t</i> -Bu)	139		4.32	144	0.344	66
PPh ₂ Et	140		4.12	140	0.328	66
PPh ₂ (<i>n</i> -Bu)	140		4.13	140	0.329	66
PEt ₂ (<i>i</i> -Pr)	141		4.64	150	0.369	75
Cy ₂ PCH ₂ CH ₂ PCy ₂	142					
PCy ₂ H	143		4.49	147	0.358	66
P(<i>i</i> -Bu) ₃	143		5.91	173	0.470	83
PPh ₂ (<i>i</i> -Bu)	144		4.54	148	0.361	71
P(<i>p</i> -ClPh) ₃	145		3.58	129	0.285	74
P(<i>p</i> -FPh) ₃	145		3.59	129	0.286	74
P(<i>p</i> -MePh) ₃	145		3.60	129	0.286	74
PPh ₃	145	120 ⁱ 123– 134 ^f	3.60 3.31– 3.82 ^f	129	0.286	75
P(<i>p</i> -OMePh) ₃	145		3.60	129	0.286	76
P(<i>m</i> -FPh) ₃	145		3.78	133	0.301	
P(<i>m</i> -ClPh)	145	165 ^g	3.91	136	0.311	78
P(<i>m</i> - <i>t</i> -BuPh) ₃	145		5.12	159	0.407	83
P(<i>i</i> -Pr) ₂ Me	146		4.72	151	0.375	78
PH(<i>i</i> -Pr) ₂		147.5 ^e	3.93	136	0.312	
P(<i>m</i> -MePh) ₃	148 ⁱ	165 ^g	4.16	140	0.331	79
PEt ₂ (<i>t</i> -Bu)	149		5.00	156	0.398	90
PPh ₂ (<i>i</i> -Pr)	150	151 ^g	4.07	139	0.324	75
P(<i>i</i> -Pr) ₂ Et	151		5.00	156	0.398	91
P(NMe ₂) ₃	152		5.40	164	0.430	
PPh ₂ Bz	152		4.06	139	0.323	74
PPh ₂ Cy	153		4.65	150	0.371	77
PPh ₂ (<i>t</i> -Bu)	157		4.60	149	0.366	97
PPh ₂ (C ₆ F ₅)	158		3.93	136	0.312	

(continued)

TABLE I (continued)

Ligand	$\theta/^\circ$ ^a	$\theta/^\circ$ ^b	Ω/sr ^c	$\Omega/^\circ$ ^c	Ω_S ^c	E_R ^d
P(<i>i</i> -Pr) ₃	160	135– 137 ^f	5.34 3.89– 4.02 ^f	163	0.425	109
P(<i>s</i> -Bu) ₃	160		5.83	172	0.464	
P(<i>t</i> -Bu) ₂ Me	161		5.33	163	0.424	113
PPhCy ₂	162		5.51	166	0.439	105
P(<i>t</i> -Bu) ₂ Et	165		5.25	161	0.418	125
PBz ₃	165		5.38	163	0.428	82
P(<i>i</i> -Pr) ₂ (<i>t</i> -Bu)	167		5.71	170	0.454	123
PPh(<i>t</i> -Bu) ₂	170	147– 155 ^f	5.61 4.50– 4.94 ^f	168	0.447	124
PCy ₃	170	163– 181 ^k 138– 149 ^f	6.33 4.02– 4.61 ^f	181	0.504	116
PPh ₂ (<i>o</i> -OMePh)		171 ^g	3.63	130	0.289	
P(<i>t</i> -Bu) ₂ (<i>i</i> -Pr)	175		6.18	178	0.492	127
P(neopentyl) ₃	~180		5.91	173	0.470	
P(<i>t</i> -Bu) ₃	182	176– 189 ^k	6.37	182	0.507	154
P(C ₆ F ₅) ₃	184		4.87	154	0.388	
P(<i>o</i> -MePh) ₃	194		4.22	142	0.336	113
P(menthyl) ₂ (<i>i</i> -Pr)	209 ^f	176.5 ^f	7.12 6.09 ^f	195	0.566	
P(mesityl) ₃	212	203– 208 ^l	6.01	175	0.479	

^a Tolman, C. A. *Chem. Rev.* **1977**, *77*, 313.^b Modifications to the Tolman cone angle.^c White, D.; Wade, P. W.; Coville, N. J. *Inorg. Chem.*, in preparation. The solid angle, Ω , is measured in steradians. The measure in degrees refers to a right circular cone with that solid angle. Ω_S is $\Omega/4\pi$ and gives the fraction of a sphere occupied.^d Brown, T. L. *Inorg. Chem.* **1992**, *31*, 1286; E_R is measured in kcal mol⁻¹.^e de Santo, J. T.; Mosbo, J. A.; Storhoff, B.-N.; Bock, P. L.; Bloss, R. E. *Inorg. Chem.* **1980**, *19*, 3086.^f Immirzi, A.; Musco, A. *Inorg. Chim. Acta* **1977**, *25*, L41; based on crystal structure data for a wide variety of metals.^g Rahman, M. M.; Liu, H. Y.; Prock, A.; Giering, W. P. *Organometallics* **1987**, *6*, 650.^h Stahl, L.; Ernst, R. D. *J. Am. Chem. Soc.* **1987**, *109*, 5673.ⁱ Mullica, D. F.; Gipson, S. L.; Sappenfield, E. L.; Lin, C. C.; Leschnitzer, D. H. *Inorg. Chim. Acta* **1990**, *177*, 89, based on Mo systems.^j White, D.; Carlton, L.; Coville, N. J. *J. Organomet. Chem.* **1992**, *440*, 15.^k Ferguson, G.; Roberts, P. J.; Alyea, E. C.; Khan, M. *Inorg. Chem.* **1978**, *17*, 2965; measurements based on Hg, Pt, Ni and Ir systems.^l Alyea, E. C.; Ferguson, G.; Somogyvani, A. *Inorg. Chem.* **1982**, *21*, 1369; measurement based on Ag system.

TABLE II
 STERIC SIZES FOR P(OR)₃, P(OR)₂A, P(OR)A₂ LIGANDS

Ligand	$\theta/^\circ$ ^a	Ω/sr ^b	$\Omega/^\circ$ ^b	Ω_s ^b	E_R ^c
P(OCH ₂) ₃ CMe	101	1.55	82	0.124	25
P(OMe) ₂ Et	106	3.30	123	0.262	69
P(OMe) ₃	107	2.83	113	0.225	52
	128 ^d				
P(OEt) ₃	109	3.01	117	0.239	59
	134 ^d				
P(OCH ₂ CH ₂ Cl) ₃	110	3.18	121	0.253	
P(O- <i>n</i> -Bu) ₃	110	4.46	146	0.355	64
P(OMe) ₂ Ph	115	2.95	116	0.235	69
P(OEt) ₂ Ph	116	3.43	126	0.273	
P(OPh)Me ₂	121	3.49	127	0.278	57
P(O- <i>p</i> -MePh) ₃	128	3.15	120	0.251	
P(OPh) ₃	128	3.85	135	0.307	65
P(O- <i>i</i> -Pr) ₃	130	4.01	138	0.319	74
P(OMe)Ph ₂	132	3.39	125	0.270	62
P(OEt)Ph ₂	133	3.18	121	0.253	62
P(O- <i>o</i> -MePh) ₃	141	4.49	147	0.357	
P(O- <i>i</i> -Pr) ₂ (O- <i>t</i> -Bu)	144	4.52	147	0.359	78
P(O- <i>o</i> - <i>i</i> -PrPh) ₃	148	5.26	161	0.418	
P(O- <i>o</i> -PhPh) ₃	152	5.42	164	0.431	
P(O- <i>i</i> -Pr)(O- <i>t</i> -Bu) ₂	158	4.69	151	0.373	90
P(O- <i>t</i> -Bu) ₃	172	5.10	158	0.406	99
P(O- <i>o</i> - <i>t</i> -BuPh) ₃	175	5.43	164	0.432	

^a Tolman, C. A. *Chem. Rev.* **1977**, 77, 313.^b White, D.; Wade, P. W.; Coville, N. J. *Inorg. Chem.*, in preparation. See Table I footnote c.^c Brown, T. L. *Inorg. Chem.* **1992**, 31, 1286; E_R is measured in kcal mol⁻¹.^d Stahl, L.; Ernst, R. D. *J. Am. Chem. Soc.* **1987**, 109, 5673.
 TABLE III
 STERIC SIZES FOR AMINES

Ligand	$\theta/^\circ$ ^a	Ω/sr ^b	$\Omega/^\circ$ ^b	Ω_s ^b	E_R ^c
NH ₂ (<i>i</i> -Bu)	106	3.34	124	0.266	33
NPh ₃	166	4.09	139	0.325	
Imidazole	82.9 ^d	1.65 ^e	84.7 ^e	0.131 ^e	
Histamine	83.5 ^d	1.99 ^e	93.6 ^e	0.158 ^e	
NH ₃	94	1.74	87	0.138	10
NH ₂ OH	45.2 ^d	1.88 ^e	91 ^e	0.149 ^e	
NH ₂ OMe		1.97 ^e	93.4 ^e	0.157 ^e	
4-Mepyridine	91.9 ^d	1.61 ^e	84.0 ^e	0.128 ^e	
Pyridine	91.9 ^d	1.61 ^e	84.0 ^e	0.128 ^e	

(continued)

TABLE III (continued)

Ligand	$\theta/^\circ$ ^a	Ω/sr ^b	$\Omega/^\circ$ ^b	Ω_s^b	E_R^c
NH ₂ Me	106	2.44	105	0.194	30
		2.90 ^e	115 ^e	0.231 ^e	
NH ₂ Et	106	2.61	109	0.208	31
NH ₂ Ph	111	2.66	110	0.212	
NH ₂ (<i>s</i> -Bu)	113	2.74	111	0.218	43
NH ₂ (<i>n</i> -Pr)	106	2.75	112	0.219	31
		3.10 ^e	119 ^e	0.247 ^e	
NH ₂ CH ₂ CO ₂ Me	68.3 ^d	3.10 ^e	119 ^e	0.247 ^e	
NH ₂ (CH ₂) ₃ OH		3.15 ^e	120 ^e	0.251 ^e	
NH ₂ CH ₂ CH ₂ OH		2.92 ^e	115 ^e	0.232 ^e	
NH ₂ (<i>i</i> -Pr)	106	2.95	116	0.235	41
NHMe ₂	119	2.96	116	0.236	64
NH ₂ CH ₂ CH(OH)CH ₂ OH		3.12 ^e	120 ^e	0.248 ^e	
NH ₂ (<i>t</i> -Bu)	123	3.11	119	0.247	53
NHEtMe	119	3.17	121	0.252	62
NH ₂ (neopentyl)	106	3.31	123	0.263	35
NMe ₃	132	3.31	124	0.263	93
NHMePh	126	3.34	124	0.265	
NHPh ₂	136	3.47	127	0.276	
NH ₂ Cy	115	3.47	127	0.276	41
NHPh ₂	136	3.47	127	0.276	
NMe ₂ Et	132	3.51	128	0.279	81
NHEt ₂	125	3.52	128	0.280	73
NHEtPh	126	3.56	129	0.284	
NMe ₂ Ph		3.58	129	0.285	
Quinuclidine	132	3.58	129	0.285	104
NH(<i>n</i> -Pr) ₂	127	4.00	137	0.319	81
NH ₂ (adamantyl)	127	4.05	138	0.322	53
Piperidine	121	4.09	139	0.326	61
NEt ₂ Me	132	4.14	140	0.329	
NMeEt ₂	145	4.14	140	0.329	93
NEt ₃	150	4.21	142	0.335	109
NH(<i>i</i> -Pr) ₂	137	4.35	144	0.346	105
NEt ₂ Ph	170	4.36	144	0.347	
NH(<i>i</i> -Bu) ₂	138	4.40	145	0.350	85
NH(<i>s</i> -Bu) ₂	158	4.45	146	0.354	88
NHBz ₂	140	4.47	146	0.356	
N(<i>n</i> -Pr) ₃	160	5.22	161	0.416	112
N(<i>i</i> -Pr) ₃	220	5.25	161	0.418	179
NHCy ₂	~133	5.39	164	0.429	113
NBz ₃	210	5.90	173	0.469	
NCy ₃		7.09	195	0.564	

^a Seligson, A. L.; Trogler, W. C. *J. Am. Chem. Soc.* **1991**, *113*, 2520, unless otherwise mentioned.

^b White, D.; Wade, P. W.; Coville, N. J. *Inorg. Chem.*, in preparation.

^c Choi, M.-G.; Brown, T. L. *Inorg. Chem.* **1993**, *32*, 1548.

^d Marques, H. M.; Bradley, J. C.; Campbell, L. A. *J. Chem. Soc., Dalton Trans.* **1992**, 2019.

^e Measured with M–N distance of 1.98 Å based on cobalamine system.

TABLE IV
STERIC SIZES OF ALKYL AND ARYL GROUPS

Substituent	$-E_s^a$	$-E_s^{t,b}$	Ω/sr^c	Ω'/sr^c	$\Omega_{\text{S,Me}}^d$	$\Omega_{\text{S,Me}}^e$	$\Omega_{\text{S,COOH}}^d$	$\Omega_{\text{S,COOH}}^e$	$\theta/^\circ f$
H	-1.24	-1.12	0°						84
F		-0.57	19.5°						90
CH ₃ C(OH)H-		-0.08							
HOCH ₂ -		-0.03			0.232				
CN	-0.73								95
Me	0.0	0.0	0.800	0.800	0.206	0.206	0.211	0.211	112
			29.2°						
Cl		0.02	28.7°						92
cyclo-C ₄ H ₇	0.06	0.03							
MeCH ₂ -	0.07	0.08							123
Et	0.07	0.08	1.638	1.324	0.256	0.256	0.259	0.259	
I	0.16								91
ClCH ₂ -	0.24	0.18	1.866	1.357	0.239				128
MeOCH ₂ -	0.19				0.240				
FCH ₂ -	0.24	0.20	1.533	1.225	0.228				119
Br		0.22	33.8°						91
BrCH ₂ -	0.27	0.24	1.992	1.407	0.242				130
ICH ₂ -	0.37	0.30	2.149	1.458	0.245				133
CH ₂ =CHCH ₂ -		0.31							
<i>i</i> -BuCH ₂ CH ₂ -		0.31							
<i>n</i> -Pr	0.36	0.31	2.017	1.702	0.269	0.273	0.274	0.274	143
<i>n</i> -Bu	0.39	0.31	2.447	1.848	0.269	0.272	0.276	0.275	143
<i>n</i> -C ₅ H ₁₁	0.40	0.31			0.270	0.272	0.278	0.275	143
PhOCH ₂ -	0.33	0.32							
<i>i</i> -PrCH ₂ CH ₂ -	0.35	0.32							
F ₂ CH-	0.67	0.32	2.262	1.646	0.248				127
Ph(CH ₃) ₄		0.33							143
<i>t</i> -BuCH ₂ CH ₂ -	0.34	0.33							

2-furylCH ₂ –		0.34								
cyclo-C ₆ H ₁₁ CH ₂ CH ₂ –		0.34								
Ph(CH ₂) ₃	0.45	0.34								143
CH ₃ (CH ₂) _n C(OH),		0.35								
<i>n</i> > 1										
PhCH ₂ CH ₂ –	0.38	0.35								
cyclo-C ₆ H ₁₁ (CH ₂) ₃		0.36								
PhCH ₂ –	0.38	0.39								
F(CH ₂) ₂ CH ₂ –	0.40									143
cyclo-C ₅ H ₉	0.51	0.41								
CH ₂ =CH(CH ₂) _m ,		0.43								
<i>m</i> > 2										
PhCH ₂ MeCH–		0.44								
<i>n</i> -C ₆ H ₁₃	0.44				0.271	0.271	0.280	0.279		143
EtMeCH–		0.449	2.855	2.226						
<i>i</i> -Pr	0.47	0.48			0.304	0.304	0.306	0.305		135
Cl(CH ₂) ₂ CH–	0.48									143
I		0.50	40.9°							
MeClCH–	0.50									139
CH ₃ (CH ₂) _n CO		0.52								
Cl ₂ CH–	1.54	0.58	2.928	1.910	0.275					144
cyclo-C ₆ H ₁₁	0.79	0.69								
3-furylCH ₂ –		0.74								
MeCOCH ₂ –	0.75				0.267					
Me ₂ (CN)C–	0.76									147
Br ₂ CH–	1.86	0.76	3.186	2.017	0.280					148
MeOCH ₂ CH ₂ –	0.77				0.267					
F ₃ C–	1.16	0.78	2.991	2.067	0.268					135
			58.4°							
NCCH ₂ –		0.89								
CNCH ₂ –	0.94 ^f	0.89			0.274					124
	1.14 ^d									

(continued)

TABLE IV (continued)

Substituent	$-E_s^a$	$-E_s'^b$	Ω/sr^c	Ω'/sr^c	$\Omega_{S,\text{Me}}^d$	$\Omega_{S,\text{Me}}^e$	$\Omega_{S,\text{COOH}}^d$	$\Omega_{S,\text{COOH}}^e$	$\theta/^\circ$
cyclo-C ₆ H ₁₁ CH ₂ -	0.98	0.89							
CNCH ₂ CH ₂ -	0.90								146
ClCH ₂ CH ₂ -	0.90				0.257				139
PhMeCH-	1.19	0.90							
cyclo-C ₇ H ₁₃	1.10	0.92							
ICH ₂ -		0.93							154
<i>i</i> -PrCH ₂ -		0.93	2.396	2.082					
I ₂ CH-		0.93	3.498	2.117					
MeBrCH-	0.93								141
<i>i</i> -Bu	0.93	0.93			0.298	0.295	0.305	0.303	
<i>s</i> -BuCH ₂ -		0.97							
<i>s</i> -Bu	1.13	1.00			0.326	0.325	0.334	0.333	154
<i>n</i> -PrMeCH-		1.02							154
ICH ₂ CH ₂ -	1.02								145
<i>n</i> -BuMeCH-		1.06							154
cyclo-C ₃ H ₅		1.09							
FluorenylCl		1.13							
BrCH ₂ CH ₂ -	1.27								142
PhEtCH-	1.50	1.32							
AnthracenylCH		1.35							
MeICH-	1.36								144
CH ₃ (CH ₂) _{<i>n</i>} C(OMe)H		1.39							
<i>t</i> -Bu	1.54	1.43	3.317 61.8°	2.374	0.352	0.352	0.354	0.354	146
Ph ₂ CH-	1.76	1.50							
<i>t</i> -BuCH ₂ -	1.74	1.63	2.774	2.460	0.331	0.331	0.338	0.338	
Cl ₃ C-	2.06	1.75	3.996 68.6°	2.469	0.318				160
BrMe ₂ C-		1.77	3.670	2.476					153
Me ₃ Si-		1.79	56.8°						

FluorenylCMe		1.81							
<i>t</i> -BuCH ₂ MeCH-	1.83	1.81							
NH ₃ CH ₂ CH ₂ -	1.82								142
Br ₂ MeC-		1.92	4.023	2.576					160
<i>i</i> -PrMeCH-		1.94	3.234	2.606					
PhC≡C-		1.97							
<i>n</i> -PrEtCH-		2.00							174
Et ₂ CH	1.98	2.00	3.234	2.606	0.356	0.355	0.373	0.368	174
<i>n</i> -BuEtCH		2.03							174
<i>n</i> -Pr ₂ CH-	2.11	2.03			0.361	0.360	0.384	0.377	174
CH ₂ =CH-		2.07							
FluorenylCEt		2.07							
<i>n</i> -Bu ₂ CH-		2.08							174
Br ₃ C-	2.43	2.24	4.376 72.3°	2.626	0.323				167
EtMe ₂ C-		2.28	3.694	2.751	0.378	0.378	0.387	0.387	
NH ₃ CH ₂ -	2.30								124
Ph		2.31							
2-furyl		2.33							
<i>i</i> -Bu ₂ CH-	2.47	2.38			0.382	0.378	0.399	0.403	
<i>t</i> -BuCH ₂ Me ₂ C-	2.57	2.48							
I ₃ C-		2.62	4.847 76.8°	2.771					175
2-furyl		2.63							
<i>o</i> -tolyl		2.82							
<i>o</i> -EtPh		2.97							
<i>o</i> -PhPh		3.01							
<i>o</i> -PrPh		3.04							
(<i>t</i> -BuCH ₃) ₂ CH-	3.18	3.06							
<i>t</i> -BuMeCH-	3.33	3.21	3.613	2.985	0.383	0.383	0.391	0.391	
FluorenylCPh		3.23							
<i>i</i> -PrEtCH-		3.23	3.613	2.985	0.386	0.389	0.401	0.402	
FluorenylC(<i>i</i> -Pr)		3.46							

(continued)

TABLE IV (continued)

Substituent	$-E_S^a$	$-E_S^b$	Ω/sr^c	Ω'/sr^c	$\Omega_{S,\text{Me}}^d$	$\Omega_{S,\text{Me}}^e$	$\Omega_{S,\text{COOH}}^d$	$\Omega_{S,\text{COOH}}^e$	$\theta/^\circ f$
<i>i</i> -PrMe ₂ C-		3.54	4.074	3.131	0.404	0.404	0.410	0.408	
Et ₃ MeC-		3.63	4.074	3.131	0.402	0.405	0.414	0.412	186
Ph ₂ MeC-	3.55	3.73							201
FluorenylC(<i>t</i> -Bu)		4.32							
Ph ₂ EtC-	4.34	4.55							221
Ph ₃ C-	4.68	4.91							228
<i>i</i> -Pr ₂ CH-		5.01	3.992	3.363	0.418	0.419	0.431	0.431	
<i>t</i> -BuEtCH-		5.21	3.992	3.363					
<i>i</i> -PrEtMeC-		5.21	4.451	3.509					
Et ₃ C-		5.29	4.451	3.509	0.429	0.429	0.437	0.437	205
<i>t</i> -BuMe ₂ C-		5.40	4.451	3.509	0.434	0.434	0.440	0.440	
<i>i</i> -PrEt ₂ C-		6.20	4.830	3.888	0.459	0.460	0.463	0.464	
<i>t</i> -Bu- <i>i</i> -PrCH-		6.53	4.371	3.742	0.453	0.454	0.459	0.460	
<i>t</i> -Bu- <i>i</i> -PrEtC-		6.62	5.587	4.645					
<i>i</i> -Pr ₃ C-		6.73	5.587	4.645	0.522	0.522	0.515	0.515	
<i>t</i> -Bu ₂ CH-		6.97	4.749	4.121	0.473	0.473	0.483	0.483	
<i>t</i> -BuEt ₂ C-		7.21	5.208	4.266	0.491	0.491	0.492	0.494	
<i>i</i> -Pr ₂ MeC-		7.38	4.830	3.888					
<i>i</i> -Pr ₂ EtC-	7.38	5.208	4.266						
<i>t</i> -Bu- <i>i</i> -PrMeC-	7.56	5.208	4.266						

^a Taft, R. W. In "Steric Effects in Organic Chemistry"; Newman, M. S., Ed.; Wiley: New York, 1956; p. 556.

^b MacPhee, J. A.; Panaye, A.; Dubois, J.-E. *Tetrahedron* **1978**, *34*, 3553.

^c Chauvin, R.; Kagan, H. B. *Chirality* **1991**, *3*, 242; solid angles measured in steradians unless indicated.

^d Komatsuzaki, T.; Sakakibara, K.; Hirota, M. *Chem. Lett.* **1990**, 1913; Akai, I.; Sakakibara, K.; Hirota, M. *Chem. Lett.* **1992**, 1317; Komatsuzaki, T.; Akai, I.; Sakakibara, K.; Hirota, M. *Tetrahedron* **1992**, *48*, 1539; measured using steric energy.

^e As for footnote *d* but measured using free energy.

^f Datta, D.; Majumdar, D. J. *Phys. Org. Chem.* **1991**, *4*, 611.

TABLE V
SOLID ANGLES OF $C_5H_5-nR_n^a$

Substituent	$\theta_1/^{\circ b}$	$\theta_2/^{\circ c}$	$\Omega_{av}/^{\circ d}$	Substituent	$\theta_1/^{\circ b}$	$\theta_2/^{\circ c}$	$\Omega_{av}/^{\circ d}$
CH=CH ₂	151	39		Me, $n = 2$			157
Ph	133	71		NHMe			150
H	128	55	131	<i>i</i> -Pr	150	107	156
	148, 150 ^e				135 ^f		
	116 ^f			NMe ₂	154	131	158
F			133	SiMe ₃	158	138	161
OMe	155	132			144 ^f		
SH			132	Me, $n = 3$			167
Cl			134	CMePh ₂	163	161	
Br			135	<i>t</i> -Bu	154	128	164
I	131	62	135		139 ^f		
NH ₂	141	64	138	Me, $n = 4$			177
SMe	154	122	139	CMe ₂ Ph	158	144	172
Me	141	64	144		145 ^f		
	128 ^f			<i>n</i> -Pr	178	172	
CO ₂ Me	132	47	141	NEt ₂	176	174	
NO ₂	142	60	141	Me, $n = 5$	182, 188 ^e		187
PMe ₃	159	143		MePh ₂			180
COMe	142	47	144	CH ₂ Ph	150	102	182
Ph			144	CPh ₃	167	178	191
PPh ₃	170	149		CHPh ₂	158	140	192
Et	146	85	150				
	132 ^f						

^a $n = 1$ unless otherwise indicated.

^b Coville, N. J.; Loonat, M. S.; White, D.; Carlton, L. *Organometallics* **1992**, *11*, 1082; measured from the ring centroid as apex, based on Fe system with Centroid-Fe distance of 1.73 Å.

^c Reference as for footnote *b* but measured from the perspective of the ring centroid.

^d White, D.; Taverner, B. C.; Leach, P. G. L.; Coville, N. J. *J. Comput. Chem.* **1993**, *14*, 1042; solid angle measured from Fe with Centroid-Fe distance of 1.73 Å.

^e Maitlis, P. M. *Chem. Soc. Rev.* **1981**, *1*; values for Rh^I and Rh^{III} complexes.

^f Möhring, P. C.; Coville, N. J. *J. Mol. Catal.* **1992**, *77*, 41; based on Zr system with Centroid-Zr distance of 2.2 Å.

TABLE VI
CLUSTER CONE ANGLES FOR SOME METAL FRAMENTS^a

	Tetrahedron	Octahedron	Icosahedron
Ideal cone angle	109.5	90.0	63.9
	M(η^5 -C ₅ H ₅)		
M-M = 2.50 Å	97	92	82
M-M = 2.90 Å	90	85	55
	M(CO) ₃		
M-M = 2.50 Å	114	108	96
M-M = 2.90 Å	108	102	90
	M(CO) ₂		
M-M = 2.50 Å	68	64	57
M-M = 2.90 Å	64	60	54
	M(CO)		
M-M = 2.50 Å	36	34	30
M-M = 2.90 Å	33	31	28
	MCl		
M-M = 2.50 Å	55	51	44
M-M = 2.90 Å	50	47	40

^a Mingos, D. M. P. *Inorg. Chem.* **1982**, *21*, 466.

TABLE VII
STERIC SIZES FOR SULFIDES

Ligand	E _R ^a	Ligand	E _R ^a
SMe ₂	42	S(<i>n</i> -Pr)(<i>n</i> -Bu)	65
S(<i>i</i> -Bu)(<i>s</i> -Bu)	55	S(<i>s</i> -Bu)(<i>t</i> -Bu)	61
SMe(<i>n</i> -Pr)	51	S(benzyl)Et	63
SMe(<i>i</i> -Pr)	54	S(benzyl)(<i>i</i> -Pr)	61
SMe(<i>s</i> -Bu)	46	SEt(<i>i</i> -Bu)	63
SMe(<i>n</i> -Bu)	52	S(<i>n</i> -Bu) ₂	63
SMeEt	51	S(<i>n</i> -Pr) ₂	64
SMe(<i>i</i> -Bu)	54	S(benzyl)(<i>s</i> -Bu)	64
SEt(<i>i</i> -Pr)	58	S(<i>n</i> -Pr)(<i>i</i> -Bu)	65
SEt(<i>n</i> -Bu)	62	S(<i>i</i> -Bu) ₂	68
S(<i>n</i> -Pr)(<i>s</i> -Bu)	55	S(benzyl)(<i>n</i> -Bu)	64
S(benzyl)(<i>i</i> -Bu)	64	SEt(<i>t</i> -Bu)	68
SMe(<i>t</i> -Bu)	57	S(<i>i</i> -Pr) ₂	71
S(<i>n</i> -Pr)(<i>i</i> -Pr)	53	S(<i>n</i> -Bu)(<i>t</i> -Bu)	72
S(<i>i</i> -Pr)(<i>i</i> -Bu)	57	S(benzyl)(<i>n</i> -Pr)	64
S(<i>n</i> -Bu)(<i>i</i> -Bu)	68	S(<i>n</i> -Pr)(<i>t</i> -Bu)	69
S(<i>n</i> -Bu)(<i>s</i> -Bu)	56	S(<i>i</i> -Bu)(<i>t</i> -Bu)	72
SEt ₂	59	S(<i>i</i> -Pr)(<i>t</i> -Bu)	73
S(benzyl)Me	56	S(<i>s</i> -Bu) ₂	61
SEt(<i>s</i> -Bu)	53	S(benzyl)(<i>t</i> -Bu)	73
SEt(<i>n</i> -Pr)	62	S(<i>t</i> -Bu) ₂	79
S(<i>i</i> -Pr)(<i>s</i> -Bu)	62		

^a Choi, M.-G.; White, D.; Brown, T. L. submitted for publication in *Inorg. Chem.* E_R is measured in kcal mol⁻¹.

TABLE VIII
 STERIC SIZES FOR MISCELLANEOUS LIGANDS

Ligand	θ^a	$\Omega/\text{sr}^{b,c}$	$\Omega/^\circ b,c$	$\Omega_s^{b,c}$	E_R^d
AsMe ₃	114	3.45	126	0.274	27
AsEt ₃	128	3.84	134	0.306	40
As(<i>n</i> -Pr) ₃	128	4.48	147	0.357	
As(<i>n</i> -Bu) ₃	128	4.70	151	0.374	44
AsPh ₃	141	3.52	128	0.280	44
AsPhMe ₂	123	3.31	124	0.263	30
AsPhEt ₂	132	3.81	134	0.303	36
As(OEt) ₃	105	2.98	117	0.237	40
As(OPh) ₃	124	3.52	128	0.280	42
PhNC	48, 77 ^e	0.528	47.3	0.0420	
<i>o</i> -MePhNC	51, 92 ^e	0.825	59.4	0.0656	
<i>o</i> -Me ₂ PhNC	53, 106 ^e	1.12	69.5	0.0892	
<i>o</i> - <i>t</i> -Bu ₂ PhNC	93, 141 ^e	2.99	117	0.238	
MeNC	52 ^e	0.352	38.5	0.0280	
EtNC	52, 64 ^e	0.586	49.9	0.0466	
<i>i</i> -PrNC		0.835	59.7	0.0664	
<i>t</i> -BuNC	68, 70 ^e	1.07	67.8	0.0850	

^a Tolman, C. A. *Chem. Rev.* **1977**, 77, 313.

^b White, D.; Wade, P. W.; Coville, N. J. *Inorg. Chem.*, in preparation. The solid angle, Ω , is measured in steradians assuming hindered rotation. The measure in degrees refers to a right circular cone with that solid angle. Ω_s is $\Omega/4\pi$ and gives the fraction of a sphere occupied.

^c Isonitrile solid angles are measured assuming a M–C distance of 2.80 Å.

^d Brown, T. L. *Inorg. Chem.* **1992**, 31, 1286; E_R is measured in kcal mol⁻¹.

^e Tamamoto, Y.; Aoki, K.; Yamazaki, H. *Inorg. Chem.* **1979**, 18, 1681; the first figure refers to the thickness and the second to the width of the group.

B. Solid Angles

Developments of quantification of steric effects using solid angles can be divided into two distinct periods: the first involves the *detection* of steric effects using molecular mechanics to produce *ligand profiles*, while in the second period *methods of quantification* were attempted. In this work we consider both of these genres in turn.

Mosbo and co-workers were the first to report the use of molecular mechanics to *assess as well as quantify* steric size (26). In an attempt to refine the Tolman cone angle, θ , for group 15 donor ligands, to allow for conformational preferences, these workers turned to molecular mechanics to calculate the weighted average of cone angles over all conformers of the ligand based on MINDO/3 calculations. The enthalpy of formation,

ΔH_f , and atomic positions for each low-energy conformer were considered and normalized according to a Boltzmann-type distribution,

$$\theta = \sum_{i=1}^m n_i \theta_i, \quad (5)$$

where n_i is the mole fraction of conformer i and θ is the Tolman cone angle of that conformer. The mole fractions were calculated as

$$n_A = \frac{g_A}{g_A + g_B e^{-\Delta E_{AB}/RT} + \dots + g_i e^{-\Delta E_{Ai}/RT}}, \quad (6)$$

where g_A is the number of conformers with conformation A and ΔE_{Ai} is the difference in enthalpy of formation between conformers A and i at 298 K. In the molecular mechanics calculation all atomic positions were allowed to optimize, but the metal atom was not considered. This is a limitation with the approach: possible conformers in which the PR_3 ligand would interact unfavorably with the ligand set can arise. In addition only a limited number of conformers were selected for study (*trans*, *gauche*-right, etc.) without attempts to determine whether these conformers corresponded to energy minima. The van der Waals radii used were: H = 1.22 Å, C = 1.55 Å, and P = 0 Å. The unusual van der Waals radius of P was chosen for two reasons: the focus was on the substituent not the phosphorus atom, and the conventional value of 1.9 Å was considered too large in organometallic complexes.

Four different θ values were defined:

$$\theta_I = 2 \left(\frac{\theta}{2} \right)_{\max}, \quad (7)$$

$$\theta_{II} = \frac{2}{3} \sum_{i=1}^3 \left\{ \left(\frac{\theta}{2} \right)_{\max} \right\}_i, \quad (8)$$

$$\theta_{III} = \frac{2}{3} \sum_{i=1}^3 \left\{ \left[\left(\frac{\theta}{2} \right)_{\max} \right]_{\text{av}} \right\}_i, \quad (9)$$

and

$$\theta_{IV} = \frac{2}{360} \sum_{i=1}^{360} \left(\frac{\theta}{2} \right)_i. \quad (10)$$

The first value, θ_I is the maximum cone angle, θ_{II} is the maximum cone angle in minimum conformation (Tolman cone angle), and θ_{III} is the averaged maximum cone angle. The value θ_{IV} , defined in Eq. (10), is proportional to the area under a ligand profile. Ligand profiles were generated

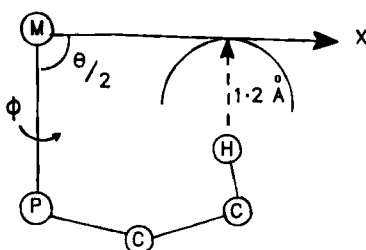


FIG. 9. Rotation about the M-P bond (ϕ) giving rise to a ligand profile. Redrawn from Ferguson *et al.* (33) with permission.

by plotting $\theta/2$ against ϕ (the angle of rotation about the M-P bond) for each 1° rotational increment (ϕ is the angle of rotation about the M-P bond—Fig. 9).

It is to be noted that the use of ligand profiles was first introduced by Ferguson and co-workers in 1978 (33) to assess the problem of steric size with respect to the *shape of the ligand* (Fig. 10). The ligand profile was developed in order to give a precise cone angle and to provide information about the spaces between atoms within a ligand. However, no attempt was made to *quantify* the area under the ligand profile to give rise to the equivalent of a solid angle. Maximum *cone angles* were generated and conformational effects were ignored. In the first paper of a series the ligand profiles for PCy_3 , $\text{P}(t\text{-Bu})_3$ and $\text{P}(o\text{-tol})_3$ were reported. In subsequent publications ligand profiles for $\text{P}(\text{mesityl})_3$ (34) and $\text{As}(\text{mesityl})_3$ (35)

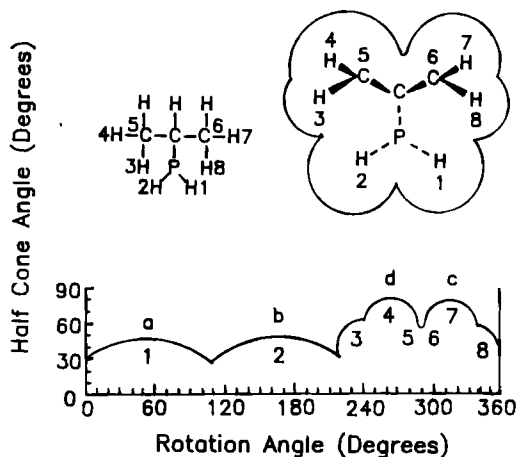


FIG. 10. Ligand profile for the $\text{PH}_2(i\text{-Pr})$ ligand generated by 1° increments of ϕ plotted in cartesian coordinates. Redrawn from Mosbo *et al.* (25) with permission.

were reported. The propeller conformations in $P(\text{mesityl})_3$ were studied further as it is one of the most sterically demanding ligands synthesized to date (Tolman cone angle 212° , Ferguson *et al.*, 200–206°) (34).

Smith and Oliver used an analogous method to examine $[(\eta^3\text{-C}_3\text{H}_5)\text{Pt}(\text{PCy}_3)_2]^+$ complexes (36). Their study was performed to specifically address the meshing problem in PCy_3 . The only difference in method between Smith and Oliver and Ferguson *et al.*, is that the former plotted the ligand profile in polar coordinates (Fig. 11) whereas the latter used cartesian coordinates. The latter method has a major advantage as the shape of the ligand is clearly visible in polar coordinates. Finally, and more recently, Mullica and co-workers have used the method of Smith and Oliver to provide the ligand profile for PPh_3 (37). This was done to rationalize the formation of *cis*- $[(\eta^5\text{-C}_5\text{H}_5)\text{Mo}(\text{CO})_2\text{PPh}_3(\text{NCCH}_3)]^+$ from the oxidative cleavage of *trans*- $[(\eta^5\text{-C}_5\text{H}_5)\text{Mo}(\text{CO})_2\text{PPh}_3]_2\text{Hg}$. These authors also used polar coordinates and noted the distinct propeller-like arms of the PPh_3 ligand in the profile.

A different type of ligand profile was proposed by Farrar and Payne in 1981 (37*b*). The authors traced the outside of the van der Waals radii of

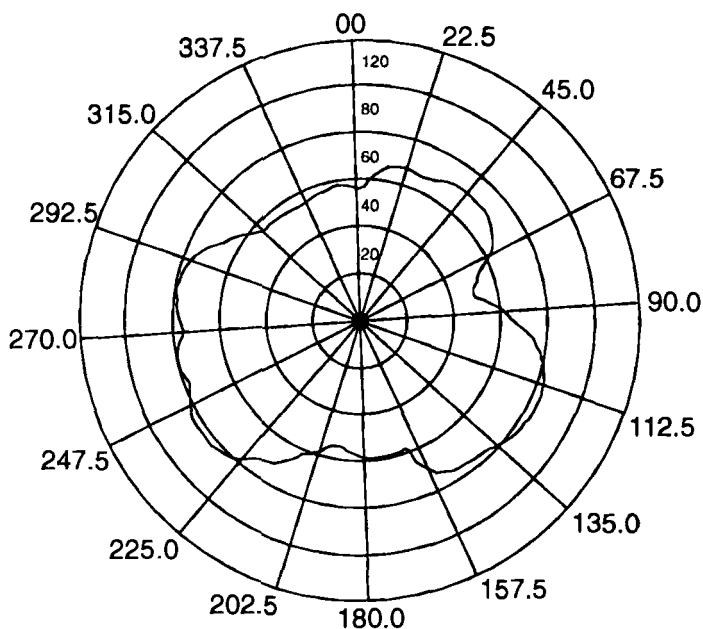


FIG. 11. Ligand profile of PCy_3 plotted in polar coordinates. Redrawn from Smith and Oliver (36) with permission.

the ligand at its widest point, yielding a view of the ligand taken from the perspective of the metal. To our knowledge this is the only report of a profile of this type in the literature.

It should be noted that a review by Clark and Hampden-Smith concerning steric effects in bulky phosphines appeared in 1987 (38).

The solid angle provides a *quantitative measure of the qualitative work described above*. The solid angle, Ω , at a point O of a surface can be represented by the integral

$$\Omega = \int_S \frac{\mathbf{r} \cdot d\mathbf{S}}{r^3}, \quad (11)$$

where \mathbf{r} is the position vector of an element of the surface with respect to O and r is the magnitude of \mathbf{r} . The integrand takes into account the three relevant factors: the size of the element of surface, its inclination to the line joining the element to O, and the distance from O (39). In essence, the solid angle can be viewed as the surface area of that part of a solid projected onto the surface of a sphere (Fig. 12). In polar coordi-

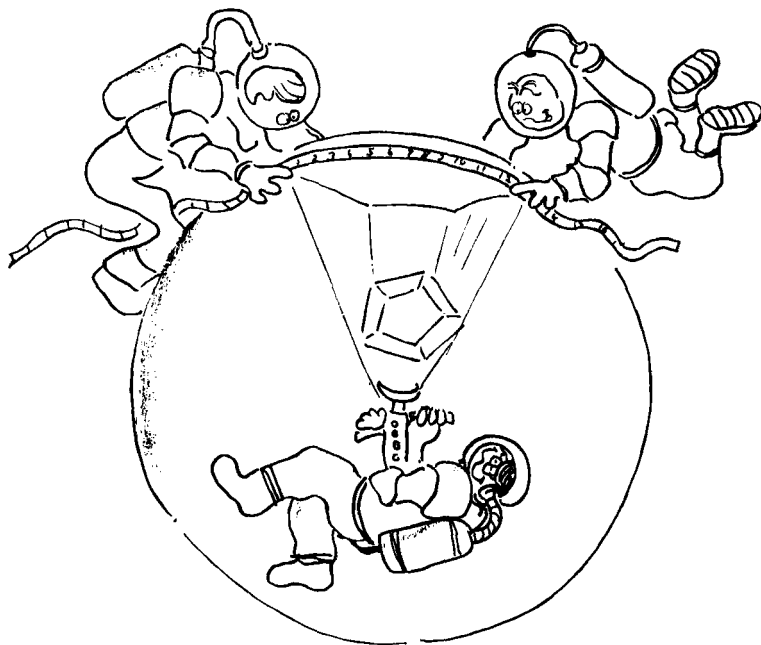


FIG. 12. Cartoon illustrating the definition of a solid angle. The area of shadow of a solid body projected onto the inside of a sphere is being measured.

nates, the expression for the solid angle can be reduced to

$$\begin{aligned}\Omega &= \int_{\phi_1}^{\phi_2} d\phi \int_{\theta_1(\phi)}^{\theta_2(\phi)} \sin \theta d\theta \\ &= \int_{\phi_1}^{\phi_2} \{\cos \theta_1(\phi) - \cos \theta_2(\phi)\} d\phi.\end{aligned}\quad (12)$$

The solid angle is measured in steradians (sr). If the solid angle is considered to be that of a cone, the vertex angle (commonly called linear or cone angle) of the cone is given by (40):

$$\Omega/^\circ = 2 \arccos \left[1 - \frac{\Omega \text{ (sr)}}{2\pi} \right]. \quad (13)$$

The solid angle takes into account the *actual shape of a group of atoms (spheres)* under investigation (Fig. 13). Unlike linear cone angles, e.g., as used by Tolman, *solid angles are additive* so that the total solid angle of, for example, three spheres is the sum of the three individual solid angles. The solid angle does encompass the entire ligand or substituent, but includes the overlap of the atomic radii of all atoms. Therefore to obtain an accurate measure of ligand size this overlap must be subtracted, a problem recently solved using both analytical (16) and numerical (41) methods.

The use of solid angles to assess steric size dates back to the work of Immirzi and Musco in 1977 (40). These authors managed to calculate a variety of *ligand compressibility values* from a variety of crystal structures. These compressibility values appear to give an indication of the number of conformational degrees of freedom in a ligand [e.g., 16% for PEt_3 vs 8% for $\text{P}(t\text{-Bu})_2\text{PL}$]. However, the methodology as reported by the authors was ultimately used to derive the equivalent linear angle giving rise to no advantages over the Tolman methodology.

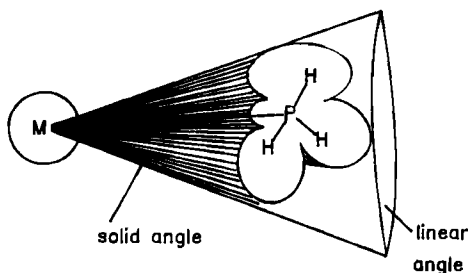


FIG. 13. Illustration of the principle difference between the linear angle (right circular cone) and the solid angle (irregularly shaped cone) shown for a PH_3 ligand.

The first workers to begin exploiting the advantages of the solid angle were Bagnall and Xing-Fu (42) in 1982 in studies on U(IV) organometallic complexes. A distinction was made between first-order and second-order steric effects: first-order effects arose from the atom or group attached directly to the metal whereas second-order effects arose from the rest of the ligand. A further distinction between global and local steric effects was noted: the former governing the stability of the complex as a whole and the latter the relative arrangements of the individual ligands. Two new terms were defined: the *fan angle* (f.a.) identical to the linear angle used by Tolman (for planar systems) and the *cone angle factor* (c.a.f.—later called the *solid angle factor* SAF). The c.a.f. was defined as follows:

$$\begin{aligned} \text{c.a.f.} &= \frac{1}{4\pi} \int_0^\theta \int_0^{2\pi} \sin \theta \, d\theta \, d\phi \\ &= \frac{1}{2} (1 - \cos \theta). \end{aligned} \quad (14)$$

By considering the sum of solid angle factors for all the ligands in $[(\eta^5\text{-C}_5\text{H}_5)_n\text{UCl}_{4-n}]$, the value of n could be rationalized exclusively from a knowledge of the sum of solid angle factors ($\Sigma\text{c.a.f.}$). The $\Sigma\text{c.a.f.}$ values indicate overall steric crowding whereas the analogous $\Sigma\text{f.a.}$ values indicate the total steric crowding in a specific plane. In a later publication, the cone angle factors were used by Fisher and Xing-Fu (43) to form the basis of the *solid angle sum* (SAS) rule to quantify the number of cyclopentadienyl groups that can be accommodated by a lanthanide metal. In attempting to measure the solid angle of a cyclopentadienyl ring the authors recognized the inaccuracies related to the use of a right circular cone as the basis for the solid angle calculation, but were unable to resolve the problem. Fisher and Xing-Fu (43) removed the C–H bond overlap problem by adding an additional term to the final calculation equation:

$$\text{SAS} = \sum_i^n \text{SAF}_i - \sum_j^n \text{SAF}_j. \quad (15)$$

Lobkovskii (44), working with similar compounds, defined the solid angle of a cyclopentadienyl ring to be the solid angle of a regular pentagon counting only carbon atoms (i.e., the van der Waals radii of the outermost H atoms or methyl groups were ignored). This approach, again, does not utilize the additive property of the solid angle and has no real advantage over the linear angle approach. The generality of the SAS rule was tested with the preparation of *trans*- $[(\eta^5\text{-C}_5\text{H}_5)_3\text{Ln}(\text{NCCH}_3)_2]$, Ln = La, Ce, Pr,

complexes (45). The concept was further expanded, in a slightly different form, in two later publications by Xing-Fu and Ao-Ling (46).

Sheeman *et al.* were the first workers to exploit the additive properties of solid angles more fully (47). By considering the kinetic data for the methylation of 2,3-dialkylpyridine and 2,5-dialkylpyridine they attempted to quantify the kinetic study by considering the point of attack of the methyl group on the organic substrate. From GEOME (MINDO/3) calculations they found the point of attack of pyridine to lie along the *para*-C-N axis, 1.75 Å from the N atom. Adding solid angles for each of the spheres visible when viewing the pyridine ring 1.75 Å from the nitrogen (ignoring the overlap) they found

$$\Omega_T = 4\pi - \Omega_{\text{OCC}}, \quad (16)$$

where Ω_{OCC} is the solid angle of the pyridine ring. To eliminate electronic effects they added a further empirical factor.

Razuvaev and co-workers (48) invoked steric effects in an attempt to rationalize the charge transfer behavior of $[(\eta^5\text{-C}_5\text{H}_4\text{R})\text{WX}_2]$ complexes (R = Me, Et, *n*-Pr, *n*-Bu, *i*-Pr, *t*-Bu; X = Cl, Br, I). The degree of transition of the complex into ion radical salts with tetracyanoethylene (TCNE) and tetracyanoquinodimethane (TCQE) was determined to be in the order $\text{Cl} > \text{Br} > \text{I}$ and $\text{Me} > \text{Et} \sim \textit{n}\text{-Pr} \sim \textit{n}\text{-Bu} > \textit{i}\text{-Pr} > \textit{t}\text{-Bu}$. It was proposed that the alkyl substituent and halogen shielded the metal atom from the attacking TCNE or TCQE molecule. Solid angles of the substituted cyclopentadienyl group and halogens were reported. The solid angle calculation was based on an algorithm used by Zakharov *et al.* (49). This latter paper presented two analogous methods (using spherical and cylindrical coordinates) for the calculation of solid angles. The precise method was not reported, but it appears that the authors simply added solid spheres for each atom in the ring without taking into account the overlap between them. The methodology must be treated with caution since (i) the authors claimed that the solid angle was not affected by addition of hydrogen atoms, (ii) the units for solid angles were quoted as radians instead of steradians, and (iii) six solid angles are in excess of 4π sr [$\text{Ti}(\text{CH}_2\text{CMe}_3)_4$, $\text{Cr}(\text{CH}_2\text{SiMe}_3)_4$, $\text{Cr}(\text{CH}_2\text{CMe}_3)_4$, $\text{V}(\text{mesityl})_3$, $\text{V}(\text{CH}_2\text{SiMe}_3)_4$, and WMe_5]. In the cylindrical coordinate calculation the cylindrical projections are unfolded to give a ligand profile. These ligand profiles were used in an attempt to rationalize metal cluster formation (50).

The calculation of cluster sizes was carried out by White using the solid angle approach (51). The assumptions used in the Mingos approach (32) were used in this analysis and consistent results were obtained. Metal cluster stability was also investigated and solid angles used to distinguish between the spatial requirements of terminal versus bridging carbonyl

groups. A bridging carbonyl group was generally found to occupy *more space* than a terminal carbonyl group. The areas of steric congestion in a cluster were studied using the *radial profile* methodology (52). This methodology is discussed further in Section IV.

Chauvin and Kagan (53) applied the solid angle concept to organic substituents and attempted to analyze stereochemical problems from this perspective. With this approach they solved the problem of differing conformations associated with the substituent. First, for symmetric tops, the total linear angle was calculated using the Tolman approach. For other types of substituents each group on the substituent was made from successive atomic layers L_0, L_1, \dots, L_n , where layer L_k has 3^k (or fewer) terminal atoms. If all the terminal atoms (X) are identical and on the same layer, then these atoms define a cone:

$$\Omega_{n,X}(3^n) = 2\pi [1 - \cos \theta(n,X)]. \quad (17)$$

The angle $\theta_{n,X}$ is the linear angle mentioned above. Now, each individual atom defines a partial cone

$$\Omega_{k,X}(N_{k,X}) = \frac{N_{k,X}}{3^k} \Omega_{k,X}(3^k), \quad (18)$$

where $N_{k,X}$ is the number of terminal atoms, X , of the k th atoms in layer L_k . Thus the solid angle of the substituent R is

$$\Omega(R) = \sum_k^n \sum_X^N \Omega_{k,X}(N_{k,X}). \quad (19)$$

The advantage of the approach is that $\Omega(R)$ is *conformation independent* and measures the bulkiness of R rather than the steric hindrance of R . In the one layer case (e.g., CHX_3) a plot of E'_s vs Ω gave a linear relationship with $R^2 = 1.000$. For two or more layers the relationship is no longer linear but parallel curves result on increasing the number of layers (Fig. 14).

A drawback to the method is that a tertiary group has less effect on the rate of a reaction than a secondary group with the same Ω . Additional parameters were required to correct for this observation;

$$\Omega' = \Omega - (a_x + a_y + a_z), \quad (20)$$

where a_x , a_y , and a_z are corrective coefficients for atoms X , Y , and Z attached directly to the first carbon atom. A plot of $\ln(-E'_s)$ versus Ω'^{-1} gives $R^2 = 0.996$. The corrective coefficients incorporate influences of the second layer onto the first that are not of steric origin.

Recently McClelland (54) used solid angles of simple spheres to rationalize reactivities of triarylmethyl and dimethyl cations with azide ions under laser flash photolysis.

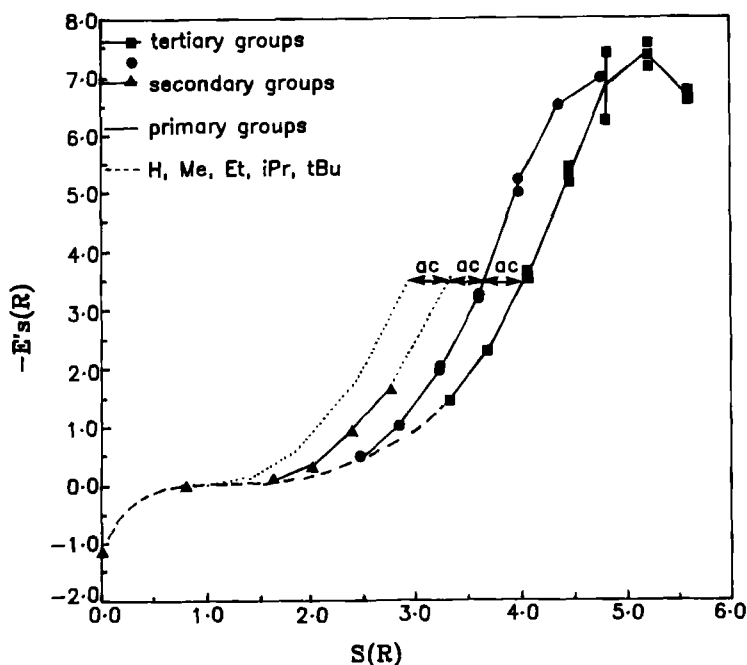


FIG. 14. Plot of $-E'_s$ against $S(R)$, the solid angle, Ω , for alkyl groups containing more than one layer of atoms. Redrawn from Chauvin and Kagan (53) with permission.

Hirota and co-workers were the first to address the atom overlap problem in a quantitative fashion without introducing "fudge" factors (41). In their approach the *entire molecule* is projected onto the inside surface of a unit sphere (Fig. 15) and the total surface area of the shadow measured *numerically*. Since the required solid angle is obtained from a numerical rather than an analytical solution, any minor modification of the substituent requires the recalculation of the entire solid angle. In addition, in its present form, the algorithm cannot calculate the solid angle of cyclic groups. The steric parameter, Ω_s , is the solid angle divided by 4π and focuses attention on the reactive center of an organic substrate. Thus Ω_s is the area of shadow divided by the total surface area of the sphere. To take into account differences in conformation a molecular mechanics (BIGSTRN-3) population mean of "every conformer" was used. The correlation coefficient, R^2 , for a plot of E_s vs Ω_s varies between 0.901 and 0.941 as one moves from primary to tertiary alkyls. As a further test, the Ω_s values were found to correlate with $\log(k/k_0)$.

Recently these authors reported the calculation of Ω_s values for a range of heteroatom-containing compounds (55). Using the Bondi data set for

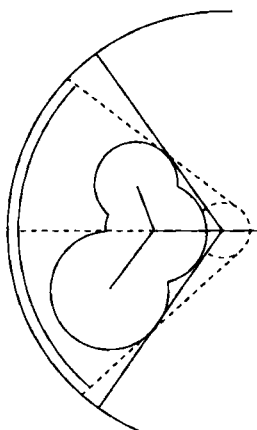


FIG. 15. Projection of an organic group onto the inside of a sphere. The solid lines indicate the solid angle from one vantage point, whereas the dotted lines indicate the small solid angle from further away. Redrawn from Komatsuzaki *et al.* (41) with permission.

atomic sizes, Hirota and co-workers again found a good correlation between Ω_s and E_s , the Taft steric parameter ($R^2 = 0.924$). Two sets of data were defined, one relative to the methyl group, $\Omega_{s,Me}$, and the other relative to a carboxylic acid, $\Omega_{s,COOH}$. The plot of Ω_s versus E_s for alkyl groups was found to lie above that of the heteroatom-containing compounds. This was rationalized on conformational grounds. In a group such as XCH_2COOH , two possible conformational extremes can be envisaged: one with X eclipsing the $C=O$ group (favored if X = alkyl) and the other with H eclipsing the carbonyl group (favored if X = halogen). The relative stabilization of one conformer relative to the other was measured using PM3 molecular orbital calculations and confirmed with MM2.

In a subsequent publication, Komatsuzaki *et al.* extensively examined the utility of the Ω_s parameter (56). The conformational analysis mentioned above was performed using MM2 (BIGSTRN-3) and was based on steric energy and free energy considerations. Again two Ω_s values were calculated to enable a thorough statistical analysis. A correlation was found between $\Omega_{s,COOH}$ and $\Omega_{s,Me}$ ($R^2 = 0.984$). The utility of Ω_s was tested using a topological statistical approach. If each carbon atom is classified according to the number of bonds between the reaction center, and N_j is the number of carbon atoms separated by j bonds, then the class, j , is evaluated through a_j defined in

$$\Omega_s = a_0 + \sum_j (a_j N_j). \quad (21)$$

In the statistical analysis, β -carbon atoms ($j = 1$) were found to contribute predominantly to Ω_s . This was in contrast to the analogous E_s system, where β and γ carbon atoms ($j = 1$ and 2) were found to contribute to E_s almost equally. A more extensive relationship was also examined,

$$\Omega_s (CR_1R_2R_3-) = \sum_k [a_k E'_s(R_k) + b_k \Delta 6_k], \quad (22)$$

where $E'_s(R_k)$ is the Taft-Dubois steric parameter for R_k and $\Delta 6_k$ is Newman's six number (57) for each k ($k = 1, 2, 3$). The R_k groups, H, Me, Et, *i*-Pr, and *t*-Bu, were chosen as they exhibit a monotonically increasing set of E'_s values, which, consequently, are independent of conformational effects. Thus, a_k and b_k give the relative importance of the E'_s and $\Delta 6_k$ parameters, respectively. Both $\Omega_{s,Me}$ and $\Omega_{s,COOH}$ showed excellent correlations in the above relationship ($R^2 = 0.9994$ and 0.998 , respectively).

In the same publication, Hirota and co-workers (56) also related Ω_s to E'_s and ϕ_f (58), the Beckhaus constant. The plots of E'_s against Ω_s were all linear with R^2 varying between 0.801 and 0.986 as was the plot of ϕ_f against Ω_s ($R^2 = 0.901$).

In an extension of the same work, Hirota and co-workers defined the probability of reaction as $1 - \Omega_s - \Omega_r$, where Ω_r is the solid angle of the rest of the molecule. This probability should be proportional to the pre-exponential factor in the Arrhenius equation. To test whether $1 - \Omega_s$ still measured steric effects, these authors found that $\log(1 - \Omega_s)$ correlated well with E'_s ($R^2 = 0.828 - 0.994$). In a kinetic study, Ω_s was found to correlate better ($R^2 = 0.978 - 0.982$) than E'_s with $\log(k/k_0)$ according to

$$\log \left(\frac{k}{k_0} \right) = \rho_s \Omega_s + a, \quad (23)$$

where ρ_s and a are constants (ρ_s measuring sensitivity to steric effects).

Recently, an *analytical* solution to the overlap problem associated with the measurement of solid angles was presented by White *et al.* (16). The assumption that permitted an analytic solution of Eq. (11) was the initial, simplifying, step of considering only a pair of atoms bound together with the required overlap between their atomic radii. An enveloping cone was placed around these two atoms, which were projected onto the base of this cone (Fig. 16). The total solid angle of the cone is trivial to calculate. By integrating from one edge of the enveloping cone to the intersection, and then to the other edge, and subtracting from the solid angle of the cone, the solid angle of the two spheres was obtained. To obtain the solid angle for a group containing many atoms, the individual atoms in the molecule were *traversed in pairs*, subtracting the relevant portions added

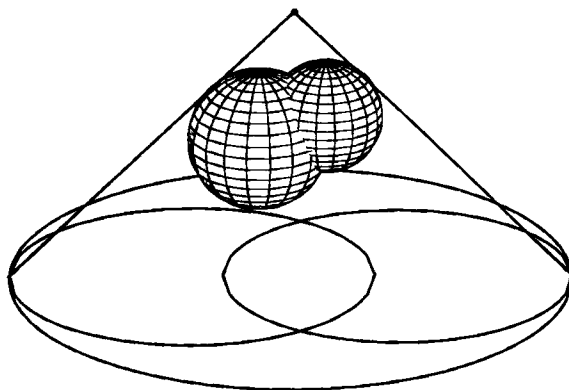


FIG. 16. Projection of two spheres onto the base of an enveloping cone to form two ellipses. The unused portion of the enveloping cone is subtracted by integration leaving the solid angle of the two ellipses.

more than once. For example: $\Omega(\text{CH}_3) = 3\Omega(\text{CH}) - 2\Omega(\text{C})$ (Fig. 17). This method for calculating solid angles (i) is general, i.e., applicable to any atom or combination of atoms in any geometrical arrangement in space; (ii) provides a measurement in units that are intuitively meaningful to practicing chemists; (iii) can be generated from a knowledge of only atomic radii, bond lengths, and angles; and (iv) takes into account group meshing.

To take into account varying conformers White *et al.* undertook a molecular mechanics study (59). The approach chosen was to keep the study consistent with the recent work by Brown (60). Thus, a typical organometallic fragment, $\text{Cr}(\text{CO})_5$, was chosen and a starting ligand conformer was allowed to minimize initially using the SYBYL force field. The choice of the starting conformer was found to be critical as the SYBYL force field was found to be insensitive to conformational effects. Initially the conformer closest to that used by Tolman was chosen. This was refined by choosing a conformer of very high energy and the geometry was allowed

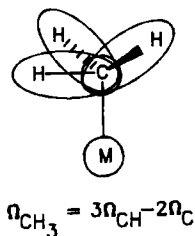


FIG. 17. Illustration of the calculation of the solid angle for CH_3 : three CH portions are added and two carbons subtracted.

TABLE IX

θ	Ω
Facile to measure. Initially required a physical scale model of the ligand for calculation. Currently possible to generate θ using molecular drawing software (e.g., ALCHEMY)	Requires algorithm which is now available.
Requires known bond lengths, angles, and atom sizes.	Requires known bond lengths, angles, and atom sizes.
Measured in degrees only.	Measured in degrees, steradians, percentage occupancy of sphere or effective radius in angstroms.
Nonadditive. Composites must be rebuilt.	Additive. A composite can be readily calculated.
Only rotation about the M-P(N, C) bond. Gives ligand profile.	Can be used to generate radial profiles, yielding variation in Ω with distance.
Does not readily take into account ligand meshing.	Readily takes into account inter- and intraligand meshing.

to optimize to a structure with minimal conformational effects. Once the minimum energy using SYBYL was obtained, this conformation was submitted to MM2 for accurate energy determination and fine tuning. No differences between the minimum conformers using the SYBYL or MM2 force fields were found. The size of the ligand was then determined using solid angles with the Cr atom at the apex of the cone. Data for a range of commonly encountered ligands (phosphines, phosphites, amines, and cyclopentadienes) were thus determined and are given in Tables I–VIII.

C. Summary

In this section the two most popular and versatile measures of steric size were presented: the linear angle, θ , and the solid angle Ω . The advantages and disadvantages associated with θ and Ω are listed in Table IX.

III

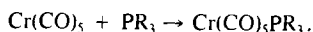
QUANTIFICATION OF STERIC SIZE USING MOLECULAR MECHANICS METHODS

A. Ligand Repulsive Energy, E_R

Two distinct molecular mechanics approaches that both *quantify* steric effects and *assess* steric size are described in this section.

To our knowledge only Brown has attempted to *quantify* steric effects using molecular mechanics (61). Brown noted that the steric effect is defined in terms of the *repulsive forces* that ligands exert on their environment, which cause distortions from ideal geometries. A ligand repulsive energy, E_R , is defined in terms of the 1,4-repulsive van der Waals interaction between atoms in a complex. To compute this effectively a prototypical metal center, $\text{Cr}(\text{CO})_5$, was chosen. This was done because the vibrational function of $\text{Cr}(\text{CO})_6$ is well defined and allows the molecular mechanics package employed (MMP2) to be thoroughly parameterized. Also, the rotational symmetry along the Cr–CO bond in $\text{Cr}(\text{CO})_5$ is fourfold as opposed to the threefold rotational symmetry that would exist about a Cr–P bond. Therefore the metal–ligand energy will not vary significantly with Cr–P bond rotation. Finally $\text{Cr}(\text{CO})_5$ is representative of the general degree of steric crowding of a metal in organometallic complexes.

The entire method involves a linear free energy approach (LFEA). The steric effect in the following reaction was investigated:



The total energy change for the process is given by

$$\Delta E = E_{\text{Cr-P}} - E_{\text{Cr}} - E_{\text{P}}, \quad (24)$$

where $E_{\text{Cr-P}}$ is the energy of $\text{Cr}(\text{CO})_5\text{PR}_3$, E_{Cr} is the energy of $\text{Cr}(\text{CO})_5$, and E_{P} is the energy of the free ligand. The molecular mechanics program MMP2 was thoroughly parametrized for both phosphine and phosphite complexes. Ultimately ΔE varies with ligand structure, but is found to be a poor measure of steric effects as it contains information about both electronic (attractive van der Waals interactions) and steric (repulsive van der Waals interactions) effects.

To employ the LFEA to define E_R the minimum number of parameters was sought. Thus only short range, 1,4-van der Waals repulsions were considered. The evaluation of E_R in every conformation was permitted, but the energy-minimized $\text{Cr}(\text{CO})_5\text{L}$ structure was used. Ligand repulsive energies were calculated starting from the energy-minimized structure, but with the conventional exponential six-form Buckingham potential being replaced by a simplified version to consider only repulsive interactions. The conventional Buckingham potential takes the form

$$E_{\text{vdw}} = D_0 \left\{ \left(\frac{6}{\gamma - 6} \right) \exp \left[\gamma \left(1 - \frac{r}{r_0} \right) \right] - \left(\frac{\gamma}{\gamma - 6} \right) \left(\frac{r_0}{r} \right)^6 \right\}, \quad (25)$$

where D_0 is the depth of the potential well at the energy minimum, γ is a scaling factor (usually 12.5), and r is the interatomic distance at the minimum potential energy (r = observed bond length, r_0 the unstrained

bond distance). The Buckingham potential was replaced by

$$E_{\text{vdW}} = \sum D_0 \left\{ \gamma \left[r_0 - \frac{r}{0} \right] \right\}, \quad (26)$$

summing over all 1,4-interactions in the complex. In the energy-minimized structure all parameters except the Cr–P bond length are kept constant; this value is varied in the vicinity of the equilibrium value, r_e . The slope of the plot of E_{vdW} versus $r_{\text{Cr-P}}$ multiplied by r_e then gives the value for E_R :

$$E_R = -r_e \left(\frac{\partial E_{\text{vdW}}(\text{repulsive})}{\partial r_{\text{Cr-P}}} \right). \quad (27)$$

The gradient is multiplied by r_e to take into account the possibility of the two slopes giving similar E_R values for different r_e values. One important point to note is that the van der Waals radius of C(sp^2) is chosen as 4.08 Å as opposed to the conventional 3.88 Å. This empirical change was introduced to accommodate aryl groups that give E_R values lower than expected (according to kinetic measurements rather than correlations with θ). Ligand repulsive energies correlate with the Tolman cone angle ($R^2 = 0.769$, for all E_R values computed, 69 data points). Steric thresholds were also noted in this measure as $E_R \rightarrow 0$ as $\theta \rightarrow \sim 82^\circ$. Thus this value, termed the *absolute steric threshold*, indicates the onset of any significant ligand–metal steric interaction. However, this value would vary with the individual metal chosen.

Both the advantages and disadvantages of this measure are well documented. The recognized disadvantages are: (i) the measure only applies to $\text{Cr}(\text{CO})_5$, but since this is representative of a “typical” organometallic fragment the results should be general; (ii) E_R depends, somewhat, on the force field employed; (iii) gas-phase conditions are assumed and hence solvent interactions are ignored; and (iv) the E_R value is problematic when different conformers with very similar energies exist. However, the advantages are significant: (i) E_R values are calculated in a conformer most appropriate to a typical metal fragment; (ii) E_R values for asymmetrically substituted phosphorus atoms are very easily calculated; (iii) the lone pairs on oxygen are included as being sterically active; (iv) the E_R values are versatile: they can be extended to organic as well as other inorganic systems by only parametrizing a suitable molecular mechanics package; and (v) an absolute steric measure can be accomplished by extending to different metal systems.

The E_R values were recently employed by Choi and Brown to relate the coefficients of the steric and electronic terms in linear free energy relationships to kinetic and thermodynamic data (62). These authors con-

sidered the effect of a ligand on the atom transfer rates in $\text{Re}(\text{CO})_4\text{L}$ radicals. The linear free energy relationship used was given by

$$\ln k = a E_i + b S_i + c, \quad (28)$$

where E_i and S_i represent the electronic and steric terms and a , b , and c are constants. This equation was related to the $\text{Re}(\text{CO})_4\text{L}$ system by application of a Marcus-type model of atom transfer (in which the free energy of activation is considered rate determining). Recently Choi and Brown have extended the initial work on the E_R measurements of P- and As-donor ligands to N-donor ligands (63) and S-donor ligands (64). The method remained identical: MM2 was parametrized for the relevant N-donor ligand set and the E_R values measured relative to the $\text{Cr}(\text{CO})_5$ fragment. To investigate the variation in E_R relative to a different metal center, a series of measurements based on the $[(\eta^5\text{-C}_5\text{H}_5)\text{Rh}(\text{CO})]$ fragment were performed (65). A good correlation between the two sets of data were found, and the authors concluded that the E_R measure was a good relative set of ligand steric parameters. A list of E_R values for phosphines, phosphites, arsines, amines, and sulfides is given in Tables I, II, III, VII, and VIII.

Rodger and Johnson have recently applied molecular mechanics to rationalize the geometries of some tris-chelate complexes (66). These authors developed an atom-atom interaction model (AAIM) with the assumption that the M-L bond strength is independent of the relative orientations of the ligand and that nonbonding electrons do not dominate the overall energy of the structure. On this basis, the authors found that both attractive and repulsive ligand-ligand interactions need to be taken into account when rationalizing the overall geometries of complexes. However, no quantitative analysis of the steric effect was presented.

B. Molecular Mechanics and Steric Size Assessment

An interesting study involving *ab initio* calculations concerning steric effects was reported by Baird in 1989 (67). This work involved the rationalization of bond angle data as an alternative to VSEPR theory. In a molecule of the form X_2A , *ab initio* molecular orbital calculations showed that the R_{AX} bond distance was the major factor influencing the X-A-X angle, particularly if A is a first-row element. For example, the HOH angle widens considerably as the OH distance is reduced. Similar effects were noted for NH_3 and singlet CH_2 . However, the rate of change was found to be slower for second-row elements (e.g., H_2S). These changes were found not to relate either to electronegativity or to the presence of lone

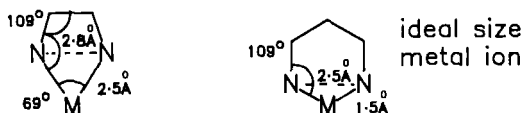


FIG. 18. Ideal size for a metal ion as part of a five- or six-membered ring. Note the differences in bond lengths and angles for the two different cases.

pairs: for example, CH_2 and H_2O behaved very similarly but PH_3 was very different. Baird found that H_2O , F_2O , $(\text{CH}_3)_2\text{O}$, and Cl_2O all showed analogous trends and concluded that the optimum XAX bond angle depends on steric rather than electronic effects.

C. Steric Effects in Macrocyclic Chemistry

The common notion that a small metal ion is best accommodated in a small macrocyclic cavity and a large metal ion in a large cavity has been questioned by Hancock (68). Thermodynamic data based on this assumption lead to a number of anomalies in the prediction of complex stability. Hancock found a different type of steric effect based on chelate ring size: small metal ions are best found as part of six-membered rings, whereas large metal ions are most stable as part of five-membered rings. These cases are illustrated with N-donor macrocycles: in a six-membered ring, the best fit involves a N–M–N bite angle of 109.5° with M–N bond lengths of 1.54 \AA , whereas for the five-membered ring the bite angle closes to 69° with M–N bond lengths of 2.5 \AA in order to preserve the 109.5° internal angle in the macrocyclic cavity (Fig. 18). On this simple basis Hancock derived a set of rules for designing ligands in order to complex metal ions of given size using molecular mechanics as a predictive tool.

IV

QUANTIFICATION OF STERIC SIZE USING CHEMICAL METHODS

A. The Modified Taft Steric Parameter, E'_s

Taft defined the steric parameter, E_s as

$$E_s = \log \left(\frac{k}{k_0} \right), \quad (29)$$

where the rate constant, k_0 , refers to the reference methyl-substituted ester and k is the rate constant for the acid-catalyzed hydrolysis of a

substituted ester (69). Taft's steric parameters were averaged from four measurements: (i) hydrolysis of ethyl esters in 70% v/v aqueous acetone at 25°C, (ii) hydrolysis of ethyl esters in 60% v/v aqueous acetone at 25°C, (iii) esterification of carboxylic acids with methanol at 25°, and (iv) esterification of carboxylic acids with ethanol at 25°. However, it was clear that the E_s parameter contained resonance effects. Attempts to modify the defining equation to exclude these effects have been made. For example Hancock *et al.* (70) proposed

$$E_s = E_s^c + (-0.306)(n - 3), \quad (30)$$

where n is the number of α -hydrogen atoms in the substituent; while Palm (71) defined

$$E_s = E_s^0 - 0.33(n_H - 3) - 0.13n_c, \quad (31)$$

where n_H is the number of α hydrogens and n_c the number of α carbons in the substituent.

Charton in 1969 (72) investigated an expanded relationship

$$E_{s,X} = \alpha \sigma_{I,X} + \beta \sigma_{R,X} + \psi r_{v,X} + h, \quad (32)$$

where σ_I and σ_R are localized and delocalized substituent constants, and r_v the van der Waals radius. Charton's approach was a simple regression analysis to determine the statistical significance of the constants α , β , and ψ . In the correlations three sets of substituents were identified: CH_2X , CHX_2 , and CX_3 with two r_v values each ($r_{v,\min}$ and $r_{v,\max}$). For substituents with internal conformational degrees of freedom, the minimum conformer was chosen. In the regression analysis only ψ was found to be statistically significant. Thus Charton concluded that the Taft steric parameter was free of electronic effects. In a parallel study Charton was able to show that E_s^0 was an electronic parameter depending on σ_I and σ_R only (73). Charton also defined an alternative steric parameter, v_X , as

$$V_X = r_{v,X} - r_{v,H}, \quad (33)$$

where r_v is the van der Waals radius (74). However, for accuracy, v_X is limited to symmetric substituents and, hence, the parameter lacks generality.

A major modification of the Taft steric parameter was made by MacPhee, *et al.* in 1978 (75). Charton's modification was rejected by these authors as it was considered to be too simple. The fundamental correctness of Taft's approach was acknowledged, but it was suggested that the calculation was not sufficiently rigorous owing to the averaging over four reactions. These authors felt the assumption of Taft that all four reactions would respond identically to a change in steric effect was erroneous.

Therefore a single standard reaction was chosen: the acid-catalyzed esterification of carboxylic acids in methanol at 40°C. The fundamental assumption in the work of these authors is that the mechanism of esterification does not change with steric effect. A comprehensive set of modified Taft steric parameters, E'_s , values was presented. To test the modified steric parameter the yardstick chosen was Charton's regression analysis (72) and a correlation of E'_s against r_v was found with $R^2 = 0.99986$.

To further expand the relationship between *chemical structure* and E'_s , Panaye *et al.* turned to a topographical analysis of the variation of the steric parameter with the addition of alkyl groups (76). Three distinct regions were noted in the plots of E'_s against the number of carbon atoms in an alkyl group: in the first region (1–7 carbon atoms) E'_s increased monotonically with the number of carbons. In the second region (8 or 9 carbon atoms) a levelling was noted with a dramatic decrease of E'_s to zero. Finally in the third region (more than 10 carbons) an inversion with change of sign was noted. To clarify the mechanism of reaction in relation to E'_s a knowledge of the precise spatial arrangements of the atoms was required. This was made difficult, however, by the lack of crystallographic data. To overcome this problem Dubois *et al.* turned to molecular mechanics to investigate the possibility of conformational effects playing a role in determining the locations of the three regions (77). Using the 1971 Allinger force field within the BIGSTRN package these authors attempted to relate the site of attack of the incoming nucleophile with the E'_s measurement. For the first region mentioned above conformational effects were predicted important by molecular mechanics since the stable *eclipsed conformers* were all *sterically active*. In the second region the presence of both *sterically active* and *sterically inactive* sites were noted. In the third region molecular mechanics predicted highly distorted geometries for very bulky substituents [e.g., C(*i*-Pr)₃ and C(*n*-Bu)(*i*-Pr)Et].

B. Use of NMR Spectroscopy to Quantify Steric Size

Staskun has *quantified* steric effects using NMR spectroscopy (78). Using ¹H NMR spectroscopy the van der Waals radius of a substituent, r_X , can be inferred from the chemical shift separation between nonequivalent benzylic protons A and B, $\Delta\delta_{AB}$, in N-substituted anilides (Fig. 19). The procedure is based on a linear regression analysis involving the equation

$$\Delta\delta_{AB} = ar_X + b, \quad (34)$$

where a and b are constants. The van der Waals radii for simple groups (e.g., halogens) and an *effective radius* for more complex organic substitu-

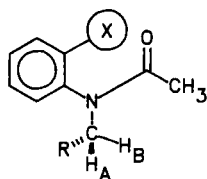


FIG. 19. The anilide used to determine the size of X on the basis of chemical shift separations between the resonances for protons H_A and H_B .

ents were taken from the literature. Correlation coefficients, R^2 , were found to vary between 0.93 and 0.97 for the series studied. In a later publication four more data points were added to the existing data (79). This model, although simple in its calculation, does require the preparation of a compound before a steric size of a substituent can be measured. As yet no data are available for very large or very small van der Waals radii.

IV

QUANTIFICATION OF THE VARIATION IN STERIC EFFECT WITH DISTANCE

A consideration of the shape of a ligand suggests that its size (as measured by θ or Ω) varies in an irregular way with distance from the apex. To date only one report that explores this variation of steric size with distance has appeared (52). In this publication the solid angle was chosen as a measure of steric size. Quantification of the *variation* in solid angle with distance from the metal center was achieved by use of a sphere of *variable radius* placed at the apex and expanded toward the ligand. As this sphere intersected the atoms in the ligand the contribution to the total solid angle could be calculated at each point *at the radius of the growing sphere*.

Consider CH_3 as an example. Three cases are encountered in determining Ω as a function of distance from the metal center: (i) the sphere intersects only one atom of the ligand (e.g., C, Fig. 20a), (ii) the sphere intersects two (or more) nonoverlapping atoms of the ligand (e.g., H and C, Fig. 20c), and (iii) the sphere intersects two (or more) atoms of the sphere which are overlapping (Fig. 20b). If the sphere intersects more than two overlapping atoms, then these atoms are traversed in a pairwise manner, identical to the method used for the calculation of the total solid angle (see Section II,B). For case (i) the portion of the atom intersected by the sphere is replaced by a sphere the cone of which has semivertex

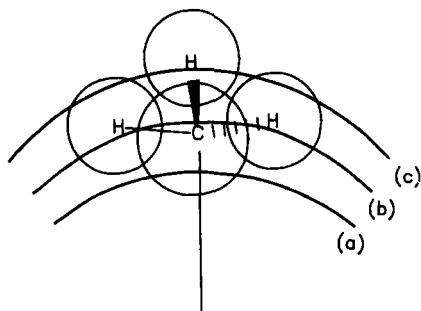


FIG. 20. Three possible interactions between a sphere of variable radius and a typical ligand; (a) the sphere intersects only one atom, (b) the sphere intersects two or more atoms that overlap, and (c) the sphere intersects two or more atoms that do not overlap.

angle γ . The solid angle, Ω_γ , is thus given by

$$\Omega_\gamma = 2\pi [1 - \cos \gamma]. \quad (35)$$

For case (ii) the same method is followed and the solid angle is given by the sum of the two (or more) semivertex angles. Case (iii) follows the procedure developed previously; i.e., all atoms in the ligand are traversed pairwise (Section II, B). A plot of the solid angle generated by the above procedure against radius gives a *radial profile* of the variation in steric effect along the ligand.

This approach can be generalized to *any* ligand or substituent once bond lengths, bond angles, and atomic radii are known.

To compare the steric demands with spatial variation of two (or more) ligands associated with the same metal a common vantage point must be chosen. If this is done, then steric interaction along a ligand can be ascertained. For systems in which the ligands are directly attached to the metal (e.g., $\text{Mo}(\text{CO})_4\text{LL}'$) the metal atom is a good vantage point (or apex) from which to examine the steric interactions between any ligands. Examples in which L and L' are varied are shown to indicate the common region in space in which L and L' are observed. From Fig. 21 the steric interaction as a function of distance from the metal center can readily be detected.

For systems such as $[(\eta^5\text{-C}_5\text{H}_3\text{R}_2)\text{Fe}(\text{CO})(\text{L})\text{I}]$ in which the ligands are not directly attached to the same metal, the metal is not a good vantage point for purposes of comparison. In this instance the point of intersection of the two vectors shown in Fig. 22 corresponds to the apex of the sphere of the variable radius. Using this approach the steric interaction between two ligands as a function of distance from the metal can be shown diagram-

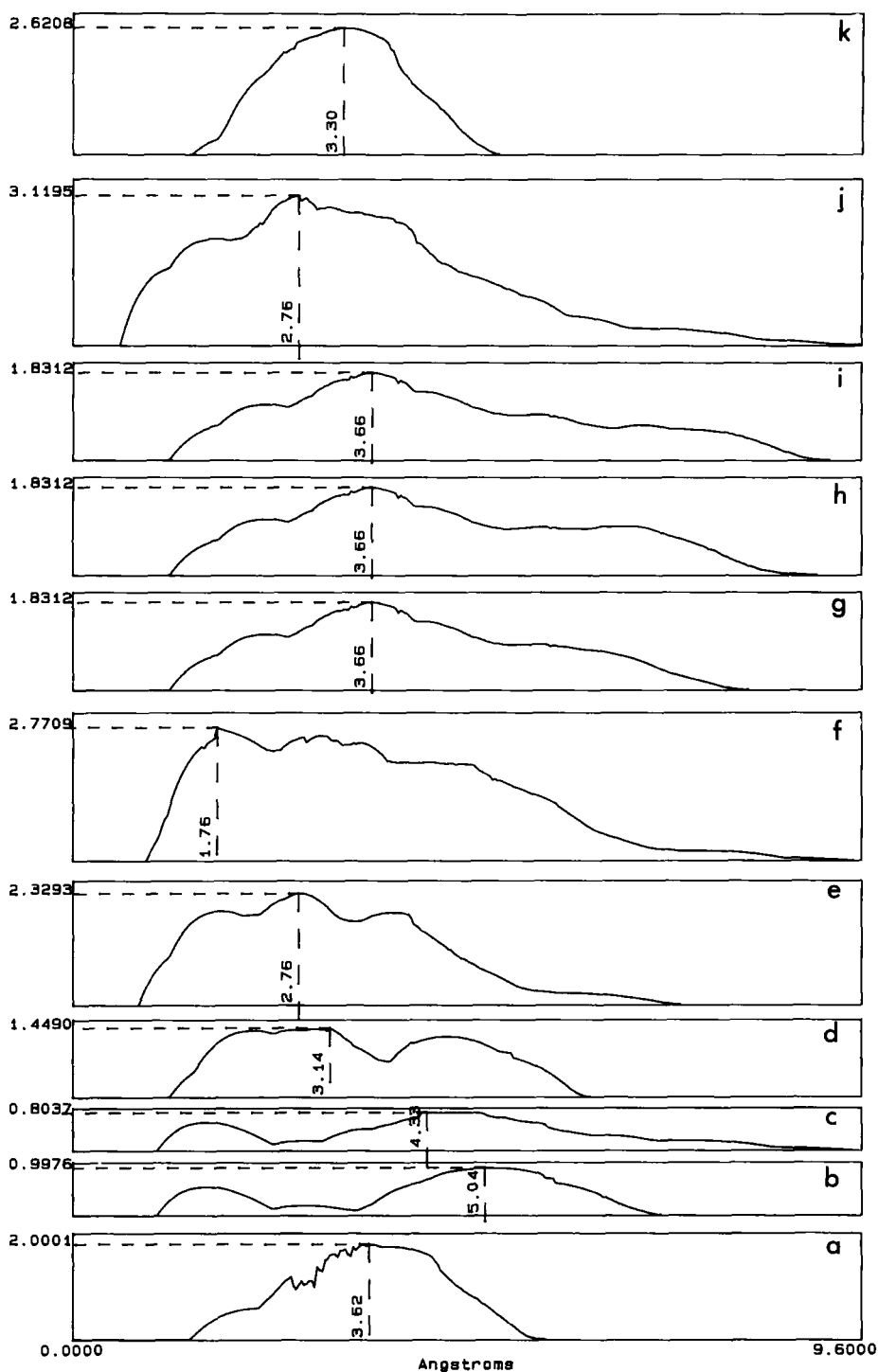


FIG. 21. Plot of growth of solid angle, Ω , against distance (\AA) for $[(\eta^5\text{-C}_3\text{H}_3\text{R}_2)\text{Fe}(\text{CO})(\text{L})]\text{I}$ complexes, (a) $\text{R} = \text{SiMe}_3$, (b) $t\text{-BuNC}$, (c) xyl-NC , (d) P(OMe)_3 , (e) PMe_2Ph , (f) $\text{P(O-}o\text{-tol)}_3$, (g) PPh_3 , (h) $\text{P}(m\text{-tol)}_3$, (i) $\text{P}(p\text{-tol)}_3$, (j) $\text{P}(\text{CH}_2\text{Ph})_3$, and (k) $\text{R} = \text{CMe}_3$.

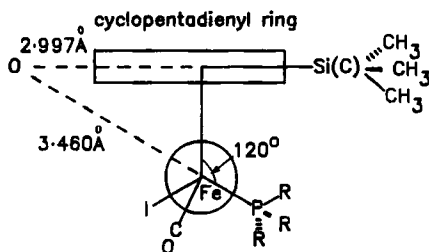


FIG. 22. Choice of vantage point in $[(\eta^5\text{-C}_5\text{H}_3\text{R}_2)\text{Fe}(\text{CO})(\text{PR}_3)\text{I}]$ ($\text{R} = \text{SiMe}_3, t\text{-Bu}$) complexes. The vector joining the centroid to $\text{Si}(\text{C})$ has been extended back by 2.997 Å to point O and the vector joining Fe to P extended back 3.460 Å to the same point. The coordinates of point O depend on the Fe-centroid distance (1.73 Å) and the centroid-Fe-P angle (120°).

matically, as below for the complexes in which L or R are varied in $[(\eta^5\text{-C}_5\text{H}_4\text{R})\text{Fe}(\text{CO})(\text{L})\text{I}]$ -type complexes (Fig. 21).

An example of the possible detection of this effect has been reported (17). In this study a ligand was specifically designed to test this suggestion. Multinuclear NMR spectroscopy, using complexes of the type $[(\eta^5\text{-C}_5\text{H}_3\text{R}_2)\text{Fe}(\text{CO})(\text{L})\text{I}]$ ($\text{R} = \text{SiMe}_3, t\text{-Bu}$; L = phosphine, phosphite or isonitrile) was employed to probe this limit. The SiMe_3 substituents in a 1,3-*pseudo-geminal* arrangement on the ring gives rise to two separate resonances for each of the atoms in the substituent in the ^1H , ^{13}C , and ^{29}Si NMR spectra. Similarly the *t*-Bu groups give rise to an analogous set of resonances in the ^1H and ^{13}C NMR spectra. Thus, moving out in space from the ring centroid to the outermost protons of the various groups, the degree of correlation between relevant NMR parameters and cone angle (or solid angle) of the ligand can be monitored. In this study it was found that the Si and C atoms on the ring interact with the ligand in a manner predicted by bulk solid or linear angle measurements. The same applies to the protons of the *t*-Bu group, but the protons of the SiMe_3

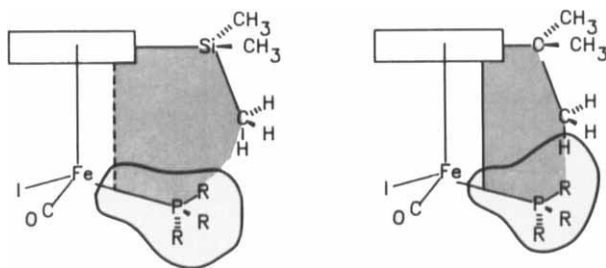


FIG. 23. Diagrammatic representation of the region in space (indicated area) in which a generalized Tolman cone angle for a PR_3 ligand is found to be meaningful for complexes of the type $[(\eta^5\text{-C}_5\text{H}_3\text{R}_2)\text{Fe}(\text{CO})(\text{PR}_3)\text{I}]$ ($\text{R} = \text{SiMe}_3, t\text{-Bu}$).

group did not (Fig. 23). Thus, it is concluded that the bulk solid angle is a poor measure of the steric demand of the ligand at certain points in space. In the case of SiMe_3 (and *t*-Bu) replacing the bulk solid angle by the solid angle at the point of the interacting protons the correlation between the chemical shift difference and the solid angle improved dramatically (Fig. 24).

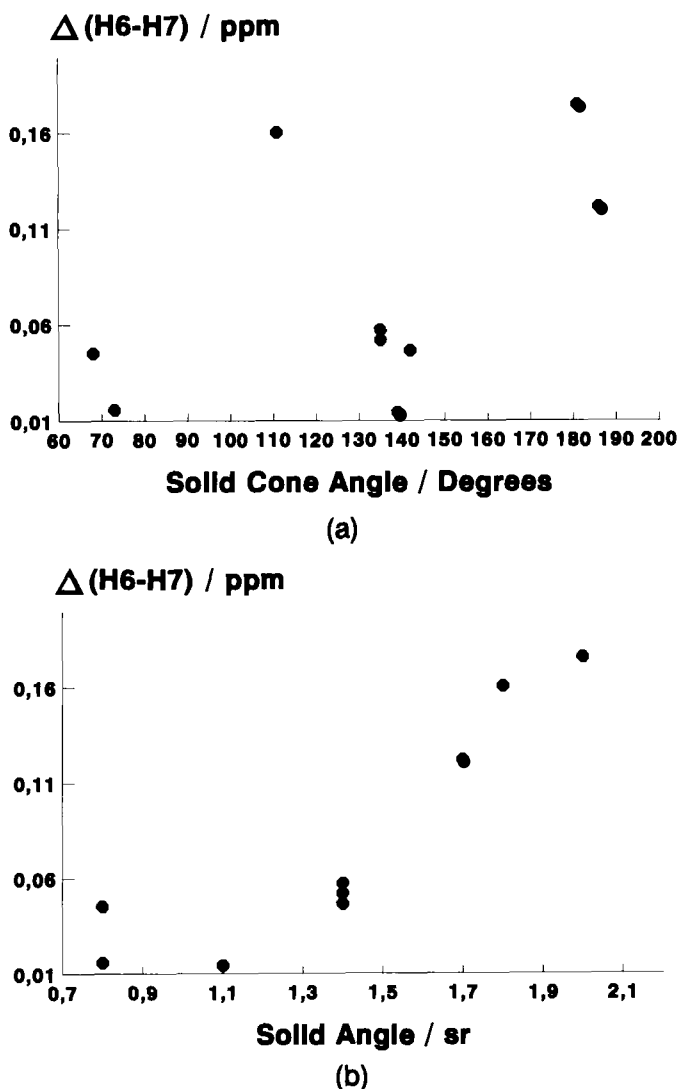


FIG. 24. Plot of $\Delta(\text{H6-H7})$ against (a) bulk solid angle, Ω and (b) solid angle at a point for $[(\eta^5\text{-C}_3\text{H}_3(\text{SiMe}_3)_2)\text{Fe}(\text{CO})(\text{L})\text{I}]$.

V

STERIC PROFILES AND THRESHOLDS

To correlate steric effects with chemical and physical properties it is necessary to differentiate between steric and electronic effects in relation to that property. In organometallic chemistry ligands have both σ and π components. The separation of the σ from the π components has a long history, which is not pertinent to this review, and is not discussed further.

Zähres and co-workers attempted a separation of steric and electronic effects based on a *regression analysis* analogous to Tolman's steric and electronic box (80). The enthalpy of the reaction between di- μ -methylbis[1-methyl-1- η^3 -(2-butenyl)]dinickel and a phosphorous ligand, L, was measured and separated into steric and electronic contributions using regression analysis.

Giering and co-workers questioned this work some years later (81). These authors achieved a *modified* separation of steric and electronic effects using a quantitative analysis of ligand effects, or QALE, approach. To measure steric effects, the Tolman cone angle was used. However, the electronic effects were separated into σ and π components. This was achieved by measurement of the reduction potential, $E_L^{0'}$, for a series of $\text{Ni}(\text{CO})_3\text{L}$ and $[(\eta^5\text{-C}_5\text{H}_4\text{Me})\text{Mn}(\text{CO})_2\text{L}]$ complexes in which L was varied. The reduction potential was found to be free of steric effects as reflected by the absence of any significant correlation between $E_L^{0'}$ and θ for the full data set. However, further analysis of the data revealed three regions: (i) below 0.40 V deviations from linearity could be attributed to a mix of σ -donor/ π -donor effects in π -basic ligands, called Class I ligands, (ii) between 0.40 and 0.51 V linearity that could be associated with pure σ -donor ligands, called Class II, was observed, and (iii) above 0.51 V nonlinearity was again observed and attributed to σ -donor/ π -acceptor, π -acid Class III ligands. Only for π bases was $E_L^{0'}$ found to correlate with θ to any significant extent.

These authors also defined electronic and steric profiles. The electronic profile is a plot of $\log k$ or $\log K$ versus $\text{p}K_a$, whereas the steric profile is a plot of the deviation from linearity in the electronic profile, $(\log k_{\text{obs}} - \log k_{\sigma})$ versus θ for Class II ligands. The deviations from linearity for Class I and III ligands were attributed to π effects. Various inferences were deduced from the electronic and steric profiles: the slope of the electronic profile gave a measure of the covalent character in the transition state, or the electron density on the metal in the transition state, whereas the steric profile revealed the steric threshold (θ_{st}). The steric threshold was interpreted as the hole size into which a ligand had to fit in a transition state. The quantity was found to be a function of the amount

of covalent bonding between the ligand in the transition state, the size of the other coordinated ligands, and the coordination number of the metal. The slope of the steric profile, once the steric threshold, θ_{st} , has been exceeded, was termed the *steric sensitivity*, which was defined as the ability of the complex to accommodate large ligands.

In a subsequent publication Prock and co-workers expanded the QALE concept to permit the separation of heats of reaction, ΔH , into σ - and π -electronic components (82). They found that σ - and π -electronic contributions to ΔH were linearly dependent upon pK_a and $E_{\pi a}$ and $E_{\pi b}$ (reduction potential for π acids and bases, respectively) both before and after θ_{st} :

$$-\Delta H_{\sigma} = a(pK_a) + c, \quad (36)$$

$$-\Delta H_{\pi} = b(E_{\pi a}) + c'. \quad (37)$$

It was noted that ΔH was dependent upon pK_a regardless of the ligand classification. However, since the data are not continuous functions (because of the Class I, II, and III classification scheme), regression analysis could not be used in such studies. Thus graphical methods were used to detect the thresholds for the onset of steric and π -electronic effects. Only when such graphical analyses were found to be impossible did the authors resort to a regression analysis. Any deviations from linearity were attributed to the onset of π effects.

This work was further explored by Rahman *et al.* (83). A number of expressions that quantified the relationships made in (81) were derived. For σ -donor ligands

$$\nu_{CO} = a\sigma_d + c, \quad (38)$$

$$E_L^{0'} = a'\sigma_d + c', \quad (39)$$

where σ_d is the σ donicity. Combining Eqs. (38) and (39) to reduce the quantities to purely measurable phenomena gave

$$\nu_{CO} = \left(\frac{a}{a'}\right) E_L^{0'} + c - \frac{ac'}{a'}. \quad (40)$$

For π -acceptor ligands

$$\nu_{CO} = A\sigma_d + B\pi_a + C, \quad (41)$$

$$E_L^{0'} = A'\sigma_d + B'\pi_a + C', \quad (42)$$

where π_a is the π acidity. Combining (41) and (42) gives

$$\nu_{CO} = \left(\frac{A}{A'}\right) E_L^{0'} + \left(B - \frac{AB'}{A'}\right) \pi_a + C - \frac{AC'}{A'}. \quad (43)$$

From these equations the authors were able to reason that for σ -donor ligands a plot of E_L^0 versus ν_{CO} is linear whereas for π acceptors a plot of ν_{CO} versus E_L^0 and π_a gives scatter.

A number of papers by Giering and co-workers expanding the above work have since appeared. Of note is the extension of the work to thioethers (84), silanes (85), applications to a study of Fe-P bond lengths (86), spectator phosphines (87), oxidative carbonylation reactions (88), and the dynamics and thermodynamics of redox-promoted carbonylation of $[(\eta^5\text{-C}_5\text{H}_5\text{Fe}(\text{CO})(\text{L})\text{Me}]$, L = group 15 donor ligand (89). In addition Moreno *et al.* have used the QALE concept to detect the steric threshold in $[(\eta^5\text{-C}_5\text{H}_4\text{COOMe})\text{Co}(\text{CO})_2]$ substitution reactions (90). Pacchioni and Bagus have used QALE to investigate the role of d orbitals in Pd-PX_3 , trans-L-Pd-PX_3 , and $(\text{CO})_3\text{-Pd-PX}_3$ complexes (X = H, Me, OMe, F; L = CO, NH_3) (91). Recently Wang *et al.* have used ^{17}O quadruple coupling constants (QCC) to investigate the π -acceptor ability of PMe_3 in $\text{W}(\text{CO})_5\text{L}$ (92). This is the first report of the relationship between π -bond strengths and the site of the ^{17}O QCC. This report managed to confirm that PMe_3 is a stronger π acid than π -neutral amines.

While the initial Giering paper (81) was in press, Poë and co-workers also proposed a method for separating steric and electronic effects (93). The main thrust of the Poë analysis was the separation of steric and electronic effects via a *steric profile* concept. Their conclusions arose from kinetic studies of the associative substitution of $\text{Ir}_4(\text{CO})_{12}$ with P-donor ligands. In the reaction the rate constant was found to depend critically upon the concentration of the ligand. A plot of $\log k_2$ against the change in half-neutralization potential, ΔHNP , yielded no regular trend. However, two ligands with similar cone angles were chosen and a straight line joining their $\log k_2$ values drawn. Deviations from this line were ascribed to steric effects, as the difference between observed values and the line was found to correlate with the Tolman cone angle, θ . A steric threshold around 101° was noted. Examination of the literature of similar reactions by Poë revealed that the form of the plots of $\log k_2$ against θ were typical of many associative substitution reactions. In subsequent publications Poë replaced the ΔHNP parameter with $\text{p}K_a$. Poë and co-workers systematically examined the literature for applications to the equation

$$\log k_2 = \alpha + \beta (\text{p}K_{a'} + 4) + \gamma (\theta - \theta_{th}) \lambda, \quad (44)$$

where λ (a switching factor) = 0 when $\theta < \theta_{th}$ (the threshold cone angle) and $\lambda = 1$ when $\theta > \theta_{th}$; $\text{p}K_{a'}$ is the σ basicity. The value of 4 in the equation was chosen as a correction factor for standard reactivity of a small, weakly basic nucleophile (94); α , β , and γ are constants. For

substitution reactions of the cluster $\text{Ru}_3(\text{CO})_{11}(\text{P}(n\text{-Bu})_3)$ with P-donor ligands little steric effect for ligands with $\theta < 130^\circ$ was noted. However, a strong relationship between θ and $\log k_2$ was found for $\theta > 130^\circ$. In contrast, the substitution of $\text{Ru}_3(\text{CO})_{12}$ by P-donor ligands showed a much more gradual change with θ . The differences between these two clusters was ascribed by Poë to a difference in *steric flexibility*. Numerous papers by Poë and co-workers have appeared exploiting and generalizing this separation of steric and electronic effects via the steric profile: kinetic studies on $\text{Ru}_3(\text{CO})_{10}(\mu\text{-Ph}_2\text{PCH}_2\text{PPh}_2)$ with P-donor ligands (95), reactions between $\text{Ru}_3(\text{CO})_{11}(\text{P}(\text{OEt})_3)$ and P- and As-donor ligands (96), reactions between $\text{Ru}(\text{CO})_4\text{L}$ and P-, As-, and Sb-donor ligands (97), a comparison of kinetics studies on $\text{Rh}_4(\text{CO})_9\{\text{P}(\text{OCH}_2)_3\text{CET}\}_3$ and $\text{Rh}_4(\text{CO})_{10}(\text{PCy}_3)_2$ (98), and the kinetics of $\text{Ru}_6\text{C}(\text{CO})_{17}$ (99).

Another detection of the steric threshold was noted by Seligson and Trogler in the study of the kinetics of olefin insertion into Pd-amine bonds (22).

In a recent work by Dunne *et al.*, the bonding properties of P-donor ligands were probed using geometric distortion parameters based on X-ray crystal structures (100). Analyzing some 1300 crystal structures these workers used molecular mechanics arguments to illustrate the geometric distortion from ideal geometries. These authors defined a mean angle deformation parameter, $S4'$:

$$S4' = \sum \alpha_i - \sum \beta_i, \quad (45)$$

where α_i is the Z–P–A angle in PA_3 (Z = any element) and β_i is the A–P–A angle. This parameter was found to correlate reasonably well with the Tolman cone angle.

VI

QUANTIFICATION OF STERIC SIZE USING MOLECULAR VOLUMES

An entirely different approach to the concept of size is given by the molecular volume approach. This involves the absolute measurement of volume occupied by a collection of atoms within a molecule.

In 1986 Meyer reviewed some of the more philosophical issues relating to the use of molecular volumes and the assumptions used in their calculation (101). The major objection to the commonly applied methods for calculating molecular volumes was that molecules do not have sharp, well-defined boundaries, but rather irregularly shaped topographies. Two extreme approaches to molecular volume measurements involve the calculation of either minimum or maximum volumes.

The calculation of molecular volumes using the minimum volume assumption assumes that the molecule is composed of overlapping spheres. However, molecules are not strictly spherical and the calculation of molecular volumes based on van der Waals radii give molecular volumes that are too small.

For the maximum volume approach a liquid is assumed to contain no interstitial sites. Hence the density, ρ , is a measure of the molecular size and the partial molar volume, v , is defined as the molar mass divided by the density. The molar volume, V_m , on the other hand, is defined as the partial molar volume divided by Avagadro's number. For *pseudo-spherical molecules* it can be shown that

$$\begin{aligned} V_m &= \frac{M}{N_A \rho} \\ &= \frac{4 \pi a^3}{3}, \end{aligned} \quad (46)$$

or

$$\frac{4 \pi a^3 N_A \rho}{3 M} = 1, \quad (47)$$

where a is the radius of the sphere. For interstitial voids, however,

$$\frac{4 \pi a^3 N_A \rho}{3 M} < 1. \quad (48)$$

In 1975 Edward and Farrell attempted to calculate the partial molar volume from the van der Waals radius for a given substituent (102). The van der Waals radius, r_w is related to the van der Waals volume, v_w , according to the equation

$$r_w = \left(\frac{3 v_w}{4 \pi} \right)^{1/3} \quad (49)$$

However, calculation of the van der Waals volume is not straightforward since an increase in volume upon dissolution of solute in solvent is not necessarily equal to the molecular volume of solute. These authors noted that the molecular volume exceeded the van der Waals volume by the volume of the solvent cage. To quantify this Edward and Farrell assumed that the solute molecules were spherical and had identical chemical properties to each other (in order to exclude any electronic effects). If Δ is the volume of the solvent cage (i.e., the separation of the solute molecule from the solvent), then the partial molar volume for one molecule, v , is

given by

$$\left(\frac{v}{v_w}\right)^{1/3} = 1 + \frac{\Delta}{r_w}. \quad (50)$$

A plot of $(v/v_w)^{1/3}$ versus r_w^{-1} gave a straight line with slope $\Delta = 0.53 \text{ \AA}$ (based on five data points). In this work the authors noted that Δ decreased with hydrophilic molecules. One severe limitation is that the methodology only applied to pseudospherically shaped molecules.

In 1978 Edward and co-workers noted that the partial molar volume, V^0 , of alkanes was greater than their van der Waals volume, V_w , by an amount V_e , the empty volume (103). In a later work this was extended to aromatic hydrocarbons (104).

In 1979 Motoc developed a different measure of steric effects based loosely on molecular volumes (105). A linear free energy relationship was employed to determine the overlapping volume of van der Waals volumes of atomic spheres reacting in the transition state. This method was called the *overlapping volume analysis* (OVA), where the overlapping volume was defined as

$$OV = \alpha \frac{|w_2|}{|w_1|}, \quad (51)$$

and α is the volume of the parallelepiped circumscribing the van der Waals envelope of any two atoms, w_2 is the set of points within the overlapping volume, and w_1 is the set of points within the parallelepiped. In a later publication Motoc *et al.* applied this analysis to a reaction involving radical addition to alkenes (106). A plot of the rate constant $\log k_r$ against OV and \mathcal{F}_c (the Swain-Lupton field constant) gave an R^2 of 0.88, whereas the same plot with E_s replacing OV gave $R^2 = 0.83$.

This method was extended to the calculation of octant volumes in a further publication (107).

In 1983 in a classical paper Gavezzotti reported the calculation of molecular volumes, providing an algorithm for these calculations (108). In the method a substituent is described by a set of vectors, S_i , connecting the nuclei to the origin, and a set of radii, R_i , defining a sphere around each nucleus. If the spheres overlap, Gavezzotti noted that the geometrical calculations became difficult. To calculate the molecular volume for a given substituent a sample envelope space containing all vectors S_i and R_i was generated. A large number of probe points, N , were added and the number of points inside at least one sphere were counted (N_{occ}). The molecular volume was then given by

$$V_m = V_{env} \frac{N_{occ}}{N}, \quad (52)$$

where V_{env} was the volume of the envelope. The volume of an interstitial site was given by

$$V_c = V_{\text{env}} \frac{N - N_{\text{occ}}}{N}. \quad (53)$$

The envelope was then divided into elementary volumes, $E_{\text{el}, i}$, and the fraction of space occupied by the i th elementary volume was defined as

$$D_i = \left(\frac{N_{\text{occ}}}{N} \right)_i \quad (54)$$

and the volume of the interstitial holes by

$$V_{\text{hole}} = \sum_{i, \text{hole}} (1 - D_i) V_{\text{el}, i}. \quad (55)$$

These formulae were applied to cryptate, inclusion compounds, and solid-state reactivity.

In 1987 Bader *et al.* used charge distribution to determine the *shapes and volumes* of molecules (109). These authors noted that an atom was fully defined by an average of its observable equations of motion obtained by generalizing quantum mechanical equations to a given subsystem. This generalization was noted to be unique as it only applied to those regions in space under the given constraints. The subsystem was chosen to be bounded by a surface with a zero flux gradient vector field of charge density for every point on the surface. Therefore each real space was partitioned into disjoint sets containing only one nucleus. The atomic surface was defined as the union of interatomic surfaces. The atomic volume was a measure of the region of space enclosed by the intersection of atomic surfaces of zero flux, and the molecular volume, v_m , was defined as

$$v_m = \sum v(\omega), \quad (56)$$

where $v(\omega)$ is the atomic volume. Meyer extended these ideas to the calculation of a molecular surface in 1988 (110).

In 1989 Higo and Gō developed an algorithm for the *rapid* calculation of molecular volumes for *large* molecules (proteins and nucleic acids) (111). The molecule was considered as a series of overlapping spheres with a rectangular box placed around the molecule. The sides of the box were an internal multiple of x , the unit cell length. The space within the box was divided into cubes of unit sides x . Three types of cube were identified: interior, exterior, and surface. The molecular volume was then defined as the sum of the volume of the interior cubes plus half the volume of the surface cubes. This *approximation* becomes asymptotically correct

as x becomes smaller. For rapid calculations x was chosen to be slightly smaller than the radii of the constituent spheres. This crude result was refined by dividing the *surface* cubes into eight smaller cubes and recalculating the volume.

The concept of molecular volume has been applied with much success to a variety of problems. Such applications include prediction of packing of molecules in a crystal (112), examination of the mutual orientation of aryl groups in a molecule (113), an examination of hydrocarbon crystals (114), evaluation of the contribution of *cavities* in protein structures (115), estimates of variable comic radii based on charge densities (116), topological analysis of histamines (117), application of void size to oxide ceramics (118), and the quantification of chirality (119).

A review by Braga appeared in 1992 (120) summarizing the applications of molecular volumes to organometallic complexes. The approach was first reported by Braga *et al.* who used *ab initio* calculations to investigate the geometries of certain clusters *in the solid state* (121). Since the metal–ligand bond strength is independent of the orientation of the ligand about the metal in the solid state, X-ray crystal data were used to provide a basis set of data for the analyses. A hard sphere approximation was used as the van der Waals radii of adjacent atoms can overlap over short distances. Three types of interaction were identified: metal–metal and metal–ligand bond interaction, intramolecular metal–metal and metal–ligand interactions, and intermolecular metal–metal and metal–ligand interactions. The intramolecular metal–metal and metal–ligand interactions are usually considered to be of steric origin and are, therefore, repulsive in nature. However, the authors found contributions from both attractive and repulsive interactions. The intermolecular interactions, which are also usually ignored, were taken into account by using a Buckingham potential [see Eq. (25)]. In the intramolecular energy calculations the 1,3-interactions were ignored and only 1,4-interactions considered. For almost all the clusters studied ($\text{Mn}_2(\text{CO})_{10}$, $\text{Re}_2(\text{CO})_{10}$, $\text{Fe}_2(\text{CO})_9$, $\text{Co}_2(\text{CO})_8$, $\text{Fe}_3(\text{CO})_{12}$, $\text{Ru}_3(\text{CO})_{12}$, red $\text{Ir}_6(\text{CO})_6$, and black $\text{Ir}_6(\text{CO})_6$) the authors found the CO groups on different metals in a cluster attract each other while the C–C interactions were repulsive.

The advantages of the solid-state analysis were recognized in a subsequent publication by Braga and Grepioni (122). The X-ray crystallographic data provide information about the molecular organization *within* the lattice. Cognisance of the ligand distribution over the cluster surface was taken in comparison with the molecular distribution within the lattice itself. These authors noted that the shape of the complex is important as it consists of *bumps* and *spaces* whereas the molecular geometry was considered as an internal parameter. Two neutral complexes, $\text{Ru}_3(\text{CO})_{12}$

(anticuboctahedral) and $\text{Fe}_3(\text{CO})_{12}$ (icosahedral) were considered and the analysis was performed using packing potential energy calculations. Later this analysis was expanded to include $\text{Fe}_2(\text{CO})_9$ and $\text{Co}_2(\text{CO})_8$ (123).

An analogous analysis was performed on charged species (124). In this study the choice of counterion was considered in response to the known criterion "solid salts separate from aqueous solution easiest for combinations of either small cation–small anion or large cation–large anion, preferably with systems having the same but opposite charges on the counterions" (125). This analysis was performed in order to answer three specific questions: (i) Is there any relation between charged and neutral systems in terms of the crystal packing? (ii) What is the relationship between ion size, shape, stoichiometry, and packing motif? and (iii) Do any preferential packing motifs exist? The methodology used was the packing potential energy calculations for rationalizing neutral solid-state behavior but at a maximum distance of 15 Å from the ion. Two different core systems were considered: $[\text{Os}_{10}\text{C}(\text{CO})_{24}]^{2-}$ and $[\text{Rh}_6\text{C}(\text{CO})_{15}]^{2-}$ in which space group symmetry was ignored. This was done in order to highlight the system from the perspective of a single ion. The authors found that, irrespective of the core nuclearity, cluster ions form monodimensional crystals within tridimensional networks. Also the intermolecular CO . . . CO distance was unaffected by the presence of the charge. The location of the site of anion–anion interlocking was found to depend on stoichiometry. When the anion : cation ratio was 1 : 2 and the cation was large, the anion pile was completely surrounded by cations, whereas when the anion : cation ratio was 1 : 1 direct interpole was found. Two factors were identified as keys to the formation of ionic crystals: the need to occupy space efficiently and the overall electrical neutrality of the material.

Mingos and Rohl quantified the above approach by recognizing the need to understand the experimental and theoretical factors governing crystallization (126,127). They calculated molecular volumes, V_m , surface areas, S_m , and shapes of ions using the method of Gavezzotti (108). To calculate the molecular volume, a parallelepiped was placed around the ion, which was constructed from a van der Waals sphere centered around the atomic position. Two variables were defined: the number of probe points, N , and a number of points inside at least one of the van der Waals spheres, N_{occ} . If the volume of the parallelepiped is V_{\parallel} , then the molecular volume is given by

$$V_m = V_{\parallel} \frac{N_{\text{occ}}}{N}. \quad (57)$$

The molecular surface area was determined from moments of inertia calculated without mass weighting (126, Ref. 8). From a computation of volumes

for cations, V_c , and anions V_a , these authors found that unusual anionic compounds may be stabilized if $V_c \geq V_a$. By examining the ratio V_a/V_c they found that cation–anion sizes need not be matched precisely in order for a complex to crystallize, but optimum crystallization occurs when V_c is slightly larger than V_a . This work used modified Bondi van der Waals radii for metal ions (128) with the Gavezzotti method for calculating molecular volumes and surfaces areas (108). An interesting correlation between molecular volume and surface area was found with $S_m = 29.8 + 1.04 V_m$. These authors also found that molecular ions do not obey strict spherical geometry and defined a geometrical parameter, $I = S_m/V_m^{2/3}$, to determine the deviations from spherical geometry of the ion under investigation. Mingos and Rohl also used moments of inertia to classify the shapes of molecular ions.

Two interesting publications relating to the size and packing of ions have appeared recently. Bouche has found that the total van der Waals volume of an ion pair is smaller than the sum of the individual volumes of the ions (129). Further, Müller has quantitatively shown that the cubic closest-packed structure is more efficient in spacial arrangement than the hexagonal close-packed structure (130). The details of these methods are beyond the scope of this review.

Recently an interesting paper by Hargittai describing steric effects in terms of VSEPR (valence shell electron pair repulsion) theory appeared (131). This descriptive paper (the details of which are beyond the scope of this review) aimed to draw attention to the importance of simple space considerations in an attempt to improve the synergic interactions between chemistry and other disciplines.

In contrast to the publications discussed above, Charton and Charton, in 1979, produced a work that questioned whether molecular volumes were indeed related to *steric effects* (132). In this work these authors considered quantitative structure activity relationships (QSAR) to determine whether van der Waals volume (V_w), molar refractivity (MR), molar volume (V_m), Traube's rule volume (V_T), and molecular weight (W_m) were interrelated. The four quantitative activity structure parameters were correlated with the Bondi values for the van der Waals volume according to the equation

$$Q = mV_w + c, \quad (58)$$

where Q is the relevant QSAR and m and c are constants. For molar refractivity three categories were considered: π bonding, partial π bonding, and no π bonding. The correlations between W_m and V_w were not significant nor was the correlation with MR, indicating that neither of these parameters is useful for the quantification of a steric effect. In a

kinetic and thermodynamic study both rate and equilibrium constants were found to depend on a steric parameter v rather than V_w , thus indicating that volume or bulk measures *do not measure steric effects*. These authors found that all the QSAR are interrelated and proposed that they measure group polarizability or hydrophobicity.

VIII

SOME APPLICATIONS OF STERIC SIZE MEASUREMENTS

The application of steric effects to rationalize physical and chemical properties in chemistry is widespread and spans such diverse realms as studies of fluxional behavior in osmium clusters (133), ^{19}F NMR spectroscopy studies of zwitterionic resonance of *para*-disubstituted arenes (134), ^{199}Hg NMR studies of dimolybdenum mercury species (135), the use of ^{17}O NMR spectroscopy to differentiate between open and triangular clusters (136), and the use of NMR spectroscopy to critically evaluate published phosphorus cone angle data using the methyl resonance (which is very sensitive to steric size) in complexes of the type $[\text{Co}(\text{L})(\text{DH})_2\text{CH}_3\text{OH}]^+$, DH = dimethylglyoximate (137). To conclude this review the authors have chosen to illustrate *some* of the applications of steric size measurements, with examples from the area of transition metal cyclopentadienyl and aryl chemistry.

In an early report of steric effects in cyclopentadienyl organometallic chemistry Dämmgen and Bürger (138) suggested that addition of larger alkyl groups R , R' , and R'' to $[(\eta^5\text{-C}_5\text{H}_5)\text{Ti}(\text{NR}_2)_3]$ resulted in a change in the metacyclopentadienyl hapticity to $[(\eta^2\text{-C}_5\text{H}_3\text{R}'\text{R}'')\text{Ti}(\text{NR}_2)_3]$. Molecular models were built to assess the steric contribution of the alkyl groups.

Werner and Hofmann (139) verified the mechanism of electrophilic substitution on the cyclopentadienyl ring as proceeding through a cationic metal intermediate. Migration of the electrophile from the ring to the metal and subsequent loss of H^+ completed the reaction. The existence of product rotamers was investigated by means of NMR spectroscopy and the conformational preferences were rationalized on steric grounds, illustrated by means of ball and stick models.

Multinuclear NMR, as well as IR, spectroscopy was used by Rausch and co-workers (140) to investigate the steric effects in $[(\eta^5\text{-C}_5\text{H}_4\text{R})\text{Rh}(\text{CO})_2]$ complexes. These authors found a significant correlation between the inductive Taft steric parameter, σ_1 , and the ^{103}Rh chemical shift. From

the IR data they were able to conclude that CO stretching frequencies were in agreement with d_{π} -electron back donation.

Bönnemann has detected a steric effect in the Co-catalyzed synthesis of pyridines only when very bulky ligands are used (141). When complexes of the type $YCoL$, $Y = \eta^5-C_5H_{5-n}R_n$, $\eta^5-C_9H_{7-n}R_n$, $L =$ olefin, diolefin, aromatic hydrocarbon, CO, or P-donor ligands were used as catalysts, electronic effects were found to dominate catalytic activity, except when $Y = \eta^5-1,2-C_5H_3(SiMe_3)_2$ and $\eta^5-C_5HPh_4$. In another catalytic study using substituted cyclopentadienyl ligands, Möhring and Coville showed that both the size and electronic effects of R in $[(\eta^5-C_5H_4R)_2ZrCl_2]$ influenced the rate of ethylene polymerization (142). Cone angle data for cyclopentadienes using the Zr system were reported.

Coville and co-workers have also detected steric effects associated with monosubstituted cyclopentadienyl iron complexes. The chemical shift difference between the ortho-cyclopentadienyl ring protons (or carbon atoms) were found to vary linearly with the cone angle of the ligand in complexes of the type $[(\eta^5-C_5H_4R)Fe(CO)(L)I]$ and $[(\eta^5-C_9H_7)Fe(CO)(L)I]$, R = Me, *t*-Bu; L = phosphine, phosphite, or isonitrile (143). Similar results were observed for complexes of the type $[(\eta^5-C_5H_4R)Ru(CO)(L)I]$ (144).

Hunter *et al.* (145) used variable-temperature ^{13}C NMR spectroscopy to calculate the energy barrier to rotation in $[(\eta^6-C_6H_6)Cr(CO)_2(PPh_3)]$, $[(\eta^6-C_6Me_6)Cr(CO)_2(PPh_3)]$, $[(\eta^6-C_6Et_6)Cr(CO)_2(PPh_3)]$, and $[(\eta^6-C_6(n-Pr)_6)Cr(CO)_2(PPh_3)]$. The steric requirements of ring rotation were assessed by means of two intersecting cones: one from the metal to the arene and the other from the metal to the phosphine. Unfortunately no value for the arene cone was reported. Subsequently Hunter and co-workers (146) extended this study to $[(\eta^6-C_6H_{6-n}Me_n)M(CO)_2(PPh_3)]$, M = Cr, Mo.

The role of bulky substituents in the chemical and physical properties of cyclopentadienyl metal complexes has been reviewed by Okuda (147) and Schumann (148). Reports of the role of bulky ring substituents on the dynamic rotational behavior of cyclopentadienyl rings have appeared (149).

Finally, a time-resolved IR study has been reported by Poliakoff and co-workers (150). The kinetics of the photochemical reactions of $[(\eta^5-C_5R_5)Mn(CO)_3]$, R = H, Me, Et, were reported. Substitution for hydrogen on the cyclopentadienyl ring was shown to effect the rate of the reaction significantly. The differences in rate between the complexes with R = Me and R = Et confirmed that the reaction was under steric rather than electronic control.

IX

CONCLUSION

Some important issues arise from this review. There are two methods presently used to quantify steric size in chemistry. These arise from either a consideration of chemical properties (Taft-Dubois steric parameter) or physical properties (cone angle, solid angle, and ligand repulsive energy). The former approach has been adopted by organic chemists, whereas the latter has been extensively used by inorganic chemists. Recent reports have indicated, not unexpectedly, that the two approaches can be interconnected.

The *physical measurement* approaches entail abstractions and are consequently based on a range of assumptions. If these are understood and appreciated, this measure can give a valuable means of quantifying the steric contribution in chemical reactions. However, there is an issue that needs to be highlighted. Presently all physical measures suffer from a fundamental limitation: comparisons between published data are not possible. This largely arises from the diversity in parameters chosen for the measurement by different authors of the same or different ligands or groups (e.g., atom size, bond lengths, bond angles, and conformation). Two solutions to this problem exist.

The first solution is to adopt and generate a uniform, standard set of data. The ability to readily measure cone angles or solid angles on a computer means that, unlike in the past where the physical measure required construction of models, any ligand or substituent size can now be measured with ease. This should result in a more sophisticated approach to the concept of structure-reactivity correlations. This procedure is, in essence, that in use today.

A second, and alternative, approach is to use different steric data sets unique to a given chemical system. Thus the steric sizes for given ligands will be different for different metals. This approach has the advantage that the steric measurements will be realistic in a specific reaction rather than relative to an arbitrary standard. In this approach a *method* rather than a specific steric value of steric demand should be formulated.

ACKNOWLEDGMENTS

We thank Professor T. L. Brown for preprints of manuscripts and Professor P. G. L. Leach for helpful suggestions in the manuscript preparation.

REFERENCES

- (1) Hofmann, A. W. *Chem. Ber.* **1872**, 5, 704.
- (2) Sachse, H. *Chem. Ber.* **1890**, 23, 1363.
- (3) Mohr, E. J. *Prakt. Chem.* **1918**, 98, 315.
- (4) Baeyer, A. *Chem. Ber.* **1885**, 18, 2269.
- (5) Kehrmann, F. *Chem. Ber.* **1888**, 21, 3315.
- (6) Meyer, V. *Chem. Ber.* **1894**, 27, 510.
- (7) Wegschneider, R. *Monatsh. Chem.* **1895**, 16, 75.
- (8) Anschütz, L. *Angew. Chem.* **1928**, 41, 691.
- (9) Newman, M. S., Ed. "Steric Effects in Organic Chemistry"; Wiley: New York, 1956.
- (10) Mosher, H. S.; Tidwell, T. T. *J. Chem. Educ.* **1990**, 67, 9.
- (11) Tolman, C. A. *J. Am. Chem. Soc.* **1970**, 92, 2953.
- (12) Cotton, F. A.; Wilkinson, G. "Advanced Inorganic Chemistry"; Wiley: New York, 1980; p. 89.
- (13) Tolman, C. A. *Chem. Rev.* **1977**, 77, 313.
- (14) Datta, D.; Sharma, G. T. *J. Chem. Res., Synop.* **1987**, 422; Datta, D.; Majumdar, D. *J. Phys. Org. Chem.* **1991**, 4, 611.
- (15) Coville, N. J.; Loonat, M. S.; White, D.; Carlton, L. *Organometallics* **1992**, 11, 1082.
- (16) White, D.; Taverner, B. C.; Leach, P. G. L.; Coville, N. J. *J. Comput. Chem.*, **1993**, 14, 1042.
- (17) White, D.; Carlton, L.; Coville, N. J. *J. Organomet. Chem.* **1992**, 440, 15.
- (18) Yamamoto, Y.; Aoki, K.; Yamazaki, H. *Inorg. Chem.* **1979**, 18, 1681.
- (19) Maitlis, P. M. *Chem. Soc. Rev.* **1981**, 1.
- (20) ALCHEMY II, Release 2.01, Tripos Associates Inc., St. Louis, Missouri, 1986, 1989.
- (21) Coville, N. J.; du Plooy, K. E.; Pickl, W. *Coord. Chem. Rev.* **1992**, 116, 1; du Plooy, K. E. Ph.D. Thesis, University of the Witwatersrand, 1993.
- (22) Seligson, A. L.; Trogler, W. C. *J. Am. Chem. Soc.* **1991**, 113, 2520.
- (23) Marques, H. M.; Bradley, J. C.; Campbell, L. A. *J. Chem. Soc., Dalton Trans.* **1992**, 2019.
- (24) Imyaninov, N. S. *Koord. Khim.* **1985**, 11, 1041, 1181.
- (25) Ounapu, L. M.; Mosbo, J. A.; Risley, J. M.; Storhoff, B. M. *J. Organomet. Chem.* **1980**, 194, 337; Boyles, M. L.; Brown, D. V.; Drake, D. A.; Hostettler, C. K.; Maves, C. K.; Mosbo, J. A. *Inorg. Chem.* **1987**, 24, 3126.
- (26) de Santo, J. T.; Mosbo, J. A.; Storhoff, B.-N.; Bock, P. L.; Bloss, R. E. *Inorg. Chem.* **1980**, 19, 3086.
- (27) Casey, C. P.; Whiteker, G. T. *Isr. J. Chem.* **1990**, 30, 299.
- (28) Casey, C. P.; Whiteker, G. T.; Campana, C. F.; Powell, D. R. *Inorg. Chem.* **1990**, 29, 3376.
- (29) Casey, C. P.; Whiteker, G. T.; Melville, M. G.; Petrovich, L. M.; Gavney, J. A., Jr.; Powell, D. R. *J. Am. Chem. Soc.* **1992**, 114, 5535.
- (30) Stahl, L.; Ernst, R. D. *J. Am. Chem. Soc.* **1987**, 109, 5673.
- (31) Kakkar, A.; Taylor, N. J.; Marder, T. B.; Shen, J. K.; Hallinan, N.; Bosolo, F. *Inorg. Chim. Acta* **1992**, 198-200, 219.
- (32) Mingos, D. M. P. *Inorg. Chem.* **1982**, 21, 464.
- (33) Ferguson, G.; Roberts, P. J.; Alyea, E. C.; Khan, M. *Inorg. Chem.* **1978**, 17, 2965.
- (34) Alyea, E. C.; Ferguson, G.; Somogyvani, A. *Inorg. Chem.* **1982**, 21, 1369.
- (35) Alyea, E. C.; Dias, S. A.; Ferguson, G.; Siew, P. Y. *Can. J. Chem.* **1983**, 61, 257.
- (36) Smith, J. D.; Oliver, J. D. *Inorg. Chem.* **1978**, 17, 2585.
- (37a) Mullica, D. F.; Gipson, S. L.; Sappenfield, E. L.; Lin, C. C.; Leschnitzer, D. H. *Inorg. Chim. Acta* **1990**, 177, 89.

- (37b) Farrar, D. H.; Payne, N. C. *Inorg. Chem.* **1981**, *20*, 821.
- (38) Clark, H. C.; Hampden-Smith, M. J. *Coord. Chem. Rev.* **1987**, *79*, 229.
- (39) Riley, K. F. "Mathematical Methods for the Physical Sciences"; Cambridge University Press: Cambridge, 1974; p. 91.
- (40) Immirzi, A.; Musco, A. *Inorg. Chim. Acta* **1977**, *25*, L41.
- (41) Komatsuzaki, T.; Sakakibara, K.; Hirota, M. *Tetrahedron Lett.* **1989**, *30*, 3309; *Chem. Lett.* **1990**, 1913; Hirota, M.; Sakakibara, K.; Komatsuzaki, T.; Akai, I. *Comput. Chem.* **1991**, *15*, 241.
- (42) Bagnall, K. W.; Xing-Fu, L. *J. Chem. Soc., Dalton Trans.* **1982**, 1365; Bagnall, K. W. *Inorg. Chim. Acta* **1984**, *94*, 3.
- (43) Fischer, R. D.; Xing-Fu, L. *J. Less-Common Met.* **1985**, *112*, 303.
- (44) Lobkovskii, E. B. *Zh. Strukt. Khim.* **1983**, *24*, 66; *J. Organomet. Chem.* **1984**, *277*, 53.
- (45) Xing-Fu, L.; Eggers, S.; Kopf, J.; Jahn, W.; Fisher, R. D.; Apostolidis, C.; Kanellakopoulos, B.; Benetollo, F.; Polo, A.; Bombieri, G. *Inorg. Chim. Acta* **1985**, *100*, 183.
- (46) Xing-Fu, L.; Ao-Ling, G. *Inorg. Chim. Acta* **1987**, *131*, 129; *134*, 143.
- (47) Sheeman, J. I.; Viers, J. W.; Schug, J. C.; Stovall, M. D. *J. Am. Chem. Soc.* **1984**, *106*, 143.
- (48) Tumanov, A.; Zakharov, L. N.; Sennikov, P. G.; Egorochkin, A. N.; Razuvaev, G. A.; Smirnov, A. S.; Dodonov, V. A. *J. Organomet. Chem.* **1984**, *263*, 213.
- (49) Zakharov, L. N.; Domrachev, G. A.; Struchkov, Yu. T. *Zh. Strukt. Khim.* **1983**, *24*, 75.
- (50) Titova, S. N.; Bychkov, V. T.; Domrachev, G. A.; Razuvaev, G. A.; Zakharov, L. N.; Alexandrov, G. G.; Struchkov, Yu. T. *Inorg. Chim. Acta* **1981**, *50*, 71.
- (51) White, D. Ph.D. Thesis, Univ. of the Witwatersrand, Johannesburg, 1993.
- (52) White, D.; Taverner, B. C.; Daniel, C. A.; Leach, P. G. L.; Coville, N. J. submitted for publication in *Inorg. Chim. Acta*.
- (53) Chauvin, R.; Kagan, H. B. *Chirality* **1991**, *3*, 242.
- (54) McClelland, R. A.; Kanagasabapathy, V. M.; Banait, N. S.; Sttenken, S. *J. Am. Chem. Soc.* **1991**, *113*, 1009.
- (55) Akai, I.; Sakakibara, K.; Hirota, M. *Chem. Lett.* **1992**, 1317.
- (56) Komatsuzaki, T.; Akai, I.; Sakakibara, K.; Hirota, M. *Tetrahedron* **1992**, *48*, 1539.
- (57) Newman, M. S. *J. Am. Chem. Soc.* **1950**, *72*, 4783; **1952**, *74*, 3929.
- (58) Beckhaus, H. D. *Angew. Chem.* **1978**, *90*, 633.
- (59) White, D.; Wade, P. W.; Coville, N. J. *Inorg. Chem.*, in preparation.
- (60) Caffery, M. L.; Brown, T. L. *Inorg. Chem.* **1991**, *30*, 3907; Lee, K. J.; Brown, T. L. *ibid.* **1992**, *31*, 289.
- (61) Brown, T. L. *Inorg. Chem.* **1992**, *31*, 1286.
- (62) Choi, M.-G.; Brown, T. L. *Inorg. Chim. Acta* **1992**, *198*, 823.
- (63) Choi, M.-G.; Brown, T. L. *Inorg. Chem.*, **1993**, *32*, 1548.
- (64) Choi, M.-G.; White, D.; Brown, T. L. submitted for publication in *Inorg. Chem.*
- (65) Choi, M.-G.; Brown, T. L. *Inorg. Chem.*, in press.
- (66) Rodger, A.; Johnson, B. F. G. *Inorg. Chim. Acta* **1992**, *191*, 109, and references therein.
- (67) Baird, N. C. *Inorg. Chem.* **1989**, *28*, 1224.
- (68) Hancock, R. D. *Prog. Inorg. Chem.* **1989**, *17*, 187.
- (69) Taft, R. W. In "Steric Effects in Organic Chemistry"; Newman, M. S., Ed.; Wiley: New York, 1956; p. 556.
- (70) Hancock, C. K.; Meyers, E. A.; Yagar, B. J. *J. Am. Chem. Soc.* **1961**, *83*, 4211.
- (71) Palm, V. A. "Fundamentals of the Quantitative Theory of Organic Reactions"; Khimlya: Leningrad, 1967; Chapter 10.
- (72) Charton, M. *J. Am. Chem. Soc.* **1969**, *91*, 615.
- (73) Charton, M. *J. Am. Chem. Soc.* **1969**, *91*, 619.

- (74) Charton, M. J. *Am. Chem. Soc.* **1975**, 97, 1552.
- (75) MacPhee, J. A.; Panaye, A.; Dubois, J.-E. *Tetrahedron* **1978**, 34, 3553.
- (76) Panaye, A.; MacPhee, J. A.; Dubois, J. E. *Tetrahedron* **1980**, 36, 759.
- (77) Dubois, J. E.; MacPhee, J. A.; Panaye, A. *Tetrahedron* **1980**, 36, 919.
- (78) Staskun, B. J. *Org. Chem.* **1981**, 46, 1643.
- (79) Boeyens, J. C. A.; Denner, L.; Painter, S.; Staskun, B. S. *Afr. J. Chem.* **1987**, 40, 60.
- (80) Schlenkluhn, H.; Scheidt, W.; Weimann, B.; Zähres, M. *Angew. Chem., Int. Ed. Engl.* **1979**, 18, 401.
- (81) Golovin, M. N.; Rahman, M. M.; Belmonte, J.; Giering, W. P. *Organometallics* **1985**, 4, 1981.
- (82) Rahman, M. M.; Liu, H.-Y.; Prock, A.; Giering, W. P. *Organometallics* **1987**, 6, 650.
- (83) Rahman, M. M.; Liu, H.-Y.; Eriks, K.; Prock, A.; Giering, W. P. *Organometallics* **1989**, 8, 1.
- (84) Tracey, A. T.; Eriks, K.; Prock, A.; Giering, W. P. *Organometallics* **1990**, 9, 1399.
- (85) Panek, J.; Eriks, K.; Giering, W. P. *Organometallics* **1990**, 9, 2175.
- (86) Liu, H.-Y.; Prock, A.; Giering, W. P. *Organometallics* **1990**, 9, 1758.
- (87) Eriks, K.; Giering, W. P.; Liu, H.-Y.; Prock, A. *Inorg. Chem.* **1989**, 28, 1759.
- (88) Prock, A.; Giering, W. P.; Greene, J. E.; Meirowitz, R. E.; Hoffman, S. L.; Woska, D. C.; Wilson, M.; Chang, R.; Chen, J.; Magnuson, R. H.; Eriks, K. *Organometallics* **1991**, 10, 3479.
- (89) Woska, D. C.; Wilson, M.; Bartholomew, J.; Eriks, K.; Prock, A.; Giering, W. P. *Organometallics* **1992**, 11, 3343.
- (90) Moreno, C.; Macazaga, M. J.; Delgado, S. *Organometallics* **1991**, 10, 1124.
- (91) Pacchioni, G.; Bagus, P. S. *Inorg. Chem.* **1992**, 31, 4391.
- (92) Wang, S. P.; Richmond, M. G.; Schwartz, M. J. *Am. Chem. Soc.* **1992**, 114, 7595.
- (93) Dahlinger, K.; Falcone, F.; Poë, A. J. *Inorg. Chem.* **1986**, 25, 2654.
- (94) Poë, A. J. *Pure Appl. Chem.* **1988**, 60, 1209.
- (95) Ambwani, B.; Chawla, S. K.; Poë, A. J. *Polyhedron* **1988**, 7, 1939.
- (96) Chen, L.; Poë, A. J. *Can. J. Chem.* **1989**, 67, 1924.
- (97) Chen, L.; Poë, A. J. *Inorg. Chem.* **1989**, 28, 3641.
- (98) Brodie, N. M. J.; Poë, A. J. *J. Organomet. Chem.* **1990**, 383, 531.
- (99) Poë, A. J.; Farrar, D. H.; Zheng, Y. *J. Am. Chem. Soc.* **1992**, 114, 5146.
- (100) Dunne, B. J.; Morris, R. B.; Orpen, A. G. *J. Chem. Soc., Dalton Trans.* **1991**, 653.
- (101) Meyer, A. Y. *Chem. Soc. Rev.* **1986**, 15, 449.
- (102) Edward, J. T.; Farrell, P. G. *Can. J. Chem.* **1975**, 53, 2965.
- (103) Edward, J. T.; Farrell, P. G.; Shahidi, F. *J. Phys. Chem.* **1978**, 82, 2310.
- (104) Shahidi, F.; Farrell, P. G.; Edward, J. T.; Canonne, P. *J. Org. Chem.* **1979**, 44, 950.
- (105) Motoc, I. *MATCH* **1979**, 4, 113.
- (106) Motoc, I.; Vancea, R.; Muscutariu, I. *MATCH* **1979**, 5, 263.
- (107) Motoc, I.; Dragomir-Fillimonescu, O.; Muscutariu, I. *MATCH* **1980**, 8, 323.
- (108) Gavezzotti, A. *J. Am. Chem. Soc.* **1983**, 105, 5220.
- (109) Bader, R. F. W.; Carroll, M. T.; Cheeseman, J. R.; Chang, C. J. *Am. Chem. Soc.* **1987**, 109, 7968.
- (110) Meyer, A. J. *Comput. Chem.* **1988**, 9, 18.
- (111) Higo, J.; Gō, N. *J. Comput. Chem.* **1989**, 10, 376.
- (112) Desiraju, G. R.; Gavezzotti, A. *Acta Crystallogr., Sect. B* **1989**, B45, 473.
- (113) Gavezzotti, A. *Chem. Phys. Lett.* **1989**, 161, 67.
- (114) Gavezzotti, A. *Acta Crystallogr., Sect. B* **1990**, B46, 275.
- (115) Alard, P.; Wodak, S. J. *J. Comput. Chem.* **1991**, 12, 918.
- (116) Arteca, G.; Grant, N. D.; Mezey, P. G. *J. Comput. Chem.* **1991**, 12, 1198.

- (117) Arteca, G.; Hernández-Laguna, A.; Ránde, J. J.; Smeyers, Y. G.; Mezey, P. G. *J. Comput. Chem.* **1991**, *12*, 705.
- (118) Thomas, N. W. *Acta Crystallogr., Sect. B* **1991**, *B47*, 588.
- (119) Meyer, A. Y.; Avnir, D. *Struct. Chem.* **1991**, *2*, 475.
- (120) Braga, D. *Chem. Rev.* **1992**, *92*, 633.
- (121) Braga, D.; Rodger, A.; Johnson, B. F. G. *Inorg. Chim. Acta* **1990**, *174*, 185.
- (122) Braga, D.; Grepioni, F. *Organometallics* **1991**, *10*, 1254.
- (123) Braga, D.; Grepioni, F.; Sabatino, P.; Gavezzotti, A. *J. Chem. Soc., Dalton Trans.* **1992**, 1254.
- (124) Braga, D.; Grepioni, F. *Organometallics* **1992**, *11*, 1256.
- (125) Bosolo, F. *Coord. Chem. Rev.* **1968**, *3*, 213.
- (126) Mingos, D. M. P.; Rohl, A. L. *Inorg. Chem.* **1991**, *30*, 3769, and references therein.
- (127) Mingos, D. M. P.; Rohl, A. L. *J. Chem. Soc., Dalton Trans.* **1991**, 3419.
- (128) Allinger, N. L. *Adv. Phys. Org. Chem.* **1976**, *13*, 1.
- (129) Bouche, G. *Angew. Chem., Int. Ed. Engl.* **1992**, *31*, 731.
- (130) Müller, U. *Angew. Chem., Int. Ed. Engl.* **1992**, *31*, 727.
- (131) Hargittai, I. *Pure Appl. Chem.* **1992**, *64*, 1489.
- (132) Charton, M.; Charton, B. I. *J. Org. Chem.* **1979**, *44*, 2284.
- (133) Einstein, F. W. B.; Johnston, V. J.; Ma, A. K.; Pomeroy, R. K. *Organometallics* **1990**, *9*, 52.
- (134) Taft, R. W.; Glick, R. E.; Lewis, I. C.; Fox, I.; Ehrenson, S. *J. Am. Chem. Soc.* **1960**, *82*, 756.
- (135) Cotton, J. D.; Miles, E. A. *Inorg. Chim. Acta* **1990**, *173*, 129.
- (136) Onaka, S.; Takagi, S.; Furuta, H.; Kato, Y.; Mizuno, A. *Bull. Chem. Soc. Jpn.* **1990**, *63*, 42.
- (137) Trogler, W. C.; Marzilli, L. G. *Inorg. Chem.* **1975**, *14*, 2942.
- (138) Dämmgen, U.; Bürger, H. J. *Organomet. Chem.* **1975**, *101*, 307.
- (139) Werner, H.; Hofmann, W. *Angew. Chem., Int. Ed. Engl.* **1977**, *16*, 794.
- (140) Graham, P. B.; Rausch, M. D.; Täschler, K.; von Philipsborn, W. *Organometallics* **1991**, *10*, 3049.
- (141) Bönnemann, H. *Angew. Chem., Int. Ed. Engl.* **1985**, *24*, 248.
- (142) Möhring, P. C.; Coville, N. J. *J. Mol. Catal.* **1992**, *77*, 41.
- (143) Johnston, P.; Loonat, M. S.; Ingham, W. L.; Carlton, L.; Coville, N. J. *Organometallics* **1987**, *6*, 2121; du Plooy, K. E.; Marais, C. F.; Carlton, L.; Hunter, R.; Boeyens, J. C. A.; Coville, N. J. *Inorg. Chem.* **1989**, *28*, 3855.
- (144) Loonat, M. S.; Carlton, L.; Boeyens, J. C. A.; Coville, N. J. *J. Chem. Soc., Dalton Trans.* **1989**, 2407.
- (145) Hunter, G.; Weakley, T. J. R.; Weissensteiner, W. *J. Chem. Soc., Dalton Trans.* **1987**, 1545.
- (146) Chudek, J. A.; Hunter, G.; MacKay, R. L.; Kremminger, P.; Schlög, K.; Weissensteiner, W. *J. Chem. Soc., Dalton Trans.* **1990**, 2001.
- (147) Okuda, J. *Top. Curr. Chem.* **1991**, *160*, 97.
- (148) Janiak, C.; Schumann, H. *Adv. Organomet. Chem.* **1991**, *33*, 291.
- (149) See, for example, Berg, U.; Roussel, C. *J. Am. Chem. Soc.* **1980**, *102*, 7848; Jones, W. D.; Feher, F. J. *Inorg. Chem.* **1984**, *23*, 2376; Armstrong, B. M.; Bowen, M. E.; Clark, M. L.; Foley, B. L.; Hamilton, J. B.; Mahaffy, C. A. I.; Rawlings, J.; Starr, T. R. *Inorg. Chim. Acta* **1990**, *170*, 37; Altbach, M. I.; Hiyama, Y.; Wittebort, R. J.; Butler, L. G. *Inorg. Chem.* **1990**, *19*, 741.
- (150) Johnson, F. P. A.; George, M. W.; Bagratashvili, V. N.; Vereschchagina, L. N.; Poliakov, M. D. *Mendeleev. Commun.* **1991**, 26.

Organotransition Metallic Chemistry of Sulfur Dioxide Analogs

ANTHONY F. HILL

*Department of Chemistry
Imperial College of Science, Technology and Medicine
South Kensington
London SW7 2AY
United Kingdom*

I.	Introduction and Scope	159
II.	General Coordination Chemistry	162
	A. Modes of Coordination	162
	B. Theoretical Considerations	162
	C. Characteristic Spectroscopic Data	164
III.	Triatomic Interchalcogens	166
	A. Selenium Dioxide	166
	B. Disulfur Monoxide	167
	C. Diselenium Monoxide	171
IV.	Sulfines (Alkylideneoxo- λ^4 -sulfuranes, Thione-S-oxides)	172
	A. Modes of Coordination	172
	B. Synthesis and Reactivity	172
	C. Structural and Spectroscopic Studies	178
	D. α -Metallasulfines	178
V.	N-Sulfinylamines (Iminooxo- λ^4 -sulfuranes)	179
	A. Simple Coordination Complexes	180
	B. Reactions of Coordinated Iminooxosulfuranes	187
	C. Reactions of Iminooxosulfuranes with Coordinated Ligands	191
VI.	Sulfur Diimides (Diimino- λ^4 -sulfuranes)	202
	A. Simple Coordination Complexes	202
	B. Reactions of Coordinated Sulfur Diimides	208
VII.	Thiazate and Related Ligands	217
VIII.	Concluding Remarks	221
	References	222

I

INTRODUCTION AND SCOPE

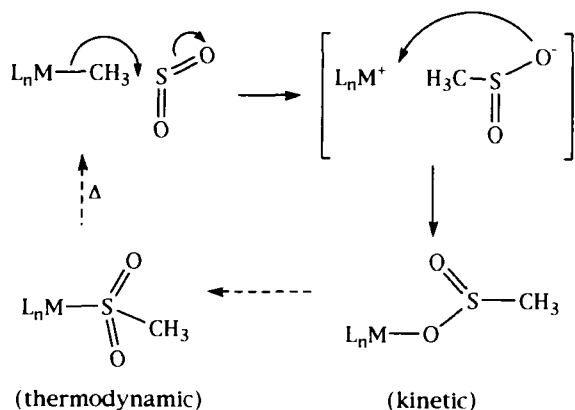
Despite the ready availability of sulfur dioxide as a substrate for transition metal chemistry, it was first observed as a ligand to a transition metal as a result of hydroxide abstraction from a coordinated bisulfite ligand by Gleu (1) in 1936. Subsequently, a plethora of complexes of sulfur dioxide has been prepared, in general, by treating coordinatively unsaturated metal-ligand fragments with free sulfur dioxide. The coordination chemis-

try of this molecule has been extensively reviewed (2–4) leading to the conclusion (2): “The diversity of bonding modes exhibited by SO_2 –metal complex interactions is unequalled by any other ligand.” The organometallic chemistry of sulfur dioxide has focused on the interactions with σ -organyl derivatives whereby apparent insertion of the cumulene into the metal–carbon bond occurs. It is now accepted that this process is, in fact, not a conventional migratory–insertion process but rather a two-stage electrophilic attack/ion-pair collapse process, which now represents one of the best understood and studied classical reactions in organometallic chemistry (5) (Scheme 1).

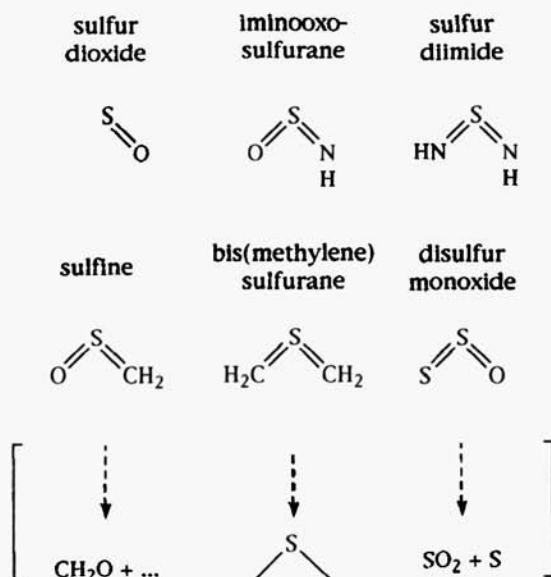
The Molecules $\text{A}=\text{S}=\text{B}$ ($\text{A}, \text{B} = \text{O}, \text{S}, \text{NR}, \text{CR}_2$)

Sulfur dioxide may be considered the parent molecule for an isolobal range of nonlinear heterocumulenes based on a central two-coordinate tetravalent (λ^4) sulfur atom. Extensive derivatization is conceivable by replacing the oxide substituents with dianionic groups to provide the molecules indicated in Scheme 2.

These molecules, derived by replacing one or both oxygen atoms with sulfur, imino ($=\text{NR}$) or alkylidene ($=\text{CR}_2$) units have varying stabilities but in many cases are isolable for suitable choices of substituent R. These heterocumulenes $\text{A}=\text{S}=\text{B}$ have a rich organic chemistry, readily entering into redox, nucleophilic, electrophilic, and cycloadditive reactions that normally lead to reduction in the $\text{A}=\text{S}$ bond orders. Both parallels and significant diversions from the reactivity associated with the “parent”



SCHEME 1. Mechanism for the insertion of sulfur dioxide into the metal–carbon bond of a metal alkyl complex $\text{L}_n\text{M}-\text{CH}_3$.



SCHEME 2. Analogs of sulfur dioxide: The molecules A=S=B (A, B = O, S, CH₂, NH).

molecule, sulfur dioxide, are observed and this chemistry has been reviewed elsewhere (6,7).

From Scheme 2 it is apparent that S₂O and the parent molecules (R = H) of these "derivatives" are in fact not stable. The stabilization of independently unstable molecules within the protective environment of a transition metal coordination sphere is, however, an endearing feature of modern coordination chemistry. The wealth of coordination chemistry shown by sulfur dioxide should be greatly enhanced by replacement of the essentially innocent oxo-groups with potentially interactive or "noninnocent" imino-, sulfido-, or alkylidene groups. The price paid (and the benefits received) for the stabilization of unstable molecules by coordination to a transition metal is often a substantial electronic relocation, orbital rehybridization, and an accompanying divergence in reactivity relative to the free molecule. This review seeks to bring together the comparatively immature fields of organometallic and coordination chemistry of these analogs of sulfur dioxide. Where possible, parallels for the guidance of future work in the area are drawn. The review does not deal specifically with the organometallic chemistry of sulfur dioxide itself, which has been adequately reviewed elsewhere (2-5); however, where appropriate, analogies are drawn for illustration.

II

GENERAL COORDINATION CHEMISTRY

A. Modes of Coordination

While the coordination chemistry of sulfur dioxide has enjoyed much more attention than that of the analogous molecules $A=S=B$, many parallels are emerging in the simple modes of coordination that are adopted. The various binding modes shown (to date) by the λ^4 -sulfur(IV) cumulenes are summarized in Scheme 3.

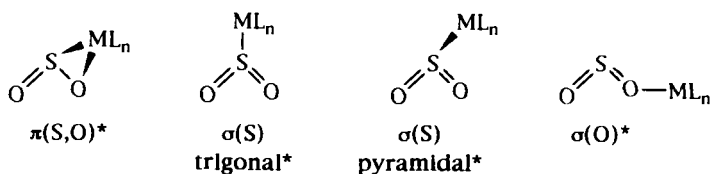
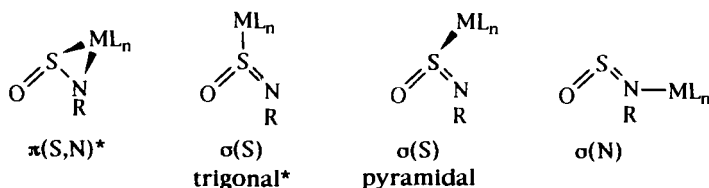
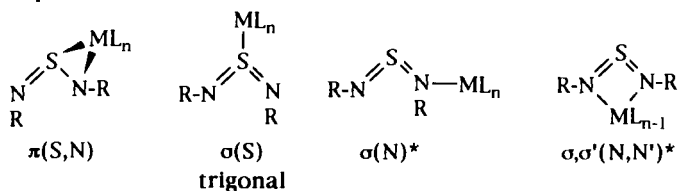
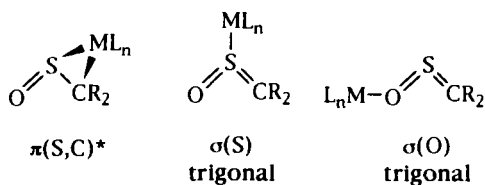
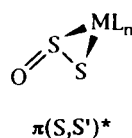
B. Theoretical Considerations

We begin with a simplified description of the frontier orbitals of sulfur dioxide (Schemes 4 and 5) relevant to transition metal coordination and then consider how these are altered by replacement of the oxygen atoms by S, NH, and CH_2 . The orbital interactions involved in the bonding of SO_2 to transition metals have been discussed in detail elsewhere (2,3).

Informative results providing valuable insights come from photoelectron spectroscopic studies by Bock and co-workers (8,9). These and other relevant data are summarized in Fig. 1 and Table I (8-16) (NB: No information about virtual unoccupied orbitals, which are of major importance in any retrodative processes with transition metals, is available from this technique.)

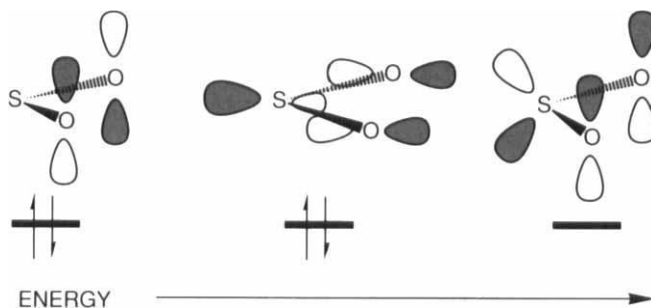
The main features of Fig. 1 and Table I may be summarized as follows:

- (i) Replacement of one oxo-group does not lead to major changes in the $A=S=O$ angle or the $S=O$ separation.
- (ii) The positive charge on sulfur decreases in the series $A=O > S \approx NH > CH_2$.
- (iii) The negative charge on oxygen decreases in the series $A=O \approx NH > CH_2 > S$.
- (iv) The negative charge remaining for A decreases in the series $A=O \approx S > NH > CH_2$.
- (v) The orbitals capable of acting as electron pair donors to a metal center are all of higher energy for the derivatives than for SO_2 . Specifically for HNSO (and presumably for HNSNH) the lone pair on nitrogen [$n(N,O)$] is more basic and therefore aza-analogs are more likely than SO_2 to coordinate in the $\sigma(N)$ mode.
- (vi) The energy of the π -HOMO increases in the order $A=O < NH \approx S < CH_2$ and the donor component of synergic bonding for the $\pi(S,A)$ mode of coordination may be expected to increase accordingly.

Sulfur dioxide**Imino-oxosulfuranes****Sulphur diimides****Sulfines****Disulfur monoxide**

SCHEME 3. Coordination modes for the analogs of sulfur dioxide (an asterisk denotes crystallographic verification).

The above data give no information about the effect of substituent variation for sulfines, imino-oxosulfuranes, and sulfur diimides, which may clearly be important in determining coordination mode. Furthermore, in the $\sigma(\text{S})$ and $\pi(\text{S},\text{A})$ coordination modes there is a very significant retrodonative component to the bonding for low-valent metal centers (more im-

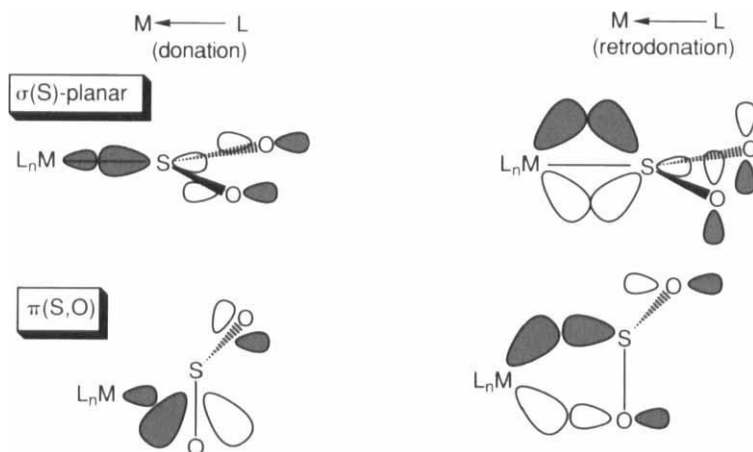


SCHEME 4. Frontier orbitals for sulfur dioxide.

portant in the latter) and the energies of the relevant acceptor orbitals are not experimentally determinable. In general, however, it can be surmised that in all cases the $A=S$ bond is more reactive than the $S=O$ bond in SO_2 and accordingly a greater propensity for $\pi(S,A)$ coordination can be expected. This will be further enhanced by electron withdrawing substituents R , which will favor retrodative processes.

C. Characteristic Spectroscopic Data

The most useful spectroscopic tool in the characterization of $A=S=B$ complexes is provided by infrared spectroscopy. The polar $A=S=B$ ligand typically shows intense absorptions the positions of which are



SCHEME 5. Orbital interactions for the coordination of sulfur dioxide to a transition metal.

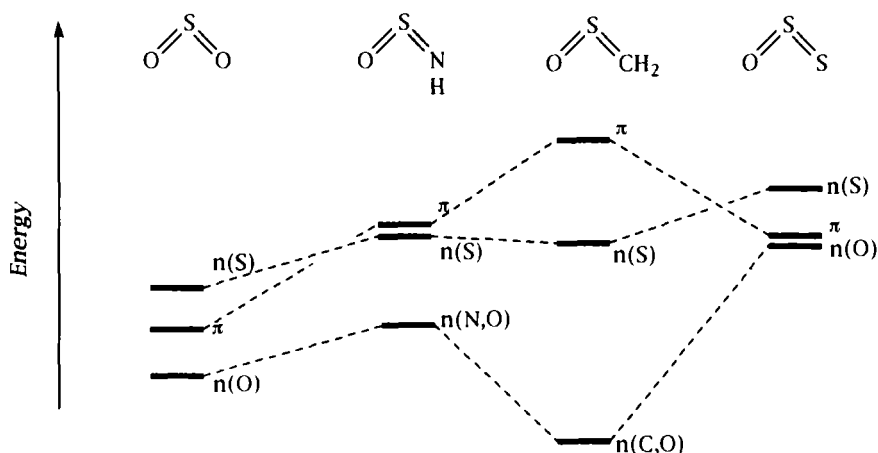


FIG. 1. Relative energies of occupied frontier molecular orbitals of the cumulenes $A=S=O$, $A = O, NH, CH_2, S$.

strongly dependent upon the coordination mode. The typical group frequency regions are shown in Fig. 2 according to the mode of coordination. It should be pointed out that in the case of iminoxosulfuranes and sulfur di-imides a strong band due primarily to $\nu_{(CN)}$ is often observed in a region overlapping with $\nu_{(SN)}$ in the $\sigma(N)$ mode of coordination and unambiguous assignment may require ^{15}N labeling studies.

The applicability of NMR spectroscopy to the assignment of coordination mode is less generally useful and dependent upon the specific ligands present. However, it should be noted that for the $\sigma(S)$ -pyramidal and $\pi(S,A)$ modes of coordination, a chiral center(S) is introduced and the resulting asymmetry may be reflected in NMR data associated with the

TABLE I
PHYSICAL DATA FOR THE CUMULENES SO_2 , $HNSO$, CH_2SO , and S_2O

$\begin{array}{c} a \quad S \quad b \\ \diagdown \quad \diagup \\ A \quad \curvearrowright \quad O \\ \diagup \quad \diagdown \\ c \end{array}$	A =			
	O	NH	CH_2	S
Mulliken charge on S	+1.05	+0.74	+0.51	+0.73
Mulliken charge on O	-0.53	-0.54	-0.37	-0.23
a (Å)	—	1.512	1.610	1.884
b (Å)	1.432	1.451	1.469	1.465
c (°)	119.5	120.4	114.7	118
Reference	(10-12)	(13)	(8,14,15)	(9,16)

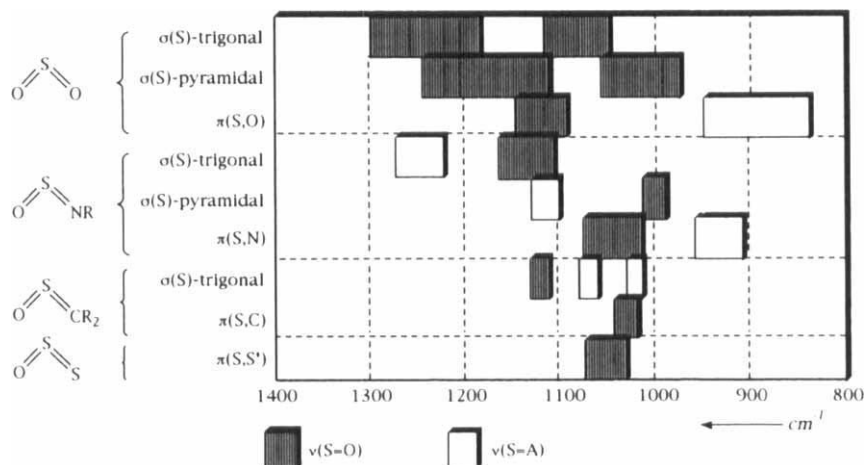


FIG. 2. Group frequencies for sulfur dioxide analogs bound to metals in various coordination modes.

coligands. It may be expected that ^{17}O and ^{15}N NMR will have roles to play in the future characterization of these complexes.

III

TRIATOMIC INTERCHALCOGENS

The coordination chemistry of chalcogen-substituted analogs of sulfur dioxide (SeO_2 , S_2O , Se_2O , and S_2O_2) remains in its infancy, in general, due to the instability of the free molecules with respect to oligomerization. Nevertheless, some promising initial results suggest that given suitable synthetic strategies, a rich chemistry may yet be accessible.

A. Selenium Dioxide

Selenium dioxide adopts a polymeric structure in the solid state; however, two reports suggest that this polymer may still serve as a source of molecular selenium oxides: The first report deals with the reaction of $[\text{Pt}(\text{PPh}_3)_2(\eta^2\text{-CH}_2\text{CH}_2)]$ and selenium dioxide. By analogy with SO_2 chemistry the complex was originally formulated as a selenium dioxide complex but subsequently shown to contain a bidentate selenite- O, O' ligand (3,17). It is not yet clear whether the product is derived from oxidation of a coordinated SeO_2 ligand or hydrolysis of the free molecule. The second

report deals with a reaction that also finds analogy in sulfur dioxide chemistry, namely the insertion of selenium dioxide into a metal–carbon σ bond. Thus treating $[\text{FeCH}_3(\text{CO})_2(\eta\text{-C}_5\text{H}_5)]$ with solid selenium dioxide leads to the methyl selenonate–*Se* complex $[\text{Fe}(\text{SeO}_2\text{CH}_3)(\text{CO})_2(\eta\text{-C}_5\text{H}_5)]$ (18). There is no obvious reason why this reaction should not be general; however, it has yet to receive significant attention. Clearly the coordination chemistry of selenium dioxide is ripe for further study. The tendency for SeO_2 to act as an oxidizing agent is, however, likely to be a continuing hindrance.

B. Disulfur Monoxide

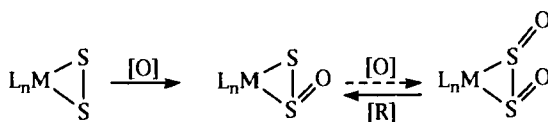
The interest in the coordination chemistry of disulfur monoxide stems from two points of view. First, such complexes are plausible intermediates in the metal mediated reduction of sulfur dioxide. Second, and perhaps less well conceived, complexes of S_2O might be considered to serve, under favorable conditions, as sources/reservoirs of the free molecule for use in subsequent syntheses. The results obtained so far would, however, suggest that dissociation of coordinated S_2O as an intact species is very unlikely.

1. Synthesis of Complexes

Disulfur monoxide is unstable with respect to formation of elemental sulfur and sulfur dioxide; however, it has been generated as a transient species of sufficient lifetime for complete spectroscopic characterization (9,19–22). The coordination chemistry of disulfur monoxide has, to date, focused on the preparation of the molecule within the metal coordination sphere from suitable precursor ligands. The most common method involves the oxidation of a coordinated disulfur ligand by air, periodate, or a peracid.

The first example of such a compound was reported by Schmid and Ritter (23) who exhaustively oxidized the cationic complex $[\text{Ir}(\eta^2\text{-S}_2)(\text{dppe})_2]^+$ (**1**) [dppe = 1,2-bis(diphenyl-phosphino)ethane] to produce $[\text{Ir}(\eta^2\text{-S}_2\text{O}_2)(\text{dppe})_2]^+$ (**2**). Subsequent careful reduction with triphenylphosphine provided the disulfur monoxide complex $[\text{Ir}(\eta^2\text{-S}_2\text{O})(\text{dppe})_2]^+$ (**3**). The reaction was subsequently refined by Rauchfuss (24) (Scheme 6), who noted a secondary role by the counteranion $[\text{Cl}^- \text{ vs } \text{PF}_6^-]$.

This general approach has been extended to include the complexes $[\text{M}(\eta^2\text{-S}_2\text{O})(\text{CO})_2(\eta\text{-C}_5\text{R}_5)]$ ($\text{R} = \text{Me}$, $\text{M} = \text{Mn}$, Re ; $\text{R} = \text{H}$, $\text{M} = \text{Re}$) (25,26), $[\text{Nb}(\eta^2\text{-S}_2\text{O})\text{Cl}(\eta\text{-C}_5\text{H}_5)_2]$ (24), and $[\text{Os}(\eta^2\text{-S}_2\text{O})\text{Cl}(\text{NO})(\text{PPh}_3)_2]$ (**9**)



SCHEME 6. Synthesis of complexes of disulfur monoxide: oxidation of coordinated disulfur. $L_nM = [Ir(dppe)_2]^+$, $[OsCl(NO)(PPh_3)_2]$, $[NbCl(\eta-C_5H_5)_2]$, $[M(CO)_2(\eta-C_5R_5)]$ ($M = Mn$, $R = Me$; $M = Re$, $R = H, Me$). $[O] = O_2$, $HO_3CC_6H_4Cl-3$, CH_3CO_3H , or IO_4^- . $[R] = PPh_3$, $-OPPh_3$.

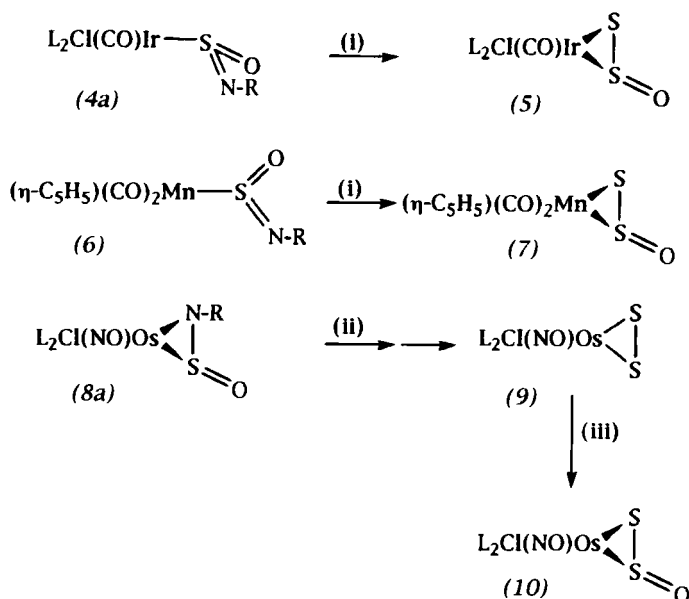
(27). In some cases the reaction may be complicated by further oxidation to the disulfur- S, S' -dioxide complex (23–25).

A dinuclear complex of S_2O viz. $[Mo_2(\mu: \sigma, \pi-S_2O)_2(S_2CNET_2-S, S')_4]$ has been isolated by aerial oxidation of a putative intermediate disulfur complex $[Mo(\eta^2-S_2)(S_2CNET_2)_2]$ obtained by the reaction of $[Mo(CO)_2(S_2CNET_2)_2]$ with elemental sulfur (28). It was suggested that the S_2O ligand is best thought of as a monoanion requiring a +3 oxidation state for molybdenum. It is, however, more reasonable to consider the ligand to be neutral $[Mo(II)]$ or dianionic $[Mo(IV)]$ given the diamagnetism of the complex and the lack of a direct Mo–Mo bond.

The drawback with this synthetic route is that the corresponding disulfur complex is required. While there are now many examples of such complexes (29), these are generally prepared by the action of elemental sulfur on suitable coordinatively unsaturated complexes and these reactions are often complicated leading to complexes of the form $[L_nM(S_x)_y]$. The factors dictating the value of x and y , however, have yet to be delineated.

An alternative strategy that should find increasingly general application involves the modification of the corresponding iminoxosulfurane complex. Iminoxosulfurane complexes are typically hydrolytically unstable and readily hydrolyzed to the corresponding sulfur dioxide complex, presumably within the coordination sphere of the metal. Extending this reaction by replacing water with hydrogen sulfide as the dibasic nucleophile leads to the corresponding disulfur monoxide complex. Thus reaction of the complexes $[L_nM(OSNSO_2C_6H_4Me-4)]$ [$L_nM = IrCl(CO)PPh_3)_2$ (**4a**) (27); $Mn(CO)_2(\eta-C_5H_5)$ (**6**) (26)] with H_2S provides tosyl amide and the corresponding disulfur monoxide complexes (**5**) and (**7**), respectively (Scheme 7).

In the case of $[OsCl(NO)(OSNSO_2C_6H_4Me-4)(PPh_3)_2]$ (**8a**) no reaction is observed with H_2S , consistent with the reduced electrophilicity of the more electron-rich complex and the $\pi(S, N)$ coordination mode (Section V,B,3). If, however, base to generate the hydrosulfide anion is present, a green disulfur complex $[OsCl(NO)(\eta^2-S_2)(PPh_3)_2]$ (**9**) is isolated, which presumably results from hydrosulfide reduction of an intermediate disulfur monoxide complex $[OsCl(NO)(\eta^2-S_2O)(PPh_3)_2]$ (**10**). The disulfur complex



SCHEME 7. Synthesis of complexes of disulfur monoxide: reaction of coordinated R-NSO with H_2S . R = $\text{SO}_2\text{C}_6\text{H}_4\text{Me-4}$, L = PPh_3 ; (i) H_2S , $-\text{RNH}_2$; (ii) H_2S /base; (iii) $\text{ClC}_6\text{H}_4\text{CO}_3\text{H-3}$.

(9) is also the product of the reaction of $[\text{OsCl}(\text{NO})(\text{PPh}_3)_3]$ (11) with elemental sulfur and this complex is readily oxidized to the disulfur monoxide (10) complex by peracid (27).

A report describing the generation of " $\text{S}_2\text{O}(\text{thf})_x$ " via the reaction of thionyl chloride with silver oxide [presumably Ag_2S was intended] has recently appeared in the secondary literature. It is claimed that this reagent reacts with $[\text{RhCl}(\text{PPh}_3)_3]$, and $[\text{MCl}(\text{CO})(\text{PPh}_3)_2]$ ($\text{M} = \text{Rh}, \text{Ir}$) to provide $[\text{RhCl}(\text{S}_2\text{O})(\text{PPh}_3)_2]$ and $[\text{MCl}(\text{CO})(\text{S}_2\text{O})(\text{PPh}_3)_2]$ (30). The only spectroscopic datum reported for the iridium complex is quite different to that previously reported (27), and therefore critical evaluation of these results must await full publication. The authors have previously suggested that the reaction of $[\text{RhCl}(\text{PPh}_3)_3]$ with stilbene episulfide provides $[\text{RhCl}(\text{SO})(\text{PPh}_3)_2]$ (31); however, it has been subsequently suggested (24) that this complex is more likely to contain disulfur monoxide.

2. Reactions of Coordinated Disulfur Monoxide

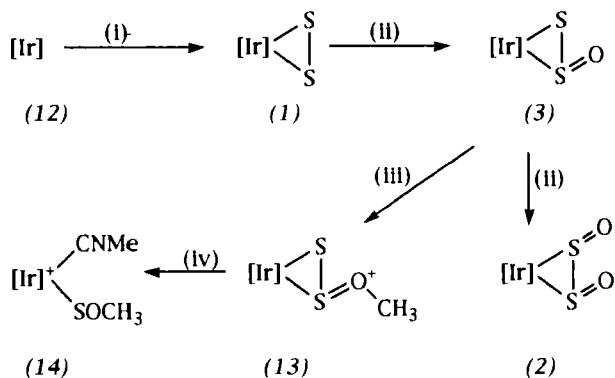
The chemistry of coordinated S_2O has yet to be studied in any detail. Simple oxidation or reduction to coordinated S_2O_2 or S_2 has been dealt with above. The bulk of information has been derived from the reactions of (3) (24). Reaction with excess triphenylphosphine leads ultimately to

loss of phosphine oxide and phosphine sulfide and regeneration of the coordinatively unsaturated cationic complex $[\text{Ir}(\text{dppe})_2]^+$ (**12**). If one equivalent of triphenylphosphine is added then triphenylphosphine sulfide is the major product with only traces of the oxide being identified. This has been taken to indicate that the sulfur atom of the S_2O ligand is the most electrophilic site. Alkylation $[\text{MeOSO}_2\text{F}]$ at the electron-rich exocyclic oxygen atom leads to the dicationic complex $[\text{Ir}(\eta^2\text{-SSOMe})(\text{dppe})_2]^{2+}$ (**13**), which undergoes an unusual reaction with methyl isonitrile involving S–S bond cleavage and formation of $[\text{Ir}(\sigma\text{-SOMe})(\text{CNMe})(\text{dppe})_2]^{2+}$ (**14**) and methyl thiocyanate (Scheme 8). The niobocene complex $[\text{Nb}(\eta^2\text{-S}_2\text{O})\text{Cl}(\eta\text{-C}_5\text{H}_5)_2]$ reacts with triphenylphosphine to provide $[\text{NbCl}(=\text{O})(\eta\text{-C}_5\text{H}_5)_2]$ (**24**) and SPPH_3 in direct contrast to the iridium reaction above. The manganese complex $[\text{Mn}(\eta^2\text{-S}_2\text{O})(\text{CO})_2(\eta\text{-C}_5\text{Me}_5)]$ reacts with $[\text{Mn}(\text{thf})(\text{CO})_2(\eta\text{-C}_5\text{Me}_5)]$ to provide the dinuclear complexes $[\text{Mn}_2(\mu\text{-S}_n)(\text{CO})_4(\eta\text{-C}_5\text{Me}_5)_2]$ ($n = 1, 2$) and $[\text{Mn}_2(\mu\text{-S}=\text{O})(\text{CO})_4(\eta\text{-C}_5\text{Me}_5)_2]$ (**26**).

While coordination of S_2O to a metal center clearly activates the molecule toward electrophilic attack, the weakening of the S–S bond is evident in the majority of the reported reactions that involve its facile cleavage. There is no evidence yet for the simple elimination of molecular S_2O from its complexes in dramatic contrast to SO_2 .

3. Structural Studies

Two disulfur monoxide complexes have been structurally characterized: the mononuclear complex $[\text{Mn}(\eta^2\text{-S}_2\text{O})(\text{CO})_2(\eta\text{-C}_5\text{Me}_5)]$ (**25**) and the dinuclear complex $[\text{Mo}_2(\mu : \sigma, \pi\text{-S}_2\text{O})_2(\text{S}_2\text{CNET}_2\text{-S, S}')_4]$ (**28**). Structural data



SCHEME 8. Reactions of coordinated disulfur monoxide. $[\text{Ir}] = [\text{Ir}(\text{dppe})_2]^+$. (i) $[\text{Ti}(\text{S}_3)(\eta\text{-C}_5\text{H}_5)_2]$; (ii) $\text{ClC}_6\text{H}_4\text{CO}_3\text{H-3}$ or $\text{Na}[\text{IO}_4]$; (iii) $\text{CH}_3\text{OSO}_2\text{F}$; (iv) 2-CNMe , $-\text{SCNMe}$.

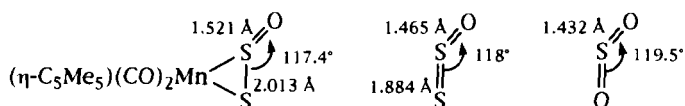


FIG. 3. Structural data for free and coordinated disulfur monoxide.

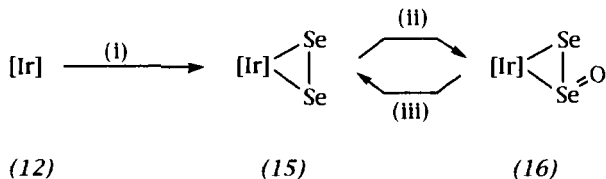
for the mononuclear complex may be compared with those for the free molecule (9,16,32) indicating that a substantial lengthening of the S-S bond occurs upon coordination, consistent with a strong π -acceptor role (Fig. 3).

C. Diselenium Monoxide

The oxidation of coordinated disulfur to disulfur monoxide has been extended by Rauchfuss to allow the isolation of a complex of diselenium monoxide viz. $[\text{Ir}(\eta^2\text{-Se}_2\text{O})(\text{dppe})_2]^+$ (**16**) (Scheme 9) (24). The reaction is surprisingly sensitive to the oxygen transfer reagent. Thus while high yields are obtained with perethanoic acid, 3-chloroperbenzoic acid leads to extensive decomposition. The generality of the reaction, however, has yet to be established. Thus, e.g., treatment of $[\text{Mn}(\eta^2\text{-Se}_2)(\text{CO})_2(\eta\text{-C}_5\text{Me}_5)]$ with either oxygen or peroxide leads to extensive decomposition and precipitation of elemental red selenium (26,33).

Unlike $[\text{Ir}(\eta^2\text{-S}_2\text{O})(\text{dppe})_2]^+$ (**3**), the diselenium monoxide (**13**) complex is very prone to deoxygenation. Thus, for example, reaction with thiols leads to clean and rapid reversion to the diselenium complex (**15**) and formation of disulfides (Scheme 9).

In conclusion, the analogy between coordinated sulfur dioxide and other triatomic interchalcogens is not a very useful one for the following reasons. (i) Coordination of S_2O does not appear to be reversible; (ii) only one coordination mode is observed [$\pi(\text{S},\text{S}')$] and this seriously perturbs the molecule relative to the free state, and (iii) the reactions of coordinated S_2O and Se_2O observed to date all involve degradation of the "molecule."



SCHEME 9. Synthesis of a complex of diselenium monoxide. $[\text{Ir}] = [\text{Ir}(\text{dppe})_2]^+$. (i) $[\text{Ti}(\text{Se}_3)(\eta\text{-C}_5\text{H}_5)_2]$; (ii) $\text{CH}_3\text{CO}_3\text{H}$; (iii) $+2 \text{HSR}, -\text{H}_2\text{O}, -\text{RSSR}$.

IV

SULFINES (ALKYLIDENEOXO- λ^4 -SULFURANES, THIONE-S-OXIDES)

Sulfines are the least reactive of the sulfur (IV) heterocumulenes and unique among these classes of compounds in being found in biological systems, e.g., the familiar lachrymator in onions. The organic chemistry of sulfines has been reviewed (7).

A. Modes of Coordination

Simple sulfines (alkylideneoxo- λ^4 -sulfuranes or thione-S-oxides) have been shown to coordinate to transition metals in two different modes, $\sigma(S)$ and $\pi(C,S)$. A weak $\sigma(O)$ coordination has been proposed for the complex $[TiCl_4(\sigma-O=S=CPh_2)]$ (34). In the case of α,β -unsaturated sulfines a tetrahapto-coordination is observed as a special case of the $\pi(C,S)$ mode (35). These complexes are notionally related to the iron tricarbonyl vinyl ketene complexes, which have enjoyed considerable application to organic synthesis in recent times (36) (Fig. 4). For α -thiolato-substituted sulfines a further mode of coordination is possible involving trihapto- or pseudo-allylic coordination of the $S-C=S$ moiety. The $\sigma(S)$ -pyramidal mode of coordination has yet to be observed.

B. Synthesis and Reactivity

Relatively few examples of sulfine complexes have been reported (35,35,37-43), and very little is known about the effect of coordination upon reactivity. This is despite the comparative simplicity of synthetic routes to the free molecules. The parent molecule, $CH_2=S=O$ is not independently stable although flash vacuum pyrolysis of suitable precursors has allowed spectroscopic characterization (8,14,15). A stable complex of sulfine (19), however, has been prepared by a stepwise assembly within the protective environment of an osmium coordination sphere.

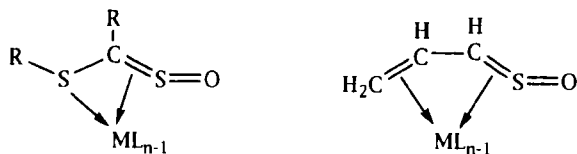
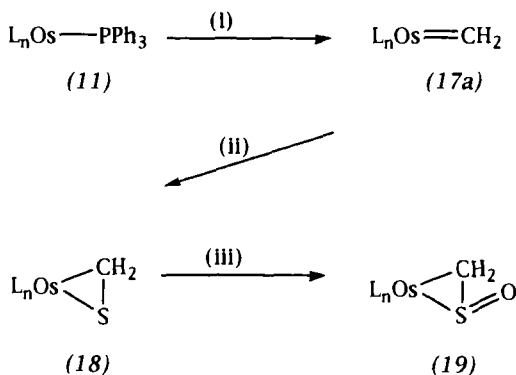


FIG. 4. α -Substituent participation in sulfine coordination. ML_{n-1} = 14 or 12 valence-electron metal ligand fragment.

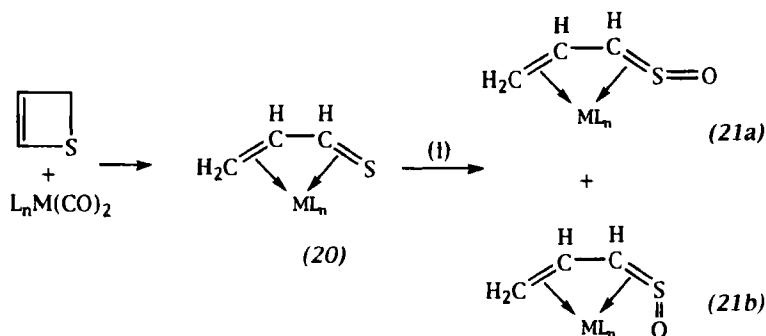
Addition of elemental sulfur to the methylene complex $[\text{OsCl}(\text{NO})(=\text{CH}_2)(\text{PPh}_3)_2]$ (**17a**) provides the thioformaldehyde complex $[\text{OsCl}(\text{NO})(\eta^2\text{-CH}_2=\text{S})(\text{PPh}_3)_2]$ (**19**) (44), which is cleanly oxidized by 3-chloro-perbenzoic acid to provide the sulfine complex $[\text{OsCl}(\text{NO})(\eta^2\text{-CH}_2\text{SO})(\text{PPh}_3)_2]$ (**19**) (Scheme 10) (37).

On the basis of spectroscopic data (IR and $^1\text{H}/^{31}\text{P}$ NMR-ABXY-spin system) the sulfine is assumed to coordinate through the carbon and sulfur atoms of the cumulene. Although this mode of coordination may reflect the synthetic route, it is more likely that this is in fact the preferred coordination mode for sulfine bound to the electron-rich $\text{OsCl}(\text{NO})(\text{PPh}_3)_2$ fragment. All other λ^4 -sulfur cumulenes bind to this fragment in a similar $\pi(\text{S},\text{A})$ manner. Attempts to oxidize the related seleno- and telluro-formaldehyde complexes $[\text{OsCl}(\text{NO})(\eta^2\text{-CH}_2=\text{A})(\text{PPh}_3)_2]$ ($\text{A} = \text{Se}, \text{Te}$) (44) to provide the heavier analogs $[\text{OsCl}(\text{NO})(\eta^2\text{-CH}_2=\text{A}=\text{O})(\text{PPh}_3)_2]$ were not successful.

The peracid or aerial oxidation of thia-acrolein complexes of iron (**20**) and cobalt have led to the formation of vinyl sulfine derivatives (**21**) (36) (Scheme 11). Free vinyl sulfine is unstable with respect to cyclization but is stabilized through coordination of the extended π -system to the iron or cobalt centers. Two isomeric possibilities exist for the vinyl sulfine ligand depending on whether the oxygen is *exo* (**21a**) or *endo* (**21b**). Surprisingly, the isomer distribution appears to be dependent upon the choice of oxidant (3-chloroperbenzoic acid or dioxygen) suggesting that these isomers do not readily convert. The coordination of the $\text{Fe}(\text{CO})_3$ to the prochiral faces of vinyl sulfines suggests the possible application to enantioselective organic synthesis, however, in contrast to the case of vinyl ketenes (36), this has yet to be addressed.



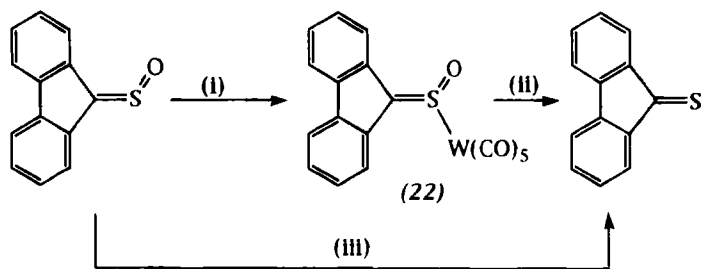
SCHEME 10. Stepwise assembly of coordinated sulfine. $\text{L}_n\text{M} = [\text{OsCl}(\text{NO})(\text{PPh}_3)_2]$. (i) CH_2N_2 , $-\text{N}_2$, $-\text{PPh}_3$; (ii) $\frac{1}{8} \text{S}_8$; (iii) $\text{ClC}_6\text{H}_4\text{CO}_3\text{H}-3$.



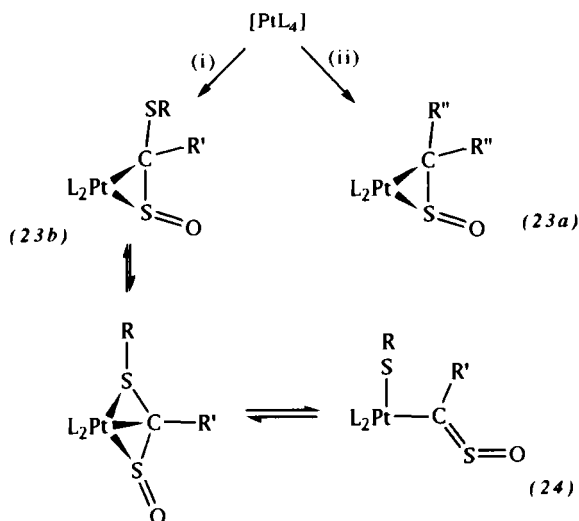
SCHEME 11. Synthesis of vinyl sulfine complexes. $L_nM = [\text{Fe}(\text{CO})_3]$, $[\text{Co}(\eta\text{-C}_5\text{H}_5)]$. (i) O_2 or $\text{ClC}_6\text{H}_4\text{CO}_3\text{H}\cdot 3$.

A binuclear derivative may also be prepared in a similar manner and as with the mononuclear derivatives, the mode of coordination is assumed on the basis of spectroscopic data and by reference to the assumed structures of the precursor complexes. Addition of suitable ligands leads to cleavage of the binuclear structure and formation of the corresponding mononuclear analog (35).

The preceding iron examples involve synthesis of the sulfine within the metal coordination sphere. This may be a necessity for iron because Alper has shown that simple diaryl sulfines are readily reduced by iron carbonyls to the corresponding thione, which may in some cases be trapped by orthometallation to provide binuclear complexes (45). If manganese carbonyl is employed simple reduction occurs with no organometallic products being isolated. The solvent-stabilized complex $[\text{W}(\text{CO})_5(\text{thf})]$ reacts with 9-sulfinyl fluorene to provide an unstable adduct formulated as $[\text{W}(\text{CO})_5(\text{O}=\text{S}=\text{CC}_{12}\text{H}_8)]$ (22), which decomposes at room temperature to provide fluorene-9-thione, $[\text{W}(\text{CO})_6]$ and CO_2 (Scheme 12) (38).



SCHEME 12. Metal-carbonyl-mediated reduction of sulfines. (i) $[\text{W}(\text{CO})_5(\text{thf})]$; (ii) $-\text{CO}_2$, $-\text{[W(CO)}_6]$; (iii) $[\text{Mn}_2(\text{CO})_{10}]$.

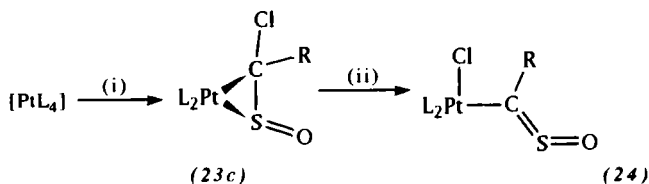


SCHEME 13. Sulfine complexes of platinum(0). L = PPh₃, R = CH₃, R' = Ph, C₆H₄Me-4; CR₂'=fluorenylidene (C₁₃H₈). (i) R'(RS)C=S=O, -2L; (ii) R₂C=S=OP, -2L.

The reactions of a variety of sulfoxes with phosphine complexes of the platinum group metals have been investigated both by van Koten and co-workers (39–43) and by Götzfried and Beck (38). Simple π adducts (23) involving the C=S double bond [π (S,C)] are observed between simple sulfoxes and the metal–ligand fragments PtL₂ (L = PPh₃, PCy₃) (Scheme 13) (38,39).

In the case of α -halosulfoxes, simple adducts (23a) may be isolated if the reaction is carried out in toluene; however, these adducts readily rearrange by oxidative addition to provide thioacyl-S-oxide complexes of platinum(II) (24) when redissolved in chloroform (Scheme 14).

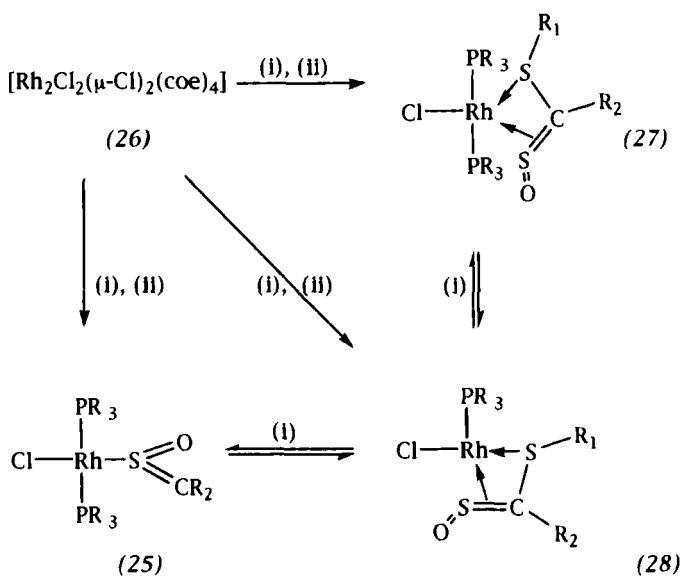
Such an interaction is also involved initially with α -mercapto-sulfoxes; however, subsequent reactions may ensue, leading to the C–S bond cleav-



SCHEME 14. Oxidative addition of α -halo sulfoxes to platinum(0). (i) ClRC=S=O, -2L, toluene; (ii) chloroform.

age with concomitant oxidative addition to the metal center and formation of σ -thioacyl-*S*-oxide complexes. It has been proposed that the C–S bond cleavage reactions may proceed via trihapto- or pseudo-allylic coordination of the S=C=S linkage (Fig. 4, Scheme 13). This is supported by the spectroscopic observation (NMR) of fluxional processes for platinum complexes of π (C,S)-bound α -thiolato sulfines, which do not proceed to complete C–S bond cleavage (40). Despite the increased electronic encouragement for oxidative addition upon replacing triphenylphosphine with the more basic tricyclohexylphosphine, oxidative addition is in fact not favored (41). This is presumably due to the increased steric constraints. Simple σ (S) coordination is proposed for the complexes (25) derived from the treatment of (26) with bulky phosphines and simple sulfines (37). In the case of the rhodium(I) complexes $[\text{RhCl}(\text{PR}_3)_2\{\eta^3\text{-O}=\text{S}=\text{C}(\text{R}^1)\text{R}^2\}]$ (27) and $[\text{RhCl}(\text{PR}_3)_2\{\eta^3\text{-O}=\text{S}=\text{C}(\text{R}^1)\text{R}^2 (\text{S}, \text{S}')\}]$ [$\text{R} = i\text{-Pr}, \text{Cy}$; $\text{R}^1 = \text{SMe}$, $\text{R}^2 = \text{C}_6\text{H}_4\text{Me-4}$; $\text{R}^1 = \text{R}^2 = \text{SC}_6\text{H}_4\text{Me-4}$] (28) the coordination of one phosphine ligand is reversible; however, this does not appear to effect the trihapto-S=C=S coordination (Scheme 15) (39). The factors determining the mode of coordination of α -thiolato-sulfines and whether or not oxidation occurs include:

(i) the nature of the metal–ligand fragment (propensity for oxidative addi-



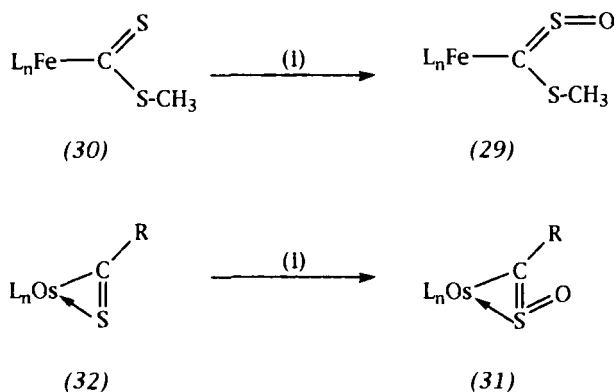
SCHEME 15. Sulfine complexes of rhodium(I). coe = cyclooctene, $\text{R} = i\text{-Pr}, \text{Cy}$; $\text{R}^1 = \text{CH}_3$, $\text{R}^2 = \text{C}_6\text{H}_4\text{Me-4}$, $\text{SC}_6\text{H}_4\text{Me-4}$ or $\text{R}^1 = \text{C}_6\text{H}_4\text{Me-4}$, $\text{R}^2 = \text{SC}_6\text{H}_4\text{Me-4}$. (i) PR_3 ; (ii) $\text{R}^1\text{R}^2\text{C}=\text{S}=\text{O}$.

- tion, i.e., coligand basicity and steric requirements, degree of coordinative unsaturation, frontier orbital symmetry) and
- (ii) stereochemistry of substitution at carbon (*Z* or *E* with respect to the cumulene spine).

A complete delineation of these factors must, however, await a broadening of this class of complexes to include more diverse metal-ligand fragments.

One possibility that may be anticipated for bis(thiolato)sulfines, but that has yet to be realized, is the three-fragment oxidative addition of both C-S bonds to provide complexes of the (to date) hypothetical thiocarbonyl-*S*-oxide ligand $[L_n M(C=S=O)(SR)_2]$, which may be considered an isomer of carbonyl sulfide. Given that three-fragment oxidative addition of thiophosgene to $[RhCl(PPh_3)_3]$ provides the thiocarbonyl complex $[RhCl_3(CS)(PPh_3)_2]$, this is an attractive possibility, which is also supported by the isolation of "thiazate" or thionitrosyl-*S*-oxide complexes $[L_n M(N=S=O)]$ (Section VII,A).

In contrast to the insertion reactions of SO_2 and its nitrogen analogs (Sections V,C,2 and VI,C,2), those of sulfines with organotransition metal complexes have yet to be investigated in any detail. One report has dealt with the presumed insertion of the parent molecule, generated *in situ* $[CH_3S(=O)Cl/Et_3N]$ with $[W(CO)_3(\eta-C_5H_5)]$, which leads to the formation of a sulfenato-*S* derivative (46). Notably, the same result is to be expected from simple nucleophilic attack at $CH_3S(=O)Cl$ by the anion $[W(CO)_3(\eta-C_5H_5)]^-$, without requiring the intermediacy of free sulfine. It should be pointed out that of the analogs of sulfur dioxide, sulfines are the least electrophilic and it can therefore be anticipated that, at least in the



SCHEME 16. α -Metallasulfine synthesis by oxidation of thioacyl complexes. $L_n\text{Fe} = [\text{Fe}(\text{CO})_2(\eta-C_5H_5)]$, $L_n\text{Os} = [\text{OsCl}(\text{CO})(\text{PPh}_3)_2]$; (i) $\text{ClC}_6\text{H}_4\text{CO}_3\text{H}$.

absence of Lewis acids, these molecules will not be particularly reactive toward insertion into metal–carbon bonds. This presumption is based on the generally accepted two-step electrophilic attack mechanism for SO_2 , RNSO , and $(\text{RN})_2\text{S}$ “insertion” reactions.

C. Structural and Spectroscopic Studies

One example of a structurally characterized sulfine complex involving 9-sulfinylfluorene (Fig. 5) has been reported (42). Although the 14- π system of the fluorenylidene group might be expected to also perturb the C–S multiple bonding (resonance form B), there is nevertheless a clear lengthening (ca. 6%) of the C–S bond length relative to that of the free parent molecule, CH_2SO (8,14,15) consistent with a π -acceptor role for sulfines bound to electron-rich metal centers in the $\pi(\text{C},\text{S})$ mode.

Clearly despite the simple synthetic accessibility of sulfines, the coordination chemistry of these molecules remains sparse and offers a fertile field for further investigation.

D. α -Metallasulfines

To date the only structurally characterized mode of coordination for sulfines in which one substituent is a transition metal involves simple $\sigma(\text{C})$ coordination (40) discussed above. This mode is also adopted in the complex $[\text{Fe}\{\sigma\text{-C}(=\text{SO})\text{SMe}\}(\text{CO})_2(\eta\text{-C}_5\text{H}_5)]$ (29) obtained by peracid oxidation of the dithiomethoxycarbonyl complex $[\text{Fe}(\sigma\text{-CS}_2\text{Me})(\text{CO})_2(\eta\text{-C}_5\text{H}_5)]$ (30) (Scheme 16) (47). The alternative bidentate coordination mode

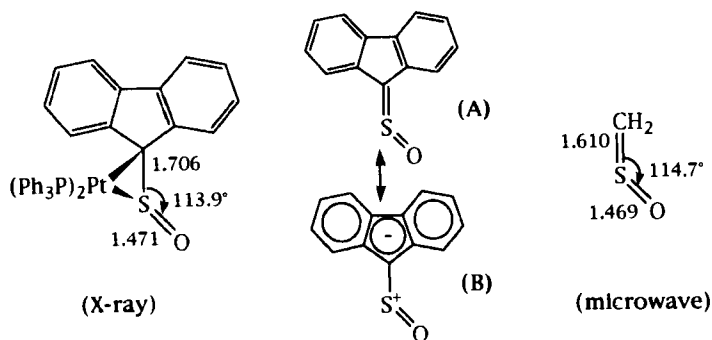
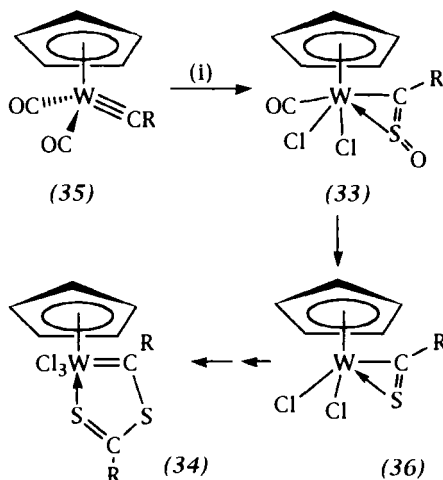


FIG. 5. Structural data for free and complexed sulfines (bond lengths in angstroms).



SCHEME 17. Proposed intermediacy of an α -metallasulfine. R = $\text{C}_6\text{H}_3\text{Me}_{2-2,6}$; (i) OSOCl_2 three-fragment oxidative addition, ($-\text{CO}$).

is proposed to occur [$^{31}\text{P}/^1\text{H}$ NMR] in the complex $[\text{OsCl}\{\eta^2\text{-C}(\text{=SO})\text{C}_6\text{H}_4\text{Me-4}\}(\text{CO})(\text{PPh}_3)_2]$ (**31**) obtained by oxidation of the thiotolulyl complex $[\text{OsCl}\{\eta^2\text{-C}(\text{=S})\text{C}_6\text{H}_4\text{Me-4}\}(\text{CO})(\text{PPh}_3)_2]$ (**32**) (Scheme 16) (48).

A related complex $[\text{W}\{\eta^2\text{-C}(\text{=SO})\text{R}\}\text{Cl}_2(\text{CO})(\eta\text{-C}_5\text{H}_5)]$ (R = $\text{C}_6\text{H}_3\text{Me}_{2-2,6}$) (**33**) has been proposed as an intermediate in the formation of the metallacyclic carbene complex $[\text{W}\{\text{=CRSCRS}\}\text{Cl}_3(\eta\text{-C}_5\text{H}_5)]$ (**34**) by addition of thionyl chloride to $[\text{W}(\text{=CR})(\text{CO})_2(\eta\text{-C}_5\text{H}_5)]$ (**35**) (Scheme 17) (49). Coordinated CO is presumed to act as an intramolecular reductant to produce the thioacyl complex (**36**) which subsequently dimerises with loss of $\text{WCl}(\eta\text{-C}_5\text{H}_5)$.

V

N-SULFINYLAMINES (IMINOXO- λ^4 -SULFURANES)

After sulfur dioxide, iminoxosulfuranes (*N*-sulfinylamines) have the most extensive organometallic and coordination chemistry among the λ^4 -sulfur(IV) cumulenes. This may be traced in part to their ease of preparation and the presence of only one reactive $\text{N}=\text{S}$ double bond, which prevents the substantial fragmentation pathways available to diiminosulfuranes (Section VI,B).

A. Simple Coordination Complexes

Iminooxosulfuranes have been observed to bond to transition metals in three modes, which are analogous to those observed for SO_2 , viz $\pi(\text{N},\text{S})$ (27,50–57), $\sigma(\text{S})$ -trigonal (26,55,58), and $\sigma(\text{S})$ -pyramidal (Scheme 3) (27,51,54). In the case of π coordination it is typically the $\text{N}=\text{S}$ multiple bond that is involved in coordination to the metal center, reflecting the greater reactivity of this linkage.

1. Factors Affecting Coordination Mode

The factors dictating the mode of coordination adopted have been discussed (55) and while the breadth of examples for comparison is not as extensive as that for sulfur dioxide complexes, it is sufficient for some preliminary generalizations to be made. Factors to consider include (i) imino substituent; (ii) metal–ligand fragment basicity and degree of coordinative saturation; and (iii) metal–ligand fragment frontier orbital symmetry.

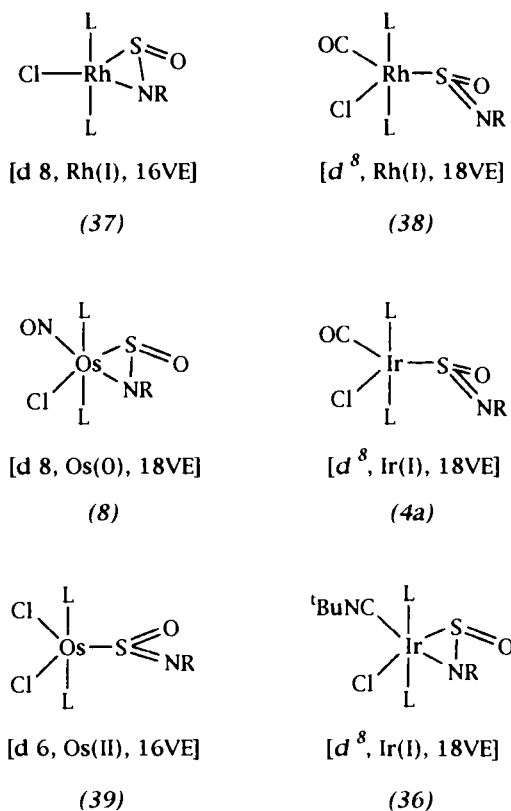
In general the more electron rich the metal–ligand fragment the greater the propensity for side-on $\pi(\text{N},\text{S})$ coordination as this most effectively alleviates excess metal d -electron density. For less electron-rich metal centers (or those with competitive strong π -acid coligands) the $\sigma(\text{S})$ -trigonal coordination mode is preferred in most cases. Although this mode of coordination also offers the metal an acceptor orbital of π symmetry, this is directed orthogonal to the metal–sulfur vector [in contrast to the $\pi^*_{(\text{SN})}$ acceptor orbital used in side-on coordination]. This is therefore presumably not as efficient in retrodonative interactions, leaving σ donation the most important interaction. Accordingly, this mode is more suitable for metals with modest retrodonative abilities.

In some cases, depending on the frontier orbital symmetry of the metal ligand fragment, the $\sigma(\text{S})$ -pyramidal mode of coordination may be adopted. It has been suggested that the orbital interactions that determine whether a nitrosyl ligand coordinates in a linear or bent manner (59) are essentially the same as those that dictate whether SO_2 adopts a $\sigma(\text{S})$ -trigonal or $\sigma(\text{S})$ -pyramidal coordination mode (2). Accordingly, for $\text{L}_4\text{M}(\text{SO}_2)$, pyramidalization at sulfur is considered to circumvent the population of a low-lying $\text{M}-\text{S}$ antibonding orbital of σ symmetry, directed along the metal–sulfur vector for coordinatively saturated complexes with d -electron counts of greater than six. Thus $\sigma(\text{S})$ -trigonal coordination is rare for d^8 SO_2 complexes and yet to be confirmed for d^{10} -electron configurations.

Within the limited range of iminooxosulfurane complexes that have been characterized, the rules for SO_2 coordination appear to be generally

applicable, notwithstanding the increased propensity for $\pi(\text{N},\text{S})$ coordination. These points are illustrated by the examples shown in Scheme 18. The effect of metal basicity on coordination mode is illustrated by comparing **(4a)** [$\sigma(\text{S})$ -pyramidal] with the isoelectronic but more basic complexes **(8)** and **(36)** [$\pi(\text{N},\text{S})$]. The effect of frontier orbital symmetry is clear from the 16-electron complex **(37)** [$\pi(\text{S},\text{N})$] and **(38)** [$\sigma(\text{S})$ -pyramidal]. Replacing the nitrosyl ligand in **(8)** with a chloride to provide **(39)** formally decreases the d occupancy and valence electron count by two. It is not clear why only one iminooxosulfurane coordinates since the complex is coordinatively unsaturated.

The coordination modes for the known complexes of iminooxosulfuranes with different metal ligand fragments are summarized in Fig. 6, which also serves to identify areas for further synthetic investigation.



SCHEME 18. Iminooxosulfurane coordination modes: Selected examples. L = PPh_3 , R = $\text{SO}_2\text{C}_6\text{H}_4\text{Me-4}$; $n\text{VE}$ = effective atomic number count for central metal.

		Increasing d-configuration			
		d ⁶	d ⁸ (16VE)	d ⁸ (18VE)	d ¹⁰
increasing oxidation state	-I				π [N,S]
	0			π [N,S]	
	+I	σ (S)-trig	σ (S)-trig π [N,S]	π [N,S] σ (S)-pyr	
	+II	σ (S)-trig			
		Increasing electron density			
		increasing electron density			

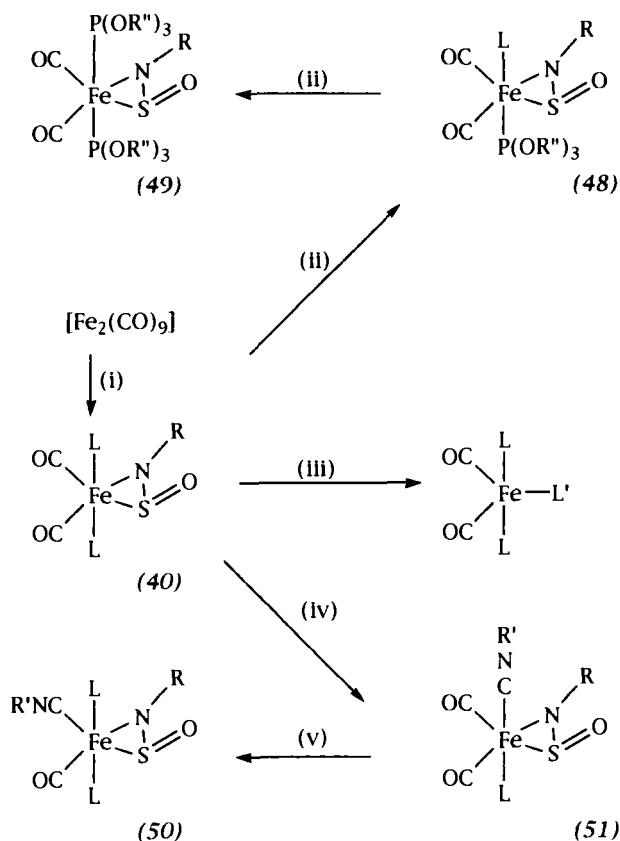
FIG. 6. Factors affecting iminoxosulfurane coordination mode.

2. Synthesis of Iminoxosulfurane Complexes

In all cases the complexes have been prepared from the free iminoxosulfurane and a suitable coordinatively unsaturated metal complex, or precursor.

a. Iron, ruthenium, and osmium The iron complexes $[\text{Fe}(\eta^2\text{-OSNAr})(\text{CO})_2(\text{PPh}_3)_2]$ (**40**) result from the reaction of the free aryliminoxosulfurane with $[\text{Fe}(\text{CO})_2(\text{PPh}_3)_3]$; however, the most conveniently prepared iron reagents are either $[\text{Fe}\{\eta^4\text{-PhCHCHC}(\text{O})\text{Me}\}(\text{CO})_3]$ or $[\text{Fe}_2(\text{CO})_9]$. These latter reagents when employed at room temperature produce intractable red oils that are presumably $[\text{Fe}(\text{OSNAr})(\text{CO})_4]$. If the reaction is carried out in the presence of suitable phosphines the thermally stable complexes (**40**) are obtained in yields of 30–55% (Scheme 19) depending on the nature of the phosphine and the aryl substituents (57). Notably, the more electron rich the phosphine and the more electron withdrawing the aryl substituent, the higher the yield. This is consistent with the assumed π (N,S) coordination mode for which the principle metal–ligand interaction is metal to ligand retrodonation. These derivatives serve as useful precursors for other iminoxosulfurane complexes of iron(0) by ligand substitution reactions. In the majority of these substitution reactions the integrity of the π (N,S) coordination is *ultimately* retained.

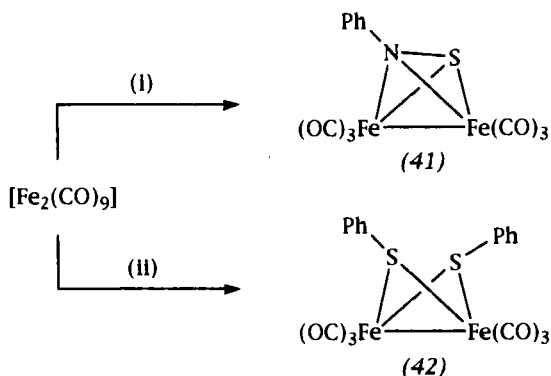
The thermolytic reaction between $[\text{Fe}_2(\text{CO})_9]$ and iminoxosulfuranes typically leads to rupture of the sulfur(IV) cumulene and isolation of fragmentation products (Scheme 20). Thus, e.g., with phenyliminoxosul-



SCHEME 19. Iminoxosulfurane complexes of iron(0). L = PPh_3 ; R = $\text{C}_6\text{H}_4\text{X}-4$ (X = H, Cl, Br, F, Me, OMe, NO_2); R' = Me, Et, C_6H_{11} , CH_2Ph ; $\text{P}(\text{OR}'')_3$ = $\text{P}(\text{OMe})_3$, $\text{P}(\text{OEt})_3$, $\text{P}(\text{O}-i\text{-Pr})_3$, $\text{P}(\text{OCH}_2)_3\text{CMe}$; L' = $(\text{NC})_2\text{C}=\text{C}(\text{CN})_2$, $^+\text{N}\equiv\text{NC}_6\text{H}_4\text{F}-4$; (i) RNSO, L; (ii) $\text{P}(\text{OR}'')_3$; (iii) $+ \text{L}'$, $-\text{RNSO}$; (iv) $+ \text{CNR}' - \text{L}$; (v) $+ \text{L}$, $-\text{CO}$.

furane, the diiron tetrahedrane complex (41) is obtained in low yield (ca. 1%) (60) while PhNHNSO provides PhSH and (42) (61).

The most convenient approach to iminoxosulfurane complexes of ruthenium and osmium involves the use of tris(triphenylphosphine) complexes. One phosphine is typically labile due to steric pressures and is readily replaced by aryliminoxosulfuranes, which have more modest steric requirements. Thus reaction of $[\text{Ru}(\text{CO})(\text{L})(\text{PPh}_3)_3]$ (L = CO, $\text{CN}(t\text{-Bu})$, $\text{CNC}_6\text{H}_3\text{Me}_2-2,6$) or (11) with aryl or tosyl iminoxosulfuranes leads to rapid and smooth replacement of one phosphine and formation of the complexes $[\text{Ru}(\eta^2\text{-OSNR})(\text{CO})(\text{L})(\text{PPh}_3)_2]$ and (8) (27,52–54). The



SCHEME 20. Cothermolysis of iron carbonyls and iminoxosulfuranes. (i) Ph-NSO; (ii) PhNHNSO.

ethene complex $[\text{OsCl}(\text{NO})(\text{PPh}_3)_2(\eta\text{-C}_2\text{H}_4)]$ (**43**) also serves as a useful precursor for simple aryliminoxosulfuranes; however, an interesting complication arises for tosyl iminoxosulfurane (Section V,C,3). This approach may also be extended to divalent complexes of ruthenium and osmium by employing the complexes $[\text{MCl}_2(\text{PPh}_3)_3]$ ($\text{M} = \text{Ru}, \text{Os}$) (**55**). While the zero-valent complexes all adopt the $\pi(\text{N},\text{S})$ coordination mode, the divalent complexes $[\text{M}(\sigma\text{-OSNAr})\text{Cl}_2(\text{PPh}_3)_2]$ (**39**) assume the $\sigma(\text{S})$ -trigonal geometry. Notably, this mode of coordination has no obvious way to stabilize the coordinative unsaturation at the metal center.

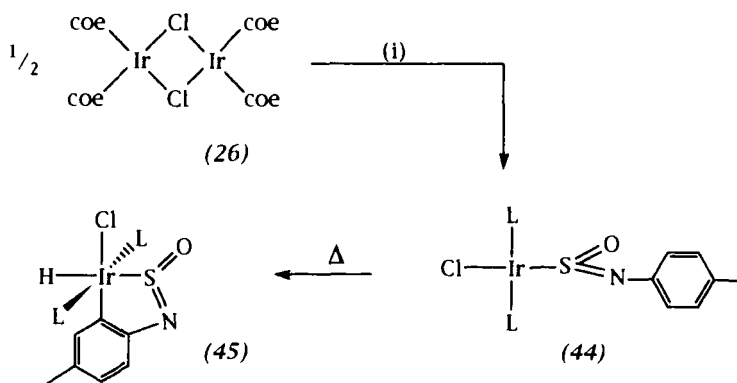
b. Rhodium and iridium The first correct report of the isolation of an iminoxosulfurane complex was that described by Blake and Reynolds (**51**) in a reinvestigation of earlier work. It had been reported (**62**) that Vaska's complex $[\text{IrCl}(\text{CO})(\text{PPh}_3)_2]$ reacted with Ph-NSO to provide aniline and $[\text{IrCl}(\text{CO})(\text{PPh}_3)_2(\text{SO}_2)]$; however, this was subsequently shown to be the result of hydrolysis of the free iminoxosulfurane by adventitious moisture. With the careful exclusion of water, no complex is formed between $[\text{IrX}(\text{CO})(\text{PPh}_3)_2]$ ($\text{X} = \text{Cl}, \text{Br}$) and Ph-NSO. If an iminoxosulfurane bearing an electron-withdrawing aryl substituent ($\text{OSNC}_6\text{H}_4\text{NO}_2\text{-4}$) is employed then an adduct may be isolated. This is nevertheless prone to dissociation upon washing with ether. The corresponding tosyliminoxosulfurane complex (**4a**) is stable with respect to dissociation; however, it is very readily hydrolyzed to the SO_2 adduct and tosyl amide (**27**). In both the above cases, spectroscopic data (IR, ^{31}P NMR) are consistent with a $\sigma(\text{S})$ -pyramidal mode of coordination, analogous to the SO_2 coordination in $[\text{IrCl}(\text{CO})(\text{PPh}_3)_2(\text{SO}_2)]$ (**63**). The rhodium analog (**38**) may be prepared

in a similar manner or by treating $[\text{RhCl}(\text{PPh}_3)_3]$ with $\text{OSNSO}_2\text{C}_6\text{H}_4\text{Me-4}$ [to provide (37)] followed by carbon monoxide (55). The more electron-rich analog of Vaska's complex $[\text{IrCl}(\text{CN-}i\text{-Bu})(\text{PPh}_3)_2]$ reacts irreversibly with tosyl-NSO to provide a 1:1 adduct (36); however, in this case the sulfur cumulene binds in the $\pi(\text{N,S})$ manner consistent with the increase in metal basicity (55).

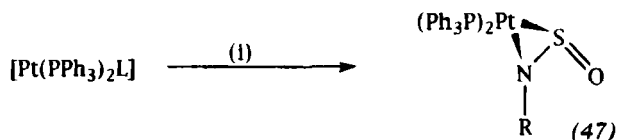
Vrieze and co-workers have investigated the interaction of aryliminoxosulfuranes with the complexes derived from addition of bulky phosphines to $[\text{M}_2(\mu\text{-Cl})_2(\text{coe})_4]$ ($\text{M} = \text{Rh}, \text{Ir}$; $\text{coe} = \text{cyclooctene}$) (26) (58). The coordinatively unsaturated complexes $[\text{MCl}(\text{PR}_3)_2(\text{OSNAr})]$ (44) ($\text{R} = i\text{-Pr}, \text{Cy}$) feature the $\sigma(\text{S})$ -trigonal coordination mode of the sulfur cumulene except for the phenyl derivative that appears to exist in an equilibrium between $\sigma(\text{S})$ -trigonal and $\pi(\text{N,S})$ isomers. It is not clear why this should be the case since neither electron withdrawing (Cl) nor releasing (CH_3) *para*-substituents on the aryl group lead to observable amounts of the $\pi(\text{N,S})$ isomer, thereby apparently excluding electronic factors. The iridium complexes $[\text{IrCl}(\text{PR}_3)_2(\text{OSNC}_6\text{H}_4\text{X-4})]$ (44) ($\text{X} = \text{Cl}, \text{Me}$) undergo an interesting orthometallation reaction of the aryl group to provide a metallacyclic derivative (45) in which the NSO linkage remains intact (Scheme 21).

One d^{10} complex of iridium $[\text{Ir}(\text{NO})(\text{PPh}_3)_2(\text{OSNSO}_2\text{C}_6\text{H}_4\text{Me-4})]$ has been prepared by the reaction of $\text{OSNSO}_2\text{C}_6\text{H}_4\text{Me-4}$ (46) with $[\text{Ir}(\text{NO})(\text{PPh}_3)_3]$ and as expected for the electron-rich $\text{Ir}(\text{I})$ center, a $\pi(\text{N,S})$ mode of coordination is adopted (55).

c. Nickel and platinum The d^{10} -electron-rich metal ligand fragments $\text{M}(\text{PPh}_3)_2$ coordinate tosyl and aryl iminoxosulfuranes irreversibly in



SCHEME 21. Orthometallation of iminoxosulfurane complexes of iridium(I). $\text{L} = \text{PCy}_3$, $\text{P-}i\text{-Pr}_3$; $\text{coe} = \text{cyclooctene}$. (i) 2.0 L , $\text{OSNC}_6\text{H}_4\text{Me-4}$.



SCHEME 22. Iminooxosulfurane complexes of platinum(0). L = PPh₃, C₂H₄. R = Ph, C₆H₂Me₃, C₆H₄Me-4, SO₂C₆H₄Me-4.

the $\pi(\text{N},\text{S})$ mode (Scheme 22) (51,55,65) and one such complex [Pt(PPh₃)₂(OSNC₆H₂Me₃-2,4,6)] (**47a**) has been the subject of a crystallographic study (vide infra).

3. Structural and Spectroscopic Studies

Three iminooxosulfurane complexes have been the investigated crystallographically and the results obtained support the analogy with sulfur dioxide coordination. The electron-rich complexes [OsCl(NO)(PPh₃)₂(OSNC₆H₄Me-4)] (**8b**) (56) and [Pt(PPh₃)₂(OSNC₆H₂Me₃-2,4,6)] (**47a**) (65) both feature the $\pi(\text{S},\text{N})$ mode of coordination as is also the case for the related sulfur dioxide complexes. Substantial lengthening (5.9%) of the N=S multiple bond occurs relative to that observed for the free molecules (Fig. 7), consistent with the operation of a pseudo-olefinic synergic bonding mechanism. In contrast the rhodium complex [RhCl(P-*i*-Pr)₂(OSNC₆H₄Me-4)] (**48a**) (63) features the $\sigma(\text{S})$ -trigonal mode of coordination. Consistent with the primary interaction being one of σ dona-

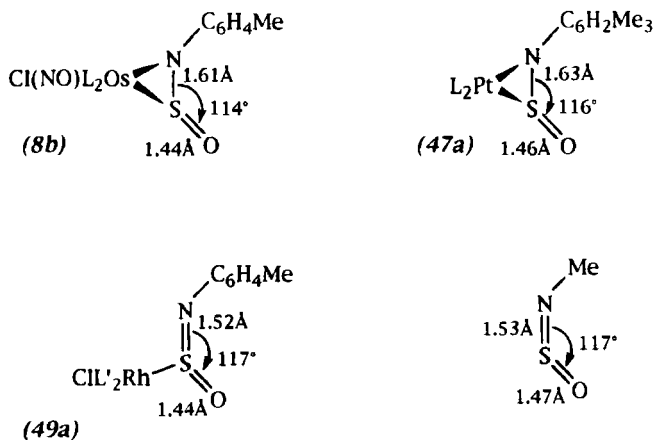


FIG. 7. Structural data for free and complexed iminooxosulfuranes. L = PPh₃, L' = P^{*i*}Pr₃.

tion there are no substantial changes in the structural parameters associated with the sulfur(IV) cumulene upon coordination.

B. Reactions of Coordinated Iminooxosulfuranes

1. Ligand Substitution Reactions

Manning has described an extensive series of iron(0) complexes of iminooxosulfuranes that derive from the complexes (**40**) by substitution of the coligands (57). With phosphites $[P(OR'')_3; R'' = \text{Me, Et, } i\text{-Pr, } (OR'')_3 = (OCH_2)_3CMe]$ either one or both phosphine ligands are replaced to provide $[Fe(\eta^2\text{-OSNR})(CO)_2(PPh_3)_n\{P(OR'')_3\}_{2-n}]$ ($n = 1$ (**48**), 0 (**49**)) depending on the reaction time. With isonitriles $[CNR'; R' = \text{Me, Et, } C_6H_{11}, CH_2Ph]$ the ultimate products involve replacement of one carbonyl ligand to provide $[Fe(\eta^2\text{-OSNR})(CO)(CNR')(PPh_3)_2]$ (**50**); however, there is spectroscopic evidence to suggest that one phosphine ligand is initially replaced and in a second, slower process liberated phosphine substitutes one carbonyl. This is supported by the observation that carrying out the reaction in the presence of a $KI/CuCl_2$ mixture (to trap PPh_3) allows the isolation of the kinetic substitution product formulated as $[Fe(\eta^2\text{-OSNR})(CO)_2(CNR')(PPh_3)]$ (**51**). These results add weight to the description of $\pi(N,S)$ -bound iminooxosulfuranes as strong π acceptors. The reagents $[N_2C_6H_4F-4]BF_4$ and tetracyanoethene lead to replacement of the iminooxosulfurane and formation of $[Fe(CO)_2(L')(PPh_3)_2]$ [$L' = N_2C_6H_4F-4^+$, $(NC)_2C = C(CN)_2$]. The iminooxosulfurane is also lost from the coordination sphere when the complexes are treated with carbon disulfide; however, the only isolated complex in the complicated reaction is $[Fe(CO)_3(PPh_3)_2]$. These transformations (57) are summarized in Scheme 19.

The rhodium complexes $[RhCl(\eta^2\text{-OSNR})(P\text{-}i\text{-Pr}_3)_2]$ ($R = \text{aryl}$) (**49**) react with carbon monoxide via dissociation of the iminooxosulfurane to provide $[RhCl(CO)(P\text{-}i\text{-Pr}_3)_2]$ (**58**). This reaction presumably proceeds via an associative pathway since (**37**) reacts with carbon monoxide to provide the coordinatively saturated complex (**38**) (55). While the highly electrophilic (**46**) is not lost from the coordination sphere, an unusual change in coordination mode from $\pi(N,S)$ to $\sigma(S)$ pyramidal accompanies the CO addition.

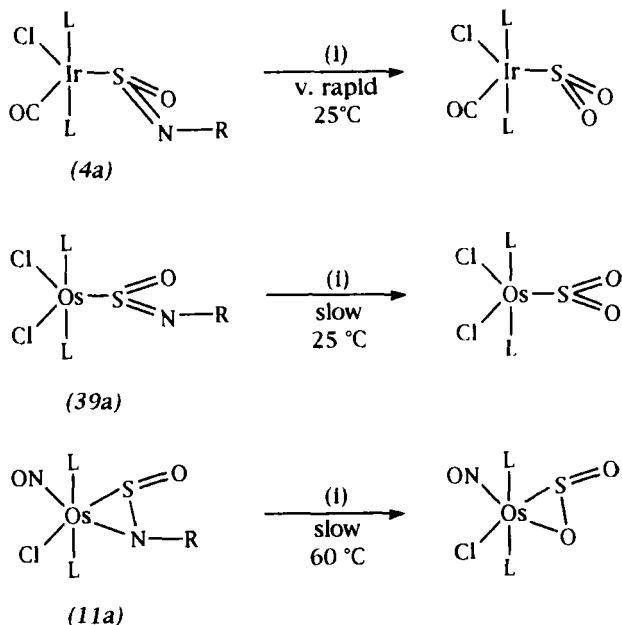
2. Fragmentation

In a study primarily concerned with the reactions of iron carbonyls with sulfur diimides, it was found that under thermal conditions, $[Fe(CO)_5]$

reacted with OSNPh to provide **(41)** (60,61) in 1% yield (Scheme 20). Iminooxosulfuranes are, however, in general much less prone to transition-metal-mediated fragmentation than the corresponding sulfur diimides (Section VI,B).

3. Hydrolysis and Reactions with Nucleophiles

The sensitivity of iminooxosulfuranes toward hydrolysis is preserved in their complexes; however, this is considerably modified depending on the mode of coordination. Thus for example the $\sigma(\text{S})$ -pyramidal complexes **(4a)** and **(38)** are very rapidly hydrolyzed by moist air. Complexes bearing the iminooxosulfurane in the $\sigma(\text{S})$ -trigonal mode of coordination appear slightly less moisture sensitive, while $\pi(\text{N,S})$ -coordinated complexes are much less reactive toward water, consistent with the substantial retrodonative transfer of metal electron density to the cumulene (Scheme 23). In all cases the product of *anaerobic* hydrolysis is the corresponding sulfur dioxide complex. If the sulfur dioxide complex is easily oxidized then the corresponding sulfato-O,O' complex is obtained under aerobic conditions.



SCHEME 23. Hydrolysis of coordinated iminooxosulfuranes. L = PPh₃, R = SO₂C₆H₄Me-4. (i) + H₂O, -H₂NR.

The assumption that the hydrolysis involves nucleophilic attack at coordinated sulfur is intriguing in that it suggests the possibility of preparing more exotic ligands within the transition metal coordination sphere by viewing $[L_nM(OSNR)]$ as being synthetically equivalent to $[L_nM(SO)]^{2+}$. This possibility has yet to be explored in any detail; however, results obtained with H_2S and SH^- (Section III,B) are promising. The possibility that hydrolysis occurs after dissociation of the iminoxosulfurane and that the SO_2 thus formed formed recoordinates cannot be excluded. The good yields of **(5)** obtained from the reaction of **(4a)** with H_2S (Scheme 7) would, however, appear to preclude this given the solution instability of disulfur monoxide. In cases where the iminoxosulfurane is bound in the $\pi(N,S)$ mode, this is particularly unlikely, given that this coordination mode is typically irreversible. The synthetic scope of this reaction is considerable, given the large number of dibasic nucleophiles that could replace H_2O or H_2S ; however, this has yet to be investigated.

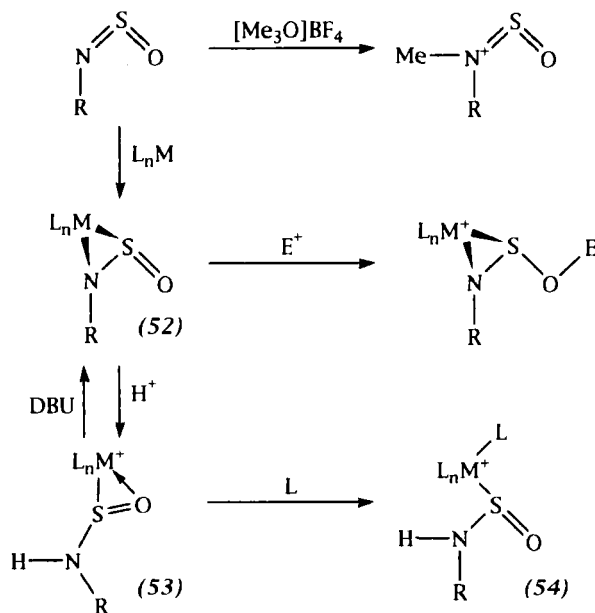
4. Oxidation

The reaction of sulfur dioxide complexes with oxygen leads to the corresponding sulfato- O,O' complex **(2)**. The analogous reaction of iminoxosulfurane complexes should provide iminosulfato-complexes; however, this has not yet been established although it has been claimed. Thus an early investigation of the reaction of $[Pt(\eta^2-O_2)(PPh_3)_2]$ with iminoxosulfuranes claimed the formation of iminosulfate- N,O complexes $[Pt(SO_3NR)(PPh_3)_2]$ **(66)**; however, it was later pointed out that the spectroscopic data for this complex were identical to the sulfato- O,O' complex $[Pt(SO_4)(PPh_3)_2]$ **(51)**. Reaction of $[IrCl(CO)(PPh_3)_2(OSNSO_2C_6H_4Me-4)]$ with air provides $[IrCl(SO_4)(CO)(PPh_3)_2]$ and while the hydrolysis of an intermediate iminosulfate complex $[IrCl(SO_3NSO_2C_6H_4Me-4)(CO)(PPh_3)_2]$ by adventitious water is plausible, no such intermediate has been isolated and it is more likely that oxidation of the ligand occurs subsequent to the (rapid) hydrolysis, which provides $[IrCl(CO)(PPh_3)_2(SO_2)]$ as an intermediate.

5. Reactions with Electrophiles

Free iminoxosulfuranes typically react with electrophiles at the nitrogen atom; indeed this feature has been employed to enhance the dienophilic reactivity by alkylation **(67)**. Prior coordination to a transition metal alters the site of electrophilic attack. Thus treatment of $[Ru(CO)(CNC_6H_3Me_2-2,6)(PPh_3)_2(OSNC_6H_4Me-4)]$ **(52)** with BF_3OEt_2 or $Me_3SiOSO_2CF_3$ leads to electrophilic attack at the exocyclic oxygen atom

(68). Notably this is also the site of electrophilic attack at coordinated disulfur monoxide (Section III,B) and sulfur dioxide (2) in related complexes. These reactions may be reversed by acetone or CsF, respectively. Alkylation also leads to attack at oxygen; however, this is not reversible. The reaction takes a different course with Brønsted acids. Acids with potentially coordinating conjugate bases lead to complete cleavage from the metal. Thus $[\text{Ru}(\text{CO})_2(\text{PPh}_3)_2(\text{OSNC}_6\text{H}_4\text{Me-4})]$ with HCl or *m*- $\text{ClC}_6\text{H}_4\text{CO}_2\text{H}$ provide $[\text{RuX}_2(\text{CO})_2(\text{PPh}_3)_2]$ ($\text{X} = \text{Cl}, \text{ClC}_6\text{H}_4\text{CO}_2$). The use of acids with noncoordinating conjugate bases $[\text{HBF}_4, \text{HSbF}_6, \text{HPF}_6]$ allows the isolation of the initial protonation products. Protonation occurs at the nitrogen atom followed by a rearrangement to provide a hemilabile sulfinamidato-*S,O* ligand (**53**). This protonation is reversed by treatment with DBU or KOH/MeOH; however, weaker, nucleophilic bases SCN^- and CN^tBu open the bidentate coordination to provide monodentate sulfinamidato-*S* derivatives (**54**). The more nucleophilic dialkyldithiocarbamate anion leads to displacement of the sulfenamide ligand (Scheme 24).



SCHEME 24. Electrophilic attack at coordinated iminoxosulfuranes. $\text{L}_n\text{M} = [\text{OsCl}(\text{NO})(\text{PPh}_3)_2], [\text{Ru}(\text{CO})_2(\text{PPh}_3)_2], [\text{Ru}(\text{CO})(\text{CNR}')(\text{PPh}_3)_2]$ ($\text{R}' = t\text{-Bu}, \text{CNC}_6\text{H}_3\text{Me}_2\text{-2,6}$); $\text{E}^+ = \text{BF}_3(\text{OEt}_2), \text{Me}_3\text{Si}^+(\text{F}_3\text{CSO}_3^-), \text{CH}_3^+(\text{F}_3\text{CSO}_3^-), \text{Et}^+(\text{FSO}_3^-)$; $\text{L} = \text{SCN}^-(\text{K}^+), \text{CN}^t\text{Bu}$; DBU = 1,8-diazabicyclo[5.4.0]undec-7-ene.

It should be noted that the limited studies of electrophilic attack have centered, quite reasonably, on complexes in which the iminoxosulfurane binds in the $\pi(\text{N},\text{S})$ mode. It is in this geometry that most electron density is transferred from the metal to the heterocumulene consistent with it being found for electron-rich complexes. The less basic nature of iron relative to ruthenium is illustrated by the failure of the analogous iron complexes (**40**) or (**50**) to react with even the potent methylating agent MeOSO_2F (**57**). Diazonium salts, e.g., $[\text{NNC}_6\text{H}_4\text{F-4}]\text{BF}_4$, lead to substitution of the iminoxosulfurane ligand. This is presumably due to initial attack at the metal, formation of the salts $[\text{Fe}(\eta^2\text{-OSNAr})(\text{CO})(\text{L})(\text{PPh}_3)_2(\text{NNC}_6\text{H}_4\text{F-4})]\text{BF}_4$, and subsequent dissociation of the iminoxosulfurane from the now electronically depleted metal center. The cleavage of ArNSO by treatment with acetic acid (**57**) would appear to proceed by the same multistep hydrogenation of the $\text{N}=\text{S}$ bond discussed above for the reactions of ruthenium(0) complexes with Brønsted acids (**68**).

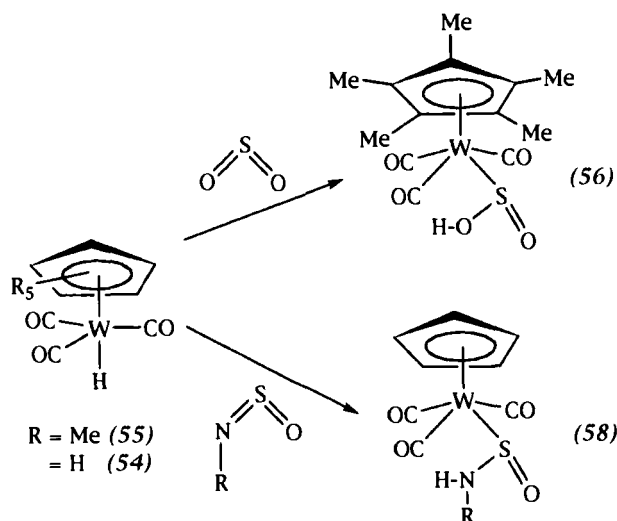
C. Reactions of Iminoxosulfuranes with Coordinated Ligands

The previously discussed organometallic complexes of iminoxosulfuranes were all prepared by reacting the free ligand with a suitable coordinatively unsaturated complex. If the complex employed is coordinatively saturated and substitution inert, ligand-based reactions may be observed. In these reactions the iminoxosulfurane appears to act primarily as an electrophile and accordingly most work has been concerned with the extremely electrophilic derivative $\text{OSNSO}_2\text{C}_6\text{H}_4\text{Me-4}$ (**46**).

1. Hydrides

The interaction of metal hydrides with sulfur(IV) heterocumulenes is of interest because of the possible relevance to metal-mediated SO_2 reduction. Thus the reaction of $[\text{WH}(\text{CO})_3(\eta\text{-C}_5\text{Me}_5)]$ (**55**) with SO_2 to initially provide $[\text{W}\{\text{S}(=\text{O})\text{OH}\}(\text{CO})_3(\eta\text{-C}_5\text{Me}_5)]$ (**56**) (**69,70**) finds analogy in the reaction of $[\text{WH}(\text{CO})_3(\eta\text{-C}_5\text{H}_5)]$ (**57**) with $\text{OSNC}_6\text{H}_4\text{Me}$ (Scheme 25) to provide the monohapto-sulfinamidato-S complex $[\text{W}\{\text{S}(\text{O})(\text{NHC}_6\text{H}_4\text{Me-4})\}(\text{CO})_3(\eta\text{-C}_5\text{H}_5)]$ (**58**) (**71**).

The two-step mechanism proposed for this insertion reaction involves initial transfer of a proton from the Brønsted-acidic tungsten center to provide an ion pair $[\text{W}(\text{CO})_3(\eta\text{-C}_5\text{H}_5)]^- [\text{OSNHR}]^+$. This subsequently collapses via nucleophilic attack at sulfur by the organometallic anion. This is supported by the failure of the weaker Brønsted acids (**55**) and $[\text{WH}(\text{CO})_2(\text{PMe}_3)\eta\text{-C}_5\text{H}_5)]$ to react with $\text{OSNC}_6\text{H}_4\text{Me-4}$. This synthetic approach to sulfenamidato-S complexes compliments the protonation of



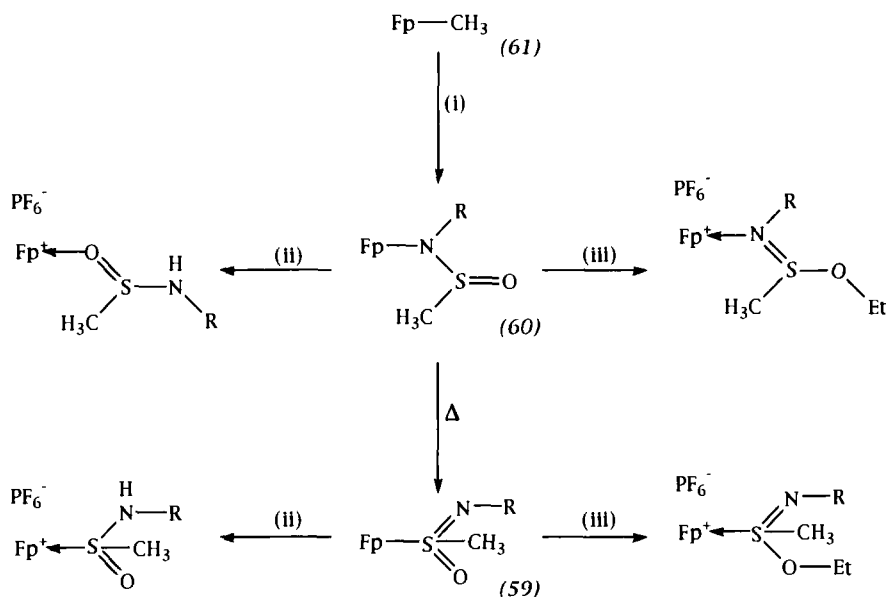
SCHEME 25. Hydrotungstenation of sulfur dioxide and iminooxosulfuranes. $\text{R} = \text{C}_6\text{H}_4\text{Me-4}$, $\text{C}_6\text{H}_4\text{Me-2}$.

electron-rich iminooxosulfurane complexes to provide (54) and (55) discussed above.

2. σ -Organyls

Wojcicki has extensively investigated the reactions of a variety of metal alkyls with iminooxosulfuranes (72–74) and found that a mechanism analogous to that established for the related insertions of sulfur dioxide operates (5). Only iminooxosulfuranes with strongly electron-withdrawing substituents enter into reactions with metal alkyls [e.g., (46)]. A wide range of coordinatively unsaturated σ -alkyl and σ -aryl complexes have been investigated and the final products typically contain (imino)alkylsulfinato-*S* ligands (59), although under favorable conditions, the kinetic products of insertion viz. alkylsulfinamido-*N* derivatives (60) may be isolated and subsequently converted thermally to the (imino)alkylsulfinato isomers. Both the kinetic and thermodynamic isomers may be trapped by reaction with suitable electrophiles (HOEt_2^+ , Et_3O^+). These transformations are summarized in Scheme 26, which illustrates the exemplary results obtained for the complex $[\text{FeCH}_3(\text{CO})_2(\eta\text{-C}_5\text{H}_5)]$ (61) (72–74).

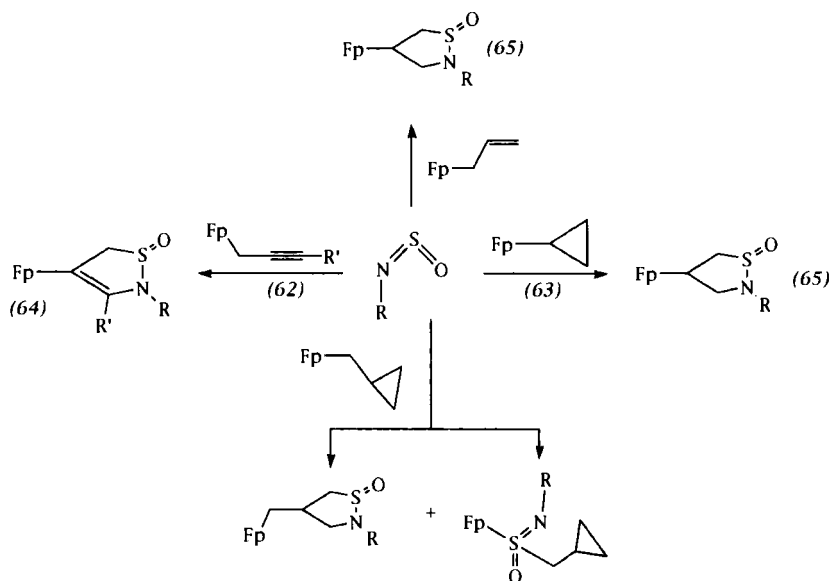
The reactions of σ -propargyl (62) and cyclopropyl (63) complexes take a different course, with the α carbon not being the site of initial electrophilic attack (75–77). The final products feature thiazacyclopentenyl-*S*-oxide



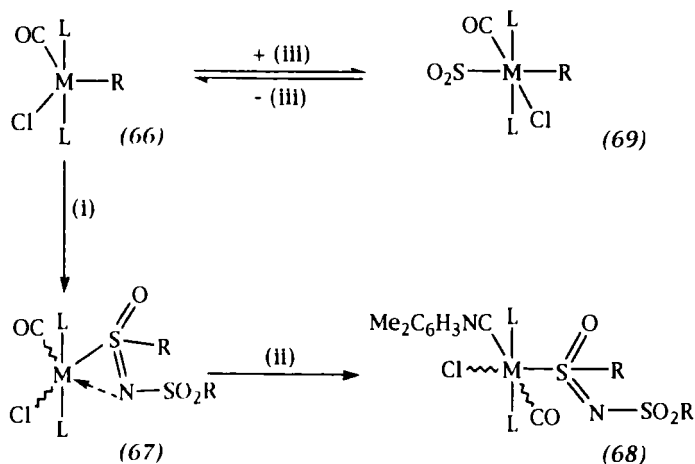
SCHEME 26. The insertion of iminoxosulfuranes into transition metal alkyl bonds. Fp = $[\text{Fe}(\text{CO})_2(\eta\text{-C}_5\text{H}_5)]$, R = SO_2Me . (i) $\text{R}-\text{NSO}$; (ii) $[\text{HOEt}_3]\text{BF}_4$; (iii) $[\text{Et}_3\text{O}]\text{BF}_4$.

(64) and thiazacyclopentyl-*S*-oxide (65) ligands (Scheme 27). The complex (64) also results from the reaction of $\text{OSNSO}_2\text{CH}_3$ with the monohapto allyl complex $[\text{Fe}(\eta^1\text{-CH}_2\text{CH}=\text{CH}_2)(\text{CO})_2(\eta\text{-C}_5\text{H}_5)]$. These reactions have parallels in the chemistry of sulfur dioxide.

The reagent complexes studied by Wojcicki (72–77) involved coordinatively saturated metal centers and accordingly the ligands produced could, under mild conditions, only occupy one coordination site. If the coordinatively unsaturated σ -tolyl complexes $[\text{M}(\text{C}_6\text{H}_4\text{Me-4})\text{Cl}(\text{CO})(\text{PPh}_3)_2]$ ($\text{M} = \text{Ru}, \text{Os}$) are treated with (46), compounds (67) having weakly bidentate *N*-(tosyl)toluenesulfinimidato-*S* ligands are obtained (78). In the absence of structural studies the mode of coordination remains equivocal; however, the spectroscopic (IR) data associated with the ligand suggest that it is coordinated through nitrogen and sulfur. Subsequent reaction of the complexes with CO or $\text{CNC}_6\text{H}_3\text{Me}_2\text{-2,6}$ leads to rapid formation of adducts (68), the infrared data for which are consistent with those reported by Wojcicki for monodentate (imino)alkylsulfinate-*S* complexes (Scheme 28). Despite the possibility of iminoxosulfurane coordination to the 16 valence electron centers prior to insertion, it is not clear that this occurs. First, no reaction (either coordination or insertion) is observed for more electron-rich iminoxosulfuranes ($\text{R}-\text{NSO}$; R = tolyl, ferrocenyl) although increas-



SCHEME 27. Reactions of iminoxosulfuranes with C-functionalized σ -alkyl complexes. Fp = $[\text{Fe}(\text{CO})_2(\eta\text{-C}_5\text{H}_5)]$, R = SO_2Me .



SCHEME 28. Reactions of coordinatively unsaturated σ -aryl complexes with iminoxosulfuranes. L = PPh_3 , M = Os, Ru; R = $\text{C}_6\text{H}_4\text{Me-4}$. (i) RSO_2NSO ; (ii) $\text{CNC}_6\text{H}_3\text{Me}_2\text{-2,6}$; (iii) SO_2 .

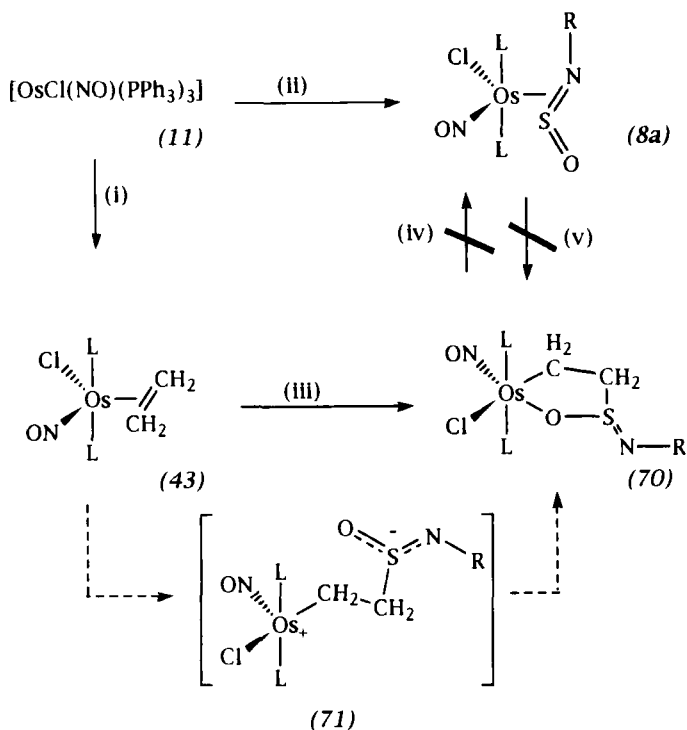
ing the donor ability of the NSO cumulene would be expected to favor coordination to ruthenium(II). Second, coordination of SO_2 to these complexes is known to occur trans to the σ -aryl ligand (79) precluding a *direct* migratory-insertion mechanism. Thus, if prior coordination occurs, this does not circumvent the electrophilicity requirements of the insertion process. No reaction is observed between (46) and the related coordinatively saturated complexes $[\text{M}(\text{C}_6\text{H}_5)\text{Cl}(\text{CO})_2(\text{PPh}_3)_2]$ ($\text{M} = \text{Ru}, \text{Os}$), $[\text{Ru}(\text{C}_6\text{H}_5)\text{Cl}(\text{CO})(\text{CNC}_6\text{H}_3\text{Me}_2-2,6)(\text{PPh}_3)_2]$, $[\text{Ir}(\text{CH}_3)\text{I}(\text{NO})(\text{PPh}_3)_2]$, and $[\text{Ru}(\text{CF}_3)\text{Cl}(\text{CO})_2(\text{PPh}_3)_2]$ (78).

3. π -Coordinated Ligands

a. *Ethene* The osmium ethene complex (43) reacts with simple iminooxosulfuranes via alkene displacement to provide the $\pi(\text{S},\text{N})$ adducts (8) (56,78). A similar result is obtained for (46) if the reaction is carried out under high dilution to provide (8a) (27). If the reaction is carried out in toluene suspension a different process ensues. The final product is a metallacycle (70) derived from the coupling of the ethene ligand and the $\text{S}=\text{O}$ bond of the R-NSO cumulene (Scheme 29) (80).

This result is somewhat surprising in that the organic chemistry of iminooxosulfuranes is dominated by the preferential disruption of the $\text{S}=\text{N}$ multiple bond rather than the sulfoxide group (6). The product formation may be explained by considering the olefin complex as a $(\sigma, \sigma'-1,2\text{-diyl})$ that undergoes conventional insertion of the iminooxosulfurane at one of the $\text{Os}-\text{C}$ bonds. The accepted mechanism for this process (Section V,C,2) would produce a zwitterionic intermediate in which the cationic osmium center is coordinatively unsaturated. Intramolecular collapse of the ion pair (71) could occur with either $\text{Os}-\text{O}$ or $\text{Os}-\text{N}$ bond formation and the former would be favored on steric grounds. The alternative mechanism involving prior coordination of the iminooxosulfurane to the osmium center (facilitated by nitrosyl bending) appears unlikely because (46) typically binds to zerovalent group 8 metal centers in the $\pi(\text{N},\text{S})$ mode and the resulting metallacycle would therefore include the $\text{S}-\text{N}$ bond and not the $\text{S}-\text{O}$ bond of the original iminooxosulfurane.

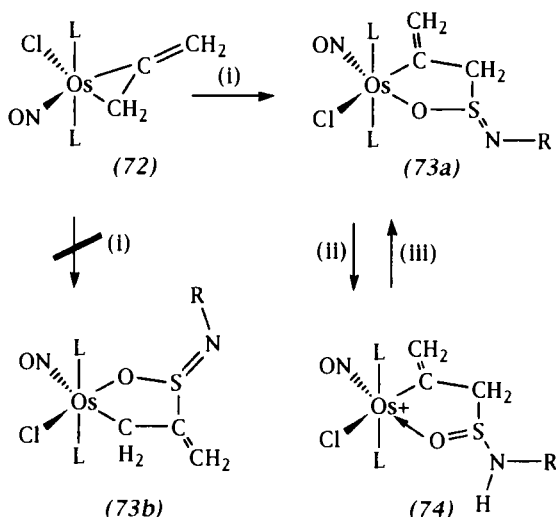
b. *Allene* The allene complex $[\text{OsCl}(\text{NO})(\eta^2\text{-CH}_2\text{CCH}_2)(\text{PPh}_3)_2]$ (72) (81,82) has two chemically distinct $\text{Os}-\text{C}$ bonds and in the reaction with (46) it is the alkyl rather than the vinylic bond into which the iminooxosulfurane cumulene inserts to provide (73a) rather than (73b) (83). As in the case of the related ethene complex (vide supra) it is the sulfoxide and not the sulfinimine group that ultimately becomes incorporated in the resulting



SCHEME 29. Coupling vs substitution reactions of an iminoxosulfurane with an ethylene complex of osmium. L = PPh₃, R = SO₂C₆H₄Me-4; (i) + C₂H₄, -L; (ii) + RNSO, -L; (iii) RNSO, toluene suspension; (iv) thf, reflux; (v) C₂H₄.

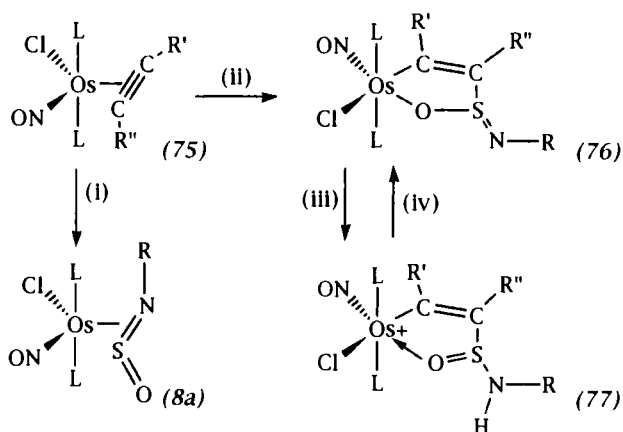
metallacycle (**73a**) (Scheme 30). The assumption that the reaction presumably proceeds by a similar mechanism to that discussed above for the ethene complex is supported by the observation that less electrophilic iminoxosulfuranes (RNSO; R = C₆H₄Me-2, C₆H₄Me-4) fail to react. The complex (**73a**) protonates reversibly (HBF₄) at the exocyclic sulfimine nitrogen to provide (**74**).

c. *Alkynes* The osmium alkyne complexes [OsCl(NO)(η -RC \equiv CR)(PPh₃)₂] (**75**) react differently with (**46**) depending on the nature of the alkyne substituents (83); The but-2-yne complex reacts by simple substitution to provide (**8a**) (Scheme 31). The more strongly bound perfluorobut-2-yne complex fails to react and the aryl alkyne derivatives [OsCl(NO)(η^2 -PhC \equiv CR)(PPh₃)₂] (R = H, Ph) react in an analogous manner to the allene and ethene complexes to provide unsaturated metallacycles (**76**). In the case of the ethynyl benzene complex the metallacycle



SCHEME 30. Coupling of R-NSO with coordinated allene. R = SO₂C₆H₄Me-4, L = PPh₃. (i) RNSO; (ii) HPF₆ or HBF₄; (iii) base or alumina.

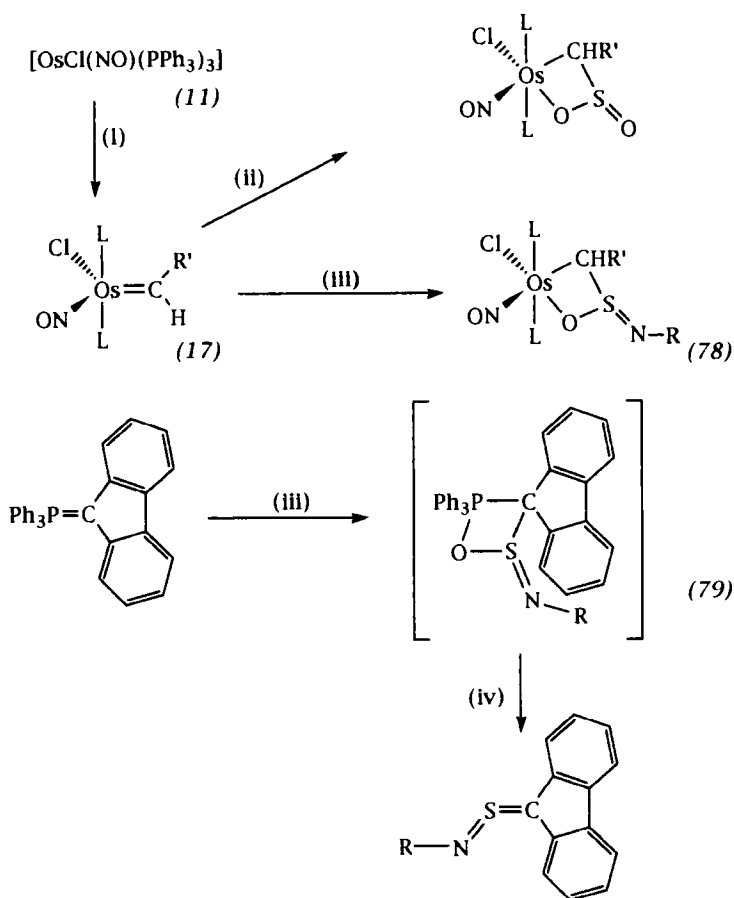
formation is regiospecific, exclusively providing the α -phenyl derivative. This is perhaps a reflection of the increased accessibility of the unsubstituted alkyne carbon toward external electrophiles. As with the allene derivative, protonation occurs reversibly at the exocyclic sulfimine nitrogen to provide (77).



SCHEME 31. Coupling of R-NSO with coordinated alkynes. R = SO₂C₆H₄Me-4, L = PPh₃. (i) RNSO R' = R'' = CH₃; (ii) RNSO R' = Ph, R'' = H, Ph; (iii) HPF₆ or HBF₄; (iv) base or alumina.

4. Metal–Carbon and Metal–Oxygen Multiple Bonds

a. *Alkylidenes* By analogy with the results obtained by Roper and Wright for sulfur dioxide (84), the osmium methylene complex $[\text{OsCl}(\text{=CH}_2)(\text{NO}(\text{PPh}_3)_2)]$ (**17a**) (44) reacts smoothly with (**46**) to provide a four-membered osmacycle (**78a**) resulting from formal coupling of the $\text{Os}=\text{C}$ and $\text{S}=\text{O}$ double bonds (Scheme 32) (85,86). A similar product (**78b**) results from the successive treatment of (**43**) or (**11**) with ethyl 2-diazoethanoate and (**46**), via the *in situ* generated alkylidene complex $[\text{OsCl}(\text{NO})(\text{=CHCO}_2\text{Et})(\text{PPh}_3)_2]$ (**17b**). Once again it is the sulfoxide and

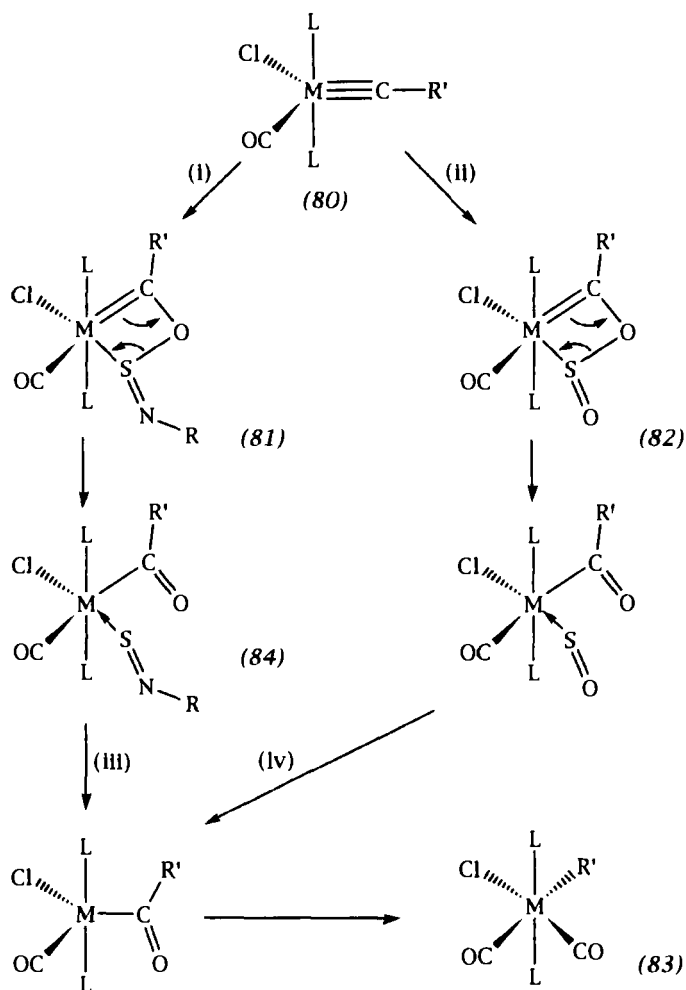


SCHEME 32. Coupling of R-NSO with alkylidene osmium complexes. $\text{R} = \text{SO}_2\text{C}_6\text{H}_4\text{Me}$ -4, $\text{L} = \text{PPh}_3$, $\text{R}' = \text{H}$, CO_2Et . (i) $\text{CHR}'\text{N}_2$, $-\text{L}$, $-\text{N}_2$; (ii) SO_2 ; (iii) RNSO ; (iv) $-\text{Ph}_3\text{PO}$.

not the sulfinimine component of the NSO cumulene that is ultimately involved. Consistent with an electrophilic role for the iminooxosulfurane, no reaction is observed with simple aryliminoxosulfuranes. The four-membered metallacycle may be viewed as a transition metal analog of the likely intermediate (**79**) in the conversion of iminoxosulfuranes to alkylidene-iminosulfuranes by a pseudo-Wittig reaction with phosphorane ylides (Scheme 32) (**87**).

b. *Alkylidyne* The alkylidyne complexes $[M(\equiv CR')Cl(CO)(PPh_3)_2]$ [$M = Ru, Os$; $R' = C_6H_5, C_6H_4Me-4$] (**81**, **82**, **88**) react with both (**46**) and simple aryliminoxosulfuranes, $R-NSO$, to provide the metallacycloadducts $[M\{CR'-OS(NR)\}Cl(CO)(PPh_3)_2]$ (**81**) (Scheme 33) (**85**). There remains some doubt as to the orientation of addition, as in the case of sulfur dioxide, which provides adducts (**82**) (**82**, **88**). The adducts (**81**) and (**82**) are not thermally stable, readily decomposing to the corresponding aryl(dicarbonyl) complexes $[MRCl(CO)_2PPh_3)_2]$ (**83**). While this decomposition precludes crystallographic verification of the orientation of cycloaddition, the nature of the products suggests a $M-C-O$ linkage in the metallacycles (**81**) and (**82**) (Scheme 33). The alternative geometries of addition should lead on thermolysis to either the thiobenzoyl-*S*-oxide complex (**31**) (Section IV,D) or the iminoacyl complex $[Ru\{C(NR)R'\}Cl(CO)(PPh_3)_2]$ (**89**), both of which have been prepared independently and are indefinitely stable. The implication of the thermolytic decomposition of the metallacycle is that an intermediate complex $[M\{C(=O)R'\}Cl(SNR)(CO)(PPh_3)_2]$ forms which subsequently loses the thionitrosoarene $S=NR$. Complexes of the form $[MR'Cl(SNR)(CO)(PPh_3)_2]$ ($M = Os, Ru$; $R' = C_6H_4Me-4$) have been isolated (**90**) and crystallographically characterized (**91**), however, only for $R = NMe_2$. In these complexes the thionitrosoamine is readily displaced by π acids, e.g., CO and isonitriles. Thionitroso-dimethylamine, $Me_2N-N=S$, is independently stable; however, simple hydrocarbyl thionitroso-compounds rapidly disproportionate in the free state to provide sulfur diimides and elemental sulfur. If sulfur diimides are produced in the decomposition of the metallacycles, these do not react with the resulting coordinatively saturated organometallic products as shown in independent experiments.

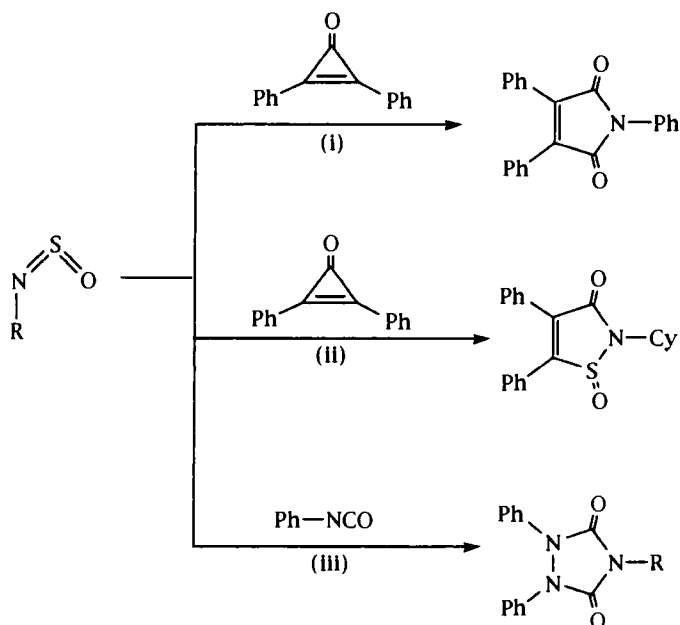
c. *Carbonyls* The thermolytic reactions of $[Fe(CO)_5]$ with iminoxosulfuranes lead to low yields of organometallic products (Section V,B,2). If the reaction is carried out in the presence of diphenylcyclopropenone, the organic product of the thermolysis is dependent upon the nature of the imino-substituent (**92**). With cyclohexyliminoxosulfurane an isothiazolone (**85**) is obtained; however, with phenyliminoxosulfurane a pyrro-



SCHEME 33. Coupling of iminoxosulfuranes with alkylidyne complexes of ruthenium and osmium. M = Ru, Os, L = PPh₃, R = SO₂C₆H₄Me-4, C₆H₄Me-4, C₆H₄Me-2; R' = C₆H₄Me-4, Ph. (i) RNSO; (ii) SO₂; (iii) -S = NR'; (iv) -"SO".

line-2,5-dione **(86)** is obtained (Scheme 34). Similar results were obtained with [Ni(CO)₄]. Aryliminoxosulfuranes may be condensed with aryl isocyanates in the presence of cobalt carbonyl to provide sulfur-free heterocycles **(93)**.

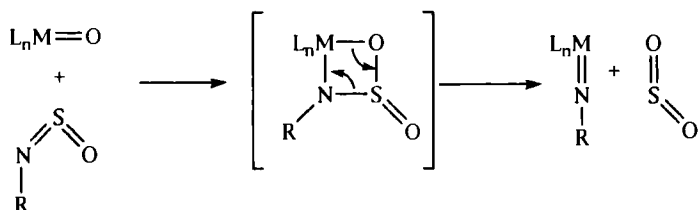
d. *Oxides* In a reaction reminiscent of olefin metathesis, the rhenium oxide complex [Re(=O)Cl₃(PPh₃)₂] reacts with iminoxosulfuranes, R -



SCHEME 34. Metal-carbonyl-mediated heterocycle syntheses. R = C₆H₅, C₆H₁₁. (i) [Fe(CO)₅]; (ii) [Ni(CO)₄]; (iii) [Co₂(CO)₈].

NSO, to provide sulfur dioxide and the corresponding imido-complex [Re(=NR)Cl₃(PPh₃)₂] (94,95) presumably via a four-membered metallacycle (Scheme 35). This type of reaction offers intriguing possibilities for the development of sulfur diimide metathesis catalysts.

Clearly the preceding results indicate that there is a rich coordination and organometallic chemistry for iminoxosulfuranes and it is sobering to reflect that this area of chemistry was theoretically, if somewhat prematurely, "written off" with the prediction "It may be concluded that PhNSO is unlikely to function generally as a ligand" (96).



SCHEME 35. Oxo-imido-metathesis of iminoxosulfuranes. L_nM = ReCl₃(PPh₃)₂, R = CMe₃.

VI

SULFUR DIIMIDES (DIIMINO- λ^4 -SULFURANES)

In contrast to sulfur dioxide and iminoxosulfuranes, sulfur diimides are much more prone to fragmentation of the sulfur(IV) cumulene and this feature has dominated the organometallic chemistry of these compounds. Such fragmentations have been employed to produce sulfido-, imido-, and thionitroso-ligands and are dealt with separately (Section VI,B,1).

A. Simple Coordination Complexes

Under mild conditions with suitable coordinatively unsaturated metal complexes, sulfur diimides may coordinate without rupture of the —N=S=N— moiety. These reactions may most conveniently be categorized according to the mode of coordination. This may be (i) through the NSN cumulene (97–108) or (ii) through donor functionalities built into the iminosubstituents and these are dealt with separately.

1. Coordination through the NSN Cumulene

Four modes of coordination have been identified or invoked as intermediates in fluxional processes. These are illustrated in Fig. 8. The factors

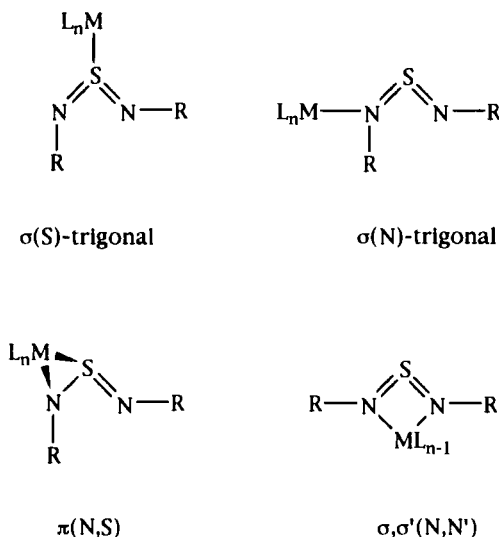
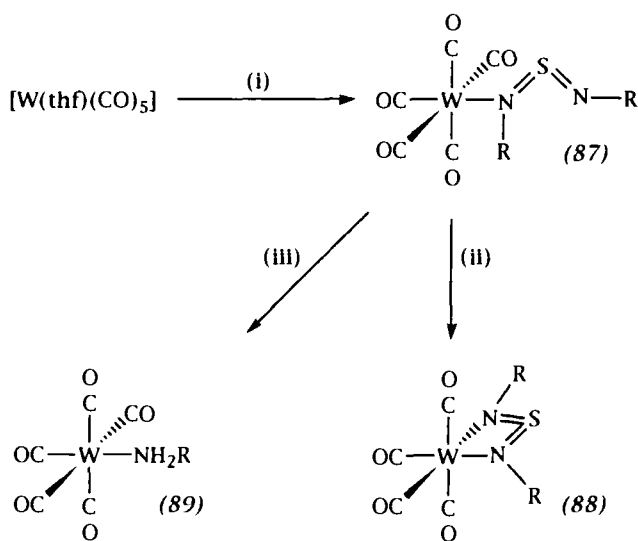


FIG. 8. Coordination modes for sulfur diimides.

dictating the mode of coordination adopted include the nature of the imino-substituent (steric and electronic properties) and the nature of the metal center (oxidation state, frontier orbital symmetry, degree of coordinative saturation, HSAB character). While the range of sulfur diimide complexes is far smaller than for iminoxosulfuranes, a similar dependence on these factors is beginning to emerge.

There is evidence that interconversion between the various modes of coordination can be facile and may be important in fluxional processes. Thus, for example, the room-temperature ^1H NMR spectrum of the complex $[\text{W}(\text{CO})_5\{\text{S}(=\text{NMe})_2\}]$ (**87a**) shows chemically equivalent methyl groups, which have been interpreted as resulting from a rapid migration of the $\text{W}(\text{CO})_5$ along the NSN cumulene between the two nitrogen donors. In the ground state, the tungsten center binds to just one of the nitrogen donors (Scheme 36) (102). The migration is presumed to involve $\pi(\text{N},\text{S})$ coordination. The corresponding di(tert-butyl)sulfur diimide complex (**87b**) readily loses CO resulting in a bidentate metallacyclic coordination $[\sigma, \sigma'(\text{N}, \text{N}')]$ (**88**) (102, 105). This type of coordination is also observed for the main-group metal halide adduct $[\text{SnCl}_4\{\text{S}(=\text{N}-t\text{-Bu})_2\}]$ (106). The hydrolytic sensitivity of free sulfur diimides is retained in the $\sigma(\text{N})$ -trigonal mode of coordination and the tungsten complexes are readily hydrolyzed to the corresponding primary amine derivatives (**89**). This enhanced hy-



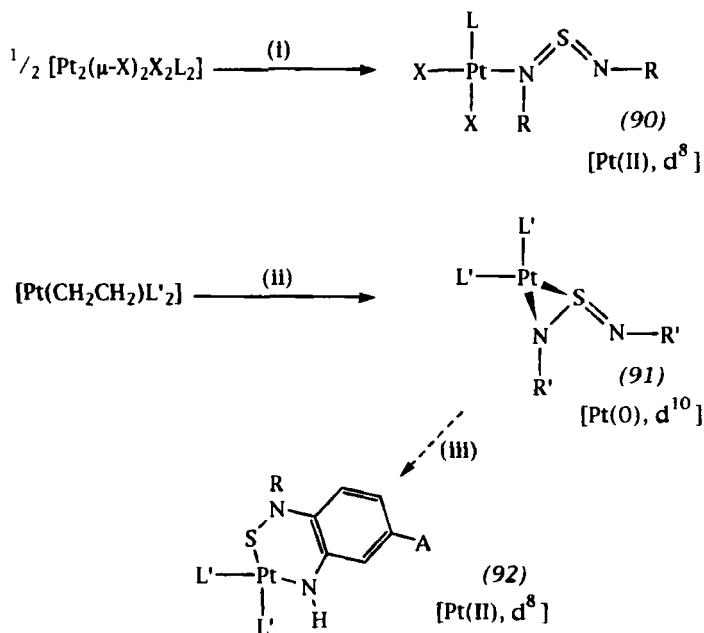
SCHEME 36. Sulfur diimide complexes of tungsten(0). R = Me, CMe_3 . (i) $\text{S}(=\text{NR})_2$; (ii) $-\text{CO}$; (iii) $+\text{H}_2\text{O}$, $-\text{SO}_2$, $-\text{RNH}_2$.

drolitic sensitivity is consistent with this mode of coordination involving a primarily σ -donor interaction.

The effect of metal basicity upon coordination mode is well illustrated by the di- and zero-valent platinum complexes $[\text{PtCl}_2(\text{PPh}_3)\{\text{S}(=\text{NR})_2\}]$ ($\text{R} = \text{alkyl, aryl}$) (**90**) (107) and $[\text{Pt}(\text{PPh}_3)_2(\eta^2\text{-RNSNR})]$ ($\text{R} = \text{C}_6\text{H}_4\text{Me-4, C}_6\text{H}_4\text{Cl-4}$) (**91**) (97,98), where, as in the case of iminoxosulfuranes, an increase in metal electron density favors the adoption of $\pi(\text{N,S})$ or pseudo-olefinic coordination. The latter complexes (**91**) are, however, not stable at ambient temperatures and rearrange with N-S bond cleavage to provide metallacyclic derivatives (**92**) (Scheme 37).

2. Coordination through the Imino Substituent

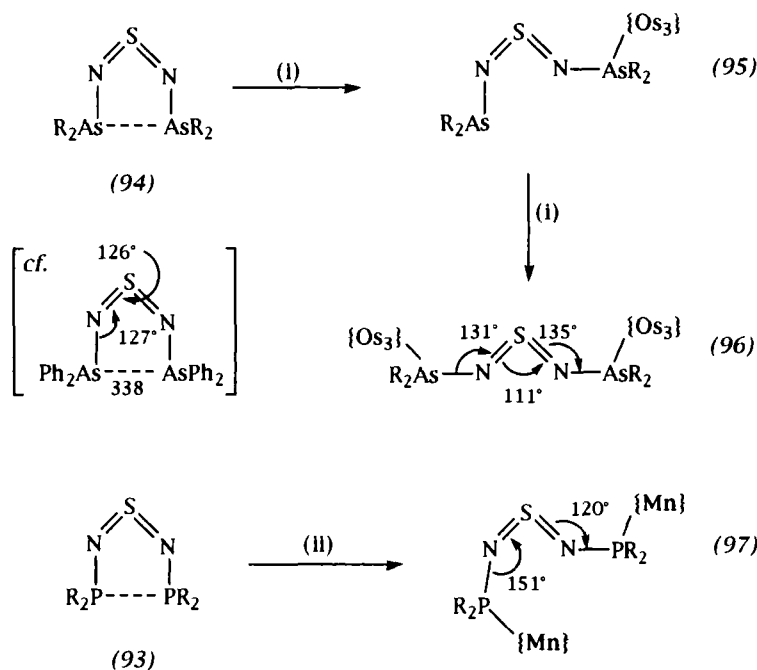
The interaction of sulfur diimides bearing pnictogeno-substituents with metal carbonyls has received considerable attention in recent times, primarily from the groups of Herberhold and Chivers. In general, phosphino-sulfur diimides are more prone to coordinative fragmentation under mild conditions than the corresponding arsino-derivatives. Thus (**93**) reacts



SCHEME 37. Sulfur diimide complexes of platinum. $\text{X} = \text{Cl, Br, I}$; $\text{R} = \text{Me, Et, } i\text{-Pr, } t\text{-Bu}$; $\text{L} = \text{PEt}_3, \text{AsEt}_3, \text{SbEt}_3, \text{PPh}_3, \text{AsPh}_3, \text{PPhMe}_2, \text{SPr}_2, \text{SeEt}_2, \text{TeEt}_2$; $\text{L}' = \text{PPh}_3$; $\text{R}' = \text{C}_6\text{H}_4\text{Me-4, C}_6\text{H}_4\text{Cl-4}$. (i) $\text{S}(=\text{NR})_2$; (ii) $\text{S}(=\text{NR}')_2$, $-\text{C}_2\text{H}_4$, $<0^\circ\text{C}$; (iii) room temperature.

with $[\text{Os}_3(\text{CO})_{11}(\text{NCMe})]$ to provide $[\text{Os}_3(\text{CO})_{11}\{\text{P}(\text{NH}_2)\text{-}t\text{-Bu}_2\}]$ (109) and with $[\text{Ru}_3(\text{CO})_{12}]$ to provide the isocyanato phosphine complex $[\text{Ru}_3\{\text{P}(\text{NCO})\text{-}t\text{-Bu}_2\}(\text{CO})_{11}]$ (110). Analogous treatment with (94) provides the arsine-coordinated 1:1 adduct $[\text{Os}_3(\text{CO})_{11}\{\text{As-}t\text{-Bu}_2\text{NSNAs-}t\text{-Bu}_2\}]$ (95) and the 1:2 adduct $[\text{Os}_3(\text{CO})_{11}]\text{As-}t\text{-Bu}_2\text{-NSN-}t\text{-Bu}_2\text{As}[\text{Os}_3(\text{CO})_{11}]$ (96) depending on reagent stoichiometry (111).

The hexanuclear cluster (96) has the unusual *E/E* configuration about the NSN cumulene, presumably for steric reasons. The free sulfur diimide adopts the *Z/Z* configuration due to a weak interarsenic interaction [3.379 Å] (112); however, simple sulfur diimides typically assume the *E/Z* configuration in the absence of any extenuating effects (6). The assumption that steric factors are responsible for the unprecedented *E/E* arrangement in the hexaoosmium example is supported by the observation that the product of reaction between (93) and $[\text{Mn}(\text{thf})(\text{CO})_2(\eta\text{-C}_5\text{H}_5)]$, viz (97), shows a severely distorted NSN cumulene (113) (Scheme 38). Similar adducts are obtained with the metal carbonyl fragments $\text{M}(\text{CO})_n$ ($n = 4$, $\text{M} = \text{Fe}$; $n = 5$, $\text{M} = \text{Cr}, \text{Mo}, \text{W}$) (112*b*). Under forcing conditions [octane,



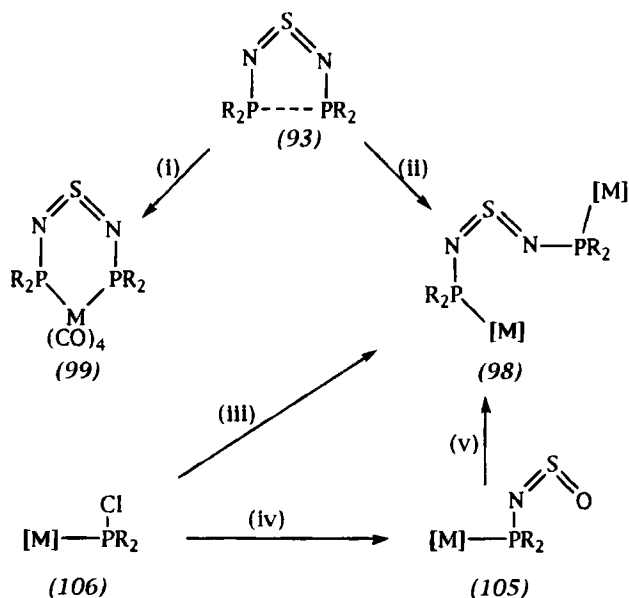
SCHEME 38. Coordination of pnictogeno-substituted sulfur diimides, $\text{R} = t\text{-Bu}$, $\{\text{Os}_3\} = \text{Os}_3(\text{CO})_{11}$, $\{\text{Mn}\} = \text{Mn}(\text{CO})_2(\eta\text{-C}_5\text{H}_5)$. (i) $[\text{Os}_3(\text{NCMe})(\text{CO})_{11}]$; (ii) $[\text{Mn}(\text{thf})(\text{CO})_2(\eta\text{-C}_5\text{H}_5)]$.

125°C] the triosmium complex is converted to the hexaosmium derivative (32%) in addition to the aminoarsine complex $[\text{Os}_3\{\text{As}(\text{NH}_2)\text{-}t\text{-Bu}_2\}(\text{CO})_{11}]$ (18%), which presumably forms via hydrolysis by adventitious moisture.

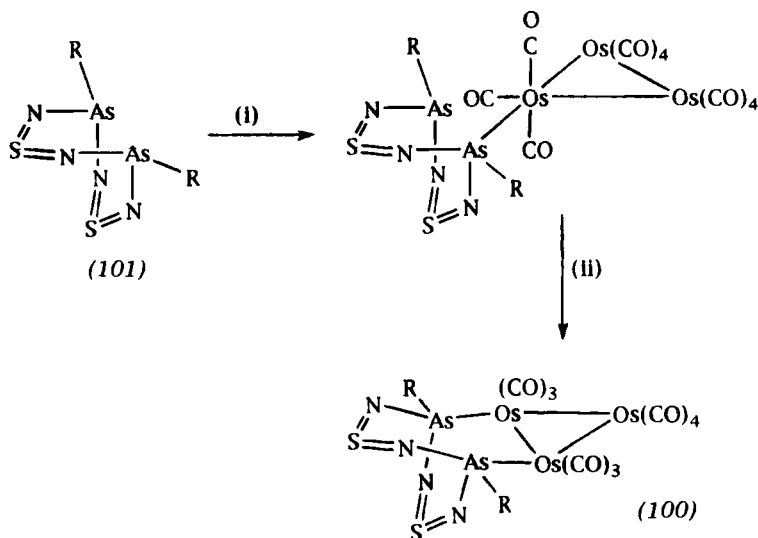
While di(*tert*-butylimino)sulfurane forms a complex with the $\text{W}(\text{CO})_4$ fragment in which coordination is through both nitrogen atoms $[\sigma, \sigma'(\text{N}, \text{N}')] (102, 105)$ the phosphino-substituted sulfur diimide (**93**) coordinates either as a bridging (**98**) (114) or chelating (**99**) (113) bis(phosphine) (Scheme 39).

A novel bicyclo-derivative (**100**) results from treating $[\text{Os}_3(\text{CO})_{11}(\text{NCMe})]$ with the cyclic sulfur diimide $t\text{-BuAs}(\text{NSN})_2\text{As-}t\text{-Bu}$ (**101**), followed by Me_3NO (Scheme 40) (115).

The related cyclic diphosphasulfur diimides $\text{RP}(\text{NSN})_2\text{PR}$ ($\text{R} = \text{Ph}$, $\text{N-}i\text{-Pr}_2$) (**102**) have been shown to coordinate in a similar manner to $\text{Cr}(\text{CO})_5$ fragments; however, in this case the binuclear complexes (**103**) were prepared via an elegant synthetic strategy involving the reactions of $[\text{Cr}(\text{PCl}_2\text{R})(\text{CO})_5]$ (**104**) with $[(\text{Me}_2\text{N})_3\text{S}][\text{NSO}]$ (116a, 116b). The mutual disposition of the $\text{Cr}(\text{CO})_5$ groups (*cis* or *trans* with respect to the ring) is dependent upon the steric bulk of the phosphorus substituents. In this reaction sequence the loss of sulfur dioxide is presumed to be induced by bases (in this case the thiazate anion). The base-induced condensation of



SCHEME 39. Coordination of pnictogeno-substituted sulfur diimides, $\text{M} = \text{Cr}$, Mo , W ; $[\text{M}] = \text{M}(\text{CO})_5$. (i) $\text{R} = t\text{-Bu}$, $[\text{M}(\text{CO})_4(\text{L})_2]$; (ii) $\text{R} = t\text{-Bu}$, $[\text{M}(\text{CO})_5(\text{thf})]$; (iii) $\text{R} = \text{Ph}$, $\text{K}_2[\text{NSN}]$; (iv) $\text{R} = \text{Me}$, Ph , $[\text{S}(\text{NMe}_2)_3][\text{NSO}]$; (v) $\text{KO-}t\text{-Bu}$.

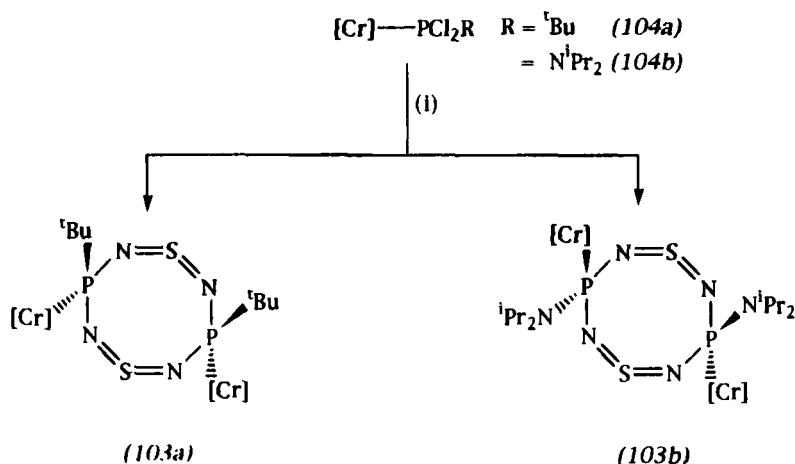


SCHEME 40. Coordination of pnictogeno-substituted sulfur diimides, R = *t*-Bu. (i) $[\text{Os}_3(\text{NCMe})(\text{CO})_{11}]$; (ii) Me_3NO , $-\text{CO}_2$, $-\text{NMe}_3$.

iminooxosulfuranes to provide sulfur diimides and sulfur dioxide is a classical route to simpler analogs of such compounds (6). The present example relies on a previous observation by Chivers (117,118) that bases induce the coupling of $[\text{Cr}\{\text{PPh}_2(\text{NSO})\}(\text{CO})_5]$ (**105**) to (**98**) with concomitant elimination of SO_2 . The thiazatophosphine complexes $[\text{M}\{\text{PR}_2(\text{NSO})\}(\text{CO})_5]$ [$\text{M} = \text{Cr}, \text{Mo}$; $\text{R} = \text{Me}, \text{Ph}$] (**105**) are readily prepared by the reaction of the corresponding chlorophosphine complex $[\text{Cr}(\text{PClR}_2)(\text{CO})_5]$ (**106**) with potassium thiazate (118). These are cleanly converted to the binuclear sulfur diimide compounds $\text{S}\{=\text{NPR}_2[\text{M}(\text{CO})_5]\}_2$ (**98**) by potassium *tert*-butoxide (Scheme 39). Such compounds are also accessible via (i) the reactions of monochlorophosphine complexes $[\text{M}(\text{PClR}_2)(\text{CO})_5]$ (**106**) with $\text{K}_2[\text{NSN}]$ (116a,116b,119,120) or (ii) the reaction of the free sulfur diimide (**93**) with complexes bearing labile ligands [typically solvent], e.g., $[\text{M}(\text{thf})(\text{CO})_5]$ (113,114,121). These transformations are summarized in Schemes 39 and 41.

The reactions of dichlorophosphine complexes with $\text{K}_2[\text{NSN}]$ do not in general lead to diphosphino-cyclic sulfur diimide complexes, but rather to mononuclear adducts of PN_2S_3 heterocycles (**107a**) (Scheme 42) (122,123).

The heterocyclic arsenic compound $[\text{Cr}(\text{As-}t\text{-BuNSNSNH})(\text{CO})_5]$ (**109**) is obtained from the reaction of $[\text{Cr}(\text{AsCl}_2\text{-}t\text{-Bu})(\text{CO})_5]$ (**110**) with $\text{K}_2[\text{NSN}]$; however, this is only as a minor product, the major product being



SCHEME 41. Coordination of pnico geno-substituted sulfur diimides, $[\text{Cr}] = \text{Cr}(\text{CO})_5$, $\text{R} = t\text{-Bu}$, $\text{N}^i\text{-Pr}_2$. (i) $[\text{S}(\text{NMe}_2)_3][\text{NSO}]$.

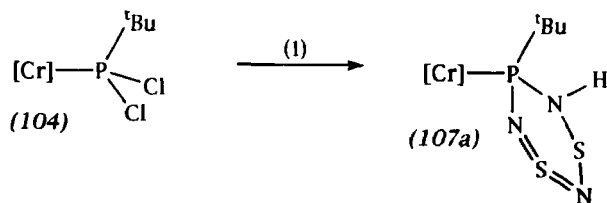
the bimetallic cyclic bis(sulfur diimide) complex $\{[(\text{OC})_5\text{Cr}\{t\text{-BuAs}(\text{NSN})_2\}]\} \text{As-}t\text{-Bu}\{\text{Cr}(\text{CO})_5\}$ (**111**) (Scheme 43) (124). The antimony-based sulfur diimides $t\text{-BuSb}(\text{NSN})_2\text{Sb-}t\text{-Bu}$ and $\text{S}(=\text{NSb-}t\text{-Bu}_2)_2$ show coordination chemistries similar to those of the arsenic analogs (125,126).

The related compound $[\text{Cr}\{\text{P}(\text{NR}_2)\text{NSNSNR}\}(\text{CO})_5]$ ($\text{R} = \text{SiMe}_3$) (**107b**) results from the reaction of $[\text{Cr}\{\text{P}(=\text{NR})\text{NR}_2\}(\text{CO})_3]$ (**108**) with S_4N_4 via a presumed double $[2 + 4]$ cycloaddition (Scheme 44) (116a).

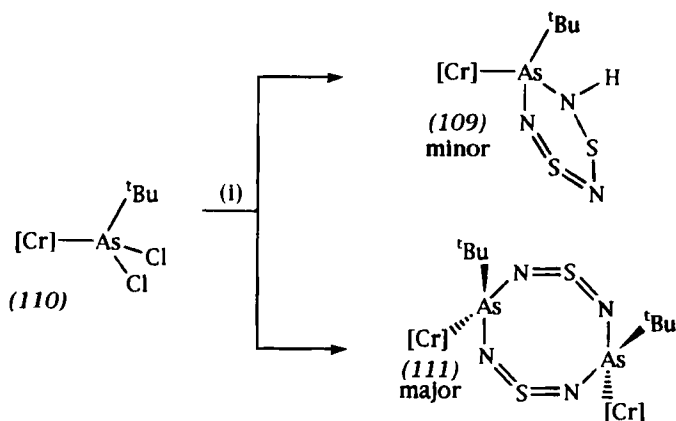
B. Reactions of Coordinated Sulfur Diimides

1. Fragmentations

Simple sulfur diimides readily fragment in the presence of transition metal carbonyl complexes. This is especially the case when the metal

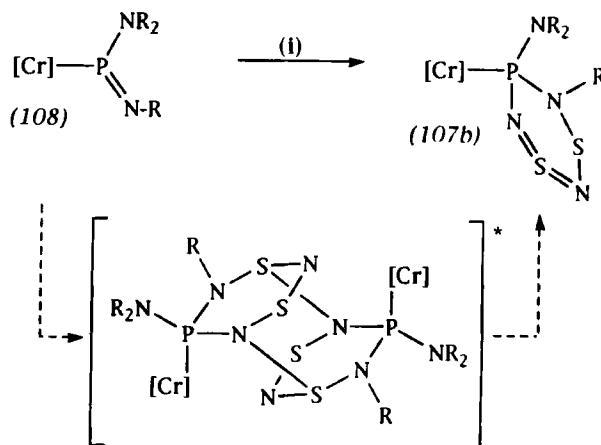


SCHEME 42. Coordination of pnico geno-substituted sulfur diimides, $[\text{Cr}] = \text{Cr}(\text{CO})_5$, $\text{R} = t\text{-Bu}$. (i) $\text{K}_2[\text{NSN}]$.

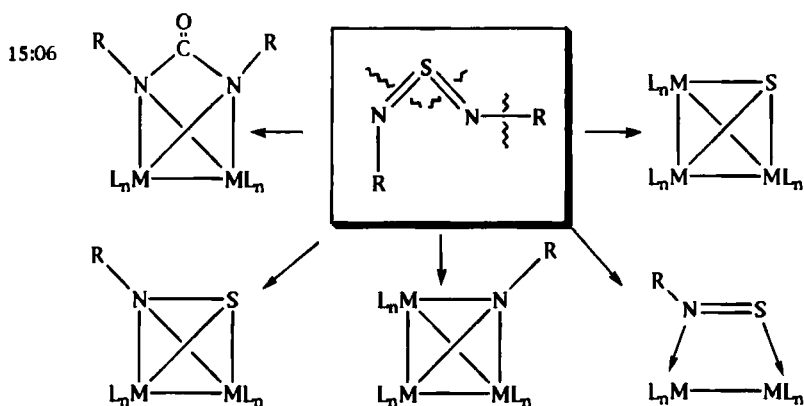


SCHEME 43. Coordination of pnictogeno-substituted sulfur diimides, $[\text{Cr}] = \text{Cr}(\text{CO})_5$, (i) $\text{K}_2[\text{NSN}]$.

reagents are capable of aggregating into cluster frameworks via bridge-assisted assembly. The clusters formed are typically supported by the bridging ligands derived from fragmentation of the NSN cumulene, i.e., $\text{R}-\text{N}$, S , or $\text{R}-\text{N}=\text{S}$ (Scheme 45). The reactions investigated, to date, have been typically carried out under thermolytic conditions and while in some favorable situations yields may be quite respectable, it is more common that this is not the case. Unfortunately, this precludes any detailed mechanistic interpretation, intellectual input being more often post-



SCHEME 44. Coordination of pnictogeno-substituted sulfur diimides, $[\text{Cr}] = \text{Cr}(\text{CO})_5$, $\text{R} = \text{SiMe}_3$, (i) $\frac{1}{2} \text{S}_4\text{N}_4$.

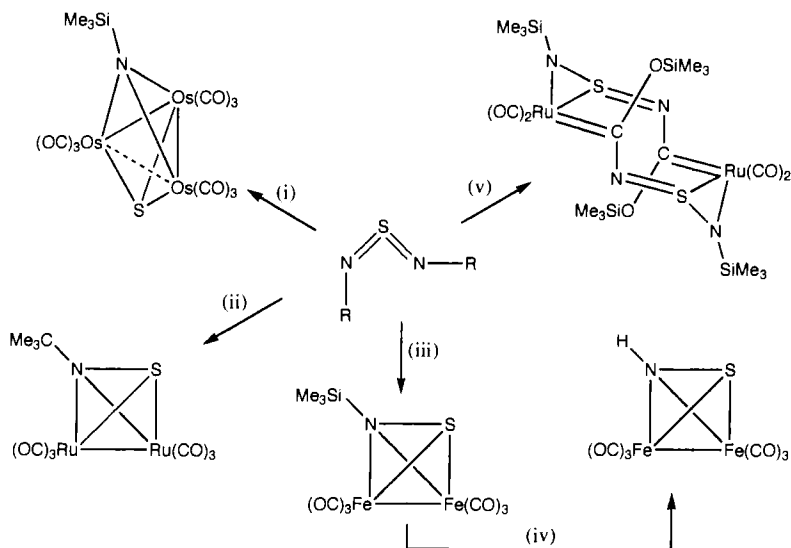


SCHEME 45. Structural motifs provided by metal carbonyl/sulfur diimide cothermolysis.

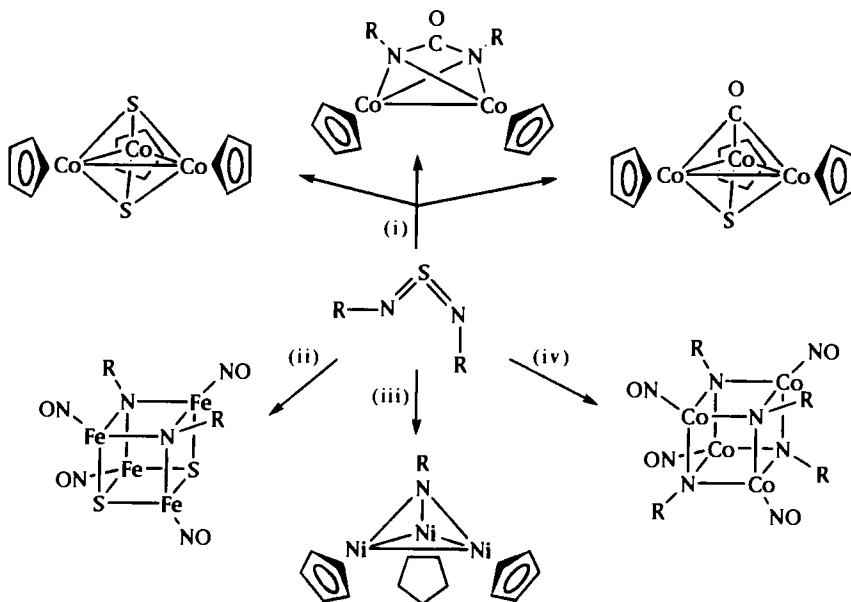
rationalist than strategic. Nevertheless, the metal-mediated fragmentation of sulfur diimides remains a useful if somewhat unpredictable approach to a host of interesting polymetallic ensembles.

It is most likely that the cleavage of the cumulene involves combination with a metal-bound carbonyl, extrusion of an isocyanate, and oligomerization of the resulting thionitrosoalkane complex via sulfur bridge-assisted clusterification. Carbon-sulfur bond cleavage is a common reaction in pyrolytic cluster synthesis and the cleavage of N-S bonds may be assumed to be at least as facile. In the absence of suitable model compounds for intermediates, these processes remain plausible conjecture. The field of bridge-assisted cluster synthesis has, however, matured considerably in recent times and the mechanistic investigation of these reactions will provide a fertile field for future study. The various imido-, sulfido-, and thionitrosoalkane-bridged clusters available through these types of reaction are summarized in Schemes 46 and 47 (127-140).

Of particular note are the reactions of $S(NR)_2$ ($R = t\text{-Bu}$, SiMe_3) with $[M_3(\text{CO})_{12}]$ ($M = \text{Fe}$, Ru , Os) (127-132), wherein the nature of the metal is surprisingly important (Scheme 46). In the case of $[\text{Fe}_3(\text{CO})_{12}]$ with $S(=\text{NSiMe}_3)_2$, the thionitrosotrimethylsilane complex $[\text{Fe}_2(\mu: \pi\text{-SNSiMe}_3)(\text{CO})_6]$ (**112**) is obtained and this may be hydrolyzed to the "parent" sulfur imide (HNS) complex $[\text{Fe}_2(\mu: \pi\text{-SNH})(\text{CO})_6]$ (**113**) by chromatography on silica gel (Scheme 46) (127). The reactions of $[\text{Fe}_3(\text{CO})_{12}]$ with $S(=\text{N-}t\text{-Bu})_2$ leads to a complicated mixture of compounds (131, 132). The reaction of $[\text{Ru}_3(\text{CO})_{12}]$ with $S(=\text{N-}t\text{-Bu})_2$, however, provides the simple 2-thionitroso-2-methyl propane-derived tetrahedrane structure $[\text{Ru}_2(\mu: \pi\text{-SN}^i\text{Bu})(\text{CO})_6]$ (**114**) (128). The reaction with $S(=\text{NSiMe}_3)_2$, however, leads to a complicated binuclear structure (**115**)



SCHEME 46. Interaction of the sulfur diimides $S(=NR)_2$ ($R = CMe_3$, $SiMe_3$) with group 8 binary carbonyls. (i) $[Os_3(CO)_{12}]$, $R = SiMe_3$; (ii) $[Ru_3(CO)_{12}]$, $R = CMe_3$; (iii) $[Fe_3(CO)_{12}]$, $R = SiMe_3$; (iv) hydrolysis; (v) $[Ru_3(CO)_{12}]$, $R = SiMe_3$.



SCHEME 47. Clusters derived from di(tert.butyl) sulfur diimide. $R = CMe_3$. (i) $[Co_2(\eta-C_5H_5)_2]$; (ii) $[Fe(NO)(CO)_3]$; (iii) $[Ni(\eta-C_5H_5)_2]$ or $[Ni_2(\mu-CO)_2(\eta-C_5H_5)_2]$; (iv) $[Co(NO)(CO)_3]$.

with bridging metallacyclic carbene ligands derived from migration of one silicon group to the oxygen of one carbonyl ligand (127). In the case of $[\text{Os}_3(\text{CO})_{12}]$, the higher temperatures required to activate the triosmium cluster lead to more extensive degradation of the NSN cumulene and the simple imido-/sulfido-capped trimetallic compounds $[\text{Os}_3(\mu_3\text{-S})(\mu_3\text{-NR})(\text{CO})_9]$ (**116**) are isolated (130).

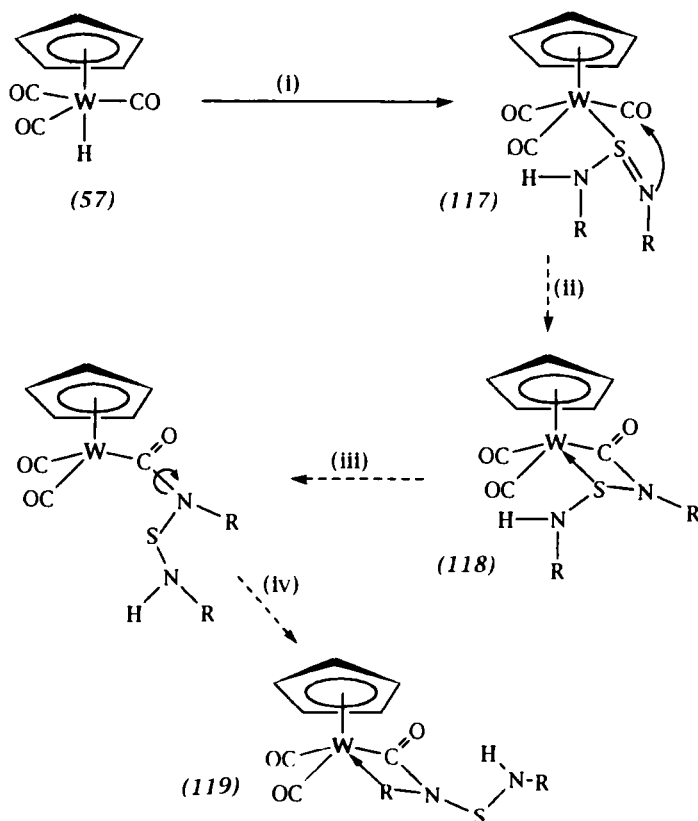
2. Reactions of Sulfur Diimides with Coordinated Ligands

The interactions of sulfur diimides with coordinated ligands have been less studied than those involving iminoxosulfuranes and concerned primarily with hydride and σ -organyl groups, although the question of implicit coupling reactions with metal carbonyls is addressed briefly in Section VI,B. This is partly due to the greater facility of sulfur diimides for cleavage reactions.

a. *Hydrides (i) Mononuclear complexes.* The reactions of sulfur diimides with the hydrido-complexes (**55**) and (**57**) are very strongly dependent on the nature of the imino-substituent although the initial steps of the reactions appear to be common (71,141,142).

Sulfur diimides bearing one or two electron-withdrawing tosylimino-substituents lead to simple 1,2-addition of the W—H bond across one S=N double bond (**117**) (71). The orientation of addition may be understood in terms of the Brønsted acidity of the W—H linkage and the related reactions with iminoxosulfuranes (Section V,C,1). Thus the sulfur diimide is protonated on one nitrogen to provide an ion pair $[\text{W}(\text{CO})_3(\eta\text{-C}_5\text{H}_5)]^-[\text{RN} = \text{S-NHR}]^+$, which collapses via nucleophilic attack by tungsten at sulfur (Scheme 47). If, however, a diaryl sulfur diimide is employed, the imino-nitrogen of the resulting complex is sufficiently nucleophilic to intramolecularly attack one of the tungsten(II)-bound carbonyl ligands to provide a metallacyclic carbamoyl derivative (**118**). Similar metallacyclic structures are observed for sulfur diimides bearing either a silyl or proton as one imino-substituent $[\text{S}(=\text{NR})(=\text{NR}')] : \text{R} = \text{H}, \text{SiMe}_3; \text{R}' = t\text{-Bu}, \text{As-}t\text{-Bu}_2]$ (141,142). A third possibility arises when the imino-substituent is itself a potentially good ligand for tungsten: Nucleophilic attack by the imino-nitrogen at one of the tungsten carbonyls is still observed; however, rotation about the carbamoyl C—N bond may occur to deliver the ligative substituent to the metal center in preference to the more weakly coordinating sulfane group. This is observed for the sulfur diimides $\text{S}(\text{NA-}t\text{-Bu}_2)_2$ ($\text{A} = \text{P}, \text{As}$) (141). These various possibilities are summarized in Scheme 48.

The heterocyclic 2,1,3-benzochalcogenadiazoles (**120**) and (**121**) may be considered as cyclic chalcogen di-imides although the incorporation of

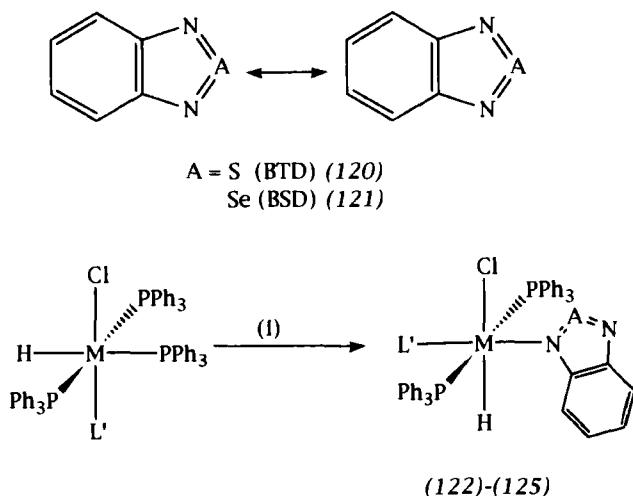


SCHEME 48. Hydrotungstenation of sulfur diimides. (i) $S(=NR)_2$, reaction stops for $R = SO_2C_6H_4Me-4$; (ii) reaction stops for $R = C_6H_4Me-4$, Ph, H, $SiMe_3$; (iii) reversible metallacycle opening; (iv) reaction proceeds if $R = P-t-Bu_2$, $As-t-Bu_2$, i.e., a better ligand for tungsten than sulfur.

the aromatic benzo-group into the cumulene electronic system leads to a substantial reduction in $N=A$ multiple bond character (Scheme 49).

This is manifest in a reduced propensity for cumulene cleavage in their reactions with transition metal hydrides. Thus, for example, $[IrCl_2H(PPh_3)_3]$ reacts with (120) or (121) to provide simple adducts $[IrCl_2H(PPh_3)_2(L)]$ [$L =$ BTD (122), BSD (123)] by phosphine substitution (143). Similar isoelectronic ruthenium complexes $[RuClH(CO)(PPh_3)_2(L)]$ [$L =$ BTD (124), BSD (125)] are obtained from $[RuClH(CO)(PPh_3)_3]$ and the mode of coordination has been established crystallographically for (124) to be through nitrogen (144).

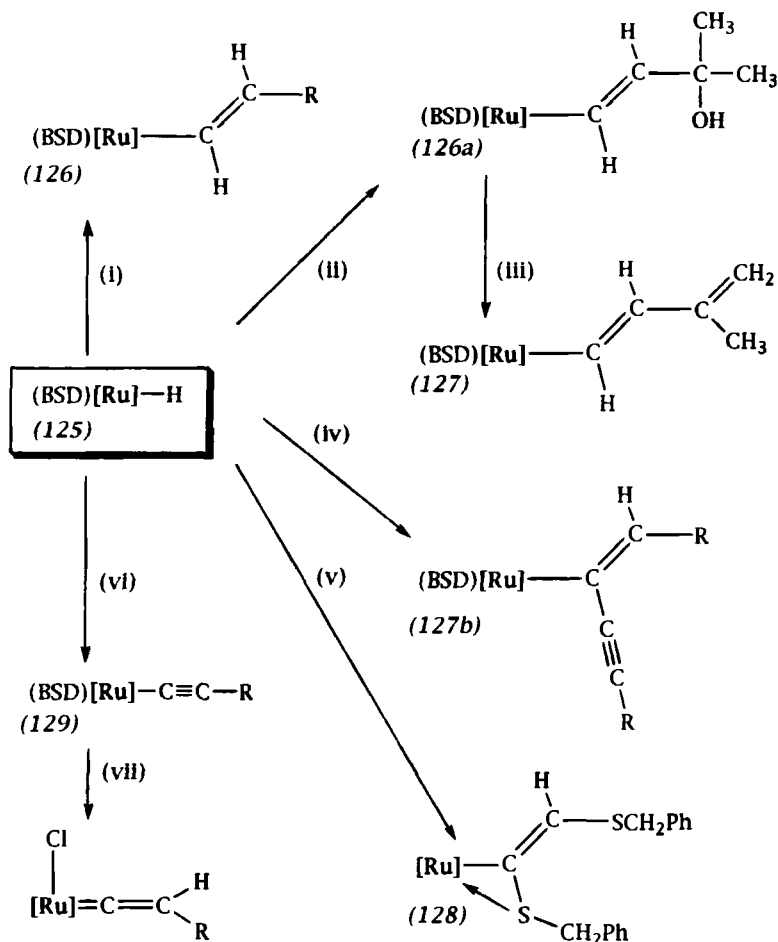
In no case has cleavage of the NSN cumulene been observed for these systems. Indeed, the innocence of these ligands is preserved in a number



SCHEME 49. Hydrido-benzochalcogenadiazole complexes. $ML' = Ru(CO), IrCl$. (i) $AN_2C_6H_4, -PPh_3$.

of subsequent reactions involving the Ru–H bond: Hydorruthenation of a wide range of alkynes and 1,3-diynes leads to σ -vinyl derivatives (145–147). These reactions require the intermediacy of a coordinatively unsaturated hydride complex and thus the facile reversibility of the BSD/BTD coordination is demonstrated. While the BSD ligand is coordinated *cis* to the hydride ligand in (124) it coordinates *trans* to the resulting σ -vinyl ligand in (126) (145). With propargylic alcohols the initially formed γ -hydroxy vinyl complexes readily dehydrate in the presence of acids or bases to provide σ -1,3-dienyl complexes (127) (146). With mercaptoalkynes the α -mercapto substituent also coordinates to the ruthenium center with displacement of the labile BSD ligand (128) (147). Reaction of (125) with bis(alkynyl)mercurials leads to formation of σ -acetylide complexes (129), which are in turn convenient precursors for octahedral vinylidene complexes of ruthenium(II) (148,149). These transformations are outlined in Scheme 50. In the resulting σ -vinyl and σ -acetylide complexes the BSD or BTD ligand fails to react with the Ru–C linkage and is readily displaced by good π -acid ligands (CO, CN-*t*-Bu, $CNC_6H_3Me_2$ -2,6).

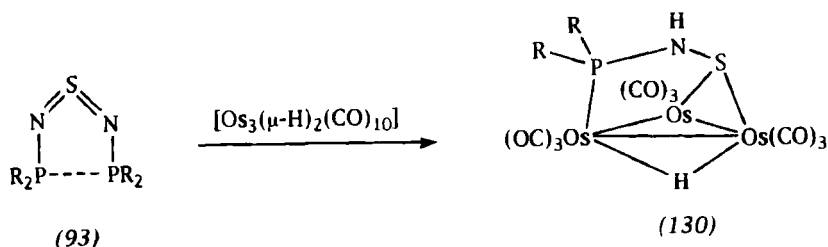
(ii) *Polynuclear complexes.* The reaction of (93) with $[Os_3(\mu-H)_2(CO)_{10}]$ leads to cleavage of the NSN cumulene, formal loss of *t*-Bu₂PNCO, and formation of the trinuclear cluster $[Os_3(\mu-H)\{\mu:\sigma,\sigma'-SN(H)P-t-Bu_2\}(S,P)(CO)_9]$ (130) (109) (Scheme 51). The reaction may proceed via similar processes to those seen for mononuclear hydrido-complexes; however, extrusion of *t*-Bu₂PNCO is presumably more facile from the polynuclear



SCHEME 50. Reactions of a ruthenium hydridobenzoselenadiazole complex. [Ru] = RuCl(CO)(PPh₃)₂, BSD = 2,1,3-benzoselenadiazole. (i) HC≡CR: R = H, *n*-Bu, Ph, C₆H₄Me-4, CH₂C(CO₂Et)PO(OEt)₂, CH₂SMe₂⁺; (ii) HC≡CCMe₂OH; (iii) base or (CF₃CO)₂O; (iv) RC≡C-C≡CR: R = H, CMe₂OH, Ph, SiMe₃; (v) PhCH₂SC≡CSCH₂Ph, -BSD; (vi) [Hg(C≡CR)₂], -Hg, -HC≡CR: R = Ph, *n*-Bu, C₆H₄Me-4; (vii) HCl, -[BSDH]Cl.

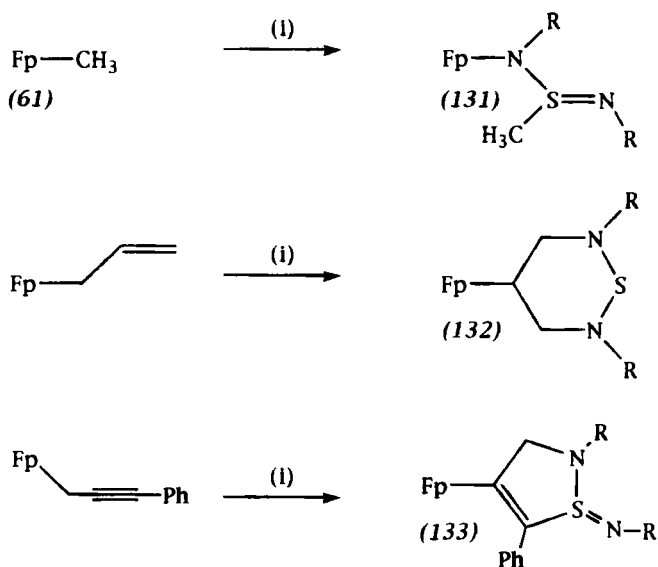
complex than from the coordinatively saturated tungsten examples (118) and (119) discussed above.

b. *σ*-Organyl complexes Wojcicki has investigated the reaction of coordinatively saturated *σ*-alkyl and *σ*-aryl complexes of groups 6–8 with sulfur diimides. Consistent with the analogous mechanism for SO₂



SCHEME 51. Osmium-hydride-mediated sulfur diimide cleavage. R = *t*-Bu.

insertion involving outer-sphere electrophilic attack by electrophilic sulfur at the metal-bound carbon atom, insertion is only observed for the exceedingly electron-deficient sulfur diimides $[\text{S}(\text{NSO}_2\text{R})_2]$: R = $\text{C}_6\text{H}_4\text{Me-Cl}$, CH_3] (72–74). The stereochemistry of these insertions is the opposite to that observed for hydrido-complexes. Thus in the case of $[\text{FeCH}_3(\text{CO})_2(\eta\text{-C}_5\text{H}_5)]$ (61) the metal initially becomes attached to the nitrogen to produce (131) (Scheme 52). The reversed orientation of kinetic addition supports the disparate mechanisms for W–CH₃ and W–H addition as well as reflecting the bond polarities [$^+\text{W}-\text{C}^-$ vs $^-\text{W}-\text{H}^+$] for the two ligands. With σ -allyl and σ -propargyl complexes, metal-substituted heterocycles (132) and (133) are obtained.



SCHEME 52. Interaction of sulfur diimides with σ -alkyl complexes of iron(II). Fp = $[\text{Fe}(\text{CO})_2(\eta\text{-C}_5\text{H}_5)]$, R = SO_2Me . (i) RNSO₂.

VII

THIAZATE AND RELATED LIGANDS

By analogy with the $\sigma(\text{O})$ coordination of sulfur dioxide to hard Lewis acids, isoelectronic thiazate complexes $[\text{L}_n\text{M}-\text{NSO}]$ and metallated sulfur diimides ($\text{L}_n\text{M}-\text{NSNR}$) (Fig. 9) have been reported, although only comparatively recently.

The reaction of $[\text{Pt}(\eta\text{-C}_2\text{H}_4)(\text{PPh}_3)_2]$ with $\text{S}(=\text{NSiMe}_3)_2$ provides the complex $[\text{Pt}(\sigma\text{-NSNSiMe}_3)_2(\text{PPh}_3)_2]$ (**134**) by an as-yet obscure mechanism (150), which is in contrast to the results obtained for simple sulfur diimides where the kinetic products are simple $\pi(\text{N},\text{S})$ zero-valent platinum complexes (**91**). A mechanism involving oxidative addition of the N-Si bond followed by olefin silylation to ultimately provide $\text{Me}_3\text{SiCH}_2\text{CH}_2\text{SiMe}_3$ seems reasonable (Scheme 53) but has yet to be confirmed. Alternatively a double N-Si oxidative addition followed by reductive elimination of Si_2Me_6 would also produce (**134**).

A related titanium complex $[\text{Ti}(\sigma\text{-NSN-}i\text{-Bu})_2(\eta\text{-C}_5\text{H}_5)_2]$ (**135a**) has been obtained from the reaction of titanocene dichloride with $\text{K}[\text{NSN-}i\text{-Bu}]$ (151); however, attempts to purify the complex by chromatography lead to N=S hydrolysis and isolation of the previously reported (152,153) bis(thiazate) complex $[\text{Ti}(\sigma\text{-NSO})_2(\eta\text{-C}_5\text{H}_5)_2]$ (**136**). This complex may be prepared more conveniently by the reaction of titanocene dichloride with a solution of thionyl chloride in liquid ammonia, which is presumed to generate $[\text{NH}_4][\text{NSO}]$ *in situ* (154). Treating (**136**) with $\text{LiN}(\text{SiMe}_3)_2$ provides the trimethylsilyl derivative (**135b**), which at first site appears an ideal candidate for the synthesis of metallacyclic NS rings. Unfortunately, the N-Ti bonds appear more labile than the N-Si bonds, generating $[\text{TiCl}_2(\eta\text{-C}_5\text{H}_5)_2]$ in reactions with main group chlorides (Scheme 54).

The $\text{OSCl}_2/\text{NH}_{3(l)}$ reagent developed by Woollins is also a convenient reagent for the synthesis of a range of bis(thiazato) complexes of platinum

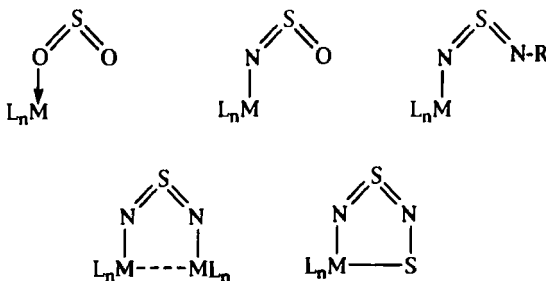
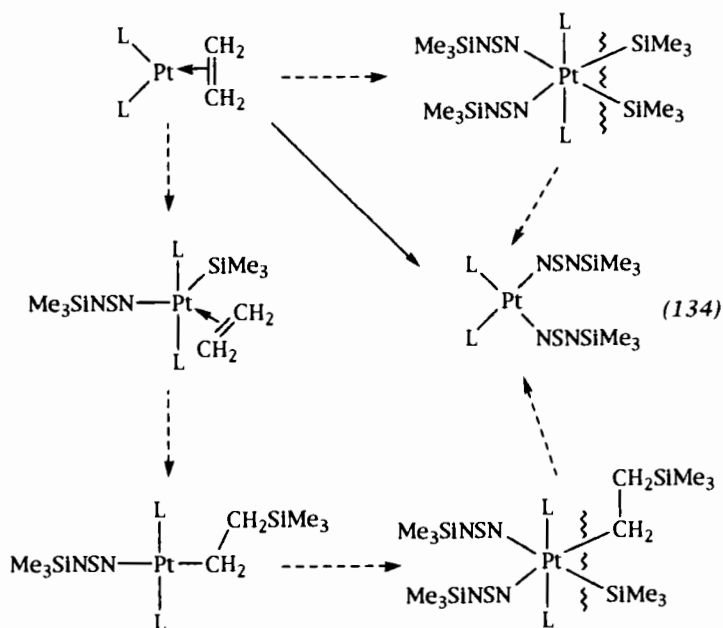
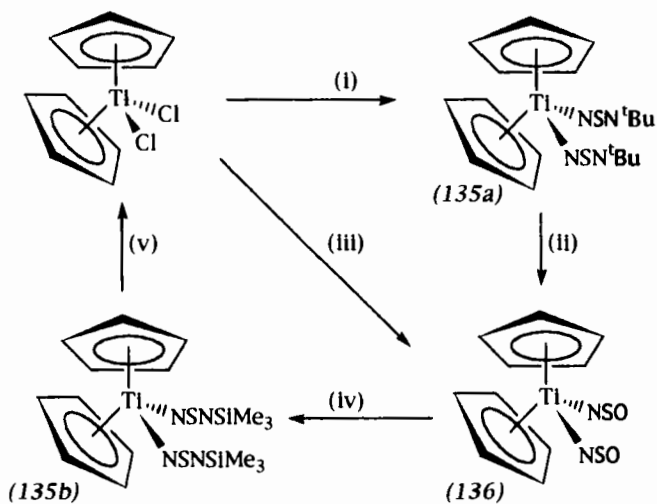


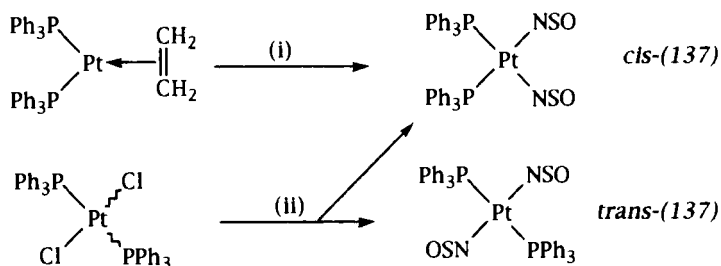
FIG. 9. Metal thiazates and related compounds.



SCHEME 53. Possible mechanisms for the interaction of $S(=NSiMe_3)_2$ with $[Pt(CH_2CH_2)L_2]$. $L = PPh_3$.



SCHEME 54. Thiatazo-complexes of titanium(IV). (i) $K[NSN-t-Bu]$; (ii) chromatography; (iii) $K[NSO]$ or $[NH_4][NSO]$; (iv) $Li[N(SiMe_3)_2]$; (v) SCl_2 .

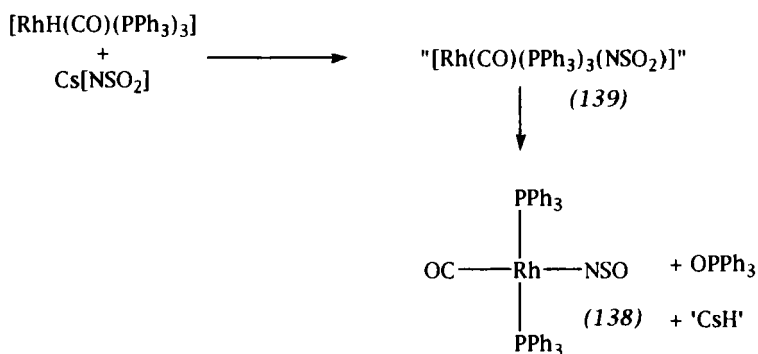


SCHEME 55. Thiazato-complexes of platinum(II). (i) $[\text{Hg}(\text{NSO})_2]$, $\text{PhAs}(\text{NSO})_2$ or $\text{S}(\text{NSO})_2$; (ii) $[\text{NH}_4][\text{NSO}]$ or $\text{S}(\text{NSO})_2/\text{NH}_3(1)$.

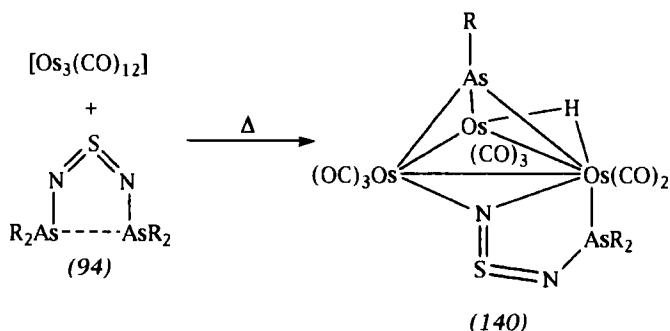
beginning with the corresponding dichlorides (Scheme 55). These complexes are also readily prepared by employing ammoniacal solutions of sulphur di(thiazate) $[\text{S}(\text{NSO})_2]$ or by treating the zerovalent ethene complex $[\text{Pt}(\eta\text{-CH}_2\text{CH}_2)(\text{PPh}_3)_2]$ with bis(thiazato)mercury(II) (152) or thiazatoarsines (153).

An unusual reaction occurs between $[\text{RhH}(\text{CO})(\text{PPh}_3)_3]$ and $\text{Cs}[\text{NSO}_2]$ to provide the structurally characterized complex $[\text{Rh}(\sigma\text{-NSO})(\text{CO})(\text{PPh}_3)_2]$ (138), and phosphine oxide (Scheme 56) (155). The initial product is presumably a $\sigma\text{-NSO}_2$ complex (139), which is subsequently reduced by triphenylphosphine.

The reaction of $[\text{CoH}\{\text{P}(\text{OPh})_3\}_4]$ with trithiazyl trichloride has been reported to provide the cobalt(III) complex $[\text{CoCl}_2(\sigma\text{-NSO})\{\text{P}(\text{OPh})_3\}_2]$ (156). The formulation was based only on infrared data and must be considered dubious, given the large number of incorrectly formulated complexes reported to result from the reactions of phosphine complexes



SCHEME 56. A thiazato-complex of rhodium(I).



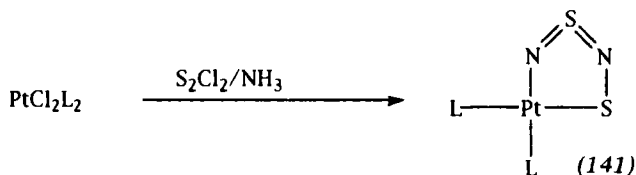
SCHEME 57. Cothermolysis of $[\text{Os}_3(\text{CO})_{12}]$ and $\text{S}(=\text{NAs-}t\text{-Bu})_2$. $\text{R} = t\text{-Bu}$.

of metals of groups 8–10 with trithiazyl trichloride (30,157). In many cases the species that is actually responsible for the infrared activity attributed to $\nu_{(\text{NS})}$ has subsequently been shown by Woollins to be $[\text{Ph}_3\text{PNH}_2]\text{Cl}$ (158).

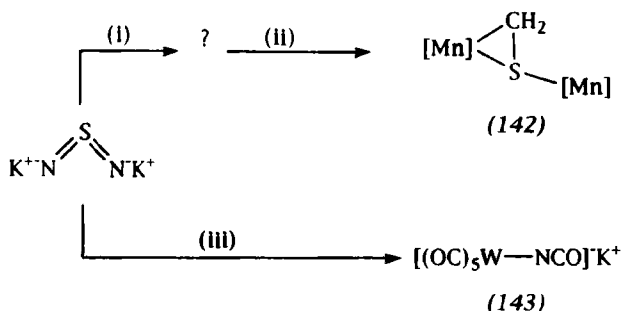
A novel trinuclear complex of the $\text{NSNAs-}t\text{-Bu}_2$ ligand (140) results from the thermolysis of osmium dodecacarbonyl with (94) (159). One nitrogen–arsenic bond is cleaved to ultimately provide a capping arsine ligand and one tert-butyl group presumably provides the hydride ligand by 2-methyl propene elimination (Scheme 57).

A range of metallacyclic complexes $[\text{L}_n\text{M}(\text{SNSN})]$ (141) of the nickel triad result from the reactions of divalent precursors with S_4N_4 or S_2Cl_2 in liquid ammonia. These compounds may be formally described as metallacyclized complexes of the $^-\text{N}=\text{S}=\text{N}-\text{S}^-$ dianion (Scheme 58) although the analogy is of limited use. The chemistry of this class of compounds has been extensively reviewed elsewhere (160).

Initial investigations into the transition metal coordination chemistry of the readily prepared, explosive salt $\text{K}_2[\text{NSN}]$ (161) have been largely disappointing (Scheme 59). Reaction of the solvent-stabilized complex $[\text{Mn}(\text{thf})(\text{CO})_2(\eta\text{-C}_5\text{H}_5)]$ with $\text{K}_2[\text{NSN}]$ leads to an intermediate complex that reacts with dichloromethane to produce the binuclear thioformaldehyde complex $[\text{Mn}_2(\sigma: \pi\text{-CH}_2\text{S})(\text{CO})_4(\eta\text{-C}_5\text{H}_5)_2]$ (142) (162). The interme-



SCHEME 58. Synthesis of platinadithiadiazoles.



SCHEME 59. Coordination chemistry of dipotassium sulfur diimide. (i) $[\text{Mn}(\text{thf})(\text{CO})_2(\eta\text{-C}_5\text{H}_5)]$; (ii) CH_2Cl_2 ; $[\text{W}(\text{CO})_6]$, $-\text{K}[\text{NS}]$.

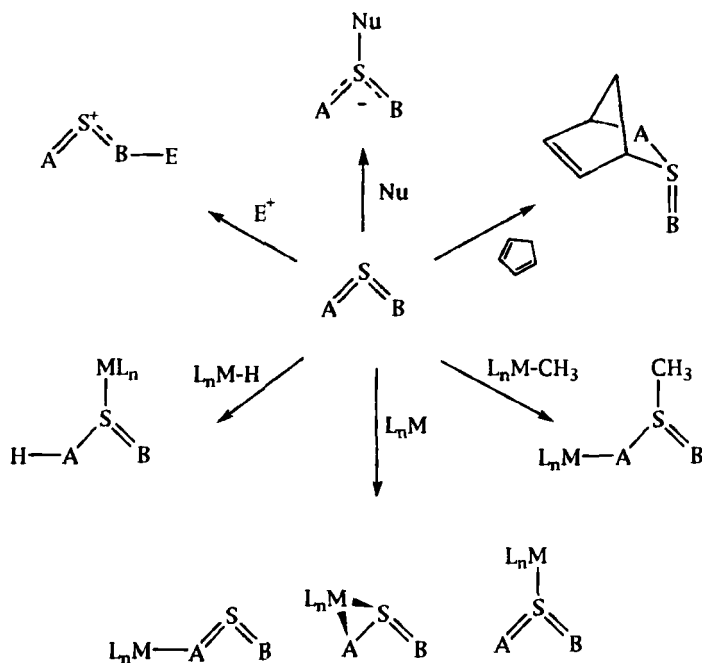
diolate is most likely of the form $\text{S}[\text{Mn}(\text{CO})_2(\eta\text{-C}_5\text{H}_5)]_n^{2-}$ ($n = 2, 3, ?$) but has yet to be identified. Reaction of $[\text{W}(\text{CO})_6]$ with $\text{K}_2[\text{NSN}]$ produces the anionic isocyanate derivative $[\text{W}(\text{NCO})(\text{CO})_5]^-$ (**143**) (163). However, both this and the preceding reaction proceed in yields too low to be mechanistically informative other than to illustrate that the salt is not incorporated intact into these coordination spheres but may serve as either a nucleophilic source of S or N, or as a potent reductant.

VIII

CONCLUDING REMARKS

The coordination and organometallic chemistry of the simple analogs of sulfur dioxide remains comparatively unexplored. The specific fields of iminoxosulfurane, sulfur diimide, and sulfine chemistry are sufficiently immature as to still reflect the particular perspectives of the few research groups involved to date. Few situations where detailed comparisons may be made for a complete range of sulfur(IV) heterocumulenes bound to the same metal–ligand fragment even exist. Even in the few situations where this is possible, both parallels and divergences are apparent. The basic analogy with sulfur dioxide will in many but not all situations be a useful one. Situations where this analogy is particularly appropriate are illustrated in Scheme 60.

A critical appraisal of the known organometallic chemistry of sulfur dioxide soon reveals a preoccupation with either the mode of coordination to be adopted or simple insertion reactions with comparatively mundane σ -alkyl ligands. It is hoped that this review, while outlining the interesting



SCHEME 60. The sulfur dioxide analogy: A, B = O, S, NR, CR₂.

results obtained so far for other sulfur(IV) cumulenes, has also highlighted potentially fruitful areas for further study.

REFERENCES

- (1) Gleu, K.; Rehm, K. *Z. Anorg. Allg. Chem.* **1936**, 227, 237; Gleu, K.; Breuel, W.; Rehm, K. *Ibid.* **1938**, 235, 201, 211.
- (2) Ryan, R. R.; Kubas, G. J.; Moody, D. C.; Eller, P. G. *Struct. Bonding (Berlin)* **1981**, 46, 47.
- (3) Mingos, D. M. P. *Trans. Met. Chem.* **1978**, 3, 1.
- (4) Livingstone, S. L. In "Comprehensive Co-ordination Chemistry"; Wilkinson, G.; Gillard, R. G.; McCleverty, J. A., Eds.; Pergamon: Oxford, 1987; Vol. 2, p. 634.
- (5) Wojcicki, A. *Adv. Organomet. Chem.* **1974**, 12, 1545.
- (6) Imino-oxosulfuranes and sulfur di-imides: Kresze, G.; Masche, A.; Albrecht, R.; Bederke, K.; Patzschke, H. P.; Smalla, H.; Trede, A. *Angew. Chem., Int. Ed. Engl.* **1962**, 1, 89; Kresze, G.; Wucherpfennig, W. *ibid.* **1967**, 6, 149; Bussas, R.; Kresze, G.; Münsterer, H.; Schwöbel, A. *Sulfur Rep.* **1983**, 2, 215. The simple co-ordination chemistry of imino-oxosulfuranes and sulfur diimides has been reviewed up till 1986: Vrieze, K.; van Koten, G. In "Comprehensive Coordination Chemistry"; Wilkinson, G.; Gillard, R. G.; McCleverty, J. A., Eds.; Pergamon: Oxford, 1987; Vol. 2, p. 190.

- (7) Sulfines: Zwanenburg, B. *Recl. Trav. Chim. Pays-Bas* **1982**, *102*, 1. NB. Bis(alkylidene) sulfuranes are unstable with respect to ring closure to produce thiiranes.
- (8) Block, E.; Bock, H.; Mohmand, S.; Rosmus, P.; Solouki, B. *Angew. Chem., Int. Ed. Engl.* **1976**, *15*, 381.
- (9) Bock, H.; Solouki, B.; Rosmus, P.; Steudel, R. *Angew. Chem., Int. Ed. Engl.* **1973**, *12*, 933.
- (10) Haase, J.; Winnewisser, M. *Z. Naturforsch., A* **1968**, *23A*, 61.
- (11) Post, B.; Schwartz, R. S.; Fankuchen, I. *Acta Crystallogr.* **1952**, *5*, 372.
- (12) Morino, Y.; Kikuchi, Y.; Saito, S.; Hirohito, E. *J. Mol. Spectr.* **1964**, *13*, 95.
- (13) Kirchhoff, W. H. *J. Am. Chem. Soc.* **1969**, *91*, 2437.
- (14) Block, E.; Penn, R. E.; Olsen, R. J.; Sherwin, P. F. *J. Am. Chem. Soc.* **1976**, *98*, 1264.
- (15) Powers, D. E.; Arrington, C. A.; Harris, W. C.; Block, E.; Kalisinsky, V. F. *J. Phys. Chem.* **1979**, *83*, 1890.
- (16) Schenk, P. W. *Z. Anorg. Allg. Chem.* **1937**, *233*, 385.
- (17) Hughes, G. R.; Minshall, P. C.; Mingos, D. M. P. *J. Less-Common Met.* **1986**, *116*, 199.
- (18) Lorenz, I.-P. *Angew. Chem., Int. Ed. Engl.* **1978**, *9*, 60.
- (19) Schenk, P. W. *Z. Anorg. Allg. Chem.* **1933**, *211*, 150; Schenk, P. W.; Steudel, R. *ibid.* **1966**, *392*, 253.
- (20) Jones, A. V. *J. Chem. Phys.* **1950**, *18*, 1263.
- (21) Meschi, D. J.; Myers, R. J. *J. Am. Chem. Soc.* **1956**, *78*, 6220; *J. Mol. Spectrosc.* **1959**, *3*, 405; Blukis, U.; Myers, R. J. *J. Chem. Phys.* **1965**, *69*, 1154.
- (22) Tang, S. Y.; Brown, C. W. *Inorg. Chem.* **1975**, *14*, 2856; Schenk, P. W.; Steudel, R. *Angew. Chem., Int. Ed. Engl.* **1965**, *4*, 402.
- (23) Schmid, G.; Ritter, G. *Angew. Chem., Int. Ed. Engl.* **1975**, *14*, 645; Schmid, G.; Ritter, G.; Debaerdemacker, T. *Chem. Ber.* **1978**, *108*, 3008.
- (24) Hoots, J. E.; Rauchfuss, T. B.; Wilson, S. R. *J. Chem. Soc., Chem. Commun.* **1983**, 1226; Hoots, J. E.; Lesch, D. A.; Rauchfuss, T. B. *Inorg. Chem.* **1984**, *23*, 3130.
- (25) Herberhold, M.; Schmidkonz, B.; Ziegler, M. L.; Zahn, T. *Angew. Chem., Int. Ed. Engl.* **1985**, *24*, 515; Herberhold, M.; Schmidkonz, B. *J. Organomet. Chem.* **1986**, *308*, 35.
- (26) Schmidkonz, B. Doktorarbeit, Universität Bayreuth, 1987.
- (27) Herberhold, M.; Hill, A. F. *J. Chem. Soc., Dalton Trans.* **1988**, 2027.
- (28) Dirand-Colin, J.; Schappacher, M.; Ricard, L.; Weiss, R. *J. Less-Common Met.* **1977**, *54*, 91.
- (29) Draganjac, M.; Rauchfuss, T. B. *Angew. Chem., Int. Ed. Engl.* **1985**, *24*, 742.
- (30) Pandey, K. K. *Prog. Inorg. Chem.* **1992**, *40*, 445.
- (31) Arulsamy, K. S.; Pandey, K. K.; Agarwala, U. C. *Inorg. Chim. Acta* **1981**, *54*, L51.
- (32) "Gmelin Handbuch für Anorganischen Chemie", 8th ed.; Springer-Verlag: Berlin, 1980; Vol. 3.
- (33) Herberhold, M.; Reiner, D.; Thewalt, U. *Angew. Chem.* **1983**, *95*, 1028.
- (34) Carsen, L. *Chem. Ind. (London)* **1977**, *16*, 733.
- (35) Dittmer, D. C.; Takahashi, K.; Iwanami, M.; Tsai, A. I.; Chang, P. L.; Bildner, B. B.; Stamos, I. K. *J. Am. Chem. Soc.* **1973**, *95*, 6113.
- (36) Alcock, N. W.; Danks, T. N.; Richards, C. J.; Thomas, S. E. *J. Chem. Soc., Chem. Commun.* **1989**, 21; Hill, L.; Richards, C. J.; Thomas, S. E. *ibid.*, **1990**, 1085; Richards, C. J.; Thomas, S. E. *ibid.*, 307.
- (37) Herberhold, M.; Hill, A. F. *J. Organomet. Chem.* **1986**, *309*, C29.
- (38) Götzfried, F.; Beck, W. *J. Organomet. Chem.* **1980**, *191*, 329.
- (39) Gosselink, J. W.; Brouwers, A. M. F.; van Koten, G.; Vrieze, K. *J. Chem. Soc., Dalton Trans.* **1982**, 397.

- (40) Gosselink, J. W.; van Koten, G.; Brouwers, A. M. F.; Overbeek, O. *J. Chem. Soc., Dalton Trans.* **1981**, 342.
- (41) Gosselink, J. W.; Bulthuis, H.; van Koten, G. *J. Chem. Soc., Dalton Trans.* **1981**, 1342.
- (42) Gosselink, J. W.; van Koten, G.; Spek, A. L.; Duisenberg, A. J. M. *Inorg. Chem.* **1981**, 20, 877.
- (43) Gosselink, J. W.; van Koten, G.; Vrieze, K.; Zwanenburg, B.; Lammerink, B. H. M. *J. Organomet. Chem.* **1979**, 179, 411.
- (44) Hill, A. F.; Roper, W. R.; Waters, J. M.; Wright, A. H. *J. Am. Chem. Soc.* **1983**, 105, 5939.
- (45) Alper, H. *J. Organomet. Chem.* **1975**, 34, 347.
- (46) Lorenz, I.-P. 9th International Conference on Organometallic Chemistry, Dijon, 1979.
- (47) Scharbert, B.; Lorenz, I.-P. *Phosphorus Sulfur*, **1987**, 34, 69.
- (48) Hill, A. F. unpublished results.
- (49) Anderson, S.; Hill, A. F.; Howard, J. A. K.; Saunders, N. submitted for publication in *Organometallics*.
- (50) Meij, R.; Stufkens, D. J.; Vrieze, K.; Roosendaal, E.; Schenk, H. *J. Organomet. Chem.* **1977**, 155, 323.
- (51) Blake, D. M.; Reynolds, J. R. *J. Organomet. Chem.* **1976**, 113, 391.
- (52) Herberhold, M.; Hill, A. F. *J. Organomet. Chem.* **1989**, 368, 111.
- (53) Herberhold, M.; Hill, A. F.; Clark, G. R.; Rickard, C. E. F.; Roper, W. R.; Wright, A. H. *Organometallics* **1989**, 8, 2483.
- (54) Herberhold, M.; Hill, A. F. *J. Organomet. Chem.* **1990**, 387, 323.
- (55) Herberhold, M.; Hill, A. F. *J. Organometallic Chem.* **1990**, 395, 195.
- (56) Hill, A. F.; Clark, G. R.; Rickard, C. E. F.; Roper, W. R.; Herberhold, M. *J. Organomet. Chem.* **1991**, 401, 357.
- (57) Ashton, H. C.; Manning, A. R. *Inorg. Chem.* **1983**, 22, 1440.
- (58) Meij, R.; Stufkens, D. J.; Vrieze, K.; van Gerresheim, W.; Stam, C. H. *J. Organomet. Chem.* **1979**, 164, 353.
- (59) Hoffmann, R.; Chem, M. M. L.; Elian, M.; Rossi, A.; Mingos, D. M. P. *Inorg. Chem.* **1974**, 13, 2666.
- (60) Otsuka, S.; Yoshida, T.; Nakamura, A. *Inorg. Chem.* **1968**, 7, 1833.
- (61) Glass, W. K.; McBreen, J. O. *J. Organomet. Chem.* **1980**, 198, 71.
- (62) DeLuca, G.; Panattoni, C.; Toniolo, L. *Chem. Ind. (London)* **1973**, 742.
- (63) LaPlaca, S. J.; Ibers, J. A. *Inorg. Chem.* **1966**, 6, 405; Vaska, L.; Bath, S. S. *J. Am. Chem. Soc.* **1966**, 88, 1333.
- (64) Walter, D.; Pfützenreuter, C. *Z. Chem.* **1977**, 17, 426.
- (65) Meij, R.; Stufkens, D. J.; Vrieze, K.; Roosendaal, E.; Schenk, H. *J. Organomet. Chem.* **1978**, 155, 323.
- (66) Kolomnikov, I. S.; Koreshkov, Y. D.; Lobura, T. S.; Volpin, M. E. *Izv. Akad. Nauk SSSR* **1972**, 1181.
- (67) Perez, M. A.; Kresze, G. *Synthesis* **1981**, 707.
- (68) Herberhold, M.; Hill, A. F. *J. Organomet. Chem.* **1990**, 395, 207.
- (69) Kubas, G. J.; Wasserman, H. J.; Ryan, R. R. *Organometallics* **1985**, 4, 2012.
- (70) Kubas, G. J.; Ryan, R. R. *J. Am. Chem. Soc.* **1985**, 107, 6138.
- (71) Ehrenreich, W. P.; Herberhold, M.; Hill, A. F. *J. Organomet. Chem.* **1989**, 371, 303.
- (72) Severson, R. G.; Wojcicki, A. *J. Organomet. Chem.* **1978**, 149, C66.
- (73) Severson, R. G.; Leung, T. W.; Wojcicki, A. *Inorg. Chem.* **1980**, 19, 915.
- (74) Leung, T. W.; Christoph, G. G.; Gallucci, J.; Wojcicki, A. *Organometallics* **1986**, 5, 366.
- (75) Leung, T. W.; Christoph, G. G.; Wojcicki, A. *Inorg. Chim. Acta* **1983**, 76, L281.

- (76) Hu, Y.-R.; Leung, T. W.; Su, S.-C. H.; Wojcicki, A.; Calligaris, M.; Nardin, G. *Organometallics* **1985**, *4*, 1001.
- (77) Leung, T. W.; Christoff, G. G.; Galluci, J.; Wojcicki, A. *Organometallics* **1986**, *5*, 846.
- (78) Herberhold, M.; Hill, A. F. *J. Organomet. Chem.* **1990**, *395*, 327.
- (79) Herberhold, M.; Hill, A. F. *J. Organomet. Chem.* **1988**, *353*, 243.
- (80) Herberhold, M.; Hill, A. F.; Clark, G. R.; Rickard, C. E. F.; Roper, W. R.; Wright, A. H. *Organometallics* **1989**, *8*, 2483.
- (81) Roper, W. R. *J. Organomet. Chem.* **1986**, *300*, 167.
- (82) Wright, A. H. Ph.D. Thesis, University of Auckland, 1983.
- (83) Herberhold, M.; Hill, A. F. *J. Organomet. Chem.* **1990**, *395*, 315.
- (84) Roper, W. R.; Waters, J. M.; Wright, A. H. *J. Organomet. Chem.* **1984**, *276*, C13.
- (85) Hill, A. F. *J. Mol. Catal.*, **1991**, *65*, 357.
- (86) Herberhold, M.; Hill, A. F. *J. Organomet. Chem.* **1988**, *354*, 227.
- (87) Saito, T.; Motoki, S. *J. Org. Chem.* **1977**, *42*, 3922.
- (88) Gallop, M. A.; Roper, W. R. *Adv. Organomet. Chem.* **1986**, *25*, 121.
- (89) Roper, W. R.; Taylor, G. E.; Waters, J. M.; Wright, L. J. *J. Organomet. Chem.* **1978**, *157*, C27.
- (90) Herberhold, M.; Hill, A. F. *J. Organomet. Chem.* **1986**, *315*, 105.
- (91) Gieren, A.; Ruiz-Perez, C.; Hübner, T.; Herberhold, M.; Hill, A. F. *J. Chem. Soc., Dalton Trans.* **1988**, 1693.
- (92) Baba, A.; Ohshiro, Y.; Agawa, T. *Chem. Lett.* **1976**, *11*; Ohshiro, Y.; Nanimoto, H.; Baba, A.; Topne, T.; Tanaka, H.; Komatsu, M.; Agawa, T. *Heterocycles* **1978**, *9*, 123.
- (93) Drapier, J.; Hubert, A. J.; Teyssie, P. *Synthesis* **1975**, 649.
- (94) LaMonica, G.; Cenini, S. *Inorg. Chim. Acta* **1978**, *29*, 183.
- (95) Cenini, S.; Pizzoli, M. *Inorg. Chim. Acta* **1980**, *42*, 65.
- (96) Collins, N. C.; Glass, W. K. *Spectrochim. Acta, Part A* **1974**, *30A*, 1335.
- (97) Meij, R.; Stufkens, D. J.; Vrieze, K.; Rosendaal, E.; Schenk, H. *J. Organomet. Chem.* **1978**, *115*, 323.
- (98) Meij, R.; Stufkens, D. J.; Vrieze, K.; Bode, J.; Heijdenrijk, Schenk, H. *J. Chem. Soc., Chem. Commun.* **1977**, 739.
- (99) Kuiper, J.; Vrieze, K. *J. Organomet. Chem.* **1985**, *86*, 127.
- (100) Kuiper, J.; van Vliet, P. I.; Vrieze, K. *J. Organomet. Chem.* **1976**, *108*, 257.
- (101) Kuiper, J.; Hubert-Pfalzgraf, L. G.; Keyser, P. C.; Vrieze, K. *J. Organomet. Chem.* **1976**, *108*, 271.
- (102) Meij, R.; Kuiper, J.; Stufkens, D. J.; Vrieze, K. *J. Organomet. Chem.* **1976**, *110*, 219.
- (103) Meij, R.; Kaandorp, T. A. M.; Stufkens, D. J.; Vrieze, K. *J. Organomet. Chem.* **1977**, *128*, 203.
- (104) Meij, R.; Stufkens, D. J.; Vrieze, K. *J. Organomet. Chem.* **1978**, *144*, 239.
- (105) Lindsell, E.; Faulds, G. R. *J. Chem. Soc., Dalton Trans.* **1975**, 40.
- (106) Roesky, H. W.; Schmidt, H.-G.; Noltemeyer, M.; Sheldrick, G. M. *Chem. Ber.* **1983**, *116*, 1411.
- (107) Kuiper, J.; Vrieze, K. *J. Organomet. Chem.* **1974**, *74*, 289.
- (108) Kuiper, J.; Vrieze, K.; Oskam, A. *J. Organomet. Chem.* **1971**, *46*, C25.
- (109) Ehrenreich, W.; Herberhold, M.; Süß-Fink, G.; Klein, H.-P.; Thewalt, U. *J. Organomet. Chem.* **1983**, *248*, 171.
- (110) Ehrenreich, W.; Herberhold, M.; Herrmann, G.; Süß-Fink, G.; Gieren, A.; Hübner, T. *J. Organomet. Chem.* **1985**, *294*, 183.
- (111) Gieren, A.; Hübner, T.; Herberhold, M.; Guldner, K.; Süß-Fink, G. *Z. Anorg. Allg. Chem.* **1986**, *539*, 21.
- (112) Gieren, A.; Betz, H.; Hübner, T.; Lamm, V.; Herberhold, M.; Guldner, K. *Z. Anorg.*

- Allg. Chem.* **1984**, 513, 160; Herberhold, M.; Ehrenreich, W.; Guldner, K. *Chem. Ber.* **1984**, 117, 1999.
- (113) Herberhold, M.; Bühlmeyer, W.; Gieren, A.; Hübner, T.; Wu, J. *J. Organomet. Chem.* **1987**, 321, 51.
- (114) Herberhold, M.; Bühlmeyer, W.; Gieren, A.; Hübner, T. *J. Organomet. Chem.* **1987**, 321, 37.
- (115) Gieren, A.; Hübner, T.; Herberhold, M.; Guldner, K.; Süß-Fink, G. *Z. Anorg. Allg. Chem.* **1987**, 544, 137.
- (116a) Chivers, T.; Dhathathreyan, K. S.; Lensink, C.; Meetsma, A.; van de Grampel, J. C.; de Boer, J. L. *Inorg. Chem.* **1989**, 28, 4150.
- (116b) Chivers, T.; Lensink, C.; Meetsma, A.; van de Grampel, J. C.; de Boer, J. L. *J. Chem. Soc., Chem. Commun.* **1988**, 335.
- (117) Chivers, T.; Lensink, C.; Richardson, J. F. *Organometallics* **1986**, 5, 819.
- (118) Chivers, T.; Lensink, C.; Richardson, J. F. *Organometallics* **1987**, 6, 1904.
- (119) Chivers, T.; Lensink, C.; Richardson, J. F. *Phosphorus Sulfur* **1987**, 30, 189.
- (120) Chivers, T.; Lensink, C.; Richardson, J. F. *J. Organomet. Chem.* **1987**, 325, 169.
- (121) Hübner, T.; Gieren, A. *Kristallogr.* **1986**, 174, 95.
- (122) Wrackmeyer, B.; Schamel, K.; Guldner, K.; Herberhold, M. *Z. Naturforsch., B: Anorg. Chem., Org. Chem.* **1987**, 42B, 703.
- (123) Gieren, A.; Ruiz-Perez, C.; Hübner, T.; Herberhold, M.; Schamel, K.; Guldner, K. *J. Organomet. Chem.* **1989**, 366, 105.
- (124) Herberhold, M.; Schamel, K. *J. Organomet. Chem.* **1988**, 346, 13.
- (125) Herberhold, M.; Schamel, K. *Z. Naturforsch., B: Anorg. Chem., Org. Chem.* **1988**, 43B, 1274.
- (126) Herberhold, M.; Schamel, K.; Gieren, A.; Hübner, T. *Phosphorus, Sulfur Silicon Relat. Elem.* **1989**, 41, 355.
- (127) Herberhold, M.; Bühlmeyer, W. *Angew. Chem., Int. Ed. Engl.* **1984**, 23, 80.
- (128) Herberhold, M.; Bühlmeyer, W.; Gieren, A.; Hübner, T.; Wu, J. *Z. Naturforsch., B: Anorg. Chem., Org. Chem.* **1987**, 42B, 65.
- (129) Gieren, A.; Hübner, T.; Wu, J.; Herberhold, M.; Bühlmeyer, W. *J. Organomet. Chem.* **1987**, 329, 105.
- (130) Süß-Fink, G.; Thewalt, U.; Klein, H.-P. *J. Organomet. Chem.* **1982**, 224, 59.
- (131) Otsuka, S.; Yoshida, T.; Nakamura, A. *Inorg. Chem.* **1968**, 7, 1833.
- (132) Meij, R.; Stufkens, D. J.; Schagen, J. D.; Zwinselman, J. J.; Overbeek, A. R.; Stam, C. H. *J. Organomet. Chem.* **1979**, 170, 337.
- (133) Gall, R. S.; Chu, C. T.-W.; Dahl, L. F. *J. Am. Chem. Soc.* **1974**, 96, 4019.
- (134) Chu, C. T.-W.; Gall, R. S.; Dahl, L. F. *J. Am. Chem. Soc.* **1982**, 104, 737.
- (135) Dahl, L. F.; Douglas-Frisch, P.; Gust, R. R. *J. Less-Common Met.* **1974**, 36, 255.
- (136) Gall, R. S.; Connelly, N. G.; Dahl, L. F. *J. Am. Chem. Soc.* **1974**, 96, 4017.
- (137) Otsuka, S.; Nakamura, A.; Yoshida, T. *Justus Liebigs Ann. Chem.* **1968**, 719, 54.
- (138) Matsu-ura, Y.; Yasuoka, N.; Ueki, T.; Kasai, N.; Kakudo, M.; Yoshida, T.; Otsuka, S. *J. Chem. Soc., Chem. Commun.* **1967**, 1122.
- (139) Otsuka, S.; Nakamura, N.; Yoshida, T. *Inorg. Chem.* **1968**, 7, 261.
- (140) Meij, R.; van der Helm, J.; Stufkens, D. J.; Vrieze, K. *J. Chem. Soc., Chem. Commun.* **1978**, 506.
- (141) Herberhold, M.; Ehrenreich, W.; Guldner, K.; Jellen, W.; Thewalt, U.; Klein, H.-P. *Z. Naturforsch., B: Anorg. Chem., Org. Chem.* **1983**, 38B, 1383.
- (142) Herberhold, M.; Jellen, W.; Bühlmeyer, W.; Ehrenreich, W. *Z. Naturforsch., B: Anorg. Chem., Org. Chem.* **1985**, 40B, 1233.
- (143) Herberhold, M.; Hill, A. F. *J. Organomet. Chem.* **1989**, 377, 151.
- (144) Alcock, N. W.; Hill, A. F.; Roe, M. S. *J. Chem. Soc., Dalton Trans.* **1990**, 1737.

- (145) Harris, M. C. J.; Hill, A. F. *Organometallics* **1991**, *10*, 3903.
- (146) Harris, M. C. J.; Hill, A. F. *J. Organomet. Chem.* **1992**, *438*, 209.
- (147) Hill, A. F.; Slawin, A. M. Z.; Williams, D. J. submitted for publication in *J. Chem. Soc., Chem. Commun.*
- (148) Hill, A. F.; Slawin, A. M. Z.; Thompson, A. R.; Williams, D. J. submitted for publication in *J. Chem. Soc., Chem. Commun.*
- (149) A. R. Thompson, Ph.D. Thesis, University of Warwick, 1993.
- (150) Walker, N. C. P.; Hursthouse, M. B.; Warrens, C. P.; Woollins, J. D. *J. Chem. Soc., Chem. Commun.* **1985**, 227.
- (151) Herberhold, M.; Neumann, F.; Süss-Fink, G.; Thewalt, U. *Inorg. Chem.* **1987**, *26*, 3612.
- (152) Short, R.; Hursthouse, M. B.; Purall, T. G.; Woollins, J. D. *J. Chem. Soc., Chem. Commun.* **1987**, 407; Parkin, I. P.; Slawin, A. M. Z.; Williams, D. J.; Woollins, J. D. *Polyhedron* **1989**, *8*, 835; Parkin, I. P.; Woollins, J. D. *J. Chem. Soc., Dalton Trans.* **1990**, 519; Parkin, I. P.; Slawin, A. M. Z.; Williams, D. J.; Woollins, J. D. *J. Chem. Soc., Chem. Commun.* **1989**, 1060.
- (153) Plenio, H.; Roesky, H. W.; Noltemeyer, M.; Sheldrick, G. M. *J. Chem. Soc., Chem. Commun.* **1987**, 1483; Plenio, H.; Roesky, H. W.; Edelman, F. T.; Noltemeyer, M. *J. Chem. Soc., Dalton Trans.* **1989**, 1815.
- (154) Chivers, T.; Dhathathreyan, K. S.; Lensink, L.; Richardson, J. F. *Inorg. Chem.* **1988**, *27*, 1570.
- (155) Roesky, H. W.; Pandey, K. K.; Dartmann, M.; Krebs, S. *J. Chem. Soc., Dalton Trans.* **1984**, 2271.
- (156) Pandey, K. K.; Agarwala, U. C. *Inorg. Chem.* **1981**, *20*, 1309.
- (157) Pandey, K. K.; Datta, S.; Agarwala, U. C. *Z. Anorg. Allg. Chem.* **1980**, *468*, 228; Pandey, K. K.; Agarwala, U. C.; Jain, K. C. *Inorg. Chim. Acta* **1981**, *48*, 23; Pandey, K. K.; Agarwala, U. C. *Indian J. Chem. Sect. A* **1981**, *20A*, 74; Pandey, K. K.; Agarwala, U. C. *ibid.* *21A*, 76; Pandey, K. K. *ibid.* *20A*, 906; Roesky, H. W.; Pandey, K. K. *Prog. Inorg. Chem.* **1983**, *26*, 337.
- (158) Hursthouse, M. B.; Walker, N. P. C.; Warrens, C. P.; Woollins, J. D. *J. Chem. Soc., Dalton Trans.* **1985**, 1043.
- (159) Süss-Fink, G.; Guldner, K.; Herberhold, M.; Gieren, A.; Hübner, T. *J. Organomet. Chem.* **1985**, 279, 447.
- (160) Kelly, P. F.; Woollins, J. D. *Polyhedron* **1986**, *5*, 607; Kelly, P. F.; Woollins, J. D.; Slawin, A. M. Z.; Williams, D. J. *Chem. Soc. Rev.* **1992**, 215, and references therein.
- (161) Herberhold, M.; Ehrenreich, W. *Angew. Chem., Int. Ed. Engl.* **1982**, *21*, 633.
- (162) Herberhold, M.; Ehrenreich, W.; Buhlmeier, W. *Angew. Chem., Int. Ed. Engl.* **1983**, *22*, 315.
- (163) Ehrenreich, W. Doktorarbeit, Universität Bayreuth, 1983.

Silaorganometallic Chemistry on the Basis of Multiple Bonding

CHRISTIAN ZYBILL, HERMANN HANDWERKER, AND
HOLGER FRIEDRICH

*Anorganisch-Chemisches Institut
Technische Universität München
D-85747 Garching
Germany*

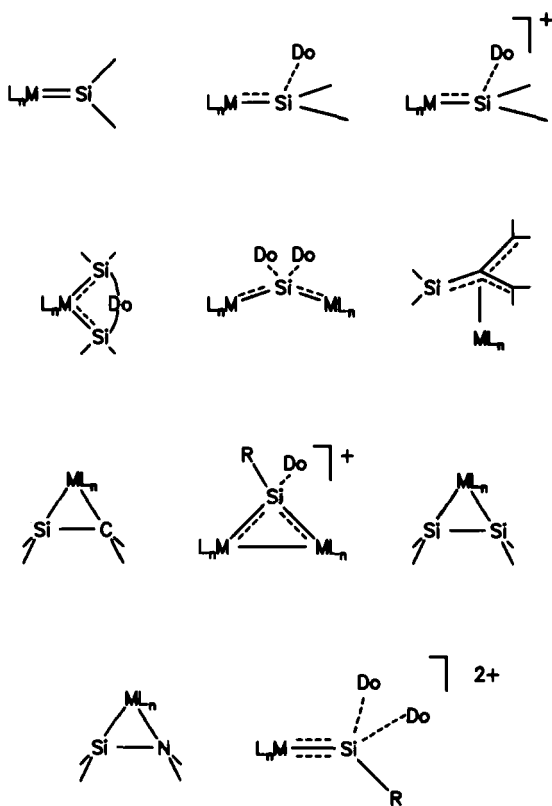
I.	Introduction	229
A.	Silylenes in the Direct Synthesis	231
B.	The Role of Silylenes in the Hydrosilation Reaction	231
C.	Dehydrogenative Coupling of Silanes	232
II.	Silylene Complexes	232
A.	Synthesis of Silylene Complexes	232
B.	Si-Si Bond Formation with Transition Metal Catalysts: Dehydrogenative Coupling Reactions	237
C.	Base Adducts of Silylene Complexes	242
D.	Reactivity of Silylene Complexes	248
E.	Intramolecular Base Stabilization in Silylene Complexes	251
F.	A Salt Adduct of the Metal-Silicon Double Bond	265
G.	Base-Free Silylene Complexes	267
III.	Silane-Induced CO-Activation Reaction	269
IV.	Cyclic Silylene Complexes	272
V.	Donor-Stabilized Silylyne Complexes	272
VI.	Silaethene Complexes	274
VII.	Silamine Complexes	275
VIII.	Disilaethene Complexes	275
IX.	Silatrimethylenemethane Complexes	276
X.	Metallasilaallenes	276
XI.	Prospects	277
	References.	278

I

INTRODUCTION

Major advances in organometallic chemistry during the past 5 years have been achieved in the area of silaorganometallic chemistry, based on silicon to metal multiple bonding and silicon with low coordination numbers (1,2). The hunt for new molecules has been carried out jointly by several research groups and has led to the discovery of fundamentally new classes of compounds, such as silylene (silanediyl) complexes

(3*a*–3*j*, 4*a*–4*c*), cationic (5*a*, 5*b*, 6) and cyclic silylene complexes (7*a*–7*f*), coordination compounds of silaethenes (8*a*–8*d*), silaimines (9), disilaethenes (10*a*–10*d*), and silatrimethylenemethane (11), as well as cationic cyclic (12) and terminal silylyne (silacarbyne) (13) complexes. These activities also included the discovery of base-stabilized metalla-2-silaallene systems (14) in which the silicon atom can be considered as zero valent. All these systems had been unknown up to their discovery and have only occasionally been postulated as reactive intermediates (Scheme 1).



The existence of such a diverse silaorganometallic chemistry is most surprising and sets stimulating new impulses for various areas of organometallic chemistry. It is now clear that coordination compounds of subvalent silicon ligands play a key role in many reactions and have important applications in industrial processes. This applies, for instance, to the hydrosilation reaction (15*a*, 15*b*), to the dehydrogenative coupling reaction of silanes to polysilanes (16), and to many metal complex catalyzed silylene

transfer reactions (17). However, coordination compounds of silylenes are also most important in heterogeneous systems and in reactions on surfaces. Coordinated silylenes are probable intermediates in the direct synthesis of Me_2SiCl_2 from MeCl and CuSi_2 (18). Furthermore, coordinated silylenes $\text{M}=\text{SiH}_2^+$ have been investigated in the gas phase by molecular beam experiments (19) and have been observed as intermediates in chemical vapor deposition reactions of silicides from volatile precursors (20). Some of these aspects are discussed in more detail in the forthcoming sections.

The exploration of silaorganometallic chemistry is still in a rudimentary state and only the first basic discoveries have been made. However, "spin-off" results of this research are already extremely interesting and include areas like asymmetric synthesis with silaorganometallic compounds for the introduction of chiral silicon atoms in pharmaceutically active compounds (21), as well as applications in materials science and semiconductor technology (22). Silaorganometallic chemistry forms an important link between organic and inorganic chemistry, and the exploration of this highly interdisciplinary field is a necessary and fascinating challenge for the future. The main development phase of the classical coordination chemistry of carbon has already passed; however, the organometallic chemistry of silicon will be a major theme in the future of organometallic chemistry!

A. Silylenes in the Direct Synthesis

The role of silylenes in the direct synthesis of methylchlorosilanes has been investigated by Clarke (18). Two types of silylene intermediates are believed to be involved.

Silylenes are physisorbed on the catalyst surface, where they react with methyl chloride yielding methylchlorosilanes (SiMeCl gives Me_2SiCl_2 ; SiCl_2 gives MeSiCl_3) in accordance with the van den Berg mechanism. Furthermore, free silylenes are released into the gas phase and can be trapped with butadiene, but these are not directly involved in methylchlorosilane production. The addition of Me_3SiH to the methyl chloride promotes radical reactions; the major product is Me_3SiCl . Me_3SiCl is believed to result from an efficient chain sequence proceeding mainly on the surface involving $\text{Me}_3\text{Si}\cdot$ radicals that scavenge surface-bound chlorine.

B. The Role of Silylenes in the Hydrosilation Process

A variety of late transition metal catalysts, which are active in hydrosilation reactions, also catalyze Si-Si bond formation of the silane component

ir. the absence of olefin. K. Brown-Wensley has shown that such reactions proceed through highly reactive silylene complex intermediates (15a). This mechanism has been confirmed recently by M. Tanaka and his research group (23).

C. Dehydrogenative Coupling of Silanes

The dehydrogenative coupling of silanes with Pt complexes such as the Speier catalyst proceeds through silylene complex intermediates. Furthermore, base adducts of related Fe- (for instance $(\text{Ph}(9\text{-Me}_2\text{NCH}_2\text{-naph})\text{Si}=\text{Fe}(\text{CO})_4)$), Cr- ($\text{Me}_2(\text{HMPA})\text{Si}=\text{Cr}(\text{CO})_5$), or dimeric Pt-silylene complexes (e.g., $[(\text{Et}_3\text{P})_2\text{PtSiHPh}]_2$) catalyze the dehydrocoupling and polymerization reaction of silanes. This observation can be considered as direct evidence for the catalytic activity of silylene complex intermediates. Evidence for the involvement of silylene complexes has also been obtained for early transition metal catalysts based on titanocene. For a detailed discussion refer to Section II,B.

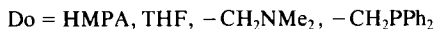
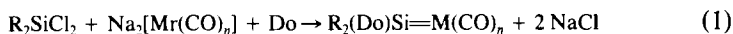
II

SILYLENE COMPLEXES

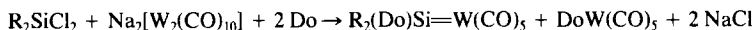
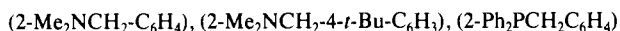
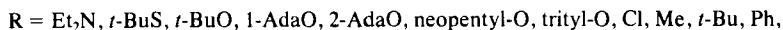
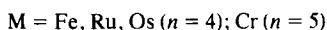
A. Synthesis of Silylene Complexes

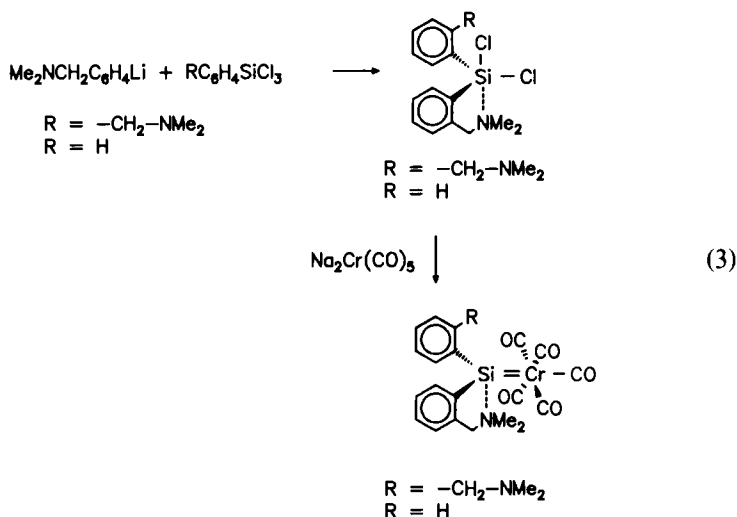
1. Salt Elimination: A One-Step Procedure

The formation of metal-silicon double bonds is most effectively accomplished in a one-step procedure by reaction of metallate dianions with dihalosilanes. This method has proven to be most effective and is widely used in many applications:



(HMPA is hexamethylphosphorotriamide, THF is tetrahydrofuran)

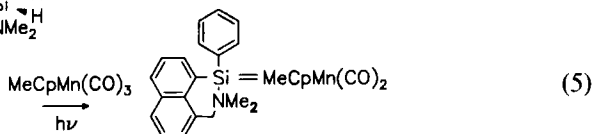
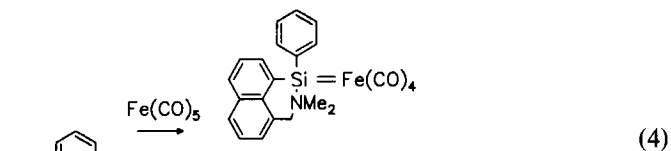




A variation of this method is the *in situ* generation of the metallate from a precursor by deprotonation (4b).

2. Insertion of Reactive $16e^-$ Metal Complexes into a Si-H Bond with H_2 Elimination

Insertion reactions of $16e^-$ metal species into a Si-H bond have been investigated extensively (24). The H_2 elimination step from the silyl metal hydride intermediate formed has been realized only recently (25):

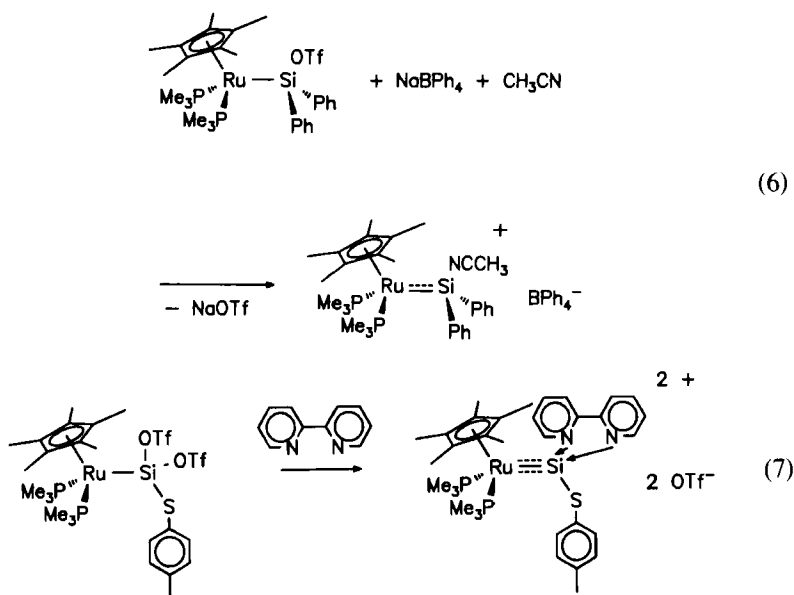


A MO calculation for the system $\text{Cp}_2\text{TiHSiH}_3 \rightarrow \text{Cp}_2\text{Ti}=\text{SiH}_2 + \text{H}_2$ gives a slightly endothermic value for the enthalpy of formation of the silylene complex of $\sim 14 \text{ kcal mol}^{-1}$. In contrast, the coordination of a base to the three-coordinated silicon atom is exothermic and yields an

additional 16 kcal mol⁻¹ (for Me₂NR), which makes the formation of a base-stabilized silylene complex by this route a thermodynamically favored process (26). Further elimination reactions from related starting materials (HCl, etc.) have not been successful.

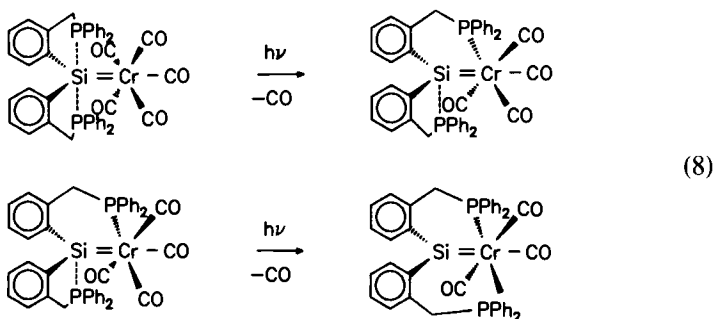
3. Substituent Displacement at Silicon: A Route to Cationic Complexes

The displacement of an anionic leaving group from silicon by a solvent molecule leads to cationic, solvent-stabilized silylene complexes. Triflates and iodides in particular have been used for the generation of both cationic silylene and silylyne complexes (5*a*,5*b*,13):



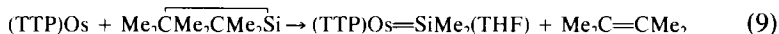
4. Base Abstraction from a Base-Stabilized Silylene Complex

The abstraction of the base from the silicon atom of a base-stabilized silylene complex seems to offer a most straightforward access to silylene complexes. This approach has, indeed, succeeded recently and involves 1,2-shifts of phosphine or amine donor groups from silicon to the metal atom. The 1,2-shift of the donor is induced by the photochemical generation of a vacant coordination site at the metal through a photolytic CO cleavage reaction. A rough estimate of the bond energies involved shows that 1,2-shift reactions are thermodynamically favored (see Section II,E, 8) (3*i*):



5. Trapping of Silylenes with Metal Complexes

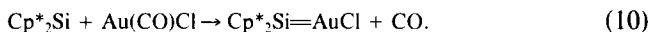
Trapping reactions of reactive silylene intermediates with appropriate metal complexes in solution have so far only rarely succeeded, since the silylenes may undergo side reactions of dimerization or polymerization. One remarkable case has been reported recently by Woo and coworkers and involves reaction of hexamethylsilirane, which was originally introduced by Seyferth, with tetratolylporphyrin (see Fig. 1) (27):



(TTP) is tetratolylporphyrin).

6. Coordination of Stable Silylenes to a Metal

The coordination of stable R_2M ($\text{M} = \text{Ge}, \text{Sn}$) species to transition metals is a common route for the synthesis of subvalent coordination compounds of tin, germanium, and lead. Stable silicon(II) compounds have only recently become available with decamethylsilicocene prepared by P. Jutzi (28) and (tri-*t*-butyl)cyclopropenyliisetyl silanediyl (isetyl = 2,6-diisopropylphenyl) by Fink (29), which opened up a new route to silylene complexes. Jutzi and Möhrke (30) also were the first to report a stable, red complex of decamethylsilicocene with gold chloride, $\text{Cp}^*_2\text{Si}=\text{AuCl}$ (^{29}Si NMR, 82.8 ppm):



This complex has not been characterized by a single crystal X-ray structure analysis, but the spectroscopic data indicate a π interaction between silicon and one cyclopentadienyl ring.

7. Cleavage of Dimeric Silylene Complexes

Cleavage reactions of dimeric complexes to form base-stabilized monomeric compounds are common in the chemistry of related Sn and Ge

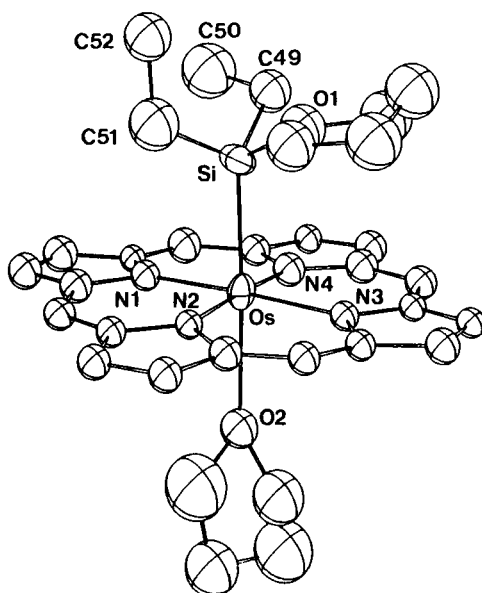
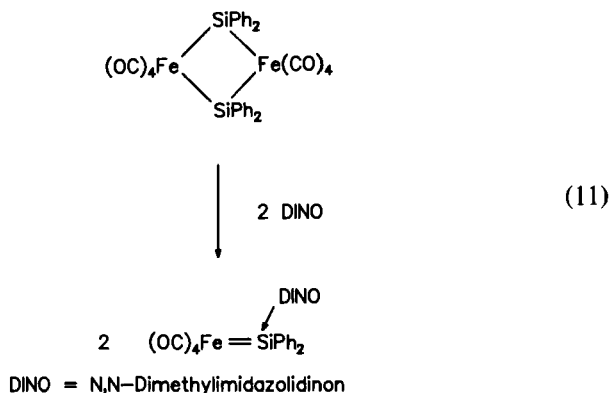


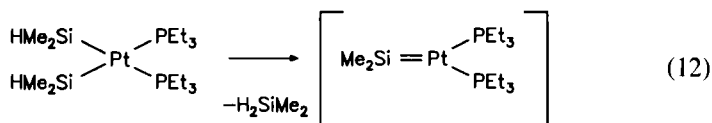
FIG. 1. ORTEP view of $(\text{TTP})\text{Os}=\text{SiEt}_2 \times 2 \text{ THF}$ (TTP is tetratolylporphyrin). Important bond distances in angstrom: Os-Si 2.40(2), Si-O1 1.853(5). Sum of bond angles at Si 348°. Reprinted with permission from Woo *et al.* (27). Copyright (1993) American Chemical Society.

complexes, but have been introduced into the chemistry of silylenes only recently. Liu *et al.* (31) obtained base adducts of silylene complexes by a cleavage reaction of a dimeric compound with THF, HMPA, and CH_3CN . A related reaction has been introduced recently by Corriu *et al.* (32), who reacted $[(\text{CO})_4\text{Fe}(\text{SiPh}_2)]_2$ with *N,N*-dimethylimidazolidinon (DINO) to give the DINO complex $\text{DINO} \rightarrow \text{Ph}_2\text{Si}=\text{Fe}(\text{CO})_4$:



8. Silane Elimination

A thermal (60°C) dimethylsilane elimination from a *cis*-dimethylsilylplatinum(II) complex gives a highly reactive silylene complex, which was trapped with phenylacetylene (23):



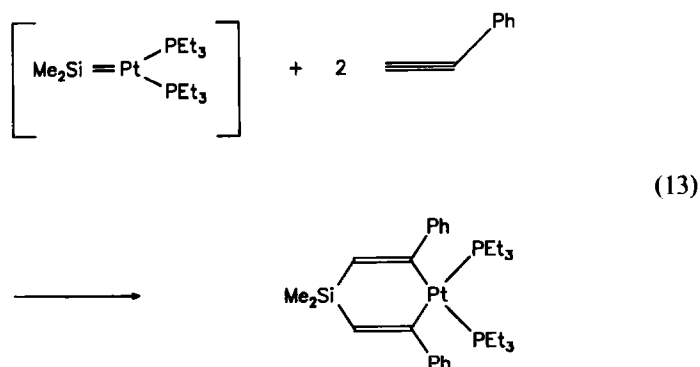
B. Si–Si Bond Formation with Transition Metal Catalysts: Dehydrogenative Coupling Reactions

The formation of Si–Si bonds by a metal complex catalyzed coupling reaction of silanes can be accomplished with a variety of transition metal catalysts. Compounds of late transition metals commonly yield disilanes or oligomeric chain silanes of relatively short chain length. The dehydrogenative coupling (in most cases) of phenylsilane with either titanocene or zirconocene-related catalysts and also lanthanide complexes gives polymeric materials with molecular weights of up to 8000 AME (33).

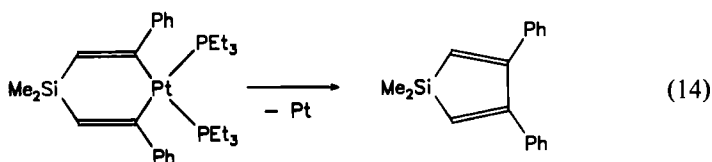
It is not completely clear whether all Si–Si coupling reactions known so far proceed by the same mechanism. Therefore, these reactions are now distinguished between those using late and those using early transition metal catalysts, with only the latter yielding highly polymeric silanes.

1. Late Transition Metals (d^n)

The dehydrogenative coupling reaction of silanes has been investigated for a variety of metal complexes, particularly with compounds that catalyze hydrosilation or hydrogenation reactions. It has been proven that the hydrosilation reaction with Speier catalysts gives Si–Si bond formation products in the absence of olefines. K. Brown-Wensley has clarified that this reaction proceeds through highly reactive silylene complex intermediates (15a). Recent investigations by Tanaka and co-workers (23) have unambiguously proven this mechanism. Thermolysis of *cis*-(Et_3P)₂Pt(SiMe_2H)₂ at 60°C gives the reactive intermediate [$(\text{Et}_3\text{P})_2\text{Pt}=\text{SiMe}_2$], with loss of Me_2SiMe_2 , as the main product, which has been trapped with phenylacetylene to give the platinasilacyclohexadiene complex $(\text{Et}_3\text{P})_2\text{PtPhC}\equiv\text{CSiMe}_2\text{CH}=\text{CPh}$. The latter has been characterized by a single-crystal X-ray structure determination:



The six-membered ring exists in a boat conformation with a nearly square planar coordination geometry at the platinum atom. Heating of the complex at 60°C affords the silacyclopentadiene $\text{Me}_2\text{SiCH}=\text{CPhCPh}=\text{CH}$ as the sole volatile product:

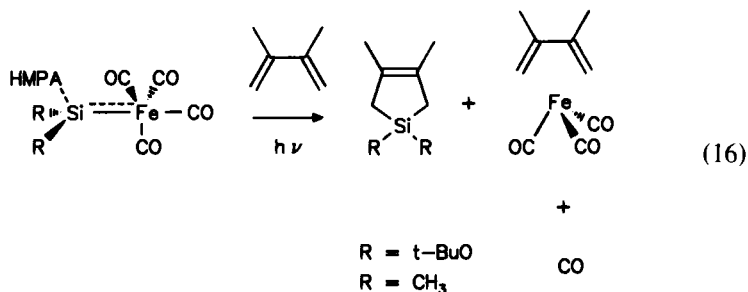
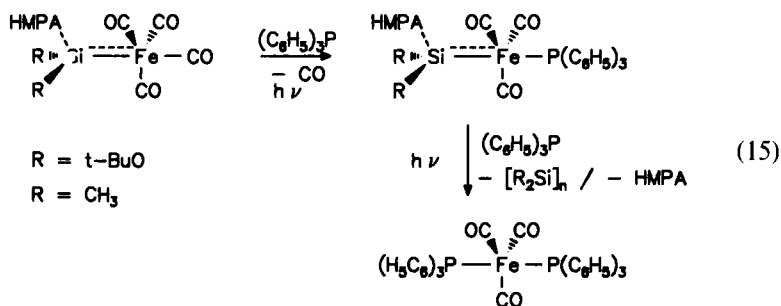


It has been shown furthermore that *cis*-(Et_3P)₂Pt(SiMe_2H)₂ catalyzes the dehydrogenative coupling reaction of $\text{HMe}_2\text{SiSiMe}_2\text{H}$, as well as the redistribution reaction of the disilane to give various linear silanes with a chain length of up to seven silicon atoms. This reaction sequence involves successive steps of dehydrogenative coupling reactions, from the oxidative addition of $\text{HMe}_2\text{SiSiMe}_2\text{H}$ to (Et_3P)₃Pt to form *cis*-(HMe_2Si)₂Pt(PEt_3)₂ up to the products of Si–Si bond formation, and is an example for a reaction of a coordinated silylene in the coordination sphere of a metal (23).

Recent results from Corriu provide similar evidence for the involvement of iron silylene complexes in the formation of polysilanes. The *N,N*-dimethylimidazolidinone adduct of phenylsilylene iron tetracarbonyl was formed by a photolytic reaction of $\text{Fe}(\text{CO})_5$ with PhSiH_3 in the presence of DINO. This complex catalyzes the dehydrogenative coupling reaction of phenylsilane to oligomeric polysilane and can therefore be used to bring about dehydrogenative coupling reactions of PhSiH_3 with $\text{Fe}(\text{CO})_5$ under conditions of photolytic induction. The diphenylsilanediyliro tetracarbonyl derivative $\text{Ph}_2(\text{DINO})\text{Si}=\text{Fe}(\text{CO})_4$ has a similar catalytic activity. In both cases, the silylenes have been eliminated from the metal complex

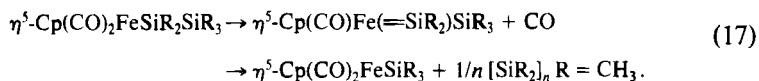
and derivatized with diethylacetylene, 2,3-dimethylbutadiene, methanol, or *t*-butanol. Furthermore, the complex $\text{Ph}_2(\text{DINO})\text{Si}=\text{Fe}(\text{CO})_4$ could be obtained by cleavage of the dimeric silylene complex $[(\text{CO})_4\text{Fe}(\text{Ph}_2\text{Si})_2]$ (32). This observation is in agreement with earlier reports of Tessier-Youngs (34), who noted the catalytic activity of the dimeric silanediyl complex $[(\text{Et}_3\text{P})_2\text{Pt}(\text{SiPhH})_2]$ in dehydrogenative coupling reactions of phenylsilane. At present, it seems likely that the dimeric complex is a stable precursor for the catalytically active monomeric compound.

It should be mentioned furthermore that the photochemical and base-induced cleavage of HMPA adducts of silylene complexes of Fe and Cr has also been demonstrated including the isolation of oligosilanes and trapping reactions of intermediate silylenes with 2,3-dimethylbutadiene (3d,3g):



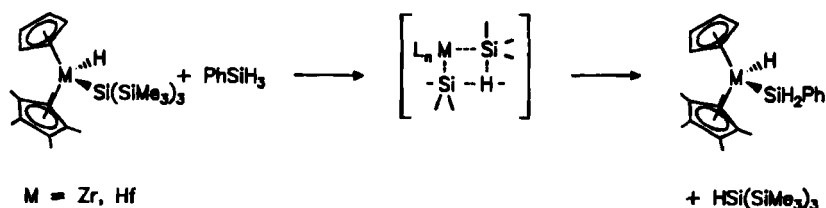
A further interesting example is given in a reaction described by Pannell. Photolysis of disilylmetal complexes leads to a silyl metal complex with a side chain shortened by one silicon unit. A Si-I unit is expelled from the complex as silylene and undergoes a polymerization reaction to polysilane in solution. A cyclic silylene complex has been isolated as an intermediate of this reaction by introduction of an intramolecular OMe-donor

function (35):



2. Early Transition Metals (d^0)

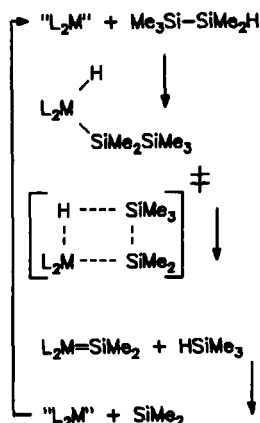
a. σ -Bond metathesis mechanism The mechanism of the dehydrogenative coupling reaction of phenylsilane with early transition metal catalysts is still controversial. Tilley and Marks have gathered a considerable amount of evidence for a σ -bond metathesis (36). This mechanism is based on two σ -bond metathesis steps that pass through four-center transition states: (1) the dehydrometallation of silane, $\text{H}(\text{SiHR})_n\text{H}$, with a metal hydride to give hydrogen and a silyl derivative, $\text{M}(\text{SiHR})_n\text{H}$, and (2) coupling of the metal silyl derivative with more hydrosilane, $\text{H}(\text{SiHR})_m\text{H}$, to produce $\text{H}(\text{SiHR})_n(\text{SiHR})_m\text{H}$ and regenerate the active metal hydride catalyst. This mechanism is based on stoichiometric σ -bond metathesis reactions involving d^0 zirconocene and hafnocene complexes. A similar reaction, which has been identified as σ -bond metathesis, is the rapid MH/SiH hydrogen exchange, for example between PhSiH_3 and CpCp^*MHCl ($\text{M} = \text{Zr}, \text{Hf}$), which was verified by deuterium labeling experiments (Scheme 2).



The thermal decomposition reaction of $\text{CpCp}^*\text{Hf}(\text{SiH}_2\text{Ph})\text{Cl}$ yields oligosilanes and $\text{CpCp}^*\text{HfHCl}$ according to second-order reaction kinetics with activation parameters of $\Delta H^\ddagger = 19.5 \pm (2) \text{ kcal mol}^{-1}$ and $\Delta S^\ddagger = -21 \pm (6) \text{ eu}$, which, furthermore, supports the proposed four-center transition state. The product distribution (chain growth process and inter-conversion of cyclic and chain oligosilanes) has been studied by gel permeation chromatography.

b. Silylene mechanism It must be pointed out, however, that recent investigations by Hengge and co-workers on the dehydrogenative coupling reaction of disilanes give evidence for a silylene complex mechanism

(16,37). The dehydrogenative coupling of 1,2,3-trimethylsilane and 1,2,3,4-tetramethyltetrasilane with Cp_2TiMe_2 was stopped after 30 sec of the polymerization reaction and yielded oligomeric chain silanes with up to 11 silicon atoms, with a large amount of branched oligomers. Kinetic investigations show that a small amount of trisilane and tetrasilane is coupled in one step without Si-Si bond cleavage to give linear hexasilane and octasilane. However, the percentage yield of a mixture of constitutional isomers of isosilanes (isohexasilane/linear hexasilane 92/8) is very high. Branched products are the result of Si-Si bond cleavage reactions and are not believed to be formed by a σ -bond metathesis reaction but by a β^* elimination from a metalsilylhydride and subsequent addition of a further monomeric silane unit to the silylene (silylene transfer). σ -bond metathesis has only been observed for "primary" silanes RSiH_3 due to steric congestion of the transition state. It has been shown by analysis of the product distribution that only this reaction sequence leads directly to highly polymeric materials within seconds. Besides the silylene reaction pathway, products of σ -bond metathesis have also been found in low yields as well as traces of cyclic silanes (cyclohexasilane). The key step of the silylene mechanism involves β^* elimination from a metal silyl hydride through a four-center transition state. It should be pointed out that σ -bond metathesis and β^* -elimination reactions should have similar activation parameters (ΔS^\ddagger) (Scheme 3).



A HFS-LCAO calculation by Harrod and Tschinke of $\text{Cp}_2\text{Ti}=\text{SiH}_2$ shows an activation barrier of ca. 60 kJ mol^{-1} for the hydrogen elimination from the hydride with a reaction enthalpy of ca. 40 kJ mol^{-1} . However, the subsequent addition of silane to the $\text{Ti}=\text{Si}$ bond is exothermic by

48 kJ mol⁻¹ with an activation barrier of ~12 kJ mol⁻¹. Taking the thermodynamic stability of the polymer into account, a silylene complex route may at least be viable (26).

C. Base Adducts of Silylene Complexes

1. Structural Aspects of Base-Stabilized Silylene Complexes

Most of the silylene complexes described so far feature a four-coordinated silicon atom due to the coordination of a solvent molecule to the silicon atom (4b). The dative bond between the solvent molecule and the silicon atom is formed by interaction of an electron pair of the donor with the LUMO of the M=Si double bond. The degree of interaction is a function of the orbital energy and coefficient of the LUMO. According to the electronic saturation of the silicon atom, different degrees of adduct formation between the silicon and the base are observed. The interplay of various electronic and steric effects is reflected in the metal–silicon and donor–silicon bond lengths and in the coordination geometry at the silicon atom. Particularly the sum of bond angles of the three covalently bonded substituents is a sensitive probe for the degree of adduct formation and varies between 352° (weak coordination) and 333° (covalent bond L–Si) (Fig. 2).

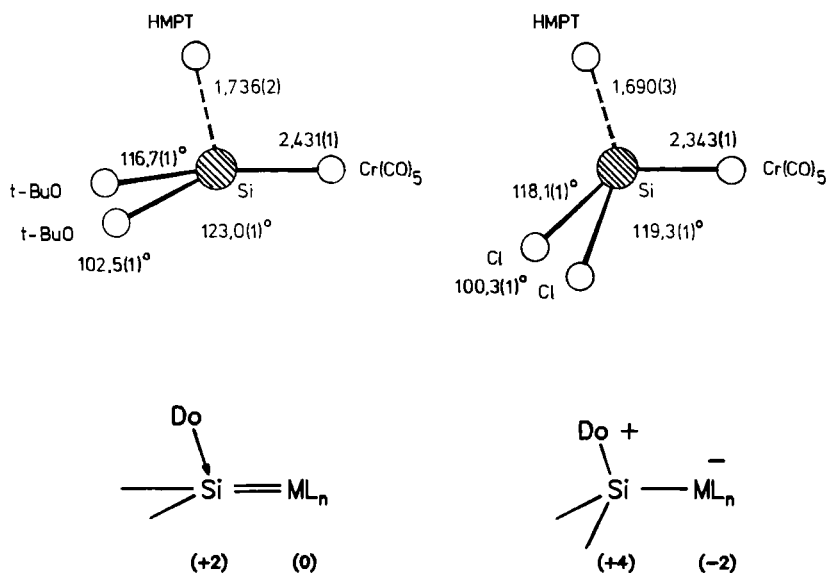


FIG. 2. Coordination geometry at silicon by incorporation of a base.

The adduct formation can be considered a general feature of polar $E=E'$ multiple bonds and as a particular characteristic of silicon chemistry. Similar solvent adducts are known from silaethenes and silaimines (2).

The structural parameters of a variety of HMPA adducts of silylene complexes are summarized in Table I. The metal-silicon bond lengths vary from 2.214 (1) angstrom to 2.572 (1) Å depending on the metal and the electronic influence of the substituents. A higher electron deficiency at silicon induces shorter metal-silicon and donor-silicon bond distances and vice versa. For a given metal and donor, the metal-silicon bond lengths can be correlated linearly with the net atomic charge at Si calculated for the free silylenes.

The following gradation for the stabilizing effect of α substituents on the silicon atom has been deduced for HMPA adducts of Fe and Cr complexes:



The N- and O-substituted complexes experience substantial stabilization

TABLE I
SELECTED STRUCTURAL PARAMETERS OF SILANEDIYL-COORDINATION
COMPOUNDS (BOND DISTANCES IN Å, BOND ANGLES IN °)

Compound	M—Si	Do—Si	P=O	Σ^a
(CO) ₄ FeSi (HMPA) (NEt ₂) ₂ 1	2.313 (1)	1.734 (1)	1.549 (2)	343.1
(CO) ₄ FeSi (HMPA) (<i>t</i> -BuO) ₂ 2	2.289 (2)	1.730 (3)	1.524 (3)	342.1
(CO) ₄ FeSi (HMPA) (<i>t</i> -BuS) ₂ 3	2.278 (1)	1.734 (2)	1.542 (2)	342.6
(CO) ₄ FeSi (HMPA)Me ₂ 4	2.280 (1)	1.735 (3)	1.528 (3)	339.0
	2.294 (1)	1.731 (3)	1.520 (3)	339.8
(CO) ₄ FeSi (HMPA)Cl ₂ 5	2.214 (1)	1.683 (3)	1.552 (3)	336.3
	2.221 (1)	1.676 (3)	1.548 (3)	337.7
(CO) ₄ RuSi (HMPA) (<i>t</i> -BuO) ₂ 6	2.414 (1)	1.731 (2)	1.525 (3)	342.1
(CO) ₅ CrSi (HMPA) (<i>t</i> -Bu) ₂ 7	2.527 (1)	1.777 (1)	1.500 (1)	340.7
(CO) ₅ CrSi (HMPA) (<i>t</i> -BuO) ₂ 8	2.431 (1)	1.736 (2)	1.527 (2)	342.2
(CO) ₅ CrSi (HMPA)Me ₂ 9	2.410 (1)	1.743 (2)	1.521 (2)	339.5
(CO) ₅ CrSi (HMPA) Cl ₂ 10	2.342 (1)	1.690 (2)	1.543 (2)	337.6
(CO) ₅ CrSi(2-Me ₂ NCH ₂ -C ₆ H ₄)C ₆ H ₅ 11	2.409 (2)	1.991 (2)	—	347.8
(CO) ₅ CrSi(2-Me ₂ NCH ₂ -C ₆ H ₄) ₂ 12	2.408 (1)	2.046 (2)	—	351.3
(CO) ₄ CrSi(2-Me ₂ NCH ₂ -C ₆ H ₅)(2-Me ₂ NCH ₂ -C ₆ H ₅) 13	2.3610 (4)	1.981 (1)	—	342.9
(CO) ₅ CrSi(2-Ph ₃ PCH ₂ C ₆ H ₄) ₂ 14	2.413 (1)	2.380 (1)	—	352.1
(CO) ₅ CrSi (<i>t</i> -Bu) ₂ × NaOTf 15	2.475 (1)	1.857 (3)	—	349.5
(CO) ₄ FeSi (HMPA) ₂ Fe(CO) ₄ 16	2.339 (1)	1.745 (2)	1.530 (2)	—
	2.341 (1)	1.748 (3)	1.526 (3)	—

^a Sum of the three bond angles at silicon without the donor as a measure for the planarization effect.

by the heteroatom; for CH_3 -substituted complexes a high hyperconjugative effect has been observed. The dimethylamino-substituted silylene complex $(\text{Et}_2\text{N})_2(\text{HMPA})\text{Si}=\text{Fe}(\text{CO})_4$ **1** eliminates HMPA in the gas phase forming the base-free complex $(\text{Et}_2\text{N})_2\text{Si}=\text{Fe}(\text{CO})_4$ (Fig. 3).

With the exception of extremely sterically hindered compounds, steric effects do not affect the coordination geometry at the silicon atom significantly and play a role only in the periphery of the molecule, influencing the conformation of the substituents at the silicon atom. In a variety of complexes, the substituents at silicon are always oriented in the crystalline phase in such a way as to minimize repulsive intramolecular interactions. This effect has been reproduced by force field calculations (3*g*,4*b*). A few cationic Ru-silylene complexes that also generally feature solvent coordination have become available recently. The observed metal-silicon bond lengths are relatively short compared to single bonds. It should be pointed out, however, that in these cases strong dipolar effects must be expected and that these will have a major influence on metal-silicon bond lengths.

A careful NMR-spectroscopical investigation of $[\text{Cp}^*(\text{PMe}_3)_2\text{RuSiPh}_2(\text{NCMe})]^+ \text{BPh}_4^-$ gives evidence for a rapid exchange of the coordinated CH_3CN with free acetonitrile in solution. A lineshape analysis of (variable temperature) VT ^1H NMR spectra of the complex in the presence of one equivalent of CH_3CN afforded activation parameters for this process of $\Delta H^\ddagger = 14.5 \pm 0.3 \text{ kcal mol}^{-1}$ and $\Delta S^\ddagger = 14 \pm 2 \text{ eu}$. The positive value for the entropy of activation is consistent with a dissociative mechanism and provides evidence for the existence of a base-free silylene complex $[\text{Cp}^*(\text{PMe}_2)_2\text{Ru}=\text{SiPh}_2]^+$ in solution (5*a*).

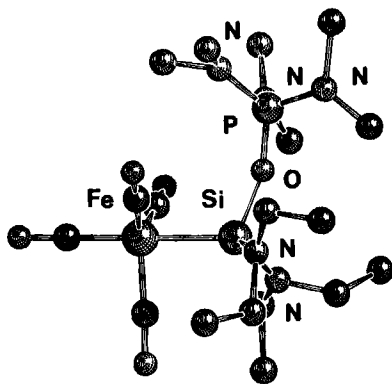


FIG. 3. SCHAKAL plot of $(\text{CO})_4\text{Fe}=\text{Si}(\text{HMPA})(\text{NEt}_2)_2$ **1**. Important bond distances in angstrom: Fe-Si 2.313 (1), Si-O5 1.734 (1).

2. Spectroscopic Parameters

^{29}Si NMR spectroscopy is a most effective method for structure assignment of silicon compounds in solution (Fig. 4). The ^{29}Si NMR shifts are strongly influenced by counteracting paramagnetic and diamagnetic shift effects (38). This situation leads in many cases to a nonlinear relationship between the ^{29}Si NMR shifts in a homologous series of $\text{SiX}_n\text{R}_{4-n}$ ($n = 0 - 4$, $\text{R} = \text{H}$, aryl, alkyl; $\text{X} = \text{halogen}$) compounds and the overall electronegativity of the substituents at silicon. Furthermore, ^{29}Si NMR shifts are indicative of the coordination number CN of the silicon atom (25).

Because of problems with relaxation times T_1 , as well as Overhauser effects of silicon compounds, certain measures such as addition of relaxation agents or use of polarization transfer with pulse sequence programs such as INEPT and DEPT, have been applied. The latter methods are independent of the sign of the gyromagnetic ratio and the T_1 time of the observed nucleus.

The observation of ^{29}Si NMR shifts has also always been possible in cases where the silicon atom is embedded in a dynamic coordination sphere. In Table II ^{29}Si NMR shifts of silylene complexes and related compounds are summarized.

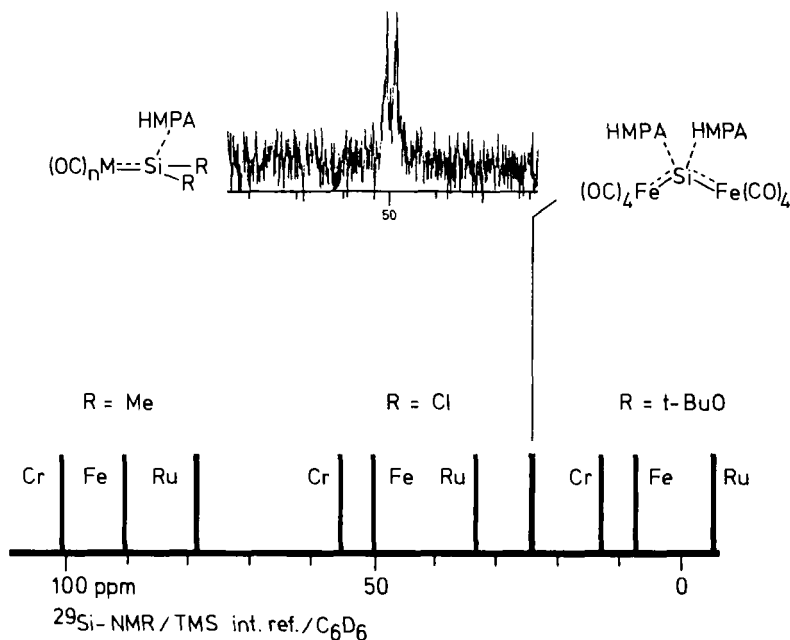


FIG. 4. NMR data of selected silanediyl complexes; see text for discussion.

TABLE II
²⁹Si NMR DATA OF SILYLENE COMPLEXES AND RELATED COMPOUNDS

Complexes	δ (ppm)	References
Silylene		
(CO) ₄ FeSi (HMPA) (NEt ₂) ₂ 1	111.0	^a
(CO) ₄ FeSi (HMPA) (<i>t</i> -BuO) ₂ 2	7.1	(3a)
(CO) ₄ FeSi (HMPA) (<i>t</i> -BuS) ₂ 3	74.7	(3d)
(CO) ₄ FeSi (HMPA)Me ₂ 4	92.3	(3d)
(CO) ₄ FeSi (HMPA)Cl ₂ 5	49.7	(3g)
(CO) ₄ RuSi (HMPA) (<i>t</i> -BuO) ₂ 6	-5.3	(3e)
(CO) ₄ RuSi (HMPA)Cl ₂ 17	33.2	(3e)
(CO) ₃ CrSi (HMPA) (<i>t</i> -Bu) 7	133.1	(56)
(CO) ₃ CrSi (HMPA) (<i>t</i> -BuO) ₂ 8	12.1	(3b)
(CO) ₃ CrSi (HMPA)Me ₂ 9	101.4	(3g)
(CO) ₃ CrSi (HMPA)Cl ₂ 10	55.0	(3g)
(CO) ₃ CrSi(2-Me ₂ NCH ₂ -C ₆ H ₄)C ₆ H ₅ 11	121.2	(3i)
(CO) ₃ CrSi(2-Me ₂ NCH ₂ -C ₆ H ₄)Cl 18	129.9	(3i)
(CO) ₃ CrSi(THF)(<i>t</i> -Bu) ₂ 19	145.3	^a
(CO) ₃ CrSi(2-Me ₂ NCH ₂ -C ₆ H ₄) ₂ 12	138.8	(3f)
(CO) ₄ CrSi(2-Me ₂ NCH ₂ -C ₆ H ₅) (2-Me ₂ NCH ₂ -C ₆ H ₅) 13	122.9	(3i)
(CO) ₃ CrSi(2-Ph ₂ PCH ₂ -C ₆ H ₄) ₂ 14	73.2	(55)
	17.5 ^b	
(CO) ₃ CrSi (<i>t</i> -Bu) ₂ × NaOTf 15	150.7	(56)
[Cp*(Me ₃ P) ₂ RuSiPh ₂ (NCMe)]BPh ₄ 20	95.75	(5b)
[Cp*(Me ₃ P) ₂ RuSiPh ₂ (OTf)] 21	112.39	(5a,b)
(TTP)Os=SiEt ₂ × 2 THF 22	24.53	(27a)
(CO) ₃ CrSi(2-Ph ₂ PCH ₂ -C ₆ H ₄)(2-Ph ₂ PCH ₂ -C ₆ H ₄) 38	159.71	(55)
Cyclic Silylene		
[(η ⁵ -C ₅ Me ₅)Fe(CO)SiMeOMe-μ-OMe-SiMe ₂] 23	127.4	(7)
Me ₂ SiOMeSiMe ₂ Mn(CO) ₄ 24	115.4	(7)
Silaethene		
Cp ₂ WCH ₂ SiMe ₂ 25	-15.66 57.1 ^c	(8c)
Cp*(<i>i</i> -Pr ₃ P)HRuCH ₂ SiPh ₂ 26	6.14	(8b)
Silaimine		
Cp ₂ (Me ₃ P)Zr(η ² -Me ₂ Si=N <i>t</i> -Bu) 27	—	(9)
Disilaethene		
Cp ₂ WSiMe ₂ SiMe ₂ 28	-48.1 50.7 ^b	(10d)
Silatrimethylenemethane		
{Me ₂ SiC[CH(<i>t</i> -Bu)CH ₂]Fe(CO) ₃ 29	43.55	(11)

(continued)

TABLE II (continued)

Complexes	δ (ppm)	References
Silylyne		
$[\text{Cp}_2\text{Fe}_2(\text{CO})_3(\mu\text{-Si-}t\text{-Bu} \times \text{NMI})]\text{I}$ 30	251.5	(12)
Metallasilalallenes		
$(\text{CO})_4\text{FeSi}(\text{HMPA})_2\text{Fe}(\text{CO})_4$ 16	24.1 22.0 ^b 4.4	(14)
$(\text{CO})_4\text{RuSi}(\text{HMPA})_2\text{Ru}(\text{CO})_4$ 31	20.2 ^b	^a

^a H. Handwerker, C. Zybill, Unpublished.^b $^1\text{J}(^{31}\text{P}^{29}\text{Si})$.^c $^1\text{J}(^{183}\text{W}^{29}\text{Si})$.

3. Electronic Structure of Transition Metal Silylene Complexes

Quantum mechanical calculations at Hartree-Fock SCF and CASSCF level for complexes $(\text{CO})_5\text{Mo}=\text{M}'\text{H}_2$, $\text{M}' = \text{C}, \text{Si}, \text{Ge}, \text{and Sn}$, allow a description of the complexes in the sense of Fischer-type carbene complexes. The $\text{Mo}=\text{M}'$ double-bond structure corresponds to the well-known sp σ -donor $p\pi$ -acceptor scheme, which becomes less efficient for the heavier elements of the series. The geometric parameters of the complexes are in agreement with the observed structures. In particular the lowering of the $\text{H}-\text{M}'-\text{H}$ bond angles appears to be related to a different mix of the M' s and p orbitals. The dissociation energies, the potential energy profiles for the dissociation process yielding $(\text{CO})_5\text{Mo}$ and $\text{M}'\text{H}_2$, the rotational barriers of the $\text{M}'\text{H}_2$ ligand around the fourfold axis of the $(\text{CO})_5\text{Mo}$ fragment, and force constants associated with the $\text{Mo}=\text{M}'$ bond stretch have been calculated (39a,39b).

An important aspect of the calculations is the reduced π contribution to the metal silicon double bond going from carbon to the heavier elements of the series C, Si, Ge, Sn due to more diffuse orbitals and less effective orbital overlap. This trend is also reflected in the bond dissociation energies and the calculated force constants of the complexes. The values significantly decrease going from carbon to silicon; however, the silicon compounds do not show unusual features compared to their Ge and Sn counterparts. Furthermore, it must be pointed out that bond dissociation energies and force constants of multiple bonds of heavier elements generally are lower than for similar carbon $\text{C}=\text{C}$ systems (Table III).

A Mulliken population analysis for $(\text{CO})_5\text{Mo}=\text{SiH}_2$ gives a total electron density of 3.583 (SCF)/3.696 (CAS) electrons at Si, which corresponds to

TABLE III
BOND DISTANCE R IN Å, DISSOCIATION ENERGY IN kcal mol⁻¹, AND FORCE
CONSTANT f IN mdyn Å⁻¹ FOR COMPLEXES (CO)₅Mo=MH₂ (39a)

M	C	Si	Ge	Sn
$R_{\text{Mo}=\text{M}} =$	2.02	2.48	2.56	2.65
$d_{\text{Mo}=\text{M}} =$	76.53	47.22	40.64	40.83
$f_{\text{Mo}=\text{M}} =$	3.234	1.270	1.132	0.898

a mean positive charge of almost 0.5 e , which makes the incorporation of a Lewis base at silicon understandable.

4. High-Valent Transition Metal Silylene Complexes

The electronic structure of complexes arising from the formation of a double bond between a silylene ligand and a high-valent transition metal fragment have been investigated recently using *ab initio* wave functions including the effects of electron correlation. These complexes may be referred to as Schrock-type silylene complexes. A description of the metal–silicon bonding requires electron correlation to adequately describe the M–Si σ bond, while the M–Si π bond is described at the Hartree–Fock level. The GVB overlap (as indicator for kinetic stability) and the MSi force constants (as indicator for thermodynamic stability) increase when electronegative substituents are present either at the metal or the silylene ligand. Furthermore, the force constants are larger for complexes of group 5 than for those of group 4 metals. A strong M–Si π backbond seems to be essential for the stabilization of high-valent silylene complexes. These results suggest strategies for the synthesis of such hitherto unknown compounds (40).

D. Reactivity of Silylene Complexes

Reactions of silylene complexes can be divided into reactions of reactive (base-free) intermediates and reactions of solvent adducts of silylene complexes. It is assumed that only minor differences exist between solvent-stabilized complexes and base-free complexes. In many cases the adduct formation between a solvent molecule and the complexes is reversible and the adducts can be considered a “storage” form of three-coordinated silicon.

Since stable complexes with a three-coordinated silicon atom have been described only recently, the chemistry of silylene complexes with a three-coordinated silicon atom is still poorly understood. Reactions of silylene

complexes with intramolecular bases coordinated to silicon are discussed in Section E.

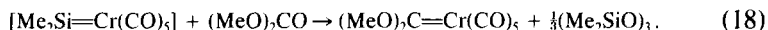
1. *M–Si Bond Cleavage and Silylene Transfer*

A variety of trapping reactions of coordinated silylenes with reagents commonly used for the identification of free silylenes, such as alcohols and dienes, have been observed. Trapping reactions are particularly valuable as proof of silylene cleavage from the metal complexes under conditions of polysilane formation. Such reactions have been reported by various authors and give evidence for the existence of silylene intermediates in metal-catalyzed dehydrocoupling reactions of silanes. However, it is not clear in all cases (different complexes or metals) whether the silylenes are still trapped in the coordination sphere of the metal, or in solution.

It should be pointed out, however, that attempts to generalize mechanistic arguments are questionable as long as the individual reaction kinetics of the systems are not known.

An interesting contribution has been made recently by the research group of Tanaka, who have for the first time isolated the derivative of a silylene complex that is functionalized at the silicon atom in the coordination sphere of the transition metal (Section II,B).

A reaction of particular value for synthetic purposes is the Sila–Wittig reaction of silanediyl complexes. The physical properties (solubility, etc.) of the single components allow the generation of the highly reactive $[\text{Me}_2\text{Si}=\text{Cr}(\text{CO})_5]$ complex at low temperatures and its further derivatization reaction with organic carbonyl compounds. The reaction with dimethyl carbonate (DMC), for instance, yields hexamethyltrisiloxane and the dimethoxycarbene complex $(\text{MeO})_2\text{C}=\text{Cr}(\text{CO})_5$ as final products. NMR–spectroscopic data clearly show a $\text{DMC} \rightarrow \text{Me}_2\text{Si}=\text{Cr}(\text{CO})_5$ adduct as intermediate:



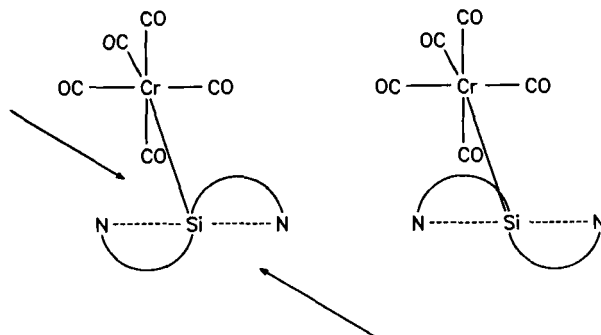
It is not to be expected that polar silicon element double bonds react according a concerted cycloaddition mechanism!

A similar Sila–Wittig reaction has been observed recently between acetone and the complex $\text{THF} \rightarrow \text{Ph}_2\text{Si}=\text{Ru}(\text{CO})_4$. Investigations on Sila–Wittig reactions will be pursued further, particularly with respect to stereoselective or asymmetric syntheses (4b).

2. *Reactions of Silylene Complexes with Retention of the Metal Silicon Bond*

Silylene complexes with two intramolecular donor functions have a C_2 -symmetric conformation in solution. This situation may provide a basis for reactions with asymmetric reagents at silicon to give access to chiral

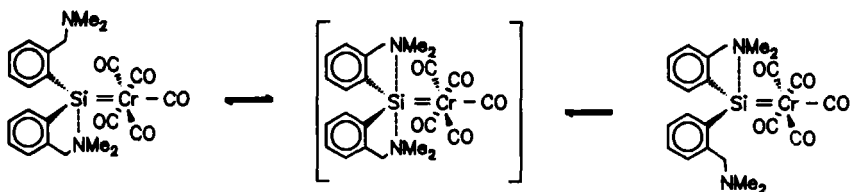
silyl metal complexes with an enantiomeric excess of one distinct enantiomer. The introduction of asymmetric reagents has not been verified experimentally so far, but the generation of chiral products has been proven by most simple reactions like the addition of water to the chromium silicon double bond (41) (Scheme 4).



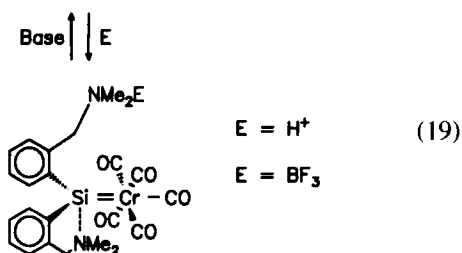
The complex obtained has the structural characteristics of a silylchromium metallate. The immobilization of silylene complexes on (silica gel) surfaces is discussed in Section II, E, 8. This reaction opens up a completely new route to surface-anchored chiral metal complexes, which are of enormous interest in heterogeneous catalysis.

a. *Si-Si bond formation reaction* The role of silylene complexes in dehydrogenative coupling reactions is discussed in Section II, B. Particularly the step of Si-Si bond formation by reaction of the silylene complex with silanes under liberation of an oligosilane has been shown for the metals Pt and Fe (3d,3g,15a,25,35).

b. *Donor functionalization* The dimethylamino-function in the complex $(2\text{-Me}_2\text{NCH}_2\text{-C}_6\text{H}_4)_2\text{Si}=\text{Cr}(\text{CO})_5$ **12** can be derivatized either by protonation or reaction with $\text{BF}_3 \times \text{Et}_2\text{O}$; the protonation reaction is reversible:



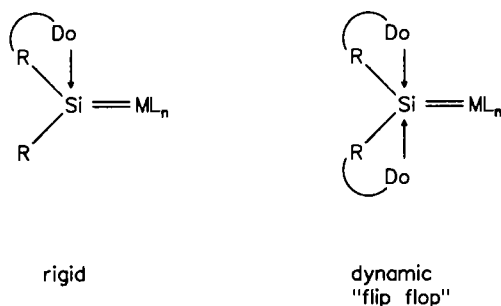
12



The photochemically induced 1,2-shift of the donor to the metal center is discussed in Section II,E,7, as well as the tandem reaction of two 1,2-donor shifts with formation of a silylene complex containing a three-coordinate silicon atom.

E. Intramolecular Base Stabilization in Silylene Complexes

Electronic and coordinative saturation of divalent silicon(II) ligands is most effectively accomplished by a reversible coordination of an intramolecular base to silicon. Examples known so far include silanediyl complexes with monodentate and bidentate donor functions (Scheme 5).



Related silanediyl complexes of iron and manganese have been introduced by Corriu *et al.* by photochemical reaction of silyldihydrides with $16e^-$ -metal complexes and have been studied extensively (42).

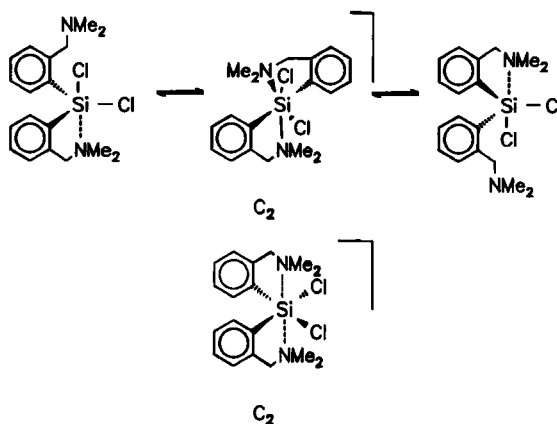
For silanediyl complexes and silanes with two symmetry equivalent intramolecular donor functions a new dynamic coordination of both donor groups to silicon by a "flip flop" mechanism was observed with variable temperature (VT) ^1H and ^{29}Si NMR spectroscopy. This dynamic $\text{N} \cdots \text{Si} \cdots \text{N}$ interaction is the basis for a variety of unexpected reactions at silicon, such as immobilization reactions of silylene complexes on silica

gel surfaces, which are a most efficient method for anchoring transition metal complexes on a solid support.

1. Silanes: Fluxionality and Penta- and Hexacoordination

Silanes with intramolecular donor functions have been investigated extensively by Corriu *et al.* (43) and related stannanes by van Koten *et al.* (44).

An investigation of the molecular dynamics of the silanes (2-Do-CH₂-C₆H₄)C₆H₅SiCl₂ and (2-Do-CH₂-C₆H₄)₂SiCl₂ (Do = Me₂N, Ph₂P) provides insight into the mechanisms of intramolecular donor coordination at the silicon atom (Table IV). For the silane (Do = Me₂N) with one intramolecular donor unit, a rigid pentacoordination of silicon is found at low temperatures (45). However, for silanes with two symmetry equivalent donor units, a new dynamic coordination mode is observed at low temperatures involving both dimethylamino-substituents simultaneously. For (2-Me₂NCH₂-C₆H₄)₂SiCl₂, decoalescence of the singlet for both CH₂ units occurs at 233 K such that one well-defined AB pattern (¹H NMR 2.79, 3.38, ²J(¹H¹H) = 12.0 Hz, 4 H, 2 × CH₂) and one singlet (1.94 ppm, s, 12 H, 4 × NCH₃) for all four methyl groups at the nitrogen atoms is seen. The signals of the N-methyl groups remain singlets because of fast exchange between both methyl substituents at each nitrogen atom by Si-N bond cleavage, rotation around the N-CH₂ bond, and inversion at nitrogen (Scheme 6).



An estimation of the Gibbs free energy of activation from the coalescence temperature for this process gives $\Delta G^\ddagger = 46.5 (\pm 0.5) \text{ kJ mol}^{-1}$ for (2-Me₂NCH₂-C₆H₄)₂SiCl₂.

TABLE IV
COALESCENCE TEMPERATURES AND GIBBS FREE ENERGIES OF ACTIVATION
FOR DETACHMENT OF THE AMINE DONORS FROM SILICON IN SILANES AND
SILANEDIYL COMPLEXES (3i)

	T_c (°C)	G (kJ mol ⁻¹)
(2-Me ₂ NCH ₂ -C ₆ H ₄)C ₆ H ₅ SiCl ₂	-60.0	40.7 ^a
(2-Me ₂ NCH ₂ -C ₆ H ₄) ₂ SiCl ₂	-40.3	46.5 ^b
(2-Me ₂ NCH ₂ -C ₆ H ₄)C ₆ H ₄ Si=Cr(CO) ₅	95.1	80.4 ^c
(2-Me ₂ NCH ₂ -C ₆ H ₄)Si=Cr(CO) ₅	58.0	67.1 ^d

^a CDCl₃, rigid pentacoordination below T_c .

^b *d*₈-toluene, dynamic hexacoordination below T_c .

^c *d*₈-toluene, rigid tetracoordination below T_c .

^d *d*₈-toluene, dynamic pentacoordination below T_c .

The general features for flip flop coordination can be summarized:

- Both dimethylaminomethylene units remain chemically equivalent below the first coalescence temperature.
- The methyl groups at each nitrogen are interconverted rapidly by a mutual displacement reaction of both amine donors, which induces Si-N bond rupture concomitant with rotation around the CH₂-N bond and inversion at one nitrogen atom. The data from VT ¹H NMR spectra clearly show a dissociative pathway via Si-N bond cleavage and exclude an intramolecular mechanism (46).
- This process does not involve any hindered rotation, since the protons of the CH₂ groups remain diastereotopic as long as one donor is still coordinated to silicon.
- The process proceeds with retention of configuration at silicon.
- The exchange involves a hexacoordinated transition state with each nitrogen atom in a *trans*-position to chlorine (capto-dative interaction) as the energetically most favored situation; conformational isomers have not been observed (3i).

These results are interpreted in terms of a dynamic coordination of both dimethylamino-substituents at silicon, one displacing the other rapidly through a hexacoordinated *C*₂-symmetric transition state. This pathway transforms the pentacoordinated isomer *A* of the silane into *A* again with retention of configuration at silicon.

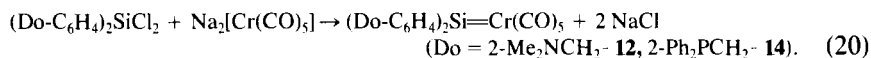
The exchange pathway can be described (Scheme 6), starting from a pentacoordinate ground state, by attack of the noncoordinated dimethylamino-group on silicon through the edge of the trigonal bipyramid to form a *C*₂-symmetric hexacoordinate transition state and formation of *A* again

by displacement of the second, coordinated dimethylamino group from silicon, and so on. The pentacoordinated ground state of **A** has been confirmed in the solid state by a single-crystal X-ray structure determination and in solution by (VT) ^1H NMR spectroscopy.

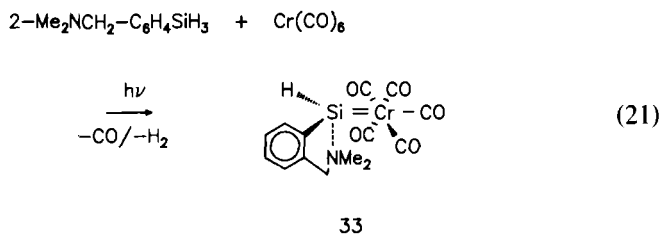
The exchange of both amine and methylene units has also been proven by a 2D EXSY exchange spectrum at -52°C . Furthermore, the ^{29}Si NMR shift of $(2\text{-Me}_2\text{NCH}_2\text{-C}_6\text{H}_4)_2\text{SiCl}_2$ is strongly temperature dependent, varying from -30.1 ppm at room temperature to -54.5 ppm at -70°C . A related mechanism has been proposed recently for the dynamic donor coordination in hexacoordinated silanes (47).

2. Silanediyl Coordination Compounds Stabilized by Intramolecular Interaction with a Base

The silanediyl complexes $(2\text{-Me}_2\text{NCH}_2\text{-C}_6\text{H}_4)\text{C}_6\text{H}_5\text{Si}=\text{Cr}(\text{CO})_5$ **11**, $(2\text{-Me}_2\text{NCH}_2\text{-C}_6\text{H}_4)_2\text{Si}=\text{Cr}(\text{CO})_5$ **12**, and $(2\text{-Me}_2\text{NCH}_2\text{-4-}t\text{-C}_4\text{H}_9\text{-C}_6\text{H}_3)_2\text{Si}=\text{Cr}(\text{CO})_5$ **32** can be prepared by a straightforward coupling reaction of chlorosilanes with anionic metallates. This has proven to be the most effective one-step access to silanediyl coordination compounds:



A valuable alternative for the generation of formal metal–silicon double bonds is the reaction of 16-electron metal complexes with dihydrosilanes (3*i*,32). This method was originally introduced by Corriu and Colomer (48) and has been applied for the synthesis of $(2\text{-Me}_2\text{NCH}_2\text{-C}_6\text{H}_4)\text{HSi}=\text{Cr}(\text{CO})_5$ **33**:



The determination of the structures of **11** and **12** in the solid state as well as an investigation into the molecular dynamics of the complexes in solution allows a detailed description of the mechanism of donor interaction between the base and the silicon atom. Depending on the substitution pattern (one or two donor units) and the temperature range, either rigid $\text{N} \rightarrow \text{Si}$ coordination or dynamic $\text{N} \cdots \text{Si} \cdots \text{N}$ (flip flop) coordination have been observed.

3. Silanediyl Complexes with One Donor Group: Rigid Coordination

Silanediyl complexes with one intramolecular donor group generally show rigid coordination of the base to silicon in solution at 22°C. The Gibbs free energies for the dissociation of the donor are relatively high, with coalescence temperatures above room temperature. For example **11** shows simultaneous coalescence of both signals of the diastereotopic Me₂N groups and the AB system of the CH₂ group at one temperature of 95°C ($\Delta G^\ddagger = 80.4 (\pm 0.5) \text{ kJ mol}^{-1}$). However, the N–Si bond can be cleaved by strong donor solvents like THF, which leads to a static equilibrium between **11** and the THF adduct **11a** with the equilibrium constant $K_{298} = 1.91 \times 10^{-1} \text{ l mol}^{-1}$. From such solutions a five-coordinate donor adduct **11a** (with THF and NMe₂ at silicon) has been frozen out below –45°C.

A single-crystal X-ray structure analysis of **11** shows the silane diyl ligand coordinated to the octahedral [Cr(CO)₅] fragment with a bond distance Cr–Si 2.409 (1) Å (Fig. 5). This bond length is indicative of a significant degree of multiple bonding in (*t*-BuO)₂(HMPA)Si=Cr(CO)₅ **8** 2.431 (1) Å, Me₂(HMPA)Si=Cr(CO)₅ **9** 2.410 (1) Å, and Cl₂(HMPA)Si=Cr(CO)₅ **10** 2.343 (1) Å. Representative Cr–Si single bond lengths are 2.4–2.7 Å (3g). An *ab initio* calculation by Nakatsuji *et al.* for H(HO)Si=Cr(CO)₅ gives 2.40 Å for a Cr=Si double bond (39b); an *ab initio* calculation recently performed by Gordon *et al.* yields 2.45 Å for the system [Cr=SiH₂]⁺ (39a,39b).

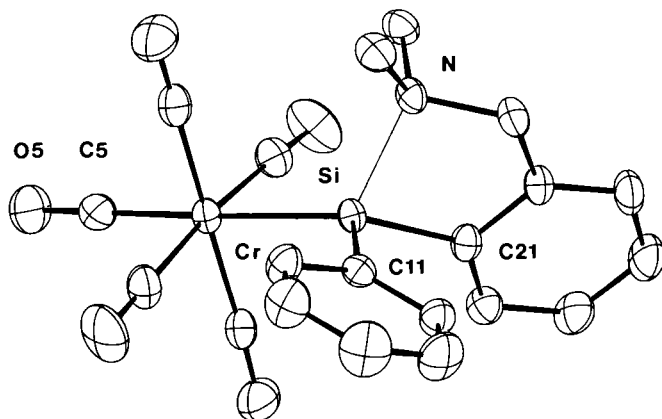
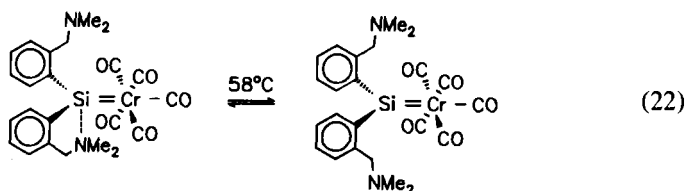


FIG. 5. ORTEP view of (2-Me₂NCH₂-C₆H₄)(C₆H₅)Si=Cr(CO)₅ **11**. Important bond distances in angstrom: Cr–Si 2.409 (2), Si–N 1.991 (2). Sum of bond angles at Si: 347.8°. Reprinted with permission from Handwerker *et al.* (3i). Copyright (1993) American Chemical Society.

The N–Si bond distance in **11** is 1.991 (2) Å, which is fairly long and out of the range of covalent bonding [1.65–1.85 Å (49)]. A further indicator for the magnitude of interaction of the base with the “silanediyl”–silicon atom is the sum of bond angles of the three covalently bonded substituents at silicon, which amounts to 347.8°. Both angles Cr–Si–C11 of 120.2 (1)° and Cr–Si–C21 of 121.3 (1)° are close to 120°, whereas the angle C11–Si–C21 of 106.3 (1)° between the phenyl rings is similar to that calculated for the free silanediyl (50).

4. Silanediyl Coordination Compounds with Two Nitrogen Donors at Silicon: Dynamic Flip Flop Coordination

Introduction of two dimethylamino donor group results in dramatic changes of the coordination mode, coordination geometry, and molecular dynamics of the complexes. Data from VT ¹H NMR spectroscopy in CDCl₃ give clear evidence for three different coordination modes in different temperature ranges (51). Below –21°C, an asymmetric coordination of one dimethylamino-substituent to silicon is observed for **12**. Above –21°C (coalescence) a dynamic coordination of both amine donor units to the silicon atom occurs, which is indicated in the ¹H NMR spectra by a singlet for all four methyl substituents at nitrogen and an AB pattern for the methylene –CH₂– units. The dynamic coordination of both nitrogen donors displacing each other rapidly on the ¹H NMR time scale takes place in a temperature range between –21°C and 58°C and proceeds through a pentacoordinate C₂-symmetrical transition state at silicon. The Gibbs free energy of activation for this process is Δ*G*‡ = 54.4 (±0.5) kJ mol^{–1}. Inversion at nitrogen and rotation around the C–N bond leads to the chemical equivalence of both methyl groups at N. Also in this case, the assumption of hindered rotation of the dimethylaminophenyl substituents is possible, but is *a priori* not necessary, since the protons H_A and H_B of the CH_AH_B groups remain diastereotopic as long as one donor unit is still coordinated to the (asymmetric) silicon atom. However, cleavage of all donor → silicon bonds occurs above 58°C (coalescence of the AB system of the CH₂ units, ²⁹Si NMR low field shift to 138.8 ppm) with formation of an essentially three-coordinated silicon atom (52):



Accordingly, the ^{29}Si NMR signals for **12** vary strongly with temperature from δ 120.9 ppm at -40.0°C for the rigidly tetracoordinated form, through δ 124.9 ppm at 22.0°C for the dynamical flip flop coordination, to δ 138.8 ppm above 58.0°C for the three-coordinated system.

A further example of a silanediyl complex with dynamic reversible intramolecular base (flip flop) coordination is provided by the *t*-butyl compound $(2\text{-Me}_2\text{NCH}_2\text{-4-}t\text{-C}_4\text{H}_9\text{-C}_6\text{H}_3)_2\text{Si}=\text{Cr}(\text{CO})_5$ **32**. The complex shows analogous temperature-dependent behavior in the VT ^1H NMR spectrum with a singlet for the dimethylamino-substituents at 22°C and an AB system for the CH_2 bridge at 22°C , with $^2J(^1\text{H}^1\text{H}) = 12.2$ Hz (C_2Cl_2). Coalescence of the AB system is observed at 61°C , which represents a Gibbs free energy of activation of $\Delta G^\ddagger = 70.1 (\pm 0.5)$ kJ mol $^{-1}$.

A single-crystal X-ray structure determination of the silanediyl complex **12** confirms the results obtained spectroscopically and provides information on the molecular structure of **12** in the solid state (Fig. 6). The complex is monomeric and the silanediyl ligand is coordinated to the octahedral chromium fragment with a short Cr–Si bond length of 2.408 (1) Å, which is similar to the one observed for **11**, indicating a considerable degree of multiple bonding. The N1–Si bond distance of 2.046 (2) Å is typical for a partially covalent interaction and somewhat shorter than in the penta-coordinated silane $(2\text{-Me}_2\text{NCH}_2\text{-C}_6\text{H}_4)_2\text{SiCl}_2$ (2.291 (2) Å), but clearly

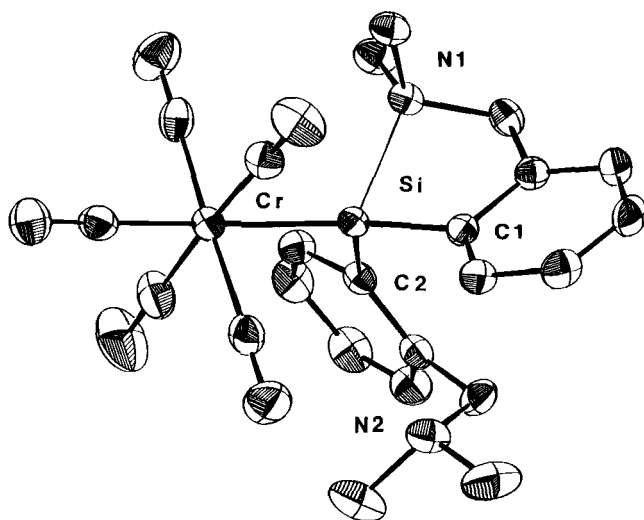


FIG. 6. ORTEP view of $(2\text{-Me}_2\text{NCH}_2\text{-C}_6\text{H}_4)_2\text{Si}=\text{Cr}(\text{CO})_5$ **12**. Important bond distances in angstrom: Si–Cr 2.408 (1), Si–N1 2.046 (2); sum of bond angles at silicon: 351.3° . Reprinted with permission of Probst *et al.* (3f). Copyright (1991) VCH-Publishers.

much longer than in any comparable silanediyl complex and out of the range of covalent bonding. The Gibbs free energy of activation for the dissociation of the Si–N1 bond is $\Delta G^\ddagger = 67.1 (\pm 0.5) \text{ kJ mol}^{-1}$. Furthermore, the UV spectrum of **12** also shows an unprecedented large bathochromic shift of $\lambda_{\text{max}} = 274 \text{ nm}$ compared to the absorption of known HMPA adducts of silanediyl complexes. This band is assigned to the $\pi \rightarrow \pi^*$ transition of the Cr=Si double bond.

The environment around the silicon atom is only slightly pyramidalized, with the sum of the bond angles of the three covalently bonded substituents around Si of 351.3° , which is close to 360° . This geometry points toward planarization at silicon, particularly considering the fact that similar pyramidalization effects are observed for three-coordinate silicon in the crystal structures of disilaethenes (*1*).

The second dimethylamino unit in **12** is also directed toward the silicon atom, but with a nonbonding distance of 3.309 \AA being representative of only a weak van der Waals interaction.

5. Phosphino-substituted Silylene Complexes

A particularly important piece of evidence in the chain of proof for the flip flop coordination mechanism is provided by the phosphino-substi-

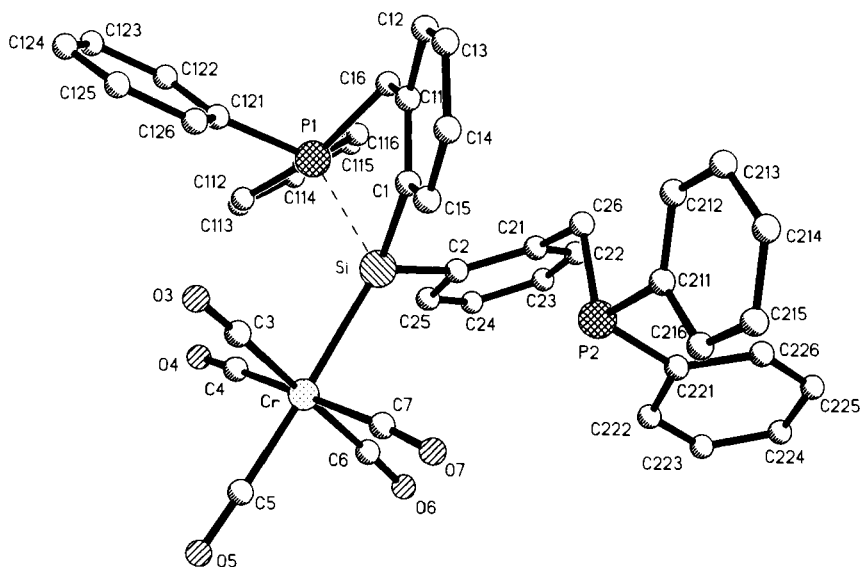


FIG. 7. Structure of $(2\text{-Ph}_2\text{PCH}_2\text{-C}_6\text{H}_4)_2\text{Si=Cr(CO)}_5$, **14**. Important bond distances in angstrom: Cr–Si 2.413 (1), Si–P1 2.380 (1). Sum of bond angles at silicon 352.1° . Reprinted with permission of Handwerker *et al.* (55). Copyright (1993) VCH-Publishers.

tuted silylene complexes $(2\text{-Ph}_2\text{PCH}_2\text{-C}_6\text{H}_4)_2\text{Si}=\text{Cr}(\text{CO})_5$ **14** and $(2\text{-Ph}_2\text{CH}_2\text{-C}_6\text{H}_4)(2\text{-Me}_2\text{NCH}_2\text{-C}_6\text{H}_4)\text{Si}=\text{Cr}(\text{CO})_5$ **34**. In the solid state, the silicon atom of **14** shows a weak asymmetric coordination to one of the phosphino-units (Si-P1 2.380 (1) Å. The second distance Si-P2 3.725(1) Å is nonbonding. Thus, a Cr—Si bond distance of 2.413 (1) Å is found with a sum of bond angles of the three covalent substituents at silicon of 352.1° (Fig. 7). It is interesting to note that the cross-polarized magic angle spinning (CP-MAS) ^{31}P NMR powder spectra of **14** show both phosphorous atoms with strongly different NMR shifts at -5.3 and 19.6 ppm (Fig. 8).

In solution, a totally different situation occurs: Both diphenylphosphino-methylphenyl substituents at the silicon atom are now chemically equivalent with a singlet at 1.8 ppm in the ^{31}P NMR spectrum, an ABX system for the CH_2 groups, and a triplet for the ^{29}Si NMR signal at 73.2 with $^1J(^{31}\text{P}^{29}\text{Si}) = 17.5$ Hz. However, the ^{13}C NMR spectrum of the $(\text{C}_6\text{H}_5)_2\text{P}$ rings shows two distinct sets of signals due to the two diastereotopic C_6H_5 substituents at each phosphorus atom. The NMR data clearly show the retention of the tetrahedrally coordinated polyhedron at phosphorous, i.e., a flip flop coordination without inversion at phosphorus.

6. Flip Flop Coordination: General Comments

Flip flop coordination describes the dynamic coordination mode of two symmetry equivalent donor ligands to an electron-deficient central atom.

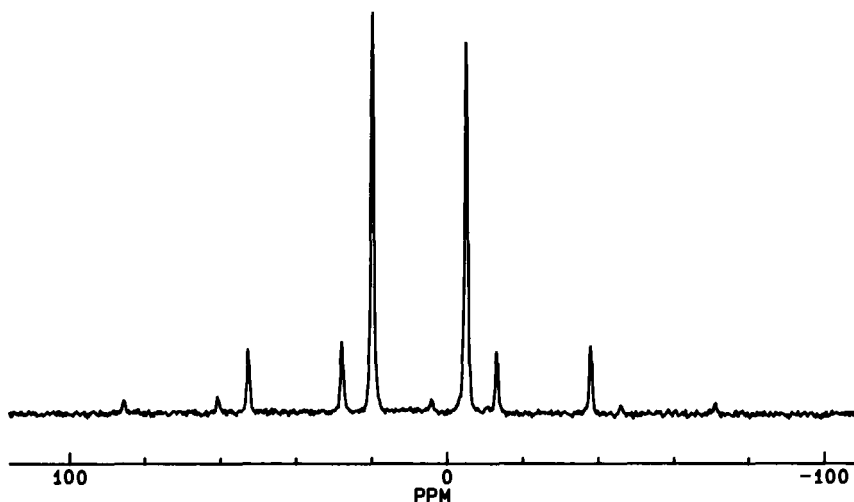
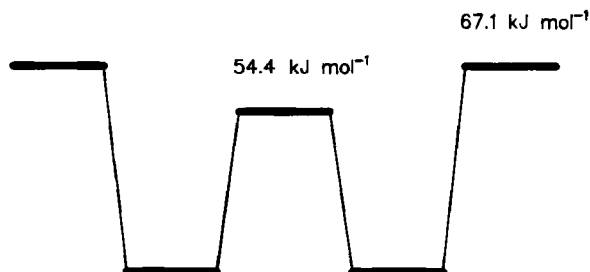
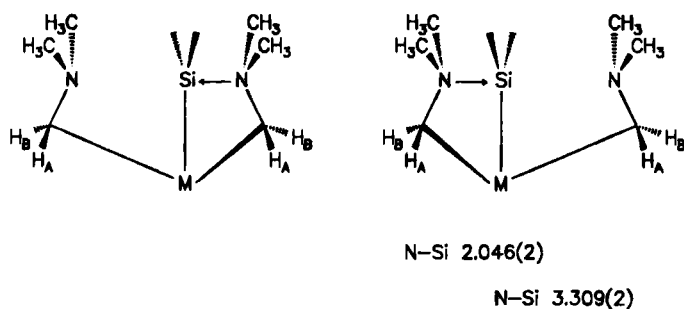


FIG. 8. CP-MAS ^{31}P NMR of $(2\text{-Ph}_2\text{PCH}_2\text{-C}_6\text{H}_4)_2\text{Si}=\text{Cr}(\text{CO})_5$ **14**. Reprinted with permission of Handwerker *et al.* (55). Copyright (1993) VCH-Publishers.

A prerequisite for a dynamic flip flop coordination mode is a geometry of two identical donor ligands, which allows mutual displacement reactions. In the observed cases, the dynamic displacement process proceeds through a C_2 -symmetrical transition state, transforming two degenerate asymmetric ground states into each other. The Gibbs free energy for the activation of the flip flop process for **12** is 54.4 kJ mol^{-1} ($13.0 \text{ kcal mol}^{-1}$). The conformation of the respective ground state is precisely known from the results of single-crystal X-ray structure determinations of $(2\text{-Me}_2\text{NCH}_2\text{-C}_6\text{H}_4)_2\text{SiCl}_2$ and $(2\text{-Me}_2\text{CH}_2\text{-C}_6\text{H}_4)_2\text{Si}=\text{Cr}(\text{CO})_5$ **12**.

In the cases investigated, flip flop coordination of the complexes is observed in a temperature range near room temperature, which clearly allows inversion at the nitrogen atom. Thus, a mechanism is proposed whereby a simultaneous $\text{N} \cdots \text{Si} \cdots \text{N}$ bond formation and rupture process, which is coupled with the inversion at nitrogen, occurs (11,53) (Scheme 7).

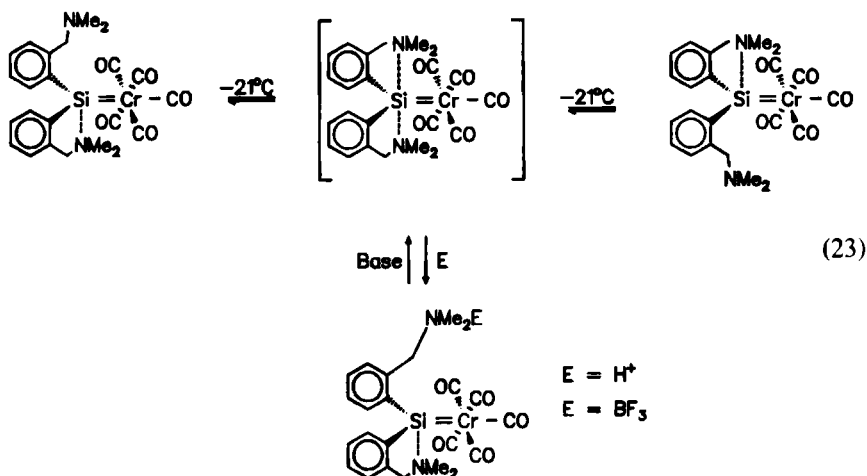


A similar observation has been made recently by van Koten and Jas-trzebski for the $\text{Sn}(\text{IV})$ cation in $(2\text{-}5\text{-bis-dimethylaminomethylphenyl})\text{-methylphenyltinchloride}$. Here too, a separation between the Sn-N bond cleavage process (which leads to inversion of the geometry at Sn) and

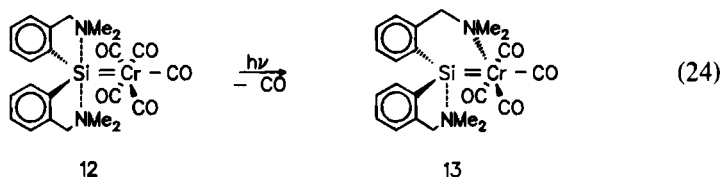
rotation around the C–C bond was possible. This process of Sn–N bond formation and rupture takes place up to 70°C and may also be described by a dynamic bond with a flip flop coordination mode (44). Further cases seem to be present in the systems (2-Me₂NCH₂–C₆H₄)₂Sn=W(CO)₅ and (2-Ph₂PCH₂–C₆H₄)₂Sn=W(CO)₅ (54).

7. Reactions of Silylene Complexes with an Intramolecular Donor

a. *Donor functionalization* The derivatization of **12** with electrophiles *E* (either H⁺ or BF₃) allows the selective blocking of one amine unit. Notably the protonation reaction is reversible and allows the on and off switching of the dynamic flip flop coordination mode in **12**:



b. *Photochemical activation of the donor: 1,2-Amine shift* Besides chemical derivatization reactions discussed in the previous section, the amine donor in **12** can also be activated by a highly selective photolysis reaction of the complex at 254 nm, which induces loss of CO and a 1,2-shift of one amine donor substituent from silicon to the metal to form (2-Me₂NCH₂–C₆H₄)(2-Me₂NCH₂–C₆H₄)Si=Cr(CO)₄ **13**:



This process also takes place in a topochemical solid-state reaction, simply by UV irradiation of crystals of **12** or **32**.

The results from an X-ray structure analysis of **13** are shown in Fig. 9. A Cr–Si bond length of 2.3610 (4) Å is found, which is the shortest so far observed for silanediyl complexes of chromium. This bond-shortening effect is caused by the increased electron density at the chromium atom due to the amine ligand and leads to a stronger metal silicon-bonding interaction by either covalent and dipolar contributions.

The N-donor ligand is coordinated slightly more strongly to the silicon atom in complex **13** than in **11**, which is indicated by a shorter N1–Si bond of 1.981 (1) Å (**13**) compared to **11**. The sum of bond angles at silicon amounts to 342.9°. The N–Cr bond length (2.291 (1) Å) lies in the expected range for N–Cr bonds of amine complexes as do the Cr–C (1.815 (2) Å–1.869 (2) Å) bonds of the carbonyl ligands. The Cr–C3 bond of the CO ligand *trans* to nitrogen is slightly shortened (1.815 (2) Å) compared to the *cis*-COs (3*i*).

c. *Immobilization of silylene complexes on a silica surface* A particularly interesting method involves the anchoring of silylene complexes on a silica gel surface. The fixation of **12** and **32** occurs quantitatively at room temperature within a few minutes and gives immobilized silyl-chromium complexes. IR spectroscopy of (2-Me₂NH⁺CH₂–C₆H₄)(2-Me₂NCH₂–

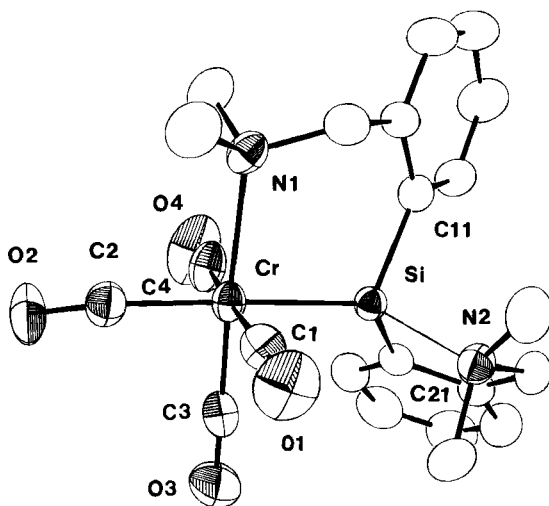
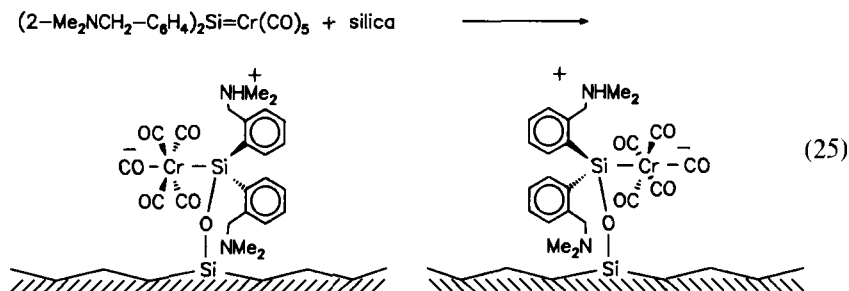


FIG. 9. ORTEP view of (2-Me₂NCH₂–C₆H₄)(2-Me₂NCH₂–C₆H₄)Si=Cr(CO)₄ **13**. Important bond distances in angstrom: Cr–Si 2.3610 (4), Si–N1 1.981 (1). Sum of bond angles at Si 342.9°. Reprinted with permission of Handwerker *et al.* (3*i*). Copyright (1993) American Chemical Society.

$\text{C}_6\text{H}_4\text{Si}(\text{silica})\text{Cr}(\text{CO})_5^-$ **35** shows bonding of the complex to the support by a Si–O linkage (ν_{SiO} 1082 cm^{-1}) and protonation of the amine function (ν_{NH} 2610 cm^{-1}) as well as an intact $\text{Cr}(\text{CO})_5$ unit:



A ^{13}C CP–MAS NMR spectrum of **35** provides further evidence for the binding of **12** to the surface (Fig. 10). The resonances of the methyl- and methylene carbon atoms are clearly visible and their chemical shifts correspond well to the values measured in solution. The signals of the phenyl carbon atoms show the typical shift anisotropy observed for aromatic ring systems. Furthermore, reactions of the complexes with buckminsterfullerene C_{60} are of interest and should be explored in the future.

d. *Reactions of silylene complexes with oxygen-containing nucleophiles* Silylene complexes with dynamic donor groups are particularly susceptible to reactions with nucleophiles. Reaction of **32** with one equivalent of water, for instance, leads to displacement of both nitrogen donors, protonation of one nitrogen atom, and formation of a hydroxysilyl complex $(2\text{-Me}_2\text{HN}^+\text{CH}_2\text{-4-}t\text{-C}_4\text{H}_9\text{-C}_6\text{H}_3)(2\text{-Me}_2\text{NCH}_2\text{-4-}t\text{-C}_4\text{H}_6\text{-C}_6\text{H}_3)\text{Si}(\text{OH})\text{Cr}(\text{CO})_5^-$ **36**. The spectroscopic parameters of **36** show a close similarity to the surface-bound complex **35**, which allows the assumption of similar structures for **35** and **36**.

A single-crystal structure analysis of **36** gives a Cr–Si bond distance of $2.469(2)\text{ \AA}$, which is still short in comparison to bond lengths of base-stabilized silylene complexes (Fig. 11). This bond shortening is presumably due to relatively strong dipolar effects. In contrast to donor adducts of silylene complexes, the Si–O6 bond distance is clearly in the range of covalent bonding ($1.695(3)\text{ \AA}$) and the coordination geometry at silicon deviates only slightly from an ideal tetrahedron (sum of bond angles Cr–Si–C101, Cr–Si–C201, C101–Si–C201: 334.4°). Both nitrogen atoms of the dimethylamino-units are directed toward oxygen O6 by hydrogen bonding, $\text{N2-H61} \cdots \text{O6}$ and $\text{N1} \cdots \text{H62-O6}$, respectively. It should be pointed out that **36** is a chiral reaction product (R-enantiomer) of C_2 -symmetric **32**.

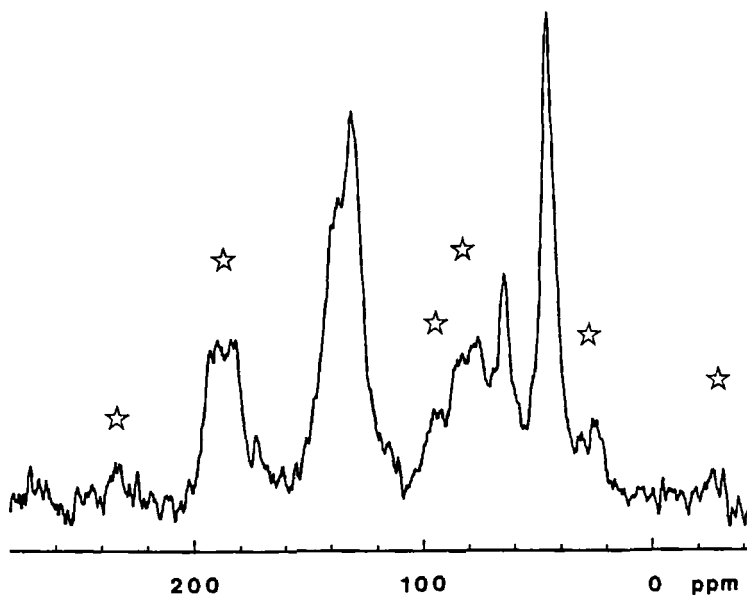


FIG. 10. CP-MAS ^{13}C NMR of $(\text{Me}_2\text{HN}^+\text{CH}_2-\text{C}_6\text{H}_4)(\text{Me}_2\text{NCH}_2-\text{C}_6\text{H}_4)(\text{silica})\text{SiCr}(\text{CO})_5^-$ **35**. Reprinted with permission of Handwerker *et al.* (3i). Copyright (1993) American Chemical Society.

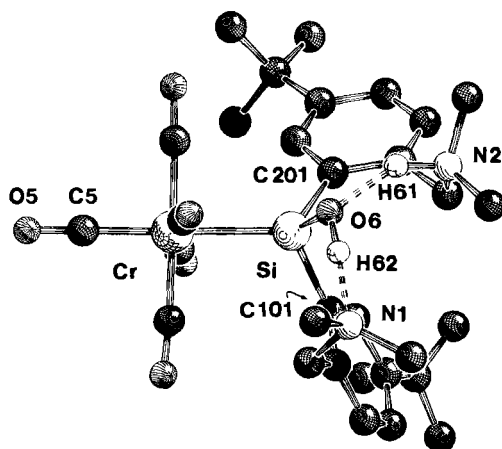
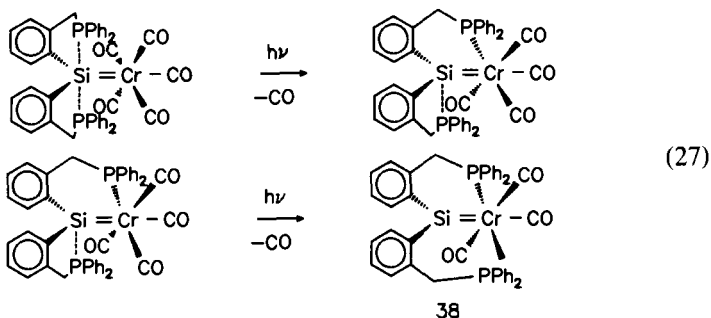
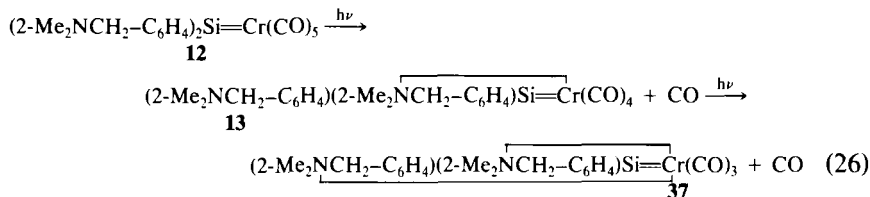


FIG. 11. SCHAKAL view of $\text{R}-(2-\text{Me}_2\text{HN}^+\text{CH}_2-4-t\text{-C}_4\text{H}_9-\text{C}_6\text{H}_3)(2-\text{Me}_2\text{NCH}_2-4-t\text{-C}_4\text{H}_9-\text{C}_6\text{H}_3)(\text{HO})\text{SiCr}(\text{CO})_5^-$ **36**. Important bond distances in angstrom: Cr–Si 2.469 (2), Si–O6 1.695 (3). Sum of bond angles at Si 334.4° . Reprinted with permission of Handwerker *et al.* (3i). Copyright (1993) American Chemical Society.

e. *Tandem reaction: Access to metal–silicon double bonds* The facile photochemical activation reaction of metal-coordinated carbonyls allows the 1,2-shift of both donor units to the metal. The amine complex obtained $(2\text{-Me}_2\text{NCH}_2\text{-C}_6\text{H}_4)(2\text{-Me}_2\text{NCH}_2\text{-C}_6\text{H}_4)\text{Si}=\text{Cr}(\text{CO})_3$ **37** is kinetically labile, but has been trapped with triethylsilane and various alcohols:

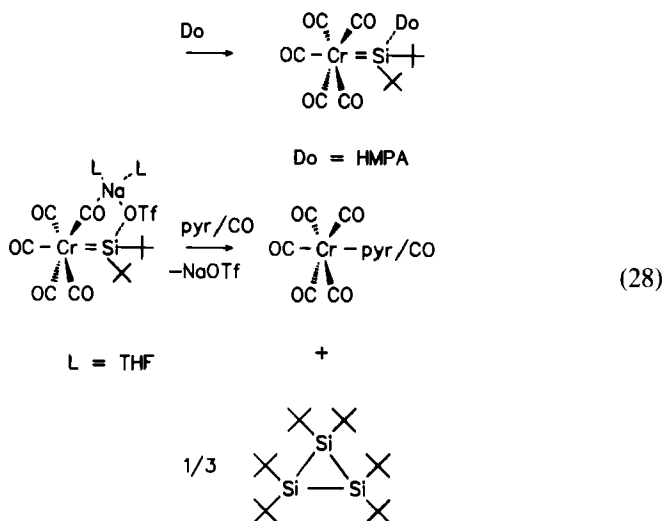


The bisphosphine complex $(2\text{-Ph}_2\text{PCH}_2\text{-C}_6\text{H}_4)(2\text{-Ph}_2\text{PCH}_2\text{-C}_6\text{H}_4)\text{Si}=\text{Cr}(\text{CO})_3$ **38** is stable and shows a *trans* geometry of both phosphine ligands with a meridional arrangement of the three CO groups. The complex has been characterized spectroscopically (^{29}Si NMR 159.7 ppm) (55).

F. A Salt Adduct of the Metal–Silicon Double Bond

A salt adduct of a neutral silanediyl complex has recently been obtained, $(t\text{-Bu})_2\text{Si}=\text{Cr}(\text{CO})_5 \times \text{NaOTf}$ **15**, with sodium triflate (trifluorosulfonate) loosely coordinated to bis-*tert*-butylsilanediyl chromium pentacarbonyl.

NMR-spectroscopic investigations indicate rapid exchange of the triflate in solution, even at low temperatures. Furthermore, the triflate is displaced by THF, which does not exchange. The reactivity of the complex is the subject of current investigations; however, di-*tert*-butylsilanediyl is eliminated from the metal under CO pressure or by addition of an excess of pyridine and forms hexa-*tert*-butylcyclotrisilane. Thus, **15** allows a facile synthesis of cyclotrisilanes:



A single-crystal X-ray structure determination gave a Cr–Si bond distance of 2.475 (1) Å in **15**. The distance Si–O7 is 1.857 (3) Å and the sum of bond angles at the silicon atom amounts to 349.5° (Fig. 12).

The molecule forms polymeric chains in the crystal with sevenfold coordinate sodium atoms (coordination to the COs of three different complexes and the O atoms of two different triflate groups and to two THF molecules). This chain structure is solvated in solution (Fig. 13).

The structure of the HMPA adduct $(t\text{-Bu})_2(\text{HMPA})\text{SiCr}(\text{CO})_5$ **7** allows a comparison with the structure of **15** and shows a significantly elongated

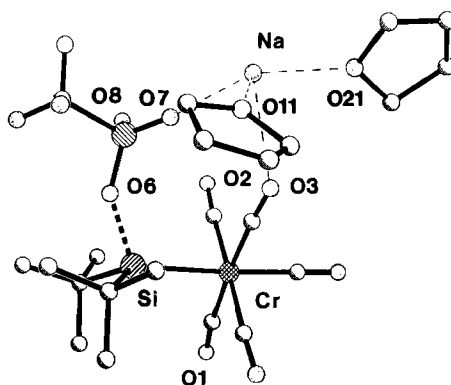


FIG. 12. Molecular structure of $(t\text{-C}_4\text{H}_9)_2\text{Si}=\text{Cr}(\text{CO})_5$ NaOTf \cdot 2 THF **15**. Important bond distances in angstrom: Cr–Si 2.475 (1), Si–O6 1.857 (3). Sum of bond angles at Si 349.5° (56).

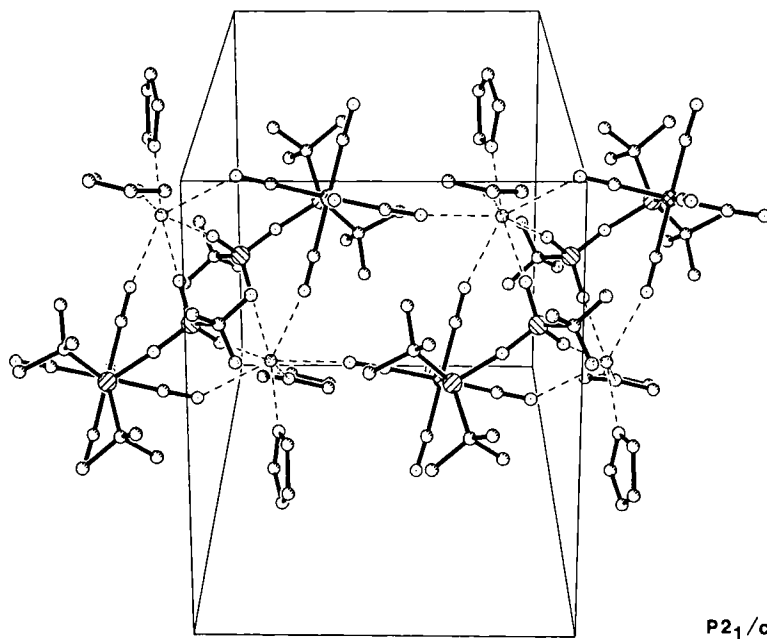


FIG. 13. View of the elemental cell of $(t\text{-C}_4\text{H}_9)_2\text{Si}=\text{Cr}(\text{CO})_5 \times \text{NaOTf} \times 2 \text{ THF}$ **15** showing a chain structure. For details refer to the text (56).

Cr–Si bond length of 2.521 (1) Å. This effect is due to electronic, but partially also to steric, interactions in the extremely crowded molecule. The Si–O6 bond distance is 1.787 (1) Å, and the sum of bond angles at silicon is 340.7° (Fig. 14) (56).

G. Base-Free Silylene Complexes

A silylene complex with a three-coordinate silicon atom, $\text{Cp}^*(\text{Me}_3\text{P})_2\text{RuSi}(\text{STol})=\text{Os}(\text{CO})_4$ **39**, has been synthesized recently and characterized by a single-crystal X-ray structure analysis and has a Os–Si bond distance of 2.419 (2) Å (equatorial silylene ligand) and a Ru–Si bond length of 2.286 (2) Å. The sum of bond angles at Si is 360.1° (57).

Also the cationic silylene complex $[\text{trans}(\text{Cy}_3\text{P})_2(\text{H})\text{Pt}=\text{Si}(\text{SEt})_2]^+ \text{BPh}_4^-$ **40** has a three-coordinate silicon atom (summation of angles at silicon 359.9°) and a Pt–Si bond length of 2.270 (2) Å, which is short in comparison to the related complex $\text{trans}(\text{Cy}_3\text{P})_2\text{Pt}(\text{H})\text{Si}(\text{SEt})_3$ [2.379 (1) Å (Fig. 15)]. The Si–S distances are unusually short [2.092 (4) and 2.074 (4)

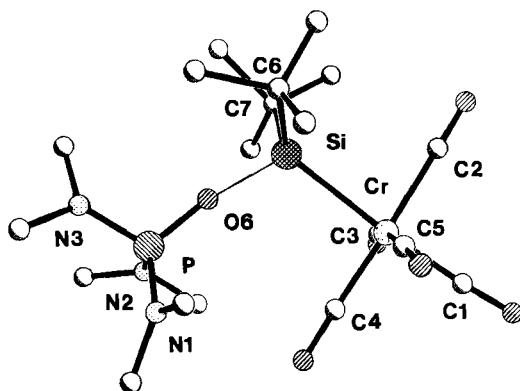


FIG. 14. Molecular structure of $(t\text{-C}_4\text{H}_9)_2(\text{HMPA})\text{Si}=\text{Cr}(\text{CO})_5$ **7**. Important bond distances in angstrom: Cr–Si 2.527 (1), Si–O6 1.777 (1). Sum of bond angles at Si 340.7° (56).

Å] and may be ascribed to some degree of π bonding. The plane of the silylene ligand is rotated 76° out of the least-squares plane of platinum donor atoms (58).

Further examples for a three-coordinate silicon atom in silanediyl-coordination compounds are given in this article.

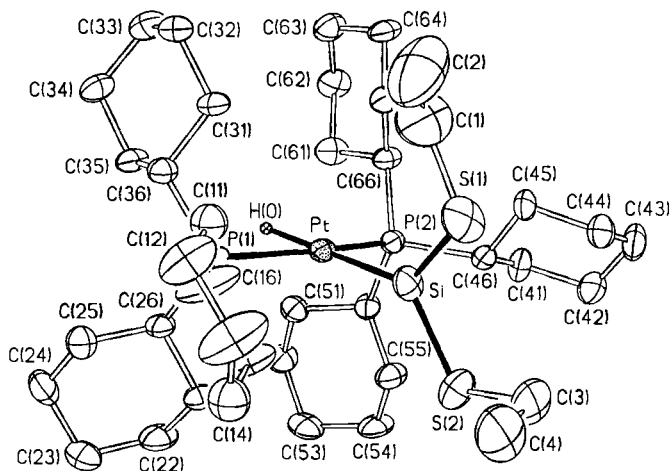
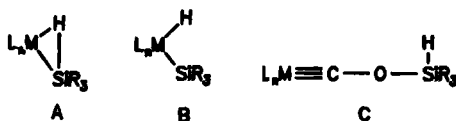


FIG. 15. ORTEP view of the cation of $[\text{trans}-(\text{Cy}_3\text{P})_2(\text{H})\text{Pt}=\text{Si}(\text{SEt})_2]\text{BPh}_4 \times \text{CH}_2\text{Cl}_2$ **40**. Important bond distances in angstrom: Pt–Si 2.270 (2), Si–S1 2.092 (4), Si–S2 2.074 (4). Sum of bond angles at Si 359.9°. Reprinted with permission of Grubbs *et al.* (57). Copyright (1993) American Chemical Society.

III

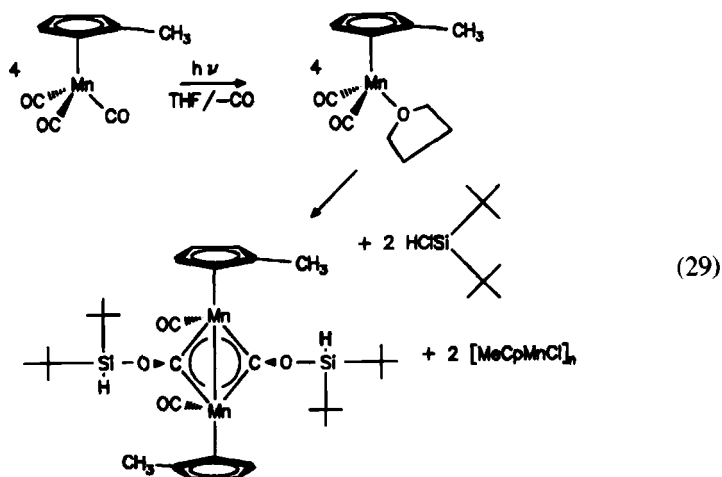
SILANE-INDUCED CO-ACTIVATION REACTION

The reaction of silanes with $16e^-$ -metal complexes leads to the formation of silylmetal hydrides by insertion of the metal complex into the Si-H bond. The mechanism of this reaction has been investigated in detail (24) (Scheme 8).



With $16e^-$ -metal carbonyl complexes, activation of the coordinated CO by the silane and formation of a siloxycarbene complex was observed. Furthermore, the carbene ligands have been coupled to acetylene by a CC-coupling reaction (59). The silane-induced CO activation and coupling reaction is an interesting variant of the processes known so far, since they require external addition of the reducing agent. Metal-mediated CC-coupling reactions are of interest in the context of Fischer-Tropsch synthesis and related reactions.

The reaction of the solvent-stabilized $16e^-$ complex $[\eta^5\text{-MeCpMn}(\text{CO})_2 \times \text{THF}]$ with $t\text{-BuSiHCl}$ allows CO activation and formation of the cyclic biscarbene complex $[\eta^5\text{-MeCp}(\text{CO})\text{Mn}(\mu\text{-CSiH}(t\text{-Bu}))_2\text{Mn}(\text{CO})(\eta^5\text{MeCp})]$ **41**:



The complex **41** is formed by O attack of the silane at a coordinated CO ligand, which induces an electron transfer from Mn to the C atom of the CO ligand under formation of a $17e^-$ -siloxycarbyne complex and a polymeric Mn(II) complex. The initially formed complex $[\eta^5\text{MeCp}(\text{CO})\text{Mn}\equiv\text{COSiH}(t\text{-Bu})_2]$ dimerizes to the closed-shell species under exclusive formation of the *cis*-isomer (^{13}C NMR of $\mu\text{-C} = 402.1$ ppm). The molecule has the bonding characteristics of a μ -carbyne complex with Mn–C 1.857 (2) Å and a Mn–Mn' bond of 2.565 (1) Å (Fig. 16). The four-membered ring is folded along the Mn–Mn' axis by 18.45° . This geometry allows the two carbyne C atoms to come into proximity [nonbonding distance 2.662 (2) Å], which is essential for the observed CC-coupling reaction of the two

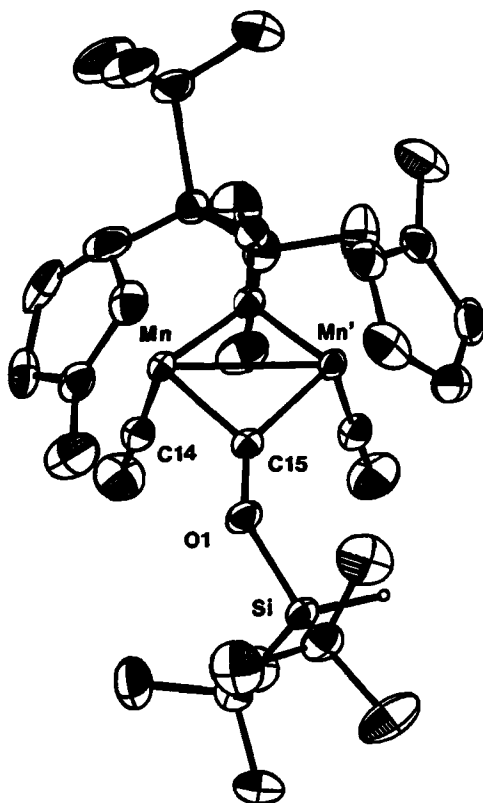


FIG. 16. ORTEP view of $(\eta^5\text{-H}_3\text{CC}_3\text{H}_4)(\text{CO})\text{Mn}(\mu\text{-COSiH}(t\text{-C}_4\text{H}_9)_2)_2\text{Mn}(\text{CO})$ ($\eta^5\text{-H}_3\text{CC}_3\text{H}_4$) **41**. Important bond distances in angstrom: Mn–C15 (carbyne) 1.857 (2), Mn–Mn' 2.565 (1). Reprinted with permission of Handwerker *et al.* (59). Copyright (1993) American Chemical Society.

carbyne units to give disiloxacyetylene (Fig. 17). As a further elimination product, the disilyl peroxide ($t\text{-Bu}_2\text{HSiO}$)₂ is found. Both processes are related to reactions of CO on metal surfaces, for which CC coupling and CO dissociation are known:

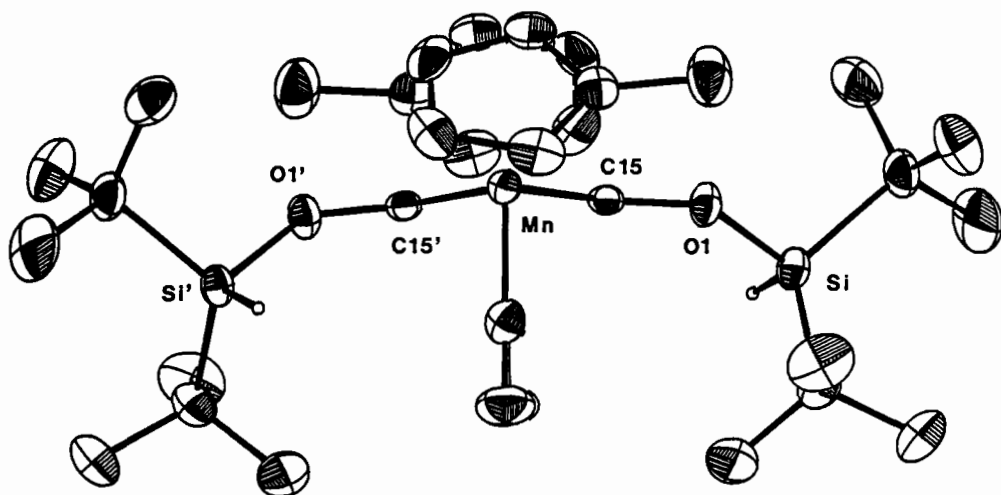
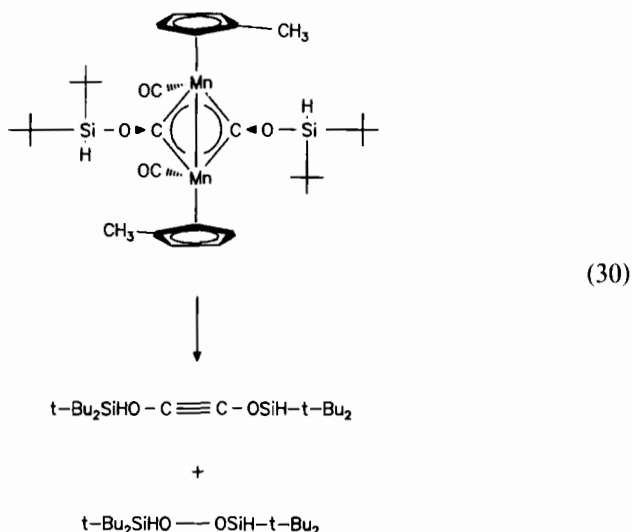


FIG. 17. Side view of ($\eta^5\text{-H}_3\text{CC}_5\text{H}_4$) (CO) $\text{Mn}(\mu\text{-COSiH}(t\text{-C}_4\text{H}_9)_2)_2\text{Mn}(\text{CO})(\eta^5\text{-H}_3\text{CC}_5\text{H}_4)$ **41** projected on the Mn–Mn' bond. The folding of the metallacycle is 18.45° . Reprinted with permission of Handwerker *et al.* (59). Copyright (1993) American Chemical Society.

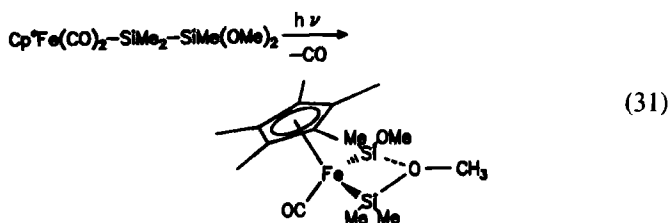
IV

CYCLIC SILYLENE COMPLEXES

Iron (Fp) derivatives of polysilanes undergo photochemical deoligomerization reactions to yield monosilyl-iron complexes. Furthermore, migration of the silyl side chain from iron to the cyclopentadienyl ligand occurs by treatment with *n*-butyllithium; the latter reaction has also been observed for a series of related indenyl-iron complexes (60).

The investigation of the photochemical deoligomerization reaction of a variety of polysilyl-Fp complexes provided evidence for a silylene expulsion process (61). The mechanism of this reaction has been clarified by matrix experiments that proved an iron-silylene complex as intermediate (62).

Stable cyclic silylene complexes could be obtained by the introduction of an intramolecular oxygen-containing donor function. For the complexes $[(\eta^5\text{-C}_5\text{Me}_5)\text{Fe}(\text{CO})\text{SiMeOMe-}\mu\text{-OMe-SiMe}_2]$ **23** (63) and $[(\text{CO})_4\text{MnSiMe}_2\text{-}\mu\text{-OMe-SiMe}_2]$ **24**, single-crystal X-ray structure determinations have been undertaken (7b):



The chemistry of these compounds is virtually unknown to date. The stereochemical behavior of alkoxy-bridged silylene-germylene iron complexes has been investigated in detail, however, and gives evidence for a ring opening and closure process via a germylene intermediate, with $\Delta G^\ddagger = 62 \text{ kJ mol}^{-1}$ for the methyl derivative (7d-7f).

V

DONOR-STABILIZED SILYLYNE COMPLEXES

The first formal silylyne complex, the cationic cyclic $\mu\text{-(SiR)}$ derivative $[\text{Cp}_2\text{Fe}_2(\text{CO})_3(\mu\text{-Si-}i\text{-Bu}) \times \text{NMI}]^+ \text{I}^-$ **30** (NMI = *N*-methylimidazole) was obtained by a displacement reaction of iodide by NMI from a neutral cyclic silylene complex (12). The Fe-Si bond distance of **30** is 2.262 (2)

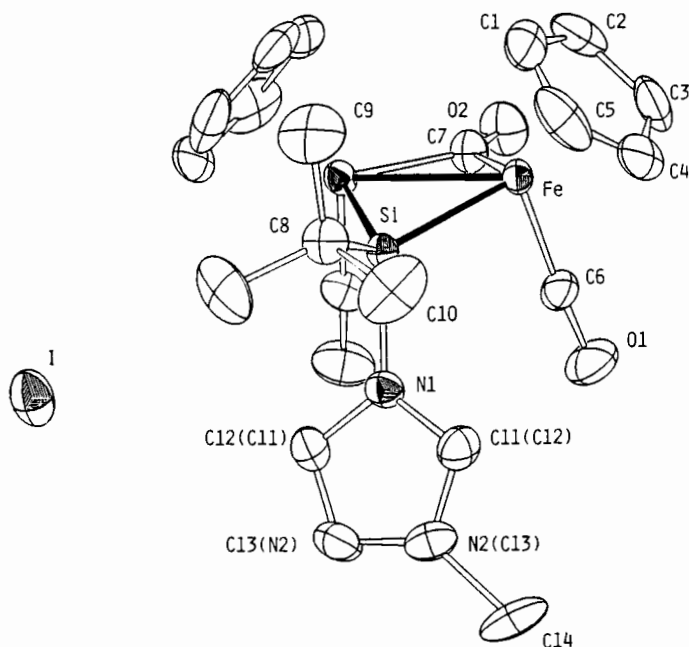
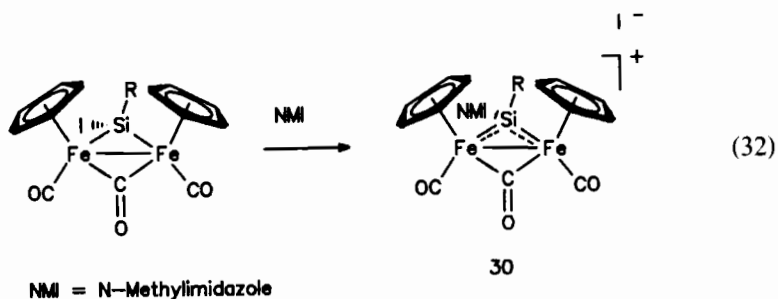
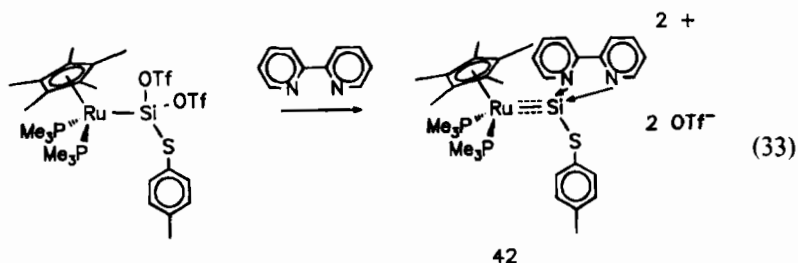


FIG. 18. ORTEP view of $[\text{Cp}_2\text{Fe}_2(\text{CO})_3(\mu\text{-Si-}i\text{-C}_4\text{H}_9) \times \text{NMI}]$ **30** (NMI is *N*-methylimidazole). Important bond distances in angstrom: Fe–Si 2.262 (2), Si–N 1.885 (7). Reprinted with permission of Ogino *et al.* (12).

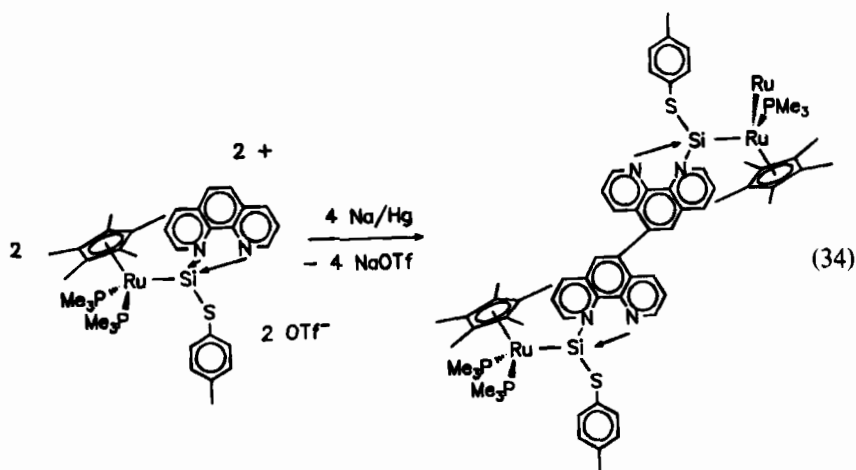
Å; the Si–N distance is only a partly bonding of 1.885 (7) Å. The ^{29}Si NMR signal of $\mathbf{30}^+ \times \text{CH}_3\text{N}$ appears at 251.5 ppm (Fig. 18):



A silylyne complex with a formally terminal $\equiv\text{SiR}$ unit $[\text{Cp}^*(\text{Me}_3\text{P})_2\text{Ru-Si}(\text{bipy})\text{STol}]^{2+} 2 \text{CF}_3\text{SO}_2^-$ **42** has been synthesized by displacement reaction of triflate with bipyridine. The Ru–Si bond length in the complex is 2.269 (5) Å, with the distances Si–N1 1.91 (1) and Si–N (2) 1.95 (1) Å:



Attempts to reduce the phenanthroline analog of **42** with Na/Hg lead to the reductive coupling of two complexes via the C atoms of the phenanthroline units. The product has been characterized by a preliminary X-ray crystal structure determination (13):



VI

SILAETHENE COMPLEXES

The first silaethene complex was characterized by Wrighton *et al.* in a matrix (8a). Stable complexes were finally obtained with the Ru complex $\text{Cp}^*(i\text{-Pr}_3\text{P})\text{HRuCH}_2\text{SiPh}_2$ **26** and the Ir compound $\text{Cp}^*(\text{Me}_3\text{P})\text{IrCH}_2\text{SiPh}_2$ **43** (Si-C 1.810 Å, sum of C-Si-C bond angles at Si 341°) (6). The synthesis of these complexes was performed by an analogous method to Wrightons original route to $\text{CpH}(\text{CO})\text{FeCH}_2\text{SiMe}_2$ by photochemical CO cleavage from the precursor complex and insertion of the 16e-metal fragment into the Si-H bond.

These complexes should have an interesting chemistry, which has yet to be explored. Furthermore, the compounds are important in the context of catalytic carbosilane formation and polymerization reactions.

Berry *et al.* recently isolated a stable silaethene complex of tungsten $\text{Cp}_2\text{WCH}_2\text{SiMe}_2$ **25**. An X-ray structure determination revealed the bond distances W–Si 2.534 (2) Å, W–C 2.329 (7) Å, Si–C 1.800 (8) Å, with a distorted (348.0°) tetrahedral coordination sphere at the silicon atom. The (DEPT)- ^{29}Si NMR shift is -15.7 ppm with $^1J(^{183}\text{W}^{29}\text{Si}) = 57.1$ Hz. The complex shows interesting reactions with ethylene, phosphine, MeOH, HX, etc., some of them undergoing ring slippage of the Cp ring. These have been summarized recently (6).

VII

SILAIMINE COMPLEXES

The first η^2 -silaimine complex $\text{Cp}_2(\text{Me}_3\text{P})\text{ZrN}(t\text{-Bu})\text{SiMe}_2$ **27** has recently been prepared by Berry and co-workers by addition of $\text{LiCH}_2\text{SiMe}_3$ to $\text{Cp}_2\text{ZrIN-}t\text{-BuSiMe}_2\text{H}$ in the presence of Me_3P , followed by the elimination of SiMe_4 from $\text{Cp}_2\text{Zr}(\text{CH}_2\text{SiMe}_3)(\text{N-}t\text{-BuSiMe}_2\text{H})$. A single-crystal X-ray structure determination shows a short Zr–Si bond of 2.654 (1) Å and a long Si–N bond of 1.687 (3) Å. The compound is highly reactive; the reactions have been partly summarized (6,9). Related systems should have an enormous potential, especially for the catalytic polymerization of monomeric SiN precursors and the design of new ceramic materials.

VIII

DISILAETHENE COMPLEXES

Disilene complexes have been observed at low temperatures in solution as intermediates of the reaction of $\text{Hg}(\text{CF}_3\text{COO})_2$ with $\text{Mes}_2\text{Si}=\text{SiMes}_2$ and *cis/trans*-*t*-BuMesSi=SiMes-*t*-Bu. The complexes decompose under expulsion of Hg and stereoselective formation of the silanes R,R/S,S; R,S/S,R $\text{CF}_3\text{COO}(t\text{-Bu})\text{MesSi-SiMes}(t\text{-Bu})\text{OOCF}_3$ (10a). Furthermore, stable π complexes of $\text{Mes}_2\text{Si}=\text{SiMes}_2$ from reactions with $\text{Pt}(\text{Et}_3\text{P})_3$ have been reported (10b). The results of an X-ray structure analysis of a stable disilaethene complex of tungsten $\text{Cp}_2\text{WSiMe}_2\text{SiMe}_2$ by Berry *et al.* show a bond distance W–Si of 2.606 (2) Å and a Si–Si bond length of 2.260 (2) Å (10d). This compound is interesting starting material for reactivity stud-

ies on coordinated disilenes, inclusive catalytic reactions, and reactions for the formation of new polymeric materials.

IX

SILATRIMETHYLENEMETHANE COMPLEXES

A η^4 complex of silatrimethylenemethane $\{\text{Mes}_2\text{SiC}[\text{CH}(t\text{-Bu})]\text{CH}_2\}$ $\text{Fe}(\text{CO})_3$ **29** was synthesized by Ando and co-workers by reaction of a silirane with diironenneacarbonyl. The silatrimethylenemethane ligand is coordinated in a η^4 mode to the $\text{Fe}(\text{CO})_3$ unit with a Fe–Si bond distance of 2.422 (2) Å and a Si–C bond length of 1.899 (8) Å. The coordination geometry at the central C atom is slightly pyramidalized so that the ligand has an umbrella-like shape (11).

X

METALLASILAALENES

Silaallene systems have been sought for a long time. Some reaction products of lithium organyls RLi with siladiimide, siladiphosphide, and silaallene have been characterized by spectroscopic methods (64). With the complexes $(\text{CO})_4\text{M}=\text{Si}(\text{HMPA})_2=\text{M}(\text{CO})_4$ ($\text{M} = \text{Fe}$ **16**, Ru **31**) the isolation and structural characterization (for $\text{M} = \text{Fe}$) of a HMPA adduct to a ferrasilallene has been undertaken with Fe–Si bond lengths of 2.339 (1) Å and 2.341 (1) Å and a Fe–Si–Fe bond angle of 122.6 (1)°. The Si–O distances are 1.745 (7) and 1.748 (3) Å with a bond angle O1–Si–O2 of 92.1 (1)°. These features support a description of the system as a base adduct of metallasilallene, with the $[(\text{OC})_4\text{Fe}=\text{Si}=\text{Fe}(\text{CO})_4]$ unit being isolobal to $\text{H}_2\text{C}=\text{C}=\text{CH}_2$. The silicon atom can formally be considered as zero valent. A qualitative description of the bonding in $[(\text{CO})_4\text{M}=\text{Si}=\text{M}(\text{CO})_4]$ ($\text{M} = \text{Fe}, \text{Ru}$) requires interaction of two occupied sp -hybridized (a) orbitals at silicon(0) with an empty d_z^2 (a) orbital of the two $\text{Fe}(\text{CO})_4$ units and a dative interaction from each $\text{Fe}(\text{CO})_4$ fragment via occupied d_{xz} and d_{yz} (b) orbitals of the metal with two empty p (b) orbitals at silicon. The electronic and coordinative unsaturation of this linear array leads to the coordination of two additional donor molecules (Fig. 19).

An exploration of the chemistry of these complexes (source of Si) will be of great interest (14).

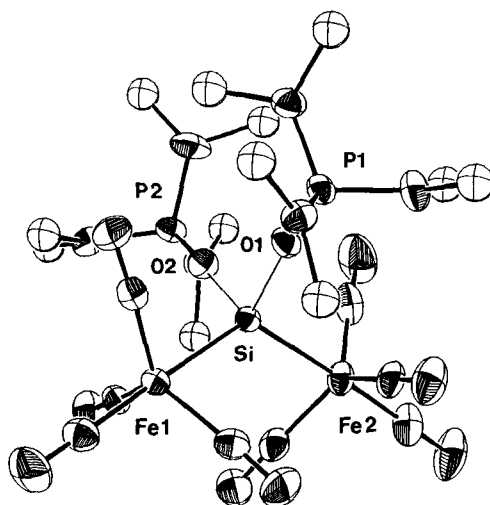


FIG. 19. ORTEP view of $(\text{CO})_4\text{Fe}=\text{Si}(\text{HMPA})_2=\text{Fe}(\text{CO})_4$ **16**. Important bond distances in angstrom: Fe1–Si 2.339 (1), Fe2–Si 2.341 (1), Si–O1 1.745 (2), Si–O2 1.748 (3). Bond angle Fe1–Si–Fe2 122.6 (1)°, O1–Si–O2 92.1 (1)°. Reprinted with permission from Zybilla *et al.* (14).

XI

PROSPECTS

Since the first discovery in 1987, silaorganometallic chemistry with subvalent silicon ligands has developed almost explosively and the number of publications and scientific meetings related to this subject is still increasing exponentially. Nevertheless, only the first basic principles have been revealed so far and numerous surprising new molecules, reactions, etc., are still likely to be discovered. Silaorganometallic chemistry is extraordinarily important since it provides a missing link between the traditional areas of organic and inorganic chemistry. The implications for material science, microelectronics, and surface science are numerous and are already beginning to take shape.

ACKNOWLEDGMENTS

The author's (C.Z.) work in this field has been financed by Deutsche Forschungsgemeinschaft, Fonds der Chemischen Industrie, and Technische Universität München. Furthermore, the author (C.Z.) is indebted to Professor W. A. Herrmann for support and to Professor

N. Auner for a collaboration on a project. Professor H. Schmidbaur encouraged us with helpful comments. One of us (H.B.F.) thanks the Alexander von Humboldt foundation (1992/1993).

REFERENCES

- (1) West, R. *Angew. Chem.* **1987**, *99*, 1231; *Angew. Chem., Int. Ed. Engl.* **1987**, *26*, 1201; West, R.; Fink, M. J.; Michl, J. *Science* **1981**, *214*, 1343; **1984**, *225*, 1109; Fink, M. J.; Michalczyk, M. J.; Haller, K. J.; West, R.; Michl, J. *Organometallics* **1984**, *3*, 793; West, R. *Pure Appl. Chem.* **1984**, *56*, 163; Masamune, S.; Tobita, H.; Murakami, S. *J. Am. Chem. Soc.* **1983**, *105*, 6524; Michalczyk, M. J.; West, R.; Michl, J. *Organometallics* **1985**, *4*, 826.
- (2) Brook, A. G.; Baines, K. M. *Adv. Organometal. Chem.* **1986**, *25*, 1; Brook, A. G.; Nyberg, S. C.; Abdesaken, F.; Gutekunst, B.; Gutekunst, G.; Kallury, R. K. M. R.; Poon, Y. C.; Chang, Y. M.; Wong-Ng, W. J. *J. Am. Chem. Soc.* **1982**, *104*, 5667; Wiberg, N.; Wagner, G.; Reber, G.; Riede, J.; Müller, G. *Organometallics* **1987**, *6*, 35; Baines, K. M.; Brook, A. G.; Ford, R. R.; Lickiss, P. D.; Saxena, A. K.; Chatterton, W. J.; Sawyer, J. F.; Behnam, B. A. *ibid.* **1989**, *8*, 693.
- (3a) Zybill, C.; Müller, G. *Angew. Chem.* **1987**, *99*, 683; *Angew. Chem., Int. Ed. Engl.* **1987**, *26*, 669.
- (3b) Zybill, C.; Müller, G. *Organometallics* **1988**, *7*, 1368.
- (3c) Zybill, C.; Wilkinson, D. L.; Leis, C.; Müller, G. *Angew. Chem.* **1989**, *101*, 206, *Angew. Chem., Int. Ed. Engl.* **1989**, *28*, 203.
- (3d) Leis, C.; Zybill, C.; Lachmann, J.; Müller, G. *Polyhedron* **1991**, *10*, 1163.
- (3e) Handwerker, H.; Leis, C.; Gamper, S.; Zybill, C. *Inorg. Chim. Acta* **1992**, *200*, 763.
- (3f) Probst, R.; Leis, C.; Gamper, S.; Herdtweck, E.; Auner, N.; Zybill, C. *Angew. Chem.* **1991**, *103*, 1155; *Angew. Chem., Int. Ed. Engl.* **1991**, *30*, 1132.
- (3g) Leis, C.; Wilkinson, D. L.; Handwerker, H.; Zybill, C.; Müller, G. *Organometallics* **1992**, *11*, 514.
- (3h) Zybill, C. *Angew. Chem.* **1992**, *104*, 180; *Angew. Chem., Int. Ed. Engl.* **1992**, *31*, 173.
- (3i) Handwerker, H.; Leis, C.; Probst, R.; Bissinger, P.; Grohmann, A.; Kiprof, P.; Herdtweck, E.; Blümel, J.; Auner, N.; Zybill, C. *Organometallics* **1993**, *12*, 2162.
- (3j) Petrova-Koch, V.; Zybill, C. *Angew. Chem.* **1993**, *105*, 887; *Angew. Chem., Int. Ed. Engl.* **1993**, *32*, 845.
- (4a) Zybill, C.; Leis, C.; Handwerker, H. *Chem. Rev.* **1993**, *93*, in press.
- (4b) Zybill, C. *Top. Curr. Chem.* **1991**, *160*, 1.
- (4c) Zybill, C. *Nachr. Chem., Tech. Lab.* **1989**, *37*, 248.
- (5a) Straus, D. A.; Zhang, C.; Quimbila, G. E.; Grumbine, S. D.; Heyn, R. H.; Tilley, T. D.; Rheingold, A. L.; Geib, S. J. *J. Am. Chem. Soc.* **1990**, *112*, 2673.
- (5b) Straus, D. A.; Tilley, T. D.; Rheingold, A. L.; Geib, S. J. *Am. Chem. Soc.* **1987**, *109*, 5872.
- (6) Tilley, T. D. In "The Silicon-Heteroatom Bond": Patai, S.; Rappoport, Z., Eds.; Wiley: New York, 1991, 309.
- (7a) Tobita, H.; Ueno, K.; Shimoi, M.; Ogino, H. *J. Am. Chem. Soc.* **1990**, *112*, 3415.
- (7b) Ueno, K.; Tobita, H.; Shimoi, M.; Ogino, H. *J. Am. Chem. Soc.* **1988**, *110*, 4092.
- (7c) Ueno, K.; Hamashina, N.; Shimoi, M.; Ogino, H. *Organometallics* **1991**, *10*, 959.
- (7d) Takeuchi, T.; Tobita, H.; Ogino, H. *Organometallics* **1991**, *10*, 835.
- (7e) Ueno, K.; Hamashina, N.; Ogino, H. *Organometallics* **1992**, *11*, 1435.
- (7f) Koe, J. R.; Tobita, H.; Ogino, H. *Organometallics* **1992**, *11*, 2479.

- (8a) Randolph, C. L.; Wrighton, M. S. *Organometallics* **1987**, *6*, 365.
- (8b) Campion, B. K.; Heyn, R. H.; Tilley, T. D. *J. Am. Chem. Soc.* **1988**, *110*, 7558.
- (8c) Campion, B. K.; Heyn, R. H.; Tilley, T. D. *J. Am. Chem. Soc.* **1990**, *112*, 4079.
- (8d) Koloski, T. S.; Carroll, P. J.; Berry, B. H. *J. Am. Chem. Soc.* **1990**, *112*, 6405.
- (9) Procopio, L. J.; Carroll, P. J.; Berry, D. H. *J. Am. Chem. Soc.* **1991**, *113*, 1870.
- (10a) Zybilla, C.; West, R. *J. Chem. Soc., Chem. Commun.* **1986**, 857.
- (10b) Pham, E. K.; West, R. *J. Am. Chem. Soc.* **1989**, *111*, 7667.
- (10c) Pham, E. K.; West, R. *Organometallics* **1990**, *9*, 1517.
- (10d) Berry, D. H.; Chey, J. H.; Zipin, H. S.; Carroll, P. J. *J. Am. Chem. Soc.* **1990**, *112*, 6405.
- (11) Ando, W.; Yamamoto, T.; Saso, H.; Kabe, Y. *J. Am. Chem. Soc.* **1991**, *113*, 2791.
- (12) Kawano, Y.; Tobita, H.; Ogino, H. *Angew. Chem.* **1991**, *103*, 877; *Angew. Chem., Int. Ed. Engl.* **1991**, *30*, 843.
- (13) Grumbine, S. D.; Chadha, R. K.; Tilley, T. D. *J. Am. Chem. Soc.* **1992**, *114*, 1518.
- (14) Zybilla, C.; Wilkinson, D. L.; Müller, G. *Angew. Chem.* **1988**, *100*, 574; *Angew. Chem., Int. Ed. Engl.* **1988**, *27*, 583.
- (15a) Brown-Wensley, K. A. *Organometallics* **1987**, *6*, 1590.
- (15b) Speier, J. L. *Adv. Organomet. Chem.* **1977**, *17*, 407.
- (16) Henge, E.; Weinberger, M. *J. Organomet.* **1993**, *443*, 167.
- (17) Curtis, M. D.; Epstein, P. S. *Adv. Organomet. Chem.* **1981**, *19*, 213; Cundy, C. S.; Kingston, B. M.; Lappert, M. F. *ibid.* **1973**, *11*, 253; Büchner, W. *J. Organomet. Chem. Lib* **1980**, *9*, 409; Yamamoto, K.; Okinoshima, H.; Kumada, J. *J. Organomet. Chem.* **1971**, *27*, C31; Ojima, I.; Inaba, S. I.; Kogure, T.; Nagai, Y. *ibid.* **1973**, *55*, C7; Kumada, M. *ibid.* **1975**, *100*, 127; Seyferth, D.; Shannon, M. L.; Vick, S. C.; Lim, T. F. O. *Organometallics* **1985**, *4*, 57; Okinoshima, H.; Yamamoto, K.; Kumada, M. *J. Am. Chem. Soc.* **1972**, *94*, 9263; Sakurai, H.; Kamiyama, Y.; Nakadaira, Y. *ibid.* **1977**, *99*, 3879.
- (18) Clarke, M. P.; Davidson, I. M. T. *J. Organomet. Chem.* **1991**, *408*, 149.
- (19) Kang, H.; Jacobson, D. B.; Shin, S. K.; Beauchamp, J. L.; Bowers, M. T. *J. Am. Chem. Soc.* **1986**, *108*, 5668.
- (20) Veprek, S.; Prokop, J.; Zybilla, C. *J. Phys. Chem.* **1993**, in press.
- (21) Wang, Y. *Acc. Chem. Res.* **1991**, *24*, 133.
- (22) Aylett, B. J. *J. Organomet. Chem. Lib.* **1978**, *9*, 327.
- (23) Yamashita, H.; Tanaka, M.; Goto, M. *Organometallics* **1992**, *11*, 3227.
- (24) Schubert, U.; Scholz, G.; Müller, J.; Ackermann, K.; Wörle, B.; Stansfield, R. F. D. *J. Organomet. Chem.* **1986**, *306*, 303; Hart-Davies, A. J.; Graham, W. A. G. *J. Am. Chem. Soc.* **1971**, *93*, 4388; Schubert, U.; Müller, J.; Alt, H. G. *Organometallics* **1987**, *6*, 469; Luo, X. L.; Crabtree, R. H. *J. Am. Chem. Soc.* **1989**, *111*, 2527; Rabaa, H.; Saillard, J. Y.; Schubert, U. *J. Organomet. Chem.* **1987**, *330*, 397; Lichtenberger, D. L.; Rai-Chaudhuri, A. *J. Am. Chem. Soc.* **1989**, *111*, 3583; **1990**, *112*, 2492.
- (25) Corriu, R. J. P.; Lanneau, G.; Priou, C. *Angew. Chem.* **1991**, *103*, 1153; *Angew. Chem., Int. Ed. Engl.* **1991**, *30*, 1130.
- (26) Harrod, J. F.; Ziegler, T.; Tschinke, V. *Organometallics* **1990**, *9*, 897.
- (27) Woo, L. K.; Smith, D. A.; Young, V. G., Jr. *Organometallics* **1991**, *10*, 3977; Seyferth, D.; Annarelli, D. C.; Vick, S. C.; Duncan, D. P. *J. Organomet. Chem.* **1980**, *201*, 179. (The mechanism of silylene transfer reactions from siliranes may also involve radical species.)
- (28) Jutzi, P.; Kanne, D.; Krüger, C. *Angew. Chem.* **1986**, *98*, 163; *Angew. Chem., Int. Ed. Engl.* **1986**, *25*, 164.
- (29) Puranik, D. B.; Fink, M. J. *J. Am. Chem. Soc.* **1989**, *111*, 5951.

- (30) Jutzi, P.; Möhrke, A. *Angew. Chem.* **1990**, *102*, 913; *Angew. Chem., Int. Ed. Engl.* **1990**, *29*, 893.
- (31) Horng, K. M.; Wang, S. L.; Liu, C. S. *Organometallics* **1991**, *10*, 631.
- (32) Corriu, R. J. P.; Lanneau, G. F.; Chauhan, B. P. *Organometallics* **1993**, *12*, 2001.
- (33) Harrod, J. F.; Mu, Y.; Samuel, E. *Polyhedron* **1991**, *10*, 1239; Tanaka, M. 24th ACS-Organosilicon Symposium, El Paso, 1991.
- (34) Zarate, E. A.; Tessier-Youngs, C.; Youngs, W. J. *J. Am. Chem. Soc.* **1988**, *110*, 4068.
- (35) Pannell, K. H.; Cervantes, J.; Hernandez, C.; Cassias, J.; Vincenti, S. *Organometallics* **1986**, *5*, 1056; Pannell, K. H.; Castillo-Ramirez, J.; Cervantes-Lee, F. *ibid.* **1992**, *11*, 3139.
- (36) Tilley, T. D. *Comments Inorg. Chem.* **1990**, *10*, 37; Woo, H. G.; Tilley, T. D. *J. Am. Chem. Soc.* **1989**, *111*, 3757; Woo, H. G.; Walzer, J. F.; Tilley, T. D. *ibid.* **1992**, *114*, 7047; Tilley, T. D. *Acc. Chem. Res.* **1993**, *26*, 22; Forsyth, C. M.; Nolan, S. P.; Marks, T. J. *Organometallics* **1991**, *10*, 2543.
- (37) Hengge, E.; Weinberger, M.; Jammegg, C. *J. Organomet. Chem.* **1991**, *410*, C1.
- (38) Blinka, T. A.; Helmer, B. J.; West, R. *Adv. Organomet. Chem.* **1984**, *23*, 193; Krentz, R.; Pomeroy, R. K. *Inorg. Chem.* **1985**, *24*, 2976.
- (39a) Márquez, A.; Sanz, J. F. *J. Am. Chem. Soc.* **1992**, *114*, 2903.
- (39b) Cundari, T. R.; Gordon, M. S. *J. Phys. Chem.* **1992**, *96*, 631.
- (40) Cundari, T. R.; Gordon, M. S. *Organometallics* **1992**, *11*, 3122.
- (41) This work has been done in cooperation with Professor G. Auner.
- (42) Corriu, R. J. P.; Priou, C. 9th International Symposium on Organo-silicon Chemistry, Edinburgh, 1990; p. 2–25.
- (43) Carré, F.; Cerveau, G.; Chuit, C.; Corriu, R. J. P.; Réyé, C. *Angew. Chem.* **1989**, *101*, 474; *Angew. Chem., Int. Ed. Engl.* **1989**, *28*, 489.
- (44) Jastrzebski, J. T. B. H. Ph.D. Thesis, Rijksuniversiteit te Utrecht, **1991**; Jastrzebski, J. T. B. H.; van der Schaaf, P. A.; Boersma, J.; van Koten, G.; Zoutberg, M. C.; Heijdenrijk, D. *Organometallics* **1989**, *8*, 1373; Jastrzebski, J. T. B. H.; van der Schaaf, P. A.; Boersma, J.; van Koten, G.; de Ridder, D. J. A.; Heijdenrijk, D. *Organometallics* **1992**, *11*, 1521.
- (45) According to ^{29}Si NMR data (-58.2 ppm), $2\text{-Me}_2\text{NCH}_2\text{-C}_6\text{H}_4\text{SiCl}_3$ has a pentacoordinated silicon atom (CDCl_3) at 22°C .
- (46) Hexacoordination has been established in silicon chemistry by Corriu and co-workers. For hexacoordinated silanes with naphthylaminosilanes, an intramolecular rearrangement has been observed: Brelière, C.; Carré, F.; Corriu, R. J. P.; Poirier, M.; Royo, G.; Zwecker, J. *Organometallics* **1989**, *8*, 1831; Brelière, C.; Corriu, R. J. P.; Royo, G.; Zwecker, J. *ibid.*, 1834; for a summary, see Corriu, R. J. P. *Pure Appl. Chem.* **1988**, *60*, 99.
- (47) Corriu, R. J. P. Münchner Silicontage, Aug. 1992; Plenary Lect. No. 1.
- (48) Colomer, E.; Corriu, R. J. P. *Top. Curr. Chem.* **1981**, *96*, 79; Colomer, E.; Corriu, R. J. P.; Lheureux, M. *Chem. Rev.* **1990**, *90*, 265.
- (49) Covalent bond length N–Si as quoted in Procopio *et al.* (9).
- (50) Maier, G.; Reisenauer, H. P.; Schöttler, K.; Wessolek-Kraus, U. *J. Organomet. Chem.* **1989**, *366*, 25.
- (51) In toluene as solvent **12** has no N \rightarrow Si donor contact and the silicon atom is threecoordinated at r.t. (^1H NMR, ^{29}Si NMR 138.8 ppm).
- (52) A C_2 -symmetrical conformer may also be a local minimum (or saddle point) on the energy hypersurface; however, a solution of this problem so far can only be obtained by extended *ab initio* calculations

- (53) An investigation of the system by molecular dynamics methods will provide further information.
- (54) Abicht, H. P.; Jurkschat, K.; Tzschach, A.; Peters, K.; Peters, E. M.; von Schnering, H. G. *J. Organomet. Chem.* **1987**, 326, 357.
- (55) Handwerker, H.; Paul, M.; Blümel, J.; Zybill, C. *Angew. Chem.* **1993**, 105, 1375; *Angew. Chem., Int. Ed. Engl.* **1993**, 32, 1313.
- (56) Handwerker, H.; Paul, M.; Riede, J.; Zybill, C. *J. Organomet. Chem.* **1993**, in press.
- (57) Grumbine, S. D.; Tilley, T. D.; Rheingold, A. J. *Am. Chem. Soc.* **1993**, 115, 358.
- (58) Grumbine, S. D.; Tilley, T. D.; Rheingold, A. L.; Arnold, F. P. *Science* **1993**, submitted for publication.
- (59) Handwerker, H.; Beruda, H.; Kleine, M.; Zybill, C. *Organometallics* **1992**, 11, 3542.
- (60) Pannell, K. H.; Lin, S. H.; Kapoor, R. N.; Cervantes-Lee, F.; Pinon, M.; Parkanyi, L. *Organometallics* **1990**, 9, 2454.
- (61) Pannell, K. H.; Rozell, J. M.; Hernandez, C. J. *Am. Chem. Soc.* **1989**, 111, 4482.
- (62) Haynes, A.; George, M. W.; Haward, M. T.; Poliakoff, M.; Turner, J. J.; Boag, N. M.; Green, M. J. *Am. Chem. Soc.* **1991**, 113, 2011.
- (63) Tobita, H.; Ueno, K.; Ogino, H. *Chem. Lett.* **1986**, 1777.
- (64) Armitage, D. A. In "The Silicon-Heteroatom Bond"; Patai, S.; Rappoport, Z., Eds.; Wiley: New York, 1991, 151.

Organometallic Chemistry of the Lanthanides

COLIN J. SCHAUVERIEN

Koninklijke/Shell Laboratorium, Amsterdam (Shell Research B.V.)
1031CM Amsterdam
The Netherlands

I. Introduction	283
II. Homoleptic Alkyl Complexes	286
III. Alkoxides	289
IV. Thiolates	293
V. Selenides and Tellurolates	293
VI. Nitrogen Donor Ligands	294
A. Porphyrins	294
B. Other Nitrogen Donors	299
VII. π Adducts	301
VIII. π -Arene Complexes	304
IX. Cyclooctatetraene Complexes	307
X. Carboranes	309
XI. Heterocyclopentadienyls	310
XII. Monocyclopentadienyl Complexes	310
XIII. Bis(cyclopentadienyl) Complexes	322
XIV. Bis(cyclopentadienyl) Ligand Variations	333
XV. Reactivity of $(C_5Me_5)_2Ln$ with Aluminum/Gallium Reagents	338
XVI. Isocarbonyls and Lanthanide Transition Metal Bonds	340
XVII. γ -C-H-Ln versus β -Si-Me-Ln Interactions	341
XVIII. Thermodynamics	343
XIX. Low-Oxidation-State Chemistry	344
XX. Tris(cyclopentadienyl)	347
XXI. Tetravalent Organolanthanide Chemistry	350
XXII. Conclusions	351
XXIII. Appendix: Abbreviations	351
References	352

INTRODUCTION

This review is intended to cover developments in organolanthanide chemistry since the review by Evans (1) in 1985. A number of general (2,3) as well as more specialized reviews on organolanthanide chemistry, including low-oxidation-state lanthanides (4), thermochemistry (5), bonding (6), C-H activation (7,8), and structural trends in bis(C_5Me_5) lanthanide complexes (9) have appeared in this period. A recent volume of *Inorganic*

Synthesis (10) covers the preparation of a range of useful organolanthanide starting materials. As well as the lanthanides, this review covers, where appropriate, relevant organoscandium and organoyttrium chemistry. These M^{3+} metals often display analogous chemistry and for comparison purposes, particularly in $(C_5Me_5)_2MR$ chemistry, are included in the scope of this review. Although of undoubted importance, solid-state lanthanide chemistry (11), as well as the gas-phase reactivity (12) of lanthanide ions with small molecules and lanthanide metals intercalated in fullerenes (13), are considered to be outside the scope of this review.

The lanthanide metals are characterized by high electropositivity (hence electrophilicity) and the ability to support high coordination numbers (8 to 12) and coordinative unsaturation. The $4f$ valence orbitals of the lanthanides probably do not protrude significantly beyond the filled $5s^2 5p^6$ orbitals. As a consequence of this limited radial extension, their interaction with ligand orbitals is less than that in transition metal chemistry. For this reason, the chemistry of the lanthanides is predominantly ionic, and governed more by electrostatic factors and steric requirements, than by filled orbital considerations. The gradual decrease in ionic radius and the limited radial extension of the valence orbitals are manifested in subtle differences in chemistry observed for complexes having different metals but analogous ligand environments. For example, one would not expect to see similar chemical environments progressing from Ti to Ni, but such chemical conformity is observed in the lanthanide series. The high charge to ionic radius ratio results in an electropositive metal center that is extremely susceptible, given the steric unsaturation, to heteroatom donor ligands. It behaves thus as a large Lewis acid. As is ubiquitously observed, water is particularly deleterious.

Furthermore, there is just one thermodynamically favorable oxidation state for the lanthanides (commonly Ln^{3+}). Cerium is unique in that it possesses an accessible $4+$ oxidation state. Other accessible nontrivalent oxidation states are Sm^{2+} ($4f^6$), Eu^{2+} ($4f^7$), and Yb^{2+} ($4f^{14}$). The effective eight-coordinate ionic radius (14) of Ln^{3+} is relatively large and gradually decreases from 1.16 Å for La^{3+} to 0.977 Å for Lu^{3+} . Nontrivalent oxidation states and their corresponding ionic radii are Ce^{4+} , 0.97; Sm^{2+} , 1.27; Eu^{2+} , 1.25; and Yb^{2+} , 1.14 Å. For Sc^{3+} and Y^{3+} these are 0.87 and 1.019 Å, respectively. Only Sm^{2+}/Sm^{3+} and Ce^{3+}/Ce^{4+} have more than one energetically accessible oxidation state. The valence state difference is, however, one, rather than the prerequisite two necessary for oxidation addition/reductive elimination. The consequence of thermodynamic stability associated with just one preferred oxidation state is that two-electron redox shuttles such as oxidative addition and reductive elimination are prohibited. The lanthanides are therefore compelled, in contrast to the transition

metals (d^n , $n \neq 0, 1$), to react with polar (i.e., alkane C–H bonds) and nonpolar (i.e., H_2) X–H bonds via a concerted σ -bond metathesis mechanism. These concerted, bimolecular reactions possess highly ordered four-centered transition states and generally have a large negative value for ΔS^\ddagger .

That lanthanide chemistry has not attracted the same attention as the transition metals is, perhaps, not surprising. Organolanthanide complexes are typically extremely air and moisture sensitive, and this, coupled with their oxophilic nature, prohibits purification by chromatography. Due to the small crystal field splitting, diamagnetic organolanthanide complexes are usually white, colors arising from forbidden $4f \rightarrow 4f$ transitions, and show little variation with ligand substitutions. This does not lend itself to separation techniques. Instead, reactions and appropriate reagents must be judiciously chosen so that one (major) product is synthesized, which can then be purified by (fractional) crystallization, or sublimation. Furthermore, these complexes are tolerant of only a limited range of solvents, this generally being confined to hydrocarbons, aromatics, and ethers. The paramagnetic elements have Laporte allowed $4f \rightarrow 5d$ transitions and have intense, variable colors that can change significantly as a consequence of ligand substitution, a clear synthetic advantage. The paramagnetism associated with many of the metals has inhibited, but certainly not prohibited, characterization by NMR spectroscopy. As this accessible, and rapid, spectroscopic technique is currently one of the favorite characterization methods, it is no surprise that many researchers have opted to investigate the chemistry of diamagnetic Y^{3+} , La^{3+} , Yb^{2+} , and Lu^{3+} . Interpretable and diagnostic, albeit paramagnetically shifted, NMR spectra for Ce^{3+} , Nd^{3+} , and $Sm^{3+/2+}$ can, however, be obtained.

As in early transition metal chemistry, β -hydrogen elimination is a common decomposition pathway. For this reason, use of the alkyl groups Me, and especially the bulky $CH(SiMe_3)_2$, have been predominant. The alkyl groups CH_2CMe_3 , CH_2SiMe_3 , and CH_2Ph , although frequently employed in early transition metal chemistry, have been less extensively utilized, possibly due to their lack of steric hindrance compared with $CH(SiMe_3)_2$. The $CH(SiMe_3)_2$ group has proved vital for the preparation of neutral, salt-free, and solvent-free precursors from which hydrides can be cleanly accessed by facile hydrogenation.

The stabilization of organolanthanide species has relied on π -donating ligands, especially cyclopentadienyl, or its pentamethyl analog. In the absence of one (or more) of these bulky ligands stability has been primarily achieved by use of chelates, or of neutral bases to increase the coordination number. In this respect, it is pertinent to note that coordination of alkali-metal halides is a ubiquitous, if undesirable, phenomenon, arising as a

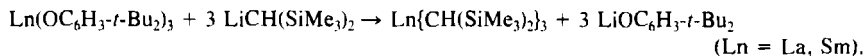
consequence of general synthetic procedures involving alkylation. This metathetical reaction of a lanthanide metal halide with (typically) a lithium alkyl results, dependent on the metal and steric bulk of its ancillary ligands, in coordination of MX to the highly electrophilic lanthanide metal.

Finally, because of the plethora of literature published (1985–1993) in this expanding field, it has not been my intention to provide a totally comprehensive survey. I have, however, attempted to address the trends that have prevailed since 1985, and to emphasize synthesis, reactivity and structure relationships.

II

HOMOLEPTIC ALKYL COMPLEXES

The stabilization of organolanthanide complexes has long relied on cyclopentadienyl ligands. In the absence of such ligands, stability has been achieved by use of chelating ligands or Lewis bases, including salt coordination, to increase the metal coordination number. Lanthanide complexes containing only alkyl ligands have been known for some time, although these have, until recently, been exclusively anionic. For example, these include $[\text{Li}(\text{THF})_4][\text{Ln}(t\text{-Bu})_4]$ ($\text{Ln} = \text{Sm}, \text{Eu}, \text{Lu}$) (15), $[\text{Li}(\text{THF})_4][\text{Lu}(\text{C}_6\text{H}_3-2, 6\text{-Me}_2)_4]$ (16), $\text{La}[(\mu\text{-Me})_2\text{Li}(\text{TMEDA})]_3$ (17), and $[\text{Lu}\{(\mu\text{-Me})_2\text{Li}(\text{TMEDA})_2\}(\mu\text{-Me})]_2$ (18). Ingenious synthetic methodology utilizing an alkyl ligand containing a pendant chelating group has been a successful way of preparing neutral alkyl species such as $\text{Lu}\{\text{C}_6\text{H}_4(\text{CH}_2\text{NMe}_2-2)\}_3$ (19), $\text{La}\{\text{CH}(\text{PPh}_2)_2\}_3$ (20), and $\text{Sc}\{\text{CH}(\text{SiMe}_2\text{C}_6\text{H}_4-2\text{-OMe})_2\}_3$ (21). In comparison with $\text{Y}(\text{CH}_2\text{SiMe}_3)_3(\text{THF})_2$ (22), coordinated THF is not necessary to stabilize $\text{Y}\{\text{CH}(\text{SiMe}_3)_2\}_3$ (22), because of the larger alkyl group. The synthesis of the first neutral homoleptic lanthanide (La–Lu) alkyl species (23) has been achieved by use of this bulky alkyl group, in conjunction with a bulky alkoxide as a “noncoordinating” leaving group:



These isostructural compounds possess a pyramidal, rather than trigonal, planar coordination geometry at the metal with $\text{La-C} = 2.515 \text{ \AA}$ and $\text{Sm-C} = 2.33 \text{ \AA}$ (Fig. 1). This deviation from planarity was proposed to minimize ligand–ligand nonbonding interactions, as well as to maximize (intramolecular) secondary C–H–Ln agostic stabilization of the electronically and coordinatively unsaturated metal center. Short $\text{Ln} \cdots \text{Me}$ γ -agostic interactions ($\text{La}, 3.121 \text{ \AA}$; $\text{Sm}, 2.85 \text{ \AA}$) were observed. $\text{Ln}\{\text{CH}$

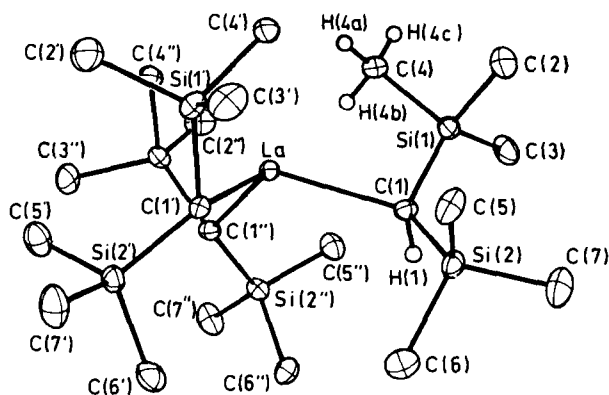
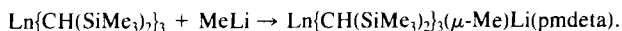


FIG. 1. Molecular structure of $\text{La}\{\text{CH}(\text{SiMe}_3)_2\}_3$. [Reproduced with permission from the Royal Society of Chemistry; from Hitchcock *et al.* (23).]

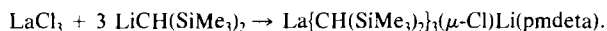
$(\text{SiMe}_3)_2\}_3$ ($\text{Ln} = \text{Y}, \text{Lu}$) (24) have also been prepared in an analogous fashion. Although highly susceptible to protonolysis by (sterically hindered) amines or phenols, to give LnX_3 ($\text{Ln} = \text{Sm}$; $\text{X} = \text{N}(\text{SiMe}_3)_2$, $\text{OC}_6\text{H}_3\text{-}t\text{-Bu}_2$) (23), $\text{Ln}\{\text{CH}(\text{SiMe}_3)_2\}_3$ is unreactive toward olefins, presumably because of the absence of a kinetically accessible initiation pathway. Although such species have potential synthetic utility via mild protonolysis to other lanthanide alkyl species, problems associated with disproportionation of $\text{Ln}\{\text{CH}(\text{SiMe}_3)_2\}_2\text{X}_2$ arise, unless X_2 is chelating [i.e., porphyrins (24) or alkoxide (25) ligands—*vide infra*].

$\text{Ln}\{\text{CH}(\text{SiMe}_3)_2\}_3$ ($\text{Ln} = \text{La}, \text{Sm}$) (23) can be alkylated by MeLi in ether in the presence of pm deta to afford the anionic “mixed” alkyl species $\text{Ln}\{\text{CH}(\text{SiMe}_3)_2\}_3(\mu\text{-Me})\text{Li}(\text{pm deta})$ (26):



This is the first example of a lanthanide complex, albeit anionic, possessing different alkyl groups, and is a rare example of a singly alkyl-bridged lithium species. The X-ray crystal structure of the Sm compound (26) shows an almost linear, asymmetric $\text{Sm-Me} \dots \text{Li}$ bridge (174°) with short Sm-Me (2.33 Å) and long Me-Li (2.42 Å) distances.

In continuing this theme, reaction of LaCl_3 with $\text{LiCH}(\text{SiMe}_3)_2$ (3 eq) in THF affords $\text{La}\{\text{CH}(\text{SiMe}_3)_2\}_3(\mu\text{-Cl})\text{Li}(\text{pm deta})$ (27), after addition of pm deta :



The La-Cl-Li bridge is almost linear (165.1°) with strong La-Cl (2.762 Å) and Li-Cl (2.28 Å) interactions. The metal environment in $\text{Ln}\{\text{CH}(\text{Si-}$

$\text{Me}_3)_2\}_3$ (23) allows coordination of the $(\mu\text{-X})\text{Li}(\text{pmdeta})$ ($\text{X} = \text{Cl}, \text{Me}$) moieties without significant distortion of the original $\text{Ln}\{\text{CH}(\text{SiMe}_3)_2\}_3$ coordination geometry. Related ionic $[\text{Li}(\text{THF})_4][\text{Yb}\{\text{CH}(\text{SiMe}_3)_2\}_3\text{Cl}]$ (28) has been structurally characterized.

Interesting differences are observed if alkylation is performed without strongly coordinating donor ligands. Reaction of LuCl_3 with the kinetically more reactive $\text{KCH}(\text{SiMe}_3)_2$ (3 eq) obviates the need for THF as solvent and in ether affords $\text{Lu}\{\text{CH}(\text{SiMe}_3)_2\}_3(\mu\text{-Cl})\text{K}(\text{ether})$ (29) (Scheme 1). This

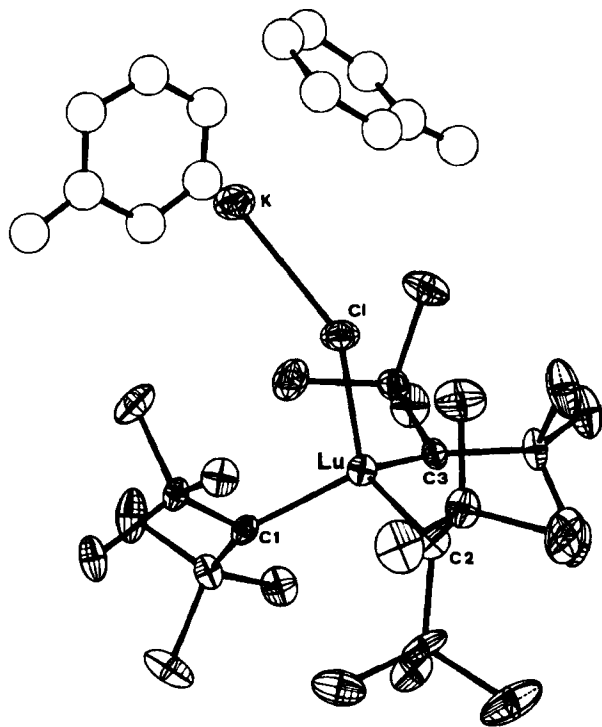
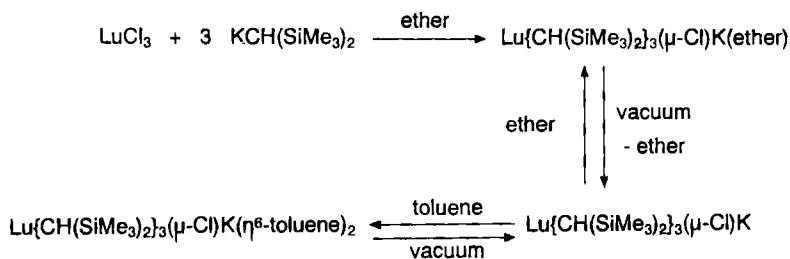


FIG. 2. Molecular structure of $\text{Lu}\{\text{CH}(\text{SiMe}_3)_2\}_3(\mu\text{-Cl})\text{K}(\eta^6\text{-C}_7\text{H}_8)_2$. [Reprinted with permission from Schaverien and Van Mechelen (29). Copyright (1991) American Chemical Society.]

can also be prepared by utilizing the electrophilicity of the Lu center by reaction of KCl with $\text{Lu}\{\text{CH}(\text{SiMe}_3)_2\}_3$ in ether. Coordination of KCl to $\text{Lu}\{\text{CH}(\text{SiMe}_3)_2\}_3$ (and to ether) compensates for the KCl lattice energy. Coordinated ether can be readily removed under vacuum to afford $\text{Lu}\{\text{CH}(\text{SiMe}_3)_2\}_3(\mu\text{-Cl})\text{K}$. Addition of even weakly coordinating solvents, such as ether or toluene, results in their coordination to potassium, to afford hydrocarbon soluble monomeric species $\text{Lu}\{\text{CH}(\text{SiMe}_3)_2\}_3(\mu\text{-Cl})\text{K}(\text{L})$ (L = ether or $(\eta^6\text{-C}_7\text{H}_8)_2$), respectively (Fig. 2). η^6 -Coordination of toluene (3.003 and 3.128 Å from the ring centroids to K) is best regarded as an induced dipole interaction (30), although still possessing predominantly ionic character (ionic radius: K^+ , 1.33 Å; half Van der Waals thickness of benzene ring, 1.70 Å). In contrast to the essentially linear Ln-X-Li unit in $\text{Ln}\{\text{CH}(\text{SiMe}_3)_2\}_3(\mu\text{-X})\text{Li}(\text{pmdeta})$ (26,27), the Lu-Cl-K unit is significantly perturbed from linearity (145.9°).

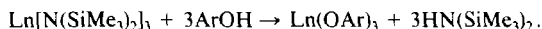
III

ALKOXIDES

The chemistry of the simple, sterically undemanding alkoxide and aryloxides (i.e., OMe, O-*i*-Pr, OPh) of Sc, Y, and the lanthanides has long been established (31–33). These species were typically insoluble in hydrocarbons, involatile, and generally considered to be polymeric. However, the small (chelating) alkoxide $\text{OCH}_2\text{CH}_2\text{OMe}$ allowed formation of a cyclic decamer $[\text{Y}(\text{OCH}_2\text{CH}_2\text{OMe})_3]_{10}$ (34) with well-defined stoichiometry.

Use of bulky aryloxides, typically O-2,6- C_6H_3 -*t*-Bu₂ (and to a much lesser extent bulky alkoxides, i.e., OC-*t*-Bu₃) has resulted in the preparation of monomeric, hydrocarbon-soluble $\text{Ln}(\text{OR})_2$ and $\text{Ln}(\text{OR})_3$ (35). Recently, such compounds have attracted attention due to their use as halide-free precursors, and their use has also been stimulated by the search for molecular precursors for the assembly of preceramic oxide aggregates, precursors to MOCVD, and to sol-gel techniques.

Homoleptic tris-alkoxides have usually been synthesized by straightforward protonolysis of $\text{Ln}[\text{N}(\text{SiMe}_3)_2]_3$ (36) with the alcohol (3 eq):



In this way, aryloxides $[\text{Y}(\text{OSiPh}_3)_3]_n$ (37) and $\text{Ce}(\text{O-2,6-C}_6\text{H}_3\text{-}t\text{-Bu}_2)_3$ (38), as well as their Lewis base adducts, have been prepared and structurally characterized. Thermolysis of monomeric $\text{Ce}(\text{OC-}t\text{-Bu}_3)_3$ (39) (prepared from $\text{Ce}[\text{N}(\text{SiMe}_3)_2]_3$ and $\text{HOC-}t\text{-Bu}_3$) afforded isobutylene and $[\text{Ce}(\text{OCH-}t\text{-Bu}_2)_3]_2$. This was structurally characterized and shown to be a dimer with alkoxide bridges (39).

A metathesis route has been used to prepare monomeric, structurally characterized $\text{Y}(\text{OC}_6\text{H}_3\text{-}t\text{-Bu}_2)_3$ (40), $\text{Y}(\text{OC}_6\text{H}_3\text{Me}_2)_3(\text{THF})_2$ (41), and dimeric $\text{Y}_2(\text{OC}_6\text{H}_3\text{Me}_2)_6(\text{THF})_2$ (41), this series demonstrating the influence of ligand bulk on metal coordination number. Use of less bulky alkoxide ligands results in the isolation of aggregates $\text{M}_5\text{O}(\text{O-}i\text{-Pr})_{13}$ (42) ($\text{M} = \text{Sc}, \text{Y}, \text{Yb}$) and $\text{Y}_3(\text{O-}t\text{-Bu})_8(\text{Cl})(\text{THF})_2$ (43). Addition of excess of a smaller alcohol in the protonolysis of $\text{M}[\text{N}(\text{SiMe}_3)_2]_3$ results in its coordination to the electrophilic metal in $\text{M}_2(\text{O-}t\text{-Bu})_9(t\text{-BuOH})_2$ ($\text{M} = \text{Y}, \text{La}$) (44). With larger alcohols the dimers $[\text{M}(\text{OR})_3]_2$ ($\text{M} = \text{Y}, \text{La}$; $\text{R} = \text{CMe}_2\text{-}i\text{-Pr}, \text{CMeEt-}i\text{-Pr}$; $\text{M} = \text{Y}, \text{R} = \text{CEt}_3$) were obtained. Unlike trigonal planar $\text{Sc}(\text{O-}2,6\text{-}t\text{-Bu}_2\text{-}4\text{-MeC}_6\text{H}_2)_3$ (35) and $\text{Y}(\text{OC}_6\text{H}_3\text{-}t\text{-Bu}_2)_3$ (40), the Ce analog has a pyramidal structure, as does $\text{M}[\text{N}(\text{SiMe}_3)_2]_3$ and $\text{Ln}\{\text{CH}(\text{SiMe}_3)_2\}_3$ (23). Reaction of the sterically hindered, phosphine-functionalized alkoxide ligands $[\text{Li}(\mu\text{-OC-}t\text{-Bu}_2\text{CH}_2\text{PMe}_2)]_2$ with LnCl_3 ($\text{Ln} = \text{Y}, \text{Nd}$) afforded the first crystallographically authenticated homoleptic alkoxide (as opposed to aryloxide) complex $\text{Ln}(\mu\text{-OC-}t\text{-Bu}_2\text{CH}_2\text{PMe}_2)_3$ (45). The three chelating phosphines are weakly coordinated to the lanthanide center. Monomeric $\text{Nd}(\text{OC-}t\text{-Bu})_3(\text{THF})$ was synthesized from $\text{Nd}[\text{N}(\text{SiMe}_3)_2]_3(\text{THF})_2$ and $\text{HOC-}t\text{-Bu}_3$ (46). Similarly, monomeric solvent-free $\text{Nd}(\text{OC-}t\text{-Bu})_3$, $\text{Nd}(\text{OSi-}t\text{-Bu}_3)_3$, and $\text{M}(\text{OCH-}t\text{-Bu}_2)_3$ ($\text{M} = \text{Nd}, \text{Dy}$) have been prepared from $\text{M}[\text{N}(\text{SiMe}_3)_2]_3$ and the corresponding alcohol (46). Until recently, only tris-alkoxides (of the trivalent lanthanides) have been prepared. Interestingly, reaction of $\text{NdCl}_3(\text{THF})_2$ with just 2 eq of $\text{LiOC-}t\text{-Bu}_3$ gave the chloro-bridged dimer $[(t\text{-Bu}_3\text{CO})_2\text{Nd}(\mu\text{-Cl})(\text{THF})]_2$ (47) (Fig. 3).

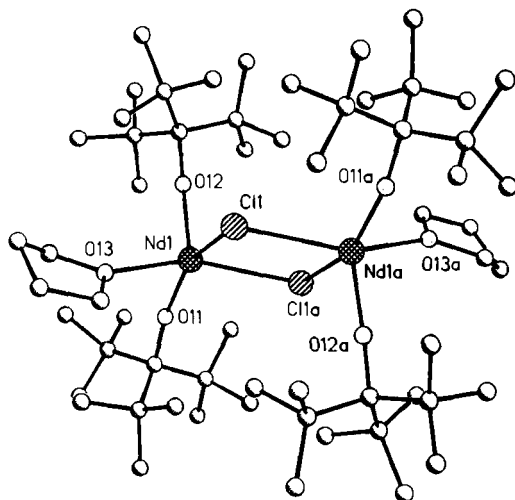


FIG. 3. Molecular structure of $[(t\text{-Bu}_3\text{CO})_2\text{Nd}(\mu\text{-Cl})(\text{THF})]_2$. [Reproduced with permission from VCH Verlagsgesellschaft; from Wedler *et al.* (47).]

There are few well-defined, hydrocarbon-soluble Ln^{II} complexes known. Monomeric Yb^{II} aryloxides have been prepared. Treatment of $\text{Yb}(\text{OAr}')_2(\text{OEt}_2)_2$ ($\text{Ar}'\text{O} = \text{O}-2,6\text{-C}_6\text{H}_2\text{-}t\text{-Bu}_2\text{-4-Me}$), prepared from addition of the phenoxide to $\text{Yb}[\text{N}(\text{SiMe}_3)_2]_2(\text{OEt}_2)_2$ in ether, with THF (2 eq or excess) affords $\text{Yb}(\text{OAr}')_2(\text{THF})_n$ ($n = 2$ or 3 , respectively) (48). Both $\text{Yb}(\text{OAr}')_2\text{L}_2$ ($\text{L} = \text{OEt}_2, \text{THF}$) display a distorted tetrahedral geometry at Yb, whereas $\text{Yb}(\text{OAr}')_2(\text{THF})_3$ is distorted square planar with two phenoxide oxygens and with two THF oxygens occupying the basal plane. A weak $\text{Yb} \cdots \text{Me}$ interaction (3.424 \AA) was observed. In comparison, the trisphenoxide $\text{Ce}(\text{O}-2,6\text{-C}_6\text{H}_3\text{-}t\text{-Bu}_2)_3(\text{CN-}t\text{-Bu})_2$ has a trigonal bipyramidal ligand arrangement (39).

Treatment of Yb metal with benzophenone in THF/hmpa afforded dimeric $[\text{Yb}(\mu\text{-}\eta^1, \eta^2\text{-OCPh}_2)(\text{hmpa})_2]_2$ (49), in which the benzophenone dianion bridges using both the alkoxide oxygen and the adjacent carbon. Reaction with $\text{HO}-2,6\text{-C}_6\text{H}_2\text{-}t\text{-Bu}_2\text{-4-Me}$ affords monomeric $\text{Yb}(\text{O}-2,6\text{-C}_6\text{H}_2\text{-}t\text{-Bu}_2\text{-4-Me})_2(\text{hmpa})_2$. Both compounds were crystallographically characterized.

In contrast to the synthetic methods described above, reaction of NdCl_3 with the smaller (relative to $\text{O}-2,6\text{-C}_6\text{H}_3\text{-}t\text{-Bu}_2$) phenoxide $\text{KO}-2,6\text{-C}_6\text{H}_3\text{-}i\text{-Pr}_2$ in THF affords the salt $\text{K}[\text{Nd}(\text{OC}_6\text{H}_3\text{-}i\text{-Pr}_2)_4]$ (50). X-ray crystallographically indicates a one-dimensional infinite chain of alternating $\text{Nd}(\text{OC}_6\text{H}_3\text{-}i\text{-Pr}_2)_4$ anions and potassium cations, which is supported by unusual $\eta^6\text{-aryl}$ interactions to K^+ between neighboring ions (Fig. 4).

Despite the well-established compatibility of alkoxides with high-valent transition metals, alkoxides, in the absence of the C_5Me_5 ligand, have been rarely used in lanthanide chemistry to support lanthanide-alkyl bonds. Because of problems associated with alkoxide exchange, or disproportionation of $\text{Ln}(\text{OR})_x\text{X}_{3-x}$, **chelating** alkoxides have been used to prepare discrete mononuclear lanthanide alkyl species. For example, reaction of $\text{La}\{\text{CH}(\text{SiMe}_3)_2\}_3$ (23) with $\text{HOC}_6\text{H}_3\text{-}t\text{-Bu}_2$ (2 eq), or reaction of $\text{La}(\text{OC}_6\text{H}_3\text{-}$

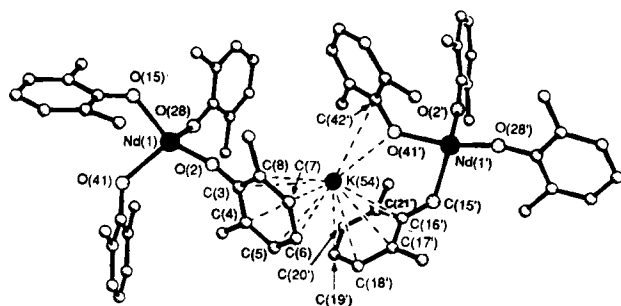
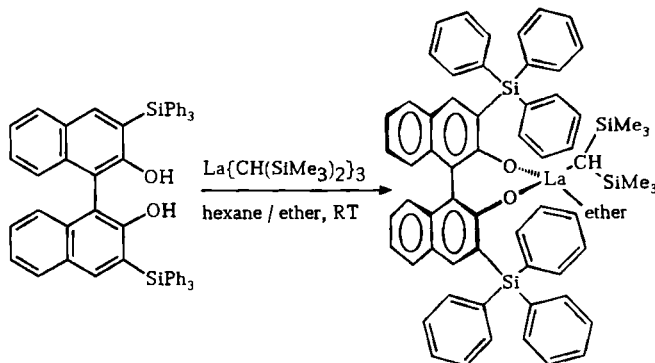


FIG. 4. Molecular structure of $\text{K}[\text{Nd}(\text{OC}_6\text{H}_3\text{-}i\text{-Pr}_2)_4]$. [Reprinted with permission from Clark *et al.* (50). Copyright (1992) American Chemical Society.]

$t\text{-Bu}_2)_3$ with $\text{LiCH}(\text{SiMe}_3)_2$ (1 eq) affords only a complex mixture of products. Mild protonolysis of $\text{La}\{\text{CH}(\text{SiMe}_3)_2\}_3$ (23) with sterically hindered, racemic, chelating biphenols and binaphthols afforded $\text{La}\{\text{CH}(\text{SiMe}_3)_2\}\{2,2'-(\text{OC}_6\text{H}_2-t\text{-Bu}_2-4,6)_2\}$ and $\text{La}\{\text{CH}(\text{SiMe}_3)_2\}\{1,1'\{2-\text{OC}_{10}\text{H}_5\text{SiPh}_3\}_2\}(\text{OEt}_2)$ (25), respectively (Scheme 2). Their intrinsic chirality is reflected



in two diastereotopic SiMe_3 ^1H , ^{13}C NMR resonances being observed. The bis-phenoxide is sterically quite undemanding, allowing coordination of three facial THFs (Fig. 5).

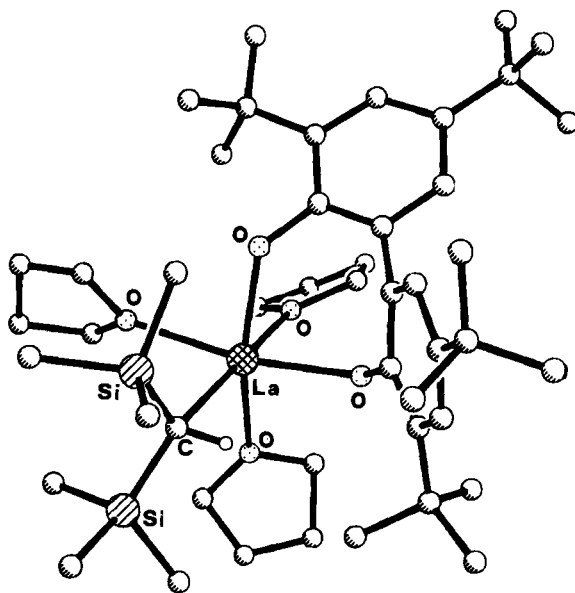


FIG. 5. Molecular structure of $\text{La}\{\text{CH}(\text{SiMe}_3)_2\}(\text{OC}_6\text{H}_2-t\text{-Bu}_2-4,6)_2(\text{THF})_3$. [Reproduced with permission from the Royal Society of Chemistry; from Schaverien *et al.* (25).]

The reactivity of organolanthanide complexes with CO has been less well studied than their actinide (51) or early transition metal counterparts. $(C_5Me_5)_2NdCH(SiMe_3)_2$ (52) reacts with CO to give a dimeric dionediolate structure $[(C_5Me_5)_2Nd(CO)_2CH(SiMe_3)_2]_2$ (52). In contrast, $(O-O)La\{CH(SiMe_3)_2\}(OEt_2)$ ($(O-O) = (C_{10}H_5SiPh_3O)_2$) reacts selectively with excess CO to give the enolate $(O-O)La\{OC(SiMe_3) = CHSiMe_3\}$ via 1,2-SiMe₃ migration from $(O-O)La\{\sigma, \eta^2-OCCH(SiMe_3)_2\}$. Similar SiMe₃ migratory insertion reactions promoted by CO insertion have been observed (53) in actinide and early transition metal chemistry. The yttrium enolate $[(MeC_5H_4)_2Y(\mu-OCH = CH_2)]_2$ has been structurally characterized (54).

IV

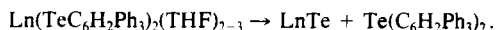
THIOLATES

In contrast to the range of discrete, mononuclear lanthanide alkoxides, the first neutral lanthanide thiolates $Sm(S-2,4,6-C_6H_2-t-Bu_3)_3$ and $Yb(S-2,4,6-C_6H_2-t-Bu_3)_2(dme)_2$ have only recently been prepared (55) by the respective protonation of $Sm\{CH(SiMe_3)_2\}_3$ and $Yb\{N(SiMe_3)_2\}_2(dme)_2$ with the thiol. Both compounds have been structurally characterized. The coordination environment of homoleptic $Sm(S-2,4,6-C_6H_2-t-Bu_3)_3$ is trigonal planar.

V

SELENIDES AND TELLUROLATES

Reaction of $Ln\{N(SiMe_3)_2\}_3$ ($Ln = La, Ce$) with $HTeSi(SiMe_3)_3$ in hexane afforded thermally unstable homoleptic $Ln\{TeSi(SiMe_3)_3\}_3$ (56). Addition of dmpe gave the adduct $Ln\{TeSi(SiMe_3)_3\}_3(dmpe)_2$. Vacuum thermolysis at 600°C gave Ln_2Te_3 . Metathesis of the halides in $LnX_2(THF)_2$ afforded $Ln(E-2,4,6-C_6H_2Ph_3)_2(THF)_2$ ($Ln = Yb, Sm, Eu$; $E = Se, Te$) (57). Pyrolysis in refluxing toluene, or at 250°C in vacuo afforded, after annealing, $LnTe$:



Protonolysis of $(C_5R_5)_2Lu(\mu-Me)_2Li(THF)_2$ ($R = H, Me$) with $t-BuSH$, $PhSeH$, Ph_2PH , and Ph_2AsH afforded $(C_5R_5)_2Lu(\mu-ER)_2Li(THF)_2$ (58), which were characterized by X-ray diffraction. A range of bridging chalcogenides $[(C_5Me_5)_2Yb]_2(\mu-E)$ ($E = S, Se, Te$) (59) can be prepared by reaction of $(C_5Me_5)_2Yb$ with the appropriate reagent, i.e., Ph_3PE ($E = S,$

Se), elemental Se or Te, or *n*-Bu₃PSe. The X-ray crystal structure of [(C₅Me₅)₂Yb]₂(μ-Se) (59) shows a nearly linear (171°) Yb–Se–Yb.

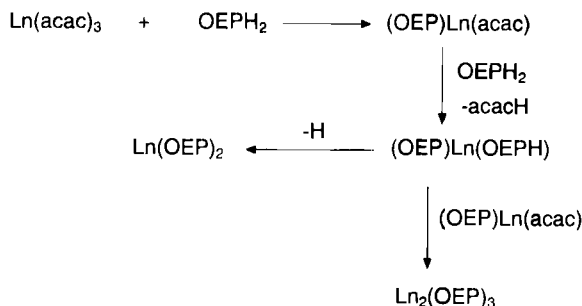
VI

NITROGEN DONOR LIGANDS

A. Porphyrins

The recent growth in organolanthanide chemistry has primarily focused on complexes stabilized by the bis(pentamethylcyclopentadienyl) ligand system although porphyrin complexes of the lanthanides have been comparatively well studied (60–66). However, their organometallic chemistry has, until recently, been limited, despite the seeming compatibility of these large, planar, hard nitrogen donor chelating ligands with the electrophilic lanthanide metals. For example, sandwich-like octaethylporphyrin complexes Ln(OEP)₂ of all lanthanides (60–64) (except Pm) are known, and tetraphenylporphyrin complexes (TPP)Ln(acac) (65) (except Ln = Pm) have also been prepared. Methods of preparation have traditionally involved heating the components in an imidazole melt, or refluxing in 1,2,4-trichlorobenzene, in the presence of an oxidant, often adventitious O₂, followed by column chromatography on alumina.

In this way double-decker complexes Ln(P)₂ and triple-decker (sometimes with mixed porphyrins) Ln₂(P)₂(P') have been prepared. Y(OEP)₂ has also been prepared from (OEP)Y(acac) with Li₂(OEP) (62). The presence of Ln^{III} in Ln(P)₂ requires that one of the porphyrin rings be the normal porphyrinate dianion, while the other is a porphyrinate monoanion radical. An occasionally isolated intermediate, written by porphyrin chemists as LnH(P)₂, is observed. This reacts with Ln(P)(acac) to give the triple-decker Ln₂(P)₃ or is dehydrogenated to the symmetrical double-decker Ln(P)₂. The intermediate is more accurately described as Ln(P)(PH) (66) (Scheme 3).



Refluxing $\text{Eu}(\text{acac})_3$ with excess OEPH_2 in 1,2,4-trichlorobenzene produces a mixture of $\text{Eu}(\text{OEP})_2$ and $\text{Eu}_2(\text{OEP})_3$, which could be separated by chromatography (61). Paramagnetic $\text{Eu}(\text{OEP})_2$ ($\mu_{\text{eff}} = 3.17 \mu_{\text{B}}/\text{Eu}$) was structurally characterized and found to be isostructural with diamagnetic $\text{Ce}(\text{OEP})_2$ (60). The crystal structures display saucer-shaped porphyrins with the metal atom displaced from the N_4 plane and the four nitrogen atoms pointing toward the bottom of the dish with its convexity toward the metal atom. This deformation serves to optimize σ and π bonding between the nitrogen atoms and the large lanthanide metal, as it allows the sp^2 hybrid lone pair to point toward the metal rather than into the N_4 porphyrin plane. Such deformation is commonly observed in porphyrin lanthanide chemistry (67). The mixed complexes $\text{Ce}(\text{OEP})(\text{TPP})$ (67), $\text{Ce}(\text{OEP})(\text{TPP})$ (68), $\text{Eu}(\text{OEP})(\text{TPP})$ (69), and $\text{La}(\text{OEP})(\text{TPP})$ (70) have been published, including the X-ray crystal structure of $\text{Ce}(\text{OEP})(\text{TPP})$ (67) (Fig. 6). Non-porphyrin-containing lanthanide sandwich species include $\text{Lu}(\text{Pc})_2$ (71) and $\text{Nd}_2(\text{Pc})_2(\text{TMPP})$ (72).

The uv-vis spectrum is a useful diagnostic tool. For lanthanide monoporphyrins the Soret band is typically found at ca. 400 nm. For the double- and triple-decker complexes this is hypsochromically shifted to ca. 375–390 nm, indicative of the presence of two (or more) porphyrin rings in a face to face arrangement. ^1H NMR spectroscopy, despite the frequent paramagnetic nature of the lanthanide compounds, has also proved useful. The methyl, methylene, and methine resonances fall in the ranges 1.8–2.0, 4.1–4.5, and 10.0–10.7 ppm, respectively, for diamagnetic mononuclear octaethylporphyrin complexes. In species possessing at least one porphy-

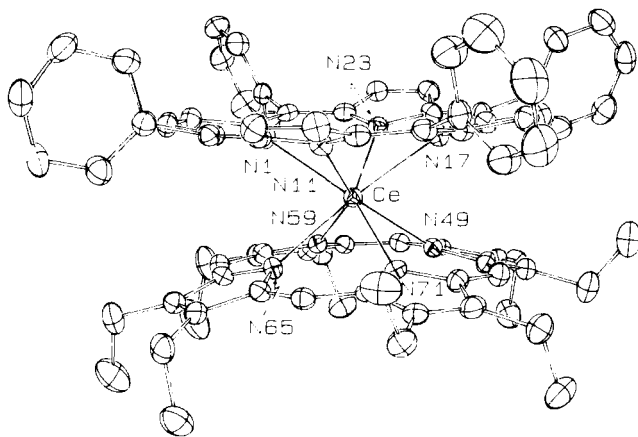


FIG. 6. Molecular structure of $\text{Ce}(\text{OEP})(\text{TPP})$. [Reproduced with permission from VCH Verlagsgesellschaft; from Buchler *et al.* (67).]

rin ring, e.g., $[(P)LnX]_2$, $Ln(P)_2$ (66), and $Ln_2(P)_3$, the methine proton, in particular, is shifted to higher field, e.g., in diamagnetic $[(OEP)LuOH]_2$, δ 9.64; $[(OEP)LuCC^tBu]_2$, δ 9.77; $Ce(OEP)_2$ (60), δ 9.11; and $La_2(OEP)_3$ (61), δ 8.19 ppm, the high field methyne chemical shift being due to the mutual influence of two porphyrin ring currents.

Despite the range of lanthanide metals for which porphyrin complexes are known (60–65), there has been, until recently, no examples that possess a lanthanide–carbon σ bond. Previous preparations have often employed synthetic methods seemingly incompatible with the synthesis of such hydrolytically sensitive species.

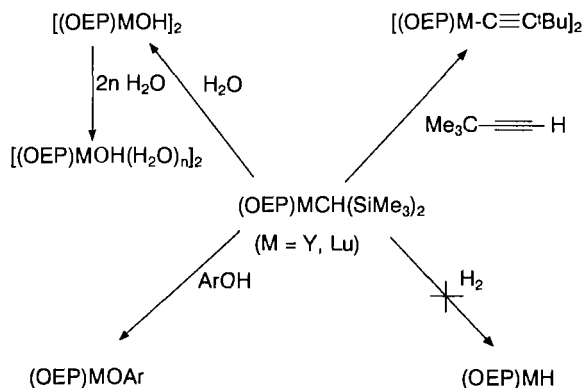
Reaction of a porphyrin (PH_2) with homoleptic solvent-free tris-alkyls $Ln\{CH(SiMe_3)_2\}_3$ or tris-alkoxides $Ln(OAr)_3$ circumvents a stepwise alkylation sequence and avoids salt or solvent coordination. Thus, reaction of MX_3 ($M = Lu$, Y ; $X = CH(SiMe_3)_2$, $O-2,6-C_6H_3-t-Bu_2$) with octaethylporphyrin ($OEPH_2$) in toluene afforded purple $(OEP)MX$ complexes ($M = Lu$, Y ; $X = CH(SiMe_3)_2$, $O-2,6-C_6H_3-t-Bu_2$) (24):



The crystal structure of $(OEP)LuCH(SiMe_3)_2$ showed a highly dished porphyrin skeleton with the square-pyramidal, five-coordinate lutetium atom 0.918 Å out of the N_4 plane of the porphyrin ligand (Fig. 7).

The 1H NMR resonances of axial groups are isotropically shifted due to the ring current of the porphyrin ring. For example, in $(OEP)MCH(SiMe_3)_2$ [$M = Sc$ (73), Y (24), Lu (24)] the $SiMe_3$ and α -CH groups resonate at δ –1.84, –1.78, and –1.76 ppm and δ –5.78, –5.33 ($J_{YH} = 2.5$ Hz), and –5.78 ppm, respectively.

$(OEP)MCH(SiMe_3)_2$ ($M = Y$, Lu) (24) proved to be a versatile starting material for a range of new lutetium porphyrin species (Scheme 4).



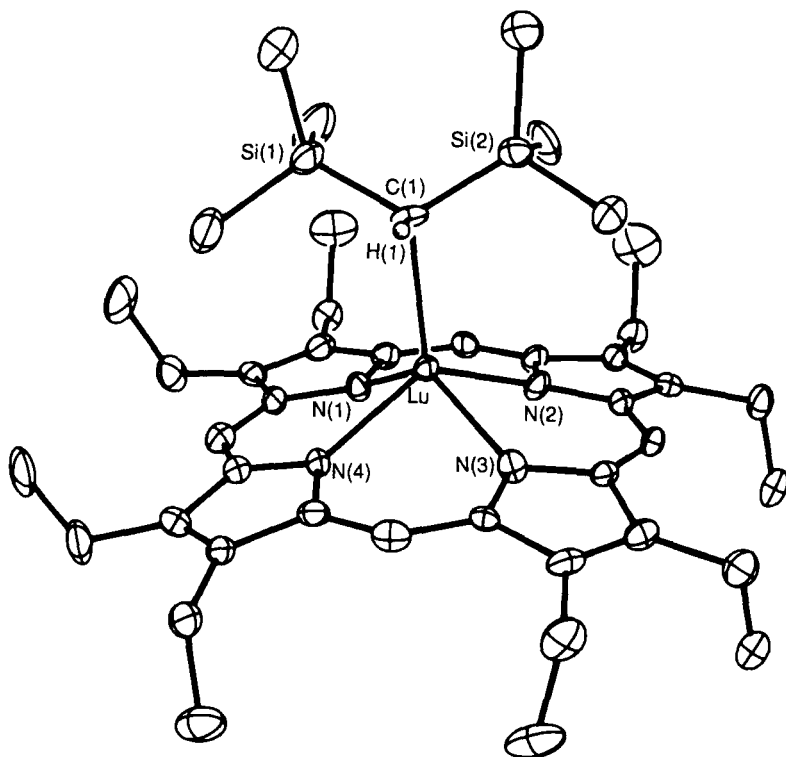


FIG. 7. Molecular structure of $(\text{OEP})\text{LuCH}(\text{SiMe}_3)_2$. [Reprinted with permission from Schaverien and Orpen (24). Copyright (1991) American Chemical Society.]

$(\text{OEP})\text{MCH}(\text{SiMe}_3)_2$ are cleanly hydrolyzed by H_2O (1 eq) to give the hydroxides $[(\text{OEP})\text{M}(\mu\text{-OH})]_2$ ($\text{M} = \text{Lu}, \text{Y}$), rather than bimolecular elimination of water to yield the thermodynamically more stable μ -oxo species [cf. $[(\text{TPP})\text{Sc}]_2(\mu\text{-O})$ (74)]. The unusually high-field chemical shift of the hydroxide (Lu , $\delta -7.18$; Y , $\delta -8.18$ ppm) is due to strong shielding by the porphyrin ring currents. The ^{17}O NMR spectrum of $[(\text{OEP})\text{M}(\mu\text{-}^{17}\text{OH})]_2$ ($\text{M} = \text{Lu}, \text{Y}$) displayed a broad peak at unusually high field ($\delta = 100$ ppm, $\text{M} = \text{Y}$; $\delta = 96$ ppm, $\text{M} = \text{Lu}$).

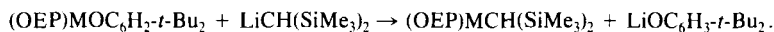
In contrast to the facile hydrogenolysis (σ -bond metathesis) of $(\text{C}_5\text{Me}_5)_2\text{MCH}(\text{SiMe}_3)_2$ [$\text{M} = \text{Y}$ (75), La (51), Nd (51), Ce (76)], $(\text{OEP})\text{MCH}(\text{SiMe}_3)_2$ ($\text{M} = \text{Lu}, \text{Y}$) did not react with H_2 (20 bar). Although, both $(\text{OEP})\text{MCH}(\text{SiMe}_3)_2$ and $\text{M}(\text{C}_5\text{Me}_5)_2\text{CH}(\text{SiMe}_3)_2$ are formally 14-electron species (assuming maximum possible π donation from the porphyrin nitrogen atoms), they possess very different electronic properties and coordination geometries. Bond dissociation enthalpies show that a late transition metal-hydride bond is ca. 20 kcal/mol stronger than the corre-

sponding M-alkyl bond (77). In d^0 transition metal and organolanthanide/actinide complexes this difference $D(\text{Ln-H})-D(\text{Ln-C})$ is reduced to ca. 5 kcal/mol due to the lack of d -electrons that would repel coordinated carbanions (78). From bond dissociation enthalpy data, hydrogenation of $\text{Sm}(\text{C}_5\text{Me}_5)_2\text{CH}(\text{SiMe}_3)_2$ has been calculated (5,79) to be thermoneutral.

The "hard" donor properties and different coordination geometry imposed by the octaethylporphyrin ligand are responsible for this marked difference in reactivity, compared to $\text{Ln}(\text{C}_5\text{Me}_5)_2\text{CH}(\text{SiMe}_3)_2$ (51,75,76). In the series $(\text{C}_5\text{Me}_5)_2\text{LnR}$, $[\text{Me}_2\text{Si}(\text{C}_5\text{Me}_4)_2]\text{LnR}$, $[\text{Et}_2\text{Si}(\text{C}_5\text{Me}_4)(\text{C}_5\text{H}_4)]\text{LnR}$ ($\text{R} = \text{CH}(\text{SiMe}_3)_2$) the decreasing Ln-R hydrogenolysis reactivity was ascribed (5) to reduce charge stabilization at the lanthanide metal in the heterolytic, four-center hydrogenolysis transition state, rather than to thermodynamic factors. Hard, electronegative ancillary ligands weaken Ln-H bonds compared to Ln-alkyl, due to the former's relative thermodynamic instability and to the additional electropositivity of the proximate lanthanide center [compared with its C_5Me_5 counterpart (5)], although the hydride may derive additional stabilization by bridging the electropositive centers. The two β silicons of $\text{CH}(\text{SiMe}_3)_2$ also help to delocalize the partial negative charge, thus increasing the thermodynamic stability of the alkyl.

The influence of ancillary ligands on the propensity for olefin insertion and hydrogenolysis in f -element chemistry has been addressed thermochemically (5) as well as theoretically (80). The additional electrophilicity at Lu, Y induced by the porphyrin ligand [compared to its bis(C_5Me_5) counterparts (51,75,76)] should strengthen M-R relative to M-H. π donation, while undoubtedly possible, is a secondary effect compared with the electronegativity of nitrogen and may not be particularly significant in comparing the influence of a porphyrin (or aryloxide) ligand with C_5Me_5 .

Aryloxides $(\text{OEP})\text{MOC}_6\text{H}_3\text{-}t\text{-Bu}_2$ are precursors useful in preparing alkyl derivatives since loss of inert $\text{LiOC}_6\text{H}_3\text{-}t\text{-Bu}_2$ circumvents problems (2,23) associated with salt coordination:



Reaction of $(\text{OEP})\text{YOC}_6\text{H}_3\text{-}t\text{-Bu}_2$ with MeLi in ether, however, afforded $(\text{OEP})\text{Y}(\mu\text{-Me})_2\text{Li}(\text{OEt}_2)$, which, on treatment with AlMe_3 (2 eq), afforded $(\text{OEP})\text{Y}(\mu\text{-Me})_2\text{AlMe}_2$:



This synthetic methodology parallels that used in the preparation of $[(\text{C}_5\text{Me}_5)_2\text{LuMe}]_2$ (81) (Section XIII). In contrast to the reactivity of $(\text{C}_5\text{R}_5)_2\text{Ln}(\mu\text{-Me})_2\text{AlMe}_2$ (82) (vide infra), reaction of $(\text{OEP})\text{Y}(\mu\text{-$

Me_2AlMe_2 with Lewis bases gave only reversible adduct formation, rather than $\text{Y}(\mu\text{-Me})\text{Al}$ bridge cleavage.

Although insertion of O_2 into early transition metal-alkyl bonds has been studied (83), selective activation of O_2 by lanthanide complexes has not been previously observed, despite their intrinsic oxophilicity and frequently observed decomposition by exposure to oxygen. $(\text{OEP})\text{Y}(\mu\text{-Me})_2\text{AlMe}_2$ selectively reacts with excess O_2 at room temperature to afford only $(\text{OEP})\text{Y}(\mu\text{-OMe})_2\text{AlMe}_2$.

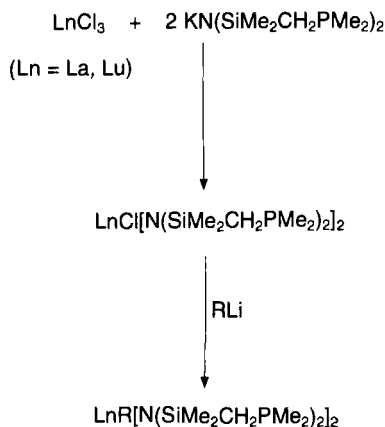
In analogous porphyrin scandium chemistry, reaction of $\text{ScCl}_3(\text{THF})_3$ with $[\text{Li}(\text{THF})_4][\text{Li}(\text{OEP})]$ (62) gave $(\text{OEP})\text{ScCl}$ (73). $(\text{OEP})\text{ScCl}$ is a useful precursor to a variety of five-coordinate alkyl, amide, and alkoxide species $(\text{OEP})\text{ScX}$ $\{\text{X} = \text{CH}(\text{SiMe}_3)_2, \text{N}(\text{SiMe}_3)_2, \text{OSiMe}_3\}$ via metathetical chloride substitution (73). The smaller size of Sc^{3+} , in comparison with Lu^{3+} or Y^{3+} , ensures that LiCl or THF coordination does not play a significant role. The larger lanthanide metals are not so amenable to such synthetic methodology, due to problems associated with salt and donor solvent coordination. Reaction of $(\text{OEP})\text{ScCl}$ with the cyclopentadienyl sources LiC_5H_5 , $\text{NaC}_5\text{H}_4\text{Me}$, and NaC_5Me_5 afforded the cyclopentadienyl complexes, of which for $\text{X} = \text{C}_5\text{H}_5$ the first cyclopentadienyl porphyrin sandwich compound has been structurally characterized. The synthesis of $(\text{TPP})\text{ScCl}$ and $(\text{TPP})\text{ScC}_5\text{Me}_5$ had been previously reported (74).

B. Other Nitrogen Donors

Cocondensation of the vaporized lanthanides Y, Nd, Sm, and Yb with excess $t\text{-BuN}=\text{CH}-\text{CH}=\text{N}-t\text{-Bu}$ ($t\text{-BuDAB}$) afforded the tris-imines $\text{Ln}(\sigma, \sigma\text{-}N, N'\text{-}t\text{-BuDAB})_3$ (84). Although these formally appear to be $\text{Ln}(0)$ compounds, spectroscopic and structural data indicate that they are better regarded as Ln^{3+} salts of the $t\text{-BuDAB}$ radical anion.

YbI_2 reacts with the heteroatom chelate $\text{Li}[\text{Me}_2\text{Si}(\text{O}-t\text{-Bu})(\text{N}-t\text{-Bu})]\{\text{Li}(\text{N}-\text{O})\}$ to give the Yb amide $(\text{N}-\text{O})_2\text{Yb}(\text{THF})_2$ (85), which contains a dative $\text{Yb}-\text{O}$ bond. The preparation and X-ray crystal structures of $\text{Nd}(\text{N}-\text{O})_3$ and $(\text{N}-\text{O})_2\text{Yb}(\mu\text{-Cl})_2\text{Li}(\text{THF})_2$ were also reported.

Fryzuk has utilized the amide $[\text{N}(\text{SiMe}_2\text{CH}_2\text{PMe}_2)_2]^-$, which allowed intramolecular coordination of the pendant phosphine arms to a lanthanide metal (86,87). Hence reaction with MCl_3 ($\text{M} = \text{Y}, \text{Lu}, \text{La}$) affords $\text{MCl}[\text{N}(\text{SiMe}_2\text{CH}_2\text{PMe}_2)_2]_2$ $((\text{N}-\text{P}) = \text{N}(\text{SiMe}_2\text{CH}_2\text{PMe}_2)_2)$ [cf. $\text{Yb}[\text{N}(\text{SiMe}_3)_2]_2(\text{Me}_2\text{PCH}_2\text{CH}_2\text{PMe}_2)$ (88)]. The M-phenyl complexes were synthesized by alkylation. These seven coordinate complexes display, as expected, highly fluxional behavior. A distorted pentagonal bipyramid geometry was favored on the basis of low-temperature ^{31}P NMR spectroscopy (Scheme 5). Hydrocarbyl derivatives $\text{YR}[\text{N}-\text{P}]_2$ ($\text{R} = \text{Ph}, \text{CH}_2\text{Ph}$)



could be prepared; however, their chemistry was dominated by hydrocarbon elimination and formation of the stable cyclometallated product $\text{Y}[\text{N}(\text{SiMe}_2\text{CHPMe}_2)(\text{SiMe}_2\text{CH}_2\text{PMe}_2)][\text{N-P}]$.

Reaction of $\text{YCl}(\text{N-P})_2$ with the allyl Grignard reagent $(\text{C}_3\text{H}_5)\text{MgCl}$ resulted in displacement of one amide-phosphine ligand and afforded the crystallographically characterized dimeric mono(ligand) complex $\{\text{Y}(\eta^3\text{-C}_3\text{H}_5)[\text{N}(\text{SiMe}_2\text{CH}_2\text{PMe}_2)_2](\mu\text{-Cl})_2\}$ (87).

N-silylated benzamidinate ligands are becoming increasingly popular as alternatives to cyclopentadienyl ligands. Anionic $[\text{ArC}(\text{NSiMe}_3)_2]^-$ is easily prepared on a large scale from the corresponding nitrile ArCN and $\text{LiN}(\text{SiMe}_3)_2$. A range of homoleptic lanthanide tris-benzamidinates $[\text{4-R-C}_6\text{H}_4\text{C}(\text{NSiMe}_3)_2]_3\text{Ln}$ ($\text{R} = \text{H, OMe, CF}_3, \text{Ph}$) were prepared by reaction of the sodium benzamidinates with LnCl_3 (89a, 89b). The X-ray crystal structure of $[\text{4-MeOC}_6\text{H}_4\text{C}(\text{NSiMe}_3)_2]_3\text{Pr}$ has been determined. It was concluded that these ligands have steric requirements similar to those of C_5H_5 . Reaction of $\text{NdCl}_3(\text{THF})_2$ with the bulkier 2,4,6-trisubstituted benzamidinate anion $\text{Li}[(\text{CF}_3)_3\text{C}_6\text{H}_2(\text{NSiMe}_3)_2]$ affords the salt complex $[(\text{CF}_3)_3\text{C}_6\text{H}_2(\text{NSiMe}_3)_2]_2\text{Nd}(\mu\text{-Cl})_2\text{Li}(\text{THF})_2$ (89c). This was considered to be a steric substitute for C_5Me_5 (89d).

Tris(pyrazolyl)borates are six-electron donors analogous to the cyclopentadienyl anion. Furthermore, their steric requirements are similar to that of the C_5Me_5 anion. Takats has reported the synthesis of a series of $[\text{HB}(\text{pz})_3]_3\text{M}$ (pz is pyrazolyl) complexes, and crystallographically characterized the eight-coordinate ytterbium complex $[\eta^3\text{-HB}(\text{pz})_3]_2\text{M}[\eta^2\text{-HB}(\text{pz})_3]$ (90). Eight-coordinate bis[hydrotris(pyrazolyl)borato] complexes of the entire lanthanide series $[\text{HB}(\text{pz})_3]_2\text{M}(\text{acac})$ have been prepared, of which the cerium and ytterbium complexes have been structurally characterized (91).

Reaction of YCl_3 with $\text{K}[\text{H}_2\text{B}(3,5\text{-R}_2\text{pz})_2]$ ($\text{R} = \text{H, Me}$) (3 eq) yields the tris(pyrazolyl)borato complexes $\text{Y}[\text{H}(\mu\text{-H})\text{B}(3,5\text{-R}_2\text{pz})_2]_3$ (92). The X-ray crystal structure shows that the six nitrogens are coordinated to yttrium in a trigonal prismatic arrangement with each rectangular face capped by a $\text{B-H} \dots \text{Y}$ agostic interaction. These molecules are fluxional in solution, with the pyrazolyl and BH_2 hydrogen atoms becoming equivalent at 25°C . Reaction of YCl_3 with $\text{K}[\text{HB}(\text{pz})_3]$ (2 eq) in THF affords unsolvated $[\text{HB}(\text{pz})_3]_3\text{YCl}$, which is in a concentration-dependent equilibrium with its dimer (92). In the presence of pyrazolyl as ligand the crystallographically monomeric pyrazolyl adduct is formed.

The amide ligand $\text{N}(\text{SiMe}_3)_2$ has allowed the preparation of salt- and solvent-free hydrocarbon-soluble $\text{Ln}[\text{N}(\text{SiMe}_3)_2]_3$ (36). These have proven to be key synthetic precursors in organolanthanide chemistry. Reaction of LnCl_3 with only two equivalents of $\text{LiN}(\text{SiMe}_3)_2$ in THF affords the dimeric chlorides $\{\text{Ln}[\text{N}(\text{SiMe}_3)_2]_2(\mu\text{-Cl})(\text{THF})\}_2$ ($\text{Ln} = \text{Eu, Gd, Yb}$) (93) and monomeric $\text{Ln}[\text{N}(\text{SiMe}_3)_2]_2\text{Cl}(\text{THF})_2$ ($\text{Ln} = \text{Y}$) (93). The X-ray crystal structures of the Gd and Yb complexes have been determined (94a). These have been utilized for preparation of the corresponding thiolates $\{\text{Ln}[\text{N}(\text{SiMe}_3)_2]_2(\mu\text{-S-}t\text{-Bu})\}_2$ ($\text{Ln} = \text{Eu, Gd, Y}$), unusual examples of relatively soft anionic donors in organolanthanide chemistry. The Gd complex was the first crystallographically characterized lanthanide thiolate complex (94a). $\{\text{Ln}[\text{N}(\text{SiMe}_3)_2]_2(\mu\text{-S-}t\text{-Bu})\}_2$ ($\text{Ln} = \text{Eu, Y}$) can alternately be prepared by reaction of $\text{Ln}[\text{N}(\text{SiMe}_3)_2]_3$ with $t\text{-BuSH}$ (1 eq) at low temperature, disproportionation only becoming significant at $> -10^\circ\text{C}$. Similarly, $\text{Ln}[\text{N}(\text{SiMe}_3)_2]_3$ ($\text{Ln} = \text{La, Eu}$) reacts with Ph_2PH (1 eq) to give the phosphido $\text{Ln}[\text{N}(\text{SiMe}_3)_2]_2\text{PPh}_2$ (94b).

Ammonolysis of melted $\text{Ln}[\text{N}(\text{SiMe}_3)_2]_3$ at 210°C , followed by annealing at 850°C resulted in the crystalline lanthanide nitrides LnN_{1-x} (95) [cf. LnTe (56,57)].

Reaction of $\text{SmI}_2(\text{THF})_2$ with $\text{NaN}(\text{SiMe}_3)_2$ in THF provides $\text{Sm}[\text{N}(\text{SiMe}_3)_2]_2(\text{THF})_2$ (96), which undergoes facile (25°C) conproportionation with $\text{SmI}_2(\text{THF})_2$ (1 eq) in THF/dme to give crystallographically characterized $\{\text{Sm}[\text{N}(\text{SiMe}_3)_2](\mu\text{-I})(\text{dme})(\text{THF})_2\}_2$. $\text{Yb}_2[\text{N}(\text{SiMe}_3)_2]_4$ reacts with AlMe_3 to give $\text{Yb}[\text{N}(\text{SiMe}_3)_2]_2(\text{AlMe}_3)_2$ (97). Two of the silicon methyl groups have short $\text{Yb} \dots \text{C}$ contacts (see Section XVII).

VII

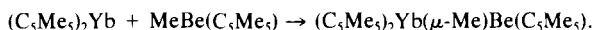
π -ADDUCTS

Organolanthanide complexes are well known to initiate the polymerization of olefins, and, in general, Ln-C bonds undergo facile hydrogenation reactions. In contrast to the wealth of literature pertaining to η^2 olefins,

and more recently, $\eta^2\text{-H}_2$ coordination to the late transition metals, there are only a small number of well-defined examples in d^0 -transition metal and organolanthanide chemistry. Due to the limited radial extension of their $4f$ orbitals, and the highly ionic nature of their bonding, it was thought that neutral hydrocarbons, or nonpolar substrates, would not coordinate to lanthanide centers, where prerequisite $\text{Ln} \rightarrow \text{olefin} (\pi^*)$ or $\text{Ln} \rightarrow \text{H}_2 (\sigma^*)$ is unavailable. Lanthanide metallocenes were shown to be able to act as Lewis acids, but not as π donors, since their HOMOs are too low in energy (98).

The first η^2 -olefin lanthanide complex $(\text{C}_5\text{Me}_5)_2\text{Yb}(\mu\text{-C}_2\text{H}_4)\text{Pt}(\text{PPh}_3)_2$ (99) was prepared by addition of $(\text{C}_5\text{Me}_5)_2\text{Yb}$ (98) to $(\text{C}_2\text{H}_4)\text{Pt}(\text{PPh}_3)_2$ (Fig. 8). The good π -donor $\text{Pt}(\text{PPh}_3)_2$ fragment makes the coordinated ethylene electron rich and maximizes the basicity of the olefin donor orbitals. A similar strategy extended this concept to the preparation and structural characterization of the first η^2 -acetylene lanthanide complex $(\text{C}_5\text{Me}_5)_2\text{Yb}(\text{MeC}\equiv\text{CMe})$ (100). The coordination of both $(\text{C}_2\text{H}_4)\text{Pt}(\text{PPh}_3)_2$ and $\text{MeC}\equiv\text{CMe}$ to $(\text{C}_5\text{Me}_5)_2\text{Yb}$ (98) is weak with little or no π backbonding, and both were regarded as Lewis acid–base adducts.

A substituted methane complex $(\text{C}_5\text{Me}_5)_2\text{Yb}(\mu\text{-Me})\text{Be}(\text{C}_5\text{Me}_5)$ (101) (Fig. 9) was prepared by judicious choice of components, $\text{MeBe}(\text{C}_5\text{Me}_5)$ having an appreciable dipole moment:



The $\mu\text{-Me}$ group geometry, and the essentially linear (177°) $\text{Yb}\text{-Me}\text{-Be}$ angle, is similar to that found in $\text{Li}_4\text{B}_4(\mu\text{-Me})\text{Me}_8$ (102), $(\text{C}_5\text{Me}_5)_2\text{Lu}(\mu\text{-$

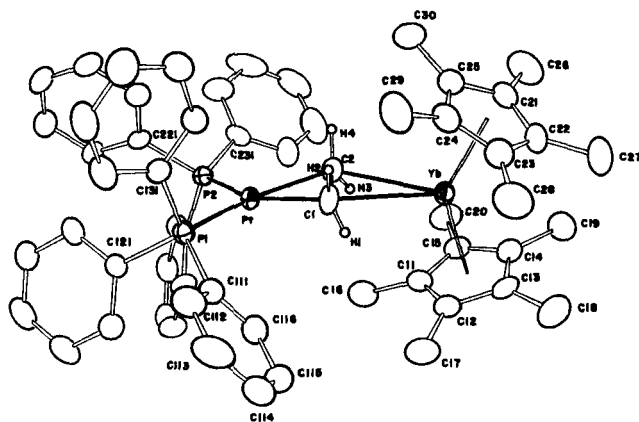


Fig. 8. Molecular structure of $(\text{C}_5\text{Me}_5)_2\text{Yb}(\mu\text{-C}_2\text{H}_4)\text{Pt}(\text{PPh}_3)_2$. [Reprinted with permission from Burns and Andersen (99). Copyright (1987) American Chemical Society.]

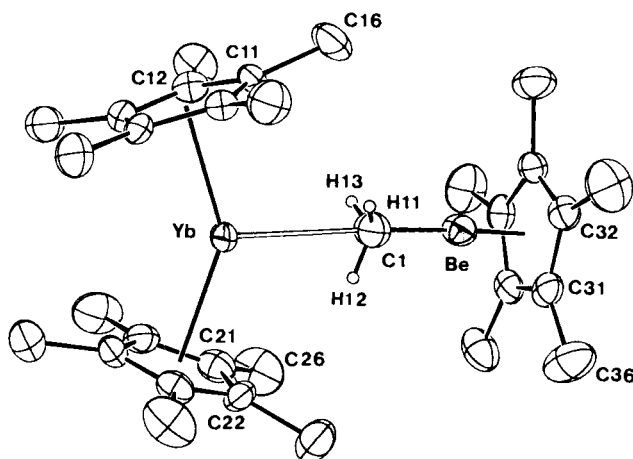


FIG. 9. Molecular structure of $(\text{C}_5\text{Me}_5)_2\text{Yb}(\mu\text{-Me})\text{Be}(\text{C}_5\text{Me}_5)$. [Reprinted with permission from Burns and Andersen (101). Copyright (1987) American Chemical Society.]

$\text{Me})\text{Lu}(\text{Me})(\text{C}_5\text{Me}_5)_2$ (81), the symmetric $\mu\text{-Me}$ in the anion $\{[(\text{C}_5\text{H}_4\text{Me})_3\text{U}]_2(\mu\text{-Me})\}^-$ (103), and with the C_{3v} methyl group in TiMeCl_3 (104).

H_2 and C_2H_4 (presumably η^2) complexes $(\text{C}_5\text{Me}_5)_2\text{Eu.L}$ have been spectroscopically detected (105) by utilization of the paramagnetic Lewis acid $(\text{C}_5\text{Me}_5)_2\text{Eu}$ (106), as a ^1H NMR probe of substrate complexation. Hence incremental addition of $(\text{C}_5\text{Me}_5)_2\text{Eu}$ to solutions of free H_2 or C_2H_4 led to signal broadening and an upfield (H_2) and downfield (C_2H_4) paramagnetic shift of their respective ^1H NMR resonances, indicative of the equilibrium $(\text{C}_5\text{Me}_5)_2\text{Eu} + \text{L} \rightleftharpoons (\text{C}_5\text{Me}_5)_2\text{Eu.L}$. No such paramagnetic shift was observed for CH_4 , indicating negligible interaction with $(\text{C}_5\text{Me}_5)_2\text{Eu}$.

Zero-valent europium–ethylene adducts were prepared by cocondensation of Eu atoms with either neat C_2H_4 or C_2H_4 diluted by a noble gas at 12 K to afford matrix-isolated $\text{Eu}(\text{C}_2\text{H}_4)_n$ (107). These were studied *in situ* by UV and IR spectroscopy. Controlled matrix annealing at 20–40 K resulted in conversion to higher stoichiometry species (increasing n). These species all decomposed readily on warming toward 77 K.

Slow crystallization of $(\text{C}_5\text{Me}_5)_2\text{Sm}$ under N_2 afforded the first organolanthanide dinitrogen complex $(\text{C}_5\text{Me}_5)_2\text{Sm}(\mu\text{-}\eta^2:\eta^2\text{-N}_2)\text{Sm}(\text{C}_5\text{Me}_5)_2$ (108) (Fig. 10). This possesses a side-on, rather than end-on [as in $((\text{C}_5\text{Me}_5)_2\text{Ti})_2(\mu\text{-N}_2)$ (109), $\mu\text{-N}_2$ ligand, with an unusual planar $\text{Sm}(\mu\text{-}\eta^2:\eta^2\text{-N}_2)\text{Sm}$ core. An $\eta^2:\eta^2$ -coordination mode of a bridging styrene, as well as an η^2 -arene lanthanide interaction, was observed (110) in the X-ray crystal structure of $(\text{C}_5\text{Me}_5)_2\text{Sm}(\mu\text{-}\eta^2:\eta^4\text{-CH}_2\text{CHPh})\text{Sm}(\text{C}_5\text{Me}_5)_2$ (Fig. 11).

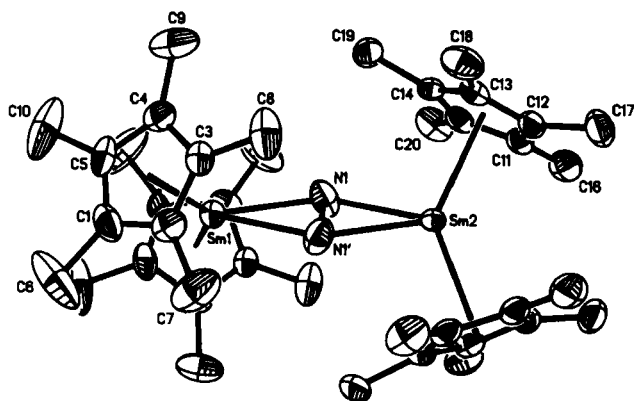


FIG. 10. Molecular structure of $(C_5Me_5)_2Sm(\mu-\eta^2:\eta^2-N_2)Sm(C_5Me_5)_2$. [Reprinted with permission from Evans *et al.* (108). Copyright (1988) American Chemical Society.]

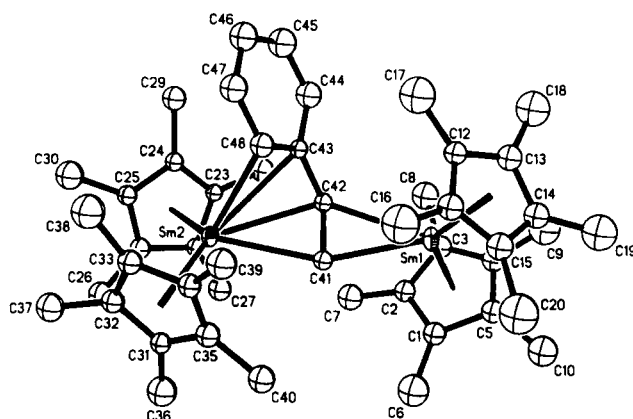


FIG. 11. Molecular structure of $(C_5Me_5)_2Sm(\mu-\eta^2:\eta^4-CH_2CHPh)Sm(C_5Me_5)_2$. [Reprinted with permission from Evans *et al.* (110). Copyright (1990) American Chemical Society.]

VIII

π -ARENE COMPLEXES

In an extension of the lanthanide π -ligand coordination above, the π interaction of aromatics with both Ln^{3+} and zero-valent lanthanides has been addressed. π coordination of arenes to lanthanides is rare. In $(\eta^6-C_6Me_6)Sm(AlCl_4)_3$ (III) the bonding between Sm^{3+} and the aromatic ring can be regarded as an electrostatically induced dipole interaction between Sm^{3+} and the π -electron density of the electron-rich arene ring (Fig. 12).

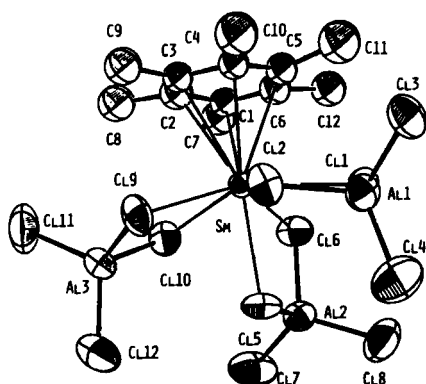


FIG. 12. Molecular structure of $(\eta^6\text{-C}_6\text{Me}_6)\text{Sm}(\text{AlCl}_4)_3$. [Reprinted with permission from Cotton and Schwotzer (111). Copyright (1986) American Chemical Society.]

η^6 coordination is not only limited to electron-rich aromatics, as $(\eta^6\text{-1,3-C}_6\text{H}_4\text{Me}_2)\text{Sm}(\text{AlCl}_4)_3$ (112) and $(\eta^6\text{-C}_6\text{H}_6)\text{Ln}(\text{AlCl}_4)_3$ (113) ($\text{Ln} = \text{La}, \text{Nd}, \text{Sm}$) can be prepared by reaction of LnCl_3 with AlCl_3 in the presence of the appropriate arene. The Sm ($\text{Sm-C}_6\text{H}_6 = 2.89\text{--}2.93 \text{ \AA}$) and Nd ($\text{Nd-C}_6\text{H}_6 = 2.93 \text{ \AA}$) compounds (3) are isostructural with $(\eta^6\text{-C}_6\text{H}_6)\text{U}(\text{AlCl}_4)_3$ (114). Similarly, the first $\text{Ln}^{\text{III}} \eta^6$ -arene complex, cyclotetrameric $[(\eta^6\text{-C}_6\text{Me}_6)\text{Er}(\text{AlCl}_4)_3]_4$ has been prepared (115). The $(\text{C}_6\text{Me}_6)\text{Er}(\text{AlCl}_4)_3$ units are connected via four $\eta^2\text{-AlCl}_4$ groups.

In comparison to these predominantly ionic interactions with Ln^{3+} , π -arene complexes of zero-valent lanthanides have been prepared by metal vapor synthesis (116*a,b*). Electron beam evaporation of Sc (116*a*), Y (116*b*), or Gd (116*b*) metal and cocondensation with excess 1,3,5- $\text{C}_6\text{H}_3\text{-}t\text{-Bu}_3$ afforded the first authentic structurally characterized $\text{Ln}(0)$ species $\text{Ln}(\eta^6\text{-C}_6\text{H}_3\text{-}t\text{-Bu}_3)_2$. The structure of the gadolinium complex was determined by X-ray crystallography ($\text{Gd-C}_{\text{average}} = 2.630 \text{ \AA}$) (Fig. 13). The benzene rings are staggered. Subsequently, the synthesis (117) of the complete range ($\text{Y} \rightarrow \text{Lu}$) was attempted, of which $\text{Ln}(\eta^6\text{-C}_6\text{H}_3\text{-}t\text{-Bu}_3)_2$ ($\text{Ln} = \text{Nd}, \text{Tb}, \text{Dy}, \text{Ho}, \text{Er}, \text{Lu}$) could be isolated and was stable at 25°C . A simple bonding model was presented on the basis of the observed stability trends and magnetism of these compounds. Three lanthanide valence electrons were proposed to be involved in bonding to the arene ring by promotion from $f^n s^2 \rightarrow f^{n-1} d^1 s^2$. This model did not hold for the larger lanthanides La or Ce, which do not form stable bis($\text{C}_6\text{H}_3\text{-}t\text{-Bu}_3$) complexes, but have $d^1 s^2$ ground-state configurations. Thermochemical data (118) quantifying these lanthanide–arene bond enthalpies supported the proposed model. Zero-valent lanthanide arene bonding is surprisingly

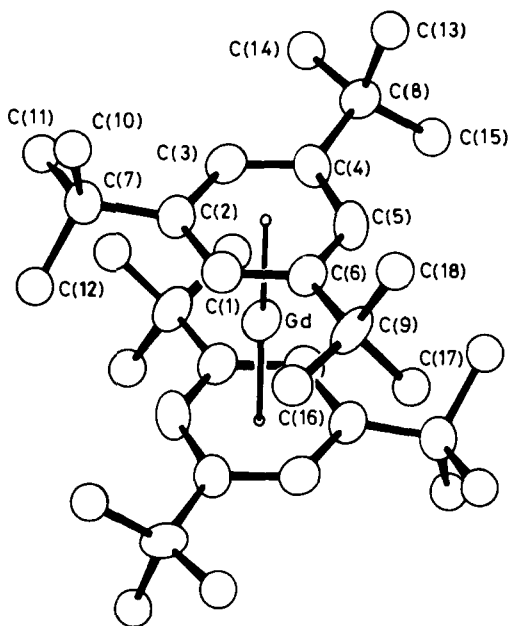


FIG. 13. Molecular structure of $\text{Gd}(\eta^6\text{-C}_6\text{H}_3\text{-}t\text{-Bu}_3)_2$. [Reproduced by permission from the Royal Society of Chemistry; from Brennan *et al.* (116b).]

strong with $\text{D}(\text{Ln-C}_6\text{H}_3\text{-}t\text{-Bu}_3) = \text{Y}$, 72; Gd, 68; Dy, 47; Ho, 56; Er, 57 kcal mol^{-1} . These enthalpies are comparable with those for $\text{M}(\eta^6\text{-arene})_2$ ($\text{M} = \text{Cr}, \text{Mo}, \text{W}$) complexes.

A more complicated example of intramolecular π -arene coordination in which a remote phenyl group lies in a position geometrically favorable for interaction with an electrophilic lanthanide center has been reported. The phenyl-substituted trisalkoxides $\text{Ln}(\text{O-2,6-C}_6\text{H}_3\text{Ph}_2)_3$ ($\text{Ln} = \text{Nd}, \text{Sm}, \text{Er}, \text{Yb}, \text{Lu}$) were prepared (119) by reaction of Ln metal powder, $\text{Hg}(\text{C}_6\text{F}_5)_2$, and the phenol in THF. In contrast to $\text{Yb}(\text{O-2,6-C}_6\text{H}_3\text{Ph}_2)_3(\text{THF})_2$, THF-free $\text{Yb}(\text{O-2,6-C}_6\text{H}_3\text{Ph}_2)_3$ possesses a novel intramolecular π -phenyl interaction ($\text{Yb-C}_{\text{average}} = 2.98 \text{ \AA}$) from one of the phenyl substituents of the aryloxy (119). A related, interesting example of $\eta^6\text{-}\pi$ -arene interaction of an aryloxy ligand occurs in $[\text{Ln}(\text{O-2,6-C}_6\text{H}_3\text{-}i\text{-Pr}_2)_3]_2$ ($\text{Ln} = \text{Nd}, \text{Sm}$) (120) has been confirmed by X-ray crystallography with $\text{Nd-C}_{\text{av.}} = 3.035 \text{ \AA}$, and $\text{Sm-C}_{\text{av.}} = 2.986, 3.016 \text{ \AA}$ (2 independent molecules in asymmetric unit cell). The centrosymmetric dimer is held together by two $\eta^6\text{-arene}$ bridges. This bonding mode is very similar to that observed in the uranium analogue (120b).

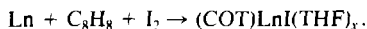
IX

CYCLOOCTATETRAENE COMPLEXES

In comparison with the extensive chemistry of cyclopentadienyl complexes of the lanthanides, relatively few lanthanide complexes of the dianionic, eight-electron donor cyclooctatetraene (COT) ligand (121) have been reported, although they have been long established, i.e., (COT)LnCl(THF)_x (Ln = Ce, Pr, Nd, Sm) (122). Reaction of LnCl₃ with K₂COT affords (COT)LnCl(THF)_x (Ln = La, Sm, Lu), which, on alkylation with LiCH₂SiMe₃ or Li(o-C₆H₄CH₂NMe₂) affords the corresponding mono-alkyl complex (COT)LnR(THF)_x (123):



The molecular structure of (COT)Lu(o-C₆H₄CH₂NMe₂)/THF was confirmed by X-ray crystallography (123). COT complexes are also accessible via reduction of COT by a lanthanide metal (Ln = La, Ce, Pr, Nd, Sm) in the presence of I₂ (124):



Whereas monomeric (COT)CeI(THF)₃ (124) has a piano-stool geometry, [(COT)Ce(μ-Cl)(THF)₂]₂ is dimeric (125). Alkylation of [(COT)Ln(μ-Cl)(THF)₂] (Ln = Y, Sm, Lu) with LiCH(SiMe₃)₂ (2 eq) afforded the zwitteranionic dialkyl species (THF)₂Li{μ-η², η⁸-C₈H₈}Ln{CH(SiMe₃)₂]₂ (126) (Fig. 14). The X-ray structure of the Sm compound showed that unusually, the (THF)₂Li fragment is η² bound to the cyclooctatetraenyl ligand.

Divalent (COT)Yb was generated by reaction of Yb metal with COT in liquid ammonia (125). Addition of pyridine afforded (COT)Yb(C₅H₅N)₃, which was crystallographically characterized (127). Reaction of the substituted cyclooctatetraene dianion [Li(THF)]₂[1,4-C₈H₆(SiMe₃)₂] with MCl₃(THF)₃ (M = Sc, Y) led to the first monocyclooctatetraene half-sandwich yttrium complex [{C₈H₆(SiMe₃)₂}Y(μ-Cl)(THF)]₂ and structurally characterized [{C₈H₆(SiMe₃)₂}Sc]₂(μ-Cl)₂(THF), which contained an unusual semibridging THF (128) (Fig. 15).

Mixed sandwich complexes (C₅Me₅)M(COT) (M = Sc, Y, La, Pr, Sm, Gd, Tb, Dy, Er, Lu) (129), C₅(CH₂Ph)₅Lu(COT) (130), and (COT)Sm(C₅H₄PPh₂)(THF)₂ (131) have been prepared by reaction of (COT)MCl(THF)_x with the appropriate cyclopentadienyl anion. Heterobimetallic SmRh species have been prepared from (COT)Sm(C₅H₄PPh₂)(THF)₂ (131) and (C₅Me₅)Rh(CO)₂.

The complexes (COT)Ln(η⁵-C₅H₅)(THF)₂ (Ln = Pr, Nd, Gd) and (COT)-Ln(η⁵-indenyl)(THF)₂ (Ln = Pr, Nd) have been synthesized, and for Ln =

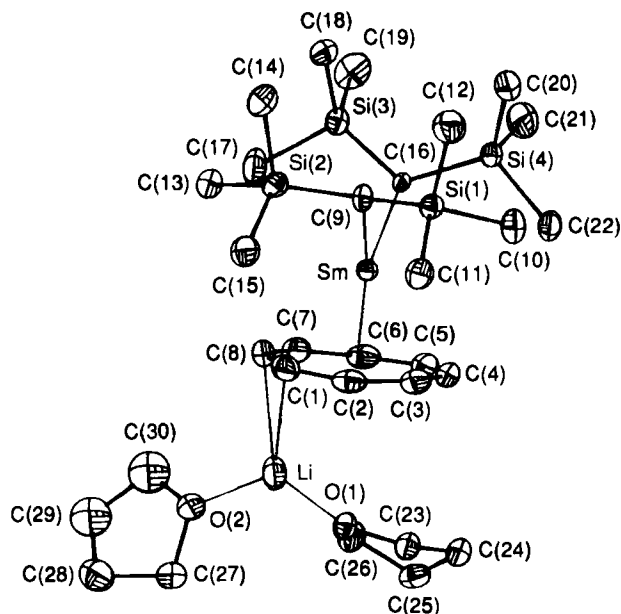


FIG. 14. Molecular structure of $(\text{THF})_2\text{Li}\{\mu\text{-}\eta^2, \eta^8\text{-C}_8\text{H}_8\}\text{Ln}[\text{CH}(\text{SiMe}_3)_2]_2$. [Reproduced by permission from the Royal Society of Chemistry; from Schumann *et al.* (126).]

Pr, both have been characterized by X-ray diffraction (132). SmCl_3 reacts with K_2COT to afford $(\text{COT})\text{SmCl}(\text{THF})_2$, which, when treated with $\text{K}(2,4\text{-dimethylpentadienyl})$ affords $(\text{COT})\text{Sm}(2,4\text{-C}_5\text{H}_5\text{Me}_2)(\text{THF})$ (133).

Typical ^1H and ^{13}C NMR chemical shifts for diamagnetic lanthanide COT complexes are δ 6.0–6.7 ppm and 92–100 ppm, respectively.

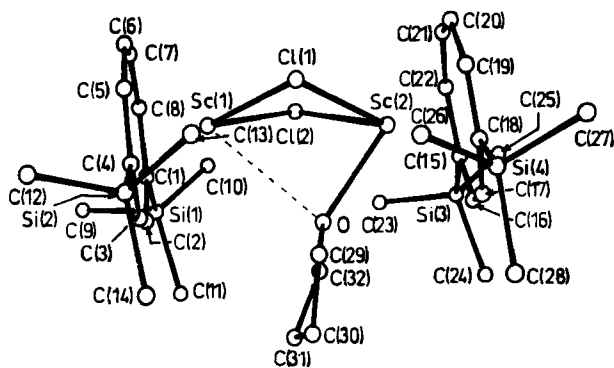


FIG. 15. Molecular structure of $[\text{C}_8\text{H}_6(\text{SiMe}_3)_2\text{Sc}]_2(\mu\text{-Cl})_2(\text{THF})$. [Reproduced by permission from the Royal Society of Chemistry; from Burton *et al.* (128).]

Examination of the UPS spectra for $(C_5Me_5)M(COT)$ ($M = Sc, Y, La$) (129) and comparison of their ionization energies with their Ti, Zr analogs (134) led to the conclusion that metal to ring bonding is almost completely ionic for the more electropositive group 3 metals.

The versatility of the $(COT)Ln$ fragment is demonstrated in that the mixed COT/pyrazolylborate and COT/benzamidinate compounds $(COT)LnX$ ($X = HBpz_3, HB(3,5-Me_2pz_3)$ and $MeOC_6H_4C(NSiMe_3)_2$) have been prepared (135).

Complexes in which cerium adopts a formal Ce^{4+} oxidation state are very scarce. Cerium could adopt a Ce^{4+} ground-state configuration in $Ce^{4+}(COT^{2-})_2$. Self-consistent field calculations (136), however, indicate that the ground state is almost entirely $4f^1$, corresponding to $Ce^{3+}(COT^{1.5-})_2$. The $4f^1$ electron forms in combination with an electron from a ligand e_{2u} orbital, a $4f^1e_{2u}^3$ HOMO, instead of a $4f^0e_{2u}^4$ (Ce^{4+}) ground state. This single-triplet splitting is ca. 0.5 eV.

X

CARBORANES

The realization of the isolobal analogy between the cyclopentadienyl anion and the dicarbollide dianion $[nido-7,8-C_2B_9H_{11}]^{2-}$ resulted in a plethora of transition metal carborane chemistry. Twenty years later, lanthanacarboranes have only recently begun to attract attention. Reaction of LnI_2 ($Ln = Sm, Yb$) with $Na_2[C_2B_9H_{11}]$ in THF afforded the mono(cage) compound $Ln(C_2B_9H_{11})(THF)_4$. The X-ray structural characterization of the first *closo*-lanthanacarborane $Yb(C_2B_9H_{11})(DMF)_4$ (137) showed that the carbollide was η^5 bound to Yb. An anionic bis(carbollide) $[PPN][Sm(C_2B_9H_{11})_2(THF)_2]$, analogous to the bent metallocenes, was prepared by reaction of $Sm(C_2B_9H_{11})(THF)_4$ with $[PPN][closo-3,1,2-TiC_2B_9H_{11}]$. Both carbollides are η^5 bound to Sm with a centroid-Sm-centroid angle of 132° . This value is similar to other trivalent $(C_5Me_5)_2SmX$ complexes (138). From this, it was proposed that C_5Me_5 and $C_2B_9H_{11}$ have similar steric requirements (137).

Reaction of equimolar quantities of Yb or Eu powder with decarborane ($B_{10}H_{14}$) in liquid NH_3 at $-40^\circ C$ gave, after heating under vacuum (desolvation), the *closo*-boranes $Ln(B_{10}H_{14})$ (139). Treatment of the NH_3 solvated reaction mixture with MeCN afforded $(MeCN)_6Yb(\mu-H)_2B_{10}H_{12}$, which was identified by X-ray crystallography. Note that the borane is bound to Yb only via B-H bridges.

The first carborane analog of an ytrocene derivative (140) $[Li(THF)_4][YCl(THF)\{(Me_3Si)_2C_2B_4H_4\}_2Li(THF)]$ was synthesized by reaction of

YCl_3 with $\text{Li}_2[2,3-(\text{Me}_3\text{Si})_2-2,3-\text{C}_2\text{B}_4\text{H}_4]$. The structure is of the bent sandwich type with each yttrium η^5 bound to the C_2B_3 face of each carborane.

XI

HETEROCYCLOPENTADIENYLS

The use of the phospholyl ($\text{C}_4\text{Me}_4\text{P}$) ligand as a C_5Me_5 substitute is attracting increasing attention. Reaction of $\text{Li}(\text{PC}_4\text{Me}_4)$ with LnCl_3 ($\text{Ln} = \text{Y}, \text{Lu}$) afforded $(\text{C}_4\text{Me}_4\text{P})_2\text{LnCl}_2\text{Li}(\text{solvent})_2$ in moderate yield (141). Bis(η^5 -phospholyl) and bis(η^5 -arsolyl) lanthanide(II) complexes $(\text{C}_4\text{Me}_4\text{P})_2\text{Ln}$ were prepared (142) by reaction of $\text{LnI}_2(\text{THF})_2$ ($\text{Ln} = \text{Sm}, \text{Yb}$) with $\text{K}(\text{EC}_4\text{Me}_4)$ ($\text{E} = \text{P}, \text{As}$), or by P–P or As–As bond cleavage of a biphospholyl or biarsolyl by the metal powders. The X-ray crystal structure of $(2,5\text{-PC}_4\text{H}_2\text{Ph}_2)_2\text{Yb}(\text{THF})_2$ was reported (Fig. 16).

XII

MONOCYCLOPENTADIENYL COMPLEXES

The growth of organolanthanide chemistry in the last decade has primarily developed around the bis(pentamethylcyclopentadienyl) ligand system. This has produced a wealth of fascinating reactions based on $\text{M}(\text{C}_5\text{Me}_5)_2\text{Me}$

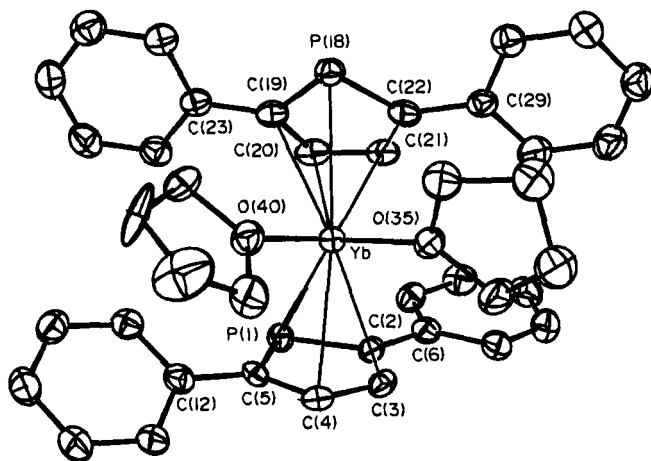


Fig. 16. Molecular structure of $(2,5\text{-PC}_4\text{H}_2\text{Ph}_2)_2\text{Yb}(\text{THF})_2$. [Reprinted with permission from Nief *et al.* (142). Copyright (1993) Pergamon Press.]

(81,143,144) and $[M(C_5Me_5)_2H]_2$ (51,75,76,145). Despite this increase in attention, relatively few mono(cyclopentadienyl) species were, until recently, known. Such species might allow increased steric and electronic unsaturation, and a broader range of neutral lanthanide alkyl coordination environments in, e.g., $(C_5Me_5)MR(X)$ (X = alkyl, alkoxide, amide). Mono(C_5Me_5) complexes, particularly of the larger, earlier lanthanides are scarce, due to facile loss of coordinating solvent, nonstoichiometric salt complexation, and a strong preference for formation of bis(C_5Me_5) lanthanide complexes. The anionic $(C_5Me_5)Lu$ alkyl complexes $[Li(TMEDA)_2][(C_5Me_5)LuMe_3]$ (146) and $[Li(TMEDA)_2][(C_5Me_5)Lu-t-Bu_2Cl]$ (147) have been long known. Some neutral monocyclopentadienyl complexes, i.e., $(C_5H_5)NdCl_2(THF)_3$, $(C_5R_5)YbCl(THF)_2$ (R = H, Me), and $(C_5H_4-t-Bu)LuCl_2(THF)_2$, have recently been synthesized and crystallographically characterized (3). These precursors have yet to display synthetic potential and are not addressed here further.

Synthetic access to monocyclopentadienyl lanthanide chemistry has relied largely on non-chloride-containing precursors, thus circumventing problems associated with salt coordination as an inevitable consequence of alkylation methodology. For this reason, lanthanide triflates, iodides, and alkoxides have been frequently used. Reaction of $Lu(OSO_2CF_3)_3$ with NaC_5H_5 affords crystallographically characterized $(C_5H_5)Lu(OSO_2CF_3)_2(THF)_3$ (148). Reaction with $LiCH_2SiMe_3$ affords the bis-alkyl $(C_5H_5)Lu(CH_2SiMe_3)_2(THF)_3$ (148). The triflates were shown to be particularly useful leaving groups, although their use has yet to become widespread.

A useful precursor to mono(C_5Me_5) lanthanide complexes is $(C_5Me_5)LnI_2(THF)_3$ (Ln = La, Ce) (149), prepared from THF-soluble $LaI_3(THF)_3$ and KC_5Me_5 . Compared to the analogous reaction of only sparingly soluble (in THF) $LnCl_3$, which favors bis(C_5Me_5) products, or gives mono(C_5Me_5) monomer-oligomer mixtures, these synthetic difficulties are effectively circumvented by use of THF-soluble $LnI_3(THF)_3$. The larger iodides assist in stabilizing $(C_5Me_5)LnI_2(THF)_3$. Additionally, the tendency for MI (M = alkali metal) salt coordination is reduced. Reaction of $(C_5Me_5)LaI_2(THF)_3$ with $KCH(SiMe_3)_2$ (2 eq) afforded thermally unstable $(C_5Me_5)La\{CH(SiMe_3)_2\}_2(THF)$ (150). THF is frequently employed to stabilize organolanthanides. Cyclic ethers, such as THF, are known to undergo electrophilic attack, with ring opening by Me_3SiI to give $Me_3SiOCH_2(CH_2)_nI$ ($n \geq 1$). THF-free $(C_5Me_5)La\{CH(SiMe_3)_2\}_2$ can be prepared either by treatment of $(C_5Me_5)La\{CH(SiMe_3)_2\}_2(THF)$ with excess Me_3SiI , or preferably, from $[(C_5Me_5)LaI_2]_n$, followed by alkylation (Scheme 6). Both $(C_5Me_5)La\{CH(SiMe_3)_2\}_2$ (Fig. 17) and its THF adduct (Fig. 18) have been crystallographically characterized (150). Their geometries differ primarily in the confor-

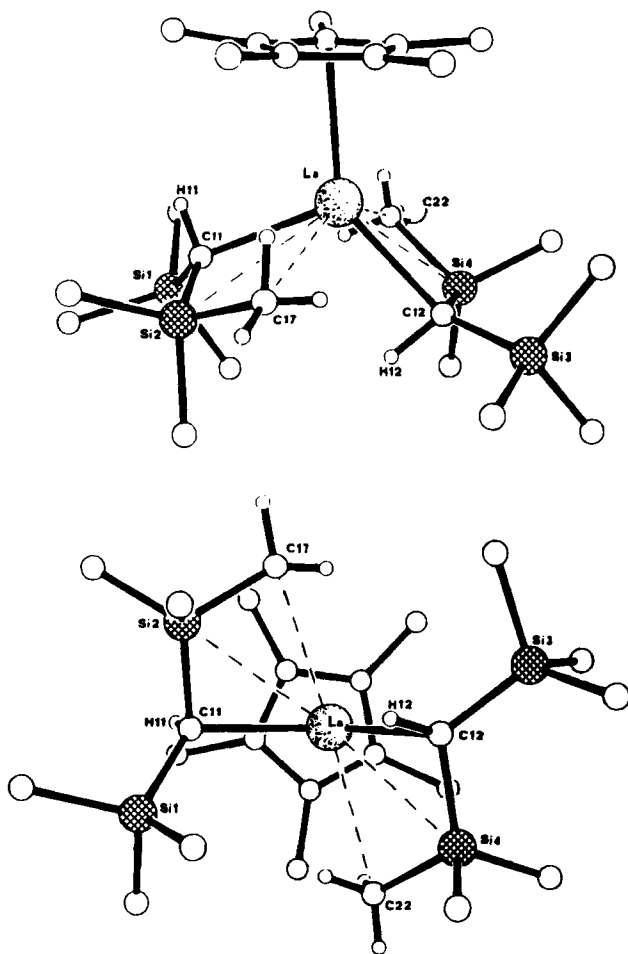
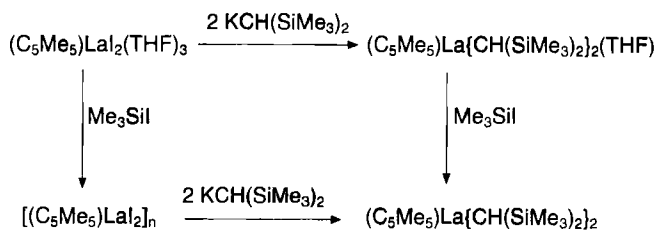


FIG. 17. Molecular structure of $(\text{C}_5\text{Me}_5)\text{La}\{\text{CH}(\text{SiMe}_3)_2\}_2$. [Reprinted with permission from van der Heijden *et al.* (150). Copyright (1989) American Chemical Society.]

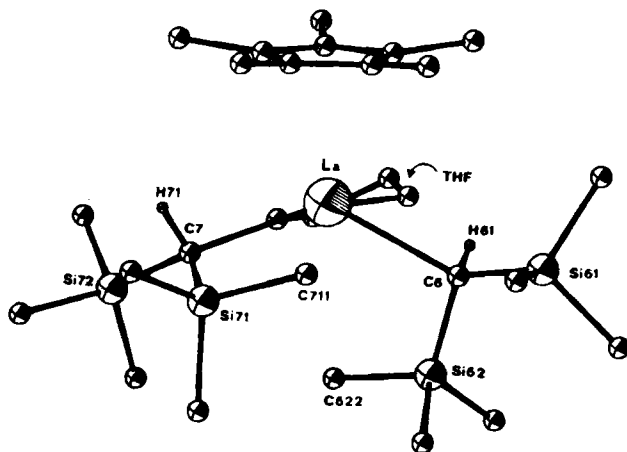
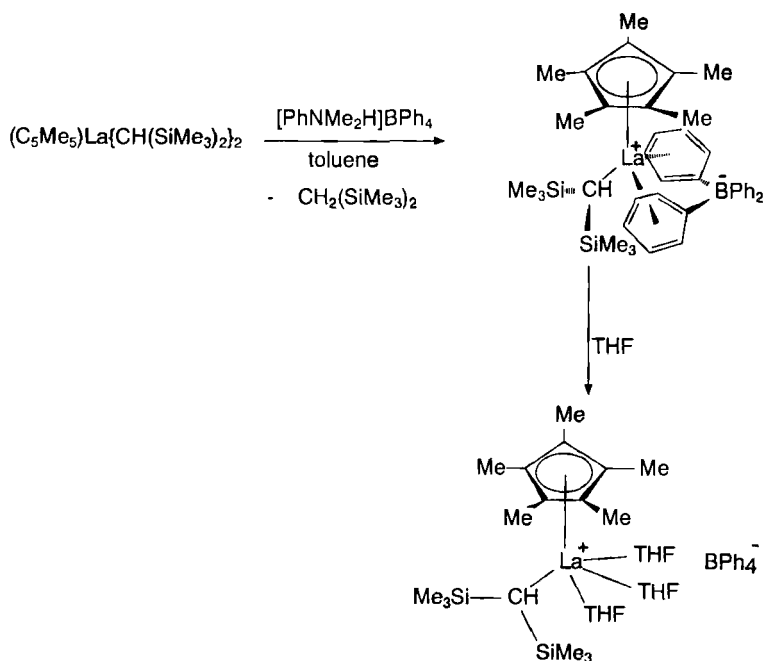


FIG. 18. Molecular structure of $(C_5Me_5)La\{CH(SiMe_3)_2\}_2(THF)$. [Reprinted with permission from van der Heijden *et al.* (150). Copyright (1989) American Chemical Society.]

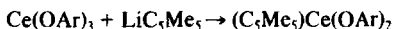
mations of the $CH(SiMe_3)_2$ ligands, and in the pyramidalization of the $(C_5Me_5)La\{CH(SiMe_3)_2\}_2$ fragment, which results from THF coordination. In both complexes, both $CH(SiMe_3)_2$ ligands are significantly distorted in a manner similar to that previously observed in $(C_5Me_5)_2MCH(SiMe_3)_2$, which is suggestive of a β -Si-Me-La interaction rather than a γ -C-H-La interaction. The subtle structural differences between these two interactions is discussed further (Section XVII). In particular, the γ -Me groups of the interacting $SiMe_3$ group are *not* oriented so as to dispose one C-H bond in the vicinity of the metal, in marked contrast to agostic β - and γ -C-H-M interactions. The near planarity of $La-C_\alpha-Si-Me_\gamma$ is reminiscent of the planar four-center intermediate postulated and observed in β -hydride elimination.

The increasing interest in cationic Ti, Zr, and Th chemistry is, in part, associated with the realization that an important prerequisite is a "noncoordinating" anion. Tetraphenylborates are, however, not necessarily innocuous. For example, phenyl π coordination (possibly η^3) has been observed in $Zr(CH_2Ph)_3(\eta^6-C_6H_5)BPh_3$ (151) and $Cp'_2ZrMe(BPh_4)$ (152), and η^6 -phenyl coordination has been established by X-ray crystallography in $Zr(CH_2Ph)_3(\eta^6-PhCH_2B(C_6F_5)_3)$ (153). Cationic lanthanide alkyl complexes were accessed by reaction of $(C_5Me_5)La\{CH(SiMe_3)_2\}_2$ with $[PhNMe_2H]BPh_4$ to afford the zwitterionic alkyl complex $La(C_5Me_5)\{CH(SiMe_3)_2\}BPh_4$, which reacts irreversibly with THF to displace the coordinated tetraphenylborate and afford the first cationic lanthanide alkyl complex $[La(C_5Me_5)\{CH(SiMe_3)_2\}(THF)_3]BPh_4$ (154) (Scheme 7). On the basis



of solid-state ^{13}C CP-MAS NMR data in which four equal intensity BPh_4 C_{ipso} resonances (all with $^{10,11}\text{B}$ coupling) were observed, the coordination mode of tetraphenylborate was proposed to be $(\eta^2\text{-C}_6\text{H}_5)_2\text{BPh}_2$ with *two* phenyl groups coordinated to La. A similar coordination environment was subsequently established by X-ray crystallography in $\text{Nb}(\eta^6\text{-C}_6\text{H}_5)_2\text{BPh}_2(\text{MeC}_2\text{Me})$ (155). Other cationic lanthanide complexes are $\{[1,3\text{-C}_5\text{H}_3(\text{SiMe}_3)_2]\text{Ln}(\text{NCMe})(\text{dme})\}\text{BPh}_4$ ($\text{Ln} = \text{La}, \text{Ce}$) (156a) and $[(\text{C}_5\text{Me}_5)_2\text{Ln}(\text{L})_2]\text{BPh}_4$ ($\text{Ln} = \text{Sm}$ (156b), Ce (156c); $\text{L} = \text{THF}$ or THT). Ab initio calculations (157) on the cations $[(\text{C}_5\text{H}_5)_2\text{Ln}]^+$ ($\text{Ln} = \text{Sc}, \text{Lu}$) show them to have bent metallocene structures. Although π bonding dominates the covalent-bonding contributions, it is the σ -bonding contributions that were found to be responsible for the bent, rather than linear, geometries.

Homoleptic phenoxide complexes were introduced by Lappert to prepare homoleptic trisalkyl complexes $\text{Ln}\{\text{CH}(\text{SiMe}_3)_2\}_3$ (23) to circumvent disproportionation or salt coordination. These also proved to be suitable for stepwise alkoxide substitution. Teuben has independently prepared (158) $\text{Ce}(\text{C}_5\text{Me}_5)\{\text{CH}(\text{SiMe}_3)_2\}_2$ (Fig. 19) via alkylation of $(\text{C}_5\text{Me}_5)\text{Ce}(\text{OAr})_2$ (158):



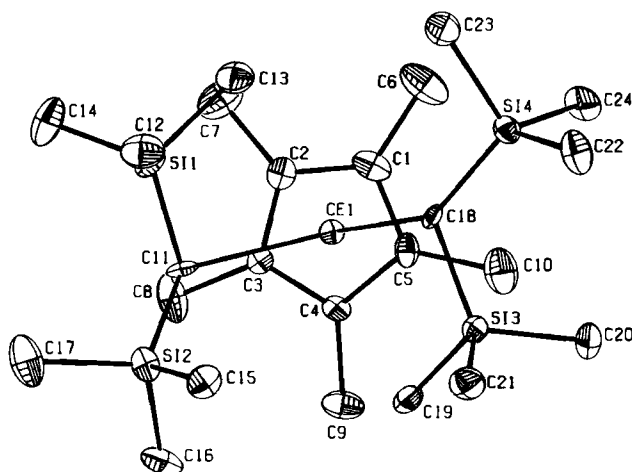


FIG. 19. Molecular structure of $(C_5Me_5)Ce\{CH(SiMe_3)_2\}_2$. [Reprinted with permission from Heeres *et al.* (158). Copyright (1989) American Chemical Society.]

The X-ray crystal structure of $(C_5Me_5)Ce(OAr)_2$ shows that one phenoxide is almost linear ($Ce-O-C = 158^\circ$), while the other is significantly bent (105°). The Y analog also displays such disparity (129° and 168°) (159). $(C_5Me_5)Ce(OAr)_2$ reacts with $LiCH(SiMe_3)_2$ and $NaN(SiMe_3)_2$ to afford $(C_5Me_5)Ce\{CH(SiMe_3)_2\}_2$, and $(C_5Me_5)Ce\{N(SiMe_3)_2\}_2$, respectively, both of which have also been structurally characterized (158).

Other routes to mono(C_5Me_5) complexes have been investigated. Reaction of $Ln\{N(SiMe_3)_2\}_3$ ($Ln = Y, La, Ce$) or $Ln\{CH(SiMe_3)_3\}_3$ ($Ln = La, Ce$) with C_5Me_5H afforded a mixture of mono and bis(C_5Me_5) complexes (160). Protonolysis of $Y(o-C_6H_4CH_2NMe_2)_3$ with C_5Me_5H was more successful, introduction of a second C_5Me_5 group being inhibited by the bulky chelating alkyl ligand:



This methodology could not be extended to the larger La and Ce analogs. X-ray crystallography showed nitrogen chelation to Ce and a geometry indicative of a Y . . C–N agostic interaction (161). Thermolysis in THF results in dimeric complex via C–H activation of one NMe_2 group on each yttrium center.

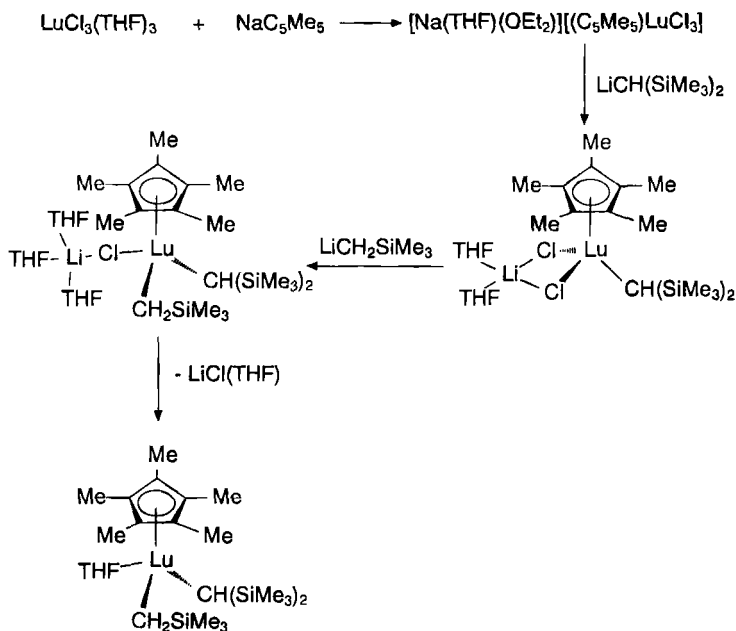
Mono(C_5Me_5) cerium complexes can be prepared by protonolysis of $(C_5Me_5)_2CeCH(SiMe_3)_2$ with *t*-BuOH (162):



Reaction of $(C_5H_5)LuCl_2(THF)_3$ with $LiCH_2CHMeCH_2NMe_2$ (1 eq) gave selective monosubstitution and affords $(C_5H_5)Lu(CH_2CHMeCH_2NMe_2)$

$\text{Cl}(\text{THF})_2$. Intramolecular chelation of N to Lu was confirmed by X-ray crystallography (163).

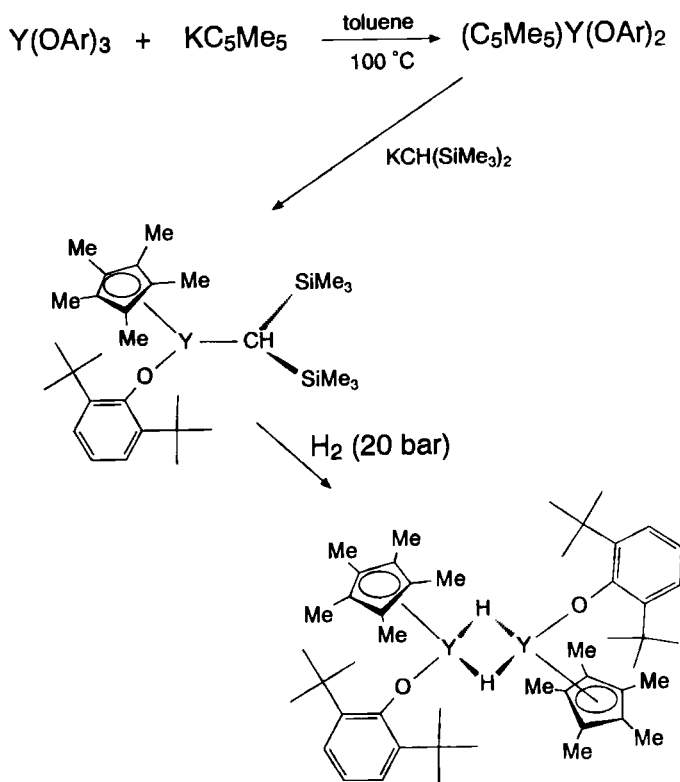
In contrast to $(\text{C}_5\text{Me}_5)\text{MR}_2$ ($\text{M} = \text{La}, \text{Ce}$) chemistry (vide supra), access to the corresponding lutetium species proved more experimentally demanding (164). This appears intuitively surprising given the smaller ionic radius of Lu^{3+} . The synthesis of the mixed bis(alkyl) complexes $(\text{C}_5\text{Me}_5)\text{LuR}'\text{R}''(\text{THF})$ was achieved according to Scheme 8. $[\text{Li}(\text{TMEDA})]$



$[(\text{C}_5\text{Me}_5)\text{Lu}\{\text{CH}(\text{SiMe}_3)_2\}\text{Cl}_2]$ and $[\text{Li}(\text{THF})_3][(\text{C}_5\text{Me}_5)\text{Lu}\{\text{CH}(\text{SiMe}_3)_2\}(\text{CH}_2\text{SiMe}_3)\text{Cl}]$ were crystallographically characterized (164). The neutral mixed-alkyl species $(\text{C}_5\text{Me}_5)\text{Lu}\{\text{CH}(\text{SiMe}_3)_2\}(\text{CH}_2\text{SiMe}_3)(\text{THF})$ could be isolated, albeit in low yield. Putative $(\text{C}_5\text{Me}_5)\text{Lu}\{\text{CH}(\text{SiMe}_3)_2\}_2$ could not be prepared, presumably for steric reasons [cf. $(\text{C}_5\text{Me}_5)\text{Ln}\{\text{CH}(\text{SiMe}_3)_2\}_2$ ($\text{Ln} = \text{La}$ (150), Ce (158))]. As well as being, as expected, very sensitive to air and moisture, these monocyclopentadienyl lutetium compounds possess limited thermal stability, with slow decomposition being observed in the solid state at 20°C and in solution $>40^\circ\text{C}$. Interestingly, the bulkier 1,3-diphenyl-2,4,5-trimethylcyclopentadienyl ligand proved useful in providing greater thermal stability and allowed synthesis of $(\text{C}_5\text{Me}_3\text{Ph}_2)\text{Lu}(\text{CH}_2\text{SiMe}_3)_2(\text{THF})$. In general, such cyclopentadienyl ligands have yet to find widespread use in organolanthanide chemistry.

The polymerization of ethylene by $[(C_5Me_5)_2MH]_2$ (2,51,75,76,145), methane transmetalation, β -methyl elimination, and propene oligomerization by $[(C_5Me_5)_2LuMe]_2$ (81) have recently led to fine tuning of the bis (C_5Me_5) ligand system in order to probe the possibilities and constraints of such catalysts. For example, variation of the cyclopentadienyl substituents, or linking the cyclopentadienyl rings, has led to α -olefin oligomerization (165), cyclization of α, ω -dienes (166), C–C σ -bond activation (167), hydroamination/cyclization of olefins (168), and isospecific α -olefin polymerization (169,170). Replacement of the six-electron π -donor $C_5Me_5^-$ by bulky four-electron donating alkoxides RO^- should provide a suitable coordination sphere for oxophilic lanthanides.

Reaction of $Y(OAr)_3$ ($OAr = O-2,6-C_6H_3-t-Bu_2$) with KC_5Me_5 (1 eq toluene, $100^\circ C$) resulted in the formation of $Y(C_5Me_5)(OAr)_2$ in 70–80% yield (159). $Y(C_5Me_5)(OAr)_2$ reacts cleanly with $KCH(SiMe_3)_2$, with loss of insoluble $KOAr$, to give $Y(C_5Me_5)(OAr)CH(SiMe_3)_2$ (Scheme 9). In contrast to the facile hydrogenation of $Ln(C_5Me_5)_2CH(SiMe_3)_2$ (51,75,76), hydrogenation of $Y(C_5Me_5)(OAr)CH(SiMe_3)_2$ to give *trans*- $[Y(C_5Me_5)_2]$

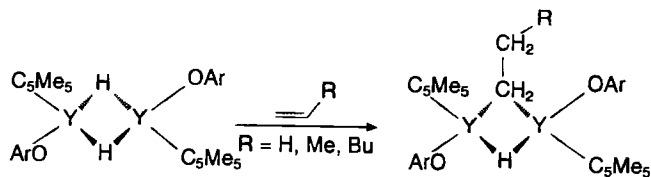


(OAr)(μ -H) $_2$ was performed under 10-bar H_2 . The hydride is constrained to bridge two yttrium centers because of the additional electropositivity of yttrium induced by the hard, electronegative ancillary alkoxide ligands (compared with its C_5Me_5 counterpart). This enables μ -H to disperse its additional negative charge resulting from Y-H bond polarization.

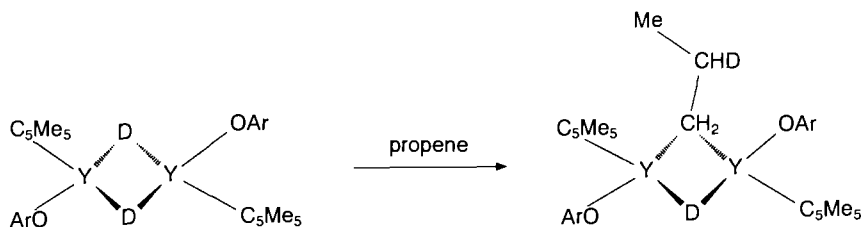
The chemical shift and Y-H coupling of the μ -H resonance (δ 5.64 ppm, $J_{YH} = 35.2$ Hz) is similar to that found in other bridging (yttrium) hydrides (171) and is consistent with a (time-averaged) symmetrical Y(μ -H) $_2$ Y bridge. Low-temperature 1H NMR ($-90^\circ C$, C_7D_8) studies provided no evidence for an asymmetric Y(μ -H) $_2$ Y dimer, as apparently observed (145b, 172) for $[(C_5Me_5)_2YH]_2$. Addition of excess THF (10 eq) to $[Y(C_5Me_5)(OAr)(\mu-H)]_2$ in C_6D_6 does not result in splitting of the dimer (173), in contrast to $[(C_5Me_5)_2YH]_2$ (145b).

^{89}Y NMR spectroscopy is a potentially useful diagnostic tool for determining the influence of the ligand environment at the yttrium center. The ^{89}Y NMR chemical shifts of $Y\{CH(SiMe_3)_2\}_3$, $Y(OAr)_3$, $(C_5Me_5)_2YCH(SiMe_3)_2$, $(C_5Me_5)Y(OAr)_2$, and $(C_5Me_5)_2YOAr$ were determined (159). From this, C_5Me_5 , OAr, and $CH(SiMe_3)_2$ group contributions to the ^{89}Y NMR chemical shift were calculated to be -100 , $+56$, and $+298$ ppm, respectively. This gives an indication of the electrophilicity of yttrium and the relative electron-donating properties of these important ligands.

Terminal olefins $H_2C=CHR$ ($R = H, Me, n-Bu$) react regiospecifically and irreversibly with $[Y(C_5Me_5)(OAr)(\mu-H)]_2$ to give the μ - n -alkyl species *trans*- $[Y(C_5Me_5)(OAr)]_2(\mu-H)(\mu-CH_2CH_2R)$ ($R = H, Me, n-Bu$), respectively (174) (Scheme 10). They are stable to β -H elimination. In all reac-



tions with terminal olefins there is no evidence for μ -isoalkyl species. In contrast to reaction of $[(C_5Me_5)_2LnH]_2$ with α olefins (Section XIII), the putative allyl species $(C_5Me_5)(OAr)Y(\eta^3-CH_2CHCH_2)$ is not formed. Reaction of $[Y(C_5Me_5)(OAr)(\mu-D)]_2$ with propene yields selectively only *trans*- $[Y(C_5Me_5)(OAr)]_2(\mu-D)(\mu-CH_2CHDMe)$, confirming the nonreversibility of olefin insertion (Scheme 11). The μ -H, μ -alkyls show disastereotopic $\alpha-CH_2$ resonances confirming idealized molecular C_2 (rather than C_s imposed by a *cis*-geometry) symmetry, indicating a mutually *trans*-geometry for the C_5Me_5 and phenoxide ligands. μ -Propyl group rotation about the μ -H, μ - C_α vector occurs. As proposed (175) for $\{Et_2Si(C_5H_4)(C_5Me_4)\}$

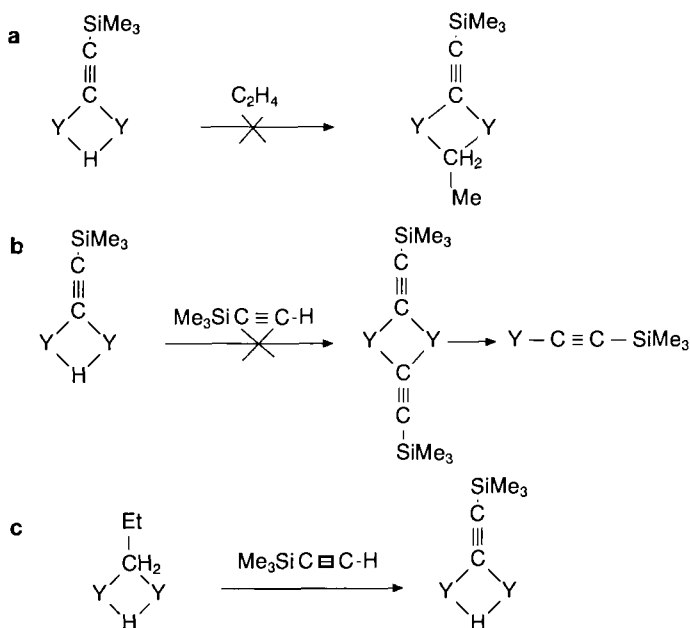


$M)_2(\mu-H)(\mu-CH_2CH_2R)$ ($M = Y, Lu$) (Section XIV), equilibration of the diastereotopic $C_\alpha H_2$'s is achieved by inversion at a planar $\mu-C_\alpha$.

Dissolution of $[Y(C_5Me_5)(OAr)(\mu-H)]_2$ in neat 1-hexene [giving $Y_2(\mu-H, \mu\text{-hexyl})$] results in slow polymerization to yield poly(1-hexene) with $M_w = 15700$, $M_w/M_n = 1.67$. The molecular weight distribution (M_w/M_n) suggests that only one active catalyst species is present, and that chain transfer occurs. Chain propagation is by 1,2-addition and termination by β -H elimination. The polymerization is slow, due to the kinetically deactivated $\mu-H$ (and μ -alkyl) (175), resulting in slow initiation.

A different reaction pathway is observed between $[Y(C_5Me_5)(OAr)(\mu-H)]_2$ and excess $Me_3SiC\equiv CH$ to afford the μ -acetylide $[Y(C_5Me_5)(OAr)]_2(\mu-H)(\mu-C\equiv CSiMe_3)$ (176).

In the $\mu-H, \mu$ -alkyls the second $\mu-H$ is significantly kinetically deactivated (Scheme 12). For example, ethylene (10 bar, 25°C) does not insert



into $\mu\text{-H}$ of $[\text{Y}(\text{C}_5\text{Me}_5)(\text{OAr})]_2(\mu\text{-H})(\mu\text{-C}\equiv\text{CSiMe}_3)$. Neither does $[\text{Y}(\text{C}_5\text{Me}_5)(\text{OAr})]_2(\mu\text{-H})(\mu\text{-C}\equiv\text{CSiMe}_3)$ react with excess $\text{Me}_3\text{SiC}\equiv\text{CH}$ to give $\text{Y}(\text{C}_5\text{Me}_5)(\text{OAr})\text{C}\equiv\text{CSiMe}_3$, although this can be prepared directly from $\text{Y}(\text{C}_5\text{Me}_5)(\text{OAr})\text{CH}(\text{SiMe}_3)_2$ and $\text{HC}\equiv\text{CSiMe}_3$. In addition, $\text{Y}_2(\mu\text{-H}, \mu\text{-propyl})$ reacts with $\text{Me}_3\text{SiC}\equiv\text{CH}$, not to give $[\text{Y}(\text{C}_5\text{Me}_5)(\text{OAr})]_2(\mu\text{-Pr})(\mu\text{-C}\equiv\text{CSiMe}_3)$, but the $\mu\text{-H}, \mu\text{-acetylide}$, the more basic $\mu\text{-alkyl}$ clearly being more susceptible to protonolysis than $\mu\text{-H}$.

Synthesis of the model compounds $[\text{Y}(\text{C}_5\text{R}_5)_2(\mu\text{-R}')_2]_2$ ($\text{C}_5\text{R}_5 = \text{C}_5\text{H}_5$, $\text{C}_5\text{H}_4\text{Me}$, $\text{C}_5\text{H}_4\text{SiMe}_3$; $\text{R}' = \text{Me}$, $n\text{-Bu}$) (173, 177) was taken as evidence to support polymerization via a $\text{Y}(\mu\text{-R}')_2\text{Y}$ intermediate. Reaction of $\text{Y}(\text{C}_5\text{Me}_5)(\text{OAr})_2$ with MeLi (1 eq) afforded the bis- $\mu\text{-Me}$ species $[\text{Y}(\text{C}_5\text{Me}_5)(\text{OAr})(\mu\text{-Me})]_2$ (174). The $\mu\text{-alkyls}$ $\text{Y}(\text{C}_5\text{Me}_5)(\text{OAr})(\text{R})$ could, however, not be prepared from $\text{Y}(\text{C}_5\text{Me}_5)(\text{OAr})_2$ and RLi (1 eq; $\text{R} = \text{Et}$, $n\text{-Bu}$, CH_2SiMe_3 , CH_2CMe_3) by similar synthetic procedures.

The $\mu\text{-Me}$ group resonates in the ^1H NMR at $\delta -0.08$ (t , $J_{\text{YH}} = 3.8$ Hz), and at $\delta 30.92$ (qt , $J_{\text{CH}} = 104$ Hz, $J_{\text{YC}} = 28$ Hz) in the ^{13}C NMR. These data are in agreement with those found in $[\text{Y}(\text{C}_5\text{Me}_5)(\text{OAr})]_2(\mu\text{-H})(\mu\text{-alkyls})$, and other symmetrically bridging $\mu\text{-Me}$ groups (82a, 173, 178) (vide supra). The synthesis of $[\text{Y}(\text{C}_5\text{Me}_5)(\text{OAr})(\mu\text{-Me})]_2$ provided an opportunity to compare the reactivity of $\text{Y}(\mu\text{-H})_2\text{Y}$ and $\text{Y}(\mu\text{-Me})_2\text{Y}$ in a system possessing otherwise identical ligand environments. In contrast to $\text{Y}(\mu\text{-H})_2\text{Y}$, $\text{Y}(\mu\text{-Me})_2\text{Y}$ is cleaved by THF to afford $\text{Y}(\text{C}_5\text{Me}_5)(\text{OAr})\text{Me}(\text{THF})_2$. The terminal methyl group resonates at $\delta 22.8$ (dq , $J_{\text{YC}} = 60$ Hz, $J_{\text{CH}} = 108$ Hz), parameters that are virtually identical to those for $\text{Y}(\text{C}_5\text{Me}_5)_2\text{Me}(\text{THF})$ (179), suggesting that such parameters are not necessarily good indicators of metal environment.

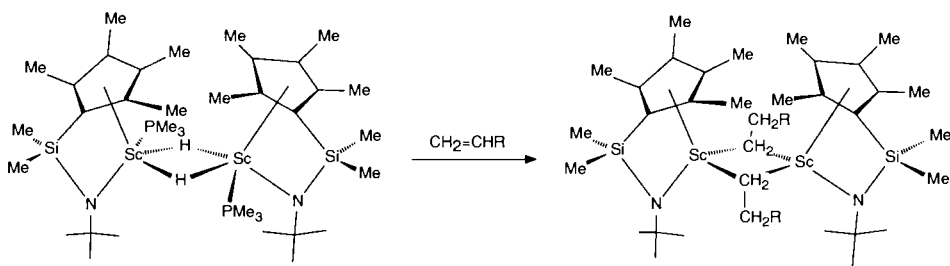
Addition of 1.6 eq MeLi to $\text{Y}(\text{C}_5\text{Me}_5)(\text{OAr})_2$, or 1 eq of MeLi to $[\text{Y}(\text{C}_5\text{Me}_5)(\text{OAr})(\mu\text{-Me})]_2$ affords the symmetrical yttrium trimer $[\text{Y}(\text{C}_5\text{Me}_5)\text{Me}_2]_3$. A related species, oligomeric $[(\text{C}_5\text{Me}_5)\text{ScMe}_2]_x$ has recently been reported (180).

Elegant fine tuning of the steric requirements in bis(cyclopentadienyl)Sc systems were performed by Bercaw in $\{(\text{C}_5\text{Me}_4)_2\text{SiMe}_2\}\text{ScR}$ and $\{(\text{C}_5\text{H}_3\text{-}t\text{-Bu})_2\text{SiMe}_2\}\text{ScR}$ (see Section XIII). Replacement of one of the cyclopentadienyl groups by a linked cyclopentadienyl–amide ligand in $(\text{C}_5\text{Me}_4\text{SiMe}_2\text{N-}t\text{-Bu})\text{ScR}$ (166) resulted in a single-component, regiospecific α -olefin oligomerization catalyst (165). The dimeric $\mu\text{-hydride}$ $[(\text{C}_5\text{Me}_4\text{SiMe}_2\text{N-}t\text{-Bu})\text{Sc}(\text{PMe}_3)]_2(\mu\text{-H})_2$ was prepared by hydrogenation of $(\text{C}_5\text{Me}_4\text{SiMe}_2\text{N-}t\text{-Bu})\text{ScCH}(\text{SiMe}_3)_2$ in the presence of PMe_3 . It possesses a C_2 symmetric structure as determined by X-ray crystallography. ^{31}P NMR studies indicated that phosphine dissociation is fast.

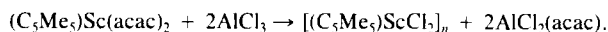
$[(\text{C}_5\text{Me}_4\text{SiMe}_2\text{N-}t\text{-Bu})\text{Sc}(\text{PMe}_3)]_2(\mu\text{-H})_2$ catalyzes the oligomerization of the α -olefins $\text{H}_2\text{C}=\text{CHR}$ ($\text{R} = \text{Me}$, Et , $n\text{-Pr}$) to the corresponding poly-

olefins with $M_w = 4000\text{--}6000$, and the polydispersity $M_w/M_n = 1.7\text{--}2.1$. Chain propagation was exclusively by 1,2-addition (i.e., "head-to-tail") and termination (chain transfer) by β -H elimination to give atactic polymers. Good evidence was obtained that the majority (if not all) of the scandium centers are active in the polymerization as the molecular weight distribution of the oligomers obtained at low propene conversion (where chain transfer effectively does not occur) corresponded well with a Poisson distribution based on the amount of monomer consumed, assuming all catalyst centers are active. As with $[(C_5Me_5)Y(OAr)(\mu-H)]_2$, polymerization rates were slow compared to Ziegler or single-component cationic Zr systems.

In contrast to the reactivity observed with both $[(C_5Me_5)Y(OAr)(\mu-H)]_2$ (174) and related $\{Et_2Si(C_5H_4)(C_5Me_4)M\}_2(\mu-H)_2$ (175) ($M = Y, Lu$), in which insertion of α -olefins occurs to give only μ -H, μ -alkyl products, $\{[(\eta^5-C_5Me_4)SiMe_2(\eta^1-NCMe_3)]Sc(PMe_3)]_2(\mu-H)_2$ (165, 166) reacts with propene (Scheme 13) to afford bis(μ -propyl) $\{[(\eta^5-C_5Me_4)SiMe_2(\eta^1-NCMe_3)]Sc\}_2(\mu-CH_2CH_2Me)_2$ (166) (Fig. 20).



In extending this theme, compounds of the type $(C_5Me_5)Sc(OR')R$ (180) were prepared. $[(C_5Me_5)ScCl_2]_n$ was prepared by reaction of $(C_5Me_5)Sc(acac)_2$ with $AlCl_3$, acetylacetonate being transferred to the more oxophilic Al:



Treatment of $(C_5Me_5)ScCl_2(PMe_3)$ with $LiOR$ ($R = 2,4,6\text{-}C_6H_2\text{-}t\text{-}Bu_3$ or $3,5\text{-}C_6H_3\text{-}t\text{-}Bu_2$) results in the (possibly dimeric) $LiCl$ adduct $(C_5Me_5)Sc(OR)Cl \cdot LiCl$ (180). The $3,5\text{-}C_6H_3\text{-}t\text{-}Bu_2$ -substituted alkoxide proved to be more amenable to alkylation; reaction of $(C_5Me_5)Sc(OR)Cl \cdot LiCl$ with $MeLi$ or protonolysis of $[(C_5Me_5)ScMe_2]_n$ (prepared from $[(C_5Me_5)ScCl_2]_n$ and $MeLi$) allowed the synthesis of $[(C_5Me_5)Sc(\mu-O\text{-}3,5\text{-}C_6H_3\text{-}t\text{-}Bu_2)Me]_2$. Its lack of reactivity is ascribed to robust alkoxide bridges. In comparison with the similar $[(C_5Me_5)Y(O\text{-}2,6\text{-}C_6H_3\text{-}t\text{-}Bu_2)(\mu-Me)]_2$, it is better formulated as $[(C_5Me_5)Sc(O\text{-}3,5\text{-}C_6H_3\text{-}t\text{-}Bu_2)(\mu-Me)]_2$. The kinetically deacti-

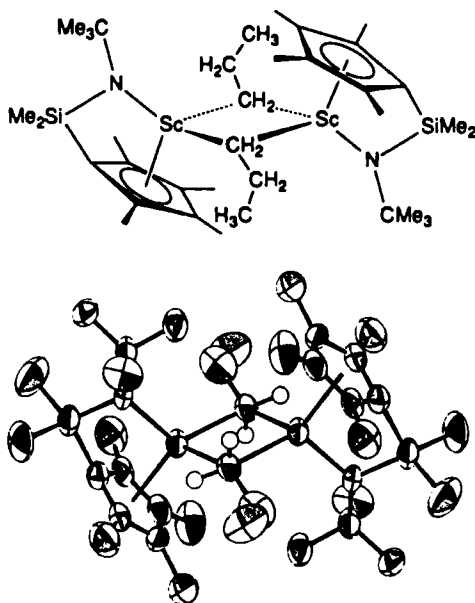


FIG. 20. Molecular structure of $[(\eta^5\text{-C}_5\text{Me}_5\text{SiMe}_2(\eta^1\text{-NCMe}_3))\text{Sc}]_2(\mu\text{-CH}_2\text{CH}_2\text{Me})_2$. [Reprinted with permission from Piers *et al.* (166). Copyright (1990) Georg Thieme Verlag.]

vated $\mu\text{-Me}$ groups do not react with ethylene, propylene, H_2 , MeC_2Me , THF, or pyridine.

In related scandium chemistry using a dianionic carborane ligand as cyclopentadienyl substitute, anionic $[\text{Li}(\text{THF})_3][(\text{C}_5\text{Me}_5)\text{Sc}(\text{C}_2\text{B}_9\text{H}_{11})\text{CH}(\text{SiMe}_3)_2]$ (181) was prepared, via alkylation of $(\text{C}_5\text{Me}_5)\text{Sc}(\text{C}_2\text{B}_9\text{H}_{11})(\text{THF})_3$, and crystallographically characterized. As in the anionic lutetium complexes above, there is little or no distortion of the $\text{CH}(\text{SiMe}_3)_2$ groups.

XIII

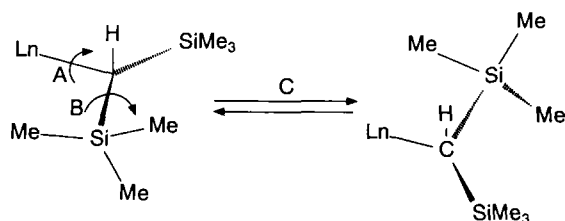
BIS(CYCLOPENTADIENYL)

The introduction of the pentamethylcyclopentadienyl ligand has revolutionized organolanthanide chemistry. More attention has been focused on, and more progress and understanding achieved in, this area than any other. Although outside the time frame of this review, it is pertinent to sketch some background. The enhanced stability and solubility caused by

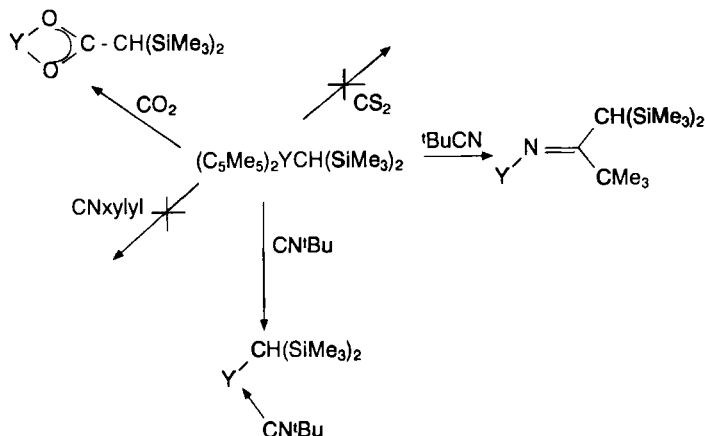
C_5Me_5 incorporation was first appreciated by Brintzinger (182) in organotitanium chemistry and was elegantly developed by Bercaw (183). Subsequent exploitation in organoactinide chemistry by Marks (184), and the brief mention of the long lifetime of $(C_5Me_4Et)_2Y(n-Bu)$ (185) toward ethylene polymerization led to seminal work by Watson (81,144). This was then developed (186), principally by Marks, Evans, and Teuben. Because of the plethora of published literature, it is not my intention to provide comprehensive coverage of this area. It is important to appreciate that compounds such as $[(C_5Me_5)_2MX]_2$ ($M = Y, Lu; X = H, Me$) (1,2,81), $[(C_5Me_5)_2SmH]_2$ (145), $[(C_5Me_5)_2YH]_2$ (187), and $(C_5Me_5)_2ScMe$ (188) have been prepared; propene oligomerization, methane transmetalation, and β -Me elimination also were established (144) prior to the period that this review covers.

Bis(pentamethylcyclopentadienyl) lanthanide precursors are commonly prepared by reaction of $LnCl_3$ with $(C_5Me_5)M$ ($M = Li, Na, K$). In this manner, virtually all the lanthanide precursors $(C_5Me_5)_2LnCl_2ML_2$ or $(C_5Me_5)_2LnCl$ are accessible. In addition, the X-ray crystal structures (3, 9) of $(C_5Me_5)_2YbCl_2Li(OEt_2)$ (189), $[(C_5Me_5)_2CeCl_2K(THF)]_n$ (190), $(C_5Me_5)_2CeCl_2Li(OEt_2)_2$ (149,191), $(C_5Me_5)_2PrCl_2Na(dme)_2$ (192), and $(C_5Me_5)_2LnCl$ [$Ln = Y$ (193), Ce (190), Nd (194), Sm (195), Ho (192), Yb (195), Lu (196)], as well as $[(C_5Me_5)_2SmCl]_3$ (197) and $(C_5Me_5)_2Y(\mu-Cl)Y(Cl)Y(C_5Me_5)_2$ (198) have been determined.

The chemistry of $(C_5Me_5)_2MCH(SiMe_3)_2$ was extended by Teuben to yttrium (75) and cerium (76). Reaction of salt-free $(C_5Me_5)_2YCl(THF)$ with $LiN(SiMe_3)_2$ or $LiCH(SiMe_3)_2$ afforded $(C_5Me_5)_2YN(SiMe_3)_2$ and $(C_5Me_5)_2YCH(SiMe_3)_2$, respectively (75). Their X-ray crystal structures have been determined. Both display γ -Me . . . Y secondary interactions (Section XVII). Solid-state ^{13}C CP-MAS spectra indicated several fluxional processes for the $X(SiMe_3)_2$ ($X = N, CH$) groups. A relative order of activation energies $E_A > E_C \gg E_B$ was proposed on the basis of pattern and intensities of the resonances (Scheme 14). These intramolecular γ -agostic, $N \rightarrow Y$ π -donation, and α -C-H-Y interactions reduce the electronic unsaturation in these formally 14-electron systems.



Facile insertion (199) of unsaturated substrates such as CO_2 and $t\text{BuCN}$ into the Y-alkyl bond of $(\text{C}_5\text{Me}_5)_2\text{YCH}(\text{SiMe}_3)_2$, and the less sterically hindered $(\text{C}_5\text{Me}_5)_2\text{YCH}_2\text{C}_6\text{H}_3-3,5\text{-Me}_2$ (200) occurs (Scheme 15). The X-

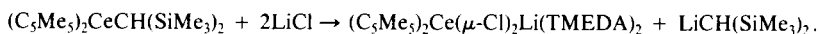


ray crystal structure of $(\text{C}_5\text{Me}_5)_2\text{Y}(\eta^2\text{-CCH}_2\text{C}_6\text{H}_3\text{Me}_2)=\text{N}(2,6\text{-xylyl})\text{THF}$ has been determined. The reaction of $(\text{C}_5\text{Me}_5)_2\text{YCH}(\text{SiMe}_3)_2$ and $(\text{C}_5\text{Me}_5)_2\text{YMe}.\text{THF}$ with acidic hydrogen-containing substrates has been investigated (200). Facile protonolysis of Y- C_α bond was observed. In this manner, alkoxides $(\text{C}_5\text{Me}_5)_2\text{YOR}(\text{OEt}_2)$ (from ROH) and acetylides $(\text{C}_5\text{Me}_5)_2\text{Y}-\text{C}\equiv\text{CR}$ (from $\text{RC}\equiv\text{CH}$) were prepared. Reaction with excess terminal acetylene resulted in the catalytic regioselective dimerization to 1-en-3-yne. As was also observed for $\{(\text{C}_5\text{Me}_5)_2\text{LuX}\}_2$ ($\text{X} = \text{H}, \text{Me}$) and $(\text{C}_5\text{Me}_5)_2\text{ScMe}$, $(\text{C}_5\text{Me}_5)_2\text{YCH}(\text{SiMe}_3)_2$ and $(\text{C}_5\text{Me}_5)_2\text{YMe}.\text{THF}$ metalate pyridine at an α -position to afford $(\text{C}_5\text{Me}_5)_2\text{Y}(\eta^2\text{-NC}_5\text{H}_4)$. Thermolysis of $(\text{C}_5\text{Me}_5)_2\text{YCH}(\text{SiMe}_3)_2$ in 1,3,5- $\text{C}_6\text{H}_3\text{Me}_3$ selectively afforded the 3,5-isomer $(\text{C}_5\text{Me}_5)_2\text{YCH}_2\text{C}_6\text{H}_3-3,5\text{-Me}_2$ (145b). A σ -bond metathesis pathway was favored, instead of (intramolecular) C-H activation of a C_5Me_5 methyl group, to afford the putative fulvene $(\text{C}_5\text{Me}_5)(\eta^6\text{-C}_5\text{Me}_4\text{CH}_2)\text{Y}$ [cf. $(\text{C}_5\text{Me}_5)(\eta^6\text{-C}_5\text{Me}_4\text{CH}_2)\text{Sc}$ (143), $(\text{C}_5\text{Me}_5)(\eta^6\text{-C}_5\text{Me}_4\text{CH}_2)\text{Ti}$ (201), and $(\text{C}_5\text{Me}_5)(\eta^6\text{-C}_5\text{Me}_4\text{CH}_2)\text{TiMe}$ (202)], and subsequent mesitylene activation. The related bridging fulvene $(\text{C}_5\text{Me}_5)_2\text{Y}(\mu\text{-}\eta^1, \eta^5\text{-CH}_2\text{C}_5\text{Me}_4)(\mu\text{-H})\text{Y}$ (C_5Me_5) (203), [cf. $(\text{C}_5\text{Me}_5)_2\text{Ti}(\mu\text{-}\eta^1, \eta^5\text{-CH}_2\text{C}_5\text{Me}_4)(\mu\text{-O})_2\text{Ti}(\text{C}_5\text{Me}_5)$ (204)], prepared from thermolysis of $[(\text{C}_5\text{Me}_5)_2\text{YH}]_2$ (145b) in cyclohexane, does not react with mesitylene under comparable conditions.

On the basis of two different $^1\text{J}_{\text{YH}}$ coupling constants, and just one observed ^1H NMR resonance, $[(\text{C}_5\text{Me}_5)_2\text{YH}]_2$ was proposed to be a dimer with *both* hydrides asymmetrically bridging (145b). This is different from that found in $(\text{C}_5\text{Me}_5)_2\text{M}(\mu\text{-X})\text{M}(\text{X})(\text{C}_5\text{Me}_5)_2$ ($\text{M} = \text{Y}, \text{Lu}$; $\text{X} = \text{H}, \text{Me}$).

$[(C_5Me_5)_2YH]_2$ was recently shown (145d) to have, after all, symmetrical μ -H ligands.

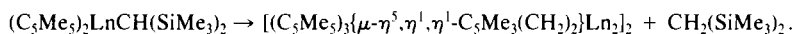
$(C_5Me_5)_2CeCH(SiMe_3)_2$ (76,205) might be expected to possess different reactivity than its yttrium counterpart because of the larger (14), hence less sterically saturated, cerium metal center. $(C_5Me_5)_2CeCH(SiMe_3)_2$ could be prepared by reaction of $(C_5Me_5)_2CeCl_2Li(THF)_n$ with $LiCH(SiMe_3)_2$. The yield is, however, poor, because the reverse reaction, metalation of $LiCl$ by $(C_5Me_5)_2CeCH(SiMe_3)_2$, occurs. In the presence of TMEDA, this is irreversible:



Thus, $(C_5Me_5)_2CeCH(SiMe_3)_2$ is better prepared from $[(C_5Me_5)_2CeCl]_n$ and $LiCH(SiMe_3)_2$:

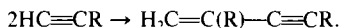


Structural characterization reveals, as well as the ubiquitous α -C-H-M interaction, a secondary β -Si-Me-Ce interaction (Section XVII). Hydrogenation is facile and affords $[(C_5Me_5)_2CeH]_2$. The thermolysis (206) of $(C_5Me_5)_2LnCH(SiMe_3)_2$ ($Ln = Y, La, Ce$) and $(C_5Me_5)_2CeCH_2C_6H_3Me_2$ in C_6D_{12} has been investigated. Loss of $CH_2(SiMe_3)_2$ (indicating hydrogen abstraction from C_5Me_5) and, for $M = La$ and Ce , a tetranuclear complex $[(C_5Me_5)_3\{\mu-\eta^5, \eta^1, \eta^1-C_5Me_3(CH_2)_2\}Ln_2]_2$ has been isolated, and for $Ln = Ce$, crystallographically characterized:



The $C_5Me_3(CH_2)_2$ ligand bridges three cerium atoms and is double metalated at two adjacent methyl groups. The fulvene $(C_5Me_5)(C_5Me_4CH_2)Ln$ was postulated as a possible intermediate. With $Ln = Y$, secondary reactions (C-H activation of solvent or $CH_2(SiMe_3)_2$ led to complex product mixtures. Because of the smaller charge/ionic radius ratio of the larger lanthanides, C-H activation of saturated substrates is less kinetically favored, and the thermodynamically stable tetranuclear products can be isolated.

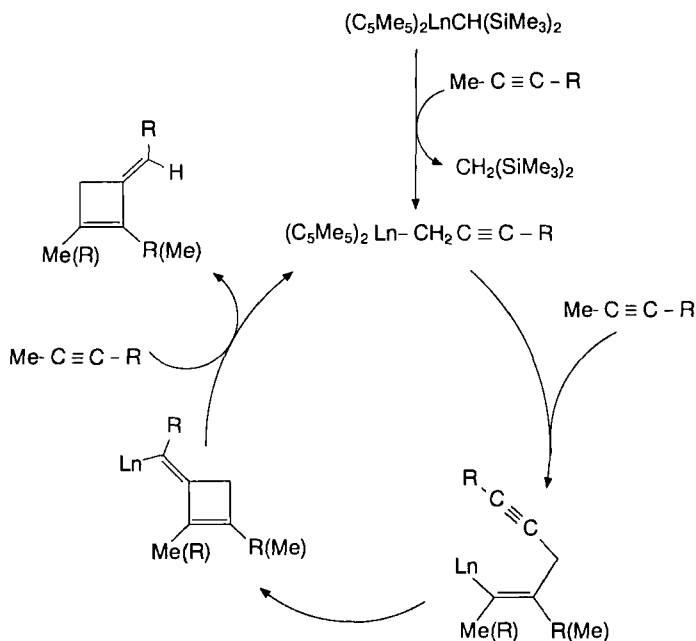
$(C_5Me_5)_2LnCH(SiMe_3)_2$ ($Ln = Y, La, Ce$) are precatalysts for the oligomerization of terminal acetylenes $HC\equiv CR$ (207). The active catalysts are $[(C_5Me_5)_2Ln-C\equiv CR]_n$. The regioselectivity and extent of oligomerization is dependent on various factors, including the size of the lanthanide metal and the substituent R. For $Ln = Y$, and with the bulky R groups *t*-Bu and *i*-Pr, regioselective head-to-tail dimerization to linear $H_2C=C(R)-C\equiv CR$ was observed:



For $Ln = La$ and Ce , higher oligomers (trimers and traces of tetramers) are

also formed. These lanthanide-mediated 1-alkyne couplings were generally less selective than for $\text{Ln} = \text{Y}$. With $\text{R} = \text{Ph}$ or SiMe_3 , the dimer $\text{RHC}=\text{C}(\text{H})-\text{C}\equiv\text{CR}$ is formed. As is typically observed for the smaller metal, yttrium, C-H activation by free 1-alkyne of $\text{Y}-\text{R}'$ (leading exclusively to dimers) is favored over 1-alkyne insertion (leading to higher oligomers). The acetylides $(\text{C}_5\text{Me}_5)_2\text{Ln}-\text{C}\equiv\text{CR} \cdot \text{L}$ ($\text{Ln} = \text{Y}, \text{Ce}, \text{Sm}$) have been isolated and monomeric $(\text{C}_5\text{Me}_5)_2\text{Sm}-\text{C}\equiv\text{CPh}(\text{THF})$ (156b) has been structurally characterized.

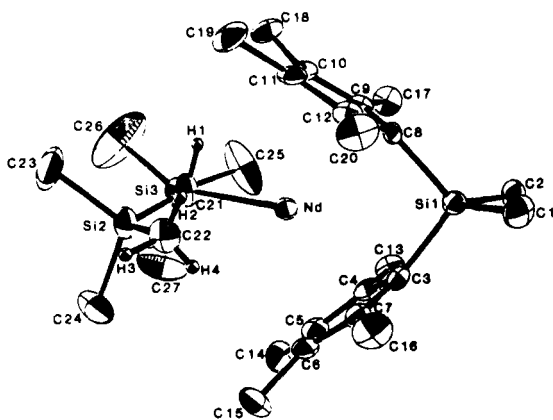
$(\text{C}_5\text{Me}_5)_2\text{LnCH}(\text{SiMe}_3)_2$ ($\text{Ln} = \text{La}, \text{Ce}$) are efficient catalysts for the cyclodimerization of alkynes $\text{MeC}\equiv\text{CR}$ ($\text{R} = \text{Me}, \text{Et}, n\text{-Pr}$) to substituted 3-alkylidenecyclobutenes (208) (Scheme 16). The initial step is for-

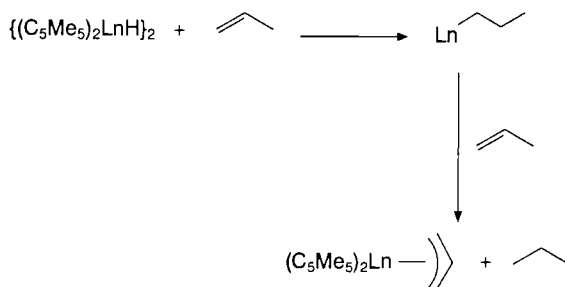


mation of $(\text{C}_5\text{Me}_5)_2\text{Ln}-\text{CH}_2\text{C}\equiv\text{CR}$ ($\text{Ln} = \text{La}, \text{Ce}$). Although $(\text{C}_5\text{Me}_5)_2\text{Y}-\text{CH}_2\text{C}\equiv\text{CR}$ could be prepared, this was inactive toward 2-butyne, presumably for steric reasons. With bulkier R groups, only stoichiometric α -methyl C-H activation was observed. A mechanism was proposed via insertion of $\text{MeC}\equiv\text{CR}$ into $\text{Ln}-\text{CH}_2\text{C}\equiv\text{CR}$, followed by intramolecular insertion of the resulting pendant $-\text{C}\equiv\text{CR}$ group. In contrast, acetonitrile reacted stoichiometrically with $(\text{C}_5\text{Me}_5)_2\text{LnCH}(\text{SiMe}_3)_2$ ($\text{Ln} = \text{La}, \text{Ce}$) to give dimeric $[(\text{C}_5\text{Me}_5)_2\text{LnCH}_2\text{CN}]_2$ (209), containing bridging CH_2CN units. Related $(\text{C}_5\text{Me}_5)_2\text{ScR}$ ($\text{R} = \text{H}, \text{Me}, p\text{-tolyl}$) react with $\text{R}'\text{CN}$ to give the azomethine complexes $(\text{C}_5\text{Me}_5)_2\text{ScNCR}'\text{R}$ (210).

Reaction of the butadiene–Mg reagent $\text{Mg}(\text{C}_4\text{H}_6)(\text{THF})_2$ with $(\text{C}_5\text{Me}_5)_2\text{La}(\mu\text{-Cl})_2\text{K}(\text{dme})_2$ afforded dimeric $(\text{C}_5\text{Me}_5)_2(\text{THF})\text{La}(\mu\text{-}\eta^1, \eta^3\text{-CH}_2\text{CHCHCH}_2)\text{La}(\text{C}_5\text{Me}_5)_2$, which was characterized by X-ray crystallography (211).

In a sequence of three important articles by Marks, $(\text{C}_5\text{Me}_5)_2\text{LnCH}(\text{SiMe}_3)_2$ ($\text{Ln} = \text{La}, \text{Nd}, \text{Sm}, \text{Lu}$) (51,212) and $\{\text{Me}_2\text{Si}(\text{C}_5\text{Me}_4)_2\}\text{LnCH}(\text{SiMe}_3)_2$ (213) were synthesized and for $\text{Ln} = \text{Nd}$, the X-ray crystal structure determined. A close Nd–Me $_{\gamma}$ interaction was observed (Fig. 21). This was described as a model for (aborted) β -Me elimination (Section XVII). The bulky $\text{CH}(\text{SiMe}_3)_2$ group has been extensively used in organolanthanide chemistry, particularly to prepare sterically saturated (hence salt- and solvent-free) precursors which can undergo subsequent facile hydrogenation to afford the corresponding dimeric hydrides. Using such methodology, $[(\text{C}_5\text{Me}_5)_2\text{LnH}]_2$ (51,212) and $[\{\text{Me}_2\text{Si}(\text{C}_5\text{Me}_4)_2\}\text{LnH}]_2$ (213) were prepared. These hydrides were shown to be extremely active for ethylene polymerization and olefin hydrogenation (214). For ethylene polymerization, activities correlated with the metal ionic radius $\text{La} > \text{Nd} \gg \text{Lu}$, and high-molecular-weight ($M_w = 3.8\text{--}15 \times 10^5$), moderate polydispersity ($M_w/M_n = 1.4\text{--}6.4$) polyethylene was manufactured. It was proposed that chain transfer and β -H elimination processes were not operable and that initiation limiting dissociation of dimeric $[(\text{C}_5\text{Me}_5)_2\text{LnH}]_2$ was responsible for the number of polymer chains produced per Ln initiator site being < 1.0 . The more “open” coordination sphere of $\text{Me}_2\text{Si}(\text{C}_5\text{Me}_4)_2$ results in an increase in activity for ethylene polymerization. Although extremely active with ethylene, reaction with α -olefins resulted in η^3 -allyl formation,





via the following insertion, hydrogen abstraction process (Scheme 17). Butadiene is not polymerized by $[(\text{C}_5\text{Me}_5)_2\text{LnH}]_2$, but afforded the η^3 -crotyl species $(\text{C}_5\text{Me}_5)_2\text{Ln}(\eta^3\text{-H}_2\text{CCHCHMe})$.

A detailed mechanistic study of olefin hydrogenation has been performed (214). For hydrogenation of 1-hexene, the rate law is $[\text{Ln}]^1[\text{H}_2]^1[\text{olefin}]^0$ suggesting rapid olefin addition and insertion into Ln-H , followed by rate-limiting Ln-R hydrogenolysis. For the larger lanthanides (La, Nd, Sm) with structures $(\text{C}_5\text{Me}_5)_2\text{Ln}(\mu\text{-H})_2\text{Ln}(\text{C}_5\text{Me}_5)_2$, the rate law for cyclohexene hydrogenation is $[\text{Ln}]^{1/2}[\text{olefin}]^1[\text{H}_2]^0$, implying that cyclohexene insertion into Ln-H now becomes rate limiting. This is consistent with the additional steric shielding of the olefin and with the small extent of dissociation of the hydride dimer. In contrast, rapid preequilibrium dissociation of the ("oversaturated") dimer $(\text{C}_5\text{Me}_5)_2\text{Lu}(\mu\text{-H})\text{LuH}$ ($\text{C}_5\text{Me}_5)_2$ ($\Delta G_{\text{dissociation}} < 2 \text{ kcal mol}^{-1}$) (144c) is facile and was thus proposed to follow a kinetic rate law for cyclohexene hydrogenation of $[\text{Lu}]^1[\text{olefin}]^1[\text{H}_2]^0$. In contrast to the trend observed for ethylene polymerization the hydrogenation activities decrease ($\text{Lu} > \text{Sm} > \text{Nd} > \text{La}$) with increasing Ln^{3+} ionic radius (14). The higher charge/radius ratio of the smaller metals accelerate H_2 activation in the concerted four-center transition state for olefin hydrogenation. The rate is also dependent on the coordination sphere, i.e., $(\text{C}_5\text{Me}_5)_2\text{Ln} > \text{Me}_2\text{Si}(\text{C}_5\text{Me}_4)_2\text{Ln}$. The rate of insertion of substituted olefins display pronounced sensitivity to the steric constraints imposed by the ligand coordination sphere. Hence the relative rates for olefin insertion are $\text{Me}_2\text{Si}(\text{C}_5\text{Me}_4)_2\text{Ln} > (\text{C}_5\text{Me}_5)_2\text{Ln}$.

On the basis of *f*-element bond enthalpies, it was proposed that for α olefins, insertion into an Ln-H bond is quite exothermic (ca. 15 kcal mol^{-1}). Conversely, this implies that β -hydrogen elimination is disfavored.

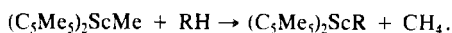
In an important contribution, the reactivity of $(\text{C}_5\text{Me}_5)_2\text{ScR}$ ($\text{R} = \text{Me}$, Ph , *p*-tolyl, CH_2Ph) (all prepared by alkylation of the corresponding chloride) was described (143). The hydride $[(\text{C}_5\text{Me}_5)_2\text{ScH}]_n$ (prepared by hydrogenation) is unstable in solution unless under an H_2 atmosphere. Nevertheless, it is a convenient source of $(\text{C}_5\text{Me}_5)_2\text{ScEt}$ and $(\text{C}_5\text{Me}_5)_2\text{Sc}(n\text{-Pr})$ by

reaction (stoichiometric) with ethene and propene, respectively. The monomeric THF adduct $(C_5Me_5)_2ScH(THF)$ is more stable and convenient to use. In general, the adducts $(C_5Me_5)_2LnH(THF)$ ($Ln = Sc, Y$) and $(C_5Me_5)_2LnMe(THF)$ ($Ln = Sc, Sm, Y, Yb, Lu$) are all stable, although the highly reactive $[(C_5Me_5)_2LuH]_2$ decomposes in diethylether, liberating ethane, to give $(C_5Me_5)_2LuOEt$. The X-ray structure of $(C_5H_5)_2YbMe(THF)$ has been reported (215) [cf. $(C_5Me_5)_2YbMe.L$ ($L = OEt_2, THF$) (144d) and $[(C_5H_5)_2Yb(\mu-Me)]_2$ (177)].

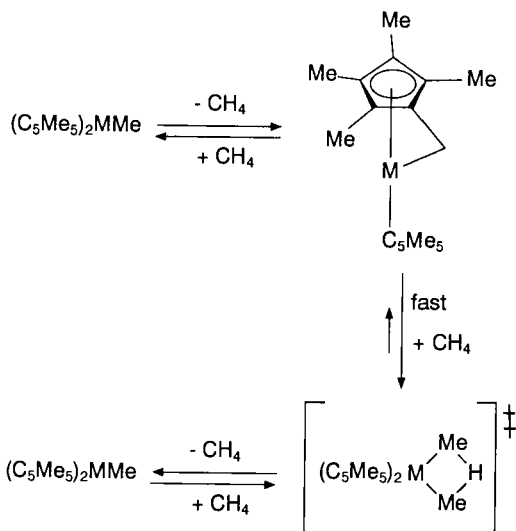
Intramolecular H/D exchange of the C_5Me_5 methyl hydrogens in $[(C_5Me_5)_2ScH]_n$ has been reported (143). In an interesting application, $[(C_5Me_5)_2ScD]_n$ (at 145°C under D_2 in C_6D_6) catalyzed the bulk synthesis of $C_5(CD_3)_5H$ from $C_5(CH_3)_5H$ in high isotopic purity (216).

$[(C_5Me_5)_2ScH]_n$ reacts with allene and metalates pyridine to afford $(C_5Me_5)_2Sc(\eta^3-C_3H_5)$ and $(C_5Me_5)_2Sc(\eta^2-C_5H_4N)$, respectively (143). The X-ray crystal structure of monomeric 14-electron $(C_5Me_5)_2ScMe$ displayed no evidence for an α -agostic C–H–Sc interaction. In addition, the isotopic perturbation of 1H NMR chemical shift $\Delta\delta$ between $(C_5Me_5)_2ScCH_3$ and $(C_5Me_5)_2ScCH_2D$ was rather small. Due to C_5Me_5 disorder, the X-ray crystal structure of $(C_5Me_5)_2ScEt$, although consistent with a β -C–H–Sc interaction, was not conclusive.

$(C_5Me_5)_2ScMe$ activates the C–H bonds of a range of hydrocarbons including $^{13}CH_4$, arenes, styrene, and alkynes:



Kinetic analysis of the degenerate C–H bond activation of $^{13}CH_4$ by $(C_5Me_5)_2MMe$ ($M = Sc$, monomer; $M = Y, Lu$, dimer) in cyclohexane as an inert solvent indicated two mechanistic pathways. Principally bimolecular kinetics were observed for Y, Lu indicating direct intermolecular C–H bond activation. For $M = Sc$, a unimolecular pathway was also observed indicating rate-determining intramolecular formation of a C_5Me_5 metalated species. The cyclometalated intermediate subsequently activates the C–H bond in a second, fast step (Scheme 18). The relative rates of C–H activation of methane by $(C_5Me_5)_2MMe$ lie in the order Y (250) > Lu (5) > Sc (1). This order was attributed to the relative electrophilicity of the metal center, but is also consistent with better substrate orbital overlap due to the increased ionic radius ($Y > Lu > Sc$). It was concluded that C–H bond activation proceeds via a concerted four-center transition state with little charge polarization. In comparison with $[(C_5H_5)_2M(\mu-Me)]_2$ ($M = Y, Lu$) (173,177) (Fig. 22), which do not react with methane, the sterically demanding C_5Me_5 ligands inhibit formation of the corresponding very stable μ -alkyl dimers. The absence of facile preequilibrium dissociation



in these very stable ground-state μ alkyls inhibits their kinetic activity, despite their apparent steric advantage.

Slow decomposition of $(C_5Me_5)_2ScCH_2(cyclo-C_5H_8)$ cleanly afforded methylcyclopentane and a crystalline scandium species containing a metalated C_5Me_5 . The X-ray crystal structure (217) showed this to be the dimer $[(C_5Me_5)_2Sc\{\mu-(\eta^1, \eta^5-C_5Me_4CH_2)\}]_2$.

In a series of papers (168,169,218,219), the organolanthanide-catalyzed regiospecific hydroamination/cyclization of unsaturated amines was addressed (Scheme 19). Rapid protonolysis of $[(C_5Me_5)_2LnH]_2$ by the (unprotected) amine, and rate-limiting ring formation involving irreversible intramolecular olefin insertion into the Ln -amide bond, is consistent with the

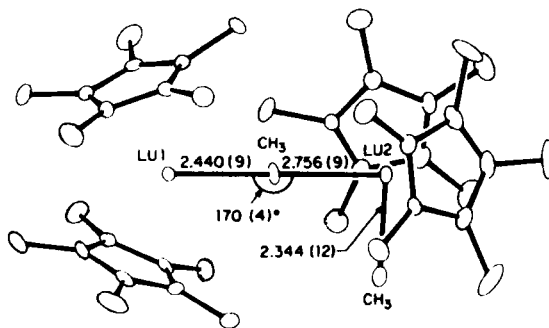
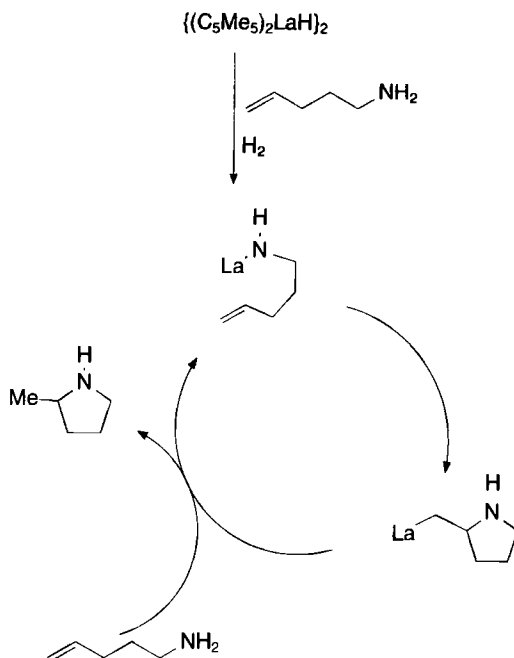
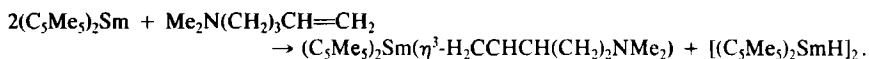


FIG. 22. Molecular structure of $(C_5Me_5)_2Lu(\mu-Me)LuMe(C_5Me_5)_2$. [Reprinted with permission from Watson and Parshall (81). Copyright (1985) American Chemical Society.]



determined rate law of $[La]^1[substrate]^0$. Protonolysis of the resulting $Ln-C$ bond by free amine, to regenerate $[(C_5Me_5)_2LnH]_2$, is also rapid. Extensive isotopic labeling supported the proposed mechanism. At low substrate concentration, the active catalyst is proposed to be $(C_5Me_5)_2LnNHR(NH_2R)$ (218). The relative activity of a number of catalysts was measured. This ordering mirrors that found for the polymerization of ethylene and correlates with the steric unsaturation at the lanthanide, i.e., $[(C_5Me_5)_2LaH]_2 > [Me_2Si(C_5Me_4)_2LuH]_2 > [(C_5Me_5)_2LuH]_2$. Diastereoselection is observed in the conversion of $H_2NCHMeCH_2CH_2CH=CH_2$ to 2,5-dimethylpyrrolidine. The *cis*/*trans*-isomer ratio was dependent on the lanthanide size, the π ligands, and the reaction temperature. Consistent with a sterically sensitive rate-limiting cyclization step, the more sterically hindered amine $H_2NCH_2CMe_2CH_2CH=CH_2$ showed marked dependency on the size of the lanthanide metal $La > Sm > Lu$ (168).

The readily accessible and conveniently prepared compounds $(C_5Me_5)_2Sm(THF)_2$ and $(C_5Me_5)_2Sm$ are also precatalysts for hydroamination/cyclization via oxidation to trivalent $(C_5Me_5)_2SmX$ species (219) via allylic C-H activation:

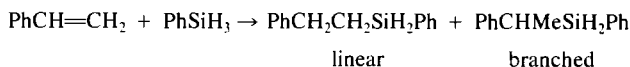


Both organosamarium species then react with primary or secondary amines to generate the (same) catalytically active $(C_5Me_5)_2SmNRR'$ complex.

Incorporation of chiral groups into the cyclopentadienyls allows the formation of chiral $\{Me_2Si(C_5Me_4)(C_5H_3R^*)\}LnCH(SiMe_3)_2$ ($Ln = La, Sm$; $R^* = (-)$ -menthyl, $(+)$ -neomenthyl). These are precatalysts for the enantioselective (with up to 74% e.e), or diastereoselective hydroamination/cyclization of unsaturated amines to piperidines or pyrrolidines, respectively. For example, the hydroamination/cyclization of $H_2NCHMeCH_2CH_2CH=CH_2$ to 2,5-dimethylpyrrolidine is mediated with >95% diastereoselectivity (for $Ln = Sm$) (169).

These chiral organolanthanide catalysts were also used for asymmetric olefin hydrogenation (220). Hydrogenation of 2-phenyl-1-butene occurred with high activity and moderate to excellent enantioselectivity, and obeyed a (hopefully, by now familiar) rate law of $[Sm]^{1/2}[H_2]^1[olefin]^0$. The two pseudoenantiomorphous catalysts yield alkanes of opposite absolute configurations and with inequivalent e.e.'s, consistent with a stereodifferentiating insertion process into the $Sm-H$ bond.

Complexes $(C_5Me_5)_2LnCH(SiMe_3)_2$ [$Ln = Y$ (145), Nd (51)] catalyze (221,222) the hydrosilylation of styrene to a mixture of branched and linear products:



With both 1-decene and the internal olefin 2-heptene regioselective hydrosilylation gave only linear products, suggesting that the Nd -alkyl (222) species isomerizes rapidly. This work was expanded (221) to a variety of substituted and functionalized olefins. The precatalyst $(C_5Me_5)_2YSiH_2Ph$ is formed *in situ*, which was proposed to further react with $PhSiH_3$ to afford the catalyst $[(C_5Me_5)_2YH]_2$, and PhH_2SiSiH_2Ph . Olefin insertion, followed by σ -bond metathesis of $Ln-R$ with $PhSiH_3$ completes the catalytic cycle. This mechanism is in agreement with the observed regioselectivity of olefin insertion (*vide supra*) (221,222).

The utility of $(C_5Me_5)_2LnCH(SiMe_3)_2$ was yet further extended to the catalytic (anti-Markownikoff) hydroboration of a wide range of unfunctionalized olefins (223). Reaction with catecholborane (as boron source) resulted not in loss of $CH_2(SiMe_3)_2$, but due to $Ln^{\delta+}-C^{\delta-}$, $B^{\delta+}-H^{\delta-}$ bond polarities results in $[(C_5Me_5)_2LnH]_2$ as catalyst, and (catechol) $BCH(SiMe_3)_2$. Olefin insertion and hydroboration of $Ln-CH_2CH_2R$, followed by oxidative workup, gave the product alcohol. As expected, the reaction rate is dependent on the steric demands at the metal center, hence $La > Sm$ and $Me_2Si(C_5Me_4)_2Ln > (C_5Me_5)_2Ln$, and on the degree

of olefin substitution. $(C_5Me_5)_2Sm(THF)_2$ is also active, by *in situ* oxidation to $(C_5Me_5)_2SmX$, as was found for catalytic hydroamination/cyclization.

Catalytic dehydrogenation of organosilanes $RSiH_3$ by organolanthanides is a convenient synthetic route to polyorganosilanes, from which ceramic precursors, etc., could be manufactured. The first lanthanide–silicon σ bond was obtained by reaction of $(C_5H_5)_2LnCl_2Na(dme)_2$ ($Ln = Sm, Lu$) with $LiSiMe_3$ to afford anionic $[Li(dme)_3][(C_5H_5)_2Ln(SiMe_3)_2]$ (224). Dehydrogenative coupling of silanes was investigated mechanistically (225). $(C_5Me_5)_2LnR$ ($Ln = La, Nd, Sm, Y, Lu$; $R = H, CH(SiMe_3)_2$) react with $PhSiH_3$, eliminating RH , and forming polysilanes according to the rate law $[(C_5Me_5)_2LaCH(SiMe_3)_2]^1 [PhSiH_3]^1$. The relative rates $La < Nd < Sm < Y < Lu$ correlated well with the metal ionic radius, as was previously observed for $[(C_5Me_5)_2LnH]_2$ -catalyzed 1-hexene hydrogenation (214). Kinetic studies for $[(C_5Me_5)_2LaH]_2$ revealed the rate law $[La]^{1/2} [PhSiH_3]^1$ implying a dimeric La–Si species $(C_5Me_5)_2LaSiH_2Ph$ in rapid preequilibrium with a reactive monomer. $(C_5Me_5)_2NdCH(SiMe_3)_2$ catalyzes the dehydrogenation condensation of $MeSiH_3$ at $90^\circ C$ to give poly(methylsilane). Pyrolysis gave β -SiC (226).

Reaction of $(C_5Me_5)_2LnCH(SiMe_3)_2$ ($Ln = Sm, Nd$) with neat $H_2Si(SiMe_3)_2$ afforded $(C_5Me_5)_2LnSiH(SiMe_3)_2$ (227). Interestingly, the X-ray crystal structure shows a dimer supported by **intermolecular** $Sm \cdots CH_3-Si$ interactions, similar to the **intramolecular** $\beta-Si-Me \cdots Ln$ interactions observed in $(C_5Me_5)_2LnCH(SiMe_3)_2$ and $(C_5Me_5)_2Ln\{CH(SiMe_3)_2\}_2$.

$[(C_5Me_5)_2SmH]_2$ and related $(C_5Me_5)_2LnMe(THF)$ complexes are precatalysts for the polymerization of methylmethacrylate (MMA) to give poly(MMA) of high $(50-550 \times 10^3)$ molecular weight and narrow polydispersity (1.02–1.04) (228). The X-ray crystal structure of the catalyst $(C_5Me_5)_2Sm\{(MMA)_2H\}$ was determined (228). The two MMA molecules form an eight-membered cyclic structure, one being bound to Sm via an alkoxide in its enolate form, the other coordinating through its $C=O$ group.

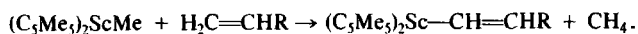
XIV

BIS(CYCLOPENTADIENYL) LIGAND VARIATIONS

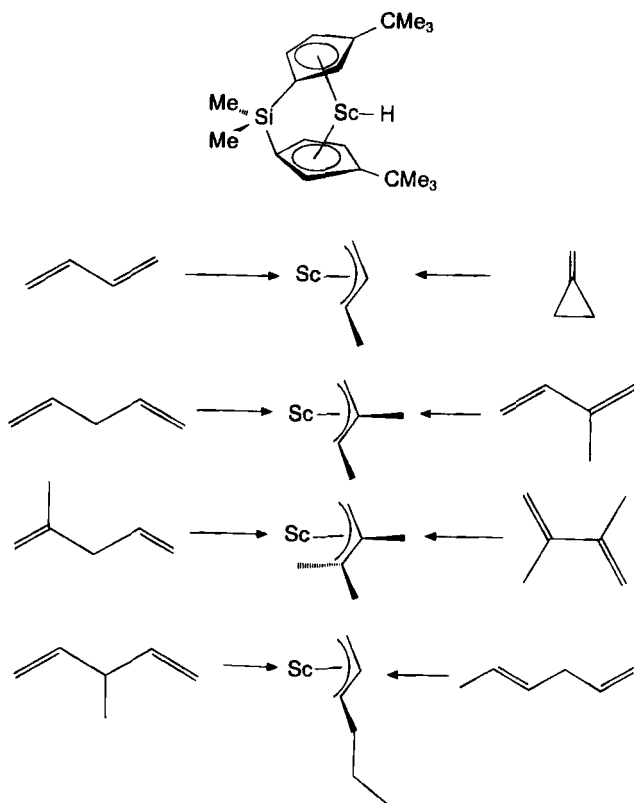
The reactivity of the organolanthanides are very sensitive to the nature and steric influence of the ancillary ligands. In seeking new stoichiometric and catalytic transformations, substantial variations within the constraints imposed by the bis(cyclopentadienyl) ligand coordination sphere have

been investigated, i.e., $[\text{Me}_2\text{Si}(\text{C}_5\text{Me}_4)_2]^{2-}$, $[\text{C}_5\text{Me}_4\text{SiMe}_2\text{N-}t\text{-Bu}]^{2-}$, $[\text{Me}_2\text{Si}(\text{C}_5\text{H}_3\text{-}t\text{-Bu})_2]^{2-}$, and $[\text{Me}_2\text{Si}\{\text{C}_5\text{H}_2\text{-}t\text{-Bu}(\text{SiMe}_3)\}_2]^{2-}$.

Although $(\text{C}_5\text{Me}_5)_2\text{ScMe}$ is active for ethene polymerization, it reacts stoichiometrically and regiospecifically at the terminal sp^2 C-H bond with substituted olefins, such as propene, to give vinylic C-H activation products:



This was assigned to unfavorable steric interactions between the olefin substituent and the C_5Me_5 ligands, preventing olefin π -bond coordination to the relatively small Sc center. Incorporation of the less sterically hindered ligand framework in $\{[\text{Me}_2\text{Si}(\text{C}_5\text{H}_3\text{-}t\text{-Bu})_2]\text{Sc}(\mu\text{-H})\}_2$ (167) allows reaction with butadiene and nonconjugated dienes (1,4-pentadiene, $\text{H}_2\text{C}=\text{CMeCH}_2\text{CH}=\text{CH}_2$, $\text{H}_2\text{C}=\text{CHCHMeCH}=\text{CH}_2$) to give allyl species $\{\text{Me}_2\text{Si}(\text{C}_5\text{H}_3\text{-}t\text{-Bu})_2\}\text{Sc}(\eta^3\text{-CH}_2\text{CRCR}'\text{R}'')$ (Scheme 20). These same allyl species were also accessible via reaction with methylenecyclopro-

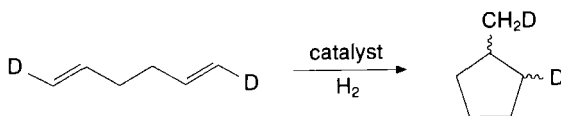


pane, isoprene, 2,3-dimethylbutadiene, and 1,4-hexadiene, respectively. These remarkable transformations, involving C–C σ -bond activation by β -alkyl elimination were probed by extensive ^{13}C -labeling studies. Catalytic, albeit a few turnovers, transformation of 1,4-pentadienes (excess) via C–C σ bond activation was also reported (167).

In related studies, using a dimeric yttrium hydride, and with a cleverly designed bridged cyclopentadienyl ligand substituted to favor the *rac*-isomer, the isospecific α -olefin polymerization catalyst [*rac*-Me₂Si(2-SiMe₃-4-*t*-BuC₅H₂)Y(μ -H)]₂ has recently been reported (170). This gave highly (97%) isotactic poly(1-olefins), with moderate molecular weights. For example, for poly(1-hexene), $M_w = 24000$, $M_w/M_n = 1.75$.

The scandium hydride {Me₂Si(C₅Me₄)₂}ScH(PMe₃) catalyzes the hydrocyclization of 1,5-hexadiene to methylcyclopentane (166). The pendant phosphine-linked cyclopentadienyl complex {Me₂Si(C₅Me₄)(C₅H₃CH₂CH₂P-*t*-Bu₂)}ScCH(SiMe₃)₂ was prepared (229) to ascertain the influence of a high effective phosphine concentration on the catalytic activity of the Sc-alkyl.

To probe the mechanism of chain propagation and transition state geometry for olefin insertion into a d^0 metal–carbon bond, the hydrocyclization of the specifically deuterated 1,5-hexadiene *trans,trans*-1,6-*d*₂-1,5-hexadiene to a mixture of *cis*- and *trans*-*d*₂-methylcyclopentane by {Me₂Si(C₅Me₄)₂}ScH(PMe₃) was investigated (230) (Scheme 21). The excess of the



trans-isomer (*trans* : *cis* = 1.19 : 1) was assigned to stereochemical partitioning due to a kinetic deuterium isotope effect in the diastereomeric intermediate Sc-CHD(CH₂)₃CH=CHD (hence prior to cyclization and hydrogenation) due to the preference for α -H rather than α -D agostic interaction. Related studies by Grubbs (231) indicated that α -activation is not significant in either the rate or stereochemistry of olefin insertion, although Brintzinger (232) found a similar product distribution to Bercaw due to a kinetic isotope effect.

In a comprehensive contribution (175), the linked bis(cyclopentadienyl) R₂Si(C₅Me₄)(C₅H₄) (R = Me, Et) was used to prepare dimeric μ -H species {R₂Si(C₅H₄)(C₅Me₄)M}₂(μ -H)₂ (M = Y, Lu) (175). In contrast to the bridged cyclopentadienyls previously used, the steric properties of each cyclopentadienyl ring (C₅Me₄ versus C₅H₄) are quite different. This resulted in some unique chemistry, with the ligand R₂Si(C₅Me₄)(C₅H₄) spanning the two lanthanide centers, in a bimolecular fashion. {Me₂Si(C₅H₄)₂Yb(μ -X)}₂

[X = Cl (233a), Br (233b)] also have such bridging structures. Monomeric, crystallographically characterized $\{R_2Si(C_5Me_4)(C_5H_4)\}MCH(SiMe_3)_2$ was prepared by standard synthetic methodology (175) (Fig. 23).

These undergo hydrogenation, a rather sterically insensitive reaction, at a rate 10^3 slower (decreased ligand electron donation leads to diminished charge stabilization at the four-center transition state) than their $(C_5Me_5)_2MCH(SiMe_3)_2$ or $\{Me_2Si(C_5Me_4)_2\}MCH(SiMe_3)_2$ counterparts to give dimeric $\{R_2Si(C_5H_4)(C_5Me_4)M\}_2(\mu-H)_2$. NMR evidence was obtained for an intermediate possessing a $\mu-CH(SiMe_3)_2$ group, of possible formulation $\{R_2Si(C_5H_4)(C_5Me_4)M\}_2\{\mu-CH(SiMe_3)_2\}H$. Reaction of μ -hydride $\{R_2Si(C_5H_4)(C_5Me_4)M\}_2(\mu-H)_2$ with α -olefins $H_2C=CHR$ (R = H, Me,

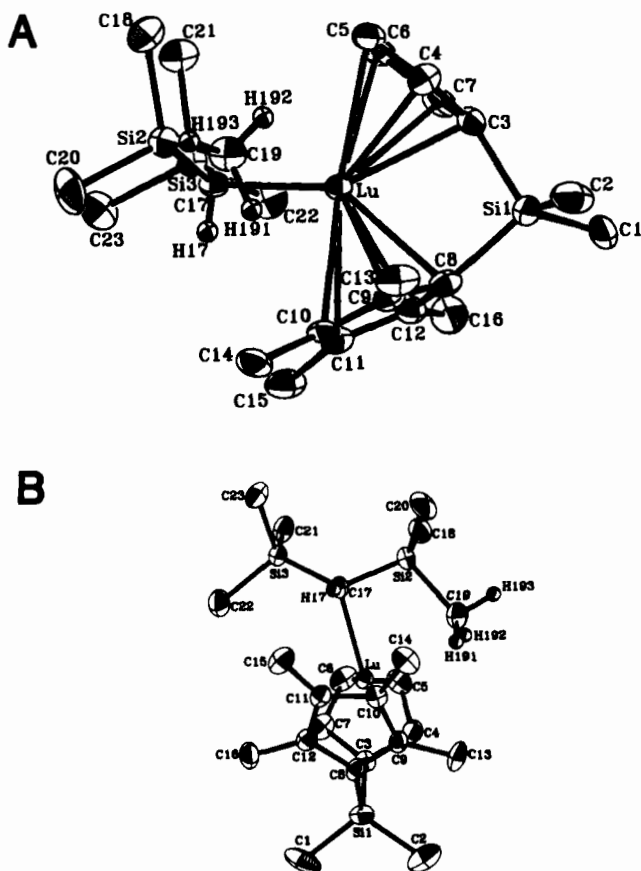
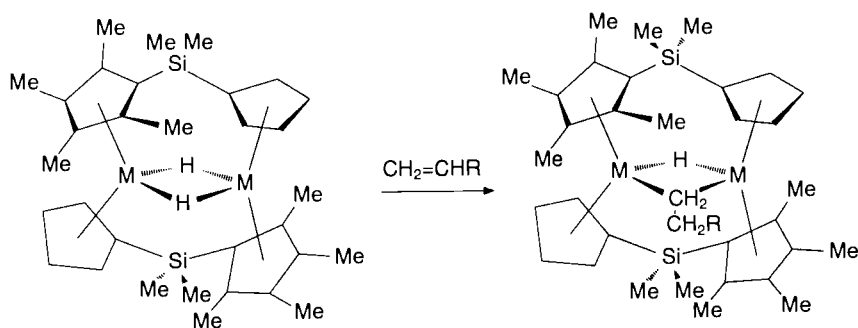


FIG. 23. Molecular structure of $\{R_2Si(C_5Me_4)(C_5H_4)\}MCH(SiMe_3)_2$. [Reprinted with permission from Stern *et al.* (175). Copyright (1990) American Chemical Society.]

n-Bu afforded the μ -H, μ -alkyl species $\{R_2Si(C_5H_4)(C_5Me_4)M\}_2(\mu-H)(\mu-CH_2CH_2R)$ (Scheme 22 and Fig. 24).



Polyolefins or bis(μ -alkyl) insertion products were not observed. [cf. olefin insertion into $[(C_5Me_5)Y(OAr)(\mu-H)]_2$ (174) and $\{(\eta^5-C_5Me_4)SiMe_2(\eta^1-NCMe_3)\}Sc(PMe_3)_2(\mu-H)_2$ (165, 166). μ -Alkyl rotation about the

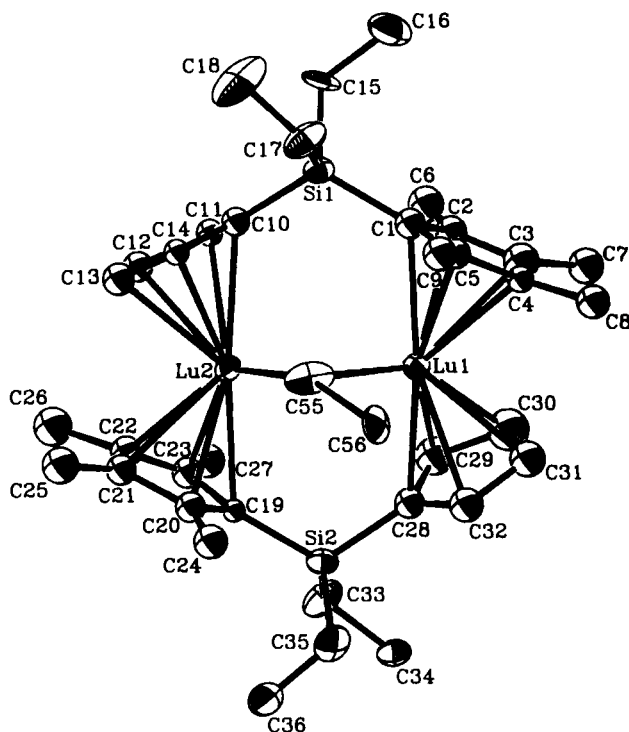


FIG. 24. Molecular structure of $\{R_2Si(C_5H_4)(C_5Me_4)M\}_2(\mu-H)(\mu-Et)$. [Reprinted with permission from Stern *et al.* (175). Copyright (1990) American Chemical Society.]

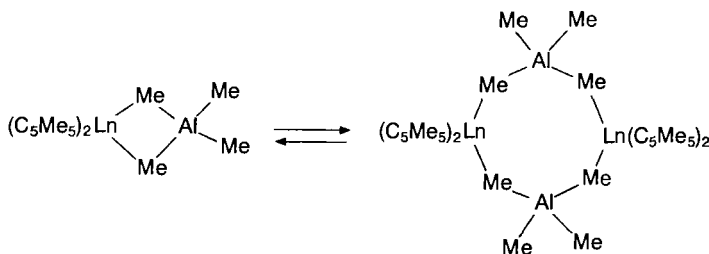
μ -H, μ -C $_{\alpha}$ vector occurs. This cannot, however, effect the equilibration of the diastereotopic α -CH $_2$ protons. Equilibration of these α -methylene protons occurs by inversion at C $_{\alpha}$ via a planar μ -alkyl group transition state.

The μ -ethyl group is bound very unsymmetrically with Lu-C $_{\alpha}$ -C $_{\beta}$ = 148° and 84.7° and Lu-C $_{\alpha}$ = 2.46 and 2.58 Å. The relatively short Lu . . . C $_{\beta}$ (2.78 Å) is suggestive of a secondary interaction. Kinetic analysis of the insertion of 1-hexene (rate law = $k[\text{dihydride}]^1[\text{olefin}]^1$) into μ -H showed that in comparison to terminal Ln-H with similar ligand coordination spheres the bridging hydrides are significantly kinetically deactivated (by 10⁸-10¹⁰) with respect to olefin insertion and that the μ -alkyls are kinetically deactivated (by 10⁸-10⁹) with respect to hydrogenolysis. In {Et $_2$ Si(C $_5$ H $_4$)(C $_5$ Me $_5$)Lu} $_2$ (μ -H)(μ -hexyl) it was concluded that β -H elimination was endothermic by 11 kcal mol⁻¹, implying that the difference in bond dissociation energy D{Lu $_2$ (μ -H)} - D{Lu $_2$ (μ -hexyl)} = 24 kcal mol⁻¹. This indicates that μ -alkyls are not necessarily more thermodynamically stable than their terminal counterparts.

XV

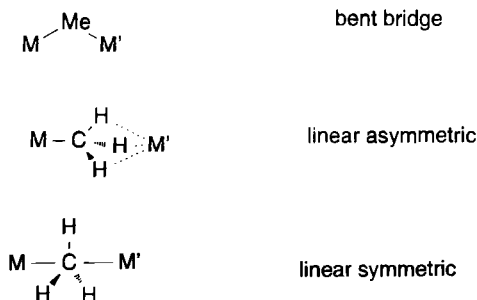
REACTIVITY OF (C $_5$ Me $_5$) $_2$ Ln WITH ALUMINUM/GALLIUM REAGENTS

The reactivity and chemistry of the methyl species (C $_5$ Me $_5$) $_2$ LnMe species with aluminum and gallium reagents has been investigated. (C $_5$ Me $_5$) $_2$ Ln(μ -Me) $_2$ MMe $_2$ (Ln = Y, Lu; M = Al, Ga) (81,82) undergoes temperature-dependent reversible dimerization to the eight-membered ring complex (C $_5$ Me $_5$) $_2$ Ln[(μ -Me) $_2$ M(μ -Me) $_2$] $_2$ Ln(C $_5$ Me $_5$) $_2$ (Scheme 23).



Similarly, reaction of (C $_5$ Me $_5$) $_2$ Sm(THF) $_2$ with excess AlMe $_3$ gave (C $_5$ Me $_5$) $_2$ Sm[(μ -Me) $_2$ Al(μ -Me) $_2$] $_2$ Sm(C $_5$ Me $_5$) $_2$ (82b). These possess a planar, square-shaped Ln(C-M-C) $_2$ Ln ring with the Ln-C-M angles being essentially linear. ¹³C NMR analysis of a range of bridged methyl species allowed (82a), on the basis of J $_{CH}$ and J $_{YC}$ coupling constants, differentiation be-

tween the various possible coordination modes of the μ -Me group (bent bridge, linear asymmetric, and linear symmetric) (Scheme 24). $(C_5Me_5)_2LnMe$ reversibly dimerizes to the symmetric linear-bridged dimer.



The C_5Me_5 groups are sufficiently bulky to inhibit formation of two bent methyl bridges as found in $(C_5H_5)_2Y(\mu-Me)_2Y(C_5H_5)_2$ (173,177). Addition of excess $AlEt_3$ to $(C_5Me_5)_2Sm$ afforded an unusual example of a μ -Et bridged species $(C_5Me_5)_2Sm(\mu-Et)_2AlEt_2$ (234a) (Fig. 25):



The μ -Et groups are highly distorted with the methyl groups pointing away from the $(C_5Me_5)_2Sm$ wedge ($Sm-C_\alpha-C_\beta = 170^\circ$). Likewise, reaction

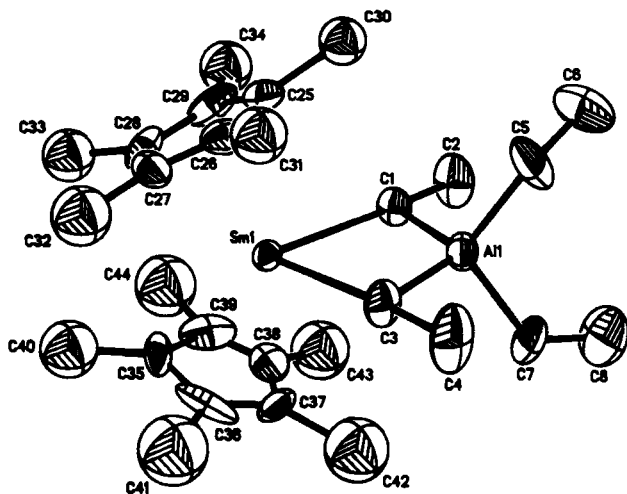


FIG. 25. Molecular structure of $(C_5Me_5)_2Sm(\mu-Et)_2AlEt_2$. [Reprinted with permission from Evans *et al.* (234a). Copyright (1987) American Chemical Society.]

of $(C_5Me_5)_2Yb(THF)$ with $AlEt_3$ afforded $(C_5Me_5)_2Yb(\mu-Et)AlEt_2(THF)$ (234*b*). Interestingly, both carbons of the $\mu-Et$ bridge were found to be within bonding distance of Yb.

Reaction of $(C_5H_5)_2LuCl$ with $LiAlH_4$ in the presence of the Lewis base NEt_3 results in the initial formation of dimeric $[(C_5H_5)_2Lu(\mu-H)_2AlH_2(NEt_3)]_2$. This dissociates in the solid state to afford monomeric $(C_5H_5)_2Lu(\mu-H)AlH_3(NEt_3)$, containing an unusual monodentate AlH_4 group (235).

XVI

ISOCARBONYLS AND LANTHANIDE-TRANSITION METAL BONDS

Reactions of transition metal carbonyl species with organolanthanides invariably results in the product (if isolated) possessing an isocarbonyl $Ln(\mu-OC)M$ moiety. Hence, in $(C_5Me_5)_2Yb(\mu-OC)_2Mn(CO)_3$ (236), $\{1,3-C_5H_3(SiMe_3)_2\}Ce(\mu-OC)_2W(CO)_2(C_5H_5)$ (237), $(C_5H_5)Yb(THF)(\mu-OC)Co(CO)_3$ (238), $[(C_5Me_5)_2Sm(\mu-OC)_2Fe(C_5Me_5)]_2$ (239) there is no lanthanide transition metal bonding, the heterobimetallic dimer being supported by the isocarbonyl ligands. The structure (240) of $\{[(MeCN)_3YbFe(CO)_4]_2 \cdot MeCN\}_x$ consists of polymeric ladders with each Yb^{2+} coordinated to two isocarbonyls. There is also a direct $Yb-Fe$ interaction. This was ascribed to a $[(OC)_4Fe]^{2-} \rightarrow Yb^{2+}$ dative bond, similar (241) to that found

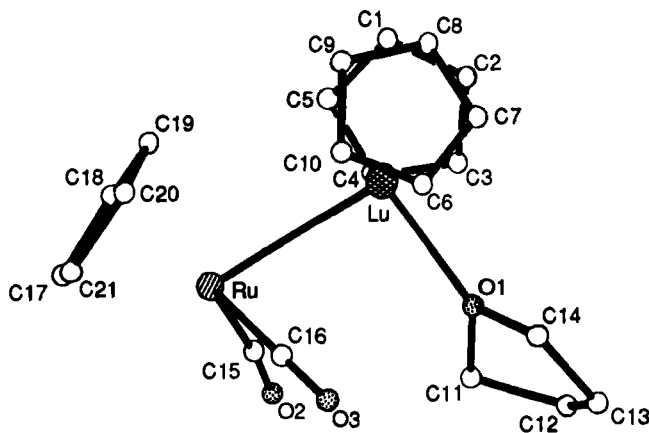


FIG. 26. Molecular structure of $(C_5H_5)_2(THF)LuRu(CO)_2(C_5H_5)$. [Reprinted with permission from Magomdeov *et al.* (245). Copyright (1993) American Chemical Society.]

in unsupported $(C_5Me_5)_2(1)Th-Ru(CO)_2(C_5H_5)$ (242). $(C_5H_5)_2(THF)YRe_2H_7(PMe_2Ph)_4$ (243) and $(C_5H_5)_2LuRe_2H_7(PMe_2Ph)_4$ (243) have open-triangular (Y–Re–Re) and closed-triangular heterotrimetallic units, respectively. These polyhydrides possess Y–Re and Lu–Re bonds bridged by two hydrides. Similarly, reaction of $K[(PMe_3)_3WH_5]$ or $K[(C_5H_5)_2NbH_2]$ (prepared *in situ* by deprotonation with KH in THF) with YbI_2 (0.5 eq) afforded $\{(PMe_3)_3WH_5\}_2Yb(diglyme)$ or $\{(C_5H_5)_2Nb(\mu-H)_2\}_2Yb(diglyme)$, respectively (244). The X-ray crystal structures of both compounds were determined and possess hydride-bridged W–Yb and Nb–Yb bonds. An elusive example of an unsupported lanthanide-transition metal bond was found in $(C_5H_5)_2(THF)Lu-Ru(CO)_2(C_5H_5)$ (245). X-ray crystallography confirmed the absence of bridging carbonyls (Fig. 26).

XVII

γ -C-H-Ln VERSUS β -Si-Me-Ln INTERACTIONS

In the structurally characterized organolanthanides containing a $N(SiMe_3)_2$ or $CH(SiMe_3)_2$ group, it has remained difficult to unequivocally differentiate between γ -C-H-Ln and β -Si-Me-Ln interactions. A β -Si-Me-Ln interaction will manifest itself by having $Ln-C_\alpha-Si(2)-Me_\gamma$ essentially coplanar and with a distorted geometry around the α -carbon atom, such that typically $Ln-C_\alpha-Si_\beta(1) = 120-135^\circ$ and $Ln-C_\alpha-Si_\beta(2) = 95-105^\circ$. This has been observed crystallographically. The consequence of this distortion allows the γ -Me group to interact with the electrophilic lanthanide center ($Ln \cdots C_\gamma = Ln-C_\alpha + 0.4-0.5 \text{ \AA}$). The $Ln-Si_\beta(2)$ distance falls well within the sum of the Van der Waals radii. A polarized, high-energy, spatially diffuse Si–Me σ bond is of a more appropriate energy to donate effectively into a lanthanide metal *d*-orbital LUMO.

In principle, 1H , ^{13}C , and ^{29}Si nuclei represent NMR probes that should be sensitive to interactions with an electrophilic lanthanide metal. In an attempt to differentiate between γ -C-H-Ln and β -Si-Me-Ln interactions, a series of related organolanthanide complexes, all containing the $CH(SiMe_3)_2$ alkyl ligand was studied by variable-temperature solution and solid-state 1H , ^{13}C , and ^{29}Si NMR spectroscopy (246). The dynamic nature of $CH(SiMe_3)_2$, even at $-90^\circ C$ in the solid state, prevented the accumulation of evidence that might have allowed differentiation between the interactions available to these flexible alkyl groups to facilitate stabilization of electrophilic lanthanide centers.

In $(C_5Me_5)Ln\{CH(SiMe_3)_2\}_2$ [$Ln = La$ (150), Ce (158), $Yb\{N(SiMe_3)_2\}_2$

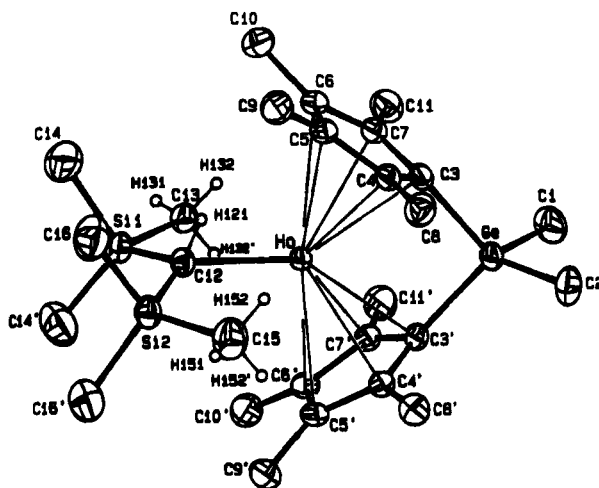


FIG. 27. Molecular structure of $\{\text{Me}_2\text{Ge}(\text{C}_5\text{Me}_4)_2\}\text{HoCH}(\text{SiMe}_3)_2$. [Reprinted with permission from Schumann *et al.* (247). Copyright (1991) American Chemical Society.]

$(\text{Me}_2\text{PCH}_2\text{CH}_2\text{PMe}_2)$ (88), $\{\text{Me}_2\text{Si}(\text{C}_5\text{Me}_4)_2\}\text{NdCH}(\text{SiMe}_3)_2$ (213), $\{\text{Me}_2\text{Si}(\text{C}_5\text{Me}_4)(\text{C}_5\text{H}_4)\}\text{LuCH}(\text{SiMe}_3)_2$ (175), and $\{\text{Me}_2\text{Ge}(\text{C}_5\text{Me}_4)_2\}\text{HoCH}(\text{SiMe}_3)_2$ (247) (Fig. 27), the γ -methyl group appears to adopt an energetically favorable (248) staggered conformation, thereby maximizing all $\text{Ln} \cdots \text{H}_\gamma$ distances that are inevitably associated with the close $\text{Ln} \cdots \text{C}_\gamma$ distance. This is in contrast to the orientation observed in C–H–M agostic interactions.

Ab initio calculations (248) on the interaction in $[\text{Ti}(\text{C}_5\text{H}_5)_2(\text{CMePh})\text{SiMe}_3]\text{AlCl}_4$ (249) suggested that the β -Si–C σ bond is the major donor to the metal center. A staggered γ -Me group conformation occupied a local minimum, while an eclipsed conformation, in which one γ -C–H bond is orientationally disposed to interact with the titanium center, is destabilized by 4 kcal mol^{-1} .

Structural parameters of crystallographically characterized neutral lanthanide species containing $\text{CH}(\text{SiMe}_3)_2$ or $\text{N}(\text{SiMe}_3)_2$ groups were collated (246), together with $[\text{Ti}(\text{C}_5\text{H}_5)_2(\text{CMePh})\text{SiMe}_3]\text{AlCl}_4$ (249) and $\text{Th}(\text{C}_5\text{Me}_5)\{\text{N}(\text{SiMe}_3)_2\}_2$ (250). The orientation of the β -Si–C σ bond, with respect to the metal center, can be defined by the parameters $\text{M}-\text{C}_\gamma$ and $\text{M}-\text{Si}_\beta$. To compare $\text{Ln} \cdots \text{X}$ distances between different lanthanides, subtraction of the effective eight-coordinate ionic radius (I) (14) affords comparable $\text{M}'-\text{C}_\gamma$ and $\text{M}'-\text{Si}_\beta$ distances. These fell in a narrow range. For $\text{CH}(\text{SiMe}_3)_2$ average $\text{M}'-\text{C}_\gamma$ and $\text{M}'-\text{Si}_\beta$ distances were $1.867 (0.11) \text{ \AA}$ and $2.244 (0.085)$

Å, respectively. For $N(\text{SiMe}_3)_2$ average $M'-C_\gamma$ and $M'-\text{Si}_\beta$ distances were 1.973 (0.11) Å and 2.205 (0.056) Å, respectively. Coordination of a $\beta\text{-Si-C}$ σ bond would lead to just such a consistency of data, given the absence of other geometric constraints on these rather flexible groups.

XVIII

THERMODYNAMICS

Concurrent with the greater understanding of the factors that determine the behavior of the organolanthanides, it has become increasingly apparent that the reactivity of the organolanthanides is not only influenced by steric or kinetic considerations, but also by thermodynamic factors (251). In extending thermochemical studies on the actinides, Marks (5,79) has examined organolanthanide bond disruption enthalpies. Clear differences in bond disruption enthalpies dependent on ligand environment were observed. In the ligand series $(\text{C}_5\text{Me}_5)_2\text{Ln}$, $[\text{Me}_2\text{Si}(\text{C}_5\text{Me}_4)_2]\text{Ln}$, and $[\text{Me}_2\text{Si}(\text{C}_5\text{Me}_4)(\text{C}_5\text{H}_4)]\text{Ln}$, the more open ligand environment accelerates sterically sensitive reactions, although, as already noted (*vide supra*), Ln-C bond hydrogenolysis is a factor 10^3 slower (175). The derived $\text{Lu-CH}(\text{SiMe}_3)_2$ bond disruption enthalpies (BDE) were found to progressively decrease for the ligand series above: 67.0, 62.4, and 55.1 kcal mol^{-1} , respectively (5). The BDE's for $\text{Sm-CH}(\text{SiMe}_3)_2$ also followed a similar trend. This trend was proposed to reflect diminishing electron donation, $(\text{C}_5\text{Me}_5)_2 > \text{Me}_2\text{Si}(\text{C}_5\text{Me}_4)_2 > \text{Me}_2\text{Si}(\text{C}_5\text{Me}_4)(\text{C}_5\text{H}_4)$, and the nature of the bond dissociation process $[\text{Ln}^{\text{III}}\text{-R} \rightarrow \text{Ln}^{\text{II}} + \text{R}\cdot]$.

The Ln-H bond disruption enthalpies in the hydride series $[(\text{C}_5\text{Me}_5)_2\text{LnH}]_2$ (La, 66.6; Nd, 56.5; Sm, 52.4; Lu, 66.7 kcal mol^{-1}) showed no apparent trend (5). In addition, the thermodynamic determinant for $\beta\text{-H}$ elimination $\{D(\text{Ln-H}) - D(\text{Ln-alkyl})\}$ was found to be small (0–9 kcal mol^{-1}) and varied in no regular fashion with Ln^{3+} ionic radius (14).

M.O. calculations indicated that the calculated bond disruption enthalpies of M-Me bonds decreased from 220 kJ mol^{-1} (52.6 kcal mol^{-1}) for $(\text{C}_5\text{H}_5)_2\text{ScMe}$, to between 100 and 170 kJ mol^{-1} (23.9–40.6 kcal mol^{-1}) for middle to late transition metal bonds. The nonpolarized bond is weakened by repulsive interactions between occupied metal orbitals and the fully occupied (mainly) $2s$ C orbital of the methyl group. This repulsive interaction in the polarized Sc-Me bond in $(\text{C}_5\text{H}_5)_2\text{ScMe}$ is reduced considerably such that Sc-Me is calculated (78) to be as strong as Sc-H .

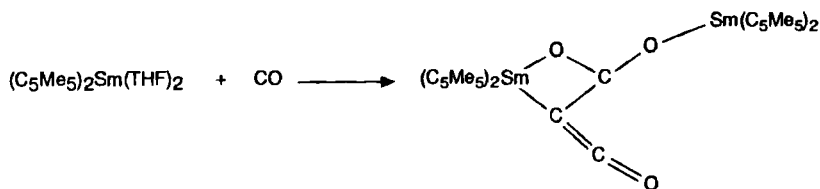
XIX

LOW-OXIDATION-STATE CHEMISTRY

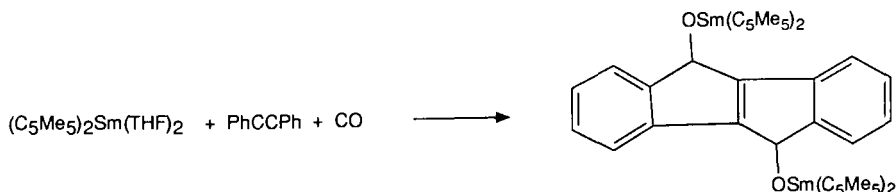
There is an extensive chemistry of the lanthanides in low oxidation states. A comprehensive review of this area was published in 1987 (4). As mentioned in the Introduction, accessible Ln^{2+} oxidation states include Sm^{2+} , Eu^{2+} , and Yb^{2+} . The X-ray crystal structures of solvent-free $(\text{C}_5\text{Me}_5)_2\text{Ln}$ [$\text{Ln} = \text{Eu}$ (252), Sm (106), Yb (98,253)] have been determined and display a bent metallocene geometry as do $(\text{C}_5\text{Me}_5)_2\text{M}$ ($\text{M} = \text{Ca}$ (254), Ba (254,255)). Calculations on $(\text{C}_5\text{H}_5)_2\text{M}$ ($\text{M} = \text{Ca}$, Sr , Ba , Sm , Eu , Yb) (256) showed that a linear geometry is favored. However, very shallow bending potentials reconciled these calculations with the experimentally determined results. Small intermolecular interactions were thought to cause the observed bent (also in the gas phase) structures. Interestingly, the bent metallocenes $[1,3\text{-C}_5\text{H}_3(\text{SiMe}_3)_2]_2\text{Ln}$ ($\text{Ln} = \text{Eu}$, Yb) (257) are polymeric with unprecedented intermolecular interactions between the lanthanide metal and the $\gamma\text{-Me}$ group of a neighboring $\text{C}_5\text{H}_3(\text{SiMe}_3)_2$ ring. $[1,3\text{-C}_5\text{H}_3(\text{SiMe}_3)_2]_2\text{Eu}$ also possesses intramolecular agostic interactions with an η^5, η^3 -bridging cyclopentadienyl ring (257). The tetramethylethylene bridged cyclopentadienyl organolanthanide(II) $[\text{Me}_4\text{C}_2(\text{C}_5\text{H}_4)_2]\text{Ln}$ ($\text{Ln} = \text{Sm}$, Yb) (258) and the *ansa*- Sm^{II} complex $[\text{Me}_4\text{C}_2(\text{C}_5\text{H}_3\text{-}t\text{-Bu})_2]\text{Sm}$ (259) were prepared by reaction of 6,6-dimethylfulvene with the lanthanide metal powder in the presence of HgCl_2 .

An extensive chemistry of $(\text{C}_5\text{Me}_5)_2\text{Sm}$ (106) and $(\text{C}_5\text{Me}_5)_2\text{Sm}(\text{THF})_2$ (138) has been developed and exploited by Evans. The strongly reducing $\text{Sm}^{\text{III}} \rightarrow \text{Sm}^{\text{II}}$ couple, and oxophilicity of $(\text{C}_5\text{Me}_5)_2\text{Sm}$ has been used to effect the reductive homologation (260) of CO to $\text{O}_2\text{CC}=\text{C}=\text{O}^{2-}$, the formation of stereospecifically substituted indenodenediolate complex (261) from $\text{PhC}\equiv\text{CPh}$ and CO, the formal insertion of CO into the $\text{C}=\text{C}$ bond of bis(2-pyridyl)ethene (262), and the double insertion of CO into the $\text{N}=\text{N}$ bond of azobenzene (263).

$(\text{C}_5\text{Me}_5)_2\text{Sm}(\text{THF})_2$ reacts with CO to give tetrameric $[(\text{C}_5\text{Me}_5)_4\text{Sm}_2(\mu\text{-}\eta^3\text{-O}_2\text{CC}=\text{C}=\text{O})(\text{THF})_2]_2$ (260) in 20% yield containing a dimetal-substituted ketenecarboxylic acid moiety (Scheme 25).

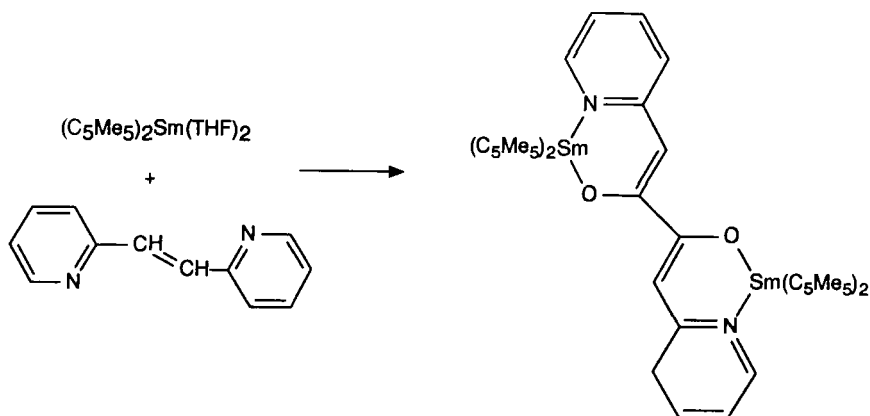


$(C_5Me_5)_2Sm(THF)_2$ reacts with $PhC\equiv CPh$ to give $(C_5Me_5)_2Sm-CPh=CPh-Sm(C_5Me_5)_2$ (145a). Further treatment with CO led to the stereospecific synthesis of the indenoindenediolate complex (261) via CO insertion and subsequent insertion of the resulting carbene centers into ortho-C-H bonds to generate the two five-membered rings (Scheme 26).

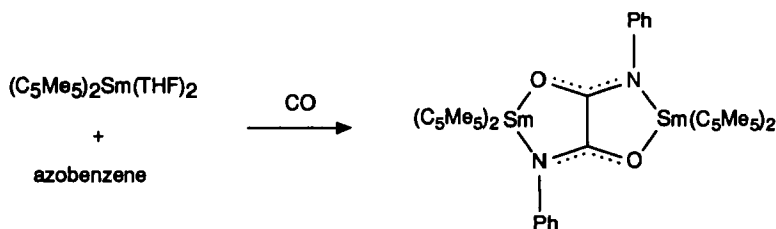


Reductive cleavage with Na/THF affords 5,10-dihydroindeno [2,1,a]indene.

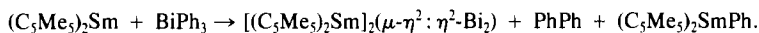
The Sm-mediated functionalization of the $C=C$ bond in bis(2-pyridyl) ethene into a bisenolate $[RCH=C(O)C(O)=CHR]^{2-}$ has been reported (262) (Scheme 27).



Reaction of $(C_5Me_5)_2Sm(THF)_2$ with azobenzene allowed the intermediate $(C_5Me_5)_2Sm-N(Ph)-N(Ph)Sm(C_5Me_5)_2$ to be isolated and crystallographically identified (264). Reaction of $(C_5Me_5)_2Sm(THF)_2$ with two equivalents of azobenzene, however, afforded $[(C_5Me_5)_2Sm]_2(N_2Ph_2)$ (264). In THF, ligand redistribution slowly occurs to give the mono- C_5Me_5 complex $[(C_5Me_5)(THF)Sm]_2(N_2Ph_2)_2$, which possesses two $\mu-\eta^2: \eta^2-N_2Ph_2$ ligands, rather than $\mu-\eta^1: \eta^1-N_2Ph_2$, as in $[(C_5Me_5)_2Sm]_2(N_2Ph_2)$. Reaction of $[(C_5Me_5)_2Sm]_2(N_2Ph_2)$ with CO was attempted to parallel the reaction of $(C_5Me_5)_2Sm(THF)_2$ with $PhC\equiv CPh$ and CO. This afforded, however, a quite different product $[(C_5Me_5)_2Sm]_2[\mu-\eta^4-(PhN)OCCO(NPh)]$ (263) (Scheme 28).

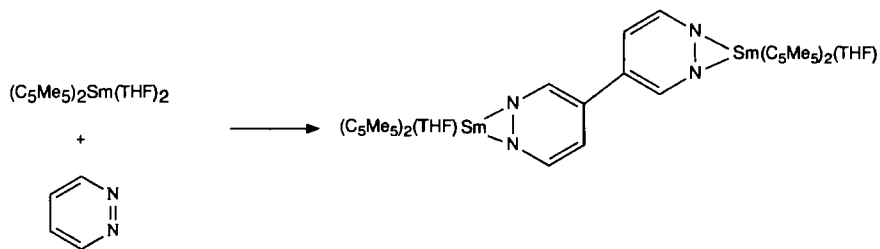


Consistent with the strongly reducing tendency of $(C_5Me_5)_2Sm$, it is readily oxidized. Thus reduction with NO , N_2O , C_3H_5NO , or preferably the epoxide 1,2-epoxybutane, affords $[(C_5Me_5)_2Sm]_2(\mu-O)$ (265). Although treatment of oxophilic, highly reducing $(C_5Me_5)_2Ln$ led to $\mu-E$ species, slow crystallization of $(C_5Me_5)_2Sm$ from toluene under N_2 gave the first dinitrogen complex of an *f* element $[(C_5Me_5)_2Sm]_2(\mu-\eta^2: \eta^2-N_2)$ (108) containing an unusual side-on bound N_2 ligand and a planar $Sm(\mu-N_2)Sm$ unit. A structurally analogous complex was obtained by reaction of $(C_5Me_5)_2Sm$ with $BiPh_3$ in an inert solvent (hexane or cyclohexane). As well as $PhPh$ and $(C_5Me_5)_2SmPh$, $[(C_5Me_5)_2Sm]_2(\mu-\eta^2: \eta^2-Bi_2)$ (266a) was formed:

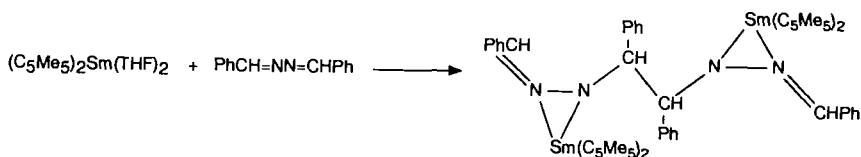


Based on a similar rationale, $(C_5Me_5)_2Sm$ was allowed to react with $Sb(n-Bu)_3$ to give a complex of the triantimony Zintl ion $[(C_5Me_5)_2Sm]_3(\mu-\eta^2: -\eta^2: \eta^1-Sb_3)(THF)$ (266b).

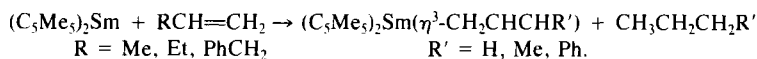
$(C_5Me_5)_2Sm(THF)_2$ reacts (267) with pyridazine ($C_4H_4N_2$) to couple the two pyridazine molecules in the 4-position via a one-electron reduction and to form crystallographically characterized $[(C_5Me_5)_2(THF)Sm]_2[(\mu-\eta^4-(CH=NNCH=CHCH-)_2)]$ (Scheme 29). $PhCH=NN=CHPh$ was also



reductively coupled via C–C bond formation to $[(C_5Me_5)_2Sm]_2[(\mu-\eta^4-(PhCH=NNCHPh-)_2)]$ (Scheme 30). In contrast, bipyridine reacts to form $(C_5Me_5)_2Sm(\eta^2-N_2C_8H_{10})$. Although inconclusive, evidence suggested that this is best described as a Sm^{3+} bipyridyl[–] species, rather than a Sm^{II} adduct.



It has been generally observed that $(\text{C}_5\text{Me}_5)_2\text{Sm}(\text{THF})_2$ reacts with unsaturated molecules to give reductive coupling. Reaction of $(\text{C}_5\text{Me}_5)_2\text{Sm}$ with $\text{PhCH}=\text{CHPh}$ or styrene affords the μ -alkene $[(\text{C}_5\text{Me}_5)_2\text{Sm}]_2(\mu-\eta^2:\eta^4\text{-alkene})$ (110). The geometries of the bridging ligand are reminiscent of the $\mu-\eta^2:\eta^2\text{-N}_2$ complex (108). Different reactivity is observed with non-phenyl-substituted alkenes that cannot interact with Sm via the phenyl group. $(\text{C}_5\text{Me}_5)_2\text{Sm}$ reacts with excess propene, 1-butene, and allylbenzene to give the allyl species (51) $(\text{C}_5\text{Me}_5)_2\text{Sm}(\eta^3\text{-CH}_2\text{CHCHR}')$ ($\text{R}' = \text{H, Me, Ph}$) (268):



Such species, were, as expected (51,75,76), also accessible from $[(\text{C}_5\text{Me}_5)_2\text{SmH}]_2$. Dimerization of 1,3-butadiene by $(\text{C}_5\text{Me}_5)_2\text{Sm}$ gave the bis-allyl $[(\text{C}_5\text{Me}_5)_2\text{Sm}(\mu-\eta^3\text{-CH}_2\text{CHCHCH}_2\text{—})]_2$ (268). Mechanisms to rationalize these transformations were proposed.

In contrast to the reaction of $(\text{C}_5\text{Me}_5)_2\text{Sm}(\text{THF})_2$ with azobenzene, reaction with PhNHNHPh in hexane cleaved the N—N bond and afforded $(\text{C}_5\text{Me}_5)_2\text{SmNHPh}(\text{THF})$ (269). Reaction of $(\text{C}_5\text{Me}_5)_2\text{Sm}$ or $[(\text{C}_5\text{Me}_5)_2\text{SmH}]_2$ with hydrazine (N_2H_4) afforded the μ -hydrazido(2-) complex $[(\text{C}_5\text{Me}_5)_2\text{Sm}]_2(\mu-\eta^2:\eta^2\text{-NHNH})$. In contrast to the geometries found in $\mu-\eta^2:\eta^2\text{-N}_2$ (108) and $\mu-\eta^2:\eta^2\text{-Bi}_2$ (266), the $\text{Sm}(\mu\text{-NN})\text{Sm}$ unit is not planar, but adopts a butterfly arrangement with the nitrogens displaced to one side of the Sm—Sm vector, rather than being symmetrically disposed. Protonation of this μ -hydrazido complex (or its THF adduct) with $\text{Et}_3\text{NHBPh}_4$ afforded cationic $[(\text{C}_5\text{Me}_5)_2\text{Sm}(\eta^2\text{-NH}_2\text{NH}_2)]\text{BPh}_4$ (270).

XX

TRIS(CYCLOPENTADIENYL)

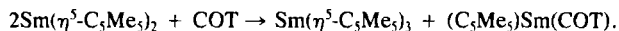
Given the aforementioned chemical uniformity of lanthanide chemistry for a given ligand environment, the solid-state structures of $\text{Ln}(\text{C}_5\text{H}_5)_3$ might have been expected to be monomeric with each cyclopentadienyl

ring η^5 bonded to the metal in a trigonal planar arrangement. However, a large structural diversity is observed.

The X-ray crystal structures of the neutral trivalent tris(cyclopentadienyl) lanthanides, polymeric $[(C_5H_5)_3La]_\infty$ (271,272), polymeric $[(C_5H_5)_3Yb]_\infty$ (273), monomeric $(MeC_5H_4)_3Yb$ (274), polymeric $[(\eta^5-C_5H_5)_2Lu(\eta^1, \eta^5-C_5H_5)]_\infty$ (275), tetrameric $[(MeC_5H_4)_3La]_4$ (276), tetrameric $[(\eta^5-MeC_5H_4)_2Ce(\mu-\eta^1, \eta^5-MeC_5H_4)]_4$ (277), $(Me_3SiC_5H_4)_3Ce$ (277), $(tBuC_5H_4)_3Ce$ (277), $\{C_5H_3(SiMe_3)_2\}_3Ce$ (277), as well as $Sm(\eta^5-C_5Me_5)_3$ (278), the mixed $Sm(\eta^5-C_5Me_5)_2(\eta^5-C_5H_5)$ (279), dimeric, mixed valence $(C_5Me_5)_2Sm(\mu-\eta^5: \eta^2-C_5H_5)Sm(C_5Me_5)_2$ (279), and $\{C_5H_3(SiMe_3)_2\}_3Sm$ (280) have been determined. The X-ray crystal structures of the Lewis base adducts $(C_5H_5)_3Nd(THF)$ (281), $(C_5H_5)_3Lu(OEt_2)$ (282), $(C_5H_5)_3Ln(NCMe)_2$ ($Ln = La, Ce, Pr$) (283), $(MeC_5H_4)_3Ce(PMe_3)$ (284), $(C_5H_5)_3La(NCet)_2$ (285), $(C_5H_5)_3Ln(NCet)$ ($Ln = La, Pr, Yb$) (286), $(C_5H_5)_3Ln(py)$ ($Ln = Sm, Nd$) (287), tris-indenyl $(C_9H_7)_3Ln(OEt_2)$ ($Ln = Nd, Gd, Er$) (288), $(C_5H_4CH_2CH_2OMe)_3Pr$ (289), $(C_5H_5)_3Dy(THF)$ (290), $(C_5H_5)_3Ce(L)$ [$L = \text{quin or } P(OCH_2)_3Cet$] (291), $(MeC_5H_4)_3Ce(NC-t-Bu)$ (277), and $\{C_5H_3(SiMe_3)_2\}_3Ce(NC-t-Bu)$ (277) have also been determined.

Synthetic routes have involved reaction of $LnCl_3$ with the appropriate cyclopentadienyl-alkali metal reagent. Exceptions to this generalization include the following: although reaction of $CeCl_3$ with $KC_5H_3SiMe_3$ gives base-free $(Me_3SiC_5H_4)_3Ce$ (277), the bulkier metallocene $\{C_5H_3(SiMe_3)_2\}_3Ce$ (277) is not available by such a metathesis route. Instead, its preparation involved protonolysis of $Ce\{N(SiMe_3)_2\}_3$ with the cyclopentadiene (277). An almost general synthetic method to base-free $Ln(C_5H_5)_3$, and solvated $Ln(C_5H_5)_3 \cdot L$, involved treating a range of lanthanide metals with $TiCl_3H_4R$ ($R = H, Me$) in THF (292) or pyridine (293).

For many years, the preparation of tris(C_5Me_5) complexes had been an elusive goal, it being considered that the steric bulk of the pentamethylcyclopentadienyl ligand precluded fitting three C_5Me_5 ligands around a lanthanide metal center. The first example of a tris(C_5Me_5) complex $Sm(\eta^5-C_5Me_5)_3$ (278) has been synthesized and structurally characterized:



The trigonal planar coordination geometry around Sm minimizes ligand steric interactions (Fig. 28). The bonding in the $Ln(C_5H_5)_3$ has been theoretically addressed (294) and compared to that of the actinide series. The $4f$ orbitals and $6s$ orbital of the lanthanides were shown to be less effective at bonding the cyclopentadienyl ligands.

Reaction of $Sm(\eta^5-C_5Me_5)_2(\eta^5-C_5H_5)$ with $(\eta^5-C_5Me_5)_2Sm$ afforded the mixed valence $(C_5Me_5)_2Sm(\mu-\eta^5: \eta^2-C_5H_5)Sm(C_5Me_5)_2$ (279), in which $\mu-$

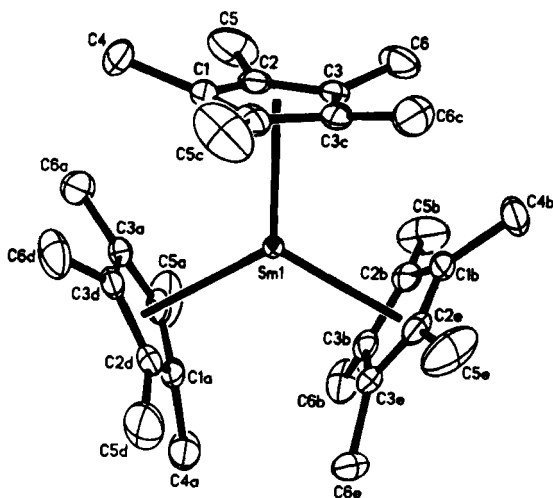
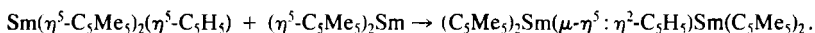


FIG. 28. Molecular structure of $(\text{C}_5\text{Me}_5)_3\text{Sm}$. [Reprinted with permission from Evans *et al.* (278) Copyright (1991) American Chemical Society.]

C_5H_5 is η^5 bonded to $(\text{C}_5\text{Me}_5)_2\text{Sm}^{\text{III}}$ and η^2 bound to $(\text{C}_5\text{Me}_5)_2\text{Sm}^{\text{II}}$ (Fig. 29):



One cyclopentadienyl ring in $\text{Ln}(\text{C}_5\text{H}_5)_3$ is particularly susceptible to cleavage either by protonolysis (295) or by alkyl lithium reagents. Hence, $(t\text{-BuC}_5\text{H}_4)_3\text{Ce}$ (277) reacts with alcohols or thiols to give the dimers $[(t\text{-BuC}_5\text{H}_4)_2\text{Ce}(\mu\text{-ER})_2]$ ($\text{E} = \text{O}, \text{S}$; $\text{R} = i\text{-Pr}$) (296). Bis(C_5H_5) species were also prepared by reaction of $\text{Ln}(\text{C}_5\text{H}_5)_3(\text{THF})$ ($\text{Ln} = \text{Nd}, \text{Lu}$) with LiR

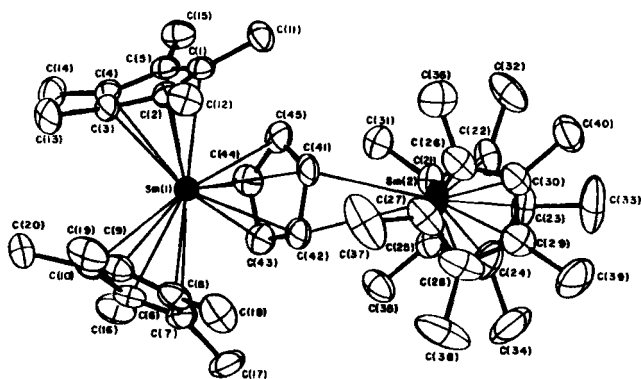


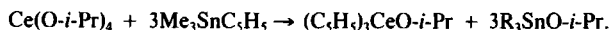
FIG. 29. Molecular structure of $(\text{C}_5\text{Me}_5)_2\text{Sm}(\mu\text{-}\eta^5\text{:}\eta^2\text{-C}_5\text{H}_5)\text{Sm}(\text{C}_5\text{Me}_5)_2$. [Reprinted with permission from Evans and Ulibarri (279). Copyright (1987) American Chemical Society.]

(R = CMe₃, CHMeEt) to afford (C₅H₅)₂LnR(THF) (297). These species decompose by β -H elimination at low temperatures to the corresponding hydrides (298). Air-stable and water-soluble complexes Ln{C₅(COOMe)₅}₃ have been prepared by treating HC₅(COOMe)₅ with the lanthanide carbonates (299). The system Ln(C₅H₅)₃/NaH in THF has been used to reduce 1-hexene, and to regioselectively reduce dienes (300). Structural data on Ln(C₅H₅)₃ complexes have been correlated (301) and therefore are not further discussed here.

XXI

TETRAVALENT ORGANOLANTHANIDE CHEMISTRY

Because of the highly oxidizing nature of Ce⁴⁺, few [in fact, just two (302)] genuine examples of an organometallic Ce⁴⁺ compound have been synthesized. Reaction of Ce(O-*i*-Pr)₄ with Me₃SnC₅H₅ led to the efficient synthesis of (C₅H₅)₃CeO-*i*-Pr (303):



Cyclic voltammetry showed that it is a relatively strong oxidizing agent and that one-electron reduction is both electrochemically and thermochemically reversible. Calculation and PES spectra indicated (303) it to be a genuine organometallic compound of Ce^{IV}, in contrast to Ce(COT)₂. The X-ray structure of (C₅H₅)₃CeO-*t*-Bu, prepared from Ce(O-*t*-Bu)(NO₃)₃(THF) and NaC₅H₅ has been determined (304) (Fig. 30).

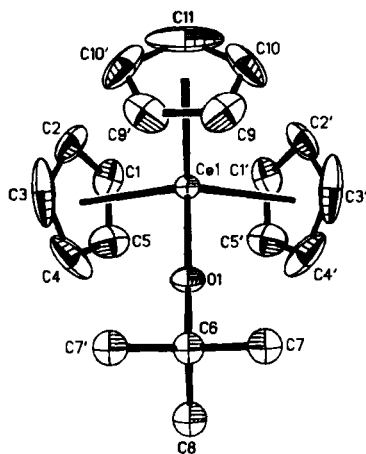


FIG. 30. Molecular structure of (C₅H₅)₃CeO-*t*-Bu. [Reprinted with permission from Evans *et al.* (303). Copyright (1989) American Chemical Society.]

XXII

CONCLUSIONS

There is no doubt that a great wealth of structural types and diverse reactivity is available to the organolanthanides (i.e., π -arene coordination to $\text{Ln}(\text{O})$, $\mu\text{-N}_2$ complexes, homoleptic trisalkyls LnR_3 , and transformations based on the $(\text{C}_5\text{Me}_5)_2\text{Sm}^{\text{II}} \rightarrow \text{Sm}^{\text{III}}$ reduction of organic substrates, asymmetric catalysis, and stereospecific polymerization, to name but a few of the late 1980s). Although the number of researchers involved in this field has not significantly expanded since the early 1980s, it certainly seems a more mature area of chemistry. This is partially afforded by a greater understanding of structural types and thermochemical data. The regular practitioners in this area have perhaps developed an intuitive "feel" for the type of ligand environments compatible with stabilizing organolanthanide species. As the work, particularly of Bercaw and Marks, has aptly demonstrated, the greater steric and mechanistic understanding afforded by the bis(cyclopentadienyl) coordination sphere still lends itself to key advances. Rational and elegant ligand variations have recently led to advances in catalysis (i.e., isotactic polyolefins, C–C σ -bond activation, enantioselective hydroamination/cyclization of unsaturated amines).

What of the future? New structural types will continue to be discovered, either serendipitously or by design, and new ligand systems able to stabilize organolanthanide coordination spheres will continue to be found.

Applications-driven research, for example, use of organolanthanides in MOCVD to manufacture thin films, will expand. A useful advance would be the efficient single-component polymerization of α olefins, without problems associated with π -allyl formation. The controlled preparation of well-defined block copolymers by single-component lanthanide catalysts is perhaps a likely candidate. The recently reported (228) polymerization of methylmethacrylate opens up new possibilities in this field.

XXIII

APPENDIX: ABBREVIATIONS

Ln , lanthanide metal
ETM, early transition metal
 M , a metal
THF, tetrahydrofuran
THT, tetrahydrothiophene
py, pyridine

hmpa, hexamethylphosphoramide
dme, dimethoxyethane
pmdeta, *N,N,N',N'',N'''*-pentamethyldiethyltri-amine
DMF, dimethylformamide
PPN⁺, bis(triphenylphosphoranylidene)ammonium cation
ArOH, 2,6-C₆H₃-*t*-Bu₂OH
Ar'OH, HO-2,6-C₆H₂-*t*-Bu₂-4-Me
disyl, CH(SiMe₃)₂
TMEDA, tetramethylethylenediamine
L, a neutral ligand
X, an anionic ligand
acac, 2,4-pentanedionate
COT, cyclooctatetraene dianion
OEP, octaethylporphyrin dianion
TTP, tetraphenylporphyrin dianion
TTP, tetratolylporphyrin dianion
TMP, tetramesitylporphyrin dianion
Pc, phthalocyanine dianion
TMPP, tetrakis(4-methoxyphenyl)porphyrin dianion

ACKNOWLEDGMENTS

I would like to thank Dr. M. Zonneville (KSLA) for an invaluable literature search.

REFERENCES

- (1) Evans, W. J. *Adv. Organomet. Chem.* **1985**, 24, 131.
- (2) Schumann, H. In "Fundamental and Technological Aspects of Organo-f-Element Chemistry", NATO ASI Ser.; Marks, T. J.; Fragalà, I. L., Eds.; D. Reidel: Boston, 1985; Vol. 155, p. 1.
- (3) Rogers, R. D.; Rogers, L. M. *J. Organomet. Chem.* **1992**, 442, 83, 225.
- (4) Evans, W. J. *Polyhedron* **1987**, 6, 803.
- (5) Nolan, S. P.; Stern, D.; Hedden, D.; Marks, T. J. *ACS Symp. Ser.* **1990**, 428, 159.
- (6) Burns, C. J.; Bursten, B. E. *Comments Inorg. Chem.* **1989**, 9, 61.
- (7) Watson, P. L. In "Selective Hydrocarbon Activation"; Davies, J. A.; Watson, P. L.; Liebman, J. F.; Greenberg, A., Eds.; VCH Publishers: New York, 1990; p. 79.
- (8) Rothwell, I. P. In "Activation of Functionalized Alkanes"; Hill, C. L., Ed.; John Wiley & Sons: New York, 1989; p. 151; In "Selective Hydrocarbon Activation"; Davies, J. A.; Watson, P. L.; Liebman, J. F.; Greenberg, A., Eds.; VCH Publishers: New York, 1990; p. 43.
- (9) Evans, W. J.; Foster, S. E. *J. Organomet. Chem.* **1992**, 433, 79.
- (10) *Inorg. Synth.* **1990**, 27, 137; Ginsberg, A. P., Ed.; Wiley (Interscience), New York.
- (11) MOVPE: Takahei, K.; Nakagome, H.; Tanaka, T.; Honma, N. *Chemtronics* **1991**, 5, 159; Takahei, K.; Nakagome, H. *Conf. Ser.—Inst. Phys.* **1990**, 106, 913; *Chem. Abstr.* **1990**, 114, 91048h; Nakagome, H.; Takahei, K. *Jpn. J. Appl. Phys.* **1989**, 28, L2098.

- (12) Ranasinghe, Y. A.; MacMahon, J. J.; Freiser, B. S. *J. Am. Chem. Soc.* **1992**, *114*, 9112; Ranasinghe, Y. A.; Freiser, B. S. *Chem. Phys. Lett.* **1992**, *200*, 135; Huang, Y.; Hill, Y. D.; Freiser, B. S. *J. Am. Chem. Soc.* **1991**, *113*, 840; Hill, Y. D.; Freiser, B. S.; Bauschlicher, C. W., Jr. *ibid.*, 1507; Sunderlin, L. S.; Armentrout, P. B. *ibid.* **1989**, *111*, 3845; Hettich, R. L.; Freiser, B. S. *ibid.* **1987**, *109*, 3543; Huang, Y.; Wise, M. B.; Jacobsen, D. B. *Organometallics* **1987**, *6*, 346.
- (13) Heath, J. R.; O'Brien, S. C.; Zhang, G.; Liu, Y.; Curl, R. F.; Kroto, H. W.; Tittel, F. K.; Smalley, R. E. *J. Am. Chem. Soc.* **1985**, *107*, 7779.
- (14) Shannon, R. D. *Acta Crystallogr., Sect. A* **1976**, *A32*, 751.
- (15) Wayda, A. L.; Evans, W. J. *J. Am. Chem. Soc.* **1978**, *100*, 7119.
- (16) Cotton, S. A.; Hart, F. A.; Hursthouse, M. B.; Welch, A. J. *J. Chem. Soc., Chem. Commun.* **1972**, 1225.
- (17) Schumann, H. *J. Organomet. Chem.* **1985**, *281*, 95.
- (18) Schumann, H.; Lauke, H.; Hahn, E.; Pickhardt, J. *J. Organomet. Chem.* **1984**, *263*, 29.
- (19) Wayda, A. L.; Atwood, J. L.; Hunter, W. E. *Organometallics* **1984**, *3*, 939.
- (20) Karsch, H. H.; Appelt, A.; Miller, G. *Angew. Chem., Int. Ed. Engl.* **1986**, *25*, 823.
- (21) Barker, G. K.; Lappert, M. F. *J. Organomet. Chem.* **1974**, *76*, C45.
- (22) Lappert, M. F.; Pearce, R. J. *J. Chem. Soc., Chem. Commun.* **1973**, 126.
- (23) Hitchcock, P. B.; Lappert, M. F.; Smith, R. G.; Bartlett, R. A.; Power, P. P. *J. Chem. Soc., Chem. Commun.* **1988**, 1007.
- (24) Schaverien, C. J.; Orpen, A. G. *Inorg. Chem.* **1991**, *30*, 4968.
- (25) Schaverien, C. J.; Meijboom, N.; Orpen, A. G. *J. Chem. Soc., Chem. Commun.* **1992**, 124.
- (26) Hitchcock, P. B.; Lappert, M. F.; Smith, R. G. *J. Chem. Soc., Chem. Commun.* **1989**, 369.
- (27) Atwood, J. L.; Lappert, M. F.; Smith, R. G.; Zhang, H. *J. Chem. Soc., Chem. Commun.* **1988**, 1308.
- (28) Atwood, J. L.; Hunter, W. E.; Rogers, R. D.; Holton, J.; McMeeking, J.; Pearce, R.; Lappert, M. F. *J. Chem. Soc., Chem. Commun.* **1978**, 140.
- (29) Schaverien, C. J.; Van Mechelen, J. B. *Organometallics* **1991**, *10*, 1704.
- (30) Bowmaker, G. A.; Schmidbauer, H. *Organometallics* **1990**, *9*, 1813.
- (31) Mazdiyasmī, K. S.; Lynch, C. T.; Smith, J. S. *Inorg. Chem.* **1965**, *4*, 342.
- (32) Brown, L. M.; Mazdiyasmī, K. S. *Inorg. Chem.* **1970**, *9*, 2783.
- (33) Bradley, D. C.; Mehrotra, R. C.; Gaur, D. P. "Metal Alkoxides"; Academic Press: London, 1978.
- (34) Poncelet, O.; Hubert-Pfalzgraf, L. G.; Daran, J.-C.; Astier, R. *J. Chem. Soc., Chem. Commun.* **1989**, 1846.
- (35) Hitchcock, P. B.; Lappert, M. F.; Singh, A. *J. Chem. Soc., Chem. Commun.* **1983**, 1499.
- (36) Bradley, D. C.; Ghotra, J. S.; Hart, F. A. *J. Chem. Soc., Dalton Trans.* **1973**, 1021.
- (37) McGeary, M. J.; Loan, P. S.; Folting, K.; Streib, W. E.; Caulton, K. G. *Inorg. Chem.* **1989**, *28*, 3283; McGeary, M. J.; Loan, P. S.; Folting, K.; Streib, W. E.; Caulton, K. G. *ibid.* **1991**, *30*, 1723.
- (38) Stecher, H. A.; Sen, A.; Rheingold, A. L. *Inorg. Chem.* **1988**, *27*, 1130.
- (39) Stecher, H. A.; Sen, A.; Rheingold, A. L. *Inorg. Chem.* **1989**, *28*, 3280.
- (40) Hitchcock, P. B.; Lappert, M. F.; Smith, R. G. *Inorg. Chim. Acta* **1987**, *139*, 183.
- (41) Evans, W. J.; Olofson, J. M.; Ziller, J. W. *Inorg. Chem.* **1989**, *28*, 4308.
- (42) Bradley, D. C.; Chudzynska, H.; Frigo, D. M.; Hammond, M. E.; Hursthouse, M. B.; Mazid, M. B. *Polyhedron* **1990**, *9*, 719; Poucelet, O.; Sartain, W. J.; Hubert-Pfalzgraf, L. G.; Folting, K.; Caulton, K. G. *Inorg. Chem.* **1989**, *28*, 263.

- (43) Evans, W. J.; Solberger, M. S. *Inorg. Chem.* **1988**, *27*, 4417; Evans, W. J.; Solberger, M. S.; Hanusa, T. P. *J. Am. Chem. Soc.* **1988**, *110*, 1841; Evans, W. J.; Olofson, J. M.; Ziller, J. W. *ibid.* **1990**, *112*, 2308.
- (44) Bradley, D. C.; Chudzynska, H.; Hursthouse, M. B.; Motevalli, M. *Polyhedron* **1991**, *10*, 1049.
- (45) Hitchcock, P. B.; Lappert, M. F.; MacKinnon, I. A. *J. Chem. Soc., Chem. Commun.* **1988**, 1557.
- (46) Herrmann, W. A.; Anwander, R.; Kleine, M.; Scherer, W. *Chem. Ber.* **1992**, *125*, 1971.
- (47) Wedler, M.; Gilje, J. W.; Pieper, U.; Stalke, D.; Noltemeyer, M.; Edelmann, F. T. *Chem. Ber.* **1991**, *124*, 1163.
- (48) Deacon, G. B.; Hitchcock, P. B.; Holmes, S. A.; Lappert, M. F.; MacKinnon, P.; Newnham, R. H. *J. Chem. Soc., Chem. Commun.* **1989**, 935.
- (49) Hou, Z.; Yamazaki, H.; Kobayashi, K.; Fujiwara, Y.; Taniguchi, H. *J. Chem. Soc., Chem. Commun.* **1992**, 722.
- (50) Clark, D. C.; Watkin, J. G.; Huffman, J. C. *Inorg. Chem.* **1992**, *31*, 1554.
- (51) Fagan, P. J.; Manriquez, J. M.; Marks, T. J.; Day, V. W.; Vollmer, S. H.; Day, C. S. *J. Am. Chem. Soc.* **1980**, *102*, 5393.
- (52) Jeske, G.; Lauke, H.; Mauermann, H.; Swepston, P. N.; Schumann, H.; Marks, T. J. *J. Am. Chem. Soc.* **1985**, *107*, 8091.
- (53) Lappert, M. F.; Raston, C. L.; Engelhardt, L. M.; White, A. H. *J. Chem. Soc., Chem. Commun.* **1985**, 521; Fachinetti, G.; Fachi, G.; Floriani, C. *J. Chem. Soc., Dalton Trans.* **1977**, 2297; Fagan, P. J.; Manriquez, J. M.; Marks, T. J. In "Organometallics of the f-elements"; Marks, T. J.; Fischer, R. D., Eds.; D. Reidel: Dordrecht, The Netherlands, 1979, pp. 137-141, and references therein; Sonnenberger, D. C.; Mintz, E. A.; Marks, T. J. *J. Am. Chem. Soc.* **1984**, *106*, 3484.
- (54) Evans, W. J.; Dominquez, R. D.; Hanusa, T. P. *Organometallics* **1986**, *5*, 1291.
- (55) Cetinkaya, B.; Hitchcock, P. B.; Lappert, M. F.; Smith, R. G. *J. Chem. Soc., Chem. Commun.* **1992**, 932.
- (56) Cary, D. R.; Arnold, J. *J. Am. Chem. Soc.* **1993**, *115*, 2520.
- (57) Strzelecki, A. R.; Timinski, P. A.; Helsel, B. A.; Bianconi, P. A. *J. Am. Chem. Soc.* **1992**, *114*, 3159.
- (58) Schumann, H.; Albrecht, I.; Gallagher, M.; Hahn, E.; Janiak, C.; Kolax, C.; Loebel, J.; Nickel, S.; Palamidis, E. *Polyhedron* **1988**, *7*, 2307.
- (59) Berg, D. J.; Burns, C. J.; Andersen, R. A.; Zalkin, A. *Organometallics* **1989**, *8*, 1865.
- (60) Buchler, J. W.; De Cian, A.; Fischer, J.; Kihn-Botulinski, M.; Paulus, H.; Weiss, R. *J. Am. Chem. Soc.* **1986**, *108*, 3652.
- (61) Buchler, J. W.; De Cian, A.; Fischer, J.; Kihn-Botulinski, M.; Weiss, R. *Inorg. Chem.* **1988**, *27*, 339.
- (62) Buchler, J. W.; Hüttermann, J.; Löffler, J. *Bull. Chem. Soc. Jpn.* **1988**, *61*, 71; Arnold, J. *J. Chem. Soc., Chem. Commun.* **1990**, 976.
- (63) Buchler, J. W.; Scharbert, B. *J. Am. Chem. Soc.* **1988**, *110*, 4272, and references therein.
- (64) Buchler, J. W.; Kihn-Botulinski, M.; Scharbert, B. *Z. Naturforsch., B: Chem. Sci.* **1988**, *43B*, 1371.
- (65) Wong, C.-P. *Inorg. Synth.* **1983**, *22*, 156.
- (66) Buchler, J. W.; Kapellmann, H.-G.; Knoff, M.; Lay, K.-L.; Pfeifer, S. *Z. Naturforsch., B: Anorg. Chem., Org. Chem.* **1983**, *38B*, 1339.
- (67) Buchler, J. W.; De Cian, A.; Fischer, J.; Hammerschmitt, P.; Löffler, J.; Scharbert, B.; Weiss, R. *Chem. Ber.* **1989**, *122*, 2219.

- (68) Bolsel, O.; Rodriguez, J.; Holten, D. *J. Phys. Chem.* **1990**, *94*, 3508.
- (69) Buchler, J. W.; Löffler, J. Z. *Naturforsch. B: Chem. Sci.* **1990**, *45B*, 531.
- (70) Buchler, J. W.; Kihn-Botulinski, M.; Löffler, J.; Scharbert, B. *New J. Chem.* **1992**, *16*, 545.
- (71) De Cian, A.; Moussavi, M.; Fischer, J.; Weiss, R. *Inorg. Chem.* **1985**, *24*, 3162.
- (72) Moussavi, M.; De Cian, A.; Fischer, J.; Weiss, R. *Inorg. Chem.* **1986**, *25*, 2107.
- (73) Arnold, J.; Hoffman, C. G. *J. Am. Chem. Soc.* **1990**, *112*, 8620.
- (74) Sewchok, M. G.; Haushalter, R. C.; Merola, J. S. *Inorg. Chim. Acta* **1988**, *144*, 47.
- (75) den Haan, K. H.; De Boer, J. L.; Teuben, J. H.; Spek, A. L.; Kojic-Prodic, B.; Hays, G. R.; Huis, R. *Organometallics* **1986**, *5*, 1726.
- (76) Heeres, H. J.; Renkema, J.; Booi, M.; Meetsma, A.; Teuben, J. H. *Organometallics* **1988**, *7*, 2495.
- (77) Collman, J. P.; Hegedus, L. S.; Norton, J. R.; Finke, R. G. "Principles and Applications of Organotransition Metal Chemistry"; University Science Books: Mill Valley, CA, 1987; Halpern, J. *Inorg. Chim. Acta* **1985**, *100*, 41; Ziegler, T.; Tschinke, V.; Versluis, L.; Baerends, E. J.; Ravenek, W. *Polyhedron* **1988**, *7*, 1625.
- (78) Ziegler, T.; Cheng, W.; Baerends, E. J.; Ravenek, W. *Inorg. Chem.* **1988**, *27*, 3458.
- (79) Nolan, S. P.; Stern, C. L.; Marks, T. J. *J. Am. Chem. Soc.* **1989**, *111*, 7844.
- (80) Burger, B. J.; Thompson, M. E.; Cotter, W. D.; Bercaw, J. E. *J. Am. Chem. Soc.* **1990**, *112*, 1566; Steigerwald, M. L.; Goddard, W. A., III. *ibid.* **1984**, *106*, 308; Rabaä, H.; Saillard, J.-Y.; Hoffmann, R. *ibid.* **1986**, *108*, 4327.
- (81) Watson, P. L.; Parshall, G. W. *Acc. Chem. Res.* **1985**, *18*, 51.
- (82a) Busch, M. A.; Harlow, R.; Watson, P. L. *Inorg. Chim. Acta* **1987**, *140*, 15.
- (82b) Evans, W. J.; Chamberlain, L. R.; Ulibarri, T. A.; Ziller, J. W. *J. Am. Chem. Soc.* **1988**, *110*, 6423.
- (82c) Den Haan, K. H.; Wielstra, J.; Eshuis, J. J. W.; Teuben, J. H. *J. Organomet. Chem.* **1987**, *323*, 181.
- (83) Han, R.; Parkin, G. *J. Am. Chem. Soc.* **1990**, *112*, 3662; Lubben, T. V.; Wolczanski, P. T. *ibid.* **1987**, *109*, 424; Cleaver, W. M.; Barron, A. R. *ibid.* **1989**, *111*, 8966.
- (84) Cloke, F. G. N.; de Lemos, H. C.; Sameh, A. A. *J. Chem. Soc., Chem. Commun.* **1986**, 1344; Cloke, F. G. N. *Chem. Rev.* **1993**, *22*, 17.
- (85) Recknagel, A.; Steiner, A.; Brooker, S.; Stalke, D.; Edelmann, F. T. *J. Organomet. Chem.* **1991**, *415*, 315.
- (86) Fryzuk, M. D.; Haddad, T. S. *J. Chem. Soc., Chem. Commun.* **1990**, 1088.
- (87) Fryzuk, M. D.; Haddad, T. S. *J. Am. Chem. Soc.* **1988**, *110*, 8263; Fryzuk, M. D.; Haddad, T. S.; Rettig, S. J. *Organometallics* **1991**, *10*, 2026; Fryzuk, M. D.; Haddad, T. S.; Rettig, S. J. *ibid.* **1992**, *11*, 2967.
- (88) Tilley, T. D.; Andersen, R. A.; Zalkin, A. *J. Am. Chem. Soc.* **1982**, *104*, 3725.
- (89a) Wedler, M.; Knösel, F.; Pieper, U.; Stalke, D.; Edelmann, F. T.; Amberger, H.-D. *Chem. Ber.* **1992**, *125*, 2171.
- (89b) Wedler, M.; Noltemeyer, M.; Pieper, U.; Schmidt, H.-G.; Stalke, D.; Edelmann, F. T. *Angew. Chem., Int. Ed. Engl.* **1990**, *29*, 894.
- (89c) Recknagel, A.; Knösel, F.; Gornitzka, H.; Noltemeyer, M.; Edelmann, F. T. *J. Organomet. Chem.* **1991**, *417*, 363.
- (89d) Wedler, M.; Knösel, F.; Noltemeyer, M.; Edelmann, F. T. *J. Organomet. Chem.* **1990**, *388*, 21.
- (90) Stainer, M. V. R.; Takats, J. *J. Am. Chem. Soc.* **1983**, *105*, 410; Moffat, W. D.; Stainer, M. V. R.; Takats, J. *Inorg. Chim. Acta* **1987**, *139*, 74.
- (91) Moss, M. A.; Jones, C. J.; Edwards, P. J. *Polyhedron* **1988**, *7*, 79.
- (92) Reger, D. L.; Lindeman, J. A.; Lebioda, L. *Inorg. Chem.* **1988**, *27*, 1890, 3923.

- (93) Aspinall, H. C.; Bradley, D. C.; Hursthouse, M. B.; Sales, K. D.; Walker, N. P. C.; Hussain, B. J. *Chem. Soc., Dalton Trans.* **1989**, 623.
- (94a) Aspinall, H. C.; Bradley, D. C.; Hursthouse, M. B.; Sales, K. D.; Walker, N. P. C. *J. Chem. Soc., Chem. Commun.* **1985**, 1585.
- (94b) Aspinall, H. C.; Bradley, D. C.; Sales, K. D. *J. Chem. Soc., Dalton Trans.* **1988**, 2211.
- (95) LaDuca, R. L.; Wolczanski, P. T. *Inorg. Chem.* **1992**, *31*, 1313.
- (96) Evans, W. J.; Drummond, D. K.; Zhang, H.; Atwood, J. L. *Inorg. Chem.* **1988**, *27*, 575.
- (97) Boncella, J. M.; Andersen, R. A. *Organometallics* **1985**, *4*, 205.
- (98) Andersen, R. A.; Boncella, J. M.; Burns, C. J.; Green, J. C.; Hohl, D.; Rösch, N. *J. Chem. Soc., Chem. Commun.* **1986**, 405.
- (99) Burns, C. J.; Andersen, R. A. *J. Am. Chem. Soc.* **1987**, *109*, 915.
- (100) Burns, C. J.; Andersen, R. A.; *J. Am. Chem. Soc.* **1987**, *109*, 941.
- (101) Burns, C. J.; Andersen, R. A. *J. Am. Chem. Soc.* **1987**, *109*, 5853.
- (102) Rhine, W. E.; Stucky, G. D.; Peterson, S. W. *J. Am. Chem. Soc.* **1975**, *97*, 6401.
- (103) Stults, S. D.; Andersen, R. A.; Zalkin, A. *J. Am. Chem. Soc.* **1989**, *111*, 4507.
- (104) Berry, A.; Dawoodi, Z.; Derome, A. E.; Dickinson, M.; Downs, A. J.; Green, J. C.; Green, M. L. H.; Hare, P. M.; Payne, M. P.; Rankin, D. W. H.; Robertson, H. E. *J. Chem. Soc., Chem. Commun.* **1986**, 520.
- (105) Nolan, S. P.; Marks, T. J. *J. Am. Chem. Soc.* **1989**, *111*, 8558.
- (106) Evans, W. J.; Hughes, L. A.; Hanusa, T. P. *Organometallics* **1986**, *5*, 1285; Tilley, T. D.; Andersen, R. A.; Spencer, B.; Ruben, H.; Zalkin, A.; Templeton, D. *Inorg. Chem.* **1980**, *19*, 2999.
- (107) Andrews, M. P.; Wayda, A. L. *Organometallics* **1988**, *7*, 743.
- (108) Evans, W. J.; Ulibarri, T. A.; Ziller, J. W. *J. Am. Chem. Soc.* **1988**, *110*, 6877.
- (109) Sanner, R. D.; Duggan, D. M.; McKenzie, T. C.; Marsh, R. E.; Bercaw, J. E. *J. Am. Chem. Soc.* **1976**, *98*, 8358.
- (110) Evans, W. J.; Ulibarri, T. A.; Ziller, J. W. *J. Am. Chem. Soc.* **1990**, *112*, 219.
- (111) Cotton, F. A.; Schwotzer, W. *J. Am. Chem. Soc.* **1986**, *108*, 4657.
- (112) Fan, B. C.; Shen, Q.; Lin, Y. H. *J. Organomet. Chem.* **1989**, *376*, 61.
- (113) Fan, B.; Shen, Q.; Lin, Y. *J. Organomet. Chem.* **1989**, *377*, 51.
- (114) Cesari, M.; Pedritti, U.; Zazetta, A.; Lugli, G.; Marconi, N. *Inorg. Chim. Acta* **1971**, *5*, 439.
- (115) Liang, H.; Shen, Q.; Jin, S.; Lin, Y. *J. Chem. Soc., Chem. Commun.* **1992**, 480.
- (116a) Cloke, F. G. N.; Khan, K.; Perutz, R. N. *J. Chem. Soc., Chem. Commun.* **1991**, 1372.
- (116b) Brennan, J. G.; Cloke, F. G. N.; Sameh, A. A.; Zalkin, A. *J. Chem. Soc., Chem. Commun.* **1987**, 1668.
- (117) Anderson, D. M.; Cloke, F. G. N.; Cox, P. A.; Edelstein, N.; Green, J. C.; Pang, T.; Sameh, A. A.; Shalimoff, G. *J. Chem. Soc., Chem. Commun.* **1989**, 53.
- (118) King, W. A.; Marks, T. J.; Anderson, D. M.; Duncalf, D. J.; Cloke, F. G. N. *J. Am. Chem. Soc.* **1992**, *114*, 9221.
- (119) Deacon, G. B.; Nickel, S.; MacKinnon, P.; Tiekink, E. R. T. *Aust. J. Chem.* **1990**, *43*, 1245.
- (120) Clark, D. C.; Gordon, J. C.; Huffman, J. C.; Vincent, R. L.; Watkin, J. G.; Zwick, B. D. unpublished results; Van der Sluys, W. G.; Burns, C. J.; Huffman, J. C.; Sattelberger, A. P. *J. Am. Chem. Soc.* **1988**, *110*, 5924.
- (121) For a review, see Streitwieser, A., Jr.; Kingsley, S. A. In "Fundamental and Technological Aspects of Organo-f-Element Chemistry"; NATO ASI Ser.; Marks, T. J.; Fragalà, I. L., Eds.; D. Reidel: Boston, 1985; Vol. 155, p. 77.
- (122) Hodgson, K. O.; Raymond, K. N. *Inorg. Chem.* **1972**, *11*, 171; Mares, F.; Hodgson, K. O.; Streitwieser, A., Jr. *J. Organomet. Chem.* **1971**, *28*, C24.

- (123) Wayda, A. L.; Rogers, R. D. *Organometallics* **1985**, *4*, 1440.
- (124) Mashima, K.; Takaya, H. *Tetrahedron Lett.* **1989**, *30*, 3697.
- (125) Hodgson, K. O.; Mares, F.; Stacks, D. F.; Streitweiser, A., Jr. *J. Am. Chem. Soc.* **1973**, *95*, 8650.
- (126) Schumann, H.; Winterfield, J.; Gorlitz, F. H.; Pickardt, J. *J. Chem. Soc., Chem. Commun.* **1993**, 623.
- (127) Wayda, A. L.; Mukerji, I.; Dye, J. L.; Rogers, R. D. *Organometallics* **1987**, *6*, 1328.
- (128) Burton, N. C.; Cloke, F. G. N.; Hitchcock, P. B.; de Lemos, H. C.; Sameh, A. A. *J. Chem. Soc., Chem. Commun.* **1989**, 1462.
- (129) Bruin, P.; Booij, M.; Teuben, J. H.; Oskam, A. *J. Organomet. Chem.* **1988**, *350*, 17; Schumann, H.; Sun, J.; Dietrich, A. *Monatsh. Chem.* **1990**, *21*, 747; Schumann, H.; Köhn, R. D.; Reier, F.-W.; Dietrich, A.; Pickardt, J. *Organometallics* **1989**, *8*, 1388.
- (130) Schumann, H.; Janiak, C.; Köhn, R. D.; Loebel, J.; Dietrich, A. *J. Organomet. Chem.* **1989**, *365*, 137.
- (131) Visseaux, M.; Dormond, A.; Kubicki, M. M.; Moise, C.; Baudry, D.; Ephritikhine, M. *J. Organomet. Chem.* **1992**, *443*, 95.
- (132) Wen, K.; Jin, Z.; Chen, W. *J. Chem. Soc., Chem. Commun.* **1991**, 680.
- (133) Jin, J.; Jin, S.; Jin, Z.; Chen, W. *J. Chem. Soc., Chem. Commun.* **1991**, 1328.
- (134) Andrea, R. R.; Terpstra, A.; Oskam, A.; Bruin, P.; Teuben, J. H. *J. Organomet. Chem.* **1986**, *307*, 307.
- (135) Kilimann, U.; Edelmann, F. T. *J. Organomet. Chem.* **1993**, *444*, C15.
- (136) Dolg, M.; Fulde, P.; Küchle, W.; Neumann, C.-S.; Stoll, H. *J. Chem. Phys.* **1991**, *94*, 3011.
- (137) Manning, M. J.; Knobler, C. B.; Hawthorne, M. F. *J. Am. Chem. Soc.* **1988**, *110*, 4458; Manning, M. J.; Knobler, C. B.; Khattar, R. F.; Hawthorne, M. F. *Inorg. Chem.* **1991**, *30*, 2009.
- (138) Evans, W. J.; Grate, J. W.; Choi, H. W.; Bloom, I.; Hunter, W. E.; Atwood, J. L. *J. Am. Chem. Soc.* **1985**, *107*, 941; Evans, W. J.; Bloom, I.; Hunter, W. E.; Atwood, J. L. *ibid.* **1981**, *103*, 6507.
- (139) White, J. P., III; Deng, H.-B.; Shore, S. G. *J. Am. Chem. Soc.* **1989**, *111*, 8946.
- (140) Oki, A. R.; Zhang, H.; Hosmane, N. S. *Organometallics* **1991**, *10*, 3964.
- (141) Nief, F.; Mathey, F. *J. Chem. Soc., Chem. Commun.* **1989**, 800.
- (142) Nief, F.; Ricard, L.; Mathey, F. *Polyhedron* **1993**, *12*, 19.
- (143) Thompson, M. E.; Baxter, S. M.; Bulls, A. R.; Burger, B. J.; Nolan, M. C.; Santarsiero, B. D.; Schaefer, W. P.; Bercaw, J. E. *J. Am. Chem. Soc.* **1987**, *109*, 203.
- (144) Watson, P. L. *J. Am. Chem. Soc.* **1982**, *104*, 337; Watson, P. L. *ibid.* **1983**, *105*, 6491; Watson, P. L.; Roe, D. C. *ibid.* **1982**, *104*, 6471; Watson, P. L.; Herskovitz, T. *ACS Symp. Ser. (Initiation Polym.)* **1983**, *212*, 459.
- (145a) Evans, W. J.; Bloom, I.; Hunter, W. E.; Atwood, J. L. *J. Am. Chem. Soc.* **1981**, *103*, 1401.
- (145b) den Haan, K. H.; Wielstra, Y.; Teuben, J. H. *Organometallics* **1987**, *6*, 2053.
- (145c) Watson, P. L. *J. Chem. Soc., Chem. Commun.* **1983**, 276.
- (145d) Booij, M.; Deelman, B.-J.; Duchateau, R.; Postma, D. S.; Meetsma, A.; Teuben, J. H. *Organometallics* **1993**, *12*, 3521.
- (146) Schumann, H.; Albrecht, I.; Pickardt, J.; Hahn, E. *J. Organomet. Chem.* **1984**, *276*, C5.
- (147) Albrecht, I.; Schumann, H. *J. Organomet. Chem.* **1986**, *310*, C29.
- (148) Schumann, H.; Meese-Marktscheffel, J. A.; Dietrich, A. *J. Organomet. Chem.* **1989**, *377*, C5.
- (149) Hazin, P. N.; Huffman, J. C.; Bruno, J. W. *Organometallics* **1987**, *6*, 23.

- (150) van der Heijden, H.; Schaverien, C. J.; Orpen, A. G. *Organometallics* **1989**, *8*, 255.
- (151) Bochmann, M.; Kargar, M.; Jaggar, A. J. *J. Chem. Soc., Chem. Commun.* **1990**, 1038.
- (152) Horton, A. D.; Frijns, J. H. G. *Angew. Chem., Int. Ed. Engl.* **1991**, *30*, 1152.
- (153) Pellecchia, C.; Grassi, A.; Immirzi, A. *J. Am. Chem. Soc.* **1993**, *115*, 1161.
- (154) Schaverien, C. J. *Organometallics* **1992**, *11*, 3476.
- (155) Calderazzo, F.; Englert, U.; Pampaloni, G.; Rocchi, L. *Angew. Chem., Int. Ed. Engl.* **1992**, *31*, 1235.
- (156a) Hazin, P. N.; Bruno, J. W.; Schulte, G. K. *Organometallics* **1990**, *9*, 416.
- (156b) Evans, W. J.; Ulibarri, T. A.; Chamberlain, L. R.; Ziller, J. W.; Alvarez, D., Jr. *Organometallics* **1990**, *9*, 2124.
- (156c) Heeres, H. J.; Meetsma, A.; Teuben, J. H. *J. Organomet. Chem.* **1991**, *414*, 351.
- (157) Kaupp, M.; Charkin, O. P.; von Schleyer, P. R. *Organometallics* **1992**, *11*, 2765.
- (158) Heeres, H. J.; Meetsma, A.; Teuben, J. H. *J. Chem. Soc., Chem. Commun.* **1988**, 962; Heeres, H. J.; Meetsma, A.; Teuben, J. H.; Rogers, R. D. *Organometallics* **1989**, *9*, 2637.
- (159) Schaverien, C. J.; Frijns, J. H. G.; Heeres, H. J.; van den Linde, J. R.; Teuben, J. H.; Spek, A. L. *J. Chem. Soc., Chem. Commun.* **1991**, 642.
- (160) Booij, M.; Kiers, N. H.; Heeres, H. J.; Teuben, J. H. *J. Organomet. Chem.* **1989**, *364*, 79.
- (161) Booij, M.; Kiers, N. H.; Meetsma, A.; Teuben, J. H.; Smmets, W. J. J.; Spek, A. L. *Organometallics* **1989**, *8*, 2454.
- (162) Heeres, H. J.; Teuben, J. H.; Rogers, R. D. *J. Organomet. Chem.* **1989**, *364*, 87.
- (163) Schumann, H.; Meese-Marktscheffel, J. A.; Dietrich, A.; Pickardt, J. *J. Organomet. Chem.* **1992**, *433*, 241.
- (164) van der Heijden, H.; Pasman, P.; de Boer, E. J. M.; Schaverien, C. J.; Orpen, A. G. *Organometallics* **1989**, *8*, 1459.
- (165) Shapiro, P. J.; Bunel, E.; Schaefer, W. P.; Bercaw, J. E. *Organometallics* **1990**, *9*, 867.
- (166) Piers, W. E.; Shapiro, P. J.; Bunel, E. E.; Bercaw, J. E. *Synlett.* **1990**, 74.
- (167) Bunel, E. E.; Burger, B. J.; Bercaw, J. E. *J. Am. Chem. Soc.* **1988**, *110*, 976.
- (168) Gagné, M. R.; Stern, C. L.; Marks, T. J. *J. Am. Chem. Soc.* **1992**, *114*, 275.
- (169) Gagné, M. R.; Brard, L.; Conticello, V. P.; Giardello, M. A.; Stern, C. L.; Marks, T. J. *Organometallics* **1992**, *11*, 2003.
- (170) Coughlin, E. B.; Bercaw, J. E. *J. Am. Chem. Soc.* **1992**, *114*, 7606.
- (171) den Haan, K. H.; Teuben, J. H. *J. Chem. Soc., Chem. Commun.* **1986**, 682; Evans, W. J.; Solberger, M. S.; Khan, S. I.; Bau, R. *J. Am. Chem. Soc.* **1988**, *110*, 439; Evans, W. J.; Meadows, J. H.; Hunter, W. E.; Atwood, J. L. *ibid.* **1984**, *106*, 1291.
- (172) See footnote 12 in Watson and Roe (144c).
- (173) Evans, W. J.; Drummond, D. K.; Hanusa, T. P.; Doedens, R. J. *Organometallics* **1987**, *6*, 2279.
- (174) Schaverien, C. J. *J. Chem. Soc., Chem. Commun.* **1992**, 11; *Organometallics*, accepted for publication.
- (175) Stern, D.; Sabat, M.; Marks, T. J. *J. Am. Chem. Soc.* **1990**, *112*, 9558.
- (176) Atwood, J. L.; Bloom, I.; Hunter, W. E.; Evans, W. J. *Organometallics* **1983**, *2*, 709, and references therein.
- (177) Holton, J.; Lappert, M. F.; Ballard, D. G. H.; Pearce, R.; Atwood, J. L.; Hunter, W. E. *J. Chem. Soc., Dalton Trans.* **1979**, 54.
- (178) Waymouth, R. M.; Santarsiero, B. D.; Grubbs, R. H. *J. Am. Chem. Soc.* **1984**, *106*, 4050; Waymouth, R. M.; Santarsiero, B. D.; Coots, R. J.; Bronikowski, M. J.; Grubbs, R. H. *ibid.* **1986**, *108*, 1427.
- (179) den Haan, K. H.; Wielstra, Y.; Eshuis, J. J. W.; Teuben, J. H. *J. Organomet. Chem.* **1987**, *323*, 181.

- (180) Piers, W. E.; Bunel, E. E.; Bercaw, J. E. *J. Organomet. Chem.* **1991**, *407*, 51.
- (181) Marsh, R. E.; Schaefer, W. P.; Bazan, G. C.; Bercaw, J. E. *Acta Crystallogr., Sect. C* **1992**, *C48*, 1416.
- (182) Bercaw, J. E.; Marvich, R. H.; Bell, L. G.; Brintzinger, H. H. *J. Am. Chem. Soc.* **1972**, *94*, 1219.
- (183) Bercaw, J. E. *J. Am. Chem. Soc.* **1974**, *96*, 5087; Manriquez, J. M.; Bercaw, J. E. *ibid.*, 6229; Threlkel, R. S.; Bercaw, J. E. *J. Organomet. Chem.* **1977**, *136*, 1, and references therein.
- (184) Manriquez, J. M.; Fagan, P. J.; Marks, T. J. *J. Am. Chem. Soc.* **1978**, *100*, 3939; also see Green, J. C.; Watts, O. *J. Organomet. Chem.* **1978**, *153*, C40.
- (185) Ballard, D. G. H.; Courtis, A.; Holton, J.; McMeeking, J.; Pearce, R. *J. Chem. Soc., Chem. Commun.* **1978**, 994.
- (186) Schumann, H. In "Fundamental and Technological Aspects of Organo-f-Element Chemistry", NATO ASI Ser.; Marks, T. J.; Fischer, R. D., Eds.; D. Reidel: Dordrecht, Holland, 1979; Vol. 44, p. 81.
- (187) den Haan, K. H.; Teuben, J. H. *Recl. Trav. Chim. Pays-Bas* **1984**, *103*, 333.
- (188) Thompson, M. E.; Bercaw, J. E. *Pure Appl. Chem.* **1984**, *56*, 1.
- (189) Watson, P. L.; Whitney, J. F.; Harlow, R. L. *Inorg. Chem.* **1981**, *20*, 3271.
- (190) Evans, W. J.; Olofson, J. M.; Zhang, H.; Atwood, J. L. *Organometallics* **1988**, *7*, 629.
- (191) Rausch, M. D.; Moriarity, K. J.; Atwood, J. L.; Weeks, J. A.; Hunter, W. E.; Brittain, H. G. *Organometallics* **1986**, *5*, 1281.
- (192) Schumann, H.; Albrecht, I.; Loebel, J.; Hahn, E.; Hossain, M. B.; van der Helm, D. *Organometallics* **1986**, *5*, 1296; Albrecht, I.; Hahn, E.; Pickardt, J.; Schumann, H. *Inorg. Chim. Acta* **1985**, *110*, 145.
- (193) Evans, W. J.; Grate, J. W.; Levan, K. R.; Bloom, I.; Petersen, T. T.; Doedens, R. J.; Zhang, H.; Atwood, J. L. *Inorg. Chem.* **1986**, *25*, 3614.
- (194) Tilley, T. D.; Andersen, R. A. *Inorg. Chem.* **1981**, *20*, 3267.
- (195) Yasuda, H.; Yamamoto, H.; Yokota, K.; Nakamura, A. *Chem. Lett.* **1989**, 1309.
- (196) Gong, L. J.; Streitweiser, A., Jr.; Zalkin, A. *J. Chem. Soc., Chem. Commun.* **1987**, 460.
- (197) Evans, W. J.; Drummond, D. K.; Grate, J. W.; Zhang, H.; Atwood, J. L. *J. Am. Chem. Soc.* **1987**, *109*, 3928.
- (198) Evans, W. J.; Peterson, T. T.; Rausch, M. D.; Hunter, W. E.; Zhang, H.; Atwood, J. L. *Organometallics* **1985**, *4*, 554.
- (199) den Haan, K. H.; Luinstra, G. A.; Meetsma, A.; Teuben, J. H. *Organometallics* **1987**, *6*, 1509.
- (200) Teuben, J. H. In "Fundamental and Technological Aspects of Organo-f-Element Chemistry", NATO ASI Ser.; Marks, T. J.; Fragalà, I. L., Eds.; D. Reidel: Boston, 1985; Vol. 155, pp. 195.
- (201) Luinstra, G. A.; Teuben, J. H. *J. Am. Chem. Soc.* **1992**, *114*, 3361.
- (202) McDade, C.; Green, J. C.; Bercaw, J. E. *Organometallics* **1982**, *1*, 1629.
- (203) den Haan, K. H.; Teuben, J. H. *J. Chem. Soc., Chem. Commun.* **1986**, 682.
- (204) Bottomley, F.; Egharevba, G. O.; Lin, I. J. B.; White, P. S. *Organometallics* **1985**, *4*, 550.
- (205) Renkema, J.; Teuben, J. H. *Recl. Trav. Chim. Pays-Bas* **1988**, *105*, 241.
- (206) Booij, M.; Meetsma, A.; Teuben, J. *Organometallics* **1991**, *10*, 3246.
- (207) Heeres, H. J.; Teuben, J. H. *Organometallics* **1991**, *10*, 1980.
- (208) Heeres, H. J.; Meetsma, A.; Teuben, J. H. *Organometallics* **1990**, *9*, 1508.
- (209) Heeres, H. J.; Meetsma, A.; Teuben, J. H. *Angew. Chem., Int. Ed. Engl.* **1990**, *29*, 420.
- (210) Bercaw, J. E.; Davies, D. L.; Wolczanski, P. T. *Organometallics* **1986**, *5*, 443.
- (211) Scholz, A.; Smola, A.; Scholz, J.; Loebel, J.; Schumann, H.; Thiele, K. H. *Angew. Chem., Int. Ed. Engl.* **1991**, *30*, 435.

- (212) Mauermann, H.; Swepston, P. N.; Marks, T. J. *Organometallics* **1985**, *4*, 200.
- (213) Jeske, G.; Schock, L. E.; Swepston, P. N.; Marks, T. J. *J. Am. Chem. Soc.* **1985**, *107*, 8103.
- (214) Jeske, G.; Lauke, H.; Mauermann, H.; Schumann, H.; Marks, T. J. *J. Am. Chem. Soc.* **1985**, *107*, 8111.
- (215) Evans, W. J.; Dominquez, R.; Hanusa, T. P. *Organometallics* **1986**, *5*, 263.
- (216) O'Hare, D.; Manriquez, J.; Miller, J. S. *J. Chem. Soc., Chem. Commun.* **1988**, 491.
- (217) Hajela, S.; Schaefer, W. P.; Bercaw, J. E. *Acta Crystallogr., Sect. C* **1992**, *C48*, 1771.
- (218) Gagné, M. R.; Marks, T. J. *J. Am. Chem. Soc.* **1989**, *111*, 4108.
- (219) Gagné, M. R.; Nolan, S. P.; Marks, T. J. *Organometallics* **1990**, *9*, 1716.
- (220) Conticello, V. P.; Brard, L.; Giardello, M. A.; Tsuji, Y.; Stern, C. L.; Sabat, M.; Marks, T. J. *J. Am. Chem. Soc.* **1992**, *114*, 2761.
- (221) Molander, G. A.; Julius, M. J. *Org. Chem.* **1992**, *57*, 6347.
- (222) Sakakura, T.; Lautenschlager, H.-J.; Tanaka, M. *J. Chem. Soc., Chem. Commun.* **1991**, 40.
- (223) Harrison, K. N.; Marks, T. J. *J. Am. Chem. Soc.* **1992**, *114*, 9220.
- (224) Schumann, H.; Nickel, S.; Hahn, E.; Heeg, M. J. *Organometallics* **1985**, *4*, 801; Schumann, H.; Meese-Marktscheffel, J. A.; Hahn, E.; *J. Organomet. Chem.* **1990**, *390*, 301.
- (225) Forsyth, C. M.; Nolan, S. P.; Marks, T. J. *Organometallics* **1991**, *10*, 2543.
- (226) Kobayashi, T.; Sakakura, T.; Hayashi, T.; Yumura, M.; Tanaka, M. *Chem. Lett.* **1992**, 1158.
- (227) Radu, N. S.; Tilley, T. D.; Rheingold, A. L. *J. Am. Chem. Soc.* **1992**, *114*, 8293.
- (228) Yasuda, H.; Yamamoto, H.; Yokota, K.; Miyake, S.; Nakamura, A. *J. Am. Chem. Soc.* **1992**, *114*, 4908.
- (229) Schaefer, W. P.; Köhn, R. D.; Bercaw, J. E. *Acta Crystallogr., Sect. C* **1992**, *C48*, 251.
- (230) Piers, W. E.; Bercaw, J. E. *J. Am. Chem. Soc.* **1990**, *112*, 9406.
- (231) Clawson, L.; Soto, J.; Buchwald, S. L.; Steigerwald, M. L.; Grubbs, R. H. *J. Am. Chem. Soc.* **1985**, *107*, 3377.
- (232) Krauledat, H.; Brintzinger, H. H. *Angew. Chem., Int. Ed. Engl.* **1992**, *29*, 1412.
- (233a) Höck, N.; Oroschin, W.; Paolucci, G.; Fischer, R. D. *Angew. Chem., Int. Ed. Engl.* **1986**, *25*, 738.
- (233b) Akhnoukh, T.; Müller, J.; Qiao, K.; Li, X.-F.; Fischer, R. D. *J. Organomet. Chem.* **1991**, *408*, 47.
- (234a) Evans, W. J.; Chamberlain, L. R.; Ziller, J. W. *J. Am. Chem. Soc.* **1987**, *109*, 7209.
- (234b) Yamamoto, H.; Yasuda, H.; Yokota, K.; Nakamura, A.; Kai, Y.; Kasai, N. *Chem. Lett.* **1988**, 1963.
- (235) Knjazhanski, S. Y.; Bulychiev, B. M.; Belsky, V. K.; Soloveichik, G. L. *J. Organomet. Chem.* **1987**, *327*, 173.
- (236) Boncella, J. M.; Andersen, R. A. *Inorg. Chem.* **1984**, *23*, 432.
- (237) Hazin, P. N.; Huffman, J. C.; Bruno, J. W. *J. Chem. Soc., Chem. Commun.* **1988**, 1473.
- (238) Beletskaya, I. P.; Voskoboynikov, A. Z.; Chuklanova, E. B.; Gusev, A. I.; Magomdeov, G.-K. I. *Metalloorg. Khim.* **1988**, *1*, 1383; Beletskaya, I. P.; Voskoboynikov, A. Z.; Magomdeov, G.-K. I. *Dokl. Akad. Nauk. SSSR* **1989**, *306*, 108.
- (239) Recknagel, A.; Steiner, A.; Brooker, S.; Stalke, D.; Edelmann, F. T. *Chem. Ber.* **1991**, *124*, 1373.
- (240) Deng, H.; Shore, S. G. *J. Am. Chem. Soc.* **1991**, *113*, 8538.
- (241) Bursten, B. E.; Novo-Gradac, K. J. *J. Am. Chem. Soc.* **1987**, *109*, 904.
- (242) Sternal, R. S.; Brock, C. P.; Marks, T. J. *J. Am. Chem. Soc.* **1987**, *107*, 8270.
- (243) Alvarez, D., Jr.; Caulton, K. G.; Evans, W. J.; Ziller, J. W. *J. Am. Chem. Soc.* **1990**, *112*, 5674.

- (244) Green, M. L. H.; Hughes, A. K.; Michaelidou, D. P.; Mountford, P. *J. Chem. Soc., Chem. Commun.* **1993**, 591.
- (245) Magomdeov, G.-K. I.; Voskoboynikov, A. Z.; Chuklanova, E. B.; Gusev, A. I.; Beletskaya, I. P. *Metalloorg. Khim.* **1990**, *3*, 706; Beletskaya, I. P.; Voskoboynikov, A. Z.; Chuklanova, E. B.; Kirillova, N. I.; Shestakova, A. K.; Parshina, I. N.; Gusev, A. I.; Magomdeov, G.-K. I. *J. Am. Chem. Soc.* **1993**, *115*, 3156.
- (246) Schaverien, C. J.; Nesbitt, G. J. *J. Chem. Soc., Dalton Trans.* **1992**, 127.
- (247) Schumann, H.; Esser, L.; Loebel, J.; Dietrich, A.; van der Helm, D.; Ji, X. *Organometallics* **1991**, *10*, 2585.
- (248) Koga, N.; Morokuma, K. *J. Am. Chem. Soc.* **1988**, *110*, 108.
- (249) Eisch, J. J.; Pitrowski, A. M.; Brownstein, S. K.; Gabe, E. J.; Lee, F. L. *J. Am. Chem. Soc.* **1985**, *107*, 7219.
- (250) Gilbert, T. M.; Ryan, R. R.; Sattelberger, A. P. *Organometallics* **1988**, *7*, 2514.
- (251) Simoes, J. A. M.; Beauchamp, J. L. *Chem. Rev.* **1990**, *90*, 629.
- (252) Evans, W. J.; Hughes, L. A.; Hanusa, T. P. *J. Am. Chem. Soc.* **1984**, *106*, 4270.
- (253) Burns, C. J. Ph.D. Thesis, University of California, Berkeley, 1987.
- (254) Williams, R. A.; Hanusa, T. P.; Huffman, J. C. *Organometallics* **1990**, *9*, 1128.
- (255) Williams, R. A.; Hanusa, T. P.; Huffman, J. C. *J. Chem. Soc., Chem. Commun.* **1988**, 1045.
- (256) Kaupp, M.; von Schleyer, P. R.; Dolg, M.; Stoll, H. *J. Am. Chem. Soc.* **1992**, *114*, 8202.
- (257) Hitchcock, P. B.; Howard, J. A. K.; Lappert, M. F.; Prashar, S. *J. Organomet. Chem.* **1992**, *437*, 177.
- (258) Recknagel, A.; Edelman, F. T. *Angew. Chem., Int. Ed. Engl.* **1991**, *30*, 693.
- (259) Edelman, F. T.; Rieckhoff, M.; Haiduc, I.; Silaghi-Dumitrescu, I. *J. Organomet. Chem.* **1993**, *447*, 203.
- (260) Evans, W. J.; Grate, J. W.; Hughes, L. A.; Zhang, H.; Atwood, J. L. *J. Am. Chem. Soc.* **1985**, *107*, 3728.
- (261) Evans, W. J.; Hughes, L. A.; Drummond, D. K.; Zhang, H.; Atwood, J. L. *J. Am. Chem. Soc.* **1986**, *108*, 1722.
- (262) Evans, W. J.; Drummond, D. K. *J. Am. Chem. Soc.* **1988**, *110*, 2772.
- (263) Evans, W. J.; Drummond, D. K. *J. Am. Chem. Soc.* **1986**, *108*, 7440; Evans, W. J.; Drummond, D. K.; Chamberlain, L. R.; Doedens, R. J.; Bott, S. G.; Zhang, H.; Atwood, J. L. *ibid.* **1988**, *110*, 4983.
- (264) Evans, W. J.; Drummond, D. K.; Bott, S. G.; Atwood, J. L. *Organometallics* **1986**, *5*, 2389.
- (265) Evans, W. J.; Grate, J. W.; Bloom, I.; Hunter, W. E.; Atwood, J. L. *J. Am. Chem. Soc.* **1985**, *107*, 405.
- (266a) Evans, W. J.; Gonzales, S. L.; Ziller, J. W. *J. Am. Chem. Soc.* **1991**, *113*, 9880.
- (266b) Evans, W. J.; Gonzales, S. L.; Ziller, J. W. *J. Chem. Soc., Chem. Commun.* **1992**, 1138.
- (267) Evans, W. J.; Drummond, D. K. *J. Am. Chem. Soc.* **1989**, *111*, 3329.
- (268) Evans, W. J.; Ulibarri, T. A.; Ziller, J. W. *J. Am. Chem. Soc.* **1990**, *112*, 2314.
- (269) Evans, W. J.; Kociok-Köhn, G.; Leong, V. S.; Ziller, J. W. *Inorg. Chem.* **1992**, *31*, 3592.
- (270) Evans, W. J.; Kociok-Köhn, G.; Ziller, J. W. *Angew. Chem., Int. Ed. Engl.* **1992**, *31*, 1081.
- (271) Rebizant, J.; Apostolidis, C.; Spirlet, M. R.; Kanellakopulos, B. *Acta Crystallogr., Sect. C* **1988**, *C44*, 614.
- (272) Eggers, S. H.; Kopf, J.; Fischer, R. D. *Organometallics* **1986**, *5*, 383.
- (273) Eggers, S. H.; Kopf, J.; Fischer, R. D. *Acta Crystallogr., Sect. C* **1987**, *C43*, 2288.
- (274) Hammel, A.; Schwarz, W.; Weidlen, J. *J. Organomet. Chem.* **1989**, *363*, C29.

- (275) Eggers, S. H.; Schultze, H.; Kopf, J.; Fischer, R. D. *Angew. Chem., Int. Ed. Engl.* **1986**, *25*, 656.
- (276) Xie, Z.; Hahn, E.; Qian, C. *J. Organomet. Chem.* **1991**, *414*, C12.
- (277) Stults, S. D.; Andersen, R. A.; Zalkin, A. *Organometallics* **1990**, *9*, 115.
- (278) Evans, W. J.; Gonzales, S. L.; Ziller, J. W. *J. Am. Chem. Soc.* **1991**, *113*, 7423.
- (279) Evans, W. J.; Ulibarri, T. A. *J. Am. Chem. Soc.* **1987**, *109*, 4292.
- (280) Evans, W. J.; Keyer, R. A.; Ziller, J. W. *J. Organomet. Chem.* **1990**, *394*, 87.
- (281) Benetollo, F.; Bombieri, G.; Castellani, C. B.; Jahn, W.; Fischer, R. D. *Inorg. Chim. Acta* **1984**, *95*, L7; Shi, L.; Shen, F.; Zhou, X.; Ye, *Zhongguo Kexue Jishu Daxue Xuebao* **1991**, *21*, 109.
- (282) Ni, C.; Deng, D.; Qian, C. *Inorg. Chim. Acta* **1985**, *110*, L7.
- (283) Li, X.-F.; Eggers, S.; Kopf, J.; Jahn, W.; Fischer, R. D.; Apostolidis, C.; Kanellakopoulos, B.; Benetollo, F.; Polo, A.; Bombieri, G. *Inorg. Chim. Acta* **1985**, *100*, 183.
- (284) Stults, S.; Zalkin, A. *Acta Crystallogr., Sect. C* **1987**, *C43*, 430.
- (285) Spirlet, M. R.; Rebizant, J.; Apostolidis, C.; Kanellakopoulos, B.; *Acta Crystallogr., Sect. C* **1987**, *C43*, 2322.
- (286) Spirlet, M. R.; Rebizant, J.; Apostolidis, C.; Kanellakopoulos, B.; *Inorg. Chim. Acta* **1987**, *139*, 211.
- (287) Deacon, G. B.; Gatehouse, B. M.; Platts, S. N.; Wilkinson, D. L. *Aust. J. Chem.* **1987**, *40*, 907.
- (288) Xia, J.; Jin, Z.; Lin, G.; Chen, W. *J. Organomet. Chem.* **1991**, *408*, 173.
- (289) Qian, C.; Wang, B.; Deng, D.; Wu, G.; Zheng, P. *J. Organomet. Chem.* **1992**, *427*, C29.
- (290) Maier, R.; Kanellakopoulos, B.; Apostolidis, C.; Nuber, B. *J. Organomet. Chem.* **1992**, *435*, 275; Ye, Z.; Wang, S.; Yu, Y.; Shi, L. *Inorg. Chim. Acta* **1990**, *177*, 97.
- (291) Brennan, J. G.; Stults, S. D.; Andersen, R. A.; Zalkin, A. *Organometallics* **1988**, *7*, 1329.
- (292) Deacon, G. B.; Koplick, A. J.; Tuong, T. D. *Aust. J. Chem.* **1984**, *37*, 517.
- (293) Deacon, G. B.; Forsyth, C. M.; Newnham, R. H.; Tuong, T. D. *Aust. J. Chem.* **1987**, *40*, 895.
- (294) Strittmatter, R. J.; Bursten, B. E. *J. Am. Chem. Soc.* **1991**, *113*, 552; also see Roesch, N. *Inorg. Chim. Acta* **1984**, *94*, 297.
- (295) Wu, Z.; Ye, Z. *Polyhedron* **1991**, *10*, 27.
- (296) Stults, S. D.; Andersen, R. A.; Zalkin, A. *Organometallics* **1990**, *9*, 1623.
- (297) Schumann, H.; Jeske, G. *Angew. Chem., Int. Ed. Engl.* **1985**, *24*, 255.
- (298) Schumann, H.; Jeske, G. *Z. Naturforsch., B: Anorg. Chem., Org. Chem.* **1985**, *40B*, 1490.
- (299) Qiu, C.; Zhou, Z. *Huaxue Xuebao* **1986**, *44*, 1058; *Chem. Abstr.* **1987**, *107*, 59165p.
- (300) Qian, C.; Ge, Y.; Deng, D.; Gu, Y.; Zhang, C. *J. Organomet. Chem.* **1988**, *344*, 175; Qian, C.; Deng, D.; Ye, C.; Xie, Z.; Ge, Y.; Li, Y.; Gu, Y. *Inorg. Chim. Acta* **1987**, *140*, 21.
- (301) Sockwell, S. C.; Hanusa, T. P. *Inorg. Chem.* **1990**, *29*, 76.
- (302) Ce(COT)₂ is best formulated as containing Ce³⁺—see Section IX.
- (303) Gulino, A.; Casarin, M.; Conticello, V. P.; Gaudiello, J. G.; Mauermann, H.; Fragalà, I.; Marks, T. J. *Organometallics* **1988**, *7*, 2360.
- (304) Evans, W. J.; Deming, T. J.; Ziller, J. W. *Organometallics* **1989**, *8*, 1581.

Index

A

- arachno*-Carboranes
 - brachiation intermediates and cations, 15–16
 - compounds, 40–47
 - 2-vertex, 46–47
 - 3-vertex, 46
 - 4-vertex, 45
 - 5-vertex, 45
 - 6-vertex, 45
 - 7-vertex, 45
 - 8-vertex, 44
 - 9-vertex, 41–42
 - 10-vertex, 42–43
 - 11-vertex, 42–43
 - 12-vertex, 42–43
 - electron counting, 31
 - geometrical systematics and electron pair relationships, 22–25, 27–28
 - Ziegler–Natta polymerization, 46
- Atom–atom interaction model, 133

B

- Bondi data set, 126–127
- Brachiation intermediates, 15–16
- Buckingham potential, 132
- Burg–Hurd hydroboration reaction, 8
- Burg–Schlesinger diborane synthesis, 7–8

C

- Carboranes
 - arachno* compounds, *see arachno*-Carboranes
 - Burg–Hurd hydroboration reaction, 8
 - Burg–Schlesinger diborane synthesis, 7–8
 - carbocations, 15–17
 - Brachiation intermediates, 15–16
 - nonclassical structures, 15
 - structures, 15–16

- classification, 22–29
 - geometrical systematics, 23–25
 - geometry, 22–24
 - most spherical deltahedra, 25–28
 - site preferences, 29
 - Wade's rules, 24–25
- closo* compounds, *see closo*-Carboranes
- early processes, 9–10
- electron counting, 31
- electron pair bonds, 18–21
 - Chop–stx, 20–21, 31, 42
 - evolution, 19
 - styx*, 19–21, 30, 32
- hypho* compounds, *see hypho*-Carboranes
- introduction, 1–8
- Keilin synthesis, 9
- lanthanide chemistry, 309–310
- nido* compounds, *see nido*-Carboranes
- nomenclature, 31–32
- polyborane Lewis base adducts, 30
- polyboranes, 17–18
- structure determinations, 10–13
- Car–Parrinello method, 83
- Chalcogens, triatomic interchalcogens, 166–171
- Charton's regression analysis, 136
- closo*-Carboranes
 - electron counting, 31
 - geometrical systematics and electron pair relationships, 22–29
 - nomenclature, 32
 - structures, 2–7, 12–15
 - thermal stability and fuel value, 17–18

D

- Diselenium monoxide, 171
- Disulfur monoxide
 - complex synthesis, 167–169
 - coordination reactions, 169–170
 - structural studies, 170–171

F**Fullerenes**

- alkali metal intercalation, 77–80
 - electrical conductivity, 79–80
 - structural studies, 78–79
 - synthesis, 78
- bond distances, 59
- doped species, symbolism, 58
- electron affinity, 59
- endohedral complexes, 63–68
 - ESR spectroscopy, 65, 67
 - EXAFS data, 65
 - formation mechanisms, 64
 - fragmentation patterns, 64
 - molecular orbital calculations, 67–68
 - Mössbauer spectroscopy, 65
 - sequestration, 65–67
 - synthesis, 63–64
- framework carbon substitution, 80–86
 - calculated structures, 84, 85
 - Car–Parrinello method, 83
 - CBN-ball structure, 84
 - computational studies, 83–86
 - heterocluster synthesis, 82–83
 - hybrid clusters, 80–81
 - polymer formation, 81
- general properties, 58–61
- Hartree-Fock method, 68
- heteroatom incorporation, 58
- HOMO orbitals, 68
- Hückel energy levels, 60
- interstitial substitution, 77–80
- introduction, 57–62
- ionization energies, 59
- isomer behaviors, 66
- LUMO orbitals, 68
- metal-containing substituents, 69–77
 - Fourier transform mass spectra, 76
 - iridium complexes, 72–75
 - iron complexes, 76–77
 - naked metal complexes, 74, 76–77
 - osmate esters, 69–71
 - platinum complexes, 71–72
 - ruthenium complexes, 74
 - structures, 70, 72, 74, 75
 - Vaska's compound, 72–73
- NMR spectroscopy, 59–60
- preparation, 61–62
- salt formation, 80

- separation, 62
- X-ray diffraction data, 58–59

G

- GEOME calculations, 124
- Grimes' isomers, 36–37

H

- Hartree-Fock method, 68
- hypho*-Carboranes
 - compounds, 47–48
 - geometrical systematics and electron pair relationships, 24, 27
- Ziegler–Natta polymerization, 48

I

- Iminooxosulfuranes
 - complexes
 - iridium, 185
 - iron, 182–184
 - nickel, 185–186
 - osmium, 183–184
 - platinum, 185–186
 - rhodium, 184–185
 - ruthenium, 183–184
 - coordinated ligands, 191–201
 - coordination modes, 180–182
 - coordination reactions, 187–191
 - coupling, 196
 - heterocycle syntheses, 201
 - hydrotungstenation, 192
 - insertion, 193
 - multiple bonds
 - alkylidynes, 199
 - carbonyls, 199–200
 - oxides, 200–201
 - σ -organyls, 192–195
 - orthometallation, 185
 - reactions, 191–192
 - π -coordinated ligands, 195–197
 - electrophiles, 189–191
 - fragmentation, 187–188
 - hydrolysis, 188–189

- ligand substitution, 187
- nucleophiles, 189
- oxidation, 189
- spectroscopic studies, 186–187
- structural studies, 186–187

Iridium complexes

- fullerenes, 72–75
- iminoxosulfuranes, 185

Iron complexes

- fullerenes, 76–77
- iminoxosulfuranes, 182–184

K

Keilin synthesis, 9

L

Lanthanides

- π -adducts, 301–304
- alkoxides, 289–293
- bis(cyclopentadienyls)
 - insertion, 324, 328–329
 - kinetics, 329
 - ligand variations, 333–338
 - mechanistic studies, 328
 - precursors, 323
 - reactivity, 325, 329, 333
 - structural studies, 325, 327, 330
- carboranes, 309–310
- characterization, 284
- γ -C-H-Ln versus β -Si-Me-Ln
 - interactions, 341–343
- (C₅Me₅)₂Ln reactivity and structure, 338–340
- complexes
 - π -arene, 304–306
 - bis(cyclopentadienyl), 322–333
 - cyclooctatetraene, 307–309
 - homoleptic alkyl, 286–289
 - homoleptic phenoxide, 314–315
 - monocyclopentadienyl, 310–322
 - tris(cyclopentadienyl), 347–350
- decomposition pathway, 285
- heterocyclopentadienyls, 310
- interactions, 341–343
- introduction, 283–286
- isocarbonyls, 340–341

- ligands, nitrogen donor, 294–301
 - porphyrins, 294–299
- low-oxidation-states, 344–347
- organolanthanides, 350
- selenides, 293–294
- stabilization, 285–286
- tellurolates, 293–294
- thermodynamics, 343
- thiolates, 293

Linear free energy approach, 131–132

M

MM2 force field, 130, 133

N

Neocarborane, 5, 13

Nickel, iminoxosulfurane complexes, 185–186

nido-Carboranes, 12

- compounds
 - 2-vertex, 39–40
 - 4-vertex, 33–34
 - 5-vertex, 34
 - 6-vertex, 32–33
 - 7-vertex, 34–35
 - 8-vertex, 34–35
 - 9-vertex, 34–35
 - 10-vertex, 35–36
 - 11-vertex, 36
 - 12-vertex, 36–39
- electron counting, 31
- geometrical systematics and electron pair relationships, 22–25, 27–29
- Grimes' isomers, 36–37
- Lewis base adducts, 30
- nomenclature, 32
- structures, 16–17

O

Organometallic chemistry, steric effects

- electronic profiles, 142–143
- introduction, 95–97
- steric effect quantification, 137–141
 - distance variation, 137–138

- possible interactions, 138
 - solid cone angle, 141
 - spatial ligand variation, 138–140
 - Tolman cone angle, 140
 - vantage point choice, 140
 - steric profiles, 142–144
 - QALE approach, 142–143
 - steric size measurements, 152–153
 - steric size quantification, *see* Steric size quantification
 - thresholds, 142–145
 - Osmate esters, fullerenes, 69–71
 - Osmium
 - iminooxosulfurane complexes, 183–184
 - mediation of sulfur diimide cleavage, 216
- P**
- Platinum complexes
 - fullerenes, 71–72
 - iminooxosulfuranes, 185–186
 - sulfines, 175
 - sulfur diimides, 204
 - with thiazate ligands, 219
 - Polymerization, Ziegler–Natta, *see* Ziegler–Natta polymerization
- Q**
- QALE approach, 142–143
- R**
- Rhodium complexes
 - iminooxosulfuranes, 184–185
 - sulfines, 176
 - with thiazate ligands, 219
 - Ruthenium complexes
 - fullerenes, 74
 - iminooxosulfuranes, 183–184
 - sulfur diimides, 215
- S**
- SCHAKAL plot, 244
 - Selenium dioxide, 166–167
 - Silaorganometallic chemistry
 - co-activation reaction, 269–271
 - complexes
 - cyclic, 272
 - disilaethene, 275–276
 - donor-stabilized, 272–274
 - silaethene, 274–275
 - silaamine, 275
 - silatrimethylenemethane, 276
 - silylene, 232–268
 - introduction, 229–232
 - metallasilaallenes, 276–277
 - prospects, 277
 - sila, 275–276
 - silaethene complexes, 274–275
 - silaamine complexes, 275
 - silylyne complexes, 272
 - Silylenes
 - base adducts
 - bond distance, 248
 - coordination geometry, 242
 - electronic structure, 247–248
 - high-valent transition metal complexes, 248
 - NMR data, 245–247
 - SCHAKAL plot, 244
 - spectroscopic parameters, 245–247
 - structural aspects, 242–244
 - structural parameters, 243
 - base-free complexes, 267–268
 - base stabilization, 251–265
 - coalescence temperatures, 253
 - flip-flop coordination, 259–261
 - fluxionality, 252–254
 - intramolecular donor reactions, 261–265
 - intramolecular interaction, 254
 - ORTEP view, 255
 - phosphino substitution, 258–259
 - silanediyl complexes, 255–256
 - silanediyl coordination, 256–258
 - complexes
 - base adducts, 242–248
 - base-free, 267–268
 - base stabilization, 251–265
 - cyclic, 272
 - donor-stabilized, 272–274
 - high-valent transition metals, 248–251
 - salt adduct, 265–267
 - Si–Si bond formation, 237–242

- synthesis, 232
- dehydrogenative coupling reactions
 - early transition metals, 240–242
 - late transition metals, 237–240
 - mechanisms, 240–241
 - silanes, 232
- hydrosilation process, 231
- methylchlorosilane synthesis by direct methods, 231
- reactivity, 248–251
 - metal silicon bond retention, 249–251
 - M–Si bond cleavage, 249
- salt adduct, 265–267
- synthesis
 - base abstraction, 234
 - dimeric cleavage, 235–236
 - insertion, 233–234
 - metal coordination, 235
 - salt elimination, 232–233
 - silane elimination, 237
 - substituent displacement, 234
 - trapping, 235
- Steric effects, in organometallic chemistry,
 - see Organometallic chemistry, steric effects
- Steric size quantification
 - alkyl groups, 110–114
 - amines, 108–109
 - aryl groups, 110–114
 - Charton's regression analysis, 136
 - cluster cone angles, 104, 116
 - cone angles, 97–117
 - bite angle, 103
 - cone measuring device, 102
 - definition, 98
 - kinetic data, 101–102
 - measurements, 97–101
 - organometallic clusters, 104–105
 - semivertex angle calculation, 102
 - Tolman angle, 97–101
 - Tolman concept, 97–104
 - value modification, 103
 - ligand repulsive energy, E_R , 130–133
 - absolute static threshold, 132
 - atom–atom interaction model, 133
 - Buckingham potential, 132
 - linear free energy approach, 131–132
- ligands, 117
 - $P(OR)_3$, 108
 - $P(OR)A_2$, 108
 - $P(OR)_2A$, 108
 - PR^3 , 105–107
- macrocyclic chemistry, 134
- molecular mechanics, 133–134
- molecular volumes, 145–152
 - applications, 149–152
 - charge distribution, 148–149
- NMR spectroscopy, 136–137
- solid angles, 115, 117–130
 - advantages, 123
 - atom overlap problem, 126–128
 - Bondi data set, 126–127
 - cluster size calculation, 124–125
 - definition, 121, 123
 - GEOME calculations, 124
 - ligand profiles, 119–121
 - MM2 force field, 130
 - molecular mechanics, 117–118, 129
 - M–P bond rotation, 119
 - SYBYL force field, 129–130
 - Taft–Dubois steric parameter, 128
 - uses, 122–126
- sulfides, 116
 - Taft steric parameter, E_s' , 134–136
- Sulfines
 - coordination modes, 172
 - metal–carbonyl mediated reduction, 174
 - α -metallasulfines, 177–179
 - oxidation addition, 175
 - platinum complexes, 175
 - reactivity, 172–178
 - rhodium complexes, 176
 - spectroscopic studies, 173, 176, 178
 - stepwise assembly, 173
 - structural studies, 178
 - α -substituent participation, 172
 - synthesis, 172–178
 - vinyl sulfine synthesis, 174
- N*-Sulfinylamines, see Iminooxosulfuranes
- Sulfur diimides
 - clusters, 211
 - coordination complexes, 202–208
 - imino substituent, 204–208
 - modes, 202
 - NSN cumulene, 202–204
 - platinum, 204
 - pnicogeno substitution, 205–208
 - tungsten, 203
- coordination reactions
 - fragmentation, 208–212, 209–212

hydrides, 212–215
 σ -organyl complexes, 215–216
 osmium-mediated cleavage, 216
 ruthenium, 215
hydrido-benzochalcogenadiazole
 complexes, 214
hydrotungstenation, 213
interactions, 211
Sulfur dioxide analogs
 cumulenes, physical data, 165
 general coordination, 162–164
 frontier orbitals, 164
 group frequencies, 166
 modes, 162
 orbital interactions, 164
 relative energies, 165
 spectroscopic data, 164–166
 theoretical considerations, 162–164
insertion mechanism, 160
introduction, 159–161
thiazate ligands, 217–221
 coordination chemistry, 221
 cothermolysis, 220
 mechanisms, 218
 metals, 217
 platinum complexes, 219
 rhodium complexes, 219

titanium complexes, 218
SYBYL force field, 129–130

T

Taft–Dubois steric parameter, 128
Taft steric parameter, E'_s , 134–136
Titanium, complexes with thiazate ligands,
 218
Tolman cone angle, 97–104, 117–118, 140,
 142
Tungsten, sulfur diimide complexes, 203

V

Vaska's compound, 72–73

W

Wade's rules, 24–25

Z

Ziegler–Natta polymerization, 46, 48

Cumulative List of Contributors

- Abel, E. W., **5**, 1; **8**, 117
 Aguiló, A., **5**, 321
 Akkerman, O. S., **32**, 147
 Albano, V. G., **14**, 285
 Alper, H., **19**, 183
 Anderson, G. K., **20**, 39; **35**, 1
 Angelici, R. J., **27**, 51
 Aradi, A. A., **30**, 189
 Armitage, D. A., **5**, 1
 Armor, J. N., **19**, 1
 Ash, C. E., **27**, 1
 Ashe III, A. J., **30**, 77
 Atwell, W. H., **4**, 1
 Baines, K. M., **25**, 1
 Barone, R., **26**, 165
 Bassner, S. L., **28**, 1
 Behrens, H., **18**, 1
 Bennett, M. A., **4**, 353
 Bickelhaupt, F., **32**, 147
 Birmingham, J., **2**, 365
 Blinka, T. A., **23**, 193
 Bockman, T. M., **33**, 51
 Bogdanović, B., **17**, 105
 Bottomley, F., **28**, 339
 Bradley, J. S., **22**, 1
 Brew, S. A., **35**, 135
 Brinckman, F. E., **20**, 313
 Brook, A. G., **7**, 95; **25**, 1
 Bowser, J. R., **36**, 57
 Brown, H. C., **11**, 1
 Brown, T. L., **3**, 365
 Bruce, M. I., **6**, 273, **10**, 273; **11**, 447; **12**, 379; **22**, 59
 Brunner, H., **18**, 151
 Buhro, W. E., **27**, 311
 Byers, P. K., **34**, 1
 Cais, M., **8**, 211
 Calderon, N., **17**, 449
 Callahan, K. P., **14**, 145
 Canty, A. J., **34**, 1
 Cartledge, F. K., **4**, 1
 Chalk, A. J., **6**, 119
 Chanon, M., **26**, 165
 Chatt, J., **12**, 1
 Chini, P., **14**, 285
 Chisholm, M. H., **26**, 97; **27**, 311
 Chiusoli, G. P., **17**, 195
 Chojinowski, J., **30**, 243
 Churchill, M. R., **5**, 93
 Coates, G. E., **9**, 195
 Collman, J. P., **7**, 53
 Compton, N. A., **31**, 91
 Connelly, N. G., **23**, 1; **24**, 87
 Connolly, J. W., **19**, 123
 Corey, J. Y., **13**, 139
 Corriu, R. J. P., **20**, 265
 Courtney, A., **16**, 241
 Coutts, R. S. P., **9**, 135
 Coville, N. J., **36**, 95
 Coyle, T. D., **10**, 237
 Crabtree, R. H., **28**, 299
 Craig, P. J., **11**, 331
 Csuk, R., **28**, 85
 Cullen, W. R., **4**, 145
 Cundy, C. S., **11**, 253
 Curtis, M. D., **19**, 213
 Darensbourg, D. J., **21**, 113; **22**, 129
 Darensbourg, M. Y., **27**, 1
 Davies, S. G., **30**, 1
 Deacon, G. B., **25**, 237
 de Boer, E., **2**, 115
 Deeming, A. J., **26**, 1
 Dessy, R. E., **4**, 267
 Dickson, R. S., **12**, 323
 Dixneuf, P. H., **29**, 163
 Eisch, J. J., **16**, 67
 Ellis, J. E., **31**, 1
 Emerson, G. F., **1**, 1
 Epstein, P. S., **19**, 213
 Erker, G., **24**, 1
 Ernst, C. R., **10**, 79
 Errington, R. J., **31**, 91
 Evans, J., **16**, 319
 Evans, W. J., **24**, 131
 Faller, J. W., **16**, 211
 Farrugia, L. J., **31**, 301
 Faulks, S. J., **25**, 237
 Fehlner, T. P., **21**, 57; **30**; **189**
 Fessenden, J. S., **18**, 275
 Fessenden, R. J., **18**, 275

- Fischer, E. O., **14**, 1
 Ford, P. C., **28**, 139
 Forniés, J., **17**, 219
 Forster, D., **17**, 255
 Fraser, P. J., **12**, 323
 Friedrich, H., **36**, 229
 Friedrich, H. B., **33**, 235
 Fritz, H. P., **1**, 239
 Fürstner, A., **28**, 85
 Furukawa, J., **12**, 83
 Fuson, R. C., **1**, 221
 Gallop, M. A., **25**, 121
 Garrou, P. E., **23**, 95
 Geiger, W. E., **23**, 1; **24**, 87
 Geoffroy, G. L., **18**, 207; **24**, 249; **28**, 1
 Gilman, H., **1**, 89; **4**, 1; **7**, 1
 Gladfelter, W. L., **18**, 207; **24**, 41
 Gladysz, J. A., **20**, 1
 Glänzer, B. I., **28**, 85
 Green, M. L. H., **2**, 325
 Grev, R. S., **33**, 125
 Griffith, W. P., **7**, 211
 Grovenstein, Jr., E., **16**, 167
 Gubin, S. P., **10**, 347
 Guerin, C., **20**, 265
 Gysling, H., **9**, 361
 Haiduc, I., **15**, 113
 Halasa, A. F., **18**, 55
 Hamilton, D. G., **28**, 299
 Handwerker, H., **36**, 229
 Harrod, J. F., **6**, 119
 Hart, W. P., **21**, 1
 Hartley, F. H., **15**, 189
 Hawthorne, M. F., **14**, 145
 Heck, R. F., **4**, 243
 Heimbach, P., **8**, 29
 Helmer, B. J., **23**, 193
 Henry, P. M., **13**, 363
 Heppert, J. A., **26**, 97
 Herberich, G. E., **25**, 199
 Herrmann, W. A., **20**, 159
 Hieber, W., **8**, 1
 Hill, A. F., **36**, 131
 Hill, E. A., **16**, 131
 Hoff, C., **19**, 123
 Hoffmeister, H., **32**, 227
 Holzmeier, P., **34**, 67
 Honeyman, R. T., **34**, 1
 Horwitz, C. P., **23**, 219
 Hosmane, N. S., **30**, 99
 Housecroft, C. E., **21**, 57; **33**, 1
 Huang, Y. Z., **20**, 115
 Hughes, R. P., **31**, 183
 Ibers, J. A., **14**, 33
 Ishikawa, M., **19**, 51
 Ittel, S. D., **14**, 33
 Jain, L., **27**, 113
 Jain, V. K., **27**, 113
 James, B. R., **17**, 319
 Janiak, C., **33**, 291
 Jastrzebski, J. T. B. H., **35**, 241
 Jenck, J., **32**, 121
 Jolly, P. W., **8**, 29; **19**, 257
 Jonas, K., **19**, 97
 Jones, M. D., **27**, 279
 Jones, P. R., **15**, 273
 Jordan, R. F., **32**, 325
 Jukes, A. E., **12**, 215
 Jutzi, P., **26**, 217
 Kaesz, H. D., **3**, 1
 Kalck, P., **32**, 121; **34**, 219
 Kaminsky, W., **18**, 99
 Katz, T. J., **16**, 283
 Kawabata, N., **12**, 83
 Kemmitt, R. D. W., **27**, 279
 Kettle, S. F. A., **10**, 199
 Kilner, M., **10**, 115
 Kim, H. P., **27**, 51
 King, R. B., **2**, 157
 Kingston, B. M., **11**, 253
 Kisch, H., **34**, 67
 Kitching, W., **4**, 267
 Kochi, J. K., **33**, 51
 Köster, R., **2**, 257
 Kreiter, C. G., **26**, 297
 Krüger, G., **24**, 1
 Kudaroski, R. A., **22**, 129
 Kühlein, K., **7**, 241
 Kuivila, H. G., **1**, 47
 Kumada, M., **6**, 19; **19**, 51
 Lappert, M. F., **5**, 225; **9**, 397; **11**, 253;
 14, 345
 Lawrence, J. P., **17**, 449
 Le Bozec, H., **29**, 163
 Lednor, P. W., **14**, 345
 Linford, L., **32**, 1
 Longoni, G., **14**, 285
 Luijten, J. G. A., **3**, 397
 Lukehart, C. M., **25**, 45
 Lupin, M. S., **8**, 211

- McGlinchey, M. J., **34**, 285
 McKillop, A., **11**, 147
 McNally, J. P., **30**, 1
 Macomber, D. W., **21**, 1; **25**, 317
 Maddox, M. L., **3**, 1
 Maguire, J. A., **30**, 99
 Maitlis, P. M., **4**, 95
 Mann, B. E., **12**, 135; **28**, 397
 Manuel, T. A., **3**, 181
 Markies, P. R., **32**, 147
 Mason, R., **5**, 93
 Masters, C., **17**, 61
 Matsumura, Y., **14**, 187
 Mayr, A., **32**, 227
 Meister, G., **35**, 41
 Mingos, D. M. P., **15**, 1
 Mochel, V. D., **18**, 55
 Moedritzer, K., **6**, 171
 Molloy, K. C., **33**, 171
 Monteil, F., **34**, 219
 Morgan, G. L., **9**, 195
 Morrison, J. A., **35**, 211
 Moss, J. R., **33**, 235
 Mrowca, J. J., **7**, 157
 Müller, G., **24**, 1
 Mynott, R., **19**, 257
 Nagy, P. L. I., **2**, 325
 Nakamura, A., **14**, 245
 Nesmeyanov, A. N., **10**, 1
 Neumann, W. P., **7**, 241
 Norman, N. C., **31**, 91
 Ofstead, E. A., **17**, 449
 Ohst, H., **25**, 199
 Okawara, R., **5**, 137; **14**, 187
 Oliver, J. P., **8**, 167; **15**, 235; **16**, 111
 Onak, T., **3**, 263
 Oosthuizen, H. E., **22**, 209
 Otsuka, S., **14**, 245
 Pain, G. N., **25**, 237
 Parshall, G. W., **7**, 157
 Paul, I., **10**, 199
 Peres, Y., **32**, 121
 Petrosyan, W. S., **14**, 63
 Pettit, R., **1**, 1
 Pez, G. P., **19**, 1
 Poland, J. S., **9**, 397
 Poliakoff, M., **25**, 277
 Popa, V., **15**, 113
 Pourreau, D. B., **24**, 249
 Powell, P., **26**, 125
 Pratt, J. M., **11**, 331
 Prokai, B., **5**, 225
 Pruett, R. L., **17**, 1
 Rao, G. S., **27**, 113
 Raubenheimer, H. G., **32**, 1
 Rausch, M. D., **21**, 1; **25**, 317
 Reetz, M. T., **16**, 33
 Reutov, O. A., **14**, 63
 Rijkens, F., **3**, 397
 Ritter, J. J., **10**, 237
 Rochow, E. G., **9**, 1
 Rokicki, A., **28**, 139
 Roper, W. R., **7**, 53; **25**, 121
 Roundhill, D. M., **13**, 273
 Rubezhov, A. Z., **10**, 347
 Salerno, G., **17**, 195
 Salter, I. D., **29**, 249
 Satgé, J., **21**, 241
 Schade, C., **27**, 169
 Schaverien, C. J., **36**, 283
 Schmidbaur, H., **9**, 259; **14**, 205
 Schrauzer, G. N., **2**, 1
 Schubert, U., **30**, 151
 Schulz, D. N., **18**, 55
 Schumann, H., **33**, 291
 Schwebke, G. L., **1**, 89
 Seppelt, K., **34**, 207
 Setzer, W. N., **24**, 353
 Seyferth, D., **14**, 97
 Shapakin, S. Yu., **34**, 149
 Shen, Y. C., **20**, 115
 Shriver, D. F., **23**, 219
 Siebert, W., **18**, 301; **35**, 187
 Sikora, D. J., **25**, 317
 Silverthorn, W. E., **13**, 47
 Singleton, E., **22**, 209
 Sinn, H., **18**, 99
 Skinner, H. A., **2**, 49
 Slocum, D. W., **10**, 79
 Smallridge, A. J., **30**, 1
 Smeets, W. J. J., **32**, 147
 Smith, J. D., **13**, 453
 Speier, J. L., **17**, 407
 Spek, A. L., **32**, 147
 Stafford, S. L., **3**, 1
 Stańczyk, W., **30**, 243
 Stone, F. G. A., **1**, 143; **31**, 53; **35**, 135
 Su, A. C. L., **17**, 269
 Suslick, K. M., **25**, 73
 Süss-Fink, G., **35**, 41

- Sutin, L., **28**, 339
Swincer, A. G., **22**, 59
Tamao, K., **6**, 19
Tate, D. P., **18**, 55
Taylor, E. C., **11**, 147
Templeton, J. L., **29**, 1
Thayer, J. S., **5**, 169; **13**, 1; **20**, 313
Theodosiou, I., **26**, 165
Timms, P. L., **15**, 53
Todd, L. J., **8**, 87
Touchard, D., **29**, 163
Traven, V. F., **34**, 149
Treichel, P. M., **1**, 143; **11**, 21
Tsuji, J., **17**, 141
Tsutsui, M., **9**, 361; **16**, 241
Turney, T. W., **15**, 53
Tyfield, S. P., **8**, 117
Usón, R., **28**, 219
Vahrenkamp, H., **22**, 169
van der Kerk, G. J. M., **3**, 397
van Koten, G., **21**, 151; **35**, 241
Veith, M., **31**, 269
Vezey, P. N., **15**, 189
von Ragué Schleyer, P., **24**, 353; **27**, 169
Vrieze, K., **21**, 151
Wada, M., **5**, 137
Walton, D. R. M., **13**, 453
Wailles, P. C., **9**, 135
Webster, D. E., **15**, 147
Weitz, E., **25**, 277
West, T., **5**, 169; **16**, 1; **23**, 193
Werner, H., **19**, 155
White, D., **36**, 95
Wiberg, N., **23**, 131; **24**, 179
Wiles, D. R., **11**, 207
Wilke, G., **8**, 29
Williams, R. E., **36**, 1
Winter, M. J., **29**, 101
Wojcicki, A., **11**, 87; **12**, 31
Yamamoto, A., **34**, 111
Yashina, N. S., **14**, 63
Ziegler, K., **6**, 1
Zuckerman, J. J., **9**, 21
Zybill, C., **36**, 229